Argonne NATIONAL LABORATORY

ANL-05/29

APS SCIENCE 2005

THE ANNUAL REPORT OF THE ADVANCED PHOTON SOURCE AT ARGONNE NATIONAL LABORATORY

MAY 2006

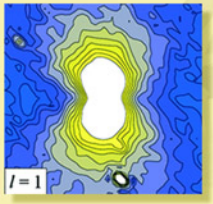

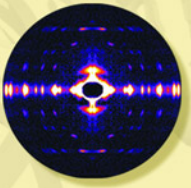

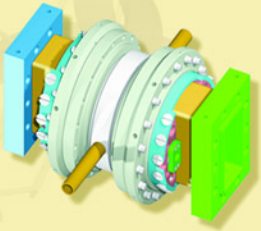

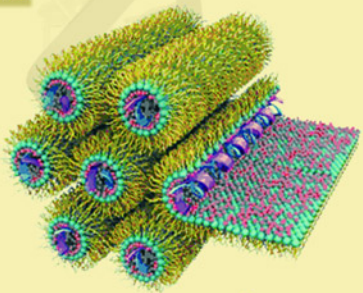

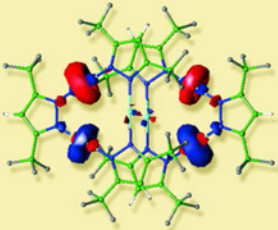

Support for the Advanced Photon Source
Argonne National Laboratory's Advanced Photon Source is supported by the
U.S. Department of Energy, Office of Science, Office of Basic Energy Sciences.

About Argonne National Laboratory
Argonne is a U.S. Department of Energy laboratory managed by The University of Chicago
under contract W-31-109-Eng-38. The Laboratory's main facility is outside Chicago, at
9700 South Cass Avenue, Argonne, Illinois 60439. For information about Argonne,
see www.anl.gov.

Availability of This Report
This report is available, at no cost, at http://www.osti.gov/bridge. It is also available
on paper to the U.S. Department of Energy and its contractors, for a processing fee, from:
U.S. Department of Energy
Office of Scientific and Technical Information
P.O. Box 62
Oak Ridge, TN 37831-0062
phone (865) 576-8401
fax (865) 576-5728
reports@adonis.osti.gov

Argonne NATIONAL LABORATORY

ANL-05/29

APS SCIENCE 2005

THE ANNUAL REPORT OF THE ADVANCED PHOTON SOURCE AT ARGONNE NATIONAL LABORATORY

The Advanced Photon Source is funded by the U.S. Department of Energy, Office of Science, Office of Basic Energy Sciences

WELCOME

J. MURRAY GIBSON...

... is Associate Laboratory Director for Scientific User Facilities at Argonne National Laboratory and Director of the Advanced Photon Source.

Murray Gibson (left), Eric Isaacs (Director, Center for Nanoscale Materials), and Brian Stephenson (Director, nanoprobe beamline, Center for Nanoscale Materials) in the 26-ID-B enclosure on the nanoprobe beamline.

Thank you for taking the time to read our annual report that aims to provide an overview of new capabilities at the Advanced Photon Source (APS) and examples of fascinating scientific research. We are very proud of the accomplishments described here, which are the fruit of dedicated work by our users and our employees. The (fiscal) year 2005 was a very successful one for the APS. The number of users grew to a record of more than 3,200, up 16% from the previous year. The number of peer-reviewed papers published by our users broke the level of 1,000 for the first time. And in this tenth anniversary year since the first light at the APS, we had our largest user meeting ever, with more than 600 participants. The machine reached its highest-ever availability and reliability, at better than 98% delivered beam, and a mean time between failures of more than 100 hours. Most important of all, the scientific impact of the research carried out here continues to broaden and deepen, as these selected highlights will show you.

This facility evolves in a healthy way. The number of beamlines operated by the APS organization grows, following the policy of the U.S. Department of Energy (DOE) to transfer to us responsibility for beamlines whose operational costs the DOE had previously funded via outside institutions. We now operate 20 beamlines through our X-ray Operations and Research (XOR) groups, with three more beamlines currently under construction. Several of these beamlines are operated jointly, either in transition with former collaborative access team (CAT) members who have become partner users, or indefinitely-for example, with the Center for Nanoscale Materials nanoprobe beamline. (The accompanying photograph was taken at this beamline, which aims to be the world's most powerful hard x-ray microscope.)

The growth in the number of beamlines under APS control has facilitated our strategic plan to optimize our beamlines and create more dedicated capabilities. This year we began—with limited funding—three of these upgrades: dedicating sector 1-ID to high-energy scattering, creating a dedicated imaging capability at sector 32 (the former COM-CAT), and optimizing the small-angle scattering beamline at sector 12. We also work closely with our partner users and CATs to optimize scientific capabilities for the entire APS facility. For example, this year we have begun installation of a special undulator for ultra-high-brightness single-pulse diffraction at BioCARS (sector 14) in collaboration with the National Institutes of Health.

"Argonne is blessed with a number of top-quality and unique facilities for materials-related research, including the APS, the Intense Pulsed Neutron Source, the Electron Microscopy Center, and the exciting new Center for Nanoscale Materials."

The growth of XOR has allowed us to reorganize our divisions and form a dedicated X-ray Science Division (XSD). Creation of this division brings the management of x-ray science at the APS to an appropriately high level, where it will be on a par with the machine and will share engineering and computing support services. This change is part of a broader reorganization intended to make us more efficient through consolidation and sharing of resources. We have three divisions as before, but with redefined roles. The "machine" division—the Accelerator Systems Division (ASD)—comprises all the technical groups that operate, develop, and carry out research with the accelerator. The "beamlines" division—the aforementioned XSD—contains the XOR groups, the User Office, and several other user-support groups. The APS Engineering Support Division (AES) will house the technical groups that maintain and develop both the machine and the beamlines, mainly mechanical engineering and computing support and development. The revised organization chart is shown on page 187.

We believe that this new organization is more efficient and promises improved safety and reliability. Safety takes precedence over all else. We have made many changes at Argonne and the APS to enhance our safety programs in the last year. One important example is electrical safety. Our awareness of the potential arc-flash risk associated with working at elevated voltages was raised by a major accident at another DOE laboratory. Argonne has implemented better safety controls for electrical work—especially at higher voltages and will inspect user equipment that is brought here. We will always take the time and care required to ensure the safety of our users, employees, contractors, and visitors.

Fiscal year 2006, which began in October 2005, has also been a challenging one for APS because of declining facility budgets across the DOE Office of Science, and this was a major driver for our reorganization. However, the budget picture for fiscal year 2007 looks much more promising ever since the U.S. President announced his "American Competitiveness Initiative" and included in his budget request to congress significant funding increases for synchrotron facilities such as the APS.

Many new beamlines are making progress at the APS; in the last year, two beamlines became operational and three took general users for the first time. The nanoprobe, inelastic x-ray scattering, and powder diffraction beamlines will be commissioned by late 2006, and the APS Scientific Advisory Committee has recommended the approval of several letters of intent for new beamlines, including The BioNanoprobe dedicated to cell biology, a high-magnetic field capability, and a beamline for soft x-rays in magnetism.

Our accelerator and support staff continue to innovate both in improving source reliability and adding new capabilities. This is an amazing accomplishment. I think of it as being akin to rebuilding an aircraft while maintaining a rigid flight schedule. Amongst the technical highlights described in this report, I want to single out the doubling of the single-bunch current to help users with timing experiments (page 176) and the development of new superconducting undulators in collaboration with both National Science Foundation and DOE laboratories (see page 180). And long term, we are very excited about developments that promise ~1 ps pulses at the APS (pages 93 and 173).

Argonne is blessed with a number of top-quality and unique facilities for materials-related research, including the APS, the Intense Pulsed Neutron Source, the Electron Microscopy Center, and the exciting new Center for Nanoscale Materials. We are continually finding new ways of working together; for example, using a centralized experiment proposal system. In 2006, all of these DOE Office of Basic Energy Sciences-funded Argonne user facilities will, for the first time, participate in a shared user meeting. A nice example of the synergy from these facilities is given in the "round the Experimental Hall" highlight (page 21, plus page 63), in which transmission electron microscopy and ex-tended x-ray absorption fine structure were used by Prof. Davidson and his collaborators in their quest to better understand Alzheimer's disease. X-ray techniques are better for finding the proverbial needle in the haystack, and then electron microscopy can examine the sharp point of the needle with atomic detail. Such synergies will be exploited here even more in the future and will help the APS, together with our sister facilities, expand Argonne's scientific impact. When you have a hammer, everything looks like a nail, but at Argonne, we have a real toolbox….

Best wishes for a productive year,

Murray Gibson

THE APS SCIENTIFIC ADVISORY COMMITTEE

PIERRE E. WILTZIUS...

... (Chair, APS Scientific Advisory Committee) is the Director of the Beckman Institute and Professor of Materials Science, Engineering, and Physics at the University of Illinois at Urbana-Champaign.

The members of the APS Scientific Advisory Committee as of January 2006. Front row (l. to r.) Murray Gibson (Argonne National Laboratory), Pierre Wiltzius, Chair, (University of Illinois at Urbana-Champaign), Michael Rowe (NIST Center for Neutron Research; retired). Center row (seated, l. to r.): Katherine Faber (Northwestern University), Richard Leapman (National Institutes of Health), Carol Thompson (Northern Illinois University), Gerhard Materlik (Rutherford Appleton Laboratory). Back row (l. to r.): James Norris (The University of Chicago), Denis McWhan (Brookhaven National Laboratory, retired), John Helliwell (University of Manchester), Joachim Stohr (Stanford Accelerator Center), Peter Ingram (Duke University Medical Center), Piero Pianetta (Stanford Linear Accelerator Center), Miles Klein (University of Illinois at Urbana-Champaign), Paul Bertsch (University of Georgia), Bruce Bunker (University of Notre Dame), William Bassett (Cornell University). Not pictured: Jennifer Doudna (University of California, Berkeley).

The Scientific Advisory Committee (SAC) of the Advanced Photon Source Meeting held its annual meeting on January 24-26, 2006.

The meeting included two days of information, updates, and discussions of APS strategic and tactical planning, as well as formulation of specific recommendations to the APS for the eight sectors reviewed during 2005, two proposals to develop new beamlines (one for a BioNanoprobe and the other for high-energy photoemission and soft x-ray resonant scattering), a proposal to further develop the bending-magnet beamline on sector 10, and responses to issues raised during the 2005 SAC meeting. In addition, a half day was spent in a cross-cut review of APS research in polymer science (http://www.aps.anl.gov/News/Meetings/APS_Cross_Cut_Reviews/index.html).

Murray Gibson, Associate Laboratory Director for Scientific User Facilities at Argonne and Director of the APS, began by presenting several scientific highlights from the past year. He then described progress for selected 2005 performance goals and outlined goals for 2006. Next, he turned to the planned administrative reorganization of the facility, explaining the relationship of the new organizational structure to the changing focus and management of APS beamlines, as well as to budget projections for FY 2006 and beyond. This information served as background to Gibson's presentation of the report on the Department of Energy's (DOE's) Office of Basic Energy Science review of the APS on May 23-25, 2005. The overall report was generally very positive, with key recommendations as follows: (1) to set priorities in consultation with the SAC and representatives of the user community, (2) continue improving general user access to the APS beamlines, and (3) establish a strong in-house scientific group with international recognition.

Gibson's presentation on the DOE review led to discussions about the relationship between the strategic plan, individual year goals, the budget, staffing, and annual priorities. Issues raised included the relationship of the new Center for Nanoscale Materials (CNM) to the APS, how to stimulate scientists/users in communities not represented on the APS staff

Please see "Science Advisory Committee" on page 7

THE APS USERS ORGANIZATION

CAROL THOMPSON...

... (Chair, APSUO Steering Committee) is Professor of Physics at Northern Illinois University.

The highlight of the year was the 2005 Users Meeting for the APS on May 2-6, held jointly for the first time with the Center for Nanoscale Materials (CNM). The Users Meeting celebrated the 10th anniversary of first light at the APS and first light at the nanoprobe beamline. Attendance grows each year, and the 2005 meeting set a new record with more than 600 attendees drawn to the excellent line-up of scientific talks, 9 outstanding workshops, 3 poster sessions (with generous prizes for best student posters), and the awarding of the 2005 Arthur H. Compton Award to Günter Schmahl and Janos Kirz for pioneering and developing the field of x-ray microscopy using Fresnel zone plates. And finishing off the week was a Friday cornerstone-laying ceremony for the CNM. (For more on the 2005 Users Meeting, see page 163.)

The Advanced Photon Source Users Organization Steering Committee (APSUOSC) continues to play an important role in representing the interests of the APS general user community. The quarterly APSUOSC meetings are the main venue for interaction with the APS management. For 2005, items that generated much discussion included the APS strategic plan and the plans for changes to existing and new X-ray Operations and Research beamlines, as the transfer of Department of Energy, Office of Basic Energy Sciences (DOE-BES) sectors to APS operations support is completed. The APSUOSC has advised the APS on policies related to the general user program and new access modes for users, and, at the request of APS management, held a special meeting in order to participate in the 2005 BES review of the APS.

The policy, initiated in 2003, to invite sector representatives to join the committee for lunch and give short presentations was continued. In 2005, it was expanded to include representatives from the Scientific Interest Groups. This provides opportunities for user groups to share issues and concerns with the steering committee, and it keeps the steering committee up to date on new developments among user constituencies.

In addition to the quarterly meetings, the APSUOSC Chair (or a representative) attends the weekly APS Operations Directorate Meeting; all Sector Review Panel meetings (where APS sectors undergo their three-year reviews), the Partner User Council Meetings, and the annual meeting of the APS Scientific Advisory Committee. At the quarterly meetings, the full APSUOSC hears summary reports from the representatives on these activities, and issues of interest or concern to users are highlighted. This has served to educate and inform the APSUOSC members and stimulates discussion between the various communities represented on the APSUOSC.

APSUOSC Chair Carol Thompson.

Advocacy continues to be a focus for the APSUOSC. In 2006, a team of APS user-group chairs, as well as those from our sister DOE labs—including the National Synchrotron Light Source, the Advanced Light Source, and the Stanford Synchrotron Radiation Laboratory—will travel to Washington, D.C., to expound on the importance of synchrotron science and other user facilities. ❍

THE APS PARTNER USER COUNCIL

BRUCE A. BUNKER...

... (Chair 2005-2006, APS Partner User Council) is Professor of Physics at the University of Notre Dame and Director of MR-CAT at the APS.

& P. JAMES VICCARO...

... (Chair 2004-2005, APS Partner User Council) is Director of the Center for Advanced Radiation Sources.

The 2005 APS Partner User Council: Bruce A. Bunker (sector 10, University of Notre Dame, Chair) • Dean R. Haeffner (sector 1, Argonne National Laboratory) • Qun Shen (sector 2, Argonne National Laboratory) • Wolfgang Sturhahn (sector 3, Argonne National Laboratory) • George Srajer (sector 4, Argonne National Laboratory) • Denis T. Keane (sector 5, Northwestern University) • Douglas S. Robinson (sector 6, Iowa State University) • Roy Clarke (sector 7, University of Michigan) • Simon G.J. Mochrie (sector 8, Yale University) • J. Kent Blasie (sector 9, University of Pennsylvania) • Mark A. Beno (sector 11, Argonne National Laboratory) • Randall E. Winans (sector 12, Argonne National Laboratory) • Mark L. Rivers (sector 13, The University of Chicago) • Keith Moffat (sector 14, The University of Chicago) • P. James Viccaro (sector 15, The University of Chicago) • David Mao (sector 16, Carnegie Institution of Washington) • Lisa J. Keefe (sector 17, The University of Chicago) • Thomas C. Irving (sector 18, Illinois Institute of Technology) • Andrzej Joachimiak (sector 19, Argonne National Laboratory) • Edward A. Stern (sector 20, University of Washington) • Wayne F. Anderson (sector 21, Northwestern University) • John J. Chrzas (sector 22, University of Georgia) • Robert F. Fischetti (sector 23, Argonne National Laboratory) • Malcolm Capel (sector 24, Cornell University) • G. Brian Stephenson (sector 26, Argonne National Laboratory) • John P. Hill (sector 30, Brookhaven National Laboratory) • Kevin L. D'Amico (sector 31, SGX Pharmaceuticals, Inc.) • Paul Zschack (sectors 33-34, University of Illinois at Urbana-Champaign)

Partner User Council Chair Bruce Bunker.

Much of the research carried out at the APS is conducted and facilitated by partner users, who have entered into agreements with the APS either to build and operate facilities at the APS or to otherwise significantly enhance APS capabilities. As a result, partner user organizations represent significant commitments and investments from non-APS and non-Department of Energy (DOE) entities. Effective communication and dialog between the partner users and the APS continues to be one of the primary goals of the Partner User Council (PUC), which was established in May 2003, replacing the Research Directorate. This continues to be the objective of the new Chair, Bruce Bunker (University of Notre Dame/Materials Research Collaborative Access Team), who was elected Chair of the PUC in July 2005 following recommendations from an *ad hoc* Nominations Committee commissioned by the then Chair, Jim Viccaro (The University of Chicago/Center for Advanced Radiation Sources).

Several important events occurred in 2005. During the DOE review of the APS in January 2005, the PUC was invited to participate in a meeting with the review panel. Approximately 12 members of the PUC participated in what proved to be a frank and productive dialog with the panel. Also in 2005, the original PUC charter was revisited by an *ad hoc* committee also commissioned by the Chair, and the PUC was officially reorganized in summer 2005 with a formal charter that was approved in a meeting in November. In the new charter, the full PUC membership was amplified to include representatives from each active Partner User Proposal (including Collaborative Access Teams, or CATs) and Collaborative Development Team (CDT), and a representative from each X-ray Operations and Research-operated sector. Because the local on-site beamline staff at the APS are crucial for the operation of the facility, each sector is asked to choose a resident user or APS staff member as an additional representative to the PUC. Similarly, the APS-recognized Scientific Interest Groups (SIGs) and the Technical Working Group (TWG) are important resources for the entire community; representatives from each of the SIGs and from the TWG are invited to be part of the PUC. Finally, to facilitate communications with the broader-based APS Users Organization (APSUO), a representative of the APSUO Steering Committee is also a member of the PUC. The full PUC meets annually, usually around the time of the APS Users Meeting.

The full PUC is large enough to be rather unwieldy for regular meetings. To address this, there is also a smaller Executive

Please see "Partner User Council " next page

"Scientific Advisory Committee" continued from page 4

(e.g., biology, and surface and interface scattering), the proper balance between research and user support by APS beamline staff, the appropriate levels and types of reviews needed for APS beamlines to facilitate the best science, and industrial access.

The eight 2005 sector reviews that were conducted by Sector Review Panels, comprising outside experts under the guidance of a SAC member, were discussed. This process has been in place for several years now and is working well, leading to a written report to the sector leadership and the formulation of specific recommendations to the Director of the APS. Many thanks are due to all those making these reviews effective.

The SAC discussed the Scientific User Access Policy, with Deputy Associate Laboratory Director for X-ray Science and Deputy APS Director Dennis Mills reviewing the four primary modes of access for APS users, as described in the draft Scientific User Access Policy. These modes (collaborative access team [CAT] member access, APS beamline staff access, general user access, and partner user access) all depend on the principle of scientific peer review that is fair, clear, expedient, and sensitive to the needs of users. A new category of GU access, known as a project proposal, was approved. General user and partner user access currently constitute the fastest-growing community at the APS. The SAC briefly reviewed reports from 20 of the 23 approved partner user proposals. Discussion of this access mode led to the consensus that it should be continued as is.

The SAC acknowledged that the Material Research-CAT (MR-CAT) has provided a strong scientific case for the development of their bending magnet line. The merger of MR-CAT with Enviro-CAT, the funding commitments from the Environmental Protection Agency and the DOE Office of Biological and Environmental Research, as well as the support from the Chemical Engineering and Biosciences divisions at Argonne, are all positive developments.

A proposal for a BioNanoprobe was enthusiastically supported by the SAC. There is an excellent scientific case for the development of such a beamline, which could lay the foundation for a center at the APS dedicated to the study of nanobiology.

A proposal for an Intermediate Energy X-ray Collaborative Development Team beamline at the APS, dedicated for high-energy photoemission and soft x-ray resonant scattering, looks highly promising. While the review process is not yet completed, the SAC is currently strongly supportive.

Paul Zschack and colleagues reported on an important "Workshop on *In Situ* Characterization of Surface and Interface Structures and Processes" held at the APS in September 2005 (see http://surface-interface.aps.anl.gov/2005workshop/index.htm and page 49 of this book).

The SAC decided that the 2007 cross-cut review should be on structural biology research at the APS. At 40%, this community represents a large and still growing fraction of the APS user community. To provide effective guidance to the APS, the SAC needs to understand current capabilities, future directions, and usage trends.

The final discussion item for the SAC was the APS strategic planning process and plan. Overall, the SAC concurred that the APS is moving forward and keeps changing, adapting to new opportunities and challenges. It will continue to fulfill its advisory role by evaluating the spectrum of the continuously changing scientific programs and techniques available around the ring. Optimizing these resources and targeting new opportunities will be an ongoing endeavor. The SAC congratulates the APS community on its achievements and looks forward to another successful year. ❍

"Partner User Council" continued from page 6

Board that meets at least quarterly. This group is a subset of the full PUC, consisting of each director or designee from each CAT or CDT sector, a representative from the APS/XOR, and a representative from the APSUO.

According to the charter, the PUC is an advisor to the Associate Laboratory Director (ALD) for the APS, with written recommendations also provided to the APSUO Steering Committee, or the APS Scientific Advisory Committee as required. The PUC provides advice and recommendations to the ALD in matters affecting current and future beamline operations, APS facility development, and the special APS-to-partner-user relationship. Additionally, the PUC serves as an advocacy group for the facility, its partners, and the user community. The Chair of the PUC Executive Committee is also an *ex-officio* member of the APS Scientific Advisory Committee (participating in annual meetings, sector reviews, and other activities as requested by the APS) and is involved in weekly and monthly operations meetings.

We believe the PUC continues to demonstrate that it is a useful resource for communication between different interest groups at the APS, and we welcome communication with the general user community. ❍

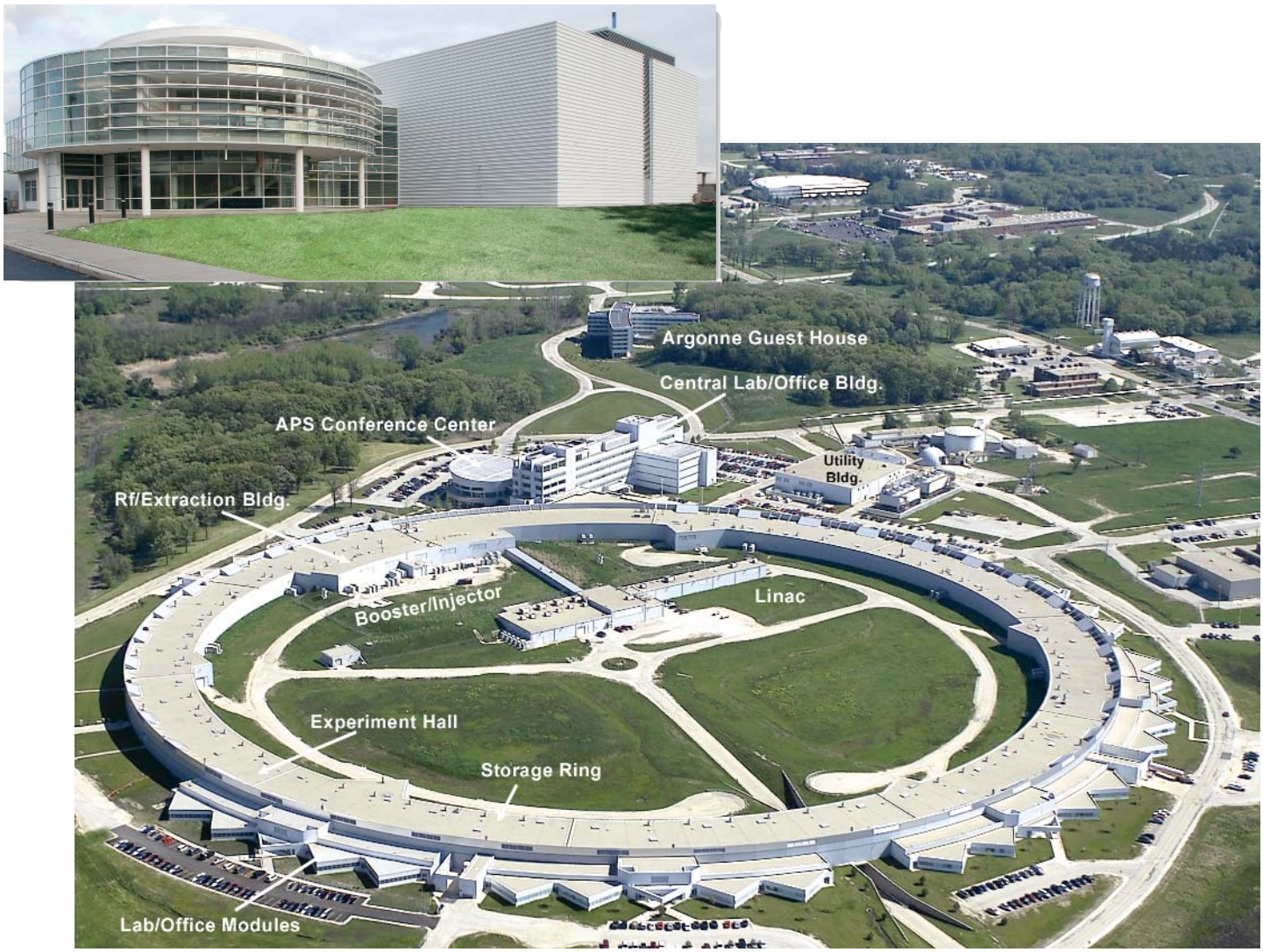

The Advanced Photon Source (APS) facility. Inset: the Center for Nanoscale Materials.
The APS occupies an 80-acre site on the Argonne National Laboratory campus,
about 25 miles from downtown Chicago, Illinois.
For maps of the Argonne/Chicago area, see http://www.aps.anl.gov/user/maps/maps.html
For directions to Argonne, see http://www.anl.gov/visiting/anlil.html

Access to Beam Time at the APS

Beam time at the APS can be obtained either as a general user (a researcher not associated with a particular beamline) or as a partner user (e.g., a member of a collaborative access team, or CAT). If you are a CAT member, contact your CAT for instructions on applying for CAT beam time. At minimum, 25% of the time at all operating beamlines is available to general users, but many offer considerably more general user time, up to 80%.

How general users can apply for beam time at the APS:
1) First-time users should read the information for new users found on our Web site at http://www.aps.anl.gov/user/ new_users.html before applying for beam time. Also, certain administrative requirements must be completed. In particular, a user agreement between the APS and each research-sponsoring institution must be in place.

2) To choose the appropriate technique(s) and beamline(s), see the beamlines directory in the “Data” section of this volume or at http://beam.aps.anl.gov/pls/apsweb/beamline_display_pkg.beamline_dir.

3) Submit a proposal via the Web-based system. Proposals are evaluated before each user run. For more information and the current proposal schedule, see the proposal system overview at http://www.aps.anl.gov/user/beam time/prop_submission.html.

Table of Contents

Contact us

For more information about the Advanced Photon Source or to order additional copies of this, or previous, issues of *APS Science*, send an e-mail to apsinfo@aps.anl.gov, or write to APSinfo, Bldg. 401, Rm. A4115, Argonne National Laboratory 9700 S. Cass Ave., Argonne, IL 60439.

APS Science is also available on line in PDF format at http://www.aps.anl.gov/News/Annual_Report/index.htm

Title-page photo: An APS laboratory/office module; the central laboratory/office building is in the background.

lightsources.org

For news from, and information about, light sources worldwide, see lightsources.org

APS Research Highlights

APS sectors:

Sectors 1-4: XOR
X-ray Operations and Research (XOR)

Sector 5: DND-CAT
DuPont-Northwestern-Dow Collaborative Access Team (CAT)

Sector 6: MU-CAT
Midwest Universities CAT

Sector 7: XOR

Sector 8: XOR (8-ID); NE-CAT (8-BM)

Sector 9: XOR/CMC
XOR/Complex Materials Consortium CAT

Sector 10: MR-CAT
Materials Research CAT

Sectors 11 and 12: XOR/BESSRC
XOR/Basic Energy Sciences Synchrotron Radiation Center

Sectors 13 through 15: CARS
Center for Advanced Radiation Sources
- GeoSoilEnviroCARS—sector 13
- BioCARS—sector 14
- ChemMatCARS—sector 15

Sector 16: HP-CAT
High Pressure CAT

Sector 17: IMCA-CAT
Industrial Macromolecular Crystallography Association CAT

Sector 18: Bio-CAT
Biophysics CAT

Sector 19: SBC-CAT
Structural Biology Center CAT

Sector 20: XOR/PNC
XOR/Pacific Northwest Consortium

Sector 21: LS-CAT
Life Sciences CAT

Sector 22: SER-CAT
South East Regional CAT

Sector 23: GM/CA-CAT
General Medicine and Cancer Institutes CAT

Sector 24: NE-CAT (plus 8-BM)
Northeastern CAT

Sector 26: CNM-CDT
Center for Nanoscale Materials
Collaborative Development Team (CDT)

Sector 30: IXS-CDT
Inelastic X-ray Scattering CDT

Sector 31: SGX-CAT
SGX CAT

Sector 32: XOR

Sectors 33 and 34: XOR/UNI
XOR/A University-National Laboratory-Industry CAT

X-ray Operations and Research sectors comprise those beamlines operated by the APS.

Collaborative access team sectors comprise beamlines operated by independent groups made up of scientists from universities, industry, and/or research laboratories.

To access the APS as **general users** (GUs), researchers submit proposals—either individual (good for one allocation of beam time) or programmatic (good for multiple beam-time allocations over a two-year period). These proposals are reviewed and rated by one of nine proposal review panels comprising scientific peers, generally not affiliated with the APS. Beam time is then allocated by either of two APS Beam Time Allocation Committees.

Those users who propose to carry out research programs beyond the scope of the GU program may apply to become **partner users** on any beamline operated by the APS. Prospective partner user proposals are peer reviewed by a subset of the APS Scientific Advisory Committee. Final decisions on the appointment of partner users are made by APS management.

Argonne NATIONAL LABORATORY

THE ADVANCED PHOTON SOURCE

Sector Allocations & Disciplines
Source Configuration

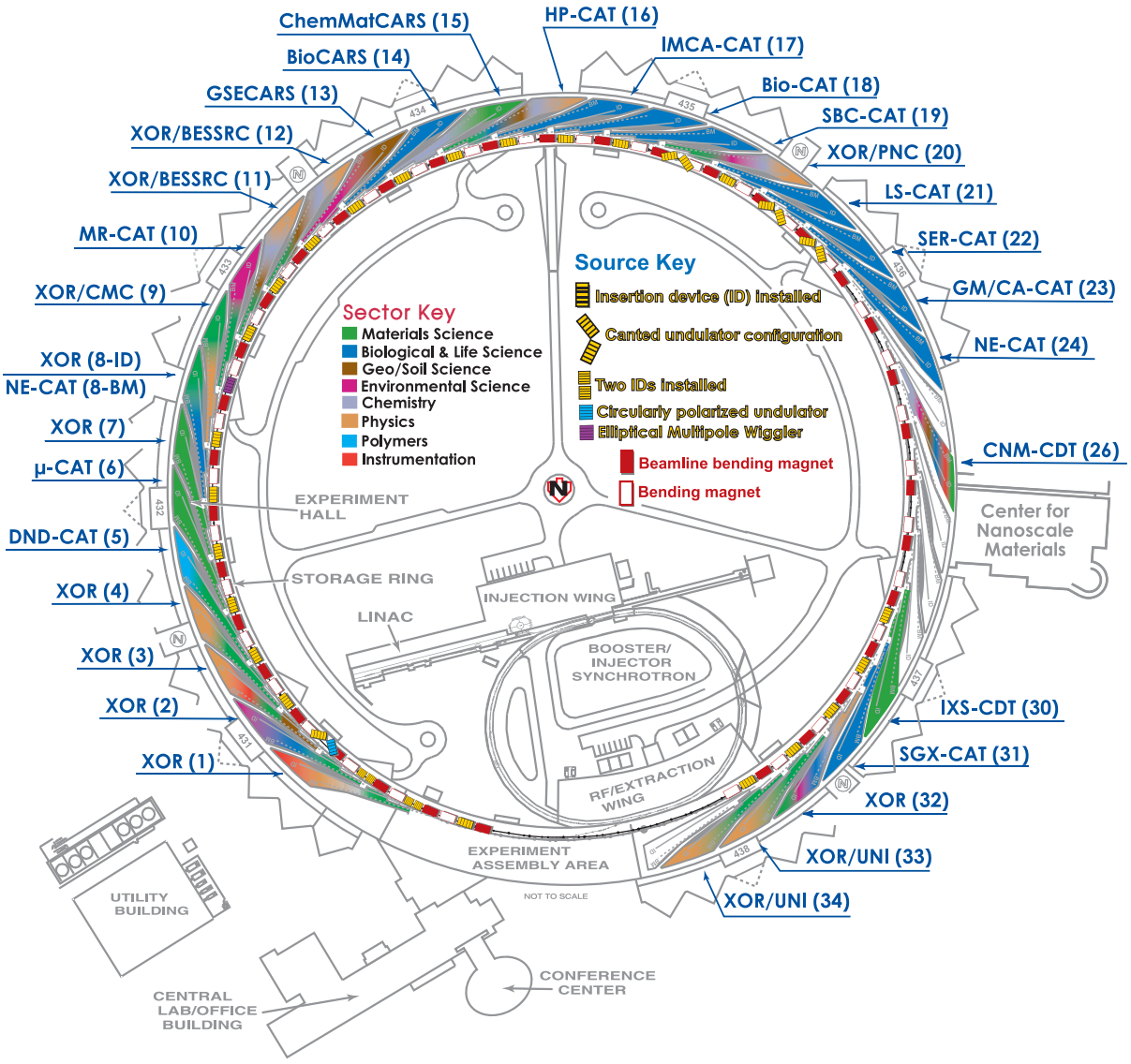

THE UNIVERSITY OF CHICAGO Office of Science U.S. DEPARTMENT OF ENERGY

U28

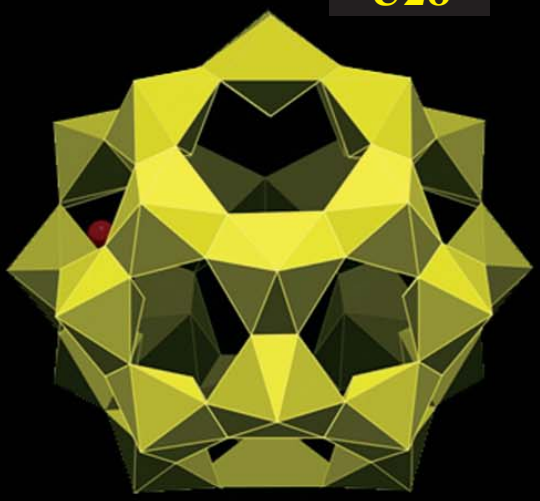

U32

U24
Np24

Self-assembling aggregate clusters known as nanospheres (or nanoparticles) that are measured in terms of atoms are proving to have a large impact on a wide array of new materials and critical applications. Nanospheres are also finding use in environmental systems because of their ability to form at low temperature while influencing heavy-metal and radionuclide transport in geological fluids. Researchers from the University of Notre Dame, the University of Windsor, and Argonne National Laboratory recently synthesized an entirely new family of self-assembling nanospheres from actinide ions in alkaline peroxide solutions. Using small-angle x-ray scattering (SAXS) data obtained at the XOR/BESSRC beamline 12-BM-B at the APS, these researchers confirmed the spherical-shell model of the structures and followed the evolution of the clusters over time in the mother liquor.

< Fig. 1. Polyhedral representations of the actinyl peroxide spherical clusters U-28, U-32, U-24 and Np-24.

A NEW SELF-ASSEMBLING NANOSPHERE FAMILY IS BORN

The laboratory conditions in which the nanospheres formed roughly approximate conditions in high-level nuclear waste storage tanks and some geologic environments where actinides have been released. Actinyl peroxide nanoparticles may form in alkaline mixtures in which alpha radiation breaks apart water molecules, forming peroxide molecules. The behavior of these minuscule clusters causes concern because they may be quite mobile and persistent in the environment. The actinide elements are also inherently intriguing because they have potentially useful chemical, structural, and electromagnetic properties.

Previous studies of main-group elements such as buckminsterfullerene (C60) and transition-metal oxides have produced nanostructures that assembled into a variety of clusters, some of which are spherical. This study revealed the first such clusters that are based upon uranium (U) and neptunium (Np). Uranyl and neptunyl peroxide polyhedra have been shown to link to form spherical clusters in peroxide solutions at room temperature (25º C).

These new species were formed from building blocks of linear actinyl ions that self-assembled into spherical clusters. Using x-ray diffraction data collected at the University of Notre Dame and Argonne National Laboratory, the team determined the molecular composition of three clusters containing uranyl ions, and one containing neptunyl ions, which ranged in size from 16.4 to 18.6 Å in diameter. The molecular units of U-24, U-32, and Np-24 all consisted of hexagonal bipyramids with identical distributions of oxygen atoms and two peroxide groups within the polyhedra, while the U-28 cluster is built from polyhedra that contain three peroxide groups (Fig. 1). Both types appear to self-assemble in a similar fashion, as each contains rings of from four to six actinyl polyhedra. The unusual geometries of the actinyl peroxide polyhedra appear to facilitate formation of the spheres.

SAXS data were used to analyze the parent solutions that yielded the U-24 cluster. Data were gathered for solutions at intervals of 2, 28, and 180 days. After just two days, spherical clusters began to form; the nanospheres increased in dominance over time, and they were the only detectable clusters in solution by 180 days. The scattering data at 180 days confirmed the spherical shell model obtained from the single-crystal x-ray studies of the crystals that formed from the solution.

Guinier analysis of the low-Q data further confirmed the spherical model, and the size was confirmed by measuring the radius of gyration, which was found to be a good fit with the structure determined from the solid. These measurements showed well-formed nanospheres with a diameter of 16.2 Å.

Further research into the properties of this new family of materials could reveal important structural, magnetic, and electrochemical characteristics of these self-assembling nanospheres. This new family of actinyl peroxide nanospheres represents apparently stable species that are persistent in the solution. These results could have important implications for understanding the transport of actinides contained in nuclear waste, when such wastes are stored in a geological repository or leak into groundwater. — *Elise LeQuire*

See: P.C. Burns[1], K.-A. Kubatko[1], G. Sigmon[1], B.J. Fryer[2], J.E. Gagnon[2], M.R. Antonio[3], and L. Soderholm[3], "Actinyl Peroxide Nanospheres," Angew. Chem. Int. Ed. **44**, 2135 (2005).
Author Affiliations: [1]University of Notre Dame, [2]University of Windsor, [3]Argonne National Laboratory
Correspondence: pburns@nd.edu

This research was supported at the University of Notre Dame; by the Environmental Management Science Program of the Office of Science, U.S. Department of Energy (DE-FG07-97ER14820); and by the National Science Foundation Environmental Molecular Science Institute at the University of Notre Dame (EAR02-21966). This research was supported at Argonne National Laboratory by the U.S. Department of Energy Office of Basic Energy Sciences–Chemical Sciences Division and by the Material Sciences Division for the Advanced Photon Source studies under Contract Number W-31-109-ENG-38. Use of the Advanced Photon Source was supported by the U.S. Department of Energy, Office of Science, Office of Basic Energy Sciences, under Contract No. W-31-109-ENG-38.31-109-ENG-38.

HIGH-QUALITY DIFFRACTION STUDIES PERFORMED ON HIGH-PRESSURE SULFUR

Sulfur (S) is a member of the group VI elements that also include oxygen, selenium, and tellurium. Sulfur has been extensively researched in the past—and continues to be a subject of much interest—in particular because it becomes a superconducting metal at very high pressures. However, past diffraction studies of nonmetallic sulfur have been complicated in part by erroneous information concerning metastability effects and re-crystallization processes. But present-day improvements in high-pressure methods and x-ray crystallographic techniques have allowed scientists to gain a better understanding of phase diagrams and material structures under high pressures. Using such techniques, investigators from the Carnegie Institution of Washington obtained high-quality diffraction data of sulfur over a wide pressure range, from 5 gigapascal (GPa) to 85 GPa. These measurements—the first of this kind—were carried out at HP-CAT beamline 16-ID-B at the APS using temperature to overcome kinetic barriers of phase transitions and to improve the quality of the diffraction data. Two important results from this study are a better understanding of the phase transition sequence of sulfur in its non-metallic state—specifically, that of high-pressure phases S-II and S-III—and the first identification of a spiral chain structure of the S-III phase.

In order to understand sulfur's high-pressure behaviors, including its phase-transition sequence, the collaborators conducted numerous structural experiments involving x-ray diffraction over wide ranges of pressures and temperatures. Samples of pure sulfur were loaded in a high-pressure diamond anvil cell, along with one of several pressure-transmitting media such as helium, neon, and nitrogen; or, in some cases, without a pressure-transmitting medium. *In situ* fluorescence measurements of ruby chips were performed to determine pressure. The sample in the pressure cell was heated using a resistive heating technique.

The ambient-pressure orthorhombic S-I phase was the starting point for the collaborators' study. The S-I phase was transformed into the S-II phase when sulfur was heated at pressures above 3 GPa and temperatures just below its melting curve, which caused the S8 molecular rings of S-I to break and form infinite helical chains of S-II. The first-order phase transformation produced distinct changes in sulfur's diffraction pattern (Fig. 1). The S-II phase, which remained stable up to 36 GPa at 300K, formed a trigonal chain structure that consisted of triangular chains running parallel to the trigonal axis with three atoms per turn (Fig. 2).

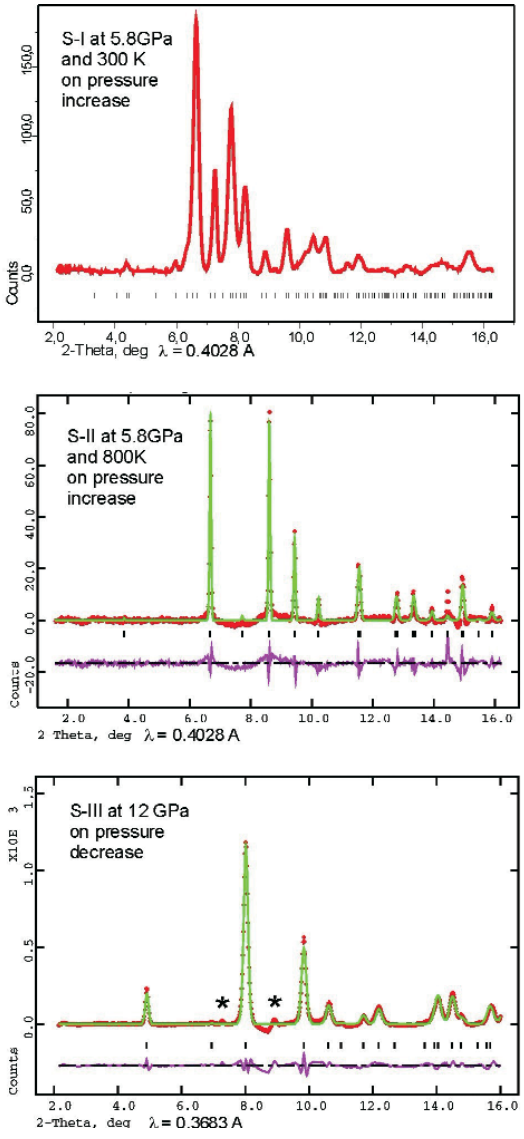

Fig. 1. *In situ* x-ray diffraction data. X-ray spectra of S-I at 5.8 GPa and 300K collected on pressure increase, S-II at 5.8 GPa and 800K collected on pressure increase, and S-III collected on pressure decrease at 12 GPa and 300K. The spectra of S-I and S-II are taken with λ = 0.4028 Å; the spectrum of S-III is taken with λ = 0.3683 Å. Full-structure Rietveld refinement is shown for the S-II and S-III phases. Red crosses, green lines, and deep purple lines represent experimental, modeled, and difference spectra, respectively. The ticks below the profiles indicate the predicted peak positions. Asterisks in the S-III profile show the reflections from the pressure-transmitting medium (N_2).

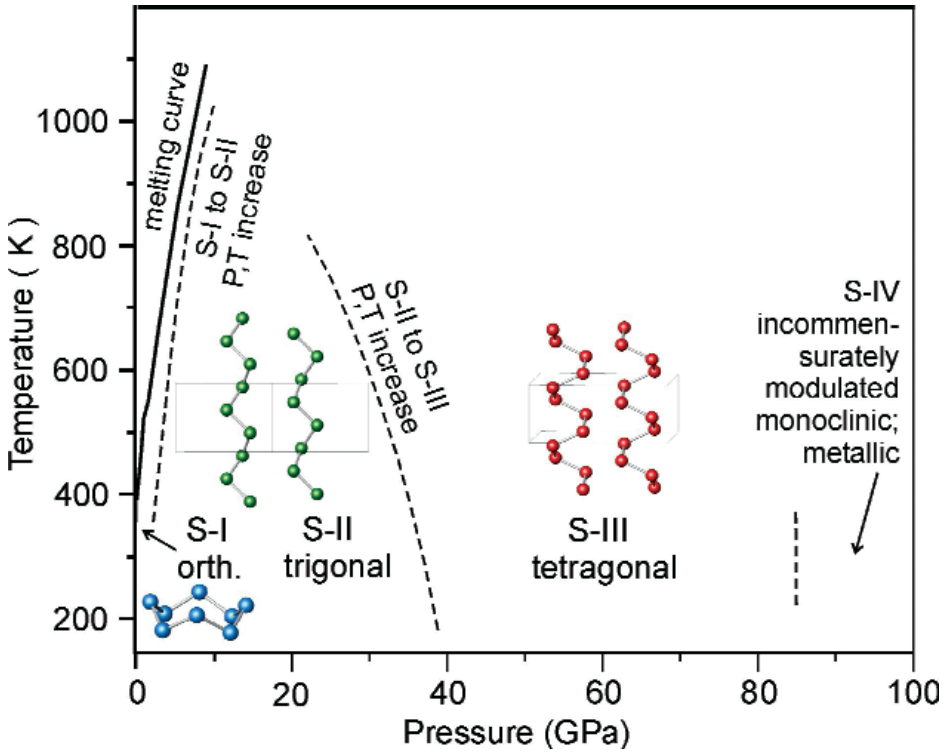

Fig. 2. Reaction and transformation diagram and crystal structures of sulfur. The boundaries for the transitions S-I to S-II, S-II to S-III, and S-III to S-IV observed in this study are shown by dashed lines. The S_8 ring molecule of S-I, trigonal chain structure of S-II, and tetragonal chain structure of S-III are shown with the interatomic bonds up to 2.10 Å.

The first-order phase transformation from S-II into S-III was observed when sulfur was subjected to pressures (1) above 36 GPa and a temperature of 300K or (2) between 22 GPa and 35 GPa and temperatures between 300K and 800K. The different pressure-transmitting media—along with the different pressure-temperature paths—led to the formation of the same S-III phase at pressures above 36 GPa and at room temperature (Fig. 2). The S-III phase, which remained stable up to 83 GPa at 300K (before transforming into the metallic S-IV phase), formed a tetragonal chain structure that consisted of squared chains running parallel to the tetragonal axis with four atoms per turn (Fig. 2). It produced a tighter spiral pitch and denser structure than S-II. The structure of S-III was solved and refined from the diffraction pattern shown in Fig 1. These results clarified the high-pressure behavior of sulfur, a subject that has been controversial until now.

The research shows that sulfur has two stable high-pressure phases (S-II and S-III) at pressures between 2 GPa and 83 GPa, while the S-II phase can only be obtained on heating to high temperatures. Both high-pressure phases form unusual chain structures. The significance of the present study centered on the collection of high-quality x-ray data over a very wide pressure range (covering the stability range of the non-metallic sulfur). For the first time, the data led to an understanding of the changes in bond lengths (among other structural parameters) of sulfur with pressure from the structure refinement.

Employing similar x-ray diffraction experiments on selenium—the next-heavier element within the group VI elements—the collaborators also learned that selenium has the same squared-chain structure as the S-III tetragonal phase of sulfur when it was subjected to high pressures (~20 GPa) and moderate temperatures (450K). This discovery proved that the chain structure of sulfur is not peculiar to sulfur alone.

The discovery of the new chain structure and the advanced diffraction data on the ring and chain structures of sulfur provide valuable information for understanding sulfur's characteristics and behavior at high pressures. These results on the sulfur phases I, II, and III reveal steady sulfur-sulfur bond lengths, similar bond angles, and conformational freedom about torsion angles. Their work supports established theory, which asserts that nonmetallic structures of sulfur (and selenium) are controlled to first order by localized bonding properties over a wide range of pressures and temperatures. — *William Arthur Atkins*

See: Olga Degtyareva[1], Eugene Gregoryanz[1], Maddury Somayazulu[2], Przemyslaw Dera[1], Ho-Kwang Mao[1], and Russell J. Hemley[1], "Novel Chain Structures in Group VI Elements," Nat. Mater. **4**, 152 (February 2005).

Author Affiliations: [1]Carnegie Institution of Washington, [2]Argonne National Laboratory
Correspondence: o.degtyareva@gl.ciw.edu

This work and HP-CAT are supported by DOE-BES, DOE-NNSA, DOD-TACOM, NSF, NASA, and the W.M. Keck Foundation. The authors acknowledge financial support from NSF, through grant EAR-0217389. Use of the Advanced Photon Source was supported by the U.S. Department of Energy, Office of Science, Office of Basic Energy Sciences, under Contract No. W-31-109-ENG-38.

CHARGE TRANSFER EXCITATIONS IN SUPERCONDUCTORS

The remarkable phenomenon of high-temperature superconductivity was discovered 20 years ago, yet the mechanism by which these materials conduct current without resistance remains unclear. What is certain, however, is that the electrons in these materials are strongly correlated and the superconducting properties depend on collective charge excitations. Researchers have sought to understand these excitations using a variety of theoretical and experimental approaches, but a suitable spectroscopic technique for investigating the charge phenomena as a function of both energy and momentum was lacking until recently. Researchers from Stanford University, Jilin University, Rutgers University, and the Brookhaven and Argonne national laboratories used resonant x-ray scattering on XOR/CMC beamline 9-ID-B at the APS to successfully study charge excitations in one of the most important cuprate high-temperature superconductors.

Previous studies with optical spectroscopy have examined some of the charge behavior found in superconductors, but these methods are limited to excitations with zero momentum transfer. Much of the charge dynamics of interest, however, lies in a broader range of momentum space. Probes such as electron energy loss spectroscopy can detect non-zero momentum exchange, but this method is strongly influenced by surface phenomena and multiple scattering events, making it less reliable for bulk studies. The recently developed technique of resonant inelastic x-ray scattering (RIXS) in the hard x-ray regime has been shown to be capable of probing charge excitations in bulk superconductors over a wide momentum range. In copper K-edge RIXS, x-rays near the absorption-edge energy are directed at a sample and the scattered x-rays are collected and analyzed. The scattering angle yields momentum information and the energy of the scattered x-rays reveals the excitation spectrum in a wide energy range.

The research team used RIXS to study charge excitations in oxygen-doped $HgBa_2CuO_4$ (also denoted Hg1201). This compound is considered a model material for such studies because of its remarkably high superconducting transition temperature, simple CuO_2 singe-layer structure, and large spacing between copper-oxygen planes. A large single-crystal sample of Hg1201 was grown at Stanford University and heat-treated in oxygen atmosphere to obtain optimal charge carrier doping with a transition temperature of 96.5K. Resonant inelastic x-ray scattering data were taken at beamline 9-ID-B with incident energy set to values near the copper K edge at 9 keV to achieve resonant enhancement of the inelastically scattered x-rays. The spectra were analyzed using a diced germanium analyzer crystal, which yielded an overall energy resolution of 300 meV.

At an incident energy of 8998 eV, the RIXS spectrum shows a scattering peak at 2.2 eV shift, along with much weaker resonances at higher energy transfer. These weaker peaks, at 3 eV, 4 eV, and 5 eV, were observed by fine-tuning the incident energy to higher values. The team finds that in the range of 2-8 eV, this multiplet of excitations, arising from electron-hole excitations, disperses only weakly across the crystalline Brillouin zone. Of particular interest is the 2-eV feature, which the team assigns to an excitation involving the formation of a collective entity called a Zhang-Rice singlet, consistent with a similar excitation found in undoped insulator compounds. The observation of this mode suggests a charge transfer energy gap in the optimally doped Hg1201 superconducting phase. To further highlight the behavior observed in Hg1201, the researchers took additional RIXS spectra of a La_2CuO_4 sample, carefully focussing on the incident photon energy dependence, and found signs of the multiplet structure and a weakly dispersive 2-eV mode.

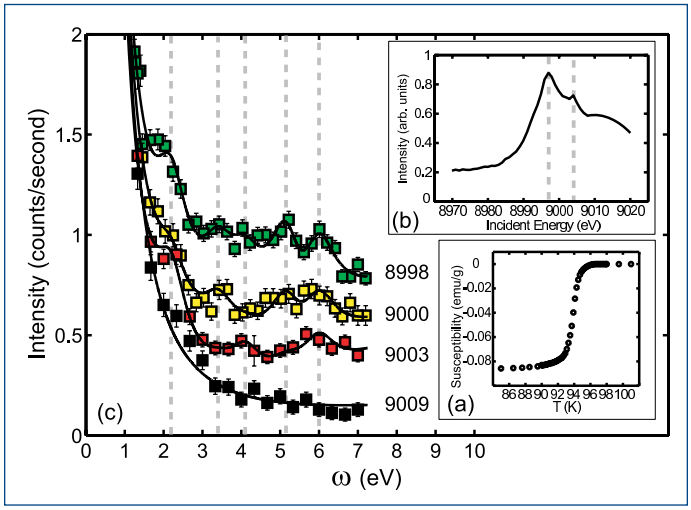

Fig. 1. (a) Measured magnetic susceptibility data showing the onset and width of the superconducting phase transition in the tetragonal high-T_c superconductor $HgBa_2CuO_{4+\delta}$. (b) Absorption spectra taken through total fluorescence yield, illustrating the resonance profile used in the RIXS process. (c) Resonant inelastic x-ray scattering spectra taken at a momentum transfer of (3,0,0) reciprocal lattice units showing the existence of multiple features in the excitation spectra.

The results show the value of employing inelastic x-ray techniques such as RIXS to correlated electron materials to understand the role charge excitations play in superconductivity and related phenomena. Moreover, the findings highlight the key role played by third-generation synchrotron facilities such as the APS, where high-energy resolution can be achieved with high brightness x-ray beams. — *David Voss*

See: L. Lu[1], G. Chabot-Couture[1], X. Zhao[2], J.N. Hancock[1], N. Kaneko[1], O.P. Vajk[1], G. Yu[1], S. Grenier[3], Y.J. Kim[4], D. Casa[5], T. Gog[5], and M. Greven[1], "Charge-Transfer Excitations in the Model Superconductor $HgBa_2CuO_{4+\delta}$," Phys. Rev. Lett. **95**, 217003 (2005).

Author Affiliations: [1]Stanford University, [2]Jilin University, [3]Rutgers University, [4]Brookhaven National Laboratory, [5]Argonne National Laboratory

Correspondence: greven@stanford.edu

The work at Stanford University was supported by the DOE under Contract Nos. DE-FG03-99ER45773 and DE-AC03- 76SF00515. Use of the Advanced Photon Source was supported by the U.S. Department of Energy, Office of Science, Office of Basic Energy Sciences, under Contract No. W-31-109-ENG-38.

CRYSTALLIZATION OF AN AMINO ACID

Knowing how to synthesize crystals is extremely important in manufacturing widely used chemicals such as pharmaceuticals and dyes. Classical theories about how complex crystals form—especially about how crystals originate—are coming under new scrutiny by researchers. The seeding of crystal formation for complex systems such as, known as nucleation, signals the beginning of crystallization and determines how further crystal growth will proceed. This initial stage is increasingly believed to consist of two steps instead of one. Focusing specifically on the nucleation of the amino acid glycine, researchers from the Illinois Institute of Technology, Glaxo Wellcome Manufacturing Pte Ltd., Argonne National Laboratory (ANL), and the Austrian Academy of Sciences used x-ray scattering (which is ideal for studying complex systems) at the Bio-CAT 18-ID beamline at the APS to determine that early formation of crystals very likely proceeds in two stages. Their work will now allow a much more sophisticated approach to using glycine in industrial applications.

The 18-ID beamline provided facilities for the small-angle x-ray scattering (SAXS) study of the crystallization of the amino acid glycine from a supersaturated aqueous solution. SAXS is well suited to study complex systems thought to contain many levels of structural features. Using the SAXS data, it is possible to learn about particle size, shape, and interactions. A supersaturated (3.6 M) solution of glycine in water provided the material for analysis. Cooling of the supersaturated solution to 10° C compensated for heating caused by the x-ray absorption and allowed glycine to crystallize within a few hours. Data collection was started during cooling of the solution and was continued until crystals were observed. Exposure time was 20 s, with a delay of 60 s between exposures. Computer programs developed at the Intense Pulse Neutron Source (IPNS) at ANL were used for data reduction. Software for Unified Fit Modeling, developed at the APS, was used for fitting the data. One advantage of using the unified fit method is that the exponential and power law regions can be fit together without introducing new parameters.

As glycine crystallizes in the supersaturated solution, the scattered intensity initially increases with time (i.e., decreasing temperature); after 3 h, the intensity is reduced over the entire range of *q* (scattering angles), a

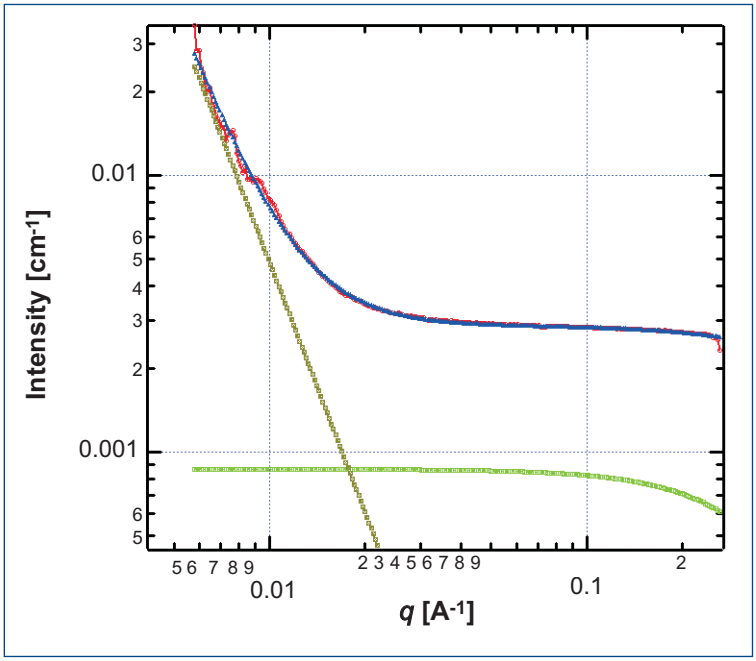

Fig. 1. Glycine data curves: red, experimental data; blue, unified fit; green, Guinier fit; olive, Porod law fit.

Continued on next page

variable that describes the difference between the incident and scattered beams. Glycine dimers appear to coexist with monomers in the solution even before supersaturation but as dimers alone after supersaturation. Scattering data from clustered dimers suggest the characteristics of fractal structure—self-similarity, scaling, universality, and aggregation formed by complex random processes. SAXS has previously been used to study fractal structure in other complex systems, such as silica particles in solution. The power law value is initially at 2.68 and increases to 2.95 in 35 min, where it remains for about 3 h (Fig. 1).

The presence of mass fractals in solution is suggested by a power law value between 2 and 3—leading the researchers to propose that, even before supersaturation occurs, the solution is a mass fractal state of monomers and dimers. The increase in the power value indicates the formation of liquid-like clusters composed primarily of dimers. This stable state exists until the power law value changes to 3.14 and then increases to a maximum of 3.21, indicating the transformation from mass fractals to surface fractals. In this latter phase, the liquid-like clusters are reorganizing, and the nucleation of glycine crystals is initiated. Once nucleation begins, surface fractal structures grow rapidly and shift x-ray scattering outside the range assessed in the present study. The transformation from mass fractals to surface fractals could be the signature of a two-step crystallization process occurring in the system.

The beauty of these new results is that the evolution of glycine from the monomeric to the crystal form can now be envisioned in some detail and with a much more sophisticated understanding of the underlying processes. Future work will investigate whether the cluster size depends on the concentration of the supersaturated solution and the effect of the presence of additives on the crystal. — *Mona Mort*

See: S. Chattopadhyay[1], D. Erdemir[1], J.M.B. Evans[2], J. Ilavsky[3], H. Amenitsch[4], C.U. Segre[1], and A.S. Myerson[1], "SAXS Study of the Nucleation of Glycine Crystals from a Supersaturated Solution," Cryst. Growth Des. **5**(2), 523 (2005).

Author Affiliations: [1]Illinois Institute of Technology, [2]Glaxo Wellcome Manufacturing Pte Ltd., [3]Argonne National Laboratory, [4]Austrian Academy of Sciences
Correspondence: segre@iit.edu

Bio-CAT is a National Institutes of Health-supported Research Center RR-08630. Use of the Advanced Photon Source was supported by the U.S. Department of Energy, Office of Science, Office of Basic Energy Sciences, under Contract No. W-31-109-ENG-38.

INSIDE THE CLATHRATE HYDRATE CAGE

Clathrate hydrates are solids that have a molecular structure in which gas molecules occupy so-called "cages" comprising hydrogen-bonded water molecules. When they are empty, the cages collapse into an ice crystal structure, but the presence of a gas molecule makes them stable. Clathrate hydrates have enormous practical importance as potential sources of energy, as hydrogen storage media, and as components of astrophysical bodies having methane molecules as the guest material inside their ice-like cage structures. Researchers using the XOR 3-ID beamline at the APS and the IN6 instrument at the neutron reactor source of the Institut Laue-Langevin have gained a better understanding of a particular clathrate hydrate that has wide implications for understanding the thermal properties of disordered solids, structural glasses, and other materials.

By using site-specific ^{83}Kr nuclear resonant inelastic x-ray scattering (NRIXS) in combination with incoherent inelastic neutron scattering (IINS) and molecular-dynamics simulations, researchers from the University of Saskatchewan, the National Research Council of Canada, Argonne National Laboratory, the Universität Kiel, the Universität Dortmund, and Institut Laue-Langevin have pinpointed the reason for the anomalously low thermal conductivity of type-II Kr clathrate hydrate: extensive mixing of the localized anharmonic "rattling" motions of "guest" ^{83}Kr atoms with host lattice phonons. Clathrate hydrates have enormous practical importance as sources of energy, as hydrogen storage media, and as components of astrophysical bodies having methane molecules as the guest material inside their ice-like cage structures. The explanation derived from this research has wide implications for understanding the thermal properties of disordered solids, structural glasses, and other materials containing localized oscillators. The NRIXS measurements were performed at the XOR 3-ID beamline of the APS, while the IINS measurements were performed on the IN6 instrument at the neutron reactor source of the Institut Laue-Langevin.

Samples of type-II Kr clathrate hydrate were prepared by continuously exposing a finely ground powder of H_2O ice to Kr gas in a reaction vessel for 7 days at a pressure of 30 bar and

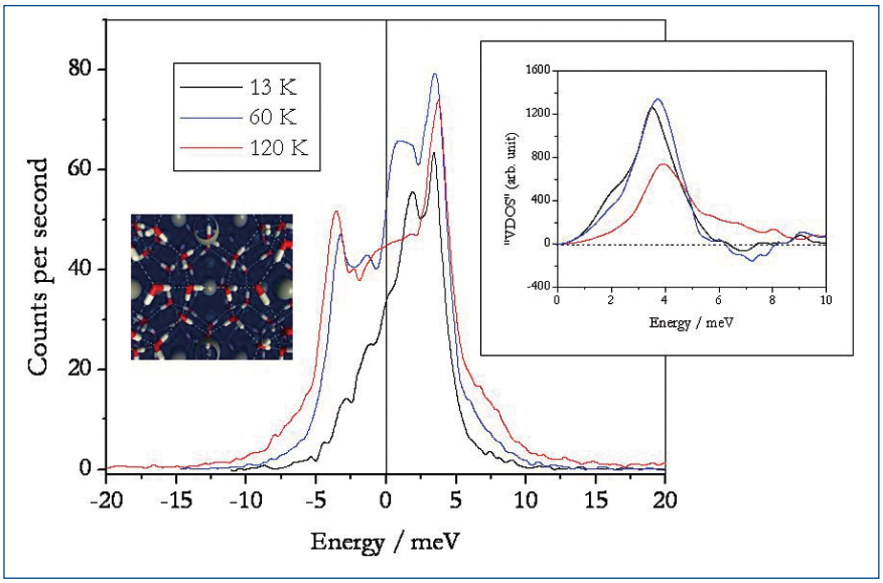

Fig. 1. Experimental NRIXS spectra (main graph) and corresponding derived photon density of states for Kr clathrate hydrate (inset graph), assuming an harmonic approximation. The unphysical negative density of states is a direct indication of the large anharmonicity of the Kr motions, which helps to scatter phonons, thus accounting for Kr hydrate's anomalous thermal behavior. Inset image shows the structure of the Kr hydrate studied.

at temperatures in the -10 to 0°C range. Samples were recovered at 77 K and then shipped in liquid nitrogen to the Institut Laue-Langevin in Grenoble.

The IINS data demonstrated a very strong coupling between guest vibrations and those of the ice-like lattice and indicated that these interactions result in the anticrossing of phonon modes with the same symmetry. The NRIXS technique was used to characterize the dynamics of the guest atom alone, in order to permit an understanding of the separate contributions of the guest and host vibrations to the IINS data. Use of the ^{83}Kr guest atom permitted this because it has a low-lying nuclear level at 9.4 keV that can be excited by synchrotron radiation (in other words, it is a Mössbauer nucleus). Nuclear resonance makes the NRIXS data sensitive only to the motions of the ^{83}Kr guest atoms in the clathrate cages, with the cage vibrations themselves being rendered essentially invisible.

The site-specific NRIXS method showed unequivocally that the phonon coupling between the guest and the host leads to unexpectedly large anharmonic motion of the guest (Fig. 1). The large anharmonicity is the cause of the very low thermal conductivity of the clathrate hydrate and is a direct indication of the nature of the coupling between the host and guest vibrations, as coupling through the anharmonic term of the interaction potential provides the means for scattering the lattice thermal phonons, leading to the marked reduction in the thermal conductivity of the clathrate.

Data were obtained at 35K, 50K, 70K, 85K, and 100K. The researchers found that the large anharmonicity persists even at very low temperatures. Although the thermal population of the rattling modes at temperatures below 38K is small, the presence of glass-like thermal conductivity at very low temperatures strongly suggests that the anharmonicity is intrinsic to the guest-host interactions. The researchers do not believe that the non-stoichiometry in the occupancy of the vacant sites is an important factor. They point out that, although the absolute thermal conductivity may change slightly with a small difference in guest concentration, such a difference does not affect the glass-like behavior of the thermal conductivity. — *Vic Comello*

See: J.S. Tse[1,2], D.D. Klug[1], J.Y. Zhao[3], W. Sturhahn[3], E.E. Alp[3], J. Baumert[4], C. Gutt[5], M.R. Johnson[6], and W. Press[4,6], "Anharmonic Motions of Kr in the Clathrate Hydrate," Nat. Mater. **4**, 917 (2005).

Author Affiliations: [1]National Research Council of Canada, [2]University of Saskatchewan, [3]Argonne National Laboratory, [4]Universitat Kiel, [5]Universität Dortmund, [6]Institut Laue-Langevin

Correspondence: john.tse@usask.ca

Use of the Advanced Photon Source is supported by the U.S. Department of Energy, Office of Basic Energy Sciences, Office of Science, under Contract No. W-31-109-ENG-38.

EXPLORING THE ATOMIC STRUCTURE OF ZIRCONIA IN THREE DIMENSIONS

Crystalline zirconia, a material with practical mechanical and electrical uses, assumes three distinct structures at different temperatures. At very high temperature—greater than 2,640K—zirconia has a cubic structure. As the temperature drops, the material takes on a tetragonal, intermediate form, and at room temperature, it assumes a monoclinic form. As the material cools, its volume increases by 3% to 5%, and structure changes cause the material to crack and become too fragile to be of practical use. In recent experiments conducted at the XOR/BESSRC beamline 11-ID-C at the APS, researchers from Central Michigan University, the University of Burdwan, India, and Argonne National Laboratory applied the power of x-ray diffraction (XRD) combined with pair distribution function (PDF) analysis to determine the atomic and spatial ordering of phases of nanocrystalline zirconium dioxide (ZrO_2) at atmospheric pressure. Using these complementary techniques, the team was able to describe the lattice arrangement at the multi-nanometer-range, or average scale, and at the local (or subnanometer) scale, providing a more complete view of the three-dimensional (3-D) structure of nanocrystalline zirconium dioxide (ZrO_2) and a better understanding of the exact properties that contribute to the stability of the cubic form of the material.

Researchers have tried various methods to stabilize ZrO_2 in its useful, cubic phase, at room temperature, by doping with such elements as calcium and yttrium, but doped zirconia still has practical limitations. A promising and cost-effective approach to stabilizing large amounts of ZrO_2 is to pulverize it to a nanocrystalline size with high-energy ball milling, but the details of the atomic structure of nanostructured zirconia have not been well understood.

In this study, specimens of low-temperature zirconia with a monoclinic structure were rotated at very high speed (450 rpm) in vials containing 10-mm chrome steel balls at time periods ranging from 1 to 3, 5, 8, and 12 h and then examined and subjected to XRD and PDF analysis.

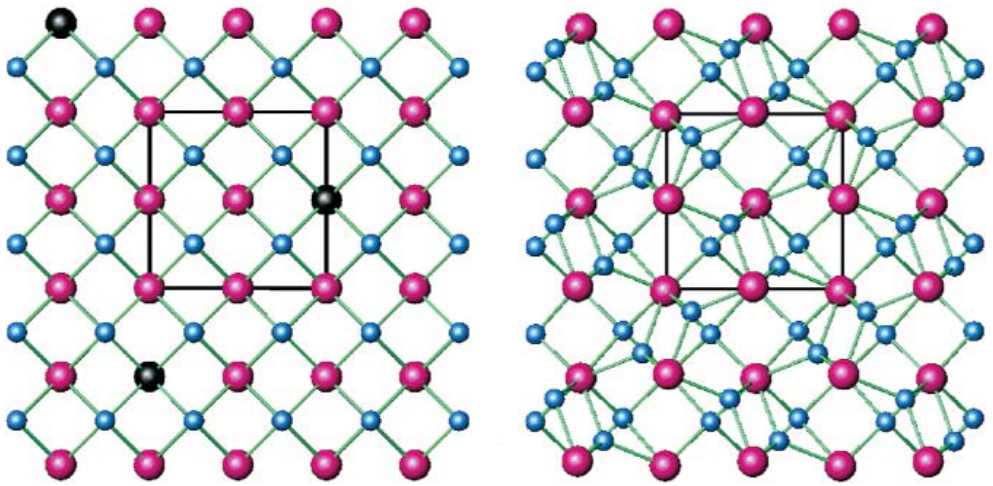

Fig. 1. The cubic structure of crystalline ZrO_2 at room temperature, stabilized by doping. The black circles represent Zr atoms that have been replaced with Ca, Y or Hf (A). Nanocrystalline ZrO_2 was obtained by high-energy ball milling of crystalline monoclinic ZrO_2. The cubic average structure is stabilized by introducing local structural disorder, which produces a local atomic order resembling the monoclinic form (B). In both figures, Zr atoms are in red, O atoms in blue, and the black lines outline the unit cell.

To determine the three-dimensional structure, diffraction data were obtained by utilizing high-energy x-rays up to high values of the wave vector Q (up to about 28 $Å^{-1}$), which makes PDF analysis possible. The diffraction studies showed well defined Bragg peaks for the unmilled samples. As milling time increased, the diffraction patterns became broader, indicating diminishing structural coherence. PDF analysis yielded information on both the average and the local, subnanometer-scale structure.

The studies confirmed that milled nanocrystalline zirconia has a long-range atomic structure (from 5 Å to approximately 2–3 nm) with a cubic lattice form, while on the local scale (shorter than 5 Å), the structure retains its less-orderly, monoclinic form. The researchers propose that it is this mismatch of orderly and disorderly structures that gives the milled nanocrystalline material its stability (Fig. 1).

Further PDF analysis and the results of complementary Rietveld studies, which use low-Q wave vectors, confirmed that nanocrystalline zirconia occurs in a single phase with cubic ordering on the average scale and distortions on the local scale, rather than in two phases, monoclinic and cubic.

The results confirm the usefulness of XRD and PDF techniques to obtain a better view of the 3-D structure and more complete data on total scattering from materials that are ordered at the nanoscale, such as nanocrystalline zirconia.

— Elise LeQuire

See: M. Gateshki[1], V. Petkov[1], G. Williams[1], S.K. Pradhan[2], and Y. Ren[3], "Atomic-scale Structure of Nanocrystalline ZrO_2 Prepared by High-energy Ball Milling," Phys. Rev. B **71**, 224107 (2005).

Author Affiliations: [1]Central Michigan University, [2]The University of Burdwan, [3]Argonne National Laboratory
Correspondence: petkov@phy.cmich.edu

This research was supported at the University of Notre Dame by the Environmental Management Science Program of the Office of Science, U.S. Department of Energy (DE-FG07-97ER14820) and the National Science Foundation Environmental Molecular Science Institute (EAR02-21966); and at Argonne National Laboratory by the U.S. Department of Energy Office of Basic Energy Sciences–Chemical Sciences Division.Use of the Advanced Photon Source was supported by the U.S. Department of Energy, Office of Science, Office of Basic Energy Sciences, under Contract No. W-31-109-ENG-38.

AROUND THE EXPERIMENT HALL

IRON AND NEURODEGENERATIVE DISEASE

Mark Davidson (left), University of Florida (UF), and Joanna Collingwood, Keele University in the United Kingdom (UK, who is supported by a UK Alzheimer's Society Research Fellowship and Dunhill Medical Trust), align a sample of Alzheimer's brain tissue at the microfocus facility, MR-CAT, beamline 10-ID.

Davidson: "Unusual iron mineral nanoscale deposits have been associated with many neurodegenerative diseases, such as Alzheimer's, Parkinson's, and Huntington's. There is indication that these deposits (containing mixed oxide phases, such as magnetite) are involved in the oxidative stress of the tissue. The only way to find and identify these minerals was by extraction from bulk tissue samples, which does not provide information on the location of the particles in tissue. These particles are so small and widely dispersed, finding just one via electron microscopy could take months or years.

"We have built a microfocus x-ray absorption spectroscopy (XAS)/x-ray fluorescence (XRF) facility at 10-ID to address this issue. Using XRF from the high intensity of the APS x-rays, we can detect a single <50-nm iron oxide particle in a 200-μm square area, allowing rapid location of biomineral particles. After locating the particle to within <5 μm, we use XAS to identify the specific iron compounds present. The sample is analyzed with transmission electron microscopy to identify the associated biological structures. To our knowledge, this technique is the only one to have located and identified these compounds within tissue. The information obtained has great significance in understanding biochemical pathogenesis mechanisms, and in the development of new iron-chelation drugs for the treatment of neurodegenerative disorders. We are now working with other beamlines (18-ID at the APS) and synchrotrons (DIAMOND) to share these techniques and expand these new powerful capabilities." (See also: page 63.)

Contact: mark@microfab.ufl.edu, j.f.collingwood@pmed.keele.ac.uk

PERMANENT MAGNETS AND RARE BREAKTHROUGHS

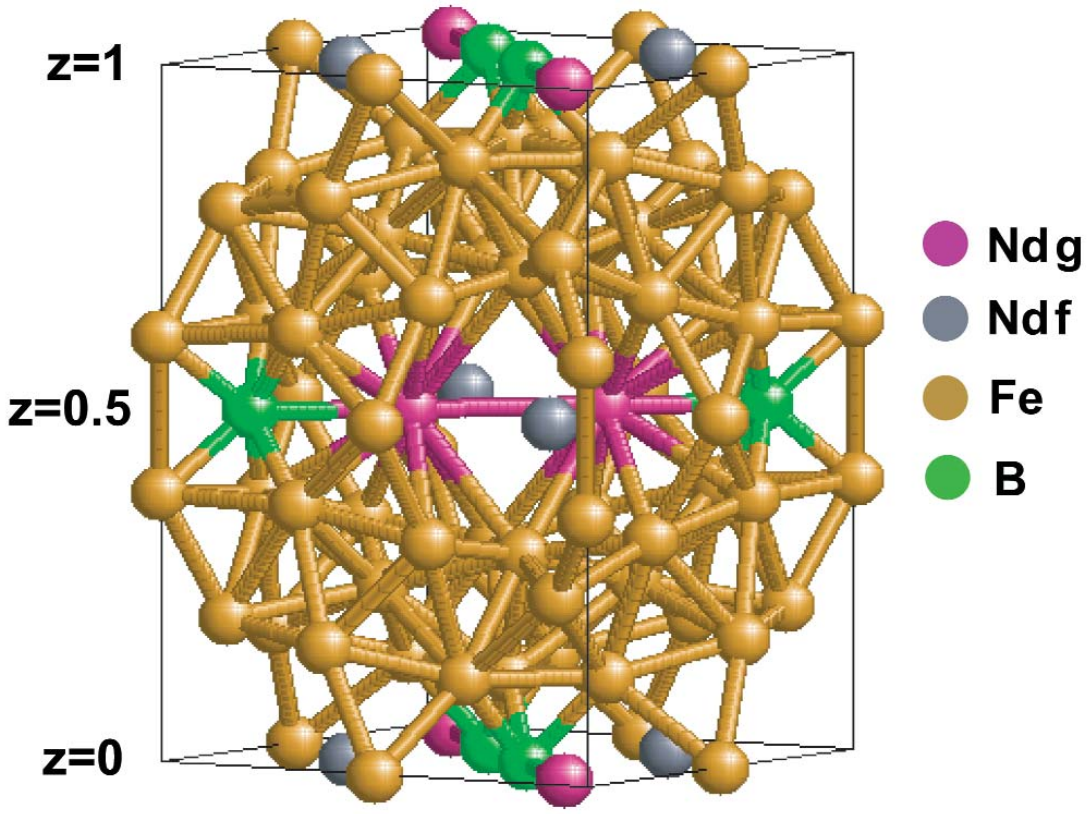

Fig. 1. Unit cell of $Nd_2Fe_{14}B$ indicating the location of the two unequal Nd crystal sites that are the focus of this study.

Much of the current technological progress in fields ranging from miniature electronics to energy conservation relies on creating stronger and more stable magnets. How to increase a magnet's strength and stability has been a major question pursued by many researchers, including a group from Argonne National Laboratory, Northern Illinois University, and Iowa State University. This research team delved deeply into how ions of rare-earth (RE) elements can be used to improve magnet performance. Their detailed work, conducted in part at XOR beamline 4-ID-D at the APS, revealed a positional effect in which two ions of the RE element neodymium (Nd) can either enhance or reduce magnetism, depending on the ions' location in a neodymium-iron-boron ($Nd_2Fe_{14}B$) crystal. This new information can guide innovation in the increasingly large number of products requiring permanent magnets.

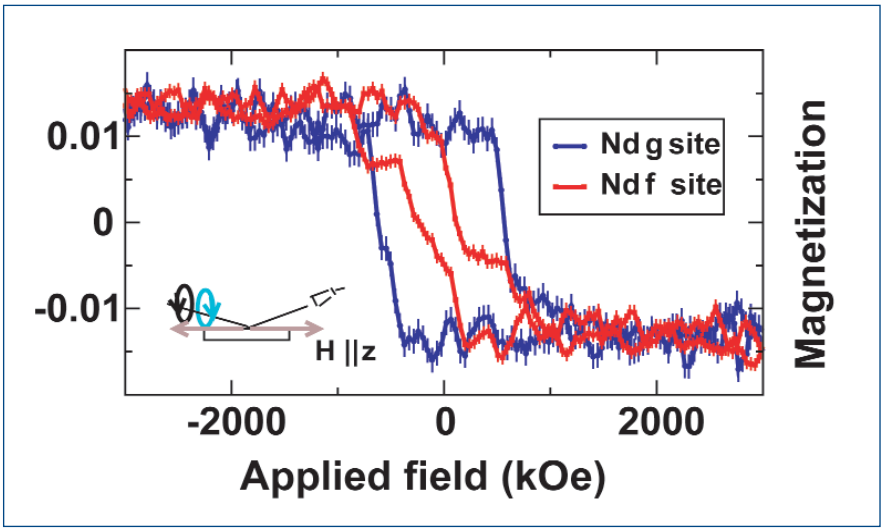

Fig. 2. Element- and site-specific Nd magnetic moment reversal loops, measured through dichroic resonant scattering of circularly polarized x-rays at (110) and (220) Bragg reflections.

The investigators studied a single crystal of $Nd_2Fe_{14}B$, a material known to have an excellent record as a permanent magnet (Fig. 1). A technique involving circularly polarized (CP) x-rays provided a tool with which to study the behavior of the two Nd sites, called *f* and *g* (Fig. 2). The Nd-*g* site turned out to be the star in terms of enhancing permanent magnetism. The Nd ion in the *g* site appears to be primarily responsible for the strong magnetic stability of this ferromagnetic material. The researchers discovered, however, that the Nd ion at the *f* site does not behave in the same way as the Nd ion at the *g* site. The Nd-*f* ion, because of the way in which it tends to influence magnetic moment orientation, actually detracts from the magnetic stability of the material. So, in looking for ways in which to make the magnet permanent, the details—in this case, the precise location of a single Nd ion—matter a lot.

To bolster their empirical evidence regarding the strong influence of the Nd-*g* site, the investigators used crystal field theory to investigate the energetics of orienting the magnetism on the different RE sites along different crystalline directions. The calculated behavior agrees well with the measurements obtained by using the x-ray techniques.

The surprisingly opposite behavior of the Nd ions in the two sites on the crystal is attributable to their dissimilar neighborhoods—unequal sites in the $P4_2/mnm$ tetragonal space group—causing *f* and *g* sites to produce alignment along different axes in the crystal structure. This difference between the Nd sites suggests one of several general applications for these findings: If *f* sites could be put out of commission by preferential chemical flooding, known as doping, then their destabilizing effect on magnetic stability could be eliminated.

Several other breakthroughs arise from the present work. First, the researchers have shown that their methods allow detailed study of the Nd sites, where the effect on magnetic stability is clear, independent of the Fe background magnetization, which is strong but apparently does not play a large role in protecting the material against demagnetization.

Second, the methods used for the present work can now be applied to study magnetic stability in other materials. The x-ray resonant scattering approach exploits the crystal's symmetry and the coupling of its magnetization to CP radiation, hence marrying site-specific diffraction to the elemental magnetic fingerprints obtained near absorption edges. The result is a remarkably fine-tuned data set that provides a clear picture of how different parts of the crystal are affecting the magnetic stability of the material.

Finally, the present work details the atomic origins of the intrinsic magnetic stability in $Nd_2Fe_{14}B$, which is currently the best permanent magnet—thus laying the groundwork for synthesis of materials that could possess the same characteristics. Because RE ions, due to their strong effects, are a preferred candidate for enhancing magnetic stability, the present work can be used as a model for the use of RE ions in technological applications. — *Mona Mort*

See: D. Haskel[1], J.C. Lang[1], Z. Islam[1], A. Cady[1], G. Srajer[1], M. van Veenendaal[1,2], and P.C. Canfield[3], "Atomic Origin of Magnetocrystalline Anisotropy in $Nd_2Fe_{14}B$," Phys. Rev. Lett. **95**(21), 217207 (2005).

Author Affiliations: [1]Argonne National Laboratory, [2]Northern Illinois University, [3]Iowa State University
Correspondence: haskel@aps.anl.gov

M. v.V. is supported by the U.S. Department of Energy Grant No. DE-FG02-03ER46097 and the U.S. Department of Education. Use of the Advanced Photon Source was supported by the U.S. Department of Energy, Office of Science, Office of Basic Energy Sciences, under Contract No. W-31-109-ENG-38.

STO THIN FILMS ON SI(001) SUBSTRATE: SQUASH ME AND I DON'T BULGE!

Transition metal oxides (TMOs), which offer substrates for the growth of new materials, are of increasing interest to the semiconductor industry for use in silicon (Si) device technology. This is especially true for strontium titanium ($SrTiO_3$, or STO) thin films grown on the 001 plane of Si [Si(001)]. It is important for materials developers to understand the thin-film epitaxy of STO with Si, as well as any uncharacteristic behavior that STO may develop when subjected to the resulting epitaxial mismatch strain that arises from growth on a substrate with a different lattice constant. Collaborators from CINVESTAV-Queretaro, the National Institute of Standards and Technology (NIST), Motorola Labs, Pennsylvania State University, the University of Illinois at Urbana-Champaign, the Stanford Synchrotron Radiation Lab, and the Naval Research Laboratory discovered such uncharacteristic behavior—a negative Poisson's ratio—for the thinnest STO films grown on Si(001) that were investigated.

When a thin film is grown coherently on a substrate with a different lattice constant (i.e., grown in such a way as to produce atom-for-atom registry across the thin-film/substrate interface), the lattice constant of the film perpendicular to the interface will respond to the strain imposed on its lattice constant in the in-plane direction. This distortion is described by the Poisson's ratio of the thin film: A film under in-plane compressive strain should expand in the out-of-plane direction. Conversely, a film that is under in-plane tensile strain should contract in the out-of-plane direction.

What the collaborators found instead was a negative Poisson's ratio for the thinnest STO films: The films were found to expand in the out-of-plane direction when they were under in-plane tensile strain (i.e., when they were stretched in the in-plane direction). (STO is a member of the transition-metal oxides [TMOs] with cubic perovskite structure at room temperature—crystals with the general pattern ABO_3, where A and B are cations of different sizes.)

The experimenters obtained this surprising result by growing STO thin films with thicknesses of 40, 60, 80, and 200 Å on Si(001) substrates using molecular-beam epitaxy. To analyze the strain state of the STO films, high-resolution x-ray diffraction measurements were performed using several Bragg reflections—in particular, out-of-plane STO(002) and in-plane STO(200). Measurements were carried out at the XOR/UNI general scattering station at beamline 33-BM. The diffraction results for the in-plane (squares) and out-of-plane (dots) lattice constants for the STO films as a function of thickness are shown in Fig. 1.

All films studied were found to be under in-plane tensile strain; that is, they were not coherent with the Si substrate. Instead, the relaxation of the films at the elevated growth temperature of 700° C, together with the differential thermal expansion of STO and Si, produced films that were stretched in plane. (The larger STO lattice constant expands much more than the smaller Si lattice constant at elevated temperature, so when the films are cooled back to room temperature, the incoherent registry achieved at elevated temperature does not allow the in-plane STO lattice constant to shrink back to its room-temperature value.) Normally, this action would produce films that had contracted out-of-plane lattice constants, and indeed this is what the researchers found for the thickest films. However, this was not the case for the thinnest films, which were found to have expanded out-of-plane lattice constants, or negative Poisson's ratios.

To understand the physics behind this intriguing phenomenon, the collaborators performed near and extended x-ray absorption fine-structure (EXAFS) measurements at the NIST beamline facility X23A2 at the National Synchrotron Light

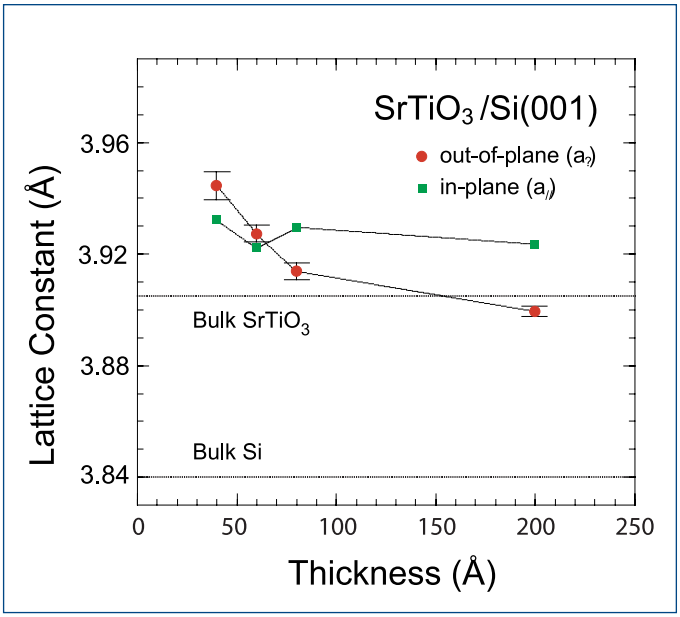

Fig. 1. In-plane (squares) and out-of-plane (dots) STO lattice constants for the 40-, 60-, 80-, and 200-Å STO thin films grown on Si(001). The dotted lines show the bulk cubic lattice constants of STO and Si. Note that all STO films are under tensile strain, and that the out-of-plane lattice constant exceeds the in-plane lattice constant for the thinnest films.

Source. These measurements were made at both glancing and normal incidence to distinguish between in- and out-of-plane Ti-O nearest-neighbor bonding.

The EXAFS data showed that the presence of the STO-Si interface for the thinnest films results in the polarization of the STO layer. This polarization was found to decrease away from the interface, likely being caused by the ionic rearrangement of the first STO layer and the surface. Thus, the collaborators found that the observed elastic anomaly (the negative Poisson's ratio) arises from the interfacial polarization of the STO films. First-principles density-functional theory calculations were also performed, resulting in the same negative Poisson's ratio for the in-plane and out-of-plane lattice constants.

The researchers in this study suggest that this phenomenon might be common to the growth of heteroepitaxial thin films that possess an ionic polarizability due to the intrinsic coupling between polarization and strain in this class of ionic compounds. — *William Arthur Atkins*

See: F.S. Aguirre-Tostado[1], A. Herrera-Gómez[1], J.C. Woicik[2], R. Droopad[3], Z. Yu[3], D.G. Schlom[4], P. Zschack[5], E. Karapetrova[5], P. Pianetta[6], and C.S. Hellberg[7], "Elastic Anomaly for $SrTiO^3$ Thin Films Grown on Si(001)," Phys. Rev. B **70**, 201403(R) (2004)

Author Affiliations: [1]CINVESTAV-Queretaro, [2]National Institute of Standards and Technology, [3]Motorola Labs, [4]Pennsylvania State University, [5]University of Illinois at Urbana-Champaign, [6]Stanford Synchrotron Radiation Laboratory, [7]Naval Research Laboratory
Correspondence: woicik@bnl.gov

This research was carried out (in part) at the National Synchrotron Light Source, Brookhaven National Laboratory, which is supported by the U.S. Department of Energy (DOE), Division of Materials Sciences and Division of Chemical Sciences, under Contract No. DE-AC02-98CH10886. The XOR/UNI facility at the APS is supported by the University of Illinois at Urbana-Champaign, Materials Research Laboratory (U.S. DOE, the State of Illinois-IBHE-HECA, and the NSF), the Oak Ridge National Laboratory (U.S. DOE under contract with UT-Battelle LLC), the National Institute of Standards and Technology (U.S. Department of Commerce), and UOP LLC. Additional support was provided by the Consejo Nacional de Ciencia y Tecnología of México (CONACyT Project No. 34721-E, 33901-U), the Stanford Linear Accelerator Center (CRADA-Project No. 158), and by the DARPA QuIST program. Computations were performed at the ASC DoD Major Shared Resource Center. Use of the Advanced Photon Source was supported by the U.S. Department of Energy, Office of Science, Office of Basic Energy Sciences, under Contract No. W-31-109-ENG-38.

A Ferromagnetic Mechanism in Insulating Co:TiO_2

Many experts predict that the development of spintronics will be the next major leap in electronics, made possible by the discovery of substances that are ferromagnetic and semiconducting at room temperature, such as cobalt-doped anatase titanium dioxide (Co:TiO_2). But completing that leap depends on finding definitive answers to some pesky questions, such as just what mechanism causes the ferromagnetism in anatase Co:TiO_2 , and is it affected by the manner in which the material is made? Is it related to the presence of free carriers—which might limit the practical usefulness of Co:TiO_2 anatase as a room-temperature semiconductor? Previous experiments seemed to suggest this scenario, at least with certain film-growth techniques. Or is the Co:TiO_2 ferromagnetism due to some other property, either inherent or resulting from the film growth process? Whatever the answers, if such materials are to be useful, we must have a better understanding of how and why they behave the way they do.

A group of researchers from the University of Washington and the Pacific Northwest National Laboratory (PNNL) set out to answer these questions at the 20-BM and 20-ID beamlines of the XOR/PNC facility at the APS, with additional work at PNNL. The investigators grew Co:TiO_2 anatase films by rf magnetron sputter deposition in a pure Ar atmosphere at a pressure of 4×10^{-3} torr. Films measuring ~85 nm in thickness were deposited at 0.01 nm/s on matching (100) $LaAlO_3$ (LAO) substrates. The films were studied both before and after a 1-h ultrahigh vacuum (UHV) annealing process at 450° C. The team employed various techniques to examine the films, including x-ray diffraction (XRD), high-resolution transmission electron microscopy (HRTEM), and selected-area diffraction. Detailed spectral analysis was done with energy-dispersive x-ray spectroscopy, and Rutherford backscattering spectroscopy (RBS).

Continued on next page

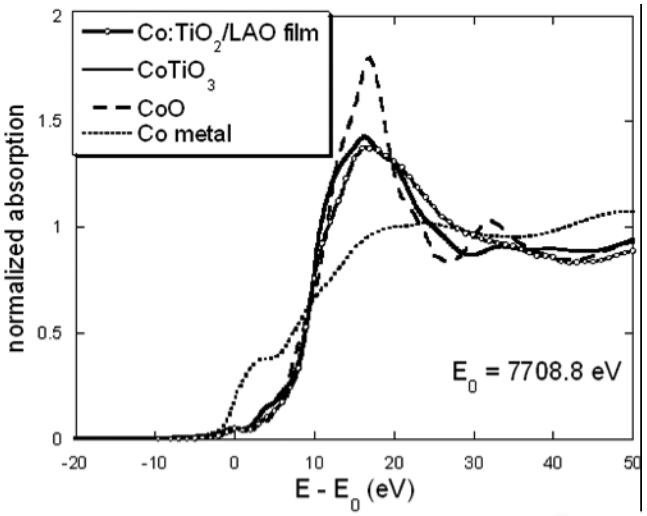

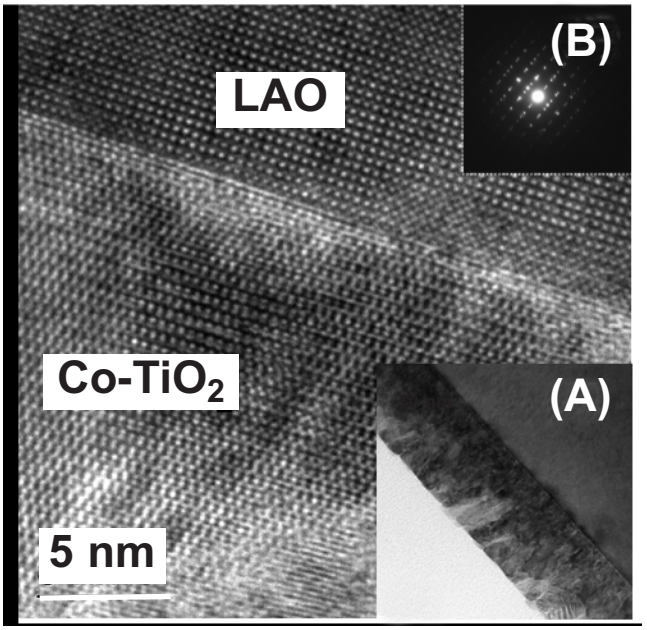

Fig. 1. Top: Co K-edge NEXAFS spectra for UHV annealed Co:TiO_2 film with reference samples: Co:TiO_2 film (open circles), $CoTiO_3$ (solid line), CoO (long dash), and Co metal (short dash) spectra. Bottom: High-resolution transmission electron microscopy image from cross-sectional specimen of annealed Co:TiO_2 film on LAO. Inset (a): Low magnification image of film (dark grey) on LAO (grey), (white area is epoxy); Inset (b): Selected area diffraction pattern.

To study the Co dopant oxidation state and geometry in the anatase lattice, near edge x-ray absorption fine structure (NEXAFS) measurements were also taken at the Co K edge.

The studies display high-quality crystalline structure in the anatase films, which was further improved with annealing. The experimenters also observed a uniform distribution of Co throughout the anatase with an average concentration of 2.8%. When the present NEXAFS measurements at the Co K edge are compared with the absorption spectra of reference samples of $CoTiO_3$ and Co metal, they seem to indicate that the Co in the anatase films is not metallic, but rather in a Co^{2+} state, because of the distorted octahedral configuration of the Co in the anatase lattice. Therefore, evidence suggests that the Co^{2+} substitutes for Ti^{4+} in the anatase with an increased presence of V_Os (oxygen vacancies) in both the as-deposited and the annealed films. Although earlier experimental results seemed to suggest that Co:TiO_2 anatase is a dilute magnetic semiconductor, the research team believes these results to be merely a byproduct of the unbound V_Os. However, most of the V_Os become bound to the Co^{2+} ions and create defects that result in a dielectric ground state that is also ferromagnetic. Thus, the annealing process that creates and diffuses these VO defects is a critical factor in the growth of Co:TiO_2 anatase films with enhanced ferromagnetism.

The researchers conclude that the bonding of these V_Os to Co^{2+} ions, along with the post-annealing high-quality crystalline structure, is the source of the enhanced ferromagnetic properties of the Co:TiO_2 anatase films. Rather than depending on free carriers in the lattice, as was previously believed, the ferromagnetism exists in conjunction with the anatase dielectric ground state. The team's work provides verification of the importance of the specific crystalline growth techniques used to create semiconducting materials and also suggests some ways in which the properties of Co:TiO_2 and similar dielectric materials could be manipulated. Such knowledge will play a vital role in turning the promise of spintronic technology into practical reality.

— Mark Wolverton

See: K.A. Griffin[1], A.B. Pakhomov[1], C.M. Wang[2], S.M. Heald[2], and Kannan M. Krishnan[1], "Intrinsic Ferromagnetism in Insulating Cobalt Doped Anatase TiO_2," Phys. Rev. Lett. **94**, 157204 (2005).

Author Affiliations: [1]University of Washington, [2]Pacific Northwest National Laboratory
Correspondence: kannanmk@u.washington.edu

This work was supported by NSF/ECS No. 0224138 and the Campbell Endowment at UW, with partial support from UWPNNLJIN (2004). The RBS and TEM work was performed at the EMSL, a national scientific user facility located at PNNL and operated for DOE by Battelle. PNC-CAT is supported by the U.S. DOE No. DEFG03-97ER45628, UW, a major facilities access grant from NSERC in Canada, and Simon Fraser University. Use of the Advanced Photon Source was supported by the U.S. Department of Energy, Office of Science, Office of Basic Energy Sciences, under Contract No. W-31-109-ENG-38.

SOLVING A PUZZLE WITH PHASE TRANSITIONS IN PEROVSKITE FERROELECTRICS

Structural phase transitions in perovskite ferroelectrics have been the subject of intense experimentation. Their simple structure, and the importance of ferroelectricity as an interesting phenomenon with many practical applications, makes them an ideal subject for detailed studies of structural phase transitions—one of the most important issues in condensed matter physics. Even after much study about perovskites, one unanswered question remains: the origin of the reciprocal lattice space diffuse x-ray scattering (DXS) sheets in the paraelectric cubic phases of barium titanate ($BaTiO_3$) and potassium niobate ($KNbO_3$). Researchers from the University of Washington, Argonne National Laboratory's Advanced Photon Source, and Rostov State University used the XOR/PNC 20-BM beamline at the APS to carry out a DXS study that settled this central issue.

The origin of diffuse x-ray scattering sheets in the paraelectric phase of two perovskite ferroelectrics—barium titanate ($BaTiO_3$) and potassium niobate ($KNbO_3$)—has been hypothesized as either the Cochran-Huller displacive model or the Comes order-disorder model. These condensed matter physics models predict that the paraelectric phase of crystals is one in which neither local displacements nor their concomitant electric dipoles exist (the displacive model) or are unaligned (the order-disorder model). At temperatures below T_C, the ferroelectric phase exhibits spontaneous macroscopic electric polarization—local dipoles are aligned (order-disorder)—or aligned spontaneous local displacements appear (displacive). To resolve the uncertainty between the two models, the researchers in this study conducted a DXS study of the paraelectric phase of single-crystal perovskite ferroelectric lead titanate ($PbTiO_3$).

Perovskite crystals possess a basic chemical formula: ABO_3, where A and B are cations of different sizes. Generally, perovskite ferroelectrics make a phase transition at T_C from a low-temperature tetragonal phase to a cubic paraelectric phase. These crystals have been extensively researched because of their simple structure and their importance in such practical applications as catalysts, sensors, and superconductors.

On the basis of the pure displacive model of William Cochran [1], the DSX sheets were explained by Adam Huller as being caused by the formation of linear chains of correlated displacements in the transverse optical soft mode [2]. The DXS sheets were also explained by R. Comes et al. through the model of order-disorder, in which the sheets are formed by linear chains of short-range correlated local displacements that existed in the paraelectric phase and have long-range order in the ferroelectric phase [3].

Recent measurements of paraelectric $BaTiO_3$ and $KNbO_3$ confirmed the presence of DSX sheets but could not clarify the reason for their existence. Because of the ambiguity of such experimental studies, the collaborators sought to resolve the uncertainty by studying paraelectric $PbTiO_3$. They decided on $PbTiO_3$ because it has similar soft-mode behavior as the other two perovskites in the paraelectric phase (as in the Cochran-Huller model), yet it has a different local displacement with respect to $BaTiO_3$ and $KNbO_3$ (as in the Comes model). $BaTiO_3$ and $KNbO_3$ have disordered local displacements along the <111> directions, while $PbTiO_3$ has disordered local displacements along the <001> directions. Thus, similar diffuse sheets should result if the Cochran-Huller model is valid, while different diffuse sheets should result if the Comes model is valid.

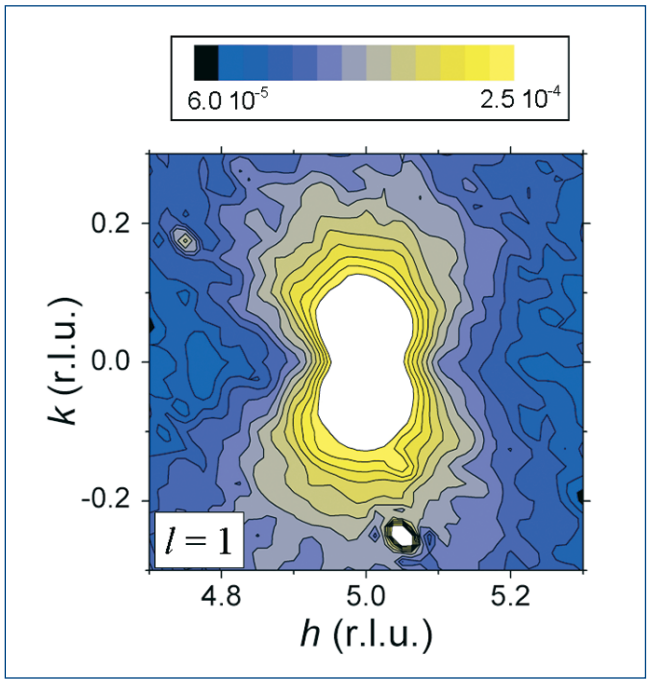

Fig. 1. The (*h, k*) plane at *l* = 1. The "hot spot" at (5.05, -0.25, 1) is due to a weak resolution-limited peak, presumably due to multiple diffraction. Note that no diffuse sheet is present along *h* = 5, as would be the case if diffuse sheets were present. Scattering from acoustic transverse and longitudinal phonons causes the diffuse signal. The white region is not shown because it was contaminated by the tails of the much more intense (*501*) Bragg peak.

Continued on next page

The collaborators grew high-quality $PbTiO_3$ single crystals from stoichiometric melts. An experimental control of thermal phonon diffuse scattering (TDS) was used through a single crystal of the nonferroelectric perovskite strontium titanate ($SrTiO_3$). Measurements were made at a fixed sample temperature of 800K (~1.05 T_C) on the PNC 20-BM beamline.

The collaborators found that diffuse scattering from the paraelectric phase of $PbTiO_3$ was dominated by TDS, revealing no evidence of diffuse scattering sheets (Fig. 1). When diffuse scattering sheets were not found in $PbTiO_3$, the collaborators concluded that, when the sheets appeared in $BaTiO_3$ and $KNbO_3$ it was not due to soft-mode contributions, but to local displacements in the <111> directions that created correlated linear chains in the <100> directions. For $PbTiO_3$, the local displacements were in the <100> directions; correlated linear chains were not created because they were energetically unfavorable. The collaborators' calculations showed that soft-mode branch contribution to the sheets was negligible in all three ferroelectric perovskites. Consequently, the DXS features of paraelectric $PbTiO_3$ were dominated by acoustic-phonon branches within TDS.

This study accomplished its goal of deciding the controversy concerning the origin of DXS sheets in the paraelectric phase of the perovskite ferroelectrics $BaTiO_3$ and $KNbO_3$: showing that differences in the diffuse scattering are explained by differences in the disordering of the local displacements, as explained through the Comes model of order-disorder.

— William Arthur Atkins

REFERENCES

[1] W. Cochran, "Crystal Stability and the Theory of Ferroelectricity," Phys. Rev. Lett. **3**, 412 (1959); W. Cochran, "Crystal Stability and the Theory of Ferroelectricity," Adv. Phys. **9**, 387 (1960).

[2] A. Huller, "Displacement correlation and anomalous x-ray scattering in $BaTiO_3$," Solid State Commun. **7**, 589 (1969); A. Huller, Z. Phys. **220**, 145 (1969).

[3] R. Comès, M. Lambert, and A. Guinier, "The Chain Structure of $BaTiO_3$ and $KNbO_3$," Solid State Commun. **6**, 715 (1968); R. Comès, M. Lambert, and A. Guíníer, "Désordre linéaire dans les cristaux (cas du silicium, du quartz, et des pérovskites ferroélectriques)," Acta Crystallogr. A **26**, 244 (1970).

See: B.D. Chapman[1], E.A. Stern[1], S.-W. Han[1], J.O. Cross[2], G.T. Seidler[1], V. Gavrilyatchenko[3], R.V. Vedrinskii[3], and V.L. Kraizman[3], "Diffuse X-ray Scattering in Perovskite Ferroelectrics," Phys. Rev. B **71**, 020102(R) (2005).

Author Affiliations: [1]University of Washington, [2]Argonne National Laboratory, [3]Rostov State University

Correspondence: stern@phys.washington.edu

This research was supported by DOE Grant No. DE-FGE03-97ER45628. PNC-CAT was supported by DOE Grant No. DE-FG03-97ER45628, the University of Washington, Pacific Northwest National Laboratory, and the Natural Sciences and Engineering Research Council of Canada. Use of the Advanced Photon Source was supported by the U.S. Department of Energy, Office of Science, Office of Basic Energy Sciences, under Contract No. W-31-109-ENG-38.

AROUND THE APS

Hispanic Educational Science and Engineering Day

Bruce Glagola (AES, at far right in photo) has the undivided attention of some of the 37 middle-school students and 6 teachers who toured several Argonne facilities, including the APS, on September 30, as the Argonne Hispanic/Latino Club held its first Hispanic Educational Science and Engineering Day. Also volunteering as tour guides at the APS were Donald C. Cronauer (CMT), Steve Davey (AES), Leo Ocola (CNM), and Mariana Varotta (ASD). After the tours were completed, the students were tasked with preparing slide presentations to answer questions about the material presented on the tours.

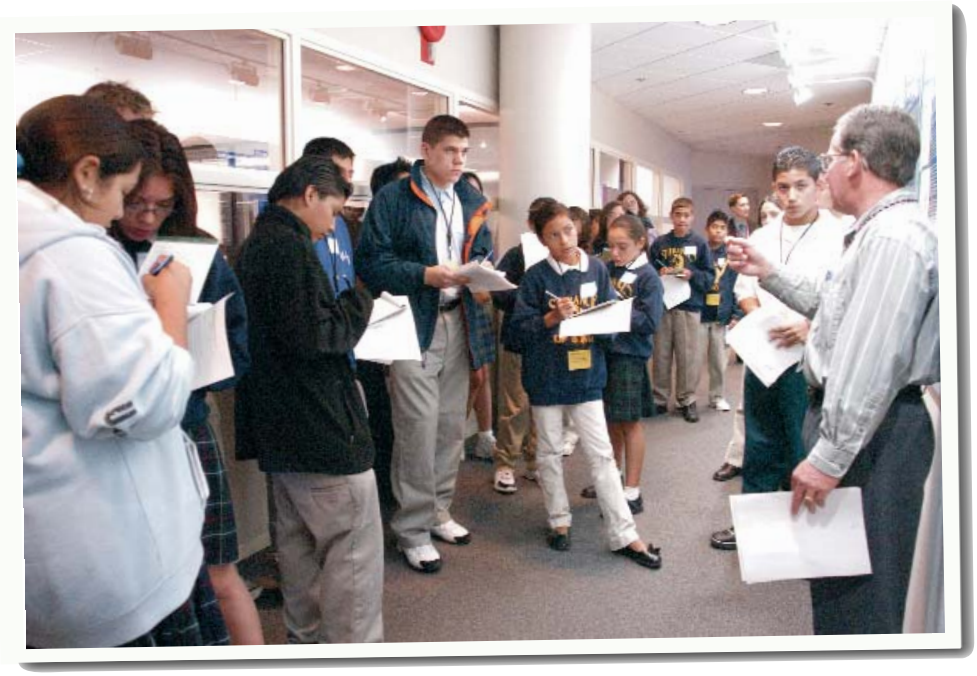

X-RAY STUDIES OF A DISORDER-ORDER TRANSITION

Microstructure is a fundamental parameter that determines the physical behavior of a material and strongly affects its mechanical and electronic properties. Controlling the microstructure and understanding its links to properties are extremely important from both fundamental and practical points of view. Understanding how long-range order develops from a disordered state has long been the subject of intense study in materials science and condensed matter physics. In particular, the evolution over time of this mesoscale ordering on length scales from nanometers to several microns has been the subject of much investigation. Most of the studies, however, have measured only an average length scale of these processes. A team of researchers from McGill University and the University of Michigan used the XOR 8-ID beamline at the APS to carry out direct measurements of fluctuations about this average behavior in a solid undergoing an order-disorder transition.

As an ordered state is approached after a material is quenched through a phase transition, the time dependence of the characteristic length scale (i.e., the average domain size) R typically follows a power law of the form $R(t) \sim t^n$. This scaling behavior applies to a wide range of systems and is not sensitive to most atomic details. In general, for first-order transitions in nonconservative systems (such as ordering in Cu-Au and Cu-Pd alloys [1]) the exponent is 1/2 (referred to as Model A), whereas for conservative systems (such as unmixing in Al-Li alloys [2]) the exponent is found to be 1/3 (Model B). This dynamic scaling hypothesis describes well the average behavior of nonequilibrium systems undergoing phase ordering, but the nature of the fluctuations around the average is harder to measure.

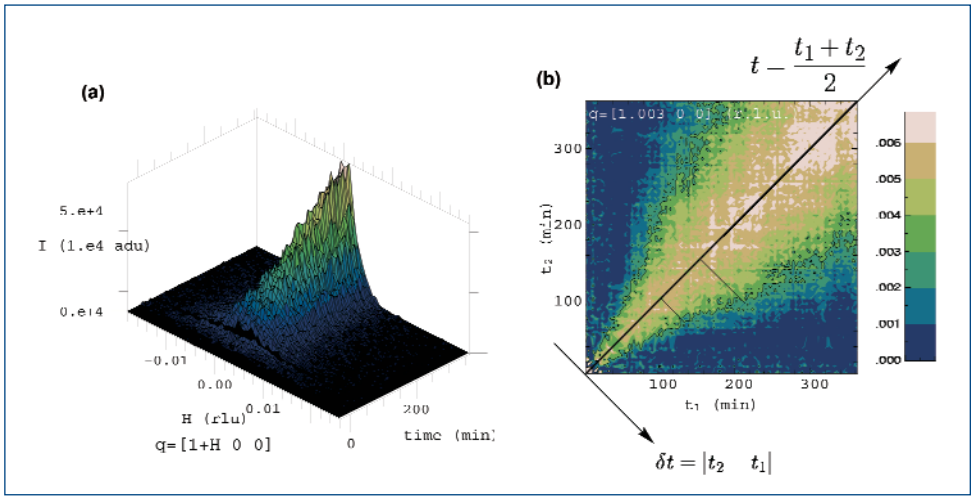

Fig. 1. (a) Growth of the [100] superlattice peak in Cu_3Au, following a quench (at t = 0) from the high-temperature, disordered phase, to a temperature below the critical temperature for ordering. (b) The autocorrelation function of the scattered intensity at two different times, t_1 and t_2, reveal the internal, mesoscale dynamics of fluctuations in the ordered material. The natural variables for analyzing these two-time correlation functions are the average time, which is measured by the distance along the "main" ($t_1 = t_2$) diagonal, and the time difference dt, which measures the distance from the "main" diagonal. The correlation functions along the $t_1 = t_2$ diagonal simply measure the degree of coherence of the beam. Along a direction perpendicular to the $t_1 = t_2$ diagonal, the two-time correlation functions decay from their maximum value to zero, for large enough time differences $dt = t_2 - t_1$. From the figure, it can be seen that the characteristic times for these decays are longer for higher average times or, in other words, the correlation times for the density-density fluctuations in the ordered material increase as the material becomes more ordered.

A specimen of the alloy Cu_3Au was chosen for the ordering experiments because it is a well-studied system for observing order-disorder phase transitions. At high temperatures the alloy has a face-centered cubic structure with each site randomly occupied by either a copper atom or a gold atom. When the temperature falls below a critical temperature (383° C in this case), the alloy exhibits a first-order ordering transition in which the gold atoms occupy the unit cell corners, while the copper atoms occupy the face sites. However, since there is a "four-fold ambiguity" in choosing the "corner," the ordered state is four-fold degenerate. As the high-temperature disordered state is quenched, regions of ordered alloy in any of the four possible states begin to form in a background of disordered phase. These ordered regions eventually grow and meet at antiphase domain walls where they occupy the entire volume of the quenched alloy. At this stage, the domains enter a coarsening regime where the average domain size follows a power law with exponent 1/2.

To study the fluctuations about this average time evolution, the researchers used x-ray intensity fluctuation spectroscopy at beamline 8-ID. In this measurement, partially coherent x-rays at 7.66 keV impinge on a single crystal of

Continued on next page

Cu_3Au and the [100] superlattice reflection is captured via a charge-coupled device array (Fig. 1a). The alloy sample is mounted on a heater attached to a water-cooled copper heat sink to achieve fast temperature quenches from 425° C to below the critical temperature. The partial coherence of the incident x-ray produces a speckle pattern that yields a two-time correlation function $C(q,t_1,t_2)$ that provides information about the dynamics of the coarsening process.

Mesoscale fluctuations in this ordering transition are different from equilibrium fluctuations as the fluctuation time increases when the solid becomes more ordered (Fig. 1b).These measurements show that the fluctuations also follow a dynamical scaling law in which the increase in correlation times is described by a power law that was observed to cross over from linear in time to an exponent of 1/2. Such studies reveal the detailed mechanisms by which the disordered state forms into ordered regions and makes the full transition to ordering. Moreover, the results demonstrate the power of x-ray fluctuation spectroscopy at third generation synchrotron facilities such as the APS, where the high x-ray brightness makes such experiments possible. — *David Voss*

REFERENCES

[1] R.F. Shannon, Jr. et al., "Time-resolved X-ray-scattering Study of Ordering Kinetics in Bulk Single-crystal Cu_3Au," Phys. Rev. B **46**, 40 (1992).
[2] F. Livet and D. Bloch, Scr. Metall. **19**, 1147 (1985).

See: Andrei Fluerasu[1*], Mark Sutton[1], and Eric M. Dufresne[2], "X-Ray Intensity Fluctuation Spectroscopy Studies on Phase-Ordering Systems," Phys. Rev, Lett. **94**, 055501 (2005).
Author Affiliations: [1]McGill University, [2]University of Michigan
*Present address: European Synchrotron Radiation Facility
Correspondence: fluerasu@esrf.fr

E.M.D. was supported by U.S. Department of Energy Grant No. DE-FG02-03ER46023. Use of the Advanced Photon Source was supported by the U.S. Department of Energy, Office of Science, Office of Basic Energy Sciences, under Contract No. W-31-109-ENG-38.

MEASURING THE MOTT TRANSITION FOR MANGANESE OXIDE

For more than half a century, the Mott transition—the phase shift in a material from an insulating state to a metallic state—could not be confirmed at room temperatures in such typical Mott insulators as 3d-transition metal monoxides (TMO, TM-Mn, Fe, Co, Ni) because of the formidably high pressures required for such transitions. Researchers from the Lawrence Livermore National Laboratory; HP-CAT; and the University of California, Davis, using high-resolution x-ray emission spectroscopy and angle-resolved x-ray diffraction data, studied manganese monoxide (MnO). their research revealed a series of electronic phase transitions in manganese monoxide: B1(PM) → dB1(AFM) → B8(PM) → B8(DM), where the last transition is the Mott insulator-metal transition, occurring at a pressure of 105 ± 5 gigapascals (GPa) and a temperature of 300K. This work represents the first time a first-order, isostructural Mott transition has been measured and reveals fundamental physics that should be incorporated in any general theory of electron-correlation-driven transitions from the insulating to metallic state.

In their experiment, the collaborators inserted nearly pure MnO powder into relatively small sample chambers that used diamond anvil cell technology and contained gaskets made of either rhenium (Re) for x-ray diffraction or beryllium (Be) for x-ray emission spectroscopy. Mineral oil, which helps in examining nearly imperceptible structural and spectral changes in highly compressed MnO, was also added. X-ray emission spectroscopy was used to investigate the 3d magnetic moments of MnO under high pressure while inside the sample chambers. Measurements were carried out with HP-CAT beamlines 16-ID-B and 16-ID-D at the APS.

The research group effected structural and spectral changes to MnO by applying high pressures; in turn, these changes provided a logical description of MnO's phase transitions (Fig.1). The three phase transitions investigated were:

1. From B1 (PM), the paramagnetic B1 phase in cubic NaCl-like structure, to dB1 (AFM), the antiferromagnetic distorted B1 phase in rhombohedral structure, at a pressure of 30 GPa;
2. From dB1 (AFM) to B8 (PM), the paramagnetic B8 phase in hexagonal NiAs-like structure at 90 GPa; and
3. From B8 (PM) to B8 (DM), the diamagnetic B8 phase at 105 ± 5 GPa, which is the Mott transition.

The results from this study agreed with earlier studies concerning MnO (at a temperature of 300K) at a pressure range of 30 GPa to 90 GPa for the dB1 (AFM) phase and at pressures

above 120 GPa for the B8 (DM) phase. In fact, the resultant Kβ emission lines for compressed MnO (with an emission energy of 6.490 keV) showed steady reductions in intensity as the experiment proceeded from the B1 (PM) phase (below 30 GPa) to the dB1 phase (from 40 GPa to 98 GPa) (Fig. 2).

Earlier structural studies, however, could not determine the phase between pressures of 90 GPa and 120 GPa. The collaborators resolved this unknown phase by identifying an isostructural phase transition at 105±5 GPa, which occurs with a large volume change. In addition, their results did not show the Kβ′ satellite feature at the B8 phase (above 108 GPa). Such a loss of the Kβ′ peak clearly indicated a significant loss of magnetic moment in MnO. At this point, the collaborators found that at the Mott transition, from the B8 (PM) state to the B8 (DM) state, the following three events simultaneously occurred: a significant loss of 3d magnetic moments, a first-order isostructural transition with an approximately 6.6 percent volume reduction, and an insulator-metal transition (i.e., metallization).

In addition, the collaborators found that the second (intermediate) phase transition became a blend between the dB1 (AFM) and B8 (PM) phases. The two phases possessed very similar energy structures that resulted in relatively large delays in responding to pressure changes, which ultimately caused the two phases to exist together over a larger-than-normal pressure range.

The results here clearly suggest that the Mott transition in MnO is more important to the scientific community that just the knowledge concerning the beginning of metallization. In fact, as previously predicted, the Mott transition in MnO describes strong parallels to the transitions in the lanthanides (the series of metallic elements commonly including lanthanum, cerium, and ytterbium) and actinides (the series of 14 radioactive elements with atomic numbers 89 through 102). The collaborators believe that such important similarities or any differences between the Mott transition in MnO and those within the lanthanide and actinide metals should be incorporated in any general theory of electron-correlation driven transitions.

— William Arthur Atkins

See: C.S. Yoo[1], B. Maddox[1], J.-H.P. Klepeis[1], V. Iota[1], W. Evans[1], A. McMahan[1], M.Y. Hu[2], P. Chow[2], M. Somayazulu[2], D. Häusermann[2], R.T. Scalettar[3], and W.E. Pickett[3], "First-Order Isostructural Mott Transition in Highly Compressed MnO," Phys. Rev. Lett. **94**, 115502 (25 March 2005).

Author Affiliations: [1]Lawrence Livermore National Laboratory; [2]HP-CAT; [3]University of California, Davis
Correspondence: yoo1@llnl.gov.

This work was supported by the LDRD-04-ERD-020 and PDRP programs at LLNL, University of California, under the auspices of the U.S. DOE under Contract No. W-7405-ENG-48, and by the Stockpile Stewardship Academic Alliances Program under DOE Grant No. DE-FG03-03NA00071. Use of the HP-CAT facility was supported by DOE-BES, DOE-NNSA (CDAC), NSF, DoD-TACOM, and the W. M. Keck Foundation. Use of the Advanced Photon Source was supported by the U.S. Department of Energy, Office of Science, Office of Basic Energy Sciences, under Contract No. W-31-109-ENG-38.

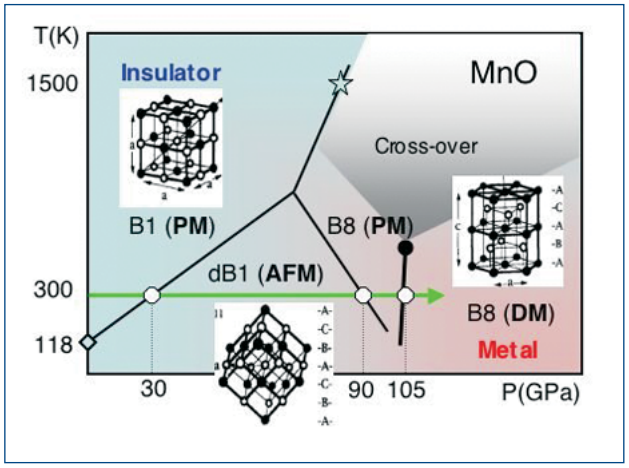

Fig. 1. The conceptual phase diagram of MnO. The thick phase line signifies the first-order isostructural Mott transition that simultaneously accompanies complete loss of magnetic moment, a large volume collapse, and metallization; the transition should end at the critical point (solid circle). The gray fan above the critical point represents a smooth cross-over to metallic behavior at high temperature.

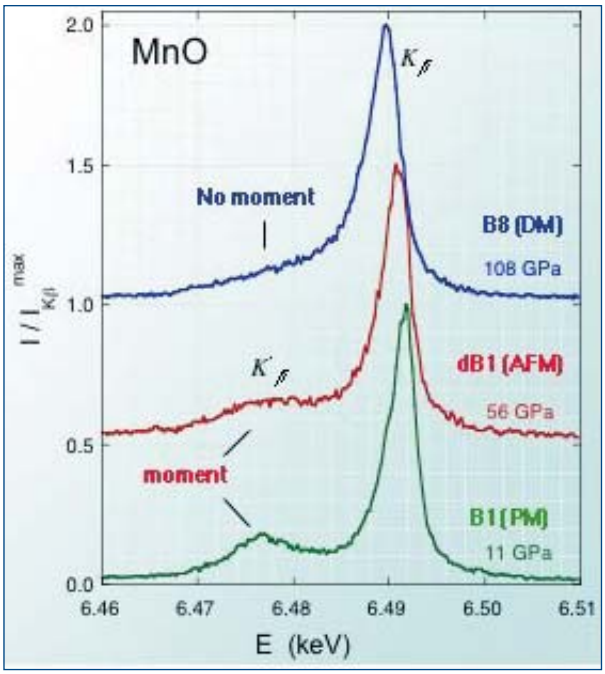

Fig. 2. Kβ x-ray emission branches of MnO at high pressures (all in GPa), showing subtle spectral changes in the Kβ 1,3 peak positions and the Kβ′ intensities at around 30 GPa and 100 GPa. The apparent absence of a Kβ′ peak above 108 GPa signifies loss of the magnetic moment.

PROBING GALLIUM NITRIDE DEFECTS USING X-RAY DIFFRACTION

Gallium nitride (GAN) and related materials have become the materials of choice for a wide range of short-wavelength, light-emitting diodes, lasers, and high-power switching devices. But when GAN is grown on conventional substrates, such as sapphire or silicon carbide, it contains a high degree of dislocations caused by mismatch of the lattices and orientational disorder. Because such defects can greatly degrade the performance of light-emitting devices, other growth methods have been developed. One technique, called pendeoepitaxy, which fosters lateral epitaxial film overgrowth on the sides of columnar structures, has been found to result in very low dislocation densities. Yet many aspects of this type of lateral growth remain unclear. Recently, a team of researchers from Oak Ridge National Laboratory, the University of Bremen, and North Carolina State University used the facilities of the XOR/UNI 34-ID-E beamline at the APS to conduct x-ray microbeam analysis of strain and dislocations in laterally grown GAN films. Their results confirmed finite element calculations about elastic properties, provided new information about dislocations, and underscored the value of high-brilliance synchrotrons for this type of experiment.

Pendeoepitaxy can be performed with or without masking. In the former case, a mask covers the top of the GAN column, whereas in the latter situation no mask covers the initial structure. When masking is used, the GAN lateral growth structures eventually grow out beyond the mask (to become "wings") and dislocations gather along the edge of the masked region. In the case of maskless pendeoepitaxy, growth occurs both laterally and from the top of the column, leading to a structure with a different crystallographic tilt. Many of the properties of strain and dislocation distribution in these kinds of GAN films remain puzzling and cannot be explained purely by elastic behavior. To sort out the factors that contribute to dislocation formation and the development of strain and tilt in the wings grown by the maskless process, the researchers used a combination of broadband white beam x-ray microdiffraction and computational finite-element analysis to gather detailed information on these technologically critical materials.

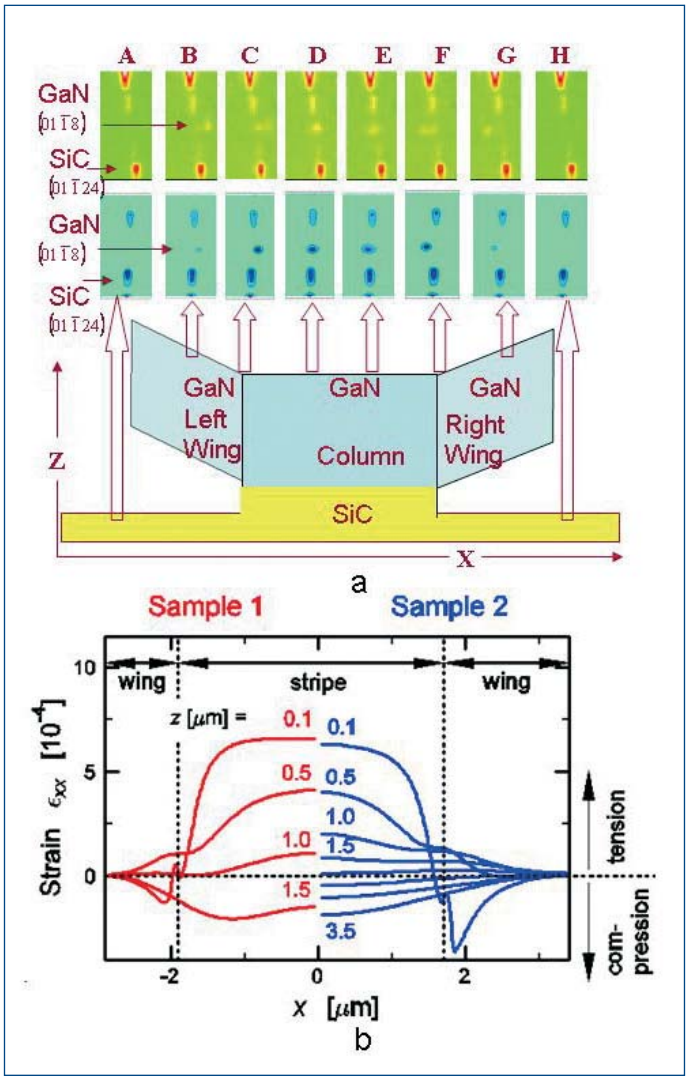

Fig. 1. Microdiffraction analysis of GaN structures grown by maskless pendeoepitaxy. (a) Schematic diagram of the starting column and growth wings on a SiC substrate. Laue diffraction patterns were obtained at points A through H across the entire structure. The topmost row of diffraction patterns is for a sample with thickness-column width-wing dimensions 1.46 x 3.8 x 0.98 μm, while the next row is for a sample with dimensions 3.53 x 3.46 x 1.74 μm. The fixed SiC peaks provide a reference for determining shifts of the GaN peaks. In the wing region, the GaN (01$\bar{1}$8) peaks are slightly shifted from the column positions owing to the tilt of the wings on either side of the column. The narrower peaks in the wing regions indicate a lower defect density and strain inhomogeneity. (b) Results of finite element calculations of strain in the GaN layers across the wing-column structure showing reduced dislocation density and strain in the wings, in agreement with the experimental data.

To create the samples for the study, the researchers etched GAN stripes from 1-μm thick single crystal layers to provide the starting columns. Overgrowth by metallorganic vapor phase epitaxy then led to growth of the lateral wings. The researchers fabricated two specimens with different strip geometries: sample 1 with a thickness of 1.46 μm, a column width of 3.8 μm, and a wing width of 0.98 μm; and sample 2 with a thickness of 3.53 μm, a column width of 3.46 μm, and a wing width of 1.74 μm. Microdiffraction data were collected at beamline ID-34-E in Laue mode to create three dimensional maps of lattice and crystallographic properties at 0.5-μm resolution (Fig. 1). The incident x-ray beam was polychromatic, with photon energy ranging from 7 keV to 25 keV, and was scanned across the sample perpendicular to the stripe axis. High-resolution x-ray diffraction was also used to obtain reciprocal space maps of the two samples.

Microdiffraction scans clearly indicated an upward tilt of the GaN wings in the lateral wings, as predicted by finite-element calculations that modeled the elastic properties of thermally induced stress in the grown structure. In particular, the amount of tilt depended on the aspect ratio of the column and the thickness of the grown layer, in agreement with calculations. Moreover, the diffraction peak broadening showed that the dislocation density was reduced in the wings compared to the column, which is especially relevant for optimizing GaN device technology. Finally, the results indicate that measurements, such as white-beam microdiffraction, requiring high source brightness across a wide spectral region, are possible at third-generation synchrotron facilities such as the APS.

— David Voss

See: R.I. Barabash[1], G.E. Ice[1], W. Liu[1], S. Einfeldt[2], D. Hommel[2], A.M. Roskowski[3], and R.F. Davis[3], "White X-ray Microbeam Analysis of Strain and Crystallographic Tilt in GaN Layers Grown by Maskless Pendeoepitaxy," Phys. Stat. Sol. (a) **202** (5), 732 (2005).

Author Affiliations: [1]Oak Ridge National Laboratory, [2]University of Bremen, [3]North Carolina State University
Correspondence: barabashr@ornl.gov

The research was supported in part by the U.S. Department of Energy (DOE), Division of Materials Sciences and Engineering through a contract with the Oak Ridge National Laboratory, which is operated by UT-Battelle, LLC, for the DOE under Contract No. DE-AC05-00OR22725. The research at NCSU was sponsored by the Office of Naval Research via Contract N00014-98-1-0654 (Harry Dietrich, monitor). The UNICAT facility at the APS is supported by the DOE under Award No. DEFG02-91ER45439, through the Frederick Seitz Materials Research Laboratory at the University of Illinois at Urbana-Champaign and Oak Ridge National Laboratory (U.S. DOE Contract No. DE-AC05-00OR22725 with UT Battelle LLC). Use of the Advanced Photon Source was supported by the U.S. Department of Energy, Office of Science, Office of Basic Energy Sciences, under Contract No. W-31-109-ENG-38.

AROUND THE APS

THE SRI2005 DETECTOR WORKSHOP

On December 8-9 more than 70 participants from the U.S. and Europe—including representatives from the National Science Foundation (NSF) and the Department of Energy, Office of Basic Energy Sciences—met at the APS for a detector workshop sponsored by the NSF, with support from the U.S. synchrotron facilities. The workshop was originally scheduled as part of the SRI2005 meeting in Baton Rouge, which had to be cancelled because of hurricane Katrina, and was a continuation of and update to the Workshop on Detectors for Synchrotron Radiation that was held in October 2000. Weather seemed to be a recurring theme with this workshop: 8 in. of snow fell on the afternoon of the first day. A major conclusion of the workshop was that the capabilities and throughput of many synchrotron beamlines could be improved dramatically if a program to provide detector upgrades and advanced detector development was initiated. It was universally acknowledged that effective detectors are one of the most efficient ways to increase scientific productivity at synchrotron sources. Talks and detailed suggestions from the workshop are at:

http://www.aps.anl.gov/News/Conferences/2005/Synchrotron_Radiation_Instrumentation/index.htm

Contact: Sol Gruner (smg26@cornell.edu), Dennis Mills (dmm@aps.anl.gov).

ORBITAL ORDERING TRANSITION DISCOVERED IN Ca_2RuO_4

The discovery of high-temperature superconductivity in layered cuprates has stimulated a great deal of interest in the electronic properties of transition metal oxides in recent years. Among these oxides, such 4*d* electron systems as Sr_2RuO_4 and Ca_2RuO_4 are particularly interesting. While Sr_2RuO_4 is metallic and exhibits superconductivity below 1.5K, Ca_2RuO_4 is insulating and becomes antiferromagnetic below its Néel temperature, T_N = 110K. Triplet pairing is known to occur in superconducting Sr_2RuO_4, but it remains unclear how strongly the 4*d* electrons are correlated and how magnetic and orbital fluctuations are related to the triplet superconductivity. Ca_2RuO_4 provides an opportunity to study the interplay between the magnetic and orbital degrees of freedom, which could provide a clue to understanding their roles in the triplet superconductivity of the layered Ru oxides.

Resonant x-ray diffraction (RXD) is well suited to delineating the interplay between these degrees of freedom. Accordingly, researchers from Max-Planck-Institut für Festkörperforschung, Brookhaven National Laboratory, Kyoto University, and Argonne National Laboratory recently performed an RXD study at the L_{II} and L_{III} absorption edges of Ru in Ca_2RuO_4 at XOR beamline 4-ID-D of the APS. The measurements were performed on single crystals grown by researchers at Kyoto University. The experimental setup at the XOR 4-ID-D station was modified to allow measurements at energies as low as 2.6 keV, and the beam path was optimized to minimize the absorption of the x-ray beam by air. The sample was mounted on an eight-circle diffractometer in a closed-cycle cryostat capable of reaching temperatures between 10K and 350K. An Si (111) crystal was used as a polarization analyzer, to help distinguish between the polarization components of the diffracted beam perpendicular (σ) and parallel (π) to the diffraction plane.

Resonant diffraction measurements at the L_{II} edge revealed a sequence of phase transitions, including the previously known magnetic transition at T_N = 110K, as well as a new transition at a much higher temperature, T_{OO} = 260K. The temperature dependence (Fig. 1) and polarization dependence (Fig. 2) of the diffracted radiation, combined with supplementary muon spin rotation (μSR) experiments performed at the General Purpose Spectrometer beamline at the Paul Scherrer Institute, in Switzerland, indicate that the latter transition originates from ordering of the 4*d* t_{2g} orbitals. The orbital order is characterized by the same propagation vector (100) as the low-temperature antiferromagnetic state. No charge scattering due to lattice distortions was observed at the orbital ordering wavevector. This illustrates the power of resonant x-ray diffraction to elucidate electronically driven orbital ordering phenomena that are only weakly coupled to the crystal lattice. — *Vic Comello*

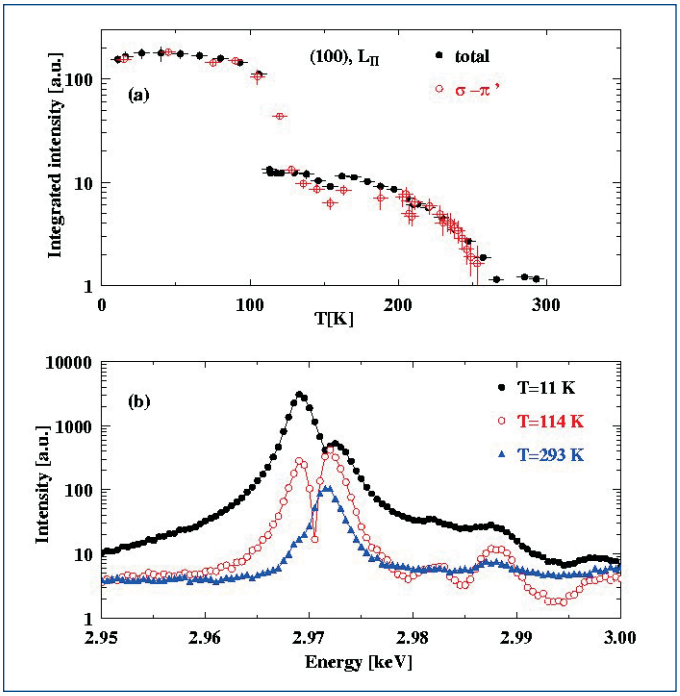

Fig. 1. (a) Temperature dependence of the integrated intensity of the (100) peak as determined from *h*-scans at the L_{II} absorption edge, both without a polarization analyzer and in σ - π′ polarization geometry (parallel to the diffraction plane; see inset, Fig. 2). Besides the antiferromagnetic phase transition at T_N = 110K, a second phase transition, attributed to the ordering of the 4*d* t_{2g} orbitals, is observed at T_{OO} = 260K. (b) Variation of the intensity of the (100) peak with energy around the L_{II} edge for selected temperatures. Besides the resonance peak directly at the absorption edge, a second peak, attributed to electronic transitions into the unoccupied e_g orbitals, is observed about 4 eV higher in energy. All scans were corrected for absorption.

See: I. Zegkinoglou[1], J. Strempfer[1], C.S. Nelson[2], J.P. Hill[2], J. Chakhalian[1], C. Bernhard[1], J.C. Lang[3], G. Srajer[3], H. Fukazawa[4], S. Nakatsuji[4], Y. Maeno[4], and B. Keimer[1], "Orbital Ordering Transition in Ca_2RuO_4 Observed with Resonant X-ray Diffraction," Phys. Rev. Lett. **95**, 136401 (23 September 2005).

Author Affiliations: [1]Max-Planck-Institut für Festkörperforschung, [2]Brookhaven National Laboratory, [3]Argonne National Laboratory, [4]Kyoto University
Correspondence: i.zegkinoglou@fkf.mpg.de

Use of the Advanced Photon Source is supported by the U.S. Department of Energy, Office of Science, Office of Basic Energy Sciences, under contract W-31-109-ENG-38. The work at Brookhaven was supported by the DOE, Division of Materials Science, under contract DE-AC02-98CH10886. The work at Kyoto was supported in part by Grants-in-Aid of Scientific Research from the Japanese Society for the Promotion of Science.

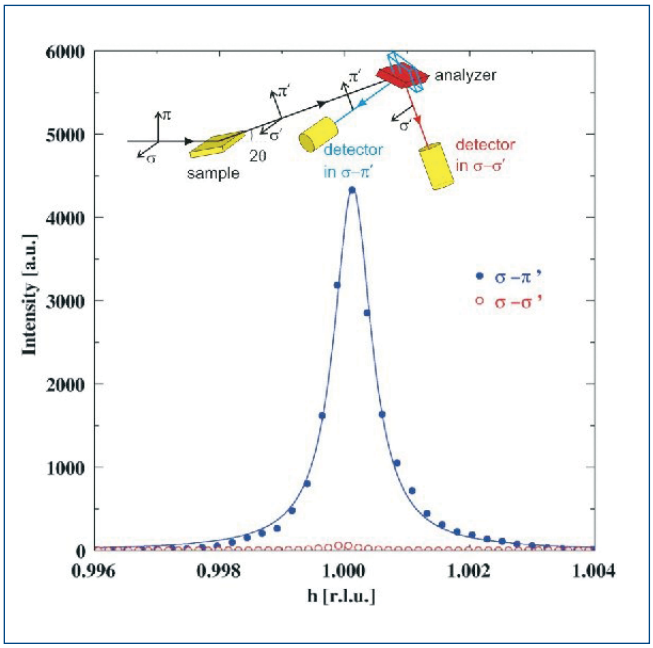

Fig. 2. Polarization dependence of the scattered intensity at (100). Significantly diffracted intensity is observed only in the σ - π′ polarization channel, indicating the absence of a charge scattering contribution at this position. The solid line is the result of a fit to a Lorentzian profile. The inset shows a schematic view of the experimental configuration.

THE THINNEST OF THE THIN: ULTRATHIN FERROELECTRIC FILMS

As cell phones, laptops, PDAs, and other electronic gizmos keep shrinking in size (but expanding in marketability), the importance of ferroelectric materials keeps growing. Many of these gadgets would not be possible without advanced materials, such as the ferroelectric perovskites, which are used in nonvolatile memories and other microelectronic applications. To maximize their potential, these materials must be very thin—in films as little as a few nanometers in thickness. But at such dimensions, poorly understood interfacial effects may take hold and impair the handy ferroelectric properties of the films. Understanding how ferroelectric films might change as they become thinner and thinner is crucial to preserving and utilizing the important benefits they offer. A research team comprising members from Argonne National Laboratory, Hebrew University, the University of Michigan, Northern Illinois University, the University of Washington, and Brookhaven National Laboratory used three beamlines at the APS to take a closer look at the nature of ultrathin ferroelectric perovskites. Their work provides some key details about how these materials behave when they are only a few atoms thick.

The experimenters prepared three samples of $PbTiO_3$ epitaxial films on $SrTiO_3$ (001) substrates using an *in situ* growth chamber at XOR/BESSRC 12-ID. The first two samples were grown to thicknesses of 4 and 9 unit cells, respectively, and slowly cooled to room temperature over a 24-h period; the third sample was 9 unit cells thick and cooled to 181° C in about 5 h in order to produce 180° stripe domains in the sample, such as those observed in other thin film experiments (180° stripe domains have been shown to significantly reduce the depolarizing field). Samples 1 and 2 were studied *ex situ* at XOR/PNC 20-ID, while sample 3 was examined inside the growth chamber. The investigators obtained electron density maps (Fig.1) of each sample by using coherent Bragg rod analysis (COBRA), an x-ray technique developed at XOR 7-ID in which complex scattering factors are calculated along substrate-defined Bragg rods and electron density is determined with Fourier transformation. Nine H, K, and L Bragg rods were studied in samples 1 and 2 with an x-ray energy of 10 keV, and three Bragg rods—22L, 30L, and 31L—were measured in sample 3 at 24 keV.

All three sample films showed polarization. In samples 1 and 2, the Pb atoms are displaced away from the $SrTiO_3$ substrate, and the Ti atoms are similarly displaced relative to the O(2) atoms. These room-temperature samples were found to be monodomain, with up polarization (away from the substrate layer). Sample 1, the 4-unit-cell-thick film, is one of the thinnest

Continued on next page

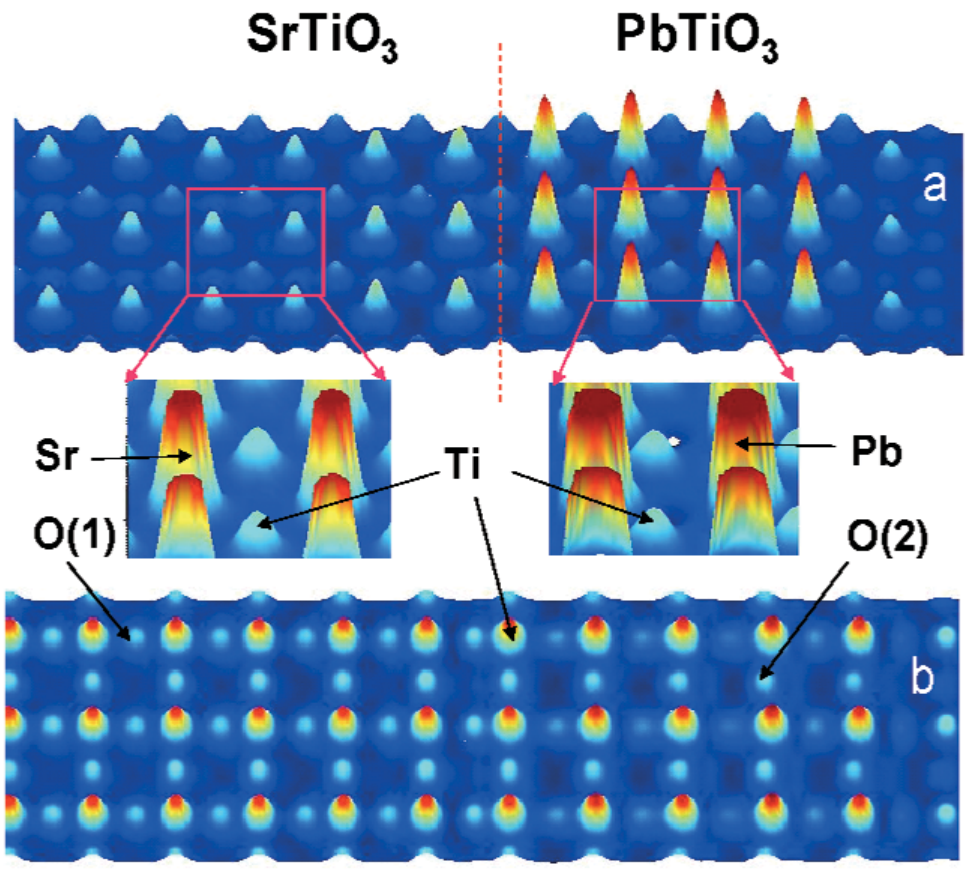

Fig. 1. Electron density maps. (a) (110) plane through the Sr, Pb, Ti, and O(1) atoms. (b) (100) plane through the Ti, O(1), and O(2) atoms. Insets: magnified regions in substrate (left) and film (right).

monodomain perovskite films yet observed in a polar phase. Sample 2, at 9-unit-cells thickness, displayed larger unit cells and displacements than sample 1. Although the Pb and Ti atoms in sample 3 are still nearly centrosymmetric, they display broader electron density peaks that indicate 180° stripe domains, with Pb and Ti atoms in a folded up and down pattern and a separation of about 0.4 + 0.1 Å, with unit cells smaller than in samples 1 and 2.

The characteristics of the first two samples (the films cooled to room temperature) show intriguing hints that their monodomain polarization may depend on interfacial effects arising from the substrate, and that there may be a greater tendency toward up polarization. The position of O(1) atoms at the interface may also be related to screening of the depolarizing field in these ultrathin films, and possible changes in bonding at this interface invite further study. With this work, the researchers have demonstrated not only that the COBRA technique is extremely effective in studying solid materials at the sub-Å level, but that the useful qualities of these ultrathin ferroelectric films may be preserved and even controlled at nanoscale dimensions. As such ferroelectric materials become thinner and more efficient, they will continue to allow the creation of even smaller and more sophisticated electronic wonders. — *Mark Wolverton*

See: D.D. Fong[1], C. Cionca[2], Y. Yacoby[3], G.B. Stephenson[1], J.A. Eastman[1], P.H. Fuoss[1], S.K. Streiffer[1], Carol Thompson[4], R. Clarke[2], R. Pindak[5], and E.A. Stern[6], "Direct Structural Determination in Ultrathin Ferroelectric Films by Analysis of Synchrotron X-ray Scattering Measurements," Phys. Rev. B **71**, 144112 (2005).

Author Affiliations: [1]Argonne National Laboratory, [2]University of Michigan, [3]Hebrew University, [4]Northern Illinois University, [5]Brookhaven National Laboratory, [6]University of Washington
Correspondence: fong@anl.gov

Work supported by the U.S. Department of Energy, Office of Science, Office of Basic Energy Sciences, under Contract No. W-31-109-ENG-38, and the State of Illinois. This project is supported in part by the US-Israel Bi-National Science Foundation under Contract No. 1999-187 and by DOE Grant No. DE-FG02-03ER46023. Use of the Advanced Photon Source was supported by the U.S. Department of Energy, Office of Science, Office of Basic Energy Sciences, under Contract No. W-31-109-ENG-38.

ORIGINS OF THE BRANCHING RATIOS AT THE *L* EDGES OF HEAVY RARE EARTHS

X-ray resonant magnetic scattering (XRMS) and x-ray magnetic circular dichroism (XMCD) have become powerful tools for investigating technologically important magnetic materials, due in large measure to the availability of modern synchrotron photon sources like the APS. Nevertheless, relating the XMCD and XRMS intensities to the electronic and magnetic structures of these materials remains a difficult task. One active area of research concerns accounting for the branching ratios of the rare earths, defined as the ratio of the XRMS (or XMCD) intensities at the L_3 and L_2 edges (for rare-earth compounds). To do this for the heavy rare-earth elements, researchers from Iowa State University utilized the MU-CAT 6-ID-B beamline at the APS to conduct a systematic study of the XRMS branching ratios at the *L* edges of the heavy rare earths in $[Gd_{1/3}Er_{1/3}Tm_{1/3}]Ni_2Ge_2$ and $[Gd_{1/4}Tb_{1/4}Dy_{1/4}Ho_{1/4}]Ni_2Ge_2$. The element-specific branching ratios across the entire heavy rare-earth series (Gd, Tb, Dy, Ho, Er, Tm) were then compared to theoretical predictions obtained through first-principles, spin-polarized band-structure calculations that were performed both without spin-orbit coupling (SOC) and with SOC as a perturbation.

X-ray resonant magnetic scattering and XMCD data are closely related, since both arise from electronic transitions between core levels to higher-lying empty orbitals at the x-ray absorption edges of magnetic ions. The *L* absorption edges of the rare-earth elements primarily involve electric dipole transitions from the 2p1/2 (*L*2 edge) and 2p3/2 (*L*3 edge) core levels to empty 5d states. Measurements of the *L*3 and *L*2 resonant scattering intensities consistently show that the *L*3 edge intensities are significantly larger than the corresponding *L*2 edge intensities for the heavy rare-earth elements, but that the reverse is true for the light rare earths. Information about the 5d electrons is important because they play essential roles in coupling the 4*f* moments with each other, which gives rise to the often exotic magnetic structures exhibited by rare-earth materials.

The researchers' experimental approach exploited similarities in the chemistries of the heavy rare-earth elements across the series, allowing the easy substitution of one rare-earth element for another in isostructural compounds. Since resonant scattering at each absorption edge is element-specific, it is possible to probe the resonant scattering associated with several different rare-earth elements using only a small number of mixed rare-earth samples. This approach helps to reduce uncertainties in the measurements arising from variations in sample quality and compositional variances from one sample to the next. These controlled experiments provided precision measurements of fundamental parameters.

Single crystals of $[Gd_{1/3}Er_{1/3}Tm_{1/3}]Ni_2Ge_2$ and $[Gd_{1/4}Tb_{1/4}Dy_{1/4}Ho_{1/4}]Ni_2Ge_2$ were produced at Ames Laboratory, using the high-temperature solution-growth technique, and mounted in thermal contact with the cold finger of a closed-cycle displex refrigerator. All XRMS measurements were carried out at the base temperature of the displex, about 7K. A liquid-nitrogen-cooled, double-crystal Si(111) monochromator and a bent mirror were used to select the incident photon energy, focus the beam, and suppress higher-order harmonics.

The researchers' calculations used the spin-polarized, scalar relativistic, self-consistent, full-potential linearized augmented plane wave (LAPW) method and employed the local-density approximation (LDA)+U approach in handling the localized 4*f* states. To isolate the effects of SOC, calculations were performed with and without SOC, which was added in each iteration by the second variation method. The magnitude of the SOC was estimated for the 5*d* states from atomic calculations, which showed that the spin-orbit splitting between $5d_{3/2}$ and $5d_{5/2}$ states remains about 0.3 eV across the heavy rare-earth elements, while the 4*f*-5*d* exchange interaction scales with the number of unpaired 4*f* electrons.

Spin-polarized band-structure calculations that included only the 4*f*-5*d* exchange interaction (no conduction-band SOC or 4*f* orbital polarization) produced branching ratios across the entire rare-earth series that were equal to unity (1:1 for XRMS and 1:1 for XMCD), which is at variance with the experimental findings. When SOC was included, however, much better agreement was found, indicating that the observed branching ratios were primarily due to SOC in the 5*d* band. The trend across the heavy rare-earth series was seen to arise from the fact that the 4f-5d exchange interaction contribution to the resonant amplitudes decreases from Gd to Tm, allowing the spin-orbit contribution in the 5d band to take on a more important role.

While the researchers did not study the light rare-earth elements, preliminary calculations suggested that the L_3 dichroic intensities of the light rare earths are strongly influenced by the unoccupied spin-up 4*f* states that hybridize with the 5d energy bands. The researchers speculate that the observed small intensities of the light rare-earth L_3 dichroic spectra may be explainable by calculations that include a careful analysis of such influences. — *Vic Comello*

Continued on next page

See: J.W. Kim, Y. Lee, D. Wermeille, B. Sieve, L. Tan, S.L. Bud'ko, S. Law, P.C. Canfield, B.N. Harmon, and A.I. Goldman, "Systematics of X-ray Resonant Scattering Amplitudes in RNi_2Ge_2 (R = Gd, Tb, Dy, Ho, Er, Tm): The Origin of the Branching Ratio at the L Edges of the Heavy Rare Earths," Phys. Rev. B **72**, 064403 (2005).

Author Affiliation: Iowa State University

Correspondence: goldman@ameslab.gov

MU-CAT and the Ames Laboratory are supported by the U.S. Department of Energy, Office of Science, under Contract No. W-7405-Eng-82. Use of the Advanced Photon Source is supported by the U.S. Department of Energy, Office of Science, Office of Basic Energy Sciences, under Contract No. W-31-109-ENG-38.

High-temperature Ferromagnetism in Bulk Ceramics with Cu Co-doping

The theoretical prediction of room-temperature ferromagnetism in Mn-doped ZnO and GaN and the discovery of ferromagnetism above room temperature in Co-doped TiO_2 anatase have triggered a worldwide search for new dilute magnetic semiconductor materials, because of their possible importance to the emerging field of spintronics. Researchers at Intematix Corp., SRI International, Argonne National Laboratory, Rowan University, and the University of Maryland joined the search for a host semiconductor that has a high solubility of magnetic ions, using a thin-film combinatorial methodology. The search led to the discovery of the ferromagnetic $(In_{1-x}Fe_x)_2O_{3-\sigma}$ bulk ceramic system with Cu co-doping. The Curie temperature of $(In_{1-x}Fe_x)_2O_{3-\sigma}$ exceeds room temperature, and the thermodynamic solubility of Fe ions in the host lattice can be higher than 20%, which makes it amenable to fabricating bulk ceramics. To confirm that the source of the magnetism is within the cation lattice rather than from an impurity phase, bulk ceramic synthesis and characterization were carried out in such a way as to carefully address the issues of structure, composition, and secondary-phase formation. This effort depended on crucial x-ray diffraction (XRD) studies at the XOR 2-BM-B beamline at the APS.

In_2O_3, the host compound used in this study, is a transparent semiconductor with a direct band gap of 2.7 eV and a cubic bixbyite crystal structure having a lattice constant of 10.12 Å and a body-centered cubic unit cell. In_2O_3 can be an n-type semiconductor having high conductivity by introducing oxygen deficiencies (σ) or by Sn doping. Ceramic synthesis was accomplished by the standard solid-state reaction method. High-purity In_2O_3, Fe_2O_3, and CuO precursors were mixed and compressed at a pressure of 120 MPa to form cylindrical ceramic samples, which were then sintered at 1100° C for 9 h. Valence variations of doped magnetic elements were induced by Cu co-doping at a level of about 2% and/or annealing in a reduced Ar atmosphere, which created the mixed-valence cations (i.e., Fe^{2+}, Fe^{3+}) necessary for charge transport and ferromagnetism.

As a check for impurity phases, an XRD study was conducted at the APS to ensure a high signal-to-noise ratio (sensitive to less than 1% impurity), as shown in Fig. 1. The diffraction peaks of $(In_{1-x}Fe_x)_2O_{3-\sigma}$ with Cu co-doping were consistent with the standard pattern of cubic In_2O_3. No significant impurity phase was

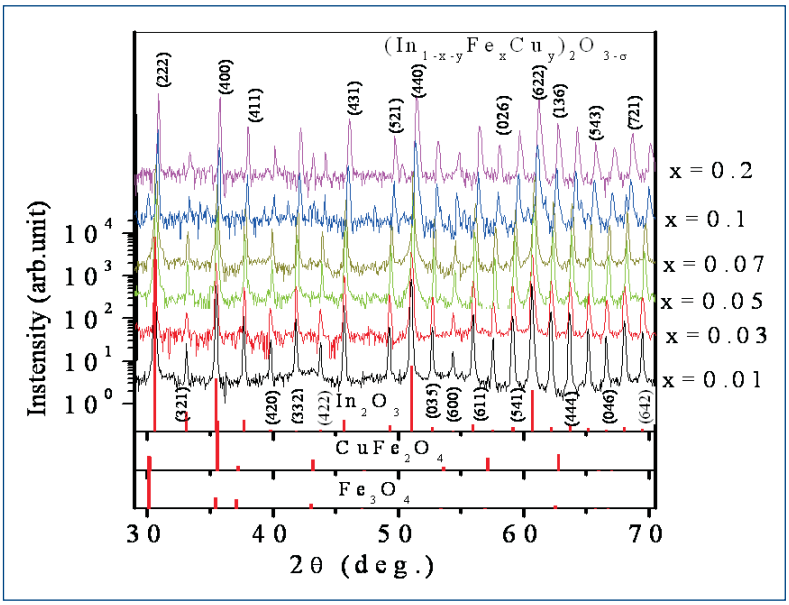

Fig. 1. Synchrotron XRD of Co-doped $(In_{1-x}Fe_x)_2O_{3-\sigma}$ bulk ceramic samples plotted on a logarithmic scale; the intensity bars representing diffraction patterns for In_2O_3, $CuFe_2O_4$, and Fe_3O_4 are shown at bottom of the figure for comparison.

detected to a level of 0.1% for most samples, except for a small impurity phase of Fe_3O_4 of about 1% in the x = 0.1 sample. More importantly, a linear decrease in d spacing was clearly observed with increasing Fe doping, suggesting the incorporation of doped elements into the cubic lattices of In_2O_3, since the Fe^{3+} ion is smaller than the In^{3+} ion.

High-resolution transmission electron microscopy (TEM) was carried out over a large-scale area across a grain boundary of a sample with Fe at 10%, in conjunction with an XRD study. The diffraction pattern was consistent with the cubic bixbyite structure of In_2O_3, and no impurity phase was observed within the grains or at the grain boundaries. The conclusion that the magnetic moment of the sample was not due to impurities of any kind was further supported by numerous other tests.

The Cu-co-doped $(In_{1-x}Fe_x)_2O_{3-\sigma}$ bulk ceramic system was found to be a thermodynamically stable solid solution of a host lattice and a high concentration (up to 20%) of magnetic ions. Also, the samples with high Fe concentration annealed under a reduced Ar atmosphere were found to be ferromagnetic, with a Curie temperature of about 750K, as shown in Fig. 2. The high concentration of magnetic ions is in sharp contrast to most previously reported magnetic semiconductors, which exhibit very low magnetic-ion solubilities in the host semiconductors. The thermodynamically stable solid solution and the large volume magnetization of the Cu-co-doped $(In_{1-x}Fe_x)_2O_{3-\sigma}$ bulk ceramic system make it a promising candidate for spintronics applications. — *Vic Comello*

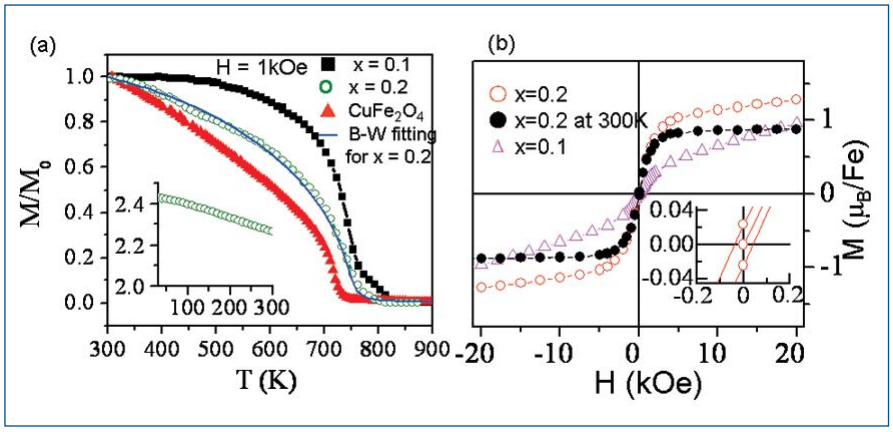

Fig. 2. (a) M-T curves for Cu-doped $(In_{1-x}Fe_x)_2O_{3-\sigma}$ bulk ceramic samples with various Fe contents and $CuFe_2O_4$. M(T) is normalized by magnetization at room temperature, Mo. Brillouin-Weiss fitting for x = 0.2 sample measured at 300K is also shown for comparison; the insert shows M-T curve for the sample with x = 0.2 measured at low temperatures (5-300K) under 1 kOe field. (b) M-H curves of Cu-doped $(In_{1-x}Fe_x)_2O_{3-\sigma}$ bulk ceramic samples at 5 K for samples with x = 0.1 and 0.2. The sample with x = 0.2 was also measured at 300 K (indicated by black solid circles). The inset is a close-up of the M-H curve for the sample with x = 0.2 at 5 K. The coercivity of the sample is 35 Oe.

See: Y.K. Yoo[1], Q. Xue[1], H.-C. Lee[1], S. Cheng[1], X.-D. Xiang[1], G.F. Dionne[1], S. Xu[2], J. He[2], Y.S. Chu[3], S.D. Preite[4], S.E. Lofland[4], and I. Takeuchi[5], "Bulk Synthesis and High-Temperature Ferromagnetism of $(In_{1-x}Fe_x)_2O_{3-\sigma}$ with Cu Co-doping," Appl. Phys. Lett. **86**, 042506 (2005).

Author Affiliations: [1]Intematix Corporation, [2]SRI International, [3]Argonne National Laboratory, [4]Rowan University, [5]University of Maryland

Correspondence: xdxiang@intematix.com

This work was supported by the Defense Advanced Research Projects Agency under Contract No. MDA972-01-C-0073. Y.Y and Q.X. acknowledge support from NSF DMI-0340438. S.E.L. acknowledges the support of the New Jersey Commission on Higher Education and NSF Grant No. DMR 00-80008. I.T. acknowledges support from NSF DMR 0231291 and DARPA DAAD 19-03-1-0038. Use of the Advanced Photon Source is supported by the U.S. Department of Energy, Office of Science, Basic Energy Sciences, under Contract No. W-31-109-ENG-38.

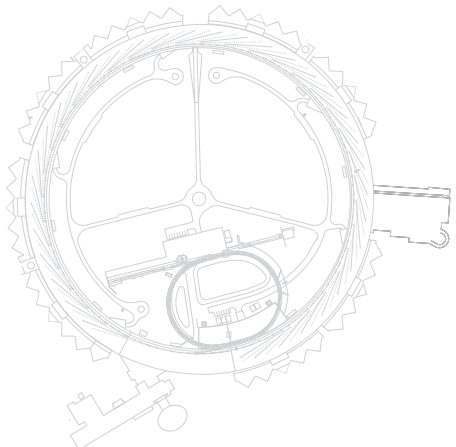

Making Solar Cells the Quick and Dirty Way

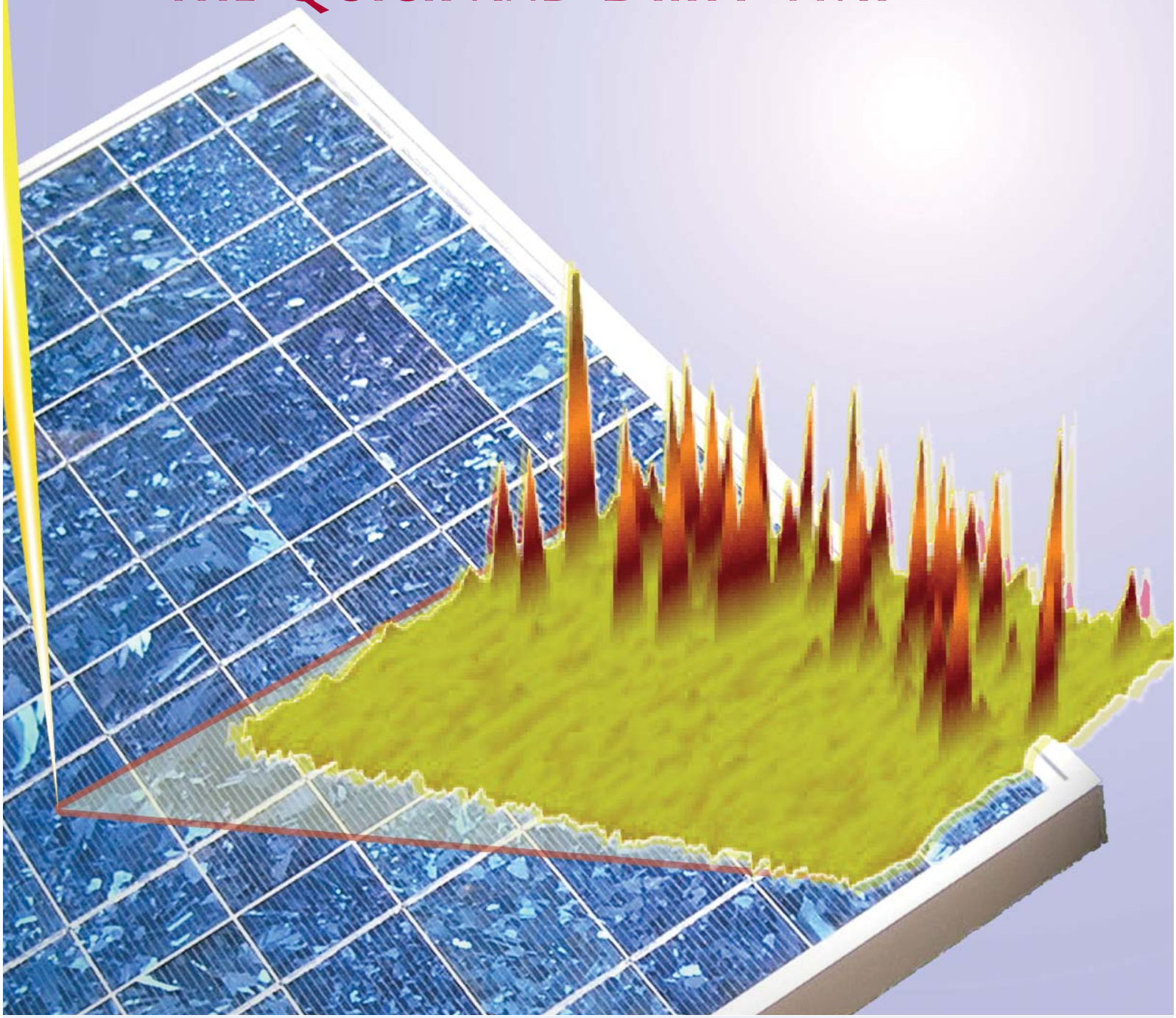

As the pressure mounts to develop energy alternatives to oil and coal, solar power has emerged as perhaps the most promising candidate. But while sunlight may be unlimited, the supply of high-quality silicon used to make solar cells—photovoltaic semiconductor devices that create electricity from sunlight— is not. Solar cells are made from semiconductor-grade crystalline silicon, which is a precious commodity that is in great demand because it is prized by the microelectronics industry for use in integrated circuits. Easier available "dirty" (metallurgical- and near-metallurgical-purity-grade) silicon usually is not suitable—given existing technologies—for making solar cells with acceptable efficiency. These factors hamper solar power's economic potential and keep it from becoming a viable, affordable energy source. But what if a way could be found to use cheaper silicon to make solar cells? Now, researchers from the University of California, Berkeley; Lawrence Berkeley National Laboratory; GE Energy; the Fraunhofer Institute for Solar Energy Systems; and Argonne National Laboratory have have demonstrated how this can be done.

< Artist's impression of an intense beam of synchrotron radiation (from the upper left) striking a solar cell, imaging the iron impurity. (Illustration: Tonio Buonassisi)

Using highly sensitive synchrotron x-ray microprobe techniques at XOR beamline 2-ID-D and XOR/PNC beamline 20-ID-B at the APS, and the 10.3.1 and 10.3.2 beamlines at the Advanced Light Source, Lawrence Berkeley National Laboratory, the experimenters studied Fe impurities in commercially available multicrystalline silicon (mc-Si) samples. Iron contamination affects solar cell performance by reducing silicon's minority carrier diffusion length, the distance that electrons can effectively move through the material. By analyzing the nature and distribution of Fe concentrations in two different varieties of mc-Si, and how the iron creeps into the silicon during the growth process, the team examined how these factors affect solar cell performance. As it happens, a little iron contamination isn't necessarily a bad thing.

The researchers studied samples of both cast mc-Si and sheet mc-Si, forms of silicon made by markedly different processes. Cast mc-Si is grown gradually from high-quality feedstock and cooled very slowly over several days (making it more expensive), while sheet mc-Si is grown quickly, using lower-quality silicon, and cooled down in only minutes (making it cheaper but more prone to defects and impurities). The team found that these differences in growth techniques affect the type and distribution of Fe impurities in predictable ways. After locating regions of Fe in the sample with x-ray induced current, the investigators used x-ray fluorescence microscopy to identify Fe particles and clusters as small as ~30 nm in diameter. Their chemical nature was then analyzed by means of x-ray absorption spectroscopy.

The team's work showed that the iron contaminants fell into two distinct groups: very small and homogeneously distributed iron silicide nanoprecipitates, and larger, more scattered Fe-rich particles and clusters of iron oxide and stainless steel. Having analyzed the morphology, distribution, and chemical makeup of the impurities, the experimenters conclude that they are largely introduced through the silicon feedstock, the crystal growth surfaces, and the furnace during the melt process. More important, the researchers found that, rather than the total Fe concentration in the silicon, it's the form and overall distribution of the iron contaminant particles that has the greatest impact on solar cell performance. As the iron clusters become larger, and thus more localized and less dense throughout the silicon material, the minority carrier diffusion length increases. Conversely, smaller and more homogeneously distributed Fe nanoprecipitates, separated by only a few microns, can severely limit the minority carrier diffusion length and thus the efficiency of the solar cell material.

The experimenters found that lower-quality, "dirty" silicon, despite its high levels of metallic contamination, can still be used to create practical solar cells, merely by controlling the size and spatial distribution of metal particles in the silicon lattice during crystallization—for example, by slowing down the silicon cooling process and allowing more time for larger Fe-rich clusters to form. This discovery comes on the heels of predictions that by 2006, the photovoltaic industry's need for silicon will exceed even that of the semiconductor world. The ability to use cheaper silicon stocks will open the door to realizing the true economic and environmental potential of solar energy.

— Mark Wolverton

See: Tonio Buonassisi[1], Andrei A. Istratov[1], Matthias Heuer[2,3], Matthew A. Marcus[3], Ralf Jonczyk[4], Joerg Isenberg[5], Barry Lai[6], Zhonghou Cai[6], Steven Heald[7], Wilhelm Warta[5], Roland Schindler[5], Gerhard Willeke[5], and Eicke R. Weber[3], "Synchrotron-based Investigations of the Nature and Impact of Iron Contamination in Multicrystalline Silicon Solar Cells," J. Appl. Phys. **97**, 074901 (2005); and Tonio Buonassisi, Andrei A. Istratov, Matthew A. Marcus, Barry Lai, Zhonghou Cai, Steven M. Heald, and Eicke R. Weber, "Engineering Metal-impurity Nanodefects for Low-cost Solar Cells," Nat. Mater. **4**, 676 (2005).

Author Affiliations: [1]University of California, Berkeley; [2]University of Leipzig; [3]Lawrence Berkeley National Laboratory; [4]GE Energy; [5]Fraunhofer Institute for Solar Energy Systems; [6]Argonne National Laboratory, [7]Pacific Northwest National Laboratory

Correspondence: buonassisi@alumni.nd.edu

This work was funded by NREL Subcontract No. AAT-2-31605-03, and the AG-Solar project of the government of Northrhein-Westfalia sNRWd, funded through the Fraunhofer Institute for Solar Energy Systems (ISE) Germany. M.H. thanks the Deutsche Forschungsgemeinschaft for funding the project HE 3570/1-1. The operations of the Advanced Light Source at Lawrence Berkeley National Laboratory are supported by the Director, Office of Science, Office of Basic Energy Sciences, Materials Sciences Division, of the U.S. Department of Energy under Contract No. DEAC03-76SF00098. PNC-CAT facilities at the Advanced Photon Source, and the research at these facilities, are supported by the US DOE Office of Science Grant No. DEFG03–97ER45628, the University of Washington, a major facilities access grant from NSERC, Simon Fraser University, and the Advanced Photon Source. Use of the Advanced Photon Source was supported by the U.S. Department of Energy, Office of Science, Office of Basic Energy Sciences, under Contract No. W-31-109-ENG-38.

PROBING THE MICROMECHANICS OF METALLIC-GLASS-MATRIX COMPOSITES

Metallic glasses can combine the high strength of metals with the processing flexibility of glasses, making them attractive candidates for a variety of load-bearing applications. Unfortunately, single-phase metallic glasses exhibit little plastic strain before fracture. For this reason, considerable effort is being directed at developing two-phase materials consisting of crystalline particles embedded in a metallic-glass matrix. The second-phase particles cause the plastic strain to be distributed over a larger volume of material, thus suppressing fracture. Researchers from Johns Hopkins University, the University of Vermont, and Argonne National Laboratory recently developed a hybrid process for making metallic-glass-matrix composites and characterized the micromechanical behavior of composite materials made this way using *in situ* x-ray scattering on the XOR 1-ID beamline at the APS, and finite element modeling (FEM). These results point the way to the development of better high-strength materials.

Typical metallic-glass-matrix composites are either *in situ* composites, in which a crystalline phase is precipitated from a melt during cooling, or *ex situ* composites, in which the reinforcing phase is physically added to the metallic glass prior to casting. *In situ* composites included crystalline phases that have fine microstructures, but the properties of the composites are quite sensitive to processing conditions. In addition, the crystalline phases are limited to particular amorphous alloy compositions. While *ex situ* composites can be produced from virtually any bulk amorphous alloy, the range of length scales of the reinforcing phase is limited.

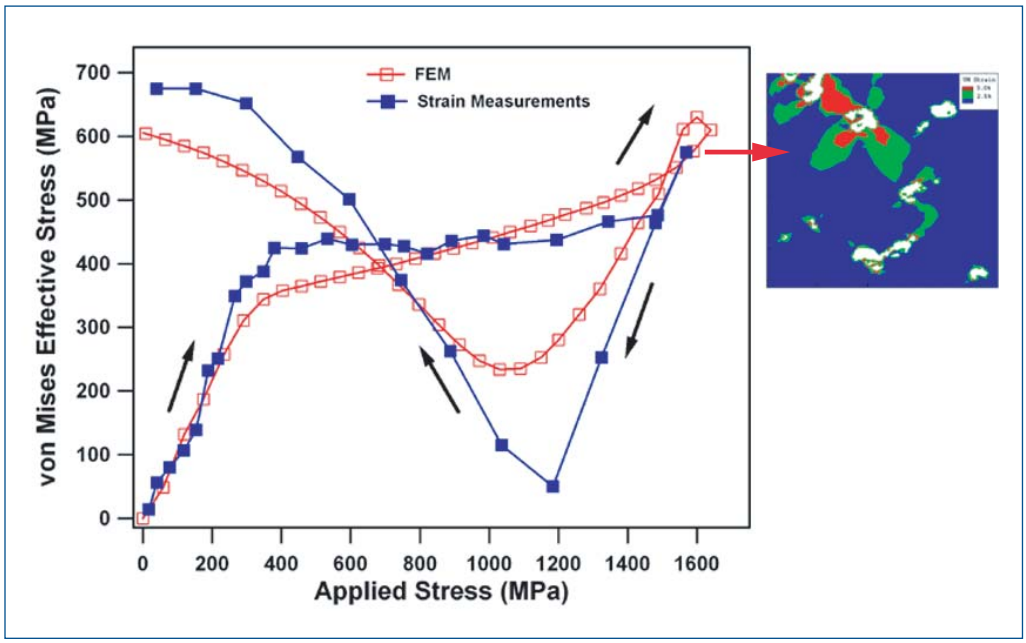

Fig. 1. Von Mises effective stress in the particles as a function of applied stress calculated from synchrotron strain measurements (solid squares) and FEM (hollow squares). The black arrows indicate the loading and unloading directions. The FEM contour map on the right shows that the strain in the matrix is concentrated around the particles, which leads to localized yielding.

The researchers developed a hybrid process for making metallic-glass-matrix composites, in which a high-melting-point crystalline phase is precipitated from a metastable crystalline solid solution in a separate step prior to casting the composite. By appropriately controlling the precipitation process, particle sizes in the composite ranging from 0.1 to 100 μm can be achieved. Although this process has been used only to produce Ta-rich particles in Zr-based metallic glasses, in principle the same basic process could be applied to any amorphous alloy in which one element shows a solid-state miscibility gap with a refractory metal, such as Ta, W, or Nb.

Composite alloys having the composition $(Zr_{70}Cu_{20}Ni_{10})_{90-x}Ta_xAl_{10}$ (x = 6, 8, and 10 at% Ta) were prepared by arc melting and suction casting. The basic procedure was to prepare a metastable Zr-Ta binary ingot, and then melt this ingot with Cu, Ni, and Al to make a master alloy ingot for casting. During the second melting step, some of the Ta precipitates out to form ~10-μm Ta-rich particles. The alloys were suction cast into a copper mold to form cylindrical rods, which were machined into prisms and polished for the synchrotron strain measurements.

The researchers performed *in situ* strain measurements at the XOR 1-ID beamline by using a screw-driven load cell to create uniaxial compressive loads from 0 to 1,800 MPa. One advantage of high-energy x-ray scattering is that it permits *in situ* transmission experiments on bulk

samples. Since the x-ray wavelength is small, the crystallographic planes satisfying the Bragg criterion are nearly parallel to the incident beam. Therefore, the lattice strain for the longitudinal (parallel to loading axis) and transverse (perpendicular to loading axis) directions can be simultaneously measured with a two-dimensional detector, along with the strain for all angles.

The researchers also developed a two-dimensional plane-strain finite element model (FEM) to examine the strain states of the particles and the amorphous matrix. The mesh-generating program ppm2oof was utilized together with scanning electron micrographs to create a mesh that captures the morphology and dimensions of the microstructure. A small-deformation plasticity model with nonlinear isotropic hardening was chosen to model the behavior of the Ta-rich particles. Fig. 1 shows a comparison between the FEM and experimental results in terms of the calculated von Mises effective stress for an 8% Ta alloy.

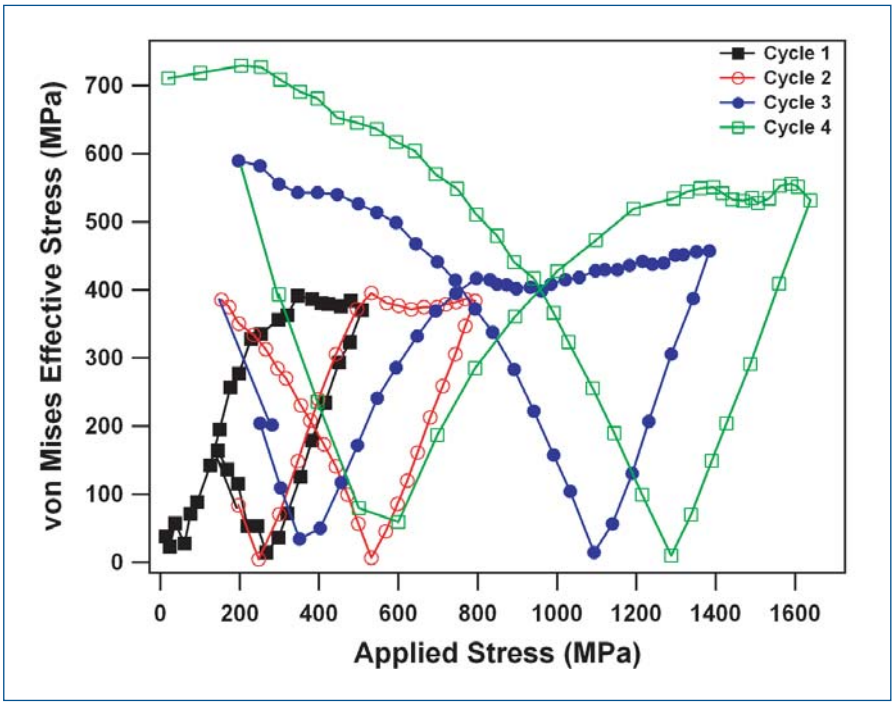

Fig. 2. Von Mises effective stress in the particles vs. applied stress for a composite alloy that has undergone four loading-unloading cycles. The residual stress that develops during unloading increases the applied stress necessary for particle yielding in each subsequent reloading.

The researchers found that the lattice strains in the particles are linear in the longitudinal and transverse directions for applied stresses below 325 MPa, indicating elastic loading of the particles. At an applied stress of approximately 325 MPa, the particles yield, causing increased load transfer to the amorphous matrix. After yielding, the particles are constrained from expanding in transverse directions by the elastic matrix, which leads to the development of compressive stresses.

The glass matrix remains elastic, since it has a much higher yield strength (~1,750 MPa) than the Ta particles (~350 MPa). This creates a plastic misfit strain between the particles and the matrix, resulting in a stress that the researchers refer to as a plastic misfit stress. The plastic misfit stress increases the load transfer to the matrix. However, at an applied stress of ~1,450 MPa, yielding in the glass matrix increases load transfer to the particles.

For the matrix, FEM results indicate that shear band initiation is not due to a mismatch in elastic properties of the matrix and the particles. Rather, yielding occurs through the development of stress concentrations resulting from the plastic misfit strain. At an applied stress of ~1,425 MPa, the yield criterion of the matrix is satisfied near the particles, leading to localized yielding by shear banding. At higher stresses approaching the macroscopic yield stress of the composite (1,725 MPa), the yield criterion is satisfied in larger regions of the matrix, allowing for macroscopic yielding. The highly inhomogeneous stress distribution in the matrix caused by the presence of the particles thus hinders shear band propagation and may delay the onset of failure. The researchers also found that the yield stress of the particles can be increased by subjecting the composite to multiple loading cycles (Fig. 2), which might provide a means of increasing the yield stress of composite alloys. — *Vic Comello*

See: R.T. Ott[1], F. Sansoz[2], J.F. Molinari[1], J. Almer[3], K.T. Ramesh[1], and T.C. Hufnagel[1], "Micromechanics of Deformation of Metallic-Glass-Matrix Composites from Synchrotron Strain Measurements and Finite Element Modeling," Acta Materialia **53**,1883 (2005).

Author Affiliations: [1]Johns Hopkins University, [2]University of Vermont, [3]Argonne National Laboratory
Correspondence: rtott@ameslab.gov

R.T.O and T.C.H. supported (for the *in situ* strain measurements) by the U.S. Department of Energy grant DE-FG02-98ER45699. Support for the finite element modeling was provided by the Center for Advanced Metallic and Ceramic Systems at the Johns Hopkins University, sponsored by the Army Research Laboratory (ARMAC-RTP), and accomplished under ARMAC-RTP Cooperative Agreement No. DAAD19-01-2-0003. Use of the Advanced Photon Source was supported by the U.S. Department of Energy, Office of Science, Office of Basic Energy Sciences, under Contract No. W-31-109-ENG-38.

CLUMPING IMPURITIES FOR LESS-COSTLY SOLAR CELLS

Less-costly solar cells may result from research carried out by experimenters from the University of California, Berkeley and the Lawrence Berkeley; Argonne; and Pacific Northwest national laboratories. The group used synchrotron-radiation-based x-ray microscopy techniques at APS and Advanced Light Source beamlines to study the size, location, and effect of metal impurities in silicon solar cells. Comparing different growth or processing methods led them to suggest a novel concept: metal-defect engineering for solar cells. If impurities can be managed rather than eliminated, dirtier (but less expensive) silicon materials could be used to make solar cells.

Most solar cells are made by using expensive electronics-grade silicon. Relatively inexpensive silicon, such as the proposed solar-grade variety, contains more metal impurities, which capture light-generated charge carriers before they reach the electrical contacts and therefore reduce efficiency. The researchers sought a way to create efficient solar cells from silicon that contains high concentrations of transition metals. Their studies suggest that metal concentration, although important, is only part of the story: the metal's chemical and structural state—and spatial distribution—also determine how long the average minority charge carrier travels before it recombines at a metal-related defect. Longer minority-carrier diffusion lengths result in higher-efficiency cells.

To study the location and effect of metal impurities in silicon, the group used x-ray fluorescence microscopy, which allows detection of metal nanoclusters with a radius as small as 16 nm; x-ray absorption microspectroscopy, which provides information on the chemical states of the clusters; and the newly developed spectrally resolved x-ray-beam-induced current, which generates a map of the minority-carrier diffusion length. They used these techniques on three beamlines: the XOR 2-ID-D and XOR/PNC 20-ID-B beamlines at the APS and the 10.3.2 beamline at the Advanced Light Source. They used beam sizes ranging from 0.2 × 0.2 μm^2 to 5 × 7 μm^2 and x-ray energies between 4 keV and 10 keV.

The researchers mapped the location and size of impurities in intentionally contaminated samples and measured the carrier diffusion length near metal clusters. They found three types of defects: micron-sized inclusions, metal silicide nanoprecipitates, and atomically dissolved metals. The relative fraction of metals in each state determines the cell efficiency. To demonstrate the impact of metal distribution on minority-carrier diffusion length, they compared three differently processed samples, all with the same total metal content.

Contaminated samples were heated to 1,200° C, then quenched (at a rate of 200° C/s), or slowly cooled (at a rate of 3° to 8° C/s), or quenched to room temperature and then re-annealed at 655° C. The first option resulted in samples with unacceptably short minority-carrier diffusion lengths (under 10 μm). The re-annealed samples were better, but the slowly cooled samples were best, with minority-carrier diffusion lengths four times longer than those of the quenched samples. This work suggests that silicon containing high concentrations of metals could be useful for solar cells if it was defect-engineered to control the distribution of metals. — *Yvonne Carts-Powell*

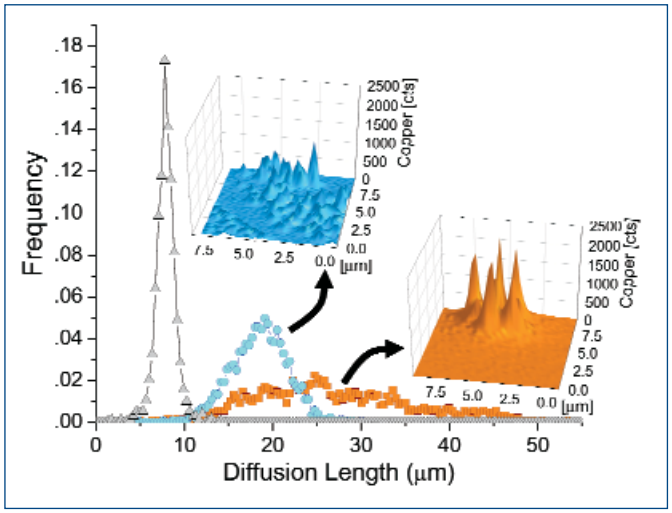

Fig. 1. The distribution of metal defects affects material performance in materials samples that are processed differently: quenched silicon (gray), quenched and re-annealed silicon (blue), and slow-cooled silicon (orange). The frequency vs. diffusion length plot shows that the slow-cooled sample has the best materials performance (longest diffusion lengths). The insets of copper counts per second at different locations show that microdefects clump more in the better material.

See: T. Buonassisi[1,2], A.A. Istratov[1,2], M.A. Marcus[2], B. Lai[3], Z. Cai[3], S.M. Heald[4], and E.R. Weber[1,2], "Engineering Metal-impurity Nanodefects for Low-cost Solar Cells" Nat. Mater. **4**, 676 (September 2005).

Author Affiliations: [1]University of California, Berkeley; Lawrence Berkeley National Laboratory; [3]Argonne National Laboratory; [4]Pacific Northwest National Laboratory
Correspondence: istratov@berkeley.edu

Work funded by National Renewable Energy Laboratory subcontract AAT-2-31605-03. Use of the Advanced Photon Source and of the Advanced Light Source is supported by the US Department of Energy, Office of Science, Office of Basic Energy Sciences, under Contract Numbers W-31-109-ENG-38 and DEAC03-76SF00098, respectively

WHERE DOES THE PLATINUM GO?

High-temperature applications need materials with special characteristics to withstand such a challenging thermal environment. These materials must conduct heat well and resist oxidation while not being prone to melting. One well-known material with these qualities is the intermetallic compound β-nickel-aluminum (β-NiAl). Adding platinum to an NiAl coating greatly increases its oxidation resistance at high temperatures, but the reasons for this unexpected bonus remain obscure. Because understanding this effect will better allow engineers to use it to enhance existing coatings, a team of researchers from Iowa State University set out to examine how platinum (Pt) behaves in the crystal structure of NiAl.

β-NiAl crystallizes in a CsCl-type (B2) structure that consists of two interpenetrating simple cubic sublattices. In its perfect stoichiometric state, one sublattice is entirely occupied by Ni atoms and the other is entirely occupied by Al atoms. When added to NiAl, Pt can occupy either the Al sites or the Ni sites. To determine the T = 0K site preference of Pt in NiAl, the researchers performed state-of-the-art first-principles calculations on 54-atom B2 supercells using the Vienna *ab initio* simulation package. The team examined Pt lattice site preferences in three types of B2 NiAl: Ni-rich, Al-rich, and stoichiometric alloys.

Under these conditions, the researchers found that, in the Al-rich alloy—with two possible lattice configurations (Pt in either the Ni or Al sublattice)—Pt displays a marked preference for the Ni sublattice, strong enough that it is unlikely to be affected by the entropic effects that come into play at higher temperatures. In the Ni-rich alloy, there are also two possible lattice configurations. Still, Pt shows a preference for the Ni sublattice, although this preference is weaker than in the Al-rich NiAl. In the stoichiometric NiAl alloy, there are three possible site configurations (Pt in either the Ni or Al sublattice, or both) but again, Pt displays a weak preference for sites in the Ni sublattice. In both the Ni-rich and stoichiometric alloys, the preference of Pt for the Ni sublattice is not only energetically favorable, but also entropically favorable at finite (i.e., higher than 0K) temperatures.

At higher temperatures, the entropy effects are also a factor in determining the site preference of Pt in NiAl. By using the statistical-mechanical Wagner-Schottky model, together with the first-principles calculated point defect formation enthalpies, the research team examined how temperature affects the Pt site preference in NiAl. In all three alloys (Al-rich, Ni-rich, and stoichiometric) at 1,273K, Pt consistently prefers

Continued on next page

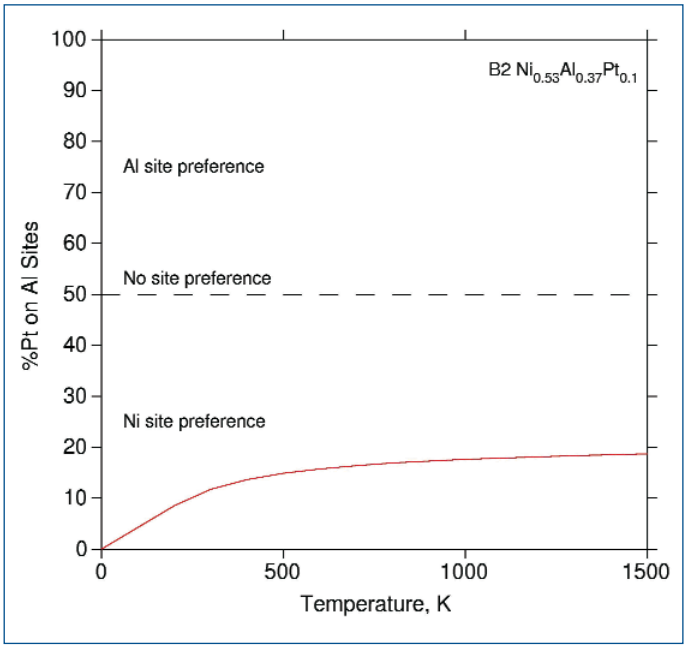

Fig. 1. Model-predicted percent of Pt atoms on Al sites in B2 $Ni_{0.53}Al_{0.37}Pt_{0.1}$ alloy as a function of temperature.

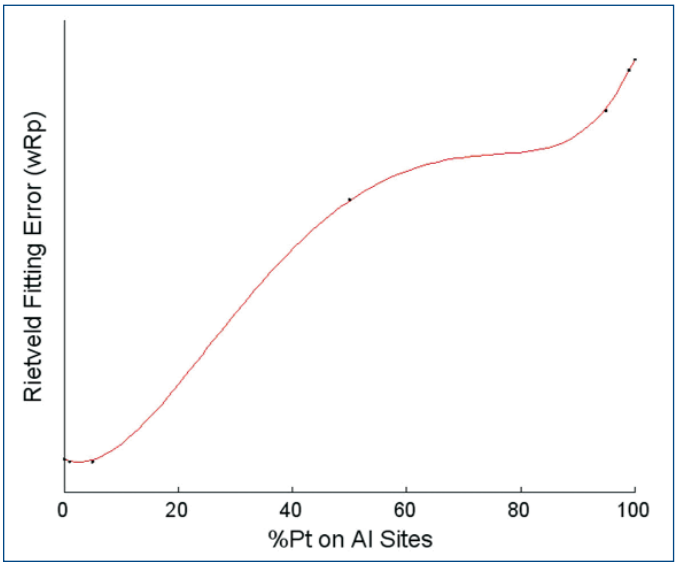

Fig. 2. Rietveld fitting error as a function of percent of Pt on Al sites at 1,273K. Such error approaches zero as the difference between the observed and calculated diffraction patterns diminishes. Clearly, putting the Pt atoms on the Ni sites more closely matches the experimental data.

the Ni sublattice. At a constant temperature, the small amount of Pt appearing in the Al sublattice increases as the Al concentration decreases, and vice versa.

The investigators further experimentally investigated the site occupancy of Pt in the B2 NiAl lattice at high temperatures by using high-energy synchrotron x-ray diffraction (HEXRD) techniques at the MU-CAT 6-ID-D beamline at the APS. Using a photon energy of 97.844 keV (wavelength 0.012643 nm), the experimenters examined powder samples of an alloy with a $Ni_{0.53}Al_{0.37}Pt_{0.1}$ composition at temperatures between 1,173K and 1,373K. The modeling techniques used to study the earlier alloys predict that as the temperature increases, a small fraction of Pt atoms enters the Al sublattice, raising the proportion of Pt to about 18% at 1,273K (Fig. 1). The researchers refined their x-ray diffraction data with Rietveld analysis software, which again demonstrated the preference of Pt for the Ni sublattice (Fig. 2).

Although these results contradict the previous work of Angenete et al., which seemed to indicate a generally equal distribution of Pt in Ni and Al sites, the HEXRD experiments give persuasive support to the conclusion of the Iowa State experimenters that Pt displays a consistent preference for the Ni sublattice in NiAl alloys. The researchers suggest that further x-ray diffraction studies with more refined techniques will only strengthen this conclusion. — *Mark Wolverton*

See: C. Jiang[1], M.F. Besser[1,2], D.J. Sordelet[1,2], and B. Gleeson[1,2], "A Combined First-principles and Experimental Study of the Lattice Site Preference of Pt in B2 NiAl," Acta Mater. **53**, 2101 (2005).

Author Affiliations: [1]Iowa State University, [2]Ames Laboratory
Correspondence: chaoisu@iastate.edu

This work was supported by the Office of Naval Research, under Contract No. N00014-02-1-0733. The MU-CAT sector is supported by the U.S. Department of Energy, Office of Science, Office of Basic Sciences, through the Ames Laboratory under Contract No. W-7405-Eng-82. Use of the Advanced Photon Source is supported by the U.S. Department of Energy, Office of Science, Office of Basic Energy Sciences, under Contract Number W-31-109-ENG-38.

PHOSPHATES TOUGHEN UP A TOOTHY PROTEIN MATRIX

As bones and teeth age, they grow larger and harder, the better to cope with life's vicissitudes. Important clues as to how specialized proteins containing bound phosphate groups (called phosphoproteins) help harden bones and teeth as they grow have been uncovered thanks to studies using the ChemMatCARS 15-ID beamline at the APS. The results show that phosphoproteins are essential in controlling the biomineralization process as teeth form. This research could ultimately help in making crystalline calcium phosphate coatings for titanium medical implants.

Mineralization of teeth and bones takes place during fetal development, when calcium salts interact with these phosphoproteins as they are synthesized, hardening these materials. However, only about half of the mass of bone and teeth is mineral, while the remaining constituents are water and a mixture of proteins. The predominant protein is collagen, which makes up 85% to 90% of the matrix. The other proteins, including the phosphoproteins, known as the noncollagenous matrix proteins (NCPs), are very tightly integrated with the mineral phase of bone and teeth and can be freed chemically only by a strong acid that demineralizes the teeth.

By itself, a collagen matrix does not mineralize. This evidence has led researchers to suggest that NCPs themselves must play an important role in the mineralization process. NCPs are composed mostly of proteins that contain large quantities of glutamic

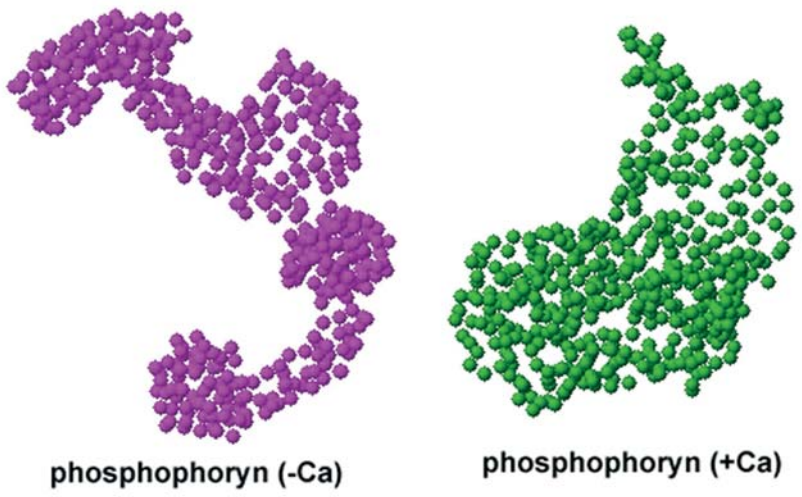

Fig. 1. Models of PP with and without calcium, generated from the SAXS data.

and aspartic acids, and serine which can bind phosphate groups, producing strongly anionic surfaces for calcium ion binding.

Now, researchers from the University of Illinois at Chicago, Northwestern University, and ChemMatCARS have investigated the role of one such NCP, the dentin matrix protein, phosphophoryn (PP). Normal PP contains a large number of repetitive amino acid sequences rich in aspartic acid and serine, and in which most of the serine is phosphorylated. The phosphate-linked serine residues are believed to act as anchors for calcium ions during mineralization.

The researchers compared the behavior of the natural form of PP with a version produced by engineered bacteria that lacks the phosphate groups of natural PP. Because of this lack of phosphates, the team predicted that it would not bind to calcium ions so effectively. To test this prediction, they used small-angle x-ray scattering (SAXS) to observe the ways both the natural and the engineered PP "fold" when they are placed in a solution rich in calcium ions. The scattering data revealed that natural PP efficiently binds calcium and folds into a compact ball shape as it does so. The engineered PP, on the other hand, does not fold at all. The detailed scattering data showed that very few calcium ions even bind to this form of the protein.

As a further test of their theory, the team investigated how well each form of the protein converted calcium phosphate into the plate-like crystalline form found in teeth. They found that ,even in a solution designed to simulate the natural chemical environment in which teeth are mineralized, only the natural PP could form these plate-like, apatite crystals. The engineered PP failed to induce this transformation.

One final test involved the collagen proteins that are present in bone and teeth together with PP and the other noncollagenous proteins. The team found that natural PP promoted the formation of aggregates of collagen molecules and fibrils similar to those found in bone and teeth. This contrasted sharply with the behavior of the engineered PP, which formed only fibrous strands of collagen.

The accrued evidence points to the phosphate groups on PP as being essential to the mineralization process in tooth formation, as predicted. Natural PP binds strongly to calcium, unlike the nonphosphorylated version. Calcium binding to PP then changes the shape of the protein to the more compact, globular protein rather than a fibrous form not found in teeth. Key to the mineralization process, however, is the way in which the phosphates on PP form a regular array of binding points for calcium that can act to seed the crystalline apatite form that is laid down in teeth to make them hard.

— David Bradley

See: Gen He[1], Amsaveni Ramachandran[1], Tom Dahl[2], Sarah George[2], David Schultz[3], David Cookson[3], Arthur Veis[2], and Anne George[1], "Phosphorylation of Phosphophoryn Is Crucial for Its Function as a Mediator of Biomineralization," J. Biol. Chem. **280** (39), 33109 (30 September 2005)

Author Affiliations: [1]University of Illinois, [2]Northwestern University, [3]ChemMatCARS

Correspondence: anneg@uic.edu

This work was supported by National Institutes of Health Grant DE 13836. Use of the Advanced Photon Source was supported by the U.S. Department of Energy, Office of Science, Office of Basic Energy Sciences, under Contract No. W-31-109-ENG-38.

AROUND THE APS

The Seventh Neutron and X-ray Scattering School

For seven years, the Neutron and X-ray Scattering School (NXS) at Argonne has provided a general background in neutron and x-ray techniques for young scientists earning their Ph.D.s In August 2005, the 60 students (at right) selected to attend the school heard lectures from top senior scientists from academia, industry, and national laboratories. They were also afforded the opportunity to carry out hands-on experiments at the Intense Pulsed Neutron Source and the APS (Argonne is the only national laboratory with both types of facilities). The school is a collaboration of several Argonne divisions: X-ray Science, Intense Pulsed Neutron Source, Materials Science, and Educational Programs.

STRESS RELAXATION IN A TITANIUM ALLOY

Titanium alloys feature prominently in products ranging from turbine blades and airframes to hip joint replacements and pacemakers. Among this family of materials, the workhorse alloy is Ti-6Al-4V—so designated because of its 6% aluminum and 4% vanadium composition. Understanding how the microstructure of this alloy changes with temperature is critical to knowing how it will behave mechanically after welding and heat treatment. Recently, a team of researchers from Lawrence Livermore National Laboratory and Oak Ridge National Laboratory made x-ray diffraction measurements on the XOR/UNI beamline 33-BM-C at the APS that show details of a crucial microstructural transformation in Ti-6Al-4V during heating.

Two different phases coexist in Ti-6Al-4V, as indicated in the microstructure shown in Fig. 1. One, called the α phase, has a hexagonal close-packed structure, whereas the β phase is a body-centered cubic lattice. At elevated temperatures, during heat-treating and welding, the α phase transforms to β. At lower temperatures, before this phase change, the usual (or normal) increase in lattice parameter occurs as a result of thermal expansion. During the phase transformation itself, the β phase undergoes an enhanced lattice expansion as vanadium migrates from α to β regions. But in the temperature regime just before the $\alpha \rightarrow \beta$ change begins, previous studies have revealed a surprising and unexplained dip in the β lattice parameter. The new x-ray diffraction studies at the APS were performed to examine the details of this lattice contraction.

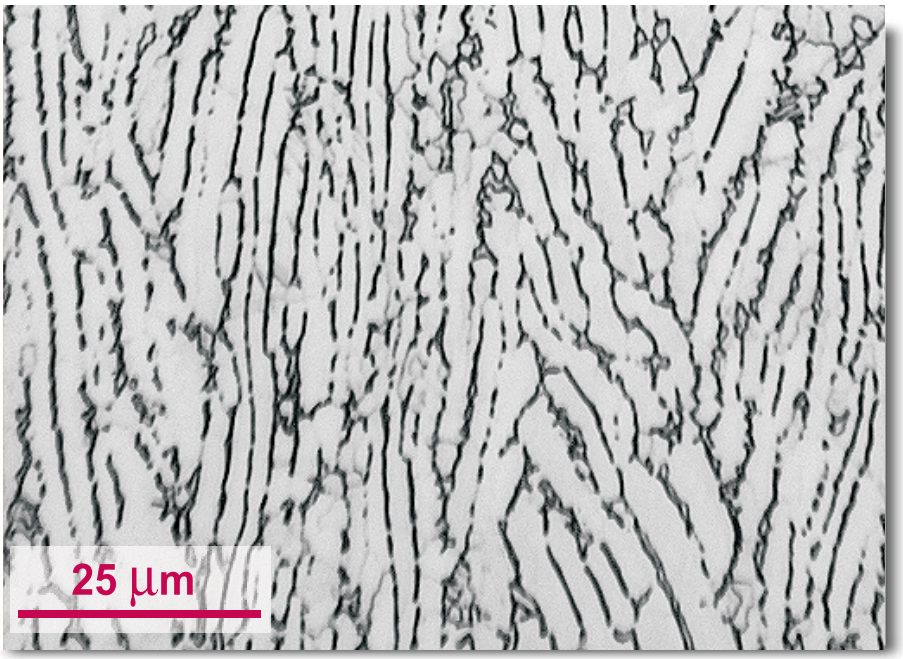

Fig. 1. Micrograph showing the starting microstructure of the Ti-6Al-4V base metal. The dark etching phase is β.

Alloy specimens were obtained from 100-mm-diameter mill-annealed bar stock and precisely analyzed for their exact composition and trace constituents. After polishing and chemical etching of the specimens, optical microscopy showed a small amount of β phase distributed among and around the elongated grains of the α alloy. Microprobe analysis, which was used to determine the compositions of these two phases, indicated an initial distribution of 87.9% α and 12.1% β. For the *in situ* x-ray diffraction measurements carried out at the 33-BM-C beamline, 30-keV x-rays from a silicon monochromator were focused to a beam of 1 mm $\times$ 0.25 mm. Diffracted x-rays were collected by using a charge-couple device detector with the samples held at temperatures ranging from 400° C to 650° C. Lattice expansion data were extracted from shifts in the Bragg peak positions.

Although the lattice parameter should increase with temperature because of conventional thermal expansion, analysis of the x-ray data for the β phase showed that its lattice parameter alone steadily decreased over a period of hours when held at 450° C (Fig. 2). In contrast, when the temperature was the phase was held at 600° C, the lattice parameter for the β phase increased slowly over a comparable duration. The α phase, on the other hand, exhibited a constant lattice parameter at 450° C and a slower increase at 600° C. As a function of temperature, the β phase lattice parameter exhibited its largest contraction at 450° C before expanding again with temperature. The α phase showed no such dip within experimental error. The researchers believe that the time-dependent change in β lattice parameter at temperatures below 550° C results from relaxation of pre-existing stress in the two-phase alloy. Above 550° C, the change in lattice parameter is caused by the α-β phase change and the subsequent redistribution of vanadium from α to β.

Such findings indicate the power of x-ray diffraction to probe, *in situ*, the fundamental physical properties of individual constituents in a multiphase alloy while temperature (and pos-

sibly other conditions) are changed. Future studies will be undertaken to investigate the formation of residual stresses in Ti-6Al-4V and other multiphase alloys that undergo simultaneous thermal contraction and phase transformations during cooling from elevated temperatures. This work required a high-brightness beam to collect data in real time during stress relaxation, a fine focal spot to resolve small changes in lattice parameter, and a high x-ray energy to penetrate deeply into the sample and avoid confounding surface effects. Thus, access to a third-generation synchrotron facility such as the APS was critical. — *David Voss*

See: J.W. Elmer[1], T.A. Palmer[1], S.S. Babu[2], and E.D. Specht[2], "Low Temperature Relaxation of Residual Stress in Ti–6Al–4V," Scripta Mater. **52**, 1051 (2005).
Author Affiliations: [1]Lawrence Livermore National Laboratory, [2]Oak Ridge National Laboratory
Correspondence: elmer1@llnl.gov

This work was performed under the auspices of the U.S. Department of Energy (DOE), Lawrence Livermore National Laboratory, under contract no. W-7405-ENG-48. Part of the research was sponsored by the U.S. DOE Division of Materials Sciences and Engineering under contract no. DE-AC05-00OR22725 with UT-Battelle, LLC. The UNI-CAT facility at the APS is supported by the U.S. DOE under Award no. DEFG02-91ER45439, through the Frederick Seitz Materials Research Laboratory at the University of Illinois at Urbana-Champaign, Oak Ridge National Laboratory (U.S. DOE contract DE-AC05-00OR22725 with UT-Battelle LLC), the National Institute of Standards and Technology (U.S. Department of Commerce) and UOP LLC. Use of the Advanced Photon Source was supported by the U.S. Department of Energy, Office of Science, Office of Basic Energy Sciences, under Contract No. W-31-109-ENG-38.

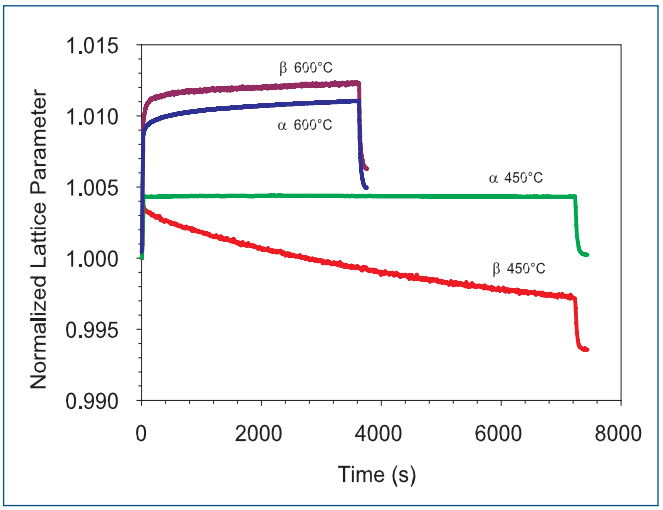

Fig. 2. Normalized lattice parameter [ratio of $a_o(t)$ to a_o initial at room temperature] for both phases as a function of time for isothermal holds at 450° C and 600° C. The rapid increase at the start of the experiment and the rapid decrease at the end correspond to heating to and cooling from the isothermal temperature.

AROUND THE APS

THE WORKSHOP ON "*IN SITU* CHARACTERIZATION OF SURFACE AND INTERFACE STRUCTURES AND PROCESSES"

A workshop on "*In Situ* Characterization of Surface and Interface Structures and Processes" was held at the APS on September 8-9. Experts in synchrotron radiation techniques and various synthesis, processing, and modeling efforts identified future directions in those areas of research. They also assessed the applicability of x-ray tools to future research problems and evaluated the interest of the research community in developing at the APS dedicated facilities for *in situ* x-ray characterization of natural processes as well as the synthesis, structure, and properties of new and technologically important materials. The more than 130 participants came from 39 different university, industrial, and research institutions (plus 8 different Argonne divisions) representing 16 U.S. states, 8 countries, and 7 synchrotron light sources. Attendees discussed a wide range of visionary concepts for the use of synchrotron radiation. One emphasis was the need to maintain a continued dialogue between the APS and the community to help develop forward-looking concepts and to continually incorporate advances into strategic and tactical planning. For the complete workshop report, See http://surface-interface.aps.anl.gov/2005workshop/index.htm. *Contact: Paul Zschack (zschack@anl.gov)*

ALLOYED FORCES LAID BARE

Nanotechnology relies on the fact that there can be significant differences between the properties of a material in the bulk and those at the sub-microscopic (nano) level. Low-melting metal alloys for instance, in the bulk, are seemingly the same throughout, behaving as near-perfect liquids when heated. However, at the nano level of metal clusters and surface atoms, several of these alloy compounds display odd behavior that seemingly goes against the grain, including surface layering, capillary action, demixing, and surface freezing. Understanding such nanoscale behavior might allow researchers to control it and exploit it in the production of novel materials with tailored properties. Such an understanding is the goal of a group of researchers from Harvard University, Bar-Ilan University, Brookhaven National Laboratory, and The University of Chicago, whose investigations into the behavior of a particular alloy provide new information about what occurs on the material's surface.

In this study, the researchers studied an alloy of bismuth and tin. The material, a less-toxic alternative to lead-based solder, has the chemical formula $Bi_{43}Sn_{57}$, and apparently behaves as a near-perfect liquid—at least when viewed on the bulk scale. However, the researchers used resonant x-ray reflectivity on the ChemMatCARS 15-ID beamline to take a much closer look at the surface of this material. Their findings suggest an altogether more deviant behavior.

They obtained a liquid $Bi_{43}Sn_{57}$ sample of 99.99% purity and prepared it under ultra-high vacuum conditions, scraping off stray impurities from the surface to render it "atomically clean" and then blasting it with high-energy argon ions to knock out any stragglers. They then carried out measurements on the liquid surface diffractometer at the ChemMatCARS beamline at a sample temperature of 142° C, which is 4 degrees above the temperature at which $Bi_{43}Sn_{57}$ melts—its eutectic point. The researchers then fitted the results to a computer model to reveal any organization in the liquid.

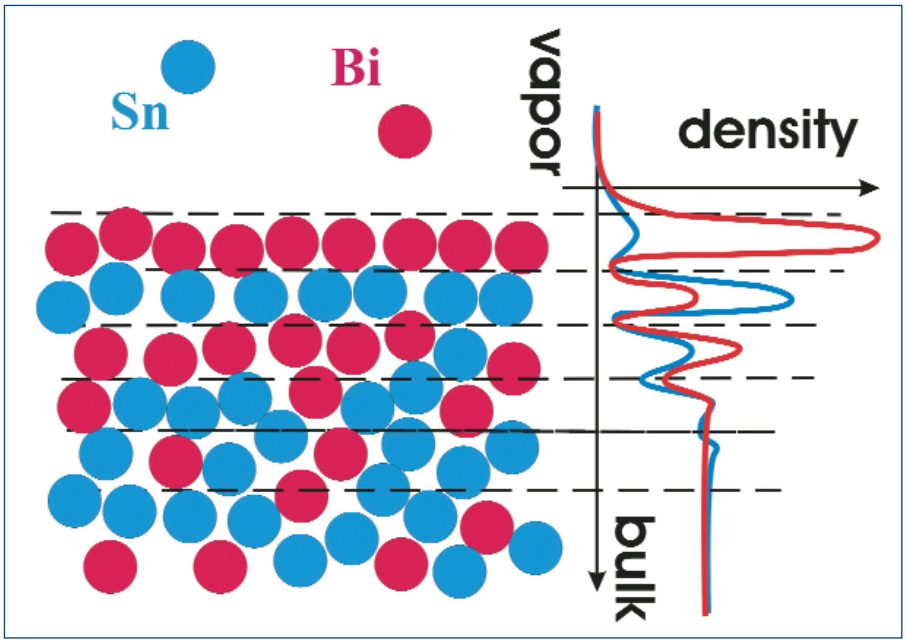

Fig. 1. On the surface, x-ray reflectivity reveals just how organized are liquid metal alloys.

In the bulk liquid, the bismuth and tin atoms are distributed evenly, albeit randomly, throughout, just as one would expect of particles in a liquid mixture. Near the surface, however, the researchers found something quite shocking for a liquid: *order*. Rather than the random metal atoms being fully mixed, they separate out into atomic layers with alternating compositions. The top layer is mostly bismuth; below that is tin, then another layer of bismuth and so on, with the atoms gradually becoming more mixed as depth increases. Their results gave an excellent fit to the model for three ordered layers, but one and two layers coincided very poorly with the model predictions.

Researchers have, in the past, observed a similar surface segregation in other liquid alloys, such as gallium induium, mercury gold, and bismuth indium, but the separating out of the two liquid-metal components was limited to a single layer at the surface. Scientists explained this phenomenon in terms of the energetics of the liquid near the surface. However, this is the first time anyone has observed such demixing extending deeper into a liquid than the uppermost monolayer. The power of synchrotron-based x-ray reflectivity using hard x-rays and atomic resolution reveals a phenomenon. On the one hand, immiscible liquids such as oil and water, which repel each other, quickly demix, but miscible liquids—ones in which the components are strongly attractive—do not.

Improved understanding of surface demixing and other phenomena—such as wetting, spreading, and reactivity—is essential to the use of novel materials, such as multicomponent alloys. Researchers might be able to tailor these materials to specific applications, such as lead-free solders and hybrid nanostructures (e.g., core-shell nanoparticles). It might also be possible to "lock-in" the surface order by cooling the liquid back

to its solid form, resulting in a modified surface. The way surfaces in the liquid interact with nanoscale particles that impinge on it could also be important in tribology applications, where significant recent research has focused on incorporating such nanoparticles into lubricants to help reduce friction and wear.

— David Bradley

See: Oleg G. Shpyrko[1], Alexei Yu. Grigoriev[1], Reinhard Streitel[1], Diego Pontoni[1], Peter S. Pershan[1], Moshe Deutsch[2], Ben Ocko[3], Mati Meron[4], and Binhua Lin[4], "Atomic-scale Surface Demixing in a Eutectic Liquid BiSn Alloy," Phys. Rev. Lett. **95**, 106103 (2005).

Author Affiliations: [1]Harvard University, [2]Bar-Ilan University, [3]Brookhaven National Laboratory, [4]The University of Chicago
Correspondence: oleg@xray.harvard.edu

This work was supported by the U.S. DOE Grants No. DE-FG02-88-ER45379 and No. DE-AC02-98CH10886 and the U.S.-Israel Binational Science Foundation, Jerusalem. ChemMatCARS Sector 15 is principally supported by the NSF/DOE Grant No. CHE0087817. Use of the Advanced Photon Source was supported by the U.S. Department of Energy, Office of Science, Office of Basic Energy Sciences, under Contract No. W-31-109-ENG-38.

NEW INSIGHTS INTO THE STRUCTURE OF SUPERCOOLED LIQUID SILICON

The structure of supercooled liquid silicon (Si) as it transforms from a metallic dense-packed structure at high temperatures to a semiconducting open network at lower temperatures has remained a controversial topic for several decades. Much of the controversy has focused on the postulated existence of a first-order liquid-liquid phase transition in the supercooled state. While some computer simulations have produced such a transition, others have not. Experimental studies using various containerless techniques have likewise yielded conflicting results. To resolve the question, researchers from Washington University, Iowa State University/Ames Laboratory, the University of Massachusetts, the University of Alabama, and the NASA Marshall Space Flight Center performed time-resolved *in situ* high-energy x-ray diffraction measurements of liquid Si by using the recently developed beamline electrostatic levitation (BESL) technique. Their results provide new insights into the existence (or lack) of a liquid-liquid phase transition.

Small spheres (2.2 to 2.5 mm in diameter) of high-purity Si, prepared by arc melting in a high-purity argon atmosphere, were levitated in a BESL chamber at high vacuum (10^{-7} to 10^{-8} torr) on the MU-CAT 6-ID-D beamline at the APS. The levitated samples were heated and melted by using 30-W diode and CO_2 lasers. Optical pyrometers with a 1.45- to 1.8-μm wavelength range were used to measure the sample temperature to an accuracy of 1K. Because of the high thermal conductivity of liquid silicon, the samples were in thermal equilibrium over the measured temperature range, with the maximum difference between the temperature at the center of the samples and that at the surface being less than 1K.

The diffraction measurements obtained at the APS offered important improvements over previous investigations. First, the use of high-energy x-rays (125 keV) ensured that the experiments were performed in a transmission geometry, so that the sample volume was probed. The use of high-energy x-rays also minimized data corrections caused by sample absorption and multiple scattering. Secondly, BESL offered a distinct advantage over electromagnetic and aerodynamic levitation, in that the processes of heating and positioning are decoupled, eliminating the need for cooling or levitating gases. The high-vacuum environment of BESL also minimizes environmental contamination of the sample, which can lead to heterogeneous nucleation. This allowed high-quality structural data to be extended more deeply into the supercooled regime of liquid silicon than has been possible before, to 316K below the melting point. Finally, the use of fast area detector technology in combination with the high-energy x-rays permitted rapid data acquisition (~100 ms for a complete pattern) over a reasonably wide momentum transfer range (q_{max} ~10 Å^{-1}), allowing the researchers to take advantage of the deep supercooling obtained in BESL without needing to hold samples at a set temperature for a prolonged period of time. Rather than obtaining only 5 to 10 data sets spaced over the entire temperature range, the researchers were able to continuously monitor structural changes over temperatures from 1815K to 1369K.

The researchers found that, in contradiction to several existing experimental studies and many simulations using the Stillinger-Weber potential, the coordination number of liquid Si

Continued on next page

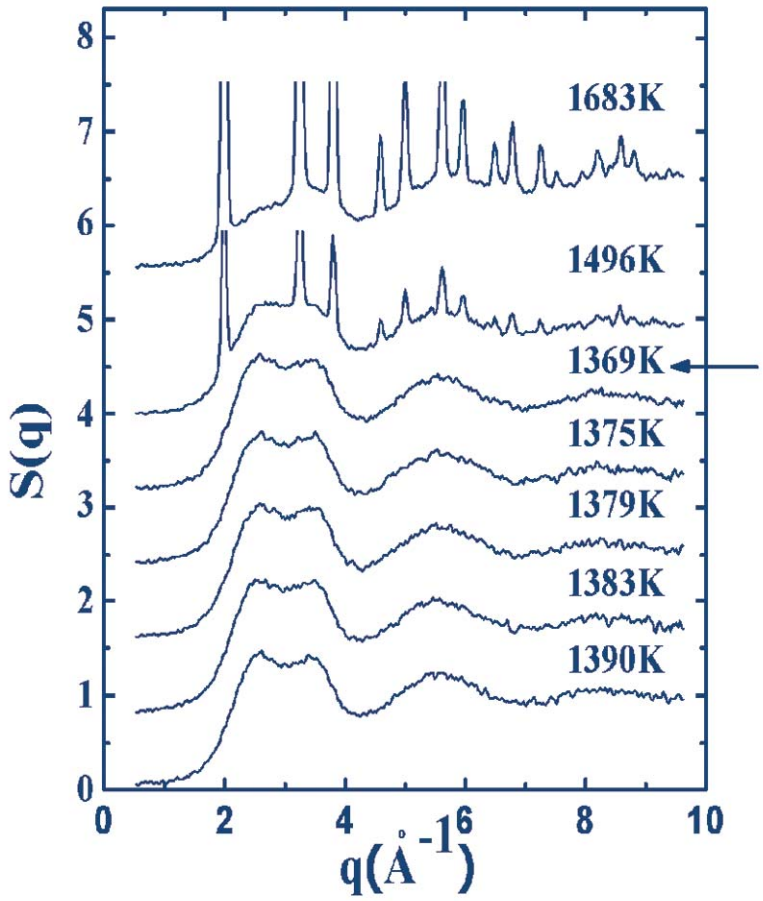

Fig. 1. Structure factors for supercooled liquid Si obtained from diffraction patterns taken at a rate of 10 Hz during free cooling. Note that upon recalescence (indicated by the arrow), the sample temperature rises.

remains unchanged (N = 6.0±0.5) down to the recalescence temperature corresponding to the nucleation and growth of the crystal phase. This result is inconsistent with the existence of a nearby liquid-liquid phase transition. Although no signal of a sharp transition in the liquid phase was observed down to the onset of crystallization, close inspection of the reduced radial distribution function revealed subtle continuous changes in the higher-order coordination shells that indicate a continuous evolution of the liquid structure with decreasing temperature. Thus, the existence of a liquid-liquid transition at a much lower temperature, such as has been recently predicted by *ab initio* molecular dynamics simulations to occur at approximately 300K below the researchers' recalescence temperature, cannot be ruled out. However, the data conclusively show that, if present, such a phase transition has no impact on first-neighbor coordination within the experimentally accessible temperature range down to recalescence (at least at standard pressure). Furthermore, while the first-order liquid-liquid phase transition predicted to occur at lower temperature could be related to the observed transformation of the higher-order coordination shells, the fact that these changes are continuous is intriguing and warrants further investigation. — *Vic Comello*

See: T.H. Kim[1], G.W. Lee[1], B. Sieve[2], A.K. Gangopadhyay[1], R.W. Hyers[3], T.J. Rathz[4], J.R. Rogers[5], D.S. Robinson[2], K.F. Kelton[1], and A.I. Goldman[2], "*In Situ* High-Energy X-Ray Diffraction Study of the Local Structure of Supercooled Liquid Si," Phys. Rev. Lett. **95**, 085501 (19 August 2005).

Author Affiliations: [1]Washington University, [2]Iowa State University, [3]University of Massachusetts, [4]University of Alabama, [5]NASA Marshall Space Flight Center
Correspondence: goldman@ameslab.gov

The work at Washington University was partially supported by the NSF under Grant No. DMR 03-07410. The work at Washington University and the University of Massachusetts was supported by NASA under Contract Nos. NAGS-1682 and NNM04AA016. MU-CAT and the Ames Laboratory are supported by the U.S. Department of Energy, Office of Science, under Contract No. W-7405-Eng-82. Use of the Advanced Photon Source is supported by the U.S. Department of Energy, Office of Science, Office of Basic Energy Sciences, under Contract No. W 31-109-ENG-38. The development and use of BESL was supported by the Marshall Space Flight Center (MSFC) Director's Discretionary Fund, the MSFC Science Directorate Internal Research and Development Program, and the NASA Microgravity Research Program.

EXCITEMENT IN LIQUID HELIUM

Excitons (quasiparticles consisting of an electron and electron "hole" bound together by Coulomb forces) are created when a photon knocks an electron out of the valence band of its clump of atoms. Although they don't stick around very long (usually the electron hole is quickly filled and the exciton disappears), they are a critical part of many physical phenomena, including semiconducting and insulating solids, substances in which they are generally observed. Because exciton formation is partially dependent on density, they are less often seen in liquid, which has a less-ordered molecular structure over shorter ranges. But under the right circumstances with the right element, excitons can be formed in liquids. One promising candidate is helium, because it can be examined as both a liquid and a solid over a wide range of densities. By using the ChemMatCARS 15-ID beamline at the APS, investigators from Argonne National Laboratory, The University of Chicago, the University of Illinois at Champaign-Urbana, and Germany's ACCEL Instruments GmbH detected excitons in bulk liquid helium (rather than in droplets, which are dominated by surface effects) for the first time, also providing insight into the nature of excitons in other states of helium.

The team used inelastic x-ray scattering (IXS) on samples of ^{4}He gas liquefied in a high-pressure Be cell with a cryostat. The x-ray beam was directed through a diamond double-crystal monochromator (used as a high-heat-load monochromator or HHLM) and through a channel-cut pair of silicon crystals (used as a high-energy-resolution monochromator or HERM). The experimenters used a germanium crystal as an analyzer, changing the angles of the HHLM and HERM crystals to vary the incident energy. Photon energy changes were measured by obtaining Stokes-shifted spectra. The energy at the analyzer was measured to be 9.487 keV. The ^{4}He liquid samples were studied under four different molar volumes (densities) with elastic and inelastic scans.

A previous similar experiment by the same researchers with lower energy resolution detected excitons in a solid crystal of hexagonal dose-packed (hdp) ^{4}He, which showed excitonic states when the crystal was subsequently melted. Compared to the current experiment, striking similarities between the excitonic peaks measured in the solid and the melted, liquefied crystal can be observed.

The current experiment with liquid ^{4}He sought to explore this connection more closely. With a temperature of 26.17 + 0.02K, the team measured exciton peaks in the ^{4}He liquid samples at molar volumes of 14.39, 13.10, 12.24, and 11.61 cm^3. The higher energy resolution reveals an apparent asymmetry in the exciton peaks, suggesting that there is more than one peak for each pressure level tested. The resulting data are best fit with two Gaussians (with amplitudes constrained to be equal), which limits the fit errors to below 10%, as seen in Fig. 1. With higher pressures, the peaks increase to higher energy levels, as do full width half maximum values.

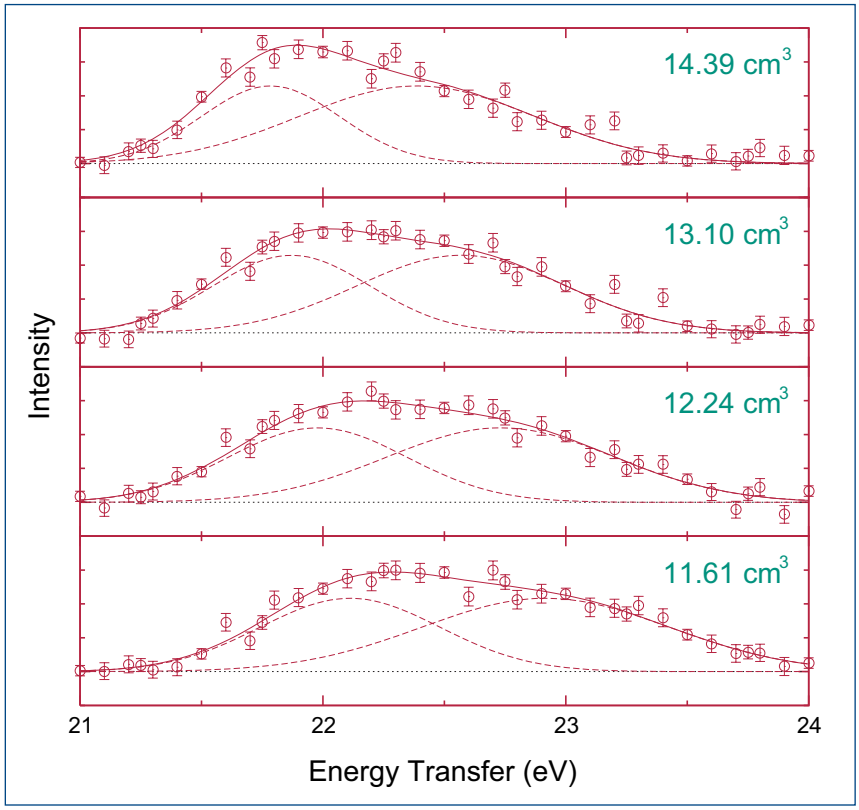

Fig. 1. Shown are the best fits to a sum of two Gaussians (with amplitudes constrained to be equal) for the four molar volumes. The range of data shown is the range used for fitting.

The experimenters infer that at least two exciton transitions are present, and perhaps more, given that the resolution of the current experimental setup is not quite high enough to fully distinguish the individual peaks. These measurements of exciton states in liquid helium, along with other experiments in solid hcp crystal helium, show that, as expected, exciton energy

Continued on next page

increases with density. Even more interesting is the fact that no notable change in the width or height of the measured exciton peaks is observed in the phase transition from solid to liquid helium. This is not the case in other elements, for example Xe, in which exciton formation is dependent on the amount of order in the sample. The experimenters conclude from these results that the formation of excitons is mostly dependent on short-range order in solid, as well as bulk liquid helium.

Further experiments with higher resolution to resolve the multiple exciton peaks will be needed to provide a theoretical basis for explaining the mechanics of the liquid helium excitons. Meanwhile, however, the researchers have provided an exciting first look at excitons in liquid helium and a demonstration of the role of short-range order and the similarities in exciton formation in both liquid and solid helium. — *Mark Wolverton*

See: D.A. Arms[1], T.J. Graber[2], A.T. Macrander[1], R.O. Simmons[3], M. Schwoerer-Böhning[4], and Y. Zhong[1], "Excitons in Bulk Liquid ^{4}He," Phys. Rev. B **71**, 233107 (2005).

Author Affiliations: [1]Argonne National Laboratory, [2]The University of Chicago, [3]University of Illinois at Urbana-Champaign, [4]ACCEL Instruments GmbH

Correspondence: dohnarms@anl.gov

ChemMatCARS is principally supported by the NSF/DOE under grant number CHE0087817 and by the Illinois Board of Higher Education. We wish to thank NSF and Professor S.M. Mini for the use of the HERM monochromator under grant number CHE9871246. Work supported by U.S. Department of Energy, Division of Materials Sciences, under contract DOEDE-FG02-91ER45439. Use of the Advanced Photon Source was supported by the U.S. Department of Energy, Office of Science, Office of Basic Energy Sciences, under Contract No. W-31-109-ENG-38.

THE PRESSING PROBLEM OF PRUSSIAN BLUE

The deeply colored pigment Prussian blue has for centuries fascinated artists and chemists alike. Its rich color results from electrons leap-frogging from metal atom to metal atom, absorbing red light as they go and reflecting just blue. Color isn't the only fascinating aspect of this complex iron salt and its related compounds. They are also of industrial importance because their sponge-like crystal structures are full of holes, tiny pores in which small molecules might nestle while others slip through. Where there are holes, there are ways to manipulate such small molecules, whether in separating mixtures, trapping gas molecules (such as hydrogen) for high-density storage purposes, or accelerating the conversion of one molecule into another. Understanding these compounds' structures and behavior could open new ways to control small molecule, and offer insights into new, porous materials. Researchers from the University of Sydney and Argonne National Laboratory used the XOR/BESSRC beamline 11-ID-C at the APS to investigate in detail the behavior of one particular analog of the archetypal Prussian blue, which can act as a nanoporous host to gas molecules.

While the original Prussian blue has the chemical formula $Fe_4[Fe(CN)_6]_3$, a vast range of analogs exist in which the iron atoms are replaced by other metal atoms, such as manganese or cobalt or both. One such analog, with the formula $Mn_3[Co(CN)_6]_2$, is of interest as a material for the reversible storage of gases—in particular, hydrogen storage for use in vehicles powered by fuel cells. The problem facing researchers studying this material is that infusing it with a gas, such as hydrogen, results in a disordered host-guest complex because the molecular guests are relatively free to move within the material's pores and do not necessarily occupy identical binding sites. Conventional x-ray diffraction techniques—based on analysis of Bragg intensities—cannot adequately resolve the structure of the gas, instead showing the smeared average of the disordered positions over the whole material and time scale of the experiment.

The research team has developed a way to obtain the local structure of the guests in the gas-loaded material by using high-energy x-ray scattering and subtracting the structural features evident in the unloaded material.

The approach, known as differential pair distribution function analysis, separates the information from *in situ* x-ray diffraction of the Prussian blue analog loaded with nitrogen gas (an experiment which may provide insight into the structure of other gases such as hydrogen). This allows the researchers to isolate the additional structural features that arise when the porous crystal structure is filled with guest molecules so that the interactions between the guest molecules, and between the guest and host, can be identified and the local structure of the guest revealed.

The information the researchers obtain using this technique allows them to see exactly how guests interact with the

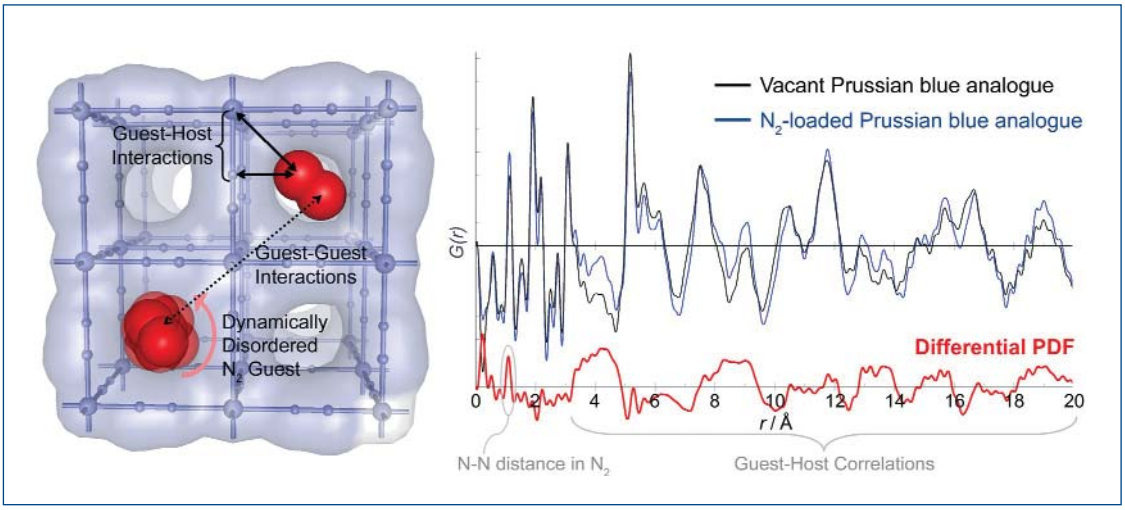

Fig. 1. Picture of the Prussian blue analog $Mn_3[Co(CN)_6]_2$ (blue) loaded with N_2 gas (red). The N_2 molecules are dynamically disordered and are averaged over the sites (lower left). The molecule, upper right, depicts the location of the molecule as a "snapshot" in time. (Right) The differential PDF (red) was calculated from the difference between the framework loaded with N2 (blue) and the empty framework (black).". (Left) Direct structure information is recoverable from the differential PDF. The intramolecular correlation in the N_2 molecule can be easily seen at about 1.2 Å, while the shortest host-guest correlation is evident at about 4 Å.

surface of the pores and how well gas molecules can be trapped. The manganese-cobalt analog can hold 20% by weight of nitrogen gas. But a clearer understanding of the role of pore shape and chemistry revealed by these studies could help guide materials scientists in designing new analogs with improved capacities. This technique has fewer limitations than other approaches, such as solid-state nuclear magnetic resonance spectroscopy, vibrational spectroscopy, and x-ray absorption spectroscopy, but with the added advantage of speed and much higher resolution. The researchers point out that the technique is not limited to a single Prussian blue analog; it could be used generally for a whole range of porous hosts loaded with guests and so provide new insights into the behavior of small molecules in materials of potential industrial use as separating agents and catalysts. — *David Bradley*

See: Karena W. Chapman[1], Peter J. Chupas[2], and Cameron J. Kepert[1], "Selective Recovery of Dynamic Guest Structure in a Nanoporous Prussian Blue through *In Situ* X-ray Diffraction: A Differential Pair Distribution Function Analysis," J. Am. Chem. Soc. **127**, 11232 (2005); and K.W. Chapman, P.D. Southon, C.L. Weeks, and C.J. Kepert, "Reversible Hydrogen Gas Uptake in Nanoporous Prussian Blue Analogues," Chem. Commun. **26**, 3322 (2005).

Author Affiliations: [1]University of Sydney, [2]Argonne National Laboratory

Correspondence: chupas@anl.gov, chapmank@aps.anl.gov

Work supported by the Australian Synchrotron Research Program, which is funded by the Commonwealth of Australia under the Major National Research Facilities Program and the Australian Research Council. K.W.C. acknowledges a Joan R. Clark Research Scholarship. Use of the Advanced Photon Source was supported by the U.S. Department of Energy, Office of Science, Office of Basic Energy Sciences, under Contract No. W-31-109-ENG-38.

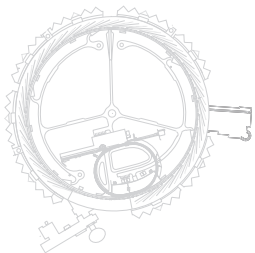

SHINING LIGHT ON FLEETING SPECIES

Light can reveal, and light can transform, and sometimes light can do both. Chemical reactions can be driven by light, as well as by the more familiar "heat and stir" approach. Indeed, countless photochemical reactions take place in the solid state. The study of photochemistry could lead to a clearer understanding of light-induced processes as diverse as electron transfer to semiconductor surfaces in photochemical cells, photosynthesis, skin damage and aging caused by sunlight, and the preservation of art exposed to light. Photochemistry also lies at the heart of novel reactions that might one day be of industrial use. It is the short-lived intermediate species that are key to such understanding, and time-resolved diffraction work is now yielding more information on the geometry of these species than ever before. Synchrotron x-ray research at the ChemMatCARS beamline 15-ID at the APS has been used to find out what happens when molecules of one such species—a trinuclear copper complex—react to light. These results reveal the way new phosphorescent materials might be developed for various photonic applications, such as chemical and temperature sensors.

Investigators from the State University of New York (SUNY) at Buffalo, the University of Toledo, The University of Chicago, and the University of North Texas have discovered that, in contrast to other compounds they have studied, the trinuclear copper complex undergoes a fast intermolecular change. Over the last few years, these researchers have studied several transition metal complexes that undergo light-induced shortening of the bond between two metal centers in the same molecule. In this new work, they used time-resolved, single-crystal diffraction to look at the cyclic trimeric $\{[3,5\text{-}(CF_3)_2\text{pyrazolate}]Cu\}_3$ complex as it reacts with light to see how the Cu-Cu separations change both within the same molecule and between adjacent molecules (Fig.1). The shape of this copper complex resembles that of a flattened doughnut, with its three copper atoms linked together through nitrogen atoms to form a nine-membered ring.

On the basis of the researchers' low-temperature results from metal complexes containing two atoms of platinum, rhodium, or copper in the same molecule, the researchers anticipated that the x-ray data would reveal that the distance between the three copper atoms shortens after the molecule absorbs light. However, this distinctive geometrical change does not take place in the case of the copper pyrazolate complex.

Instead, when the researchers chilled this molecule and exposed it to pulses of ultraviolet light, the time-resolved data they obtained revealed that the excited molecule forms through a so-called excimer, or an excited state dimer, in which two molecules in close proximity inside the crystal form an intermolecular Cu-Cu bond. This finding contrasts sharply with the contraction of metal-metal distances within a single molecule that the team observed in other metal complexes they have studied. Computational modeling of a dimer-of-trimer structure corroborates these results as a transient bond between copper atoms in adjacent molecules forms. The computations show that this change is a result of photoexcitation to an intermolecularly Cu-Cu bonding molecular orbital. This bonding can only be possible, explain the researchers, if the copper pyrazolate molecules are stacked together in the solid state.

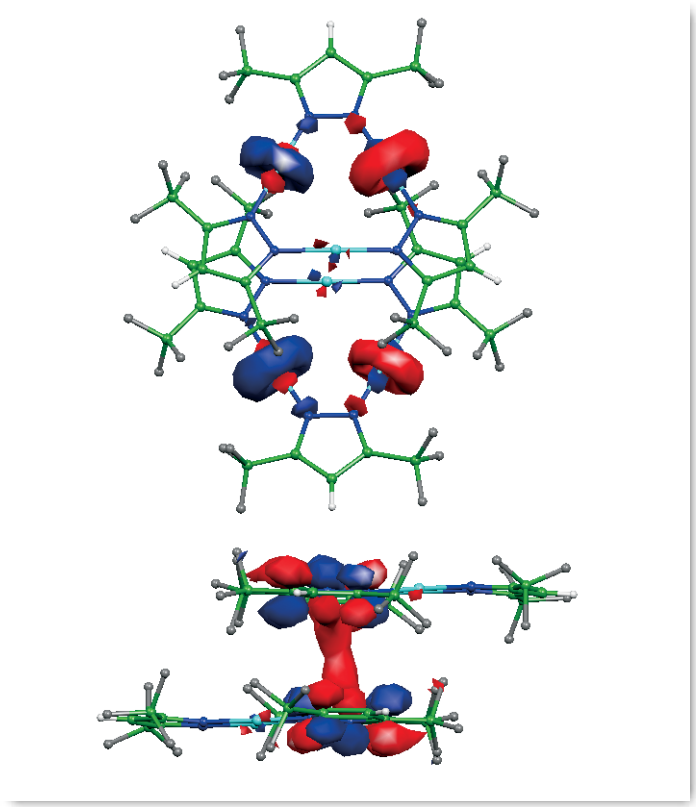

Fig.1. Top: The molecular orbital from which the photoelectron is transferred when ultraviolet light is shone onto the copper complex. Bottom: The acceptor orbital receives said photoelectron. The bridge between the two copper atoms indicates that a weak bond has formed in the excited state.

This unusual behavior has important implications for the potential use of copper pyrazolates and related materials in technological applications. These complexes can produce strong emissions at various wavelengths of light and so might be useful in molecular light-emitting devices (MOLEDs). Most

molecular materials used in this technology suffer "self-quenching," which reduces the efficiency of their luminescence due to packing in the solid state. In contrast, the bright orange phosphorescence in {[3,5-$(CF_3)_2$pyrazolate]Cu}$_3$ and similar molecules is caused by their association in the solid state, as the research team has clearly proven. Thus, the problematic self-quenching in typical emitters is turned into "self-sensitization" in these novel phosphors.

The fact that the emission in such materials is sensitive to various stimuli—such as solvent, temperature, excitation wavelength, and pressure—promises a myriad of potential applications, including optical sensing of environmental pollutants such as solvent vapors, pressure and temperature sensors; photomagnetic switching devices; and non-linear optical materials. The group is evaluating such applications in parallel with photocrystallographic studies aimed at characterizing the structural changes in the excited states upon application of the various stimuli. These studies will help the researchers fine-tune materials for the many practical applications. — *David Bradley*

See: Ivan I. Vorontsov[1], Andrey Yu. Kovalevsky[1], Yu-Sheng Chen[2], Tim Graber[3], Milan Gembicky[1], Irina V. Novozhilova[1], Mohammad A. Omary[4], and Philip Coppens[1], "Shedding Light on the Structure of a Photoinduced Transient Excimer by Time-Resolved Diffraction," Phys. Rev. Lett. **94**, 193003 (2005).
Author Affiliations: [1]SUNY at Buffalo, [2]University of Toledo, [3]The University of Chicago, [4]University of North Texas
Correspondence: coppens@buffalo.edu

The time-resolved experiments at APS were supported through Grant No. DE-FG02-02ER15372. Theoretical calculations were performed at the Center for Computational Research of the University at Buffalo. The 15-ID beamline is funded through NSF Grant No. CHE0087817. M.A.O. acknowledges support of his contribution by NSF through CAREER Grant No. CHE-0349313 and the Robert A. Welch Foundation through Grant No. B-1542. Use of the Advanced Photon Source was supported by the U.S. Department of Energy, Office of Science, Office of Basic Energy Sciences, under Contract No. W-31-109-ENG-38.

GREEN SOLVENTS SHOW THEIR TRUE COLORS

Many chemical processes occur at surfaces and interfaces between materials. For instance: chemical reaction fronts between different species, catalytic reactions, nucleation and growth of crystals from solutions and melts. Knowledge of the interface's structure is crucial to understanding such processes. The surface structure and thermodynamics of two so-called ionic liquids, an emerging class of industrially important "green" (i.e., environmentally friendly) solvents, have been determined by researchers from Bar-Ilan University, Brookhaven National Laboratory, and Argonne National Laboratory using the XOR/CMC 9-ID beamline at the APS and beamline X22B at the National Synchrotron Light Source. Their findings could help explain the properties of these materials as well as point to new applications and ways to use them.

Ionic materials are usually solids at room temperature. Think of regular table salt, otherwise known as sodium chloride. Most ionic materials melt only upon heating to hundreds of degrees above room temperature. However, some ionic materials don't follow this simplistic rule because the energy barrier to forming solid crystals can be too high for those ionic materials composed of bulky and irregularly shaped ions. These have low melting points and remain liquid near room temperature.

As chemists search for environmentally benign alternatives to volatile, flammable, and toxic organic solvents, and for less corrosive and more stable electrolytes for batteries and general applications, such room-temperature ionic liquids have become the focus of much research. Imidazole-based ionic liquids, for instance, developed over the last decade, turned out to be almost ideal for these applications. Unlike common organic solvents, they are nonvolatile, nontoxic, nonflammable, stable against water and air, and can be easily recycled. Additionally, chemists can fine-tune the properties of such ionic liquids for a particular application by varying the chemical structure of the material's constituent positive and negative ions. Indeed, more than 500 different ionic liquids have been synthesized and tested so far, each representing a variation on the theme.

The team studied two well-known ionic liquids consisting of a 1-butyl-3-methylimidazolium [bmim+] cation, and either a hexafluorophosphate (PF_6) or a tetrafluoroborate (BF_4) anion, using x-ray reflectivity and surface tensiometry. The high intensities, good collimation, and world-class liquid surface diffractometers available at beamlines 9-ID and X22B allowed the researchers to resolve the spatial structure of the surfaces with sub-nanometer resolution.

The researchers found that, unlike aqueous salt solutions—where the surface is depleted of ions—ionic liquids' surfaces are

Continued on next page

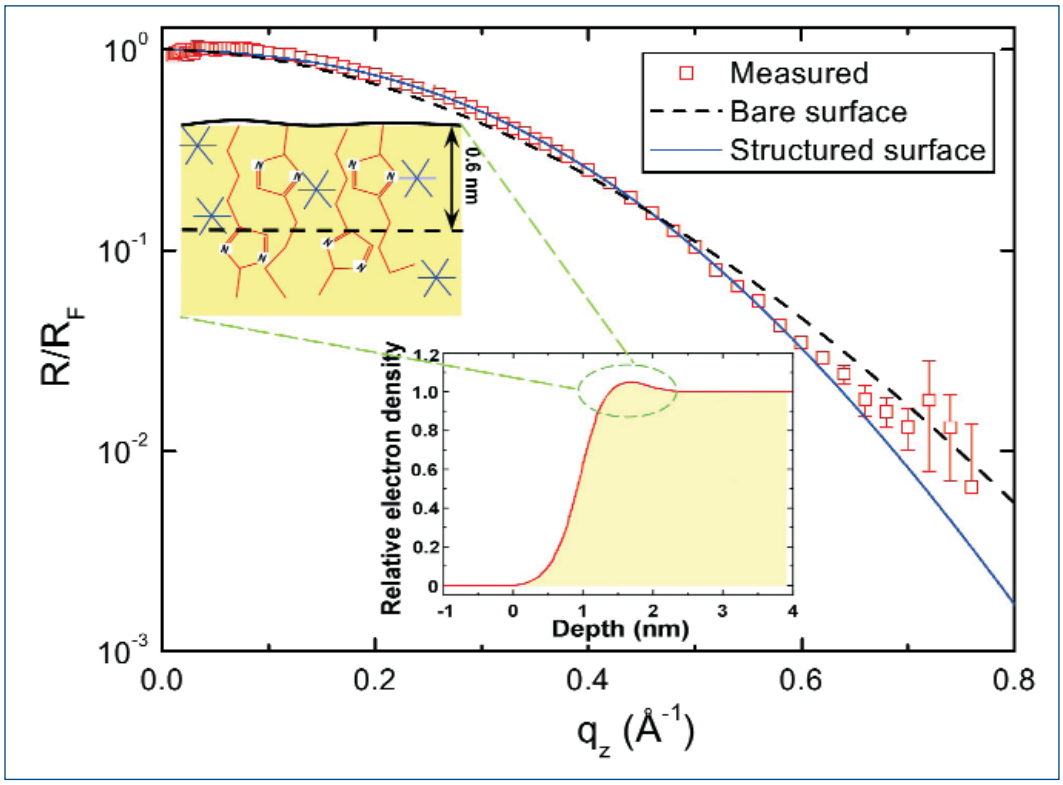

Fig. 1. The measured (squares) variation of the intensity of x-rays reflected off the ionic liquid's surface with increasing momentum transfer in the surface-normal direction (q_z), which is a measure of the incidence angle of the x-rays onto the liquid surface. The dashed line shows the intensity expected for an unstructured surface, while the solid line is the intensity expected for a liquid surface with a dense surface layer. The measured intensity clearly agrees better with the latter. The liquid's density variation with depth, z, in the lower inset, depicts the dense layer as a "bump" close to the surface (z = 0). A schematic of the likeliest molecular arrangement in the surface layer is shown in the upper left-hand inset.

enriched by anions, relative to their bulk. The only previous measurement of the surface structure of any ionic liquid, by neutron reflectivity on the same materials, hinted at a surface layering in these ionic liquids. However, the low neutron flux and limited angular range did not provide conclusive results. Moreover, spectroscopic studies led to contradictory results regarding the orientation of the surface molecules; one suggested that the imidazole ring of the cation lies parallel to the surface, while the other suggested that it is situated at right angles to the surface.

For both of the ionic liquids studied, the new measurements revealed a 15% enrichment of the surface by the anions, forming a 0.6-nm-thick surface layer. This surface layer was negatively charged, and is 10% to 12% denser than the bulk liquid. Although the orientation of the cations at the surface could not be unambiguously determined, the researchers identified two possible arrangements and ruled out several other possibilities. Whichever of the two arrangements turns out to be correct, both are very different from the surface ordering seen in liquid metals, polymer melts, and liquid crystals. This may hint at ordering mechanisms and dominant interactions that differ from those observed to date at liquid surfaces. The team suggests that future studies on other ionic liquids may lead to the identification and elucidation of these mechanisms.

— David Bradley

See: Eli Sloutskin[1], Benjamin M. Ocko[2], Lilach Tamam[1], Ivan Kuzmenko[3], Thomas Gog[3], and Moshe Deutsch[1], "Surface Layering in Ionic Liquids: An X-ray Reflectivity Study," J. Am. Chem. Soc. **127**, 7796 (2005).

Author Affiliations: [1]Bar-Ilan University, [2]Brookhaven National Laboratory, [3]Argonne National Laboratory
Correspondence: deutsch@mail.biu.ac.il

Support to M.D. by the U.S.-Israel Binational Science Foundation, Jerusalem is gratefully acknowledged. B.N.L. is supported by U.S. DOE Contract No. DE-AC02-98CH10886. Work at the CMC-CAT beamlines is supported in part by the Office of Basic Energy Sciences of the U.S. Department of Energy and by the National Science Foundation Division of Materials Research. Use of the Advanced Photon Source was supported by the U.S. Department of Energy, Office of Science, Office of Basic Energy Sciences, under Contract No. W-31-109-ENG-38.

RAXR REVEALS STRUCTURES FROM AQUEOUS-ION-OXIDE INTERACTIONS

The role of interfacial reactions is of growing importance in understanding the interaction between a mineral surface and aqueous metal ions at the liquid-solid interface. This role is especially important due to the ability of interfacial reactions to regulate a large range of reaction and transport processes in various natural systems, as well as in such industrial and technological applications as contaminant transport, catalyst preparation, corrosion inhibition, ore extraction and processing, and water treatment and purification. A key uncertainty about the interaction is whether the ion's hydration sphere is disrupted, yielding strong chemical bonds with oxygen atoms of the substrate (i.e., innersphere surface complex) or whether the ion retains its hydration sphere. If the latter case is true, there will be one or more water layers between the ion and substrate. Utilizing resonant anomalous x-ray reflectivity (RAXR), researchers from Argonne National Laboratory and the University of Illinois at Chicago have successfully examined the adsorption of aqueous metal complexes at the oxide mineral-water interface. They determined that RAXR is a viable way to make direct, simultaneous examinations of geometric and spectroscopic structures of weakly bound (outer-sphere) adsorbate materials at the mineral-water interface, and have verified that the adsorption of aqueous metal complexes show complex characteristics that are understandable only after resolving their geometric and spectroscopic substructures.

A key consideration guiding this study was the nature of the interaction of metal oxide surfaces with aqueous metal. These interactions are critical to the first step of noble metal catalyst preparation, where platinum tetraammine (PTA, $Pt(NH_3)_4^{2+}$) on silica was chosen as a model system. Previous studies have suggested that the interaction of ionic platinum complexes with an oxide support results in one or more water layers between it and the substrate, preserving the integrity of the ion hydration shell, either as a discrete outer-sphere surface complex or as a continuous Gouy-Chapman diffuse ion distribution.

A second critical factor for the study concerned the limited ability of conventional spectroscopic-based techniques to probe weakly adsorbed species *in situ*, in the presence of solution ions. In the past, such fluorescence-based methods by themselves could not accurately examine mineral-water interfaces because of spectroscopic interference from the ions in solution (or, in many cases, the solid substrate). This is a common limitation for *in situ* studies of the solid-liquid interface. These researchers, however, overcame the limitations by utilizing RAXR together with conventional surface x-ray reflectivity.

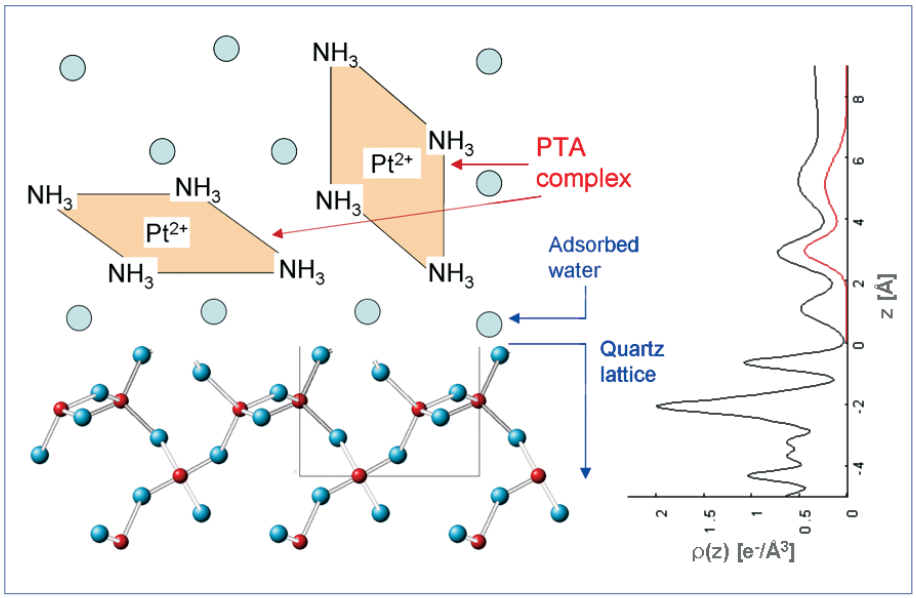

Fig. 1. The interaction of $Pt(NH_3)_4^{2+}$ (PTA) ions with quartz single crystal surfaces is obtained with RAXR. Electron density profiles, shown at right, are derived from the experimental data and include the total interfacial electron density (black) and Pt-specific electron density (red). A structural model consistent with the experimental data is shown at left, including two distinct adsorbed PTA complexes, separated from the quartz surface by a layer of adsorbed water.

By utilizing the XOR/BESSRC beamline 12-BM-B at the APS for their measurements, the group probed the physical structure and spectroscopic properties of PTA after it was adsorbed at the quartz (100)-water interface from dilute (~200 parts per million) platinum tetraammine (II) chloride $[Pt(NH_3)_4Cl_2]$ solutions at a pH of about 10. The quartz (100) surface was selected because its geometric structure (when exposed to water) is well verified and its surface functional groups share similar characteristics with amorphous silica used as a catalyst support.

Continued on next page

The group found that PTA (Fig. 1) adsorbs at a height above the surface hydration layer (i.e., as an outer-sphere species). Specifically, when the RAXR spectra of adsorbed PTA were measured near the Pt L_{III} edge, they were found to have (1) an interface-specific x-ray absorption near-edge profile that exhibits a significant white-line enhancement when compared to the bulk and (2) an unexpected geometric structure containing two distinct outer-sphere adsorbed layers above the quartz surface. These characteristics are unexpected with respect to the standard picture that outer-sphere species are only weakly ordered at the solid-liquid interface. They suggest to the collaborators that these outer-sphere adsorbates may have a more complex structure than earlier presumed.

As a result of their experiments, the researchers confirmed that resonant scattering is useful as an element-specific approach for examining ion adsorption at the oxide-water interface. They verified that the adsorption of aqueous metal complexes, which are electrostatically held at the oxide-water interface, show complex characteristics that are understandable only after resolving their geometric and spectroscopic substructures.

Thus, RAXR measurements led to a better understanding of the complex structural and chemical changes within these aqueous-ion-oxide interactions. The promising results provide the scientific community with new prospects for examining interfacial reactions that were previously unattainable.

— William Arthur Atkins

See: Changyong Park[1], Paul A. Fenter[1], Neil C. Sturchio[1,2], and John R. Regalbuto[2], "Probing Outer-sphere Adsorption of Aqueous Metal Complexes at the Oxide-Water Interface with Resonant Anomalous X-Ray Reflectivity," Phys. Rev. Lett. **94**, 076104-1 (2005).

Author Affiliations: [1]Argonne National Laboratory [2]University of Illinois at Chicago

Correspondence: cypark@anl.gov; fenter@anl.gov

This work and use of the Advanced Photon Source were supported by the U.S. Department of Energy, Office of Science, Geoscience Research Program of the Office of Basic Energy Sciences, under Contract No. W31-109-ENG-38 and by the NSF through Grant No. DMR 0304391 (NIRT).

AROUND THE EXPERIMENT HALL

ATOMIC MODELS OF PLANT VIRUSES

Amy Kendall (left), Michele McDonald, and Sarah Tiggelaar—all with the Stubbs Lab in the Department of Biological Sciences at Vanderbilt University—taking data at the Bio-CAT 18-ID beamline.

Kendall: "Our lab uses fiber diffraction data from oriented sols and dried fibers to determine the structures of flexible filamentous plant viruses. Our long-term goal is to produce atomic models based on diffraction data at resolutions close to 3 Å, but a great deal of information can be obtained at lower resolution, including the size, shape, and symmetry of the viruses.

"These viruses are of great significance as models for fundamental virology and cell biology, They have enormous potential as vectors in biotechnology and they are of considerable importance because of the damage they cause to agriculture. We also use the filamentous plant viruses as important model systems for developments in fiber diffraction."

Contact: amy.k.kendall@vanderbilt.edu

Storing the Power to Fly

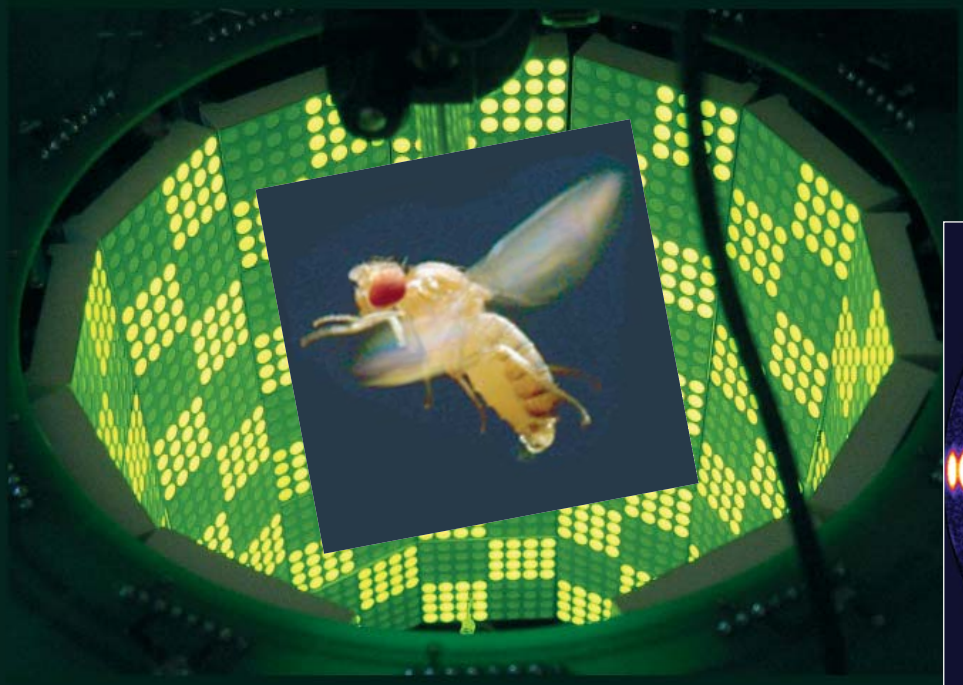

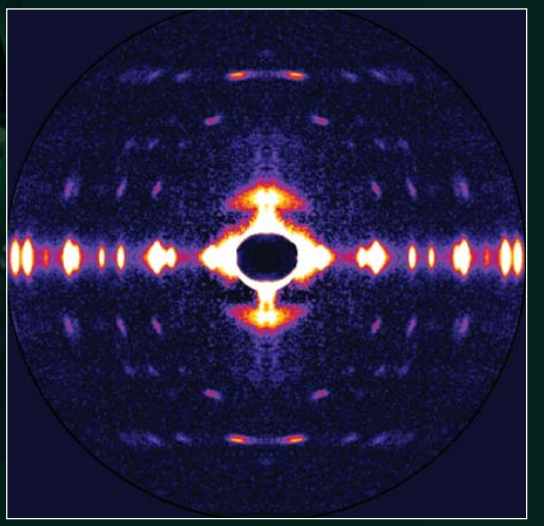

Fig. 1 (above). Smaller than the flashing green lights on its flight simulator, a fruit fly (inset) uses spring-like flight muscle proteins to beat its wings. Fig. 2 (right). All the muscle components diffract high-intensity x-rays that are captured on the detector in colorful patterns.

Fruit flies beat their wings faster than their cellular powerplants can generate the energy needed for flapping. To resolve this energetic discrepancy, researchers from the California Institute of Technology, the Illinois Institute of Technology, and the University of Vermont used the Bio-CAT beamline 18-ID at the APS to obtain a series of x-ray photographs that revealed the flies' secret: A muscle protein used to power wings acts like a spring, storing energy while stretched before snapping back. Not only did this finding surprise researchers who study muscle, but the results might also help scientists better understand the human heart.

Drosophila, the fruit fly, beats its wings up and down once every 5 milliseconds. Two layers of muscle control this action: when one layer contracts, it stretches the other. The stretched muscle is then primed to contract; when it does, it stretches the first layer and completes the cycle. These cycles occur faster than nerve impulses can stimulate them; hence, the muscles themselves must keep the beat going.

To find out how muscles do this, the research team needed to visualize the proteins that make muscle contract. Within the flight muscle cells, two proteins cooperate to do this. Myosin proteins have flexible heads and long tails that bundle together. The heads grab filaments made of the protein actin that ultimately connect at either end to opposite cell walls. Like a bunch of hands pulling on a rope, the myosin heads drag actin inward, making the muscle cell shorter. Methods to visualize what proteins look like often require purifying the protein or killing the organism in which it exists. Not only did the team want to keep the flies alive, but they wanted to watch myosin and actin in action. Short bursts of APS's high-intensity x-rays allowed them to achieve both goals.

The researchers tethered flies inside a box (a “flight simulator”) and used air and moving lights to convince the bugs that they were buzzing around. Then the team took x-ray snapshots of the proteins responsible for beating the wings. They synchronized the beam's shutter speed with the wing beat's frequency. Much like a strobe light reveals the status of a dancer instantaneously, synching the wing beat to the synchrotron x-rays allowed the scientists to view the positions of the muscle proteins at one point in time. The team put together a series

Continued on next page

of these images taken at different points of the beat to create a stop-action film of the protein movements within muscle cells.

After exposure in the beam, myosin and the other muscle components diffract x-rays onto a detector in specific patterns. From this pattern, researchers can tell if myosin is grabbing onto the actin filament, pulling, or releasing its grasp. In contracted muscle, the researchers saw myosin dragging the actin filament as expected.

But when the muscles relaxed, the team saw an unanticipated movement. Instead of completely releasing its grasp as myosin does in other relaxed muscles, the myosin briefly let go, but then snagged the filament again. And the bundle of myosin tails—long believed to be stiff for pulling during contractions—stretched a bit, due to the second layer of contracting flight muscle. This finding suggested to the researchers that myosin stores elastic energy in its tail that can be used in the next contraction, much like a stretched spring holds onto energy and releases it when the spring recoils. The stretching also appears to stimulate the myosin and actin filaments to again contract the muscle.

In addition to this novel finding, the technological advancement that allows scientists to view the composition of a living muscle will now let them study muscle contraction in greater detail. Fruit flies are well suited for genetic studies that might eventually illuminate how human heart muscle, which is similar to a fly's muscle, can fail when diseased. — *Mary Beckman*

See: M. Dickinson[1], G. Farman[2], M. Frye[1*], T. Bekyarova[2], D. Gore[2], D. Maughan[3], and T. Irving[2], "Molecular Dynamics of Cyclically Contracting Insect Flight Muscle *In Vivo*," Nature **433**, 330 (20 January 2005)

Author Affiliations: [1]California Institute of Technology, [2]Illinois Institute of Technology, [3]University of Vermont. [*]Current address: University of Illinois

Correspondence: irving@iit.edu

This work was supported by the National Institutes of Health. The APS is supported by the U.S. Department of Energy. Bio-CAT is an NIH-supported Research Center. Use of the Advanced Photon Source was supported by the U.S. Department of Energy, Office of Science, Office of Basic Energy Sciences, under Contract No. W-31-109-ENG-38.

IRON ON THE BRAIN

Everyone needs iron, but too much of it in the wrong place in the body can be a very bad thing. Neurodegenerative disorders, such as Alzheimer's, Huntington's, and Parkinson's disease, have all been shown to be closely related to the presence of too much iron in brain tissue, which is the result of disturbances in normal iron metabolism. But discovering how much iron is present in the brain, and in what particular compounds, has proven to be a challenge. The chief methods used at present rely on staining of tissue samples, a technique that provides poor resolution and does not provide any data on the makeup of specific iron compounds. Clearly, a more precise and accurate strategy for locating and identifying iron anomalies in brain tissue is needed. Now, researchers from the University of Florida, the University of Minnesota, Keele University, and Argonne National Laboratory, using the MR-CAT insertion device beamline at the APS, may have found just that strategy.

Using the MR-CAT 10-ID beamline at the APS, the team has developed a technique that combines the technique of x-ray absorption near-edge spectroscopy (XANES) with with iron-edge area scanning. The process not only allows individual, minute iron anomalies to be detected with much greater resolution and sensitivity than ever before, but it also makes possible their identification and specific characterization *in situ*.

The experimenters used tissue samples from the midbrain of a homing pigeon for this initial demonstration of the technique. The samples were fixed and sealed between two sheets of Kapton film containing gridlines of zinc wire for use as an orientation tool. The researchers ensured that the methods and materials used to prepare the samples, including the fixing solutions, Kapton sheets, and slides, were fully cleaned and purified to prevent the detection of extraneous impurities during the experimental procedures. Comparing the x-ray fluorescence of the tissue samples above the iron K absorption edge at 7,112 eV with their fluorescence below the iron absorption edge, the team was able to generate an iron concentration map for each sample (Fig. 1). A detection limit of less than 1 ppm is possible because of the high intensity of the APS microfocused synchrotron x-rays. Because of the extreme sensitivity this affords, a single particle of nanometer scale can be detected in a 500-μm spot.

The tiny areas of iron concentration found were then examined at even higher resolution— down to 5 μm—followed by XANES analysis. The data obtained from the XANES studies were compared with measured standards and published results for magnetite, ferritin, haemosiderin, and haemoglobin. This revealed that the iron anomalies detected in the tissue samples consisted of ferritin, magnetite, and haemoglobin. The researchers also confirmed that the sample preparation tech-

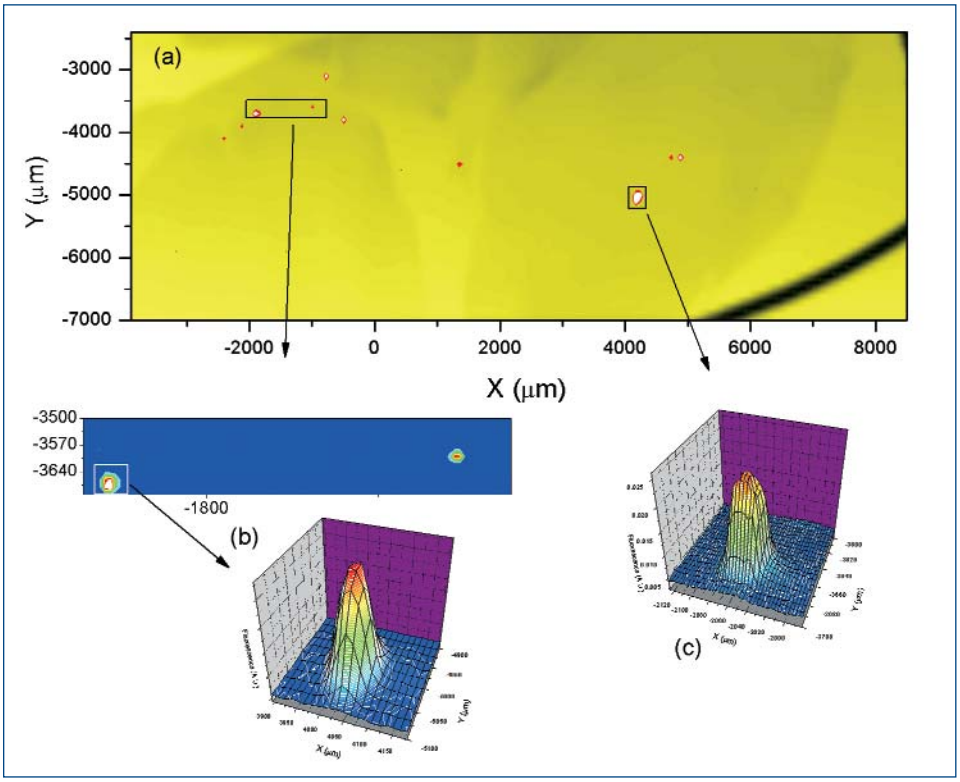

Fig. 1. Maps of the coronal section of a pigeon brain consisting of (a) x-ray transmission map (black–yellow) with superimposed iron fluorescence map (red–white) with 500-μm resolution; (b) iron fluorescence map at 20-μm resolution, with 5-μm resolution wireframe image inset of iron anomaly A consisting primarily of ferritin-like iron compounds; and (c) iron fluorescence wireframe map at 5-μm resolution of iron anomaly D, consisting primarily of magnetite.

niques did not affect the iron compounds detected, and that any trace metallic contamination introduced during the preparation process can be distinguished from biogenic iron anomalies with XANES.

The research team's work provides a powerful demonstration of the potential of highly focused synchrotron x-ray beams to detect and identify *in situ* iron deposits in brain tissue with very high resolution and with only a few hours of study. The use of the zinc wire gridlines on the sample slides also allows the identification and location of anomalies for comparison study by other techniques, including electron and light microscopy. Other metals that have been tied to neurological abnormalities, such as aluminum and zinc, can also be detected and analyzed via this method. Another interesting potential use of this technique is the study of magnetoreception in animals—how certain species (such as pigeons) may use magnetic fields to orient themselves and navigate over great distances.

The researchers believe that their work is the first step in the development of even more sophisticated techniques to find, map, and precisely characterize abnormal iron and other metallic compounds within brain tissue (they have now demonstrated the technique in human tissue from Alzheimer's patients). This new tool promises to provide crucial information on the specific cells and structures containing such anomalies, and clues about the ways in which these metallic deposits do their neurological dirty work. — *Mark Wolverton*

Reference

[1] J.F. Collingwood, A. Mikhailova, M. Davidson, C. Batich, W.J. Streit, J. Terry, and J. Dobson, "In-situ Characterization and Mapping of Iron Compounds in Alzheimer's Tissue," J. Alzh. Dis. **7**, 267 (2005).

See: A. Mikhaylova[1], M. Davidson[1], H. Toastmann[2], J.E.T. Channell[1], Y. Guyodo[3], C. Batich[1], and J. Dobson[4], "Detection, Identification and Mapping of Iron Anomalies in Brain Tissue Using X-ray Absorption Spectroscopy," J. Roy. Soc. Interface **2**, 33 (18 January 2005).

Author Affiliations: [1]University of Florida, [2]Argonne National Laboratory, [3]University of Minnesota, [4]Keele University
Correspondence: bea22@keele.ac.uk

This work was supported by the University of Florida Opportunity Fund, a McKnight Brain Institute Seed Fund grant, NIH/NIA grant no. R01 AG02030-01 A1, and by the Alzheimer's Society (United Kingdom). J.D. acknowledges the support of a Royal Society/ Wolfson Foundation Research Merit Award. Use of the Advanced Photon Source was supported by the U.S. Department of Energy, Office of Science, Office of Basic Energy Sciences, under Contract No. W-31-109-ENG-38.

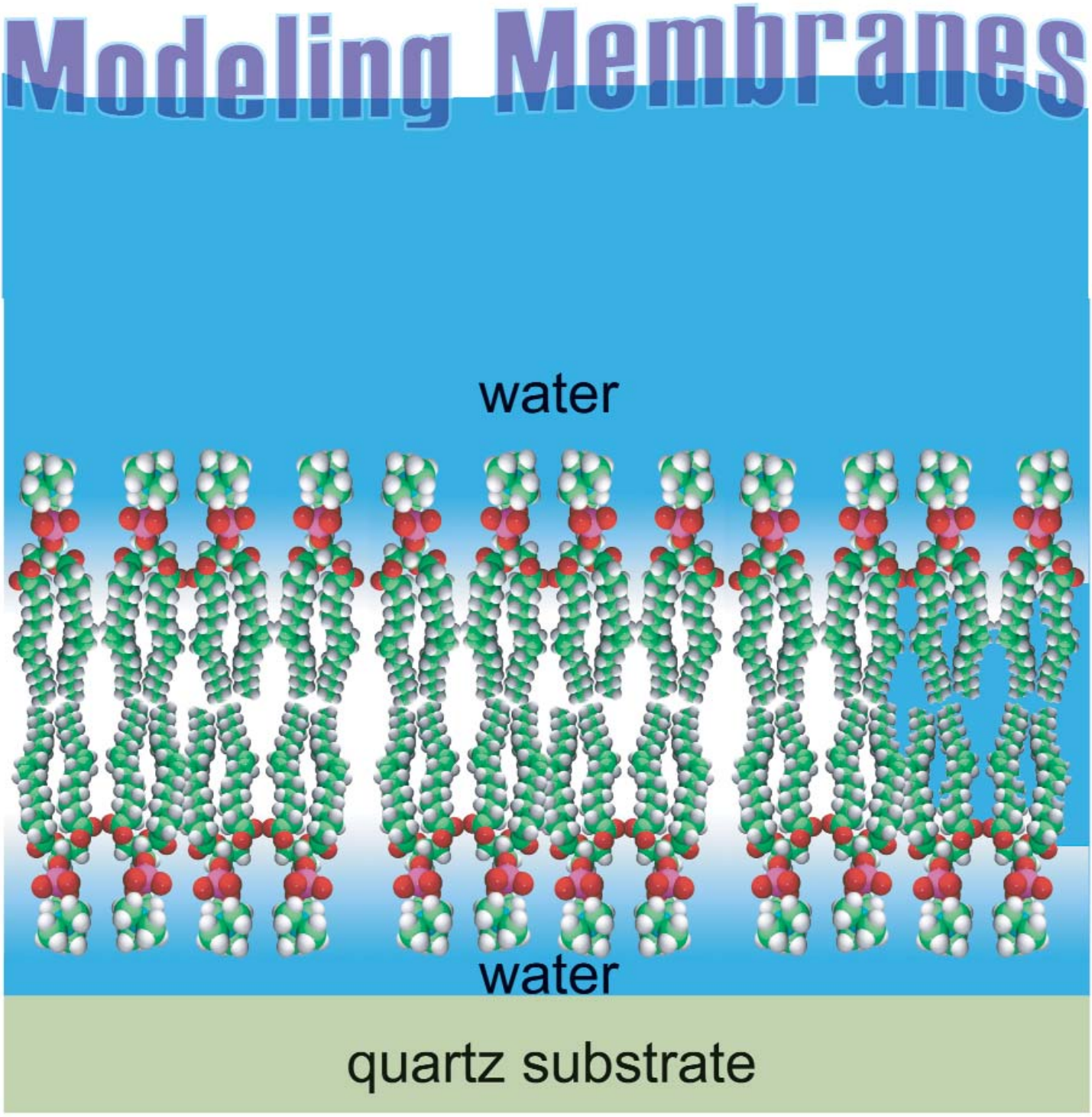

Fig. 1. Phospholipid head-groups and hydrocarbon tail region of the bilayer can be seen using x-ray reflectivity and a water cushion layer between the bilayer and the substrate revealed.

Cell membranes are incredibly complex, which makes studying their structure and function difficult. Model systems—thin films formed from the building blocks of cell membranes without the myriad of other components of a real cell—can offer a simplified view and so provide crucial insights into this important area of biology. However, earlier methods of studying such model membranes either reveal only low-resolution details or else cannot penetrate far beneath the surface. Specular x-ray reflectivity (XR) studies of biological membranes carried out at XOR/CMC beamline 9-ID at the APS have demonstrated that XR can reveal details that are hidden during related lower-power neutron studies and so provide an unprecedented picture of how phospholipids structurally assemble in thin films. The detailed observations obtained by researchers from the University of California, Davis; Los Alamos National Laboratory; and Argonne National Laboratory will provide biomedical researchers with new targets for pharmaceutical discovery and aid in understanding how toxins function.

Earlier research into model cell membranes has exploited the penetrating power of neutrons to investigate structure perpendicular to a buried interface. The research team knew that neutrons did not provide them with the resolution they could obtain by using x-rays. Conventional x-ray techniques, however, lacked the penetrating power needed to give them a more detailed view of model membranes at the interface between solid and liquid. The researchers' aim is ultimately to mimic the cell membrane with a view to creating model systems for medicine and drug screening, as well as mapping new avenues for materials science. High-power x-rays might point the way.

The investigators used the 9-ID beamline to probe their model membranes by increasing the x-ray photon energy to 18 keV, allowing them to penetrate the bulk-water environment to which the membrane is exposed. Before, XR studies were limited to examining monolayers at the air-liquid interface. In addition to providing better resolution, x-rays are also cheaper, more accessible, and quicker than neutrons.

Now, instead of studying monolayers, the researchers can investigate the more biologically relevant bilayer systems with increased resolution over neutron reflectivity. They made membranes from the phospholipids found in natural cell membranes and characterized a fluid-phase bilayer and a predominantly gel-phase bilayer formed at the interface between a solid support and liquid water. The phospholipid bilayers stabilize themselves by lining up their water-repellant “tails” of the phospholipid molecules to “hide” themselves from water, while the water-loving, hydrophilic “heads” sit happily exposed to the water. These lipid structures thus mimic more complicated real cell membranes.

This is the first time scientists have studied such phospholipid bilayers using synchrotron XR, which typically utilizes an incident flux that is ten orders of magnitude greater than current neutron fluxes. With such power on tap, the team could probe the molecular orientation of the bilayers with unparalleled detail.

Their high-resolution results confirmed that membranes may be more complex than imagined: arranging themselves into non-symmetrical groups or slabs with different lipid molecules preferentially segregated into the leaflet of the bilayer that faces the solid support or that is exposed to bulk water. The researchers could clearly distinguish the phospholipid head-groups and hydrocarbon tail region in the bilayer as well as observing a 4-Å-thick cushion of water formed between the bilayer and the solid support, or substrate. The much higher resolution afforded by x-rays enables clear resolution of the subtle differences in the packing of the lipid leaflets, as demonstrated by the increased electron density of the lipid head-groups closest to the substrate.

Structural details like these will have a significant impact on the development of membrane-based sensors for toxin detection and drug screening. Such a straightforward and elegant approach to studying cell membranes could also revolutionize structural investigations of membranes and their interactions with proteins. — *David Bradley*

See: C.E. Miller[1], J. Majewski[2], T. Gog[3], and T.L. Kuhl[1], “Characterization of Biological Thin Films at the Solid-Liquid Interface by X-Ray Reflectivity,” Phys. Rev. Lett **94**, 238104 (2005)

Author Affiliations: [1]University of California, Davis; [2]Los Alamos National Laboratory; [3]Argonne National Laboratory
Correspondence: cemiller@ucdavis.edu

This work was supported by University of California directed research and development funds, by Los Alamos National Laboratory under DOE Contract No. W7405-ENG-36, and by the DOE Office of Basic Energy Sciences. The work at the CMC-CAT beamline is supported in part by the Office of Basic Energy Sciences of the U.S. Department of Energy and by the National Science Foundation Division of Materials Research. Use of the Advanced Photon Source was supported by the U.S. Department of Energy, Office of Science, Office of Basic Energy Sciences, under Contract No. W-31-109-ENG-38.

EXPLORING THE STRUCTURE OF BONE

X-rays and bones have a long history. The bones in a human hand were revealed in one of the very first x-ray images captured by Wilhelm Conrad Röntgen when he discovered the x-ray more than 110 years ago. From that day on, x-rays have been used to image bones for medical purposes. But probing the structure of bone materials itself required the high-brilliance x-rays from a synchrotron light source such as the APS. Bone is one of the most intriguing composite materials. Engineers have yet to create a structure that rivals its strength and toughness pound for pound. Tough materials can be heavily damaged before they fail, and a tough skeleton improves an animal's chances of survival. So, studies that provide new insights into the characteristics that make bone so strong and tough, but keep it lightweight, are keenly followed by structural researchers hoping to emulate this natural material. Such insights are also important to medical researchers hoping to better understand bone diseases, such as osteoporosis. Scientists from Argonne National Laboratory and Northwestern University have turned to high-energy synchrotron x-ray scattering at the XOR 1-ID beamline to glean new insights into the way bone carries the stresses and strains encountered during everyday life.

Bone consists of very tiny mineral particles of calcium phosphate, packed with collagen fibers. The mineral phase is very strong but brittle. Collagen is a very ductile connective tissue that, combined with the mineral phase, produces a tough material with some flexibility. Certain diseases, such as osteoporosis, increase the overall porosity of bone and decrease its mineral density. Not all low-density bone suffers fractures, however, nor is all high-density bone safe from fracture. Clinical researchers face a challenge in discriminating between healthy bone and bone susceptible to fracture. After all, physicians cannot test their patients' bones to destruction. Animal models of bone strength and changes that occur in disease have improved our understanding, but what constitutes bone quality remains elusive

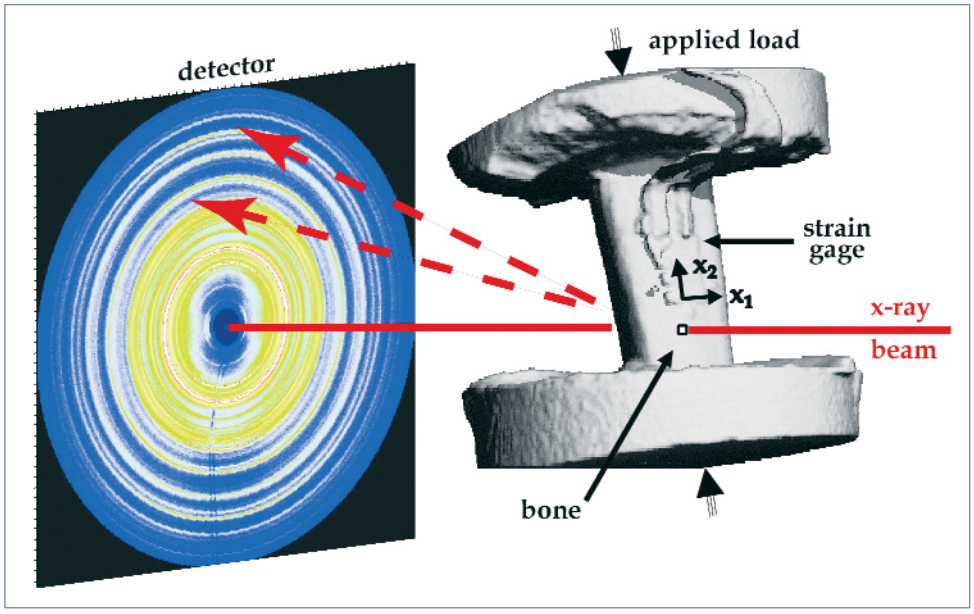

Fig. 1. A small x-ray beam is used to follow compression of a bone specimen (right) via changes in the pattern of x-ray scattering measured by the area detector (left, with the colors indicating different scattered x-ray intensities). The small attached strain gauge provides supplementary information.

As x-rays pass through the soft and hard (mineral containing) tissues of the body, they commonly produce “shadow” images of bone. The nanoparticles of mineral are tiny crystals, and the building blocks or unit cells of these crystals scatter x-rays. When bone is compressed, the unit cells distort in response, changing the pattern of scattered x-rays. The Argonne and Northwestern University team used the calcium phosphate crystal unit cells as microscopic strain gauges for testing a bone. This approach avoids invasive procedures, such as affixing external, millimeter-sized strain gauges to the bone.

With assistance from XOR beamline 1-ID, the team used 80.7-keV x-radiation to investigate the internal stresses in an intact bone under compressive loading. They found that, using this technique, the changes in the crystal unit cells under loading could be easily quantified. The researchers noted that when they applied a compressive stress to the bone, the crystal unit cells—however they are oriented—compressed in the direction of the stress and expanded in the directions at right-angles to it. This is analogous to squeezing a piece of foam rubber with each “cell” distorted by the squeeze so that it gets shorter in the direction of the squeeze and bulges out sideways.

The distortion of the crystal unit cells in bone appeared as small, but clear differences in the x-ray scattering patterns between unstressed and stressed bone. The researchers then

inferred the changes in the crystal unit cells from the altered x-ray patterns and related these to the stress applied and to the internal forces carried by the bone. By combining wide-angle diffraction and small-angle scattering from the bone sample they were able to glean far more information than has so far been possible with other techniques. Their results demonstrate that measuring the internal strain on bone's mineral phase—and the corresponding stress it feels—should be possible on intact bones or vertebrae. The same approach might even allow studies to be carried out on the limbs of anesthetized animals in model studies to help improve our understanding of bone's behavior. — *David Bradley*

See: J.D. Almer[1] and S.R. Stock[2], "Internal Strains and Stresses Measured in Cortical Bone Via High-Energy X-ray Diffraction," J. Struct. Biol. **152**, 14 (2005).

Author Affiliations: [1]Argonne National Laboratory, [2]Northwestern University

Correspondence: s-stock@northwestern.edu

Use of the Advanced Photon Source was supported by the U.S. Department of Energy, Office of Science, Office of Basic Energy Sciences, under Contract No. W-31-109-ENG-38. Use of the Northwestern University MicroCT Facilities Scanco MicroCT-40 is also acknowledged.

How Attractive Is That DNA?

Long, linear DNA molecules bend and fold into three-dimensional shapes. The electrochemical forces that dictate the conformation adopted by nucleic acid are central to understanding how DNA and RNA carry out their tasks within cells. Researchers from Stanford University used the XOR/BESSRC beamline 12-ID at the APS and Stanford Synchrotron Radiation Laboratory's 4-2 beamline to test how different electrochemical environments influence the way DNA molecules structure themselves. The measurements will help scientists enhance their understanding of the forces that shape DNA and RNA.

Negative charges riddle the backbones of DNA and RNA molecules. The negativity creates repulsion that should prevent nucleic acids from interacting (Fig.1). And yet often, within cells (such as when DNA condenses into chromosomes before cell division), nucleic acids have to contact other nucleic acids. Ions with one or two positive charges normally coat the negative charges, forming a so-called ion atmosphere near the molecule's surface. Ions with two or more positive charges interact to a greater extent with the negative charges on DNA and RNA. For example, magnesium ions with two positive charges are commonly required for folding DNA and RNA. Researchers have found that in very long molecules such as chromosomes, these divalent and multivalent cations line up between two DNA helices in a way that allows the molecules to attract each other. This arrangement could also allow a DNA molecule to fold in upon itself.

To explore whether the same mechanism prompts the folding of small DNA and

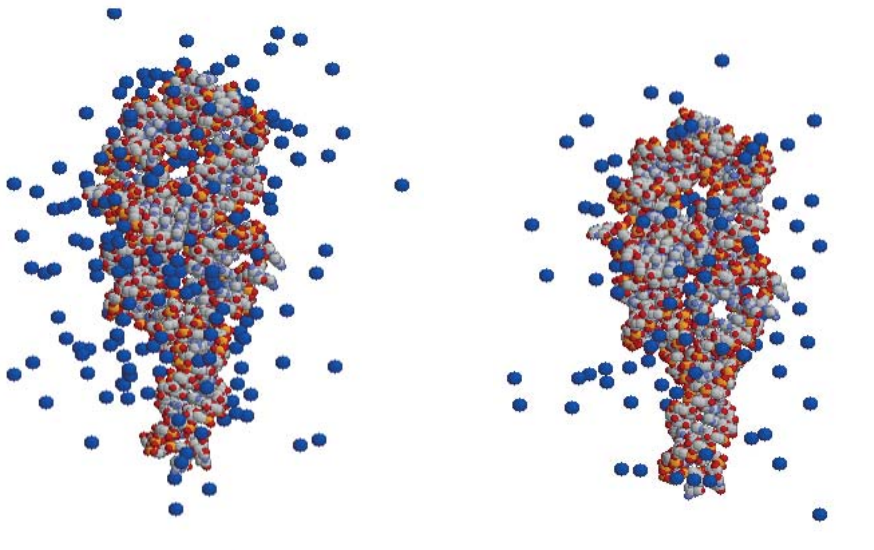

Fig.1. Positively charged ions (blue orbs) surrounding negatively charged molecules of DNA or RNA (red and gray structures).

Continued on next page

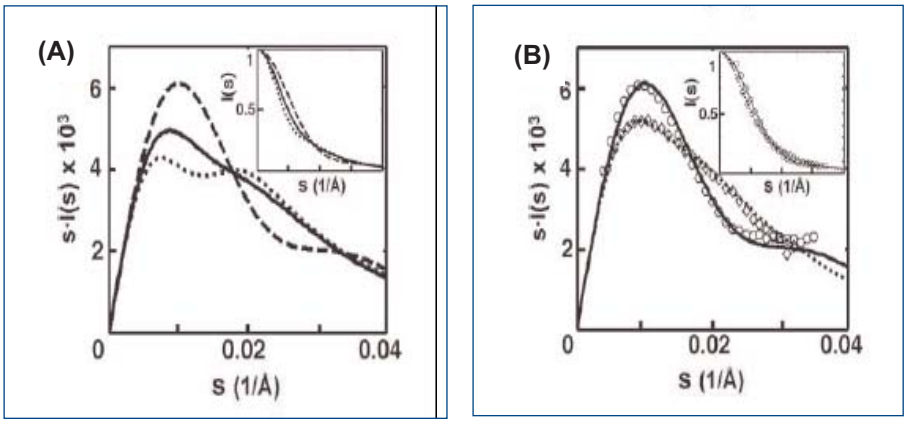

Fig. 2. Monitoring conformational states of the tethered DNA duplexes by SAXS. (A) Predicted SAXS profiles of the extended (dotted line), random (solid line), and collapsed (dashed line) states of 12-bp tethered DNA. Scattering intensity *I*(s) has been multiplied by the scattering angle *s* to help illustrate SAXS profile differences; inset shows the unweighted profile with intensity normalized to unity at s = 0. (B) Experimental SAXS profiles of 24-bp duplex DNA (diamonds) and circular DNA (circles) compared to the predicted SAXS profiles of the duplex (dotted line) and circular (solid line) DNA. (Inset) Plots of *I*(s), normalized as in (A). SAXS data were obtained with 0.2-mM DNA in 1.2 M NaCl/100-mM Na-Mops, pH 7.0.

RNA molecules, scientists must better understand the shape and charge of the ion atmosphere, whose constant flux makes it unsuitable for crystallography. Neutron scattering and small-angle x-ray scattering (SAXS) can provide information about the shape of the ion atmosphere, and researchers have used these methods to narrow down its breadth. But to determine how positive or negative the atmosphere becomes with the buildup of positive ions, the Stanford scientists tied two DNA molecules together to see what close company they would keep.

The researchers first tested whether structures derived from SAXS profiles can be distinguished from one another. To do so, they used a small DNA helix to represent DNA that is long and extended. They compared this to a circular DNA molecule that takes the shape of folded, collapsed DNA. The two conformations resulted in distinct SAXS profiles.

Next, the group wanted to determine the shapes that two independent, yet linked, helices would take under electrochemical conditions replete with positive ions. If repulsive forces kept the helices apart, the researchers would see SAXS profiles that indicated an extended molecule. If the helices were neither repulsed by nor attracted to each other, the SAXS profile would indicate a relaxed, floppy molecule (a third shape in addition to the extended and collapsed forms). If, however, large amounts of positive ions caused an attraction, the SAXS profiles would appear more like the collapsed DNA molecule.

To keep the two DNA helices close enough to test how they react to one another yet still able to move about in solution, the team linked them together with a polymer that had no charge. The researchers mixed the linked helices with low or high concentrations of positively charged ions and took SAXS snapshots (Fig. 1). The DNA helices with low levels of positive ions milling about appeared as extended molecules, indicating high repulsive forces, as expected. High levels of singly charged ions resulted in floppy molecules, also consistent with previous data. However, in contrast to the evidence that divalent cations can induce DNA collapse on long molecules, the researchers found that ion concentrations higher than those normally found within cells do not beget such an attractive force for the smaller molecule (Fig. 2). The researchers concluded that biologists modeling possible structures of small nucleic acids can ignore the attractive force. The team has applied this finding to subsequent work on ribozymes, small enzymes made of RNA and cations, and used the linked DNA helices to further study repulsive forces. — *Mary Beckman*

See: Y. Bai, R. Das, I. S. Millett, D. Herschlag, and S. Doniach, "Probing Counterion Modulated Repulsion and Attraction between Nucleic Acid Dplexes in Solution," Proc. Natl. Acad. Sci. U S A. **102**, 1035 (25 January 2005).

Author Affiliation: Stanford University
Correspondence: herschla@cmgm.stanford.edu

This work was supported by National Institutes of Health Grant PO1 GM066275 and U.S. Department of Energy Contract W-31-109-ENG-38 (to the Advanced Photon Source, beamline 12-ID, University of Chicago, and Intense Pulsed Neutron Source). Y.B. and R.D. were partially supported by Stanford Graduate Fellowships and a National Science Foundation graduate fellowship, respectively. Beamline 4-2 of the Stanford Synchrotron Radiation Laboratory and beamline 12-ID of the Advanced Photon Source are supported by the National Institutes of Health and U.S. Department of Energy.

ZINC CONCENTRATIONS IN ESOPHAGEAL TISSUE AND THE RISK OF ESOPHAGEAL CANCER

Studies in rats have shown that zinc deficiency enhances the effects of certain nitrosamines that act as esophageal carcinogens, and that the mechanisms that increase the incidence of esophageal cancers operate locally inside esophageal tissues, rather than through changes in carcinogenic metabolism at other sites, such as the liver. To study the relationship between zinc levels in esophageal tissues and the risk of developing esophageal squamous-cell carcinoma in humans, researchers from the National Cancer Institute, Argonne National Laboratory, and the Chinese Academy of Medical Sciences measured zinc concentrations in human tissue directly, using x-ray fluorescence spectroscopy at the XOR 2-BM beamline at the APS. X-ray fluorescence spectroscopy can nondestructively measure multiple-element concentrations in very small amounts of tissue. This was the first prospective study to determine the association between elemental zinc levels in human esophageal tissues and the incidence of esophageal squamous-cell carcinoma.

X-ray fluorescence spectroscopy has advantages over other methods of measurement, such as quantifying serum zinc levels or estimating dietary zinc intake, precisely because it can directly measure elemental levels inside tissues. Serum zinc concentrations are maintained homeostatically, so serum zinc is a weak marker of zinc concentrations in human tissues. Estimating zinc intake on the basis of nutrient density in diet is likewise complicated by the fact that other dietary constituents can have dramatic effects on zinc bioavailability. For example, phytate in whole grain prohibits the uptake of dietary zinc.

The subjects were from Linzhou, People's Republic of China, which has one of the highest rates of esophageal squamous-cell cancer in the world. They were selected from a group of 440 healthy subjects that had filled out demographic questionnaires and had endoscopies and tissue samples taken in 1985. All of these subjects were followed over the years to check their vital status and incidence of cancer through May 31, 2001. Sixty of the initially screened subjects were chosen for study because they had developed esophageal squamous-cell carcinomas and had sufficient tissue remaining in their biopsy specimens for x-ray fluorescence analysis. From those who had not developed cancer, the researchers selected 72 subjects who were matched to the cancer subjects on the basis of their esophageal health at baseline and who had sufficient tissue remaining in their biopsy material. X-ray fluorescence measurements were completed on tissue samples from a total of 132 people. Levels of copper, iron, nickel, and sulfur were also assessed, in part to eliminate the possibility of confounding effects. High concentrations of iron, for example, are known to be associated with an increased risk of esophageal cancer, and metallic nickel and certain nickel compounds are suspected human carcinogens.

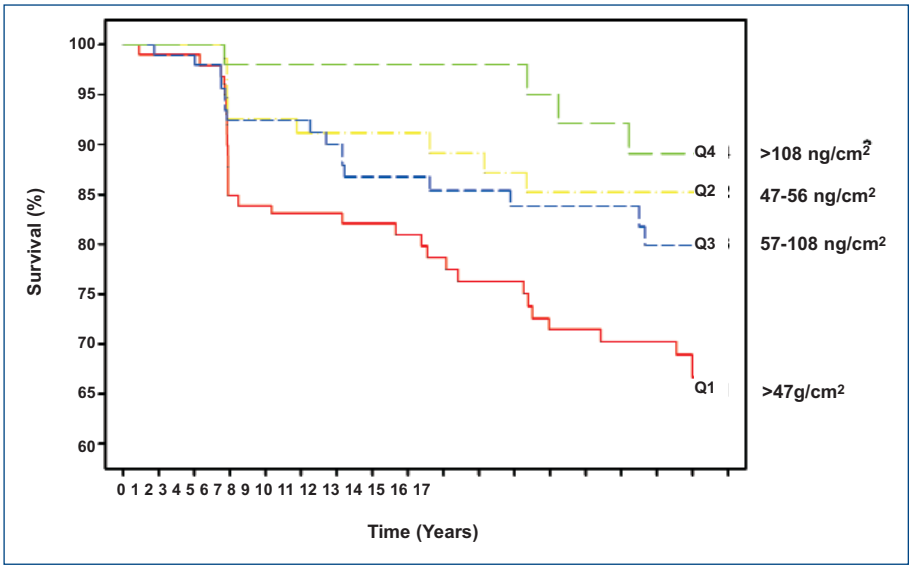

Fig. 1. Percentage of incident esophageal squamous-cell carcinoma-free survival among study subjects. Q1 through Q4 refer to tissue zinc concentration quartiles, with Q1 having the lowest concentrations of zinc and Q4 having the highest. Individuals in Q1 had a much lower probability of being disease-free at the end of the follow-up than individuals in Q4.

A single 5-μm-thick section was cut from each tissue block, and 10.5-keV x-rays were focused to a 100-μm-diameter spot at two randomly selected sites within each tissue specimen. National Institute of Standards and Technology standards NBS 1832 and NBS 1833 were subjected to similar x-ray exposures to provide a basis for quantitative estimates of elemental concentrations.

Approximately 90% of the individuals in the highest zinc quartile (Q4) were alive without esophageal cancer after 16

Continued on next page

years. By contrast, only 65% of the individuals in the lowest zinc quartile (Q1) were alive without esophageal cancer. Individuals in the second (Q2) and third (Q3) quartiles of zinc concentration showed intermediary disease-free survival rates of 85% and 80%, respectively (Fig. 1). The results for copper, iron, nickel, and sulfur were equivocal, leading the researchers to conclude that the importance of these elements in the risk of developing esophageal squamous-cell carcinoma requires further study.

The research strengthened the hypothesis that zinc deficiency is a contributing factor to the development of esophageal squamous-cell carcinoma in humans. It also demonstrated a method to accurately measure elemental concentrations in small esophageal biopsy specimens. Prospectively collected tissue samples are precious resources that must be used sparingly to address important hypotheses via analytical techniques that have sufficient sensitivity and reproducibility. One advantage of the researcher's analytical method is the high sensitivity and multiple-element capabilities of x-ray fluorescence spectroscopy, which requires only a single tissue section from each subject. The study, therefore, provides a model for other prospective studies of the potential associations between nutritional or toxic elements and the risk of subsequent disease.

— Vic Comello

See: C.C. Abnet[1], B. Lai[2], Y.-L. Qiao[3], S. Vogt[2], X.-M. Luo[3], P.R. Taylor[1], Z.-W. Dong[3], S.D. Mark[1], and S.M. Dawsey[1], "Zinc Concentration in Esophageal Biopsy Specimens Measured by X-ray Fluorescence and Esophageal Cancer Risk," J. Natl. Cancer I. **97**(4), 301 (16 February 2005).

Author Affiliations: [1]National Cancer Institute, [2]Argonne National Laboratory, [3]Chinese Academy of Medical Sciences
Correspondence: abnetc@mail.nih.gov

This study was supported by the Intramural Research Program of the National Institutes of Health and the National Cancer Institute and the following contracts from the U.S. Department of Health and Human Services, National Institutes of Health: N01-SC-91030, N01-CP-40540, 263-MQ-822420, 263-MQ-731789. Use of the Advanced Photon Source was supported by the U.S. Department of Energy, Office of Science, Office of Basic Energy Sciences, under Contract No. W-31-109-ENG-38.

Negatively-charged Lipids for Gene Therapy

Gene therapy, using either viral or synthetic DNA delivery systems, is one of the most promising strategies for curing many hereditary and acquired diseases. Among the synthetic DNA delivery systems, those based on negative ion fatty acids (anionic lipids, or ALs) are being examined as an alternative to cationic lipid (CL)-DNA complexes because the former are less likely to damage cells. Although ALs can be complexed with anionic DNA via interactions with multivalent cations, such as Ca^{2+}, and have been shown to successfully transfer oligonucleotides (molecules made up of a small number of the nucleotide units that are building blocks of DNA or RNA), the inefficient association between the ALs and DNA molecules remains an outstanding problem with this approach. To help provide a basis for the rational design of AL-DNA vectors, researchers used small-angle x-ray scattering (SAXS) and confocal microscopy at the Frederick Seitz Materials Research Laboratory, the Stanford Synchrotron Radiation Laboratory, and the XOR/UNI 34-ID beamline at the APS.

The researchers, from the University of Illinois at Urbana-Champaign and the National Institutes of Health, used SAXS and confocal microscopy to systematically investigate the anionic lipid (AL)-DNA complexes induced by a wide range of divalent ions, to show how different ion-mediated interactions are expressed in the self-assembled structures. The SAXS measurements were made at the Frederick Seitz Materials Research Laboratory, the Stanford Synchrotron Radiation Laboratory, and the XOR/UNI 34-ID beamline at the APS. The governing interactions in AL-DNA systems were found to be complex, as divalent ions can mediate strong attractions between the components in various combinations. Moreover, divalent cations can coordinate non-electrostatically with lipids, thereby modifying the resultant membrane structure. It was found that at low membrane charge densities, AL-DNA complexes self-assemble into a lamellar structure having alternating layers of like-charged DNA and anionic membranes bound together with divalent cations. This is the condensed DNA-ion-membrane lamellar phase. As the membrane charge density is increased, a new phase appears having no analog in cationic lipid (CL)-DNA systems. In this phase, DNA is expelled from the complex, and the divalent ions mediate attractions between anionic membrane sheets to form a lamellar stack of membranes and intercalated ions. This is the condensed ion-membrane lamellar phase.

Divalent ions differ in their tendency to coordinate non-electrostatically with lipids. Zn^{2+} ions are known to have strong non-electrostatic interactions with lipids, involving significant

dehydration of the lipid headgroups. The researchers found that both lamellar phases are destabilized as the global Zn^{2+} concentration is increased. The system in this case forms an inverted hexagonal phase, comprising a hexagonal array of divalent cation-coated DNA strands wrapped in turn by anionic membrane monolayers (see Fig. 1). Although Zn^{2+} is known to adhere to both lipids and DNA, the researchers believe that the change in AL-DNA structure is caused primarily by a cation-induced change in the membrane's spontaneous curvature. A simple theoretical model that takes into account the electrostatic interactions and the membrane's elastic contributions to the free energy shows that this transition is consistent with an ion-induced change in the membrane's spontaneous curvature. Moreover, the crossover between the lamellar and inverted hexagonal phases occurs at a critical curvature that agrees well with experimental values. — *Vic Comello*

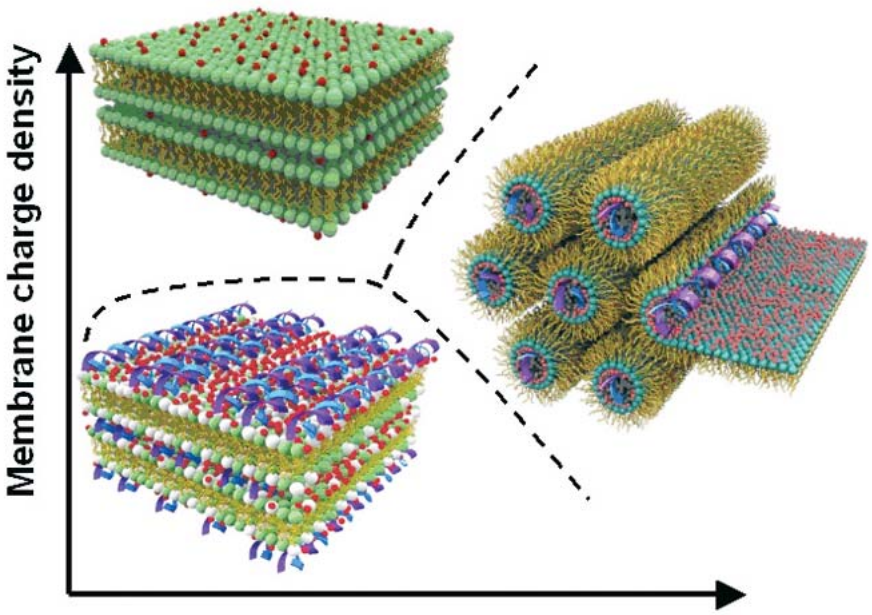

Fig. 1. A phase diagram for anionic lipid-DNA complexes, showing the two distinct lamellar phases (left) and the inverted hexagonal phase (right).

See: H. Liang[1], D. Harries[2], and G.C.L. Wong[1], "Polymorphism of DNA-anionic Liposome Complexes Reveals Hierarchy of Ion-mediated Interactions," Proc. Nat. Acad. Sci. USA, **102** (32), 11173 (9 August 2005).

Author Affiliations: [1]University of Illinois at Urbana-Champaign, [2]National Institutes of Health
Correspondence: gclwong@uiuc.edu

This work was supported in part by the U.S. Department of Energy, Division of Materials Sciences, under Award DEFG02-91ER45439, through the Frederick Seitz Materials Research Laboratory at the University of Illinois at Urbana-Champaign, the National Science Foundation Nanoscience and Engineering Initiative, and the Petroleum Research Fund. Use of the Advanced Photon Source was supported by the U.S. Department of Energy, Office of Science, Office of Basic Energy Sciences, under Contract No. W-31-109-ENG-38.

AROUND THE EXPERIMENT HALL

A LEAD TO THE ROOT CAUSE OF BEETHOVEN'S DEMISE

What killed famed composer Ludwig von Beethoven? On December 6, Argonne researchers Francesco De Carlo, Ken Kemner, and Derrick Mancini;, and Bill Walsh from the Pfeiffer Treatment Center in Warrenville, Ill., provided insight into this 178-year-old mystery. X-ray fluorescence spectroscopy at the XOR sector 2 bending magnet beamline revealed that the lead content in Beethoven's hair at the time of his death was 60 ppm, about 100 times higher than normal. Analysis of bone fragments from the composer's skull showed that they, too, had a greatly elevated lead content. The same state-of-the-art x-ray equipment and techniques that were used to quantify the lead in Beethoven's hair and bones are being employed at the APS and other DOE synchrotron x-ray facilities to guide researchers toward, for instance, ways of cleaning up the environment, improving existing energy technology, looking for alternative energy sources, furthering the cause of national security, and designing new pharmaceuticals. In the photo, Kemner meets the press in the APS atrium.
For more information, see http://www.anl.gov/Media_Center/News/2005/news051206.html.
Contact: decarlo@aps.anl.gov, kemner@anl.gov, mancini@aps.anl.gov, bill.walsh@hriptc.org

Structure of a Human Sex Hormone

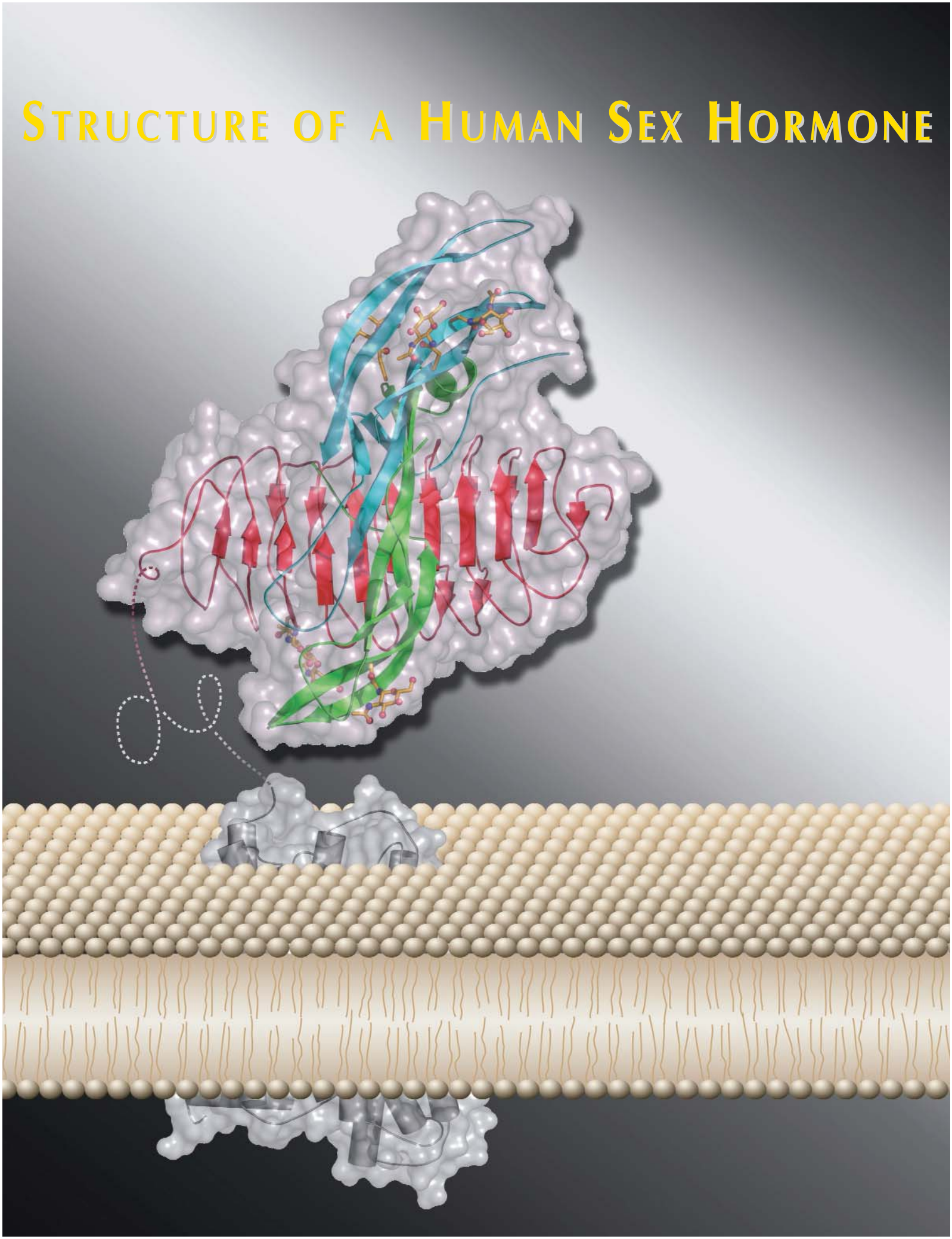

AND ITS RECEPTOR

Synchrotron x-rays have provided the closest-ever look at the active form of a human hormone used to treat infertility. Called human follicle-stimulating hormone (FSH), it induces the development of eggs in women and the formation of sperm in men. FSH works by latching onto a receptor protein on the surface of certain ovarian or testicular cells. Using x-ray crystallography, investigators from Columbia University solved the structure of the hormone and its receptor, both bound together. Greater understanding of the structural details of this joining could help in the design of new contraceptives and infertility treatments.

FSH is part of a family of "glycoprotein" hormones, which consist of a protein core studded with sugar molecules. The receptors for these hormones project from and extend through the cell membrane. When hormones stick to them, the receptors experience shape changes that propagate through the cell membrane and send signals inside the cell, altering its behavior in some way. To try to understand how such receptors accomplish both binding and signaling, researchers from Columbia University crystallized FSH, together with the hormone-binding region of its receptor. They and other groups had solved the structures of several of these hormones alone, without the receptor.

The hormone lies across an elongated, curved receptor, like hands clasping each other (Fig. 1). The x-ray crystallographic structure derived from studies on SGX-CAT beamline 31-ID at the APS and beamline X4A of the National Synchrotron Light Source at Brookhaven National Laboratory reveals the receptor to be a solid, bent tube. The hormone lies on the tube's concave side, perpendicular to its long axis. The hormone bends slightly, twists at one end, and becomes more rigid upon receptor binding, the authors conclude from a comparison of the structures of the free and bound hormone. The contact area between the two proteins is dense with positively charged amino acids on the hormone's side and negatively charged amino acids on the receptor's side. Atomic details of the contact interface explain how the FSH hormone uniquely recognizes its specific receptor. No sugars are sandwiched between them, indicating that the hormone's sugars are not important for receptor binding. The hormone-receptor complex forms a roughly symmetric dimer, or bound pair, in the crystal. This dimer formation may play a role in turning on the receptor, the researchers speculate.

The structure is consistent with a model of receptor activation, in which the receptor-bound hormone contacts an additional site in the membrane-spanning domain for activation. The authors argue, based on many similarities in structure and amino acid sequence and on comparisons with results from biochemical studies, that all hormones in this class should bind and activate their receptors in the same way. — *JR Minkel*

< Fig. 1. Human follicle-stimulating hormone (green, teal) bound to the hormone-binding region of its receptor (red), which is depicted as it would project from the cell membrane. The proteins bind each other in a perpendicular "hand-clasp" orientation.

See: Qing R. Fan[1] and Wayne A. Hendrickson[1,2], "Structure of Human Follicle-Stimulating Hormone in Complex with Its Receptor," Nature **433**, 269 (20 January 2005).

Author Affiliation: Columbia University
Correspondence: wayne@convex.hhmi.columbia.edu

Beamline X4A at the National Synchrotron Light Source is supported by the New York Structural Biology Center, and beamline 31-ID at the APS is supported by SGX Pharmaceuticals, Inc. NSLS and APS are U.S. Department of Energy facilities. Work was supported in part by an NIH grant. Q.R.F. is an Agouron Institute fellow of the Jane Coffin Childs Memorial Foundation. Use of the Advanced Photon Source was supported by the U.S. Department of Energy, Office of Science, Office of Basic Energy Sciences, under Contract No. W-31-109-ENG-38.

CAVITY CONSTRUCTION

To understand how biological processes—from antibiotics to reproduction—work, scientists need to understand how protein enzymes speed up chemical reactions within and between molecules. But protein engineers have difficulty designing the three-dimensional structures in proteins that hold onto molecules and make them react. To investigate the issue, researchers from The Scripps Research Institute used the GM/CA-CAT beamline 23-ID at the APS and the 9-1 beamline at the Stanford Synchrotron Radiation Laboratory (SSRL) to determine whether spacious pockets could be engineered within protein coils. The ability to make such pockets is the first step in eventually customizing enzymes to perform a variety of natural and artificial chemical reactions.

Proteins are chains of amino acid building blocks that twist and fold into a variety of shapes, depending on how the building blocks fit together. These shapes include helices, flat sheets, and disorganized blobs. Enzymes often have clefts or canyons into which other molecules can fit. Inside these cavities, the chemically reactive "active site" performs the magic enzymatic reaction. A common architectural feature of active site clefts are helices, which often form the walls of the active site cleft.

To find out whether it is possible to design clefts from scratch that would hold a small molecule, the Scripps researchers turned to a bit of protein called GCN4-pLI. This peptide is a 33-amino-acid-long piece of a larger, well-studied protein called GCN4. Inside cells, the peptide forms a helix, and two helices wrap around each other to become a so-called "coiled coil." Two coiled coils team up to allow GCN4 to perform its reaction. The researchers chose GCN4-pLI because it is small, easy to work with, and can assemble even with a few mutations. The team chemically synthesized 15 different versions of GCN4-pLI. Each contained a change to one amino acid. Because scientists know the three-dimensional shape of the peptide, the Scripps group was able to alter amino acid positions that fell within the interior core of the peptide coils. Like designers eliminating clutter, they replaced large bulky amino acids with smaller ones, hoping to open up some space in the core.

To determine the three-dimensional structure, the team produced the mutant peptides, spurred them to crystallize, and collected data at the Scripps Institute (larger crystals) and the SSRL and APS (smaller crystals). After determining the three-dimensional structures of the peptides, the team found that all of the mutants had structural differences compared with the original GCN4-pLI. Most had open spaces surrounded by four sides, though some had more of a tunnel running though the coils. The researchers were unable to accurately measure some of the cavities, but the remaining dozen ranged in volume from 80 $Å^3$ to 370 $Å^3$, compared with spaces of 20 to 40 $Å^3$ found in normal GCN4-pLI. To determine whether a small molecule could fit comfortably within the spaces, the group added iodobenzene to two mutants with cavities measuring about 220 $Å^3$ in size. One iodobenzene molecule fit well in either of the spaces, proving that appropriately engineered cavities for molecules could be successfully designed (Fig.1). — *Mary Beckman*

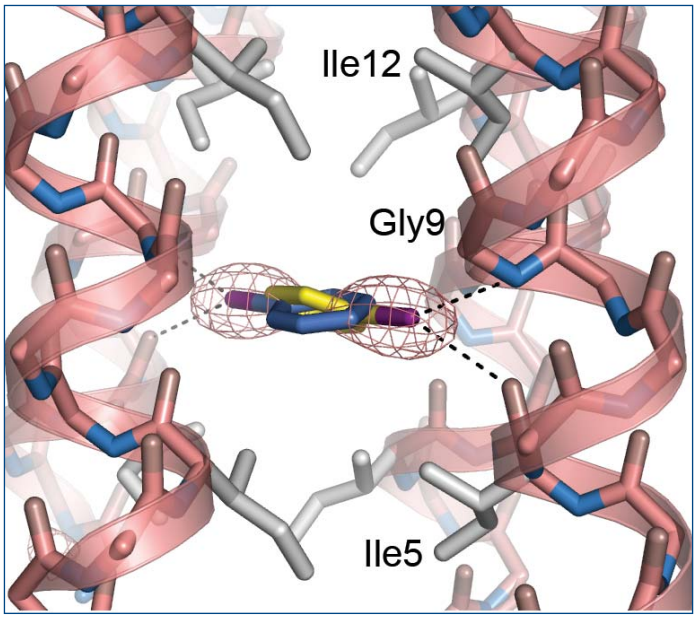

Fig. 1. Amid the helices of congregating peptides, a small molecule hangs in an engineered space. Two overlapping molecules are shown because the molecule can be in one of two positions.

See: M.K. Yadav, J.E. Redman, L.J. Leman, J.M. Alvarez-Gutierrez, Y. Zhang, C.D. Stout, and M.R. Ghadiri, "Structure-Based Engineering of Internal Cavities in Coiled-Coil Peptides," Biochem. **44**, 9723 (19 July 2005).

Author Affiliation: The Scripps Research Institute
Correspondence: ghadiri@scripps.edu

This work was supported by National Institutes of Health Grant GM52190. J.E.R., J.M.A.-G., and L.J.L. were supported by the Wellcome Trust (061454/Z/00/Z), the Spanish Ministerio de Ciencia y Tecnología, and the National Science Foundation, respectively. GM/CA-CAT has been funded in whole or in part with Federal funds from the National Cancer Institute (Y1-CO-1020) and the National Institute of General Medical Sciences (Y1-GM-1104). Use of the Advanced Photon Source was supported by the U.S. Department of Energy, Office of Science, Office of Basic Energy Sciences, under Contract No. W-31-109-ENG-38.

BETRAYING THE NEUROTOXIC TROJAN HORSE

Botulinum neurotoxin (BoNT) paralyzes its victims, and if it doesn't soon kill them, renders them helpless and dependent on mechanical breathing devices for months until the toxin clears the body. Although the medical community has found the toxin helpful (for example, in ameliorating muscle spasms in cerebral palsy and migraines), the defense community would like to better prepare against its use as a weapon. Researchers from The Scripps Research Institute used the GM/CA-CAT beamline 23-ID at the APS to determine the three-dimensional shape of one of the seven BoNT variants. The structure appears to be slightly different from the three variants that researchers have already uncovered, providing insight into the toxin's deadly game.

People catch botulism from contaminated food or an infection that lets in *Clostridium botulinum*. The bacteria exude a neurotoxin into the blood, where the toxin floats around inconspicuously, until it finds and enters neurons. Inside the nerve cells, the toxin, a protein, reveals its Trojan Horse leanings: a chunk of the toxin known as the light chain splits off and activates, chewing up another protein needed by neurons and causing neuromuscular paralysis. Of the seven BoNT variations, three chop up the same neural protein, although one of those three can also gnaw down a second neural protein. The remaining four types—B, D, F, and G—destroy a third neural protein. The overall shapes of three of these toxin light chains are known, including A—more famously known as Botox®. Determining the three-dimensional forms of the remaining four will help explain how each toxin recognizes, grabs, and chews up the neural proteins of its choice.

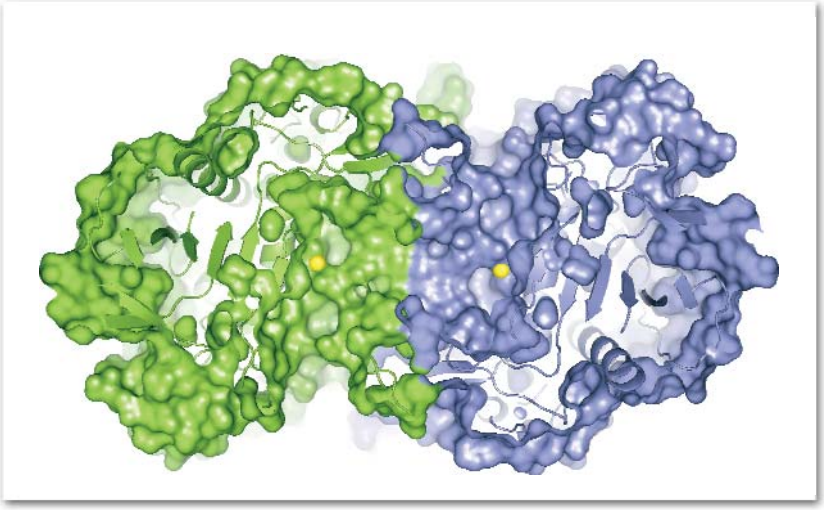

Fig. 1. Channel surfing: Two copies of light chain G (green and purple) nestle side-by-side, creating a channel with their central clefts, seen here with zinc atoms (yellow) resting inside.

The Scripps team decided to tackle light-chain G, a variant recently discovered in soil. To do so, they first had to form crystals of the toxin protein. Diffraction data collected at beamline 23-ID, at a wavelength of 1.009 Å, allowed the group to determine the overall shape of the toxin, as well as to view the cleft in which the toxin snags and cuts its victim, a neural protein called VAMP.

The team found that the structure of G on its own differed from the other types, and from when it is contained within the entire toxin complex. This result could help explain how the light chain gets turned on only after losing its toxin partner. The researchers also found that the clefts between two light chains sitting side by side in the crystal connected, forming one long channel. The biological significance to this particular feature, if any, is still under study.

Within the cleft, the team located a single zinc atom. It is known that BoNT uses zinc to axe neural proteins, so the site where the atom resides is likely important for the chemical reaction used to snip VAMP. Although the Scripps group did not add VAMP to the crystal mix, a computer-generated model of VAMP appeared to fit quite nicely in the toxin's cleft.

Lastly, comparing the G light chain to other BoNT light chains allowed the team to identify regions similar in all versions. This suggested which regions on the light chains were more important than others—leads that can be followed up by biochemical experiments. — *Mary Beckman*

See: J.W. Arndt, W. Yu, F. Bi, and R.C. Stevens, "Crystal Structure of Botulinum Neurotoxin Type G Light Chain: Serotype Divergence in Substrate Recognition," Biochem. **44**, 9574 (19 July 2005).

Author Affiliation: The Scripps Research Institute
Correspondence: stevens@scripps.edu

This work is supported in part by the PSWRCE (U54 GM AI065359). Portions of this research were carried out at the General Medicine and Cancer Institutes Collaborative Access Team (GM/CA-CAT) beamlines of the Advanced Photon Source (APS). GM/CA-CAT has been funded in whole or in part with Federal funds from the National Cancer Institute (Y1-CO-1020) and the National Institute of General Medical Sciences (Y1-GM-1104). Use of the APS was supported by the U.S. Department of Energy, Basic Energy Sciences, Office of Science, under Contract W-31-109-ENG-38.

Making Protein Production a Lean Machine

Assembling proteins in a cell is much like assembling cars in a factory—all of the necessary components must be present in order for production to go forward. Just as current manufacturing methods are lean and depend on "just-in-time" delivery of parts, cellular processes for manufacturing protein are very efficient. One example of this efficiency is the way mammal and yeast cells behave when they are starved and when certain amino acids needed to make proteins are in low supply or unavailable. An enzyme system that regulates protein synthesis slows overall protein production even while production of proteins that help combat cellular stress continues. How these wonder enzymes accomplish such a feat is made elegantly clear by the structural data collected at the SGX-CAT beamline 31-ID.

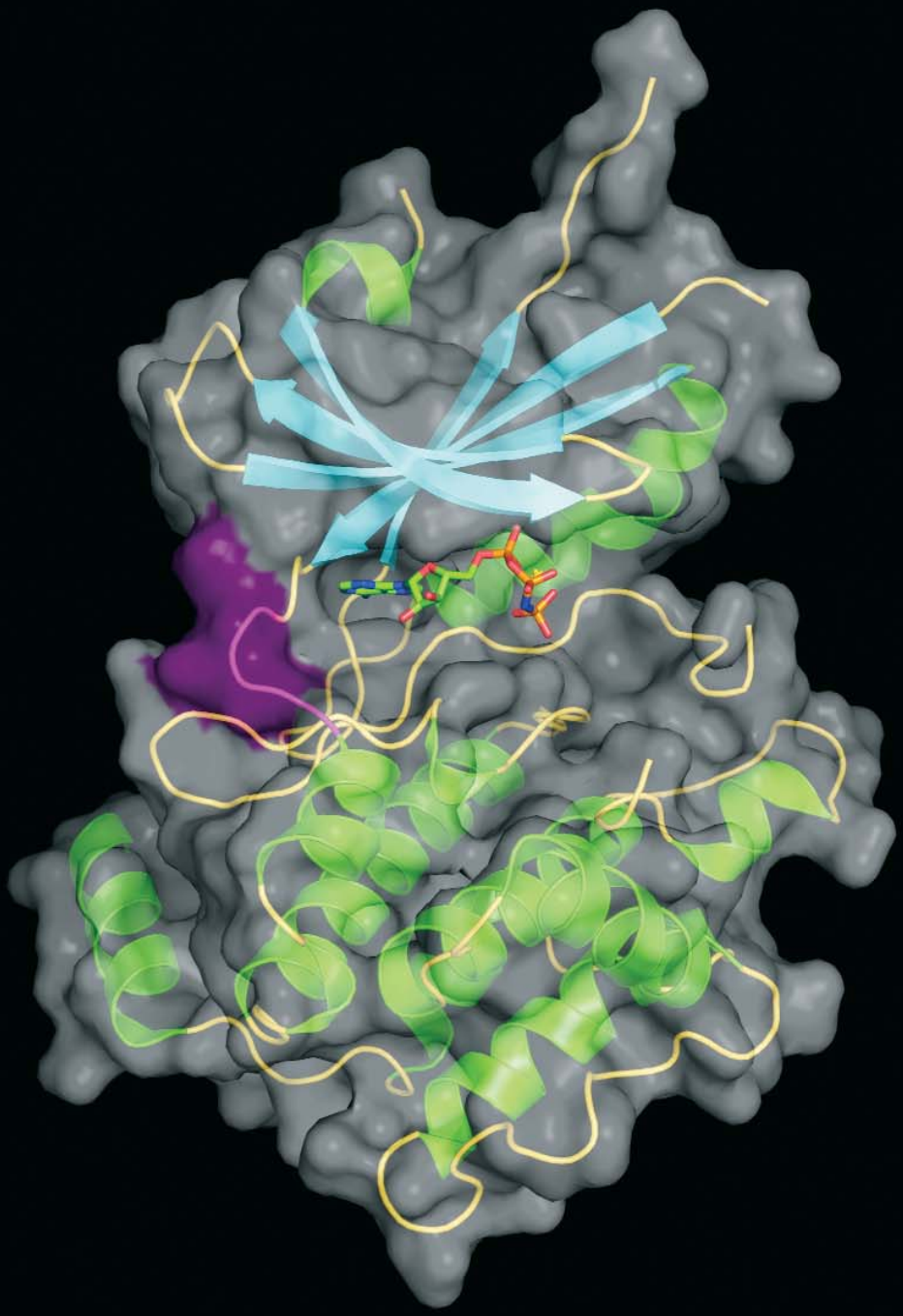

New knowledge about the subtleties of protein production makes it easier to understand what happens when the mechanisms go awry, cells malfunction, and a disease state ensues. The researchers from SGX Pharmaceuticals, Inc.; The Rockefeller University; The National Institutes of Health; and the University of California, San Francisco, took a unique approach to this particular enzyme system. They studied the structure of a mutant form of the protein kinase GNC2 from yeast cells in order to understand the behavior of the normal form. By doing so, they were able to determine that a two-step activation process, and its regulation, nicely explains both activation and slowing of protein production.

Protein kinases help keep protein assembly efficient by controlling whether phosphate is added to an initiation factor. GCN2 is a protein kinase that is inactive, or autoinhibited, in normal cells, and activated when cells are under stress, such as amino acid starvation or UV irradiation. So, GCN2 is called into play when the cell is slowing down total protein production and in need of those proteins that help the cell respond to stress. To bring GCN2 back into an active state requires binding of an empty transfer RNA molecule, one that should be carrying an amino acid but isn't because the cellular supply is low. The main question in the work conducted by the research team centered on exactly how all of this activity is manifested in structural changes.

To answer that question, the team determined x-ray structures of normal and mutant GNC2 from yeast cells (Fig. 1). By doing so, they came up with a tantalizing two-step model for activating GNC2. The first step involves rearranging the shape of the hinge region. The shape change in the first step allows the second step, binding of an adenosine triphosphate (ATP) molecule, to occur. In the inactive, autoinhibited form of GNC2, the shape of the hinge area is such that the second step, ATP binding, cannot occur. The necessary remodeling of the GNC2 hinge region, which is mediated by binding of the empty transfer RNA molecule, was clear in the mutant form of the enzyme, where a way to activate GNC2 independent of transfer RNA binding could be used.

A detailed comparison of the shape changes in the normal and mutant GNC2 made it easy to see why ATP binding could not occur when the enzyme is in its autoinhibited state. The mutant form also showed interesting flexibility resulting from loss of amino acid interactions that would be present in the normal form. These interactions within a molecule appear to be important for the hinge area remodeling that occurs after binding of transfer RNA. Knowledge of such differences could be used to great benefit in the design of pharmaceuticals.

By studying the mutant form of GCN2, the behavior of the normal form comes into focus. What the researchers discovered fits well with existing data, paves the way for increasingly sophisticated studies of this protein kinase involved in the stress response, and is downright beautiful. The magnificent efficiency of the protein assembly line has just become much easier to understand. — *Mona Mort*

See: A.K. Padyana[1,2], H. Qiu[3], A. Roll-Mecak[2,4], A.G. Hinnebusch[3], and S.K. Burley[1,2], "Structural Basis for Autoinhibition and Mutational Activation of Eukaryotic Initiation Factor2a Protein Kinase GCN2," J. Biol. Chem. **280**(32), 29289 (2005).

Author Affiliations: [1]SGX Pharmaceuticals, Inc.; [2]The Rockefeller University; [3]National Institutes of Health; [4]University of California, San Francisco

Correspondence: sburley@sgxpharma.com and anil_padyana@yahoo.com

This work was supported by the National Institutes of Health, the U.S. Department of Energy, and SGX Pharmaceuticals, Inc. Use of the Advanced Photon Source was supported by the U.S. Department of Energy, Office of Science, Office of Basic Energy Sciences, under Contract No. W-31-109-ENG-38.

< Fig. 1. Structure of the mutant form of GCN2 protein kinase. The white monomer surface is rendered semi-transparent and shown with an embedded protein ribbon containing α-helices (green), β-strands (cyan), and loops (gold). The magenta-colored portion of the surface incorporates the mutation site and exhibits structural flexibility to regulate the GCN2 kinase activity. The small molecule that is at the surface crevice is a non-hydrolysable analog of ATP shown in stick representation.

How SUMO Grapples with a Target

The first complete picture of the crystal structure of a cluster of proteins that helps regulate the life cycle of a cell has been determined by researchers from the Sloan-Kettering Institute. The structure suggests the mechanism by which one of these proteins, a molecular "tag" called SUMO (small ubiquitin-related modifier), attaches to its target. Knowing how the proteins interact provides important clues about how they carry out their collective function, which includes transport of cargo into and out of the nucleus and maintaining the integrity of the cell's chromosomes during cell division. Errors in this latter process are believed to contribute to cancer, although researchers have not yet observed direct evidence suggesting that this particular set of proteins malfunctions in tumor cells.

The key protein is SUMO. When cells want to get rid of a protein or send it to a new location, they will often tag it with a small protein called ubiquitin, or a related protein such as SUMO. This tagging process requires two helper proteins: a "conjugating protein" that primes SUMO for attachment to the target protein, and a "ligase" that assists in fusing SUMO to its target. The Sloan-Kettering Institute researchers crystallized a complex between SUMO, its conjugating protein, a ligase, and a target protein that participates in moving cargo in and out of the nucleus when the entire complex is bound to the membrane surrounding the nucleus. They determined the crystal's structure from x-ray studies carried out on the SGX-CAT beamline 31-ID at the APS.

The structure shows how SUMO and its target interact through a pair of narrow projections, much like fingers (Fig. 1). The conjugating protein snugly encircles these projections like a gasket, while the ligase cradles SUMO and the conjugating protein. Because ligases generally work by touching the substrate, the authors argue that this ligase works indirectly by tethering SUMO and the conjugating protein to promote an alignment that is better able to form the chemical bond between SUMO and its target. Tethering also reduces flexibility in the proteins' shapes, which enhances the SUMO conjugation to the target. Another possible mechanism would be that the ligase binds to the active site where chemistry takes place or to key structural locations on the conjugating protein to change its shape in such a way as to promote the reaction.

To distinguish among these possibilities, the researchers prepared a series of biochemical assays using complexes incorporating different mutant forms of the ligase. The presence or absence of ligase had no effect on the chemical reactivity of the bond between SUMO and its conjugating protein, suggesting that the ligase plays no direct role in the reaction. But by deleting a portion of the ligase, researchers were able to alter interactions between the conjugating protein, SUMO, and its target, as well as the rate at which it catalyzes the linking of the two proteins. These results suggested that ligase simply stabilizes the bond between SUMO and conjugates in an optimal orientation for interaction with the target, which in turn speeds up the linking reaction. — *JR Minkel*

See: David Reverter and Christopher D. Lima, "Insights into E3 Ligase Activity Revealed by a SUMO–RanGAP1–Ubc9– Nup358 Complex," Nature. **435**, 687 (2 June 2005).

Fig. 1. Transparent surface and ribbon representation of the protein complex containing SUMO. SUMO is yellow, the conjugating protein Ubc9 is blue, the ligase Nup358/RanBP2 is magenta, and the substrate RanGAP1 is colored pink. The figure was generated using PyMOL. (http://www.pymol.org).

Author Affiliation: Sloan-Kettering Institute
Correspondence: limac@mskcc.org

Use of the SGX-CAT beamline facilities at Sector 31 of the APS was provided by SGX Pharmaceuticals, Inc., which constructed and operates the facility. D.R. and C.D.L. were supported in part by a National Institutes of Health grant. C.D.L. acknowledges support from the Rita Allen Foundation. Use of the Advanced Photon Source was supported by the U.S. Department of Energy, Office of Science, Office of Basic Energy Sciences, under Contract No. W-31-109-ENG-38.

SOLVING THE STRUCTURE OF A MYSTERY ENZYME

Just as its name implies, the protein ubiquitin is ubiquitous in cells. Many different kinds of biochemical pathways appear to be regulated by adding ubiquitin to target proteins. Exactly what the purpose of this ubiquitous addition of ubiquitin might be is still a mystery. But that hasn't stopped biochemists from studying how the mysterious ubiquitin actually attaches to proteins. What has received less attention, and is still nearly as mysterious as ubiquitin itself, is the process by which enzymes remove ubiquitin from proteins. Understanding both the attaching and detaching of ubiquitin could lead to important clues about its real function. To that end, a research team from Harvard Medical School and Harvard University determined the structure of an enzyme involved in detaching ubiquitin. The mystery enzyme is a type of ubiquitin C-terminal hydrolase (UCH) that appears only in certain tissues and, when mutated, is associated with disease in humans. Solving the enzyme's structure can further our understanding of ubiquitin's role in disease.

Using the NE-CAT 8-BM beamline at the APS, the researchers studied the crystal structure of human UCH-L3 that was attached to an inhibitor called ubiquitin vinylmethylester. This inhibitor was expected to interfere with the active site on the ubiquitin-specific UCHs. Using the inhibitor allowed the investigators not only to confirm how the inhibitor (and by, extension, the enzyme functions), but also to compare the structure of the UCH enzyme when it was attached and unattached to ubiquitin. Detailed analysis of this UCH interacting with its inhibitor led the team to determine a detailed structure for the UCH enzyme. The researchers were then able to show how the UCH enzyme may remove a protein (one that was 13 amino acids long) from ubiquitin. This aspect of the work showed that the UCH enzyme could perform its detaching function with proteins of varying size; the enzyme appears to be quite flexible in this respect. The team then proposed a satisfying model that shows how the UCH enzyme and other members of the same enzyme family act to remove ubiquitin from other proteins by a process called hydrolysis.

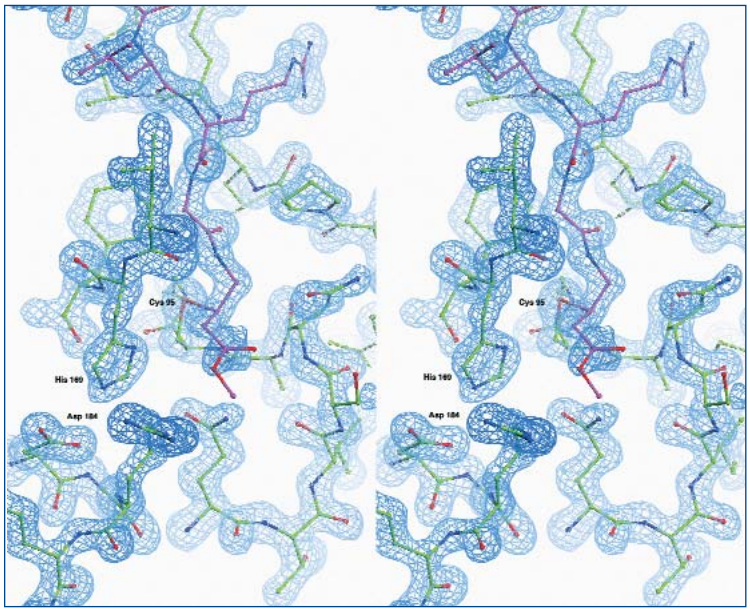

Fig. 1. Electron density of the active site of UCH-L3 (green) bound to the inhibitor ubiquitin vinylmethylester (magenta).

By facilitating hydrolysis—breaking bonds by adding a water molecule—the de-ubiquinating enzymes, also known as DUBs, act to sever the link between ubiquitin and the protein to which it is attached. In the DUB family of enzymes, there are four subclasses, one of which is the UCH group. Previous data from yeast showed a size limit on the protein that could be accommodated in the UCH detaching pathway, suggesting that a different form of the enzyme handles detaching larger proteins. In particular, a crossover loop at the active site of UCH would have to be quite flexible before attaching to the protein-ubiquitin complex. Though such a trait was suggested by previous studies, it took the careful analyses in the present study to demonstrate that this was actually the case.

The choice of the inhibitor allowed the researchers to extrapolate the mechanism by which the UCH enzyme activates the detaching of protein from ubiquitin (Fig. 1). The team also synthesized a branched protein that, from purely structural considerations, the UCH enzyme should not have been able to accommodate. Nonetheless, the team was able to show that the UCH enzyme could, in fact, hydrolyze the protein bonds and proceed with its function in the detaching of the protein from ubiquitin. This last piece of evidence strongly supports the existence of a flexible active-site crossover loop for the enzyme.

Combining the carefully collected data, the researchers proposed a model that elegantly illustrates how UCH functions to activate the detaching of ubiquitin from its attached protein. By studying the UCH enzyme both in its free state and attached

Continued on next page

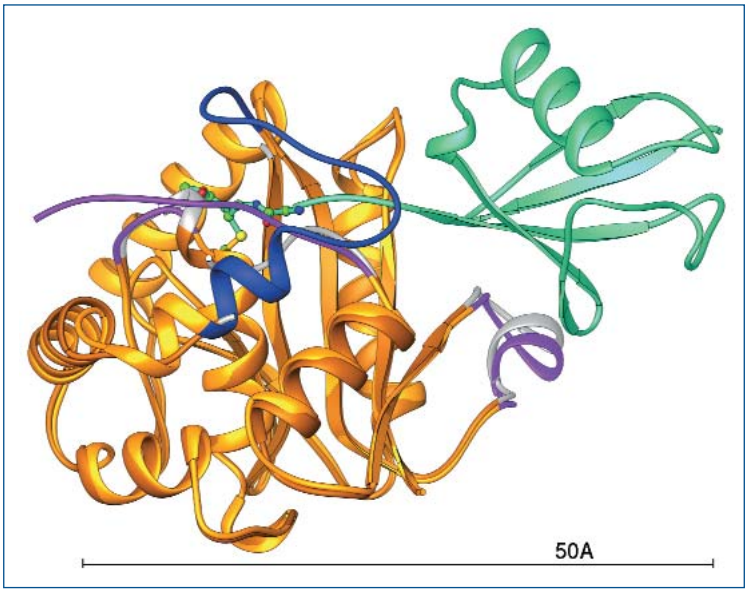

Fig. 2. Superimposed ribbon structures of UCH-L3 in the presence (gold) and absence (yellow) of the inhibitor ubiquitin vinylmethylester (green). Regions that change with binding are shown in gray, purple, and blue.

to the inhibitor, the team could precisely define the changes that occur when it binds to the ubiquitin-protein complex (Fig. 2). Knowing so much more about how the UCH enzyme behaves in the detaching of ubiquitin allows future work to concentrate on pinpointing the cellular function of the ubiquitin-protein complexes, and brings us that much closer to figuring out why ubiquitin is so ubiquitous. — *Mona Mort*

See: S. Misaghi[1], P.J. Galardy[1], W.J.N. Meester[1], H. Ovaa[1], H.L. Ploegh[1], and R. Gaudet[2], "Structure of the Ubiquitin Hydrolase UCH-L3 Complexed with a Suicide Substrate," J. Biol. Chem. **280**, 1512 (2005).

Author Affiliations: [1]Harvard Medical School, [2]Harvard University

Correspondence: misaghi@wi.mit.edu

This work was supported by grants from the National Institutes of Health (to S. M., P. J. G., and H. L. P.) and The Netherlands Organization for Scientific Research (to W. J. N. M. and H. O.). The NE-CAT is supported by Award RR-15301 from the National Center for Research Resources at the National Institutes of Health. Use of the Advanced Photon Source was supported by the U.S. Department of Energy, Office of Science, Office of Basic Energy Sciences, under Contract No. W-31-109-ENG-38.

THE AMAZING RNA AS ENZYME

More than 20 years ago, the news from Kruger et al. [1] and C. Guerrier-Takada et al. [2] rocked the biochemistry world: RNA was not only the well-known middle player in converting DNA's message to protein, but it could also act like an enzyme, catalyzing important steps in that reaction system. Since this discovery, the architecture of RNAs that act as enzymes—also known as ribozymes—has been a hotly pursued topic in molecular biology. Now, by solving the crystal structure of a natural ribozyme, ribonuclease P (RNase P), a research group from Northwestern University and The University of Chicago, using several APS beamlines, has made the astonishing abilities of these enzymatic RNAs easier to comprehend.

The research group chose to study RNase P, an important ribonucleoprotein enzyme that is necessary for proper formation of transfer RNA (tRNA), the molecule that carries amino acids to the site of protein synthesis. Without this particular ribonuclease, tRNA will not mature properly and will not be able to perform its critical role of making sure that amino acids destined to become part of proteins are in the right place at the right time. RNase P is doubly intriguing because it is present in all life forms. In fact, the structural work shows that RNase P's function is closely tied to its structure, and that the strong universal conservation of certain regions of its RNA sequence has occurred in order to maintain this particular functional RNA structure.

The team focused on producing a crystal structure for the RNA component of a RNase P from the bacterium *Thermotoga maritima*. Given the flexible nature of RNA, it is often very difficult to obtain diffraction-quality crystals. The crystals obtained from the 338-nucleotide molecule were small and diffracted weakly and differently in each direction (anisotropically), and there were often crystal-to-crystal variations (non-isomorphous). Given also the tendency of RNA molecules to bind large numbers of heavy metal ions non-specifically, a large number of potential derivatives had to be tested. It was thus essential for the team to be able to access several APS beamlines and their robotic crystal-mounting systems, wherever possible. The data were collected primarily on APS beamlines 5-ID (DND-CAT) and 32-ID (LS-CAT), with some additional work done on beamlines 17-ID (IMCA-CAT) and 22-ID (SER-CAT). The structure could be solved to a resolution of 3.85 Å from a MIRAS diffraction experiment by using Os- and Co-hexamine

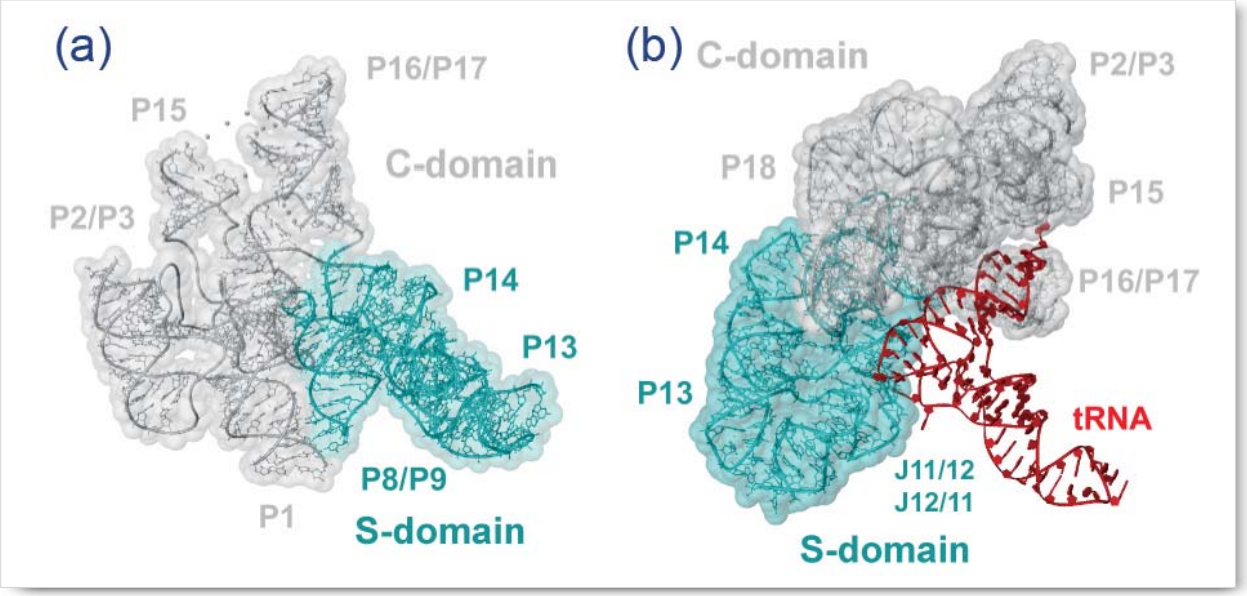

Fig. 1. A: Overall structure of *T. maritima* RNase P RNA showing the two structural domains: the catalytic domain or C-domain (gray) and the specificity domain or S-domain (cyan). B: Model of the RNase P interaction with its tRNA substrate. The tRNA T C stem loop is recognized by the S-domain, and the catalytic reaction is carried out by the C-domain. The relevant functions of both domains are carried out in the vicinity of two patches of universally conserved nucleotides.

as derivatives, aided by a molecular replacement solution found by using the specificity domain structure of *T. thermophilus*, which was solved previously by the same research groups also using the APS.

The researchers were able to describe the structure of the entire molecule and show how the structural domains are arranged. The structure revealed a two-layer architecture for the ribonuclease, where each layer is one helix thick. Most of the regions that appear to be the same in all life forms are found on one side of the larger layer.

The structure is divided into a specificity domain, one that is responsible for recognizing the correct binding partners, and the catalytic domain, the part that drives the reaction (Fig. 1). Their data show what the overall structure of the RNA is, how interactions occur within and between domains, where the universally conserved regions are, and where the recognition sites for the precursor tRNA are. Additionally, since this is one of the larger RNA molecules that have been solved, it provides new information on how different RNA domains and helices can be brought together by intricate, highly structured connecting regions.

To narrow down the region where the active site is located, the investigators built a molecular model in which tRNA was bound to the RNase P RNA (Fig. 1). Their model not only agrees with all known data, but it also suggests ways in which the two RNA molecules could recognize each other and points to where the active site is likely to be.

From this structure, it is clear that certain structural details of this ribonuclease must remain the same from one organism to another, while other characteristics are allowed to vary between organisms. Now that the overall architecture of this ribonuclease is known, future research can delve into atomic-level studies, where secrets about even more amazing traits are sure to reside. — *Mona Mort*

Reference

[1] K. Kruger, P.J. Grabowski, A.J. Zaug, J. Sands, D.E. Gottschling, and T.R. Cech, "Self-splicing RNA: Autoexcision and Autocyclization of the Ribosomal RNA Intervening Sequence of Tetrahymena," Cell **31**(1), 147 (31 November 1982).

[2] C. Guerrier-Takada, K. Gardiner, T. Marsh, N. Pace, and S. Altman, "The RNA Moiety of Ribonuclease P Is the Catalytic Subunit of the Enzyme," Cell **35**, 849 (1983).

See: A. Torres-Larios[1], K.K. Swinger[1], A.S. Krasilnikov[1,3], T. Pan[2], and A. Mondragón[1], "Crystal Structure of the RNA Component of Bacterial Ribonuclease P," Nature **437**, 584 (2005).

Author Affiliations: [1]Northwestern University, [2]The University of Chicago, [3]Pennsylvania State University
Correspondence: a-mondragon@northwestern.edu

This research was supported by an NIH grant to A.M. Support from the R.H. Lurie Cancer Center of Northwestern University to the Structural Biology Center is acknowledged. DND-CAT is supported by DuPont, Dow, and the NSF. Use of the Advanced Photon Source was supported by the U.S. Department of Energy, Office of Science, Office of Basic Energy Sciences, under Contract No. W-31-109-ENG-38.

AN ENZYME'S MANY RELATIVES

Proteins come in a bewildering array. In humans alone, researchers estimate the number of proteins to be about 30,000. Other species have similarly large complements of proteins. For researchers trying to understand the form-and-function relationship of protein shapes, that is a daunting variety. Luckily, all proteins in existence today have descended from older proteins, which were copied, mixed, matched, and tweaked along the evolutionary path. As a result, different species share many of the same proteins or very similar ones, and many proteins in a single species also share common structural pieces. Studying a single protein's structure can, therefore, fill in many gaps. Researchers from Argonne National Laboratory and The University of Chicago had this strategy in mind when they decided to scrutinize pyrroline carboxylate reductase (PCR), whose protein family numbers over 400, with representatives in bacteria, plants, and animals (including people).

X-ray studies have revealed the first structure of the enzyme pyrroline carboxylate reductase, part of a large family of proteins spread across the kingdoms of life. The result is part of an ongoing effort to catalog the most fundamental structural types from among all known proteins. The researchers crystallized PCR from two bacteria and compared the structures, to help explain how the enzyme performs its task of synthesizing proline, a key amino acid.

An enzyme that synthesizes proline ought to have an ancient lineage and therefore lots of relatives. Proline is one of the 20 amino acids, the building blocks of proteins. Bulky and rigid, it plays a unique structural function, helping flexible proteins fold properly and maintain their shape even in unfavorable conditions. Many species respond to environmental stresses, such as cold or salt, by building more proline. Pyrroline carboxylate reductase requires a so-called co-factor to catalyze the reaction that results in proline. Accordingly, the enzyme is also active in cellular metabolism, in which co-factors harness the energy locked in sugar molecules.

The researchers in this study have determined that two identical PCR molecules link to form a kidney-bean-shaped enzyme, with a crevice on each end for holding co-factor. The group extracted the enzyme from 14 different species and managed to crystallize it from two bacteria that infect humans—*Neisseria meningitides*, which causes meningitis, and *Streptococcus pyogenes*, the source of strep throat. The structures were derived from x-ray diffraction patterns measured on the SBC-CAT beamline 19-ID at the APS.

The enzyme forms proline by transferring two hydrogen atoms from the co-factor and protein to pyrroline carboxylate, a molecule very close in structure to proline. To carry out this reaction, the enzyme must bring the pyrroline carboxylate and co-factor snugly together in a precise orientation. The group studied this interaction by superimposing the *N. meningitides* enzyme, minus co-factor and pyrroline carboxylate, on two structures of the *S. pyogenes* enzyme, one bound to co-factor and the other to proline. (The proline-bound enzyme reveals pyrroline carboxylate's location before the reaction occurs.) When the three structures were lined up as well as possible, co-factor and pyrroline carboxylate were indeed close enough for hydrogen ions to jump from one to the other. Most of the amino acids responsible for binding the substrate molecules are conserved throughout PCR's family of proteins, the researchers find, suggesting that the same reaction mechanism may be common to them all. — *JR Minkel*

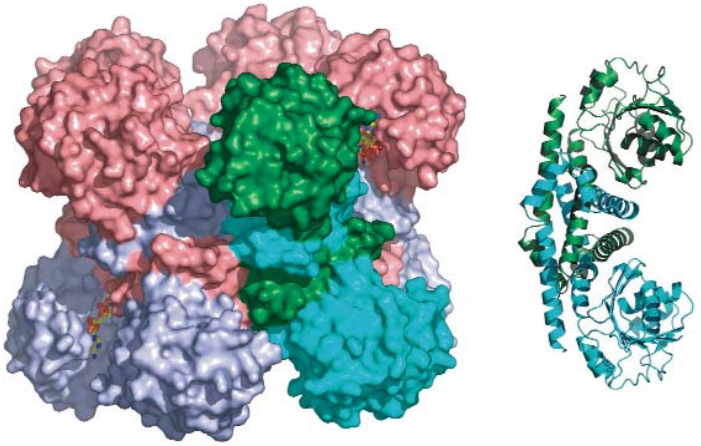

Fig. 1. The crystal structure of pyrroline carboxylate reductase from bacterium *S. pyogenes* (left, surface view) and from *N. meningitides* (right, schematic). Both enzymes consist of paired protein molecules (right), but they differ in how they cluster together in solution. Co-factor molecules (shown as a stick model) indicate the location of the active site, where the enzymatic reaction takes place that forms the amino acid proline.

See: B. Nocek[1], C. Chang[1], H. Li[1], L. Lezondra[1], D. Holzle[1], F. Collart[1], and A. Joachimiak[1,2], "Crystal Structures of Δ^1-Pyrroline-5-carboxylate Reductase from Human Pathogens *Neisseria meningitides* and *Streptococcus pyogenes*," J. Mol. Biol. **354**, 91 (2005).

Author Affiliations: [1]Argonne National Laboratory, [2]The University of Chicago **Correspondence:** andrzejj@anl.gov

This work was supported by National Institutes of Health grant GM62414 and by the U.S. Department of Energy, Office of Biological and Environmental Research, under contract W-31-109-ENG-38. Use of the Advanced Photon Source was supported by the U.S. Department of Energy, Office of Science, Office of Basic Energy Sciences, under Contract No. W-31-109-ENG-38.

ENZYME STRUCTURE SHEDS LIGHT ON ANTIBIOTIC SYNTHESIS

The widespread use of antibiotics is creating strains of bacteria that have developed resistance—they are not eliminated by drug therapy. In such cases, another antibiotic can be used for treatment, but that could lead to bacterial strains with multiple resistances. Since most prescribed antibiotics have been isolated from natural sources, it makes sense that bacteria would be genetically well equipped for developing resistance. One way around this dilemma would be to figure out how the antibiotics are made in nature and then to design a synthetic form with a few structural changes, making it harder for microbes to develop resistance. It turns out that the biochemical pathways for making antibiotics can be unusual, with unexpected twists and turns, and can take extensive labor to unravel. Thanks to experimentation by a research team from the Massachusetts Institute of Technology and the University of Texas at Austin, we are now much closer to understanding the synthetic pathway for the important antibiotic fosfomycin, which is used in treating lower urinary tract infections and against strains of *Staphylococcus aureus* that have become resistant to other antibiotics. This elegant work determined the structure of a mononuclear iron enzyme, revealing several features that are rare in biochemistry.

The biosynthetic pathway for fosfomycin includes the enzyme hydroxypropylphosphonic acid epoxidase (HppE), a member of a new subfamily of enzymes in the group called non-haem mononuclear iron enzymes. With the help of the NE-CAT 8-BM beamline at the APS, and a beamline at the National Synchrotron Light Source at Brookhaven National Laboratory, the researchers determined and studied six x-ray structures of the enzyme—in its free state and bound to iron or cobalt—ranging in resolution from 1.8 Å to 2.5 Å (Fig. 1). The high level of detail in the resulting structural data allowed the team to suggest a mechanism by which the enzyme recognizes the molecules to which it must bind and the necessary changes in shape, or conformation, that are necessary for the enzyme to carry out its assigned role in the reaction (Fig. 2).

To achieve a deeper understanding of the enzyme's unusual attributes, the investigators compared the enzyme to other members of the same family. By doing so, they were able to explain why this particular mononuclear iron enzyme can prime an iron molecule for binding of two oxygens without α-ketoglutarate—the presence of which is required in many other mononuclear iron enzymes.

By taking their analysis yet a step further, the research team also explained how the final epoxidation reaction in fosfomycin biosynthesis, which may be unique in living systems, could occur. The enzyme studied by the group—an iron-dependent epoxidase—is responsible for catalyzing the last step in making fosfomycin. Fosfomycin is an important molecule to study not only because of its importance as an antibiotic, but also because it is one of the few natural compounds with a carbon-phosphorous bond in its structure.

A look at the overall structure of the enzyme, with its β-barrel fold, explains why it is in the cupin superfamily: the Latin term for small barrel is *cupa*. Particular challenges posed by the cupin family include the question of how to activate iron for binding two oxygens. Comparing the structure of the free HppE enzyme with one bound to iron showed how the area around the metal binding site in the β-domain becomes ordered when metal binds. Because of the high level of detail in the analysis, it was possible to see that the binding process might involve two steps before catalysis occurs. Intricate molecular movements, involving a hairpin substructure and a cantilever, appear to be responsible for creating the final conformation.

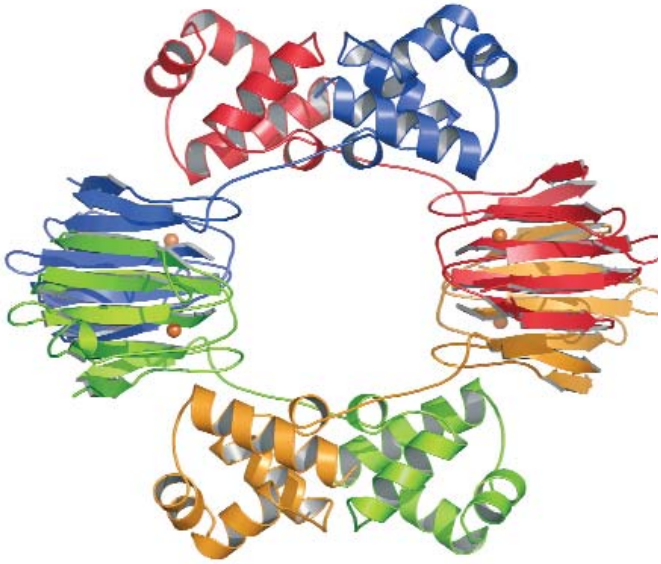

Fig. 1. The tetrameric structure of HppE.

By determining the first structures for HppE, the research team gained insight into co-factor independent mononuclear iron enzymes. Careful analysis of the structures resulted in a picture of binding and catalysis in the final stages of making fosfomycin. Using this new knowledge, synthetic production of fosfomycin-like molecules can now move forward—and with it the battle against antibiotic resistance. — *Mona Mort*

Continued on next page

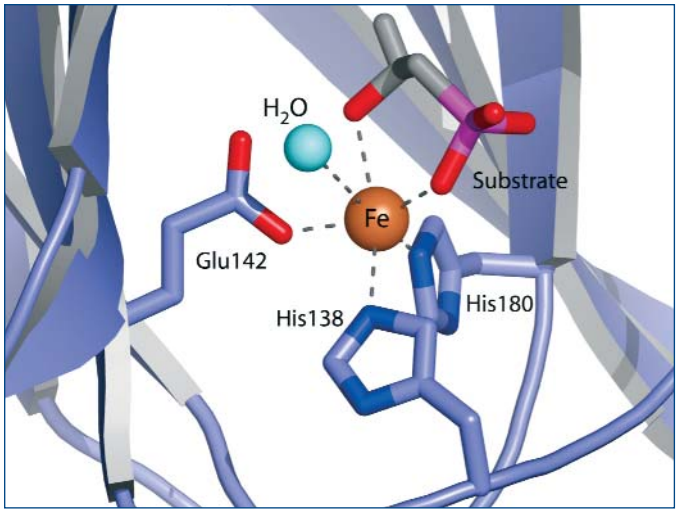

Fig. 2. Substrate—hydroxypropylphosphonic acid—bound in HppE active site.

See: L.J. Higgins[1], F. Yan[2], P. Liu[1,2], H-w. Liu[2], and C.L. Drennan[1], "Structural Insight into Antibiotic Fosfomycin Biosynthesis by a Mononuclear Iron Enzyme," Nature **437**, 838 (2005).

Author Affiliations: [1]Massachusetts Institute of Technology, [2]University of Texas at Austin

Correspondence: cdrennan@mit.edu

This research was supported in part by the National Institutes of Health (C.L.D. and H-W.L.), the National Institute of Environmental Health Sciences (L.J.H.), the Searle Scholars Program (C.L.D.), Alfred P. Sloan Foundation (C.L.D.), and a Lester Wolfe Predoctoral Fellowship (L.J.H.). Synchrotron facilities are funded by the NIH National Center of Research Resources (NE-CAT 8-BM) and the U.S. Department of Energy, Division of Materials Sciences and Division of Chemical Sciences (National Synchrotron Light Source, Brookhaven National Laboratory). Use of the Advanced Photon Source was supported by the U.S. Department of Energy, Office of Science, Office of Basic Energy Sciences, under Contract No. W-31-109-ENG-38.

How an RNA Enzyme Joins Small Organic Molecules

The catalytic activity of protein enzymes as biological macromolecules has been the subject of extensive study. Structural information on other types of catalysts, such as ribonucleic acid (RNA)-containing enzymes, or ribozymes, is scarce and limited to a few natural ribozymes. An international team led by researchers at the Memorial Sloan-Kettering Cancer Center in New York, New York, crystallized and determined the first three-dimensional structure of a synthetic ribozyme catalyzing a chemical reaction between two small organic molecules. The ribozyme fuses together two ring-shaped molecules in a highly specific way, forming chemical bonds between carbon atoms. To figure out how the ribozyme accomplishes this task, researchers crystallized the enzyme with and without its reaction product. The result establishes the catalytic potential of small RNA molecules.

For decades, researchers thought that all enzymes—molecules that speed up chemical reactions—were made of protein. Ribonucleic acid was thought to be just a temporary store of genetic information from which cells build those proteins. Then, in the 1980s, some RNAs were found to catalyze reactions for cleaving and joining of RNA molecules. In these ribozymes, the chain-like RNA twists into a shape capable of rearranging chemical bonds in the target RNA molecules. Although the mechanisms that drive ribozyme catalysis are still under debate, some protein enzymes likely work in a similar way, despite proteins being composed of twenty different amino acids, whereas RNAs are built from just four base types.

Researchers have since created ribozymes that perform various chemical reactions, including the ribozyme that forges bonds between carbon atoms through the famous Diels-Alder reaction. (see Fig. 1a). The reaction, which garnered its discoverers a Nobel Prize, is commonly used in organic chemistry laboratories to make biologically active compounds. The Diels-Alder ribozyme forms a compact, puckered structure, like a pasta shell with three corners (Fig. 1b), based on x-ray diffraction data collected on beamlines X25 and X12c at the National Synchrotron Light Source (Brookhaven National Laboratory) and supported by studies at the BioCARS beamline 14-BM and SBC-CAT beamline 19-BM at the APS. The ribozyme's interior houses a wedge-shaped, water-repellent catalytic pocket, almost perfectly suited to carry and freely release only one type of water-averse reaction product. Free and product-bound ribozyme structures are nearly identical, indicating that the

enzyme is rigid and that the pocket is formed before catalysis. Most other RNAs are more flexible, wrapping around their substrates upon binding.

The structure suggests that the ribozyme grips its two substrates in a precise orientation, quelling motion that would interfere with their joining. The catalytic pocket contains a crevice that fits one substrate snugly, probably stacking it atop the other substrate, the group reports. The crevice would permit the substrates to approach each other from only one direction, which would explain why the reaction product is twisted in one direction rather than another. Additionally, the pocket's shape precisely complements the high-energy transition structure formed by the two substrates in the course of becoming the reaction product. Such complementarity would aid the reaction by stabilizing its intermediate stages, as certain Diels-Alder protein enzymes are known to do.

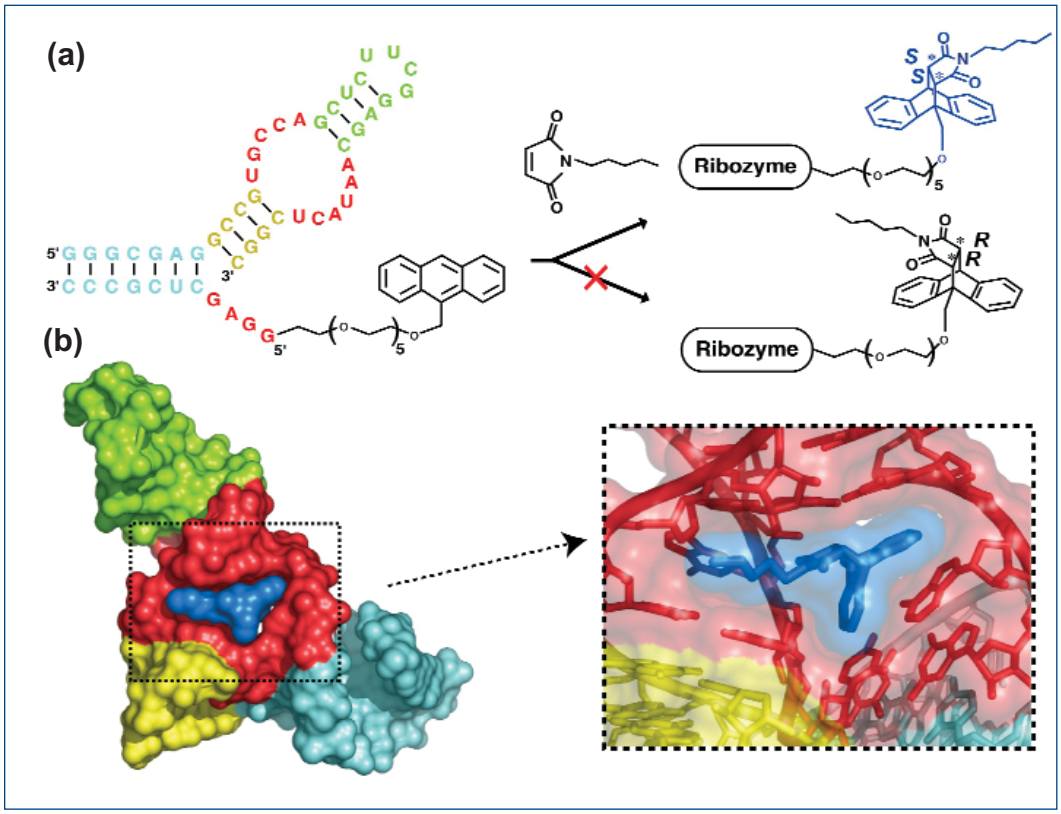

Fig. 1. (a) Simplified structure of the Diels-Alder ribozyme catalyzing the reaction between anthracene and maleimide, which forms a single geomeric form of the complex (blue). (b) Surface representation of the Diels-Alder ribozyme bound to the reaction product. Inset: catalytic pocket with reaction product surrounded by RNA shown in stick representation.

The researchers compared the ribozyme's structure to that of antibodies that catalyze the Diels-Alder reaction. The only antibody that works on the same substrates also forms a water-averse pocket shaped like the ribozyme's, so similar structural principles and catalytic mechanisms probably underlie both types of enzyme, the group argues.

This similarity highlights RNA's structural versatility. With fewer chemical tools compared to proteins, RNA has independently evolved the same way of efficiently and selectively joining carbon atoms. The structure of the Diels-Alder ribozyme revealed a simple RNA scaffold, which can be used to create catalytic pockets in RNA molecules, and clearly defines the principles that could be applied in the search for novel ribozymes for custom chemical synthesis. — *JR Minkel*

See: Alexander Serganov[1], Sonja Keiper[2], Lucy Malinina[1], Valentina Tereshko[1], Eugene Skripkin[1], Claudia Hobartner[3], Anna Polonskaia[1], Anh Tuân Phan[1], Richard Wombacher[2], Ronald Micura[3], Zbigniew Dauter[4], Andres Jäschke[2], and Dinshaw J. Patel[1], "Structural Basis for Diels-Alder Ribozyme-Catalyzed Carbon-Carbon Bond Formation," Nat. Struct. Biol. **12**(3), 218 (March 2005).

Author Affiliations: [1]Memorial Sloan-Kettering Cancer Center, [2]Ruprecht-Karls-University, [3]Leopold Franzens University, [4]Brookhaven National Laboratory

Correspondence: jaeschke@uni-hd.de or pateld@mskcc.org

This research was supported by the National Institutes of Health, the DeWitt Wallace Foundation, and the Abby Rockefeller Mauze Trust D.J.P.); the Bundesministerium fiir Bildung and Forschung (BioFuture program), the Deutsche Forschungsgemeinschaft, HFSP and the Fonds der Chemischen Industrie (A.J.); and the Austrian Science Fund FWF (R.M.). Use of the Advanced Photon Source was supported by the U.S. Department of Energy, Office of Science, Office of Basic Energy Sciences, under Contract No. W-31-109-ENG-38.

BUILDING BEAUTIFUL RNA

When regarding a magnificent cathedral, such as the Cathédrale Notre Dame de Paris, it is the overall effect of the elegant and intricate architecture that delights one's eye. To reach that final form, all great structures must be assembled from intermediate stages. The RNA molecule, an important component of cellular architecture, is no exception. The complexity of the end-state of RNA comes from the folding together of many intermediate stages. Identifying those intermediates, which are often difficult to discover and visualize, makes the end structure—and malfunctioning—of RNA easier to understand. Thanks to work done by researchers from The University of Chicago and Université Louis Pasteur, using the Bio-CAT 18-ID beamline at the APS, the structure of an RNA folding intermediate is now available. Because of this new knowledge, reasons for the stability of the final RNA structure become clear and provide a way to approach the cellular difficulties caused by RNA instability.

Just as the flying buttresses at Notre Dame support the main building, the structure of the RNA folding intermediate studied by the team makes clear how the core and peripheral elements of the molecule interact. In fact, the particular folding intermediate that they studied, part of RNA (RNase P RNA) from the bacterium *Bacillus subtilis*, turned out to have an intricate structure of its own. The researchers studied the molecule in fine detail, down to the level of its sugar-phosphate backbone. They used a variety of techniques, including the x-ray work done at the APS, to determine the three-dimensional (3-D) structure of the RNA intermediate. Amazingly complex in its own right, the intermediate consists of several structural components. Some of the two- and three-dimensional components are built in such a way as to suggest a certain sequence of events for creating the final 3-D form of the intermediate. It is as if the intermediate has a dance that must be performed for its own folding before it can participate in the assembly of the final RNA molecule. Just like with flying buttresses, the intermediate must be properly constructed before it can contribute to the stability of the final architecture.

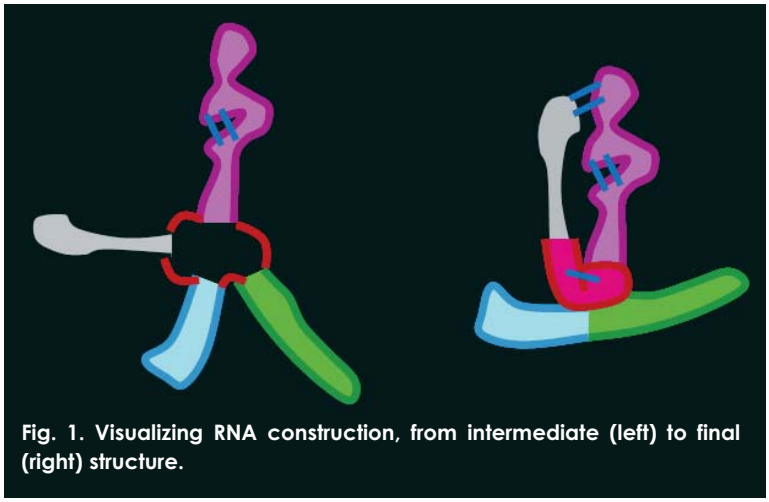

Fig. 1. Visualizing RNA construction, from intermediate (left) to final (right) structure.

If one looks at the intermediate in terms of how it compares to the final RNA, you would see that it does not have the core region or other peripheral, long-range interactions that the final form has. So, the intermediate is truly only a part of the final structure and not a miniature of it. The large data set produced by the research team allowed them to visualize some of the steps required for folding—steps leading from the intermediate form to the final form (Fig. 1). The process is stunning in the large amount of cooperation required by all of the structural players in order to achieve the final form. By studying the intermediate RNA in such detail, the investigators were able to dispel certain notions about how the final RNA structure comes into being. Scientists previously believed that the folding intermediates exhibited a lot of two-dimensional structure, but perhaps not so much 3-D structure, which was believed to arise only from the final form. But the 3-D structure of intermediates can be harder to find, especially because it is not likely to crystallize.

A combination of methods—including chemical and nuclease mapping, circular dichromism spectroscopy, small-angle x-ray scattering, and molecular modeling—provides strong support for the presence of at least short-range 3-D structure in the intermediate, including a four-way junction and an unusual set of two interacting loops. The structure itself contains information suggesting the next steps in building from the intermediate to the final form of the RNA. Although it is not yet possible to simulate exactly how the folding dance proceeds in forming the final RNA, the current work constitutes significant progress in that direction and makes possible calculations to determine the stability of the magnificent final structure. — *Mona Mort*

See: N.J. Baird[1], E. Westhof[2], H. Qin[1], T. Pan[1], and T.R. Sosnick[1], "Structure of a Folding intermediate Reveals the Interplay between Core and Peripheral Elements in RNA Folding," J. Mol. Biol. **352**, 712 (2005).

Author Affiliations: [1]The University of Chicago, [2]Université Louis Pasteur **Correspondence:** taopan@uchicago.edu, trsosnic@uchicago.edu

This work was supported by a NIH grant (GM57880). Bio-CAT is a National Institutes of Health-supported Research Center RR-08630. Use of the Advanced Photon Source was supported by the U.S. Department of Energy, Office of Science, Office of Basic Energy Sciences, under Contract No. W-31-109-ENG-38.

WORKING TOGETHER TO MODIFY RNA

A three-protein complex known to be essential for protein manufacturing and cell division in a wide variety of organisms can take a deadly turn in humans. Mutations in the human version of this complex cause a rare disease, called dyskeratosis congenita, which leads to cancer and other complications early in life. Researchers from Florida State University and the University of Georgia, using the NE-CAT beamline 8-BM and the SER-CAT beamline 22-ID at the APS, have determined the first three-dimensional structure of the three proteins. On the basis of the new structure, the group created a model of the relevant human protein and identified the sites where disease-causing malfunctions commonly occur. Besides illuminating a key cellular process, the results could be used to design ways of restoring the cluster's function in those who have the illness.

The key player of the three proteins in the cluster, called Cbf5 in some species, introduces subtle changes to the structure of certain RNA molecules, which are similar to DNA and used by cells to perform various basic tasks. Cbf5 needs a so-called "guide RNA" to discriminate between different potential target RNAs. It also must touch two other proteins: Nop10 and Gar1. Previous studies offered inconclusive evidence about how these two helper proteins might affect Cbf5. To better understand how the cluster functions, its three-dimensional structure was needed.

The Cbf5 protein consists of two RNA-binding domains, one of which modifies the bound RNA, according to the new structure. The researchers in this study crystallized the three proteins from a species of archaeon, a type of single-celled organism that thrives in extreme environments. The structure was derived from x-ray crystallography studies performed on the NE-CAT and SER-CAT beamlines. Based on the behavior of similar proteins, the group predicts that Cbf5 binds to RNAs that play important roles in constructing all the cell's proteins and in maintaining the ends of chromosomes, which allow cells to keep dividing. Its two helper proteins bind near each other but independently (Fig. 1).

Cbf5's two helpers seem to increase the number of contacts it makes with the guide and target RNAs, judging from several lines of evidence. Gar1 binds to a protrusion of Cbf5 that is likely involved in orienting the guide and target RNAs. In solution, Gar1 protects this protrusion from degraded by a protein-digesting enzyme, the group reports, indicating that Gar1 stabilizes the region's structure. Nop10 attaches near the catalytic site of Cbf5 and seems to mold its shape to fit that of the larger protein. This rearrangement suggests that Nop10 acquires new functions upon binding—perhaps serving as structural glue for the RNA and protein. In a model based on a related protein-RNA complex, Nop10 is in a position to bend the guide RNA to better fit its target RNA.

Given the structure of Cbf5, the group also modeled the analogous human protein, dyskerin, which is always mutated in people with dyskeratosis congenita. Most of the known dyskerin mutations cluster on the domain that serves only to bind RNA, suggesting that the disease would result in a lack of important RNA molecules. The finding is consistent with studies indicating that mutated dyskerin disrupts both protein synthesis and chromosome maintenance systems. This region of Cbf5 or dyskerin could still play an as-yet unknown role. Figuring out its exact function will be key to understanding its precise function in the cell. — *JR Minkel*

Fig. 1. Schematic structural drawing of a three-member protein complex responsible for ribosome biogenesis: Cbf5 (Blue), a homolog of human dyskerin responsible for a rare genetic disease, chemically alters ribosomal RNA (grey ovals) with the help of its two helper proteins, Gar1 (yellow) and Nop10 (red).

See: Rumana Rashid[1], Bo Liang[1] Daniel L. Baker[2], Osama A. Youssef[2], Yang He[1], Kathleen Phipps[1], Rebecca M. Terns[2], Michael P. Terns[2], and Hong Li[1], "Crystal Structure of a Cbf5-Nop10-Gar1 Complex and Implications in RNA-guided Pseudouridylation and Dyskeratosis Congenita," Mol. Cell **21**, 249 (20 January 2006).

Author Affiliations: [1]Florida State University, [2]University of Georgia

Correspondence: hongli@sb.fsu.edu

This work was supported by the National Institutes of Health (NIH) grant R01 GM66958-01 (to H.L.) and NIH grant RO1 GM54682 (to M.P.T. and R.M.T.). R.R. is a predoctoral fellow of the American Heart Association, Florida/Puerto Rico Affiliate (0415201B). Use of the Advanced Photon Source was supported by the U.S. Department of Energy, Office of Science, Office of Basic Energy Sciences, under Contract No. W-31-109-ENG-38.

How a Viral RNA Self-Splices

Although most of the chemical reactions in a cell are performed by protein molecules, some RNA molecules (close relatives of DNA) catalyze biological reactions. Introns, first discovered in the mid-1970s, are members of one family of catalytic RNA molecules. While geneticists have known that introns are capable of splicing out segments of themselves from the larger whole, they have been puzzled for more than 30 years about the method chemically reactive introns use to excise themselves without help from other molecules. Now, a group of researchers using the NE-CAT beamline 8-BM and the BioCARS beamline 14-ID-B at the APS has provided an important clue by solving the three-dimensional (3-D) structure of a viral intron bound to its reaction product. The structure reveals a ring enveloping the RNA enzyme's snug active pocket, a hollow in which the chemical reactions that split and rejoin RNA molecules take place.

Genes are coded in DNA and then copied into RNA, but not all of the sequence coded in DNA makes it into the final RNA molecule, which serves as a template for protein synthesis. A process called splicing shortens the RNA molecule by removing introns interspersed along it. Sometimes a single RNA molecule can be spliced in multiple ways, giving a cell greater flexibility in the proteins it can manufacture from its store of genes. The splicing reaction first transfers a molecule of guanosine to one end of the intron, making the first break in the RNA. The released piece of RNA then attacks a guanosine at the far end of the intron, making the second break and linking the broken ends.

X-ray crystallography has illuminated the precise mechanisms by which some self-splicing introns work. Biochemists at Purdue University in West Lafayette, Indiana, decided to study an intron from a virus that infects bacteria to see whether different introns share the same mechanism. They shortened the viral RNA molecules and exposed one end of the intron, leaving a short RNA enzyme—or ribozyme—capable of catalyzing repeated reactions on RNA molecules. They added a small RNA segment that is structurally similar to the ribozyme's reaction product and crystallized the mix.

On the basis of x-ray studies carried out at beamlines 8-BM and 14-ID-B, the researchers found that the ribozyme adopts a complicated 3-D shape (Fig. 1) that buries the active site in a pocket near the center.

The active site forms a pocket that complements the shape of the nucleotide base guanosine, one of RNA's four subunits. The binding site for guanosine is nestled between two base triplets in a structure similar to that of other introns of known structure. Binding of guanosine forms yet a third base triplet, sandwiched between the other two, that stabilizes the binding between enzyme and substrate.

The splicing reaction transfers guanosine from one end of the intron to the interior of the intron, and then to the base flanking the other end of the intron. Each reaction proceeds through an intermediate stabilized by a cluster of two to three magnesium ions. To identify these sites, the researchers added manganese to the crystallization mix. One manganese ion was incorporated into a location appropriate for coordinating the intermediate, and the researchers found that modeling of the other two locations was possible. Comparison of the structure to that of another known intron structure suggests that guanosine binding brings the metal ions to their active configuration.

Structures of three different classes of introns at different points in the splicing reaction are now known. Their catalytic cores are all markedly similar, suggesting that the structures can be used to help model those of the more than 1500 introns currently identified by sequence searches. — *JR Minkel*

< Fig 1. The 3-D structure of an RNA enzyme capable of removing itself from a large RNA molecule.

See: Barbara L. Golden, Hajoeng Kim, and Elaine Chase, "Crystal Structure of a Phage Twort Group I Ribozyme-product Complex," Nature Struct. Biol. **12**, 82 (January 2005).
Author Affiliation: Purdue University
Correspondence: barbgolden@purdue.edu

This work was supported by NASA (NAG8-1833), the Pew Scholars Program in Biomedical Sciences, and the Purdue University Cancer Center. Use of the Advanced Photon Source was supported by the U.S. Department of Energy, Office of Science, Office of Basic Energy Sciences, under Contract No. W-31-109-ENG-38.

CATALOGING NEW PROTEIN PARTS

A team of structural biologists from the Center for Eukaryotic Structural Genomics at the University of WIsconsin is on a hunt. The databases that hold information about the three-dimensional forms of proteins are chock-full of proteins with similar shapes and structures. That's because over the years, scientists have chosen to study related proteins; otherwise, the workload would be unbearable. But with today's technology, researchers can rapidly determine the form of proteins about which little is known—even if all the information they have on a particular protein is the slip of DNA that codes it in an organism's chromosomes. The researchers from Wisconsin used the GM/CA-CAT beamline 23-ID and SER-CAT beamline 22-BM at the APS to determine the overall shape of an unsung protein made by a gene found in a small plant. The protein surprised them, though, by turning out to be similar to a known protein family that includes neurotoxins.

As part of a larger goal of identifying all the different structural ways proteins hold their shapes and perform their duties in the biological world, some scientists are determining what unknown proteins look like in three dimensions. Some spans of proteins—long chains of amino-acid building blocks that twist and fold into shapes that depend on the chemical nature of the particular sequence of blocks—will twirl into helices; groupings of other blocks will form spheres, stuffing chemically similar blocks inside while packing others on the outside. Substructures, such as helices, compose different architectural chunks of proteins, and scientists predict the substructure that amino-acid sequences take based on what exists in the databases. But the Wisconsin team wanted to learn about the vast array of proteins that remain unexplored. Perhaps amino acid sequences have yet-to-be-discovered ways of forming the same substructures, or perhaps substructures exist that scientists have not yet seen.

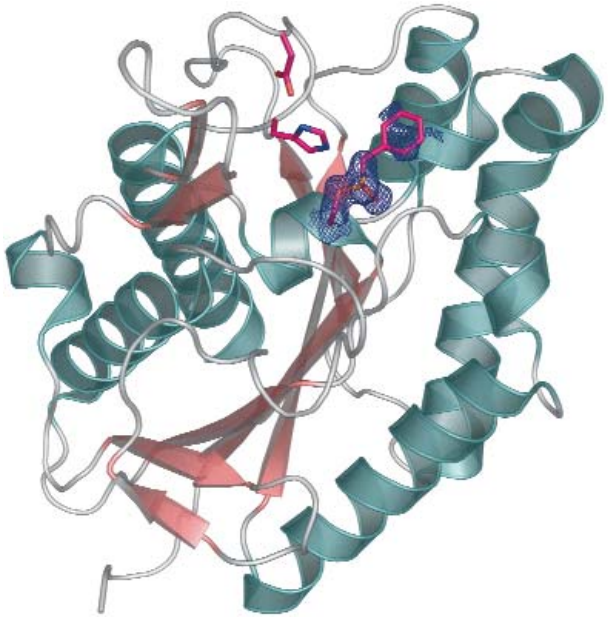

Fig. 1. The hitherto unknown protein At4g34215 showed itself by grabbing onto a certain kind of inhibitor (red hexagon), revealing its roots in a family of protein-choppers.

First, the researchers searched the DNA databases of various organisms, looking for genes that were the most unlike anything already studied. One such gene, At4g34215 from the plant *Arabidopsis thaliana*, had less than 30% of its sequence in common with other proteins.

Native crystals grown by the researchers were studied using x-ray diffraction extending to 2.6 Å and 1.6 Å at the SER-CAT and GM/CA-CAT beamlines, respectively. Studies of the electron-density map for At4g34215 revealed an unaccounted-for electron density. The mystery density was located in close proximity to a serine amino acid. In addition, the team had added a compound known as PMSF to the protein during crystallization. PMSF inhibits enzymes that break down other proteins by using a serine amino acid in the biochemical reaction. A close look at the At4g34215 structure revealed that At4g34215 likely holds onto the proteins it chews up in a slightly different manner than other members of the family. These results confirm that At4g34215 belongs to a well-known superfamily of enzymes known as the SGNH-hydrolases, which includes some neurotoxins. Not only did At4g34215 surprise the researchers by turning out to be less unusual than expected, but it was also a little different than it appeared. — *Mary Beckman*

See: E. Bitto, C.A. Bingman, J.G. McCoy, S.T.M. Allard, G.E. Wesenberg, and G.N. Phillips, Jr., "The Structure at 1.6 A° Resolution of the Protein Product of the At4g34215 Gene from *Arabidopsis thaliana*," Acta Crystallogr. D **61**, 1655 (December 2005).

Author Affiliation: University of Wisconsin, Madison
Correspondence: phillips@biochem.wisc.edu

This work is supported by National Institute for General Medical Sciences grants P50 GM64598 and U54 GM074901 (John L. Markley, PI, and Brian G. Fox and George N. Phillips, Co-PI's). The work of all members of the CESG team is acknowledged. GM/CACAT is funded by the National Cancer Institute (Y1-CO-1020) and the National Institute of General Medical Science (Y1-GM-1104). Use of the Advanced Photon Source was supported by the U.S. Department of Energy, Office of Science, Office of Basic Energy Sciences, under Contract No. W-31-109-ENG-38.

LOADING AND UNLOADING A CHOLESTEROL SHUTTLE

The structure of a cholesterol-sensing protein, based on studies carried out SER-CAT at the APS and beamline X25 at the National Synchrotron Light Source, has revealed how such proteins might transfer cholesterol molecules back and forth between the membranes of cells. The result marks the first structure and possible mechanism of action for a class of proteins essential to the survival of cells from yeast to human. Researchers crystallized the yeast protein, called Osh4, and found that it forms a cylinder-like structure with a flexible lid. When cholesterol is lodged inside the cylinder, the protein structure is suited for traveling through liquid. In a structure lacking cholesterol, Osh4 appears primed to latch onto a cellular membrane and spring open its lid to disgorge the cylinder's contents.

Cholesterol does more than clog arteries. The compact, rigid molecule is an essential component of animal cells, making their outer cell membranes sturdier and less prone to leaking. It works by wedging itself between more fluid and flexible molecules called phospholipids, which make up most of a cell membrane. Cells need machinery to incorporate cholesterol or cholesterol-like molecules called sterols into membranes and to present them to other machinery in the cell to shut down sterol production, for example. Accordingly, sterol-binding proteins have been found in organisms from yeast to people, and they tend to be key players in the proper functioning of those organisms. Embryonic mice, for instance, fail to develop without them. In keeping with the role of transporter, some sterol-binding proteins change location in the cell after latching onto a sterol. Researchers had no detailed understanding, however, of how this type of protein binds and transports its target molecule.

The Osh4 protein—one of seven in yeast—forms a greasy, water-repelling tunnel that is plugged at one end and has a flexible lid at the other end (Fig. 1), report researchers from the National Institutes of Health (NIH, who crystallized the protein mixed with several different sterols, including cholesterol and ergosterol, the yeast counterpart of cholesterol. On the basis of x-ray crystallography studies performed at SER-CAT beamline ID-22 at the APS and beamline X25 at the National Synchrotron Light Source, the researchers found that the Osh4 lid closes snugly around a sterol, making it inaccessible from the outside.

The researchers were unable to crystallize the full-length protein without a bound sterol molecule, to study how structural changes might serve to expel the sterol. Instead, they crystallized a mutant form of the protein, in which the lid had been removed. The lidless structure displays a flat, unobstructed surface around the mouth of the tunnel, which is well suited to release the sterol. The shift in structure causes several positively charged, or basic, amino acids to face out from the tunnel mouth.

The researchers hypothesize that the release of a sterol is driven by the affinity of these basic amino acids for the acidic,

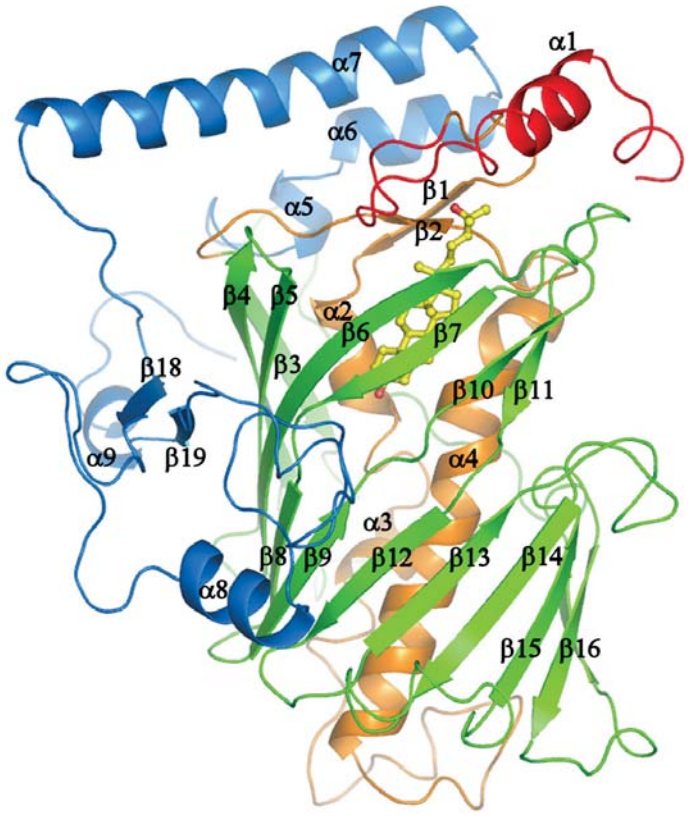

Fig. 1. The schematic structure of Osh4, a yeast protein that binds and transports cholesterol and related sterol molecules. An oxysterol molecule (yellow) is shown lodged inside the protein's water-repelling tunnel (orange, green), which is kept closed by an otherwise flexible lid (red).

negatively charged phosphate groups projecting from the phospholipids of cellular membranes. In Osh4's lidded form, two of the basic amino acids are very near to each other. Their close proximity creates a strain in the protein structure, because like charges repel. The lid wants to open and relieve the strain, but

Continued on next page

it can only stay open when these basic amino acids have something else to bind onto, such as phosphate groups on a membrane surface. The researchers therefore propose that the empty Osh4 uses its flexible lid to help bind to a membrane and then sucks up a cholesterol molecule, which causes the lid to shut tight until it reaches a second membrane, into which it injects the cholesterol, relieving the strained configuration.

— JR Minkel

See: Young Jun Im, Sumana Raychaudhuri, William A. Prinz, and James H. Hurley, "Structural Mechanism for Sterol Sensing and Transport by OSBP-related Proteins," Nature **437**, 154 (1 September 2005).

Author Affiliation: National Institutes of Health
Correspondence: hurley@helix.nih.gov

This research was supported by the intramural program of the NIDDK. Y.J.I. was partly supported by the Korea Science and Engineering Foundation. Research carried out at the National Synchrotron Light Source is supported by the U.S. Department of Energy, Division of Materials Sciences and Division of Chemical Sciences. Use of the Advanced Photon Source is supported by the U.S. Department of Energy, Office of Science, Office of Basic Energy Sciences, under Contract No. W-31-109-ENG-38.

UNTRACKING INTERMEDIATES IN PHOTOACTIVE REACTIONS

Figuring out how molecules morph during reactions is not always easy, especially if it happens in less than a second. We can surmise that intermediate molecules exist but never really know—unless there is a way to visualize those intermediates. Such a technique would be particularly useful for photoactive proteins, where the form and function of energy carriers is critical to understanding the reaction. A beautiful set of intermediate molecules appeared in an analysis recently performed with help from the facilities at the APS. An international team—led by the Korea Advanced Institute of Science and Technology (KAIST)—used the BioCARS 14-ID-B beamline at the APS and beamline ID09B at the European Synchrotron Radiation Facility (ESRF) to study a bacterial photoreceptor protein at time points up to one second, producing a major breakthrough in our knowledge of photocycle reaction mechanisms.

The researchers determined three-dimensional (3-D) intermediate structures—in real time and under ambient conditions—of the blue-light photoreceptor photoactive yellow protein (PYP) from the bacterium *Halorhodospira halophila*. A comprehensive set of Laue data collected during the PYP photocycle allowed tracking of all atoms, as well as observation of how a blue-light photon absorbed by its *p*-coumaric acid (pCA) chromophore triggered a reversible photocycle. This event is a complex chemical mechanism, in which five distinct structural intermediates emerged. In the early appearing, red-shifted intermediates, structural changes at the chromophore shift to the exterior of the protein in the late, blue-shifted intermediates. The shift is mediated by an initial "volume-conserving" isomerization of the chromophore followed by progressive disruption of hydrogen bonds between the chromophore and its surrounding binding pocket. The intermediates discovered in this study, when combined with previous biophysical data, allow a satisfyingly complete view of the PYP reaction system.

BioCars 14-ID-B beamline (APS) and beamline ID09B (ESRF) allowed time-resolved crystallographic data to be collected on the crystallized wild-type protein. Data collected at ESRF covered the early to middle time range of the reaction, from 1 ns to 10 μs; the APS data covered the middle to late time range of 6 μs to 1.33 s. The total of 47 measured time points spanned the complete photocycle and were analyzed with singular value decomposition (SVD). By using laser illumination from both sides of the crystal, the APS measurements occurred with increased photoactivation. Performing a 10-μs time point in all data sets facilitated comparison of the APS and ESRF data sets. SVD analysis aided in resolution of density maps, in which coexisting intermediates can create a mixture of density differences.

When a blue-light photon is absorbed by the *H. halophila* PYP pCA chromophore, a rapid trans-cis isomerization creates a structural signal leading to a negative phototactic response. Previous spectroscopic studies of the PYP system showed that it participates in a reversible photocycle from the dark state through intermediates that decay to a red-shifted intermediate, then to a blue-shifted state, finally returning to the dark state, but they gave limited information about the 3-D structure of intermediates, exhibited low signal-to-noise, or did not cover the complete photo cycle. The present study of 3-D intermediates fills in important details about events in the PVP photocycle. Four relaxation times (at 20 ns, 180 μs, 5 ms, and 52 ms) occurred in the 47 time points and yielded four proposed intermediate states (α, β, γ, and δ). The β state required two inter-

mediate structures to resolve the observed difference electron density, thus bringing the total number of intermediates to five (Fig. 1). Because the intermediates were studied at high resolution, the wild-type PYP chromophore isomerization can now be visualized in stunning detail. To capture the energy of the blue-light photon, PYP uses a strained chromophore conformation to maintain the hydrogen bond network and harness the energy for subsequent steps in the photo cycle. Finding ways to clearly "see" intermediates in the PYP reaction pathway represents a breakthrough in the study of reaction mechanisms.

— *Mona Mort*

See: H. Ihee[1,2], S. Rajagopal[2], V. Šrajer[2], R. Pahl[2], S. Anderson[2], M. Schmidt[3], F. Schotte[4], P.A. Anfinrud[4], M. Wulff[5], and K. Moffat[2], "Visualizing Reaction Pathways in Photoactive Yellow Protein from Nanoseconds to Seconds," PNAS **102**, 7145 (2005).

Author Affiliations: [1]Korea Advanced Institute of Science and Technology, [2]The University of Chicago, [3]Technische Universitaet München, [4]National Institutes of Health, [5]European Synchrotron Radiation Facility

Correspondence: hyotcherl.ihee@kaist.ac.kr

This work was supported by the National Institutes of Health (K.M., BioCARS facility), the Deutsche Forschungsgemeinschaft (M.S.), the European Union (M.W.), the Korea Research Foundation (H.I.), and the Damon Runyon Cancer Research Foundation (H.I.). Use of the Advanced Photon Source was supported by the U.S. Department of Energy, Office of Science, Office of Basic Energy Sciences, under Contract No. W-31-109-ENG-38.

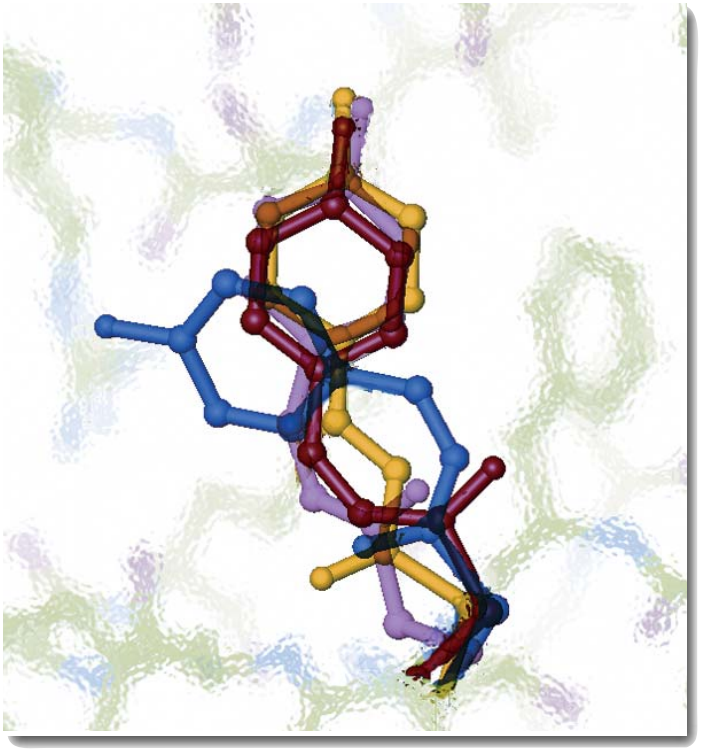

Fig. 1. Overlay of intermediates on one of the reaction pathways determined from SVD and posterior analysis of time-resolved Laue crystallographic data from wild-type Photoactive Yellow Protein. Yellow denotes structural intermediates pG, red I_{CP}, purple R_{CW}, and blue pB_1.

AROUND THE APS

THE APS SHORT-PULSE WORKSHOP

The primary purpose of the workshop on "Generation and Use of Short X-ray Pulses at APS" held on May 6, in conjunction with the APS User Meeting, was to present preliminary results of accelerator and optics calculations leading to the production of short (~1 ps) x-ray pulses from the APS storage ring. In addition to presentations pertaining to the generation of short pulses—and of equal import and interest—the workshop afforded an opportunity to summarize the science driving this project. National and international experts were invited to hear the presentations and provide critical comments regarding all aspects of the proposal. The workshop attendees concluded that a special configuration at the APS for 1-ps to 2-ps x-ray pulses is not only feasible, but affords unprecedented opportunities for probing picosecond dynamics.

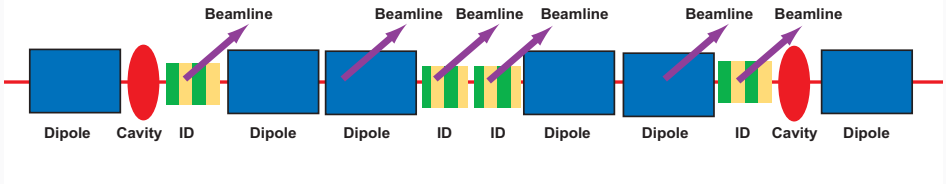

Schematic of a short-pulse configuration at the APS. Minimum implementation shown is for insertion devices and two bending magnets.

The workshop summary and copies of the presentations are on the Web at:
http://www.aps.anl.gov/News/Conferences/2005/Generation_and_Use_of_Short_Xray_Pulses/index.html.
Contact: Kwang-Je Kim (kwangje@aps.anl.gov), Dennis Mills (dmm@aps.anl.gov)

ACTIN' LIKE A RATCHET

Actin filaments, the long, thin filaments that allow cells to change shape, could grow by a ratchet-like process, according to new structural data obtained by investigators from the University of Texas Southwest Medical Center using the SBC-CAT beamline 19-ID at the APS. Utilizing x-ray crystallography, the researchers studied the structure of a piece of protein known to play a role in filament growth, called formin homology domain 2 (FH2), wrapped around an actin filament. Based on this structure and biochemical assays of FH2, they hypothesize that fluctuations in the protein's structure capture actin subunits as they randomly join and fall off of the nascent filament.

Actin filaments, which consist of two alternating subunits, are a key part of a cell's internal "skeleton." If a concentrated group of filaments grows in one direction, for example, they will drag part of the cell with them, creating an appendage for grabbing food or attaching to a surface. Cells can assemble actin filaments quite rapidly despite the fact that free actin molecules join together very slowly by themselves. Researchers have found that FH2 seeds the formation of filaments and speeds up their growth, but until now, no group had determined the structure of one of these seeds. To see how FH2 works its magic, investigators from the University of Texas Southwest Medical Center at Dallas crystallized the protein along with actin, and gathered x-ray crystallographic data on SBC-CAT beamline 19-ID at the APS.

The researchers carrying out this study found that FH2 is a short, bow-shaped protein with a knob on one end and a loop on the other. In their structure, FH2 molecules string together and wind around the actin filament like the red band of a candy cane, with the loop of each molecule bound to the knob of the next. FH2 forms a bound pair in solution, not a string, so based on the new structure, the researchers modeled a pair of FH2 molecules encircling a trio of actin subunits (Fig. 1). The FH2 molecules form a ring that has four binding sites for actin, two on each side of the ring. One half of the ring, called a “bridge element,” binds the middle and upper actin subunits; the other binds the middle and lower subunits.

The structure has one snag. Actin filaments are asymmetric; they have a pointy end and a “barbed” end, like a harpoon. Prior experiments indicated that actin filaments grow from the barbed end, but the modeled FH2 pair obstructs that end, whereas the pointy end is completely accessible. To account for this apparent obstacle, the researchers propose that the bridge element stuck to the middle and upper actins slips down

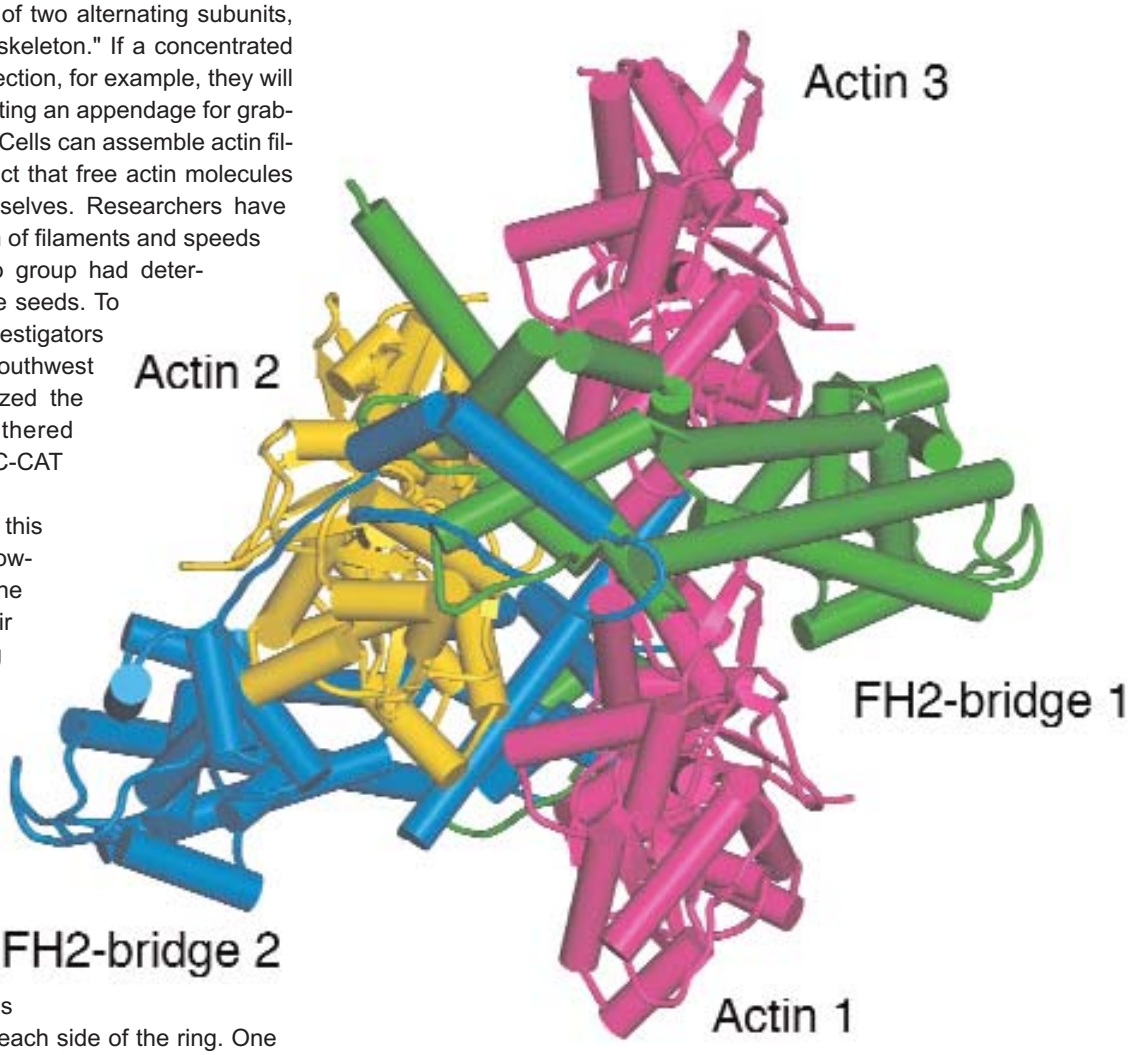

Fig. 1. Modeled structure of a nascent actin filament made of three subunits (magenta, gold) encircled by a pair of proteins critical for the filament's formation and rapid growth (green, blue). Based on this structure, researchers proposed that a new actin subunit attaches from below when the top “bridge element” (green) slips downward.

so it binds just the middle subunit and has one free binding site. This slippage would allow a new actin subunit to come along, join the existing filament, and leave again at random. This new actin subunit gets caught when the other bridge element slips down, and the process repeats.

The driving force behind this growth would be the stability of the actins once FH2 has completely released them into the filament. The structure shows that FH2 distorts the bound actins, putting them in a high-energy state. Once both bridge elements release an actin subunit into the bulk filament, they cannot back up easily because this action would require the addition of significant energy. The mechanism proposed by these researchers is consistent with the group's results using mutant FH2 pairs that lack activity in one or two binding sites, they note. Deactivating either actin binding site on either of the bridge elements blocks filament growth, as would be expected if both bridge elements work in tandem. — *JR Minkel*

See: Takanori Otomo, Diana R. Tomchick, Chinatsu Otomo, Sanjay C. Panchal, Mischa Machius, and Michael K. Rosen, "Structural Basis of Actin Filament Nucleation and Processive Capping by a Formin Homology 2 Domain," Nature **433**, 488 (3 February 2005).

Author Affiliation: University of Texas Southwestern Medical Center

Correspondence: mrosen@biochem.swmed.edu

This work was supported by grants from the NIH to M.K.R. T.O. was supported by the Human Frontier Science Program. Use of the Argonne National Laboratory Structural Biology Center beamlines at the Advanced Photon Source was supported by the US Department of Energy, Office of Energy Research. Use of the Advanced Photon Source was supported by the U.S. Department of Energy, Office of Science, Office of Basic Energy Sciences, under Contract No. W-31-109-ENG-38.

ESTROGEN RECEPTOR BINDING: SMALL CHANGES WITH BIG EFFECTS

Hormones are powerful biological molecules capable of directing major metabolic rearrangements. It came as no surprise, then, to find estrogen activity linked to uterine and breast cancer. In particular, selective estrogen receptor modulators (SERMs), and a subtype (selective estrogen receptor alpha modulators, SERAMs), show promise in terms of designing drugs that can treat estrogen-related cancers. Building on their earlier work, a research group from Merck Research Laboratories, using the IMCA-CAT 17-ID beamline at the APS, recently discovered that minor changes in one class of SERAM markedly affect hormone activity in uterine tissue. The new data will facilitate creation of pharmaceuticals to battle related diseases.

The Merck researchers prepared several dihydrobenzoxathiin SERAMs with alkylated pyrrolidine side chains or alkylated linkers. The series of compounds started with analog 1, which previous studies characterized as retaining potency while reducing the oxidative metabolism of the side chain. The fused cyclopropyl analog 2, when compared to analog 1, exhibited even better potency and subtype selectivity, and similar uterine activity, but still exhibited side chain oxidation. Using analog 1 as a starting point, the search for a pyrrolidine analog that exhibited an improved SERM profile and lower susceptibility to oxidation resulted in synthesis of alkylated pyrrolidine side chain and linker analogs, with accompanying assays for estrogen receptor (ER) binding and uterine activity. The analyses reveal that the dihydrobenzoxathiin SERAMs exhibit a SERM profile that depends on the size of the side chains as well as their location. Several of the new compounds were an improvement over compound 1, especially compounds 4, 15, and 18, and suggest modifications that could further enhance the selectivity and activity of these SERAMs. This systematic approach could very likely lead to improved treatment of diseased uterine tissue.

X-ray analysis of 15, 16, 18, and 19 bound to the ligand-binding domain of ER occurred at the APS IMCA-CAT 17-ID beamline. Crystals, obtained by means of vapor diffusion, were in the space group P6522 (cell dimensions, 15: $a = b = 58.62$, $c = 276.79$; 16: $a = b = 58.57$, $c = 276.31$; 18: $a = b = 58.64$, $c = 275.77$; and 19: $a = b = 58.69$, $c = 277.18$). A series of assays using the newly synthesized compounds measured cyanide adduct formation after microsomal oxidation, estrogen receptor ligand binding, breast cancer cell proliferation, and estrogen agonism and antagonism in rat uterine tissue.

An ethylene linker is the usual way in which SERM side chains are connected to the core structure. Because methylated pyrrolidines exhibited superior uterine profiles, the research team investigated the effect of adding a methyl group

Continued on next page

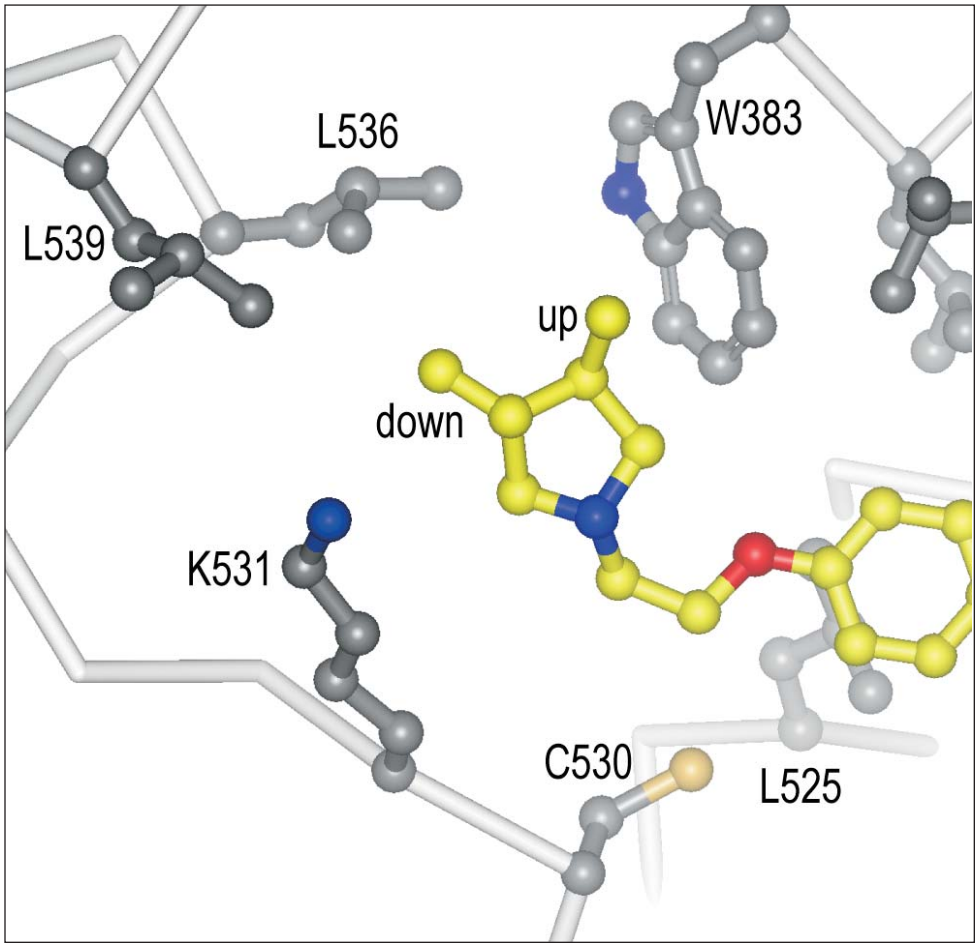

Fig. 1. Compound 15 bound to ERa, showing nitrogen (blue); oxygen (red); sulfur (gold); and carbon atoms in the ligand (yellow) and protein (gray). "Up" and "down" refer to stereochemistry of methyl substitutions.

to the linker. As long as the stereochemistry was conserved, addition of a methyl group to the position of the ethylene linker improved the SERM profile (Fig. 1). The size of the substitution greatly influenced the metabolic profile, as was also the case with the alkylated pyrrolidines. Increased oxidation—as measured by cyanide adduct formation—resulted from larger substitutions. The novel alkylated pyrrolidine analogs (4–16) exhibited the high ER potency found in analogs 1–3. Analog 4 demonstrated that smaller side chain substitutions yielded greater metabolic stability and a better uterine profile. Extreme uterine antagonism was observed with compound 15, probably due to stabilization of helix 12 in the antagonist conformation. In contrast, structural shifts in compound 16, which result in suboptimal contacts with helix 12, appear to partially eliminate this positive effect. In compounds 18 and 19, the methyl substitutions are on the linker instead of on the ring. Compound 18 has better contacts with residues in helix 12, and, as expected, stronger uterine antagonism than compound 19.

A major contribution of this careful and detailed analysis of SERAMs is demonstrating that the size and location of side chain substitutions greatly influence SERM profile. In addition, seemingly minor changes in side chains or linkers can have a great impact on biological activity.— *Mona Mort*

See: T.A. Blizzard, F. DiNinno, J.D. Morgan, II, H.Y. Chen, J.Y. Wu, S. Kim, W. Chan, E.T. Birzin, Y.T Yang, L-Y. Pai, P.M.D. Fitzgerald, N. Sharma, Y. Li, Z. Zhang, E.C. Hayes, C.A. DaSilva, W. Tang, S.P. Rohrer, J.M. Schaeffer, and M.L. Hammond, "Estrogen Receptor Ligands. Part 9: Dihydrobenzoxathiin SERAMs with Alkyl Substituted Pyrrolidine Side Chains and Linkers," Bioorg. Med. Chem. Lett. **15**, 107 (2005).

Author Affiliation: Merck Research Laboratories
Correspondence: tim_blizzard@merck.com

The Industrial Macromolecular Crystallography Association, by contract with the Illinois Institute of Technology, supported use of the APS beamline 17-ID. Use of the Advanced Photon Source was supported by the U.S. Department of Energy, Office of Science, Office of Basic Energy Sciences, under Contract No. W-31-109-ENG-38.

PICTURING MYOSIN: A MIGHTY MOLECULAR MOTOR

Imagine a massive chain-tread tractor lumbering over rugged terrain at a construction site, pushing forward yards of soil. Now shrink that image to the cellular level, where the tractor and the terrain are the proteins myosin and actin, and the payload is a starch bundle that needs to be moved from one part of the cell to another. Just like the tractor itself, myosin is a motor that, in concert with actin, gets things moving in cells. Unlike the steel in the tractor, the myosin motor is constructed of molecules, an intriguing and complex system of proteins and associated linkers—a true engineering feat. It is not surprising that, for decades, biophysicists and biochemists have been busy unraveling the wonders of the actin-myosin system. One such group of researchers, based at the Boston Biomedical Research Institute, used the BioCARS beamline 14-BM-C at the APS to produce a structure for a portion of the myosin molecule. Their results make it much easier to understand how this molecular motor, so critical to normal functioning of the cell, functions.

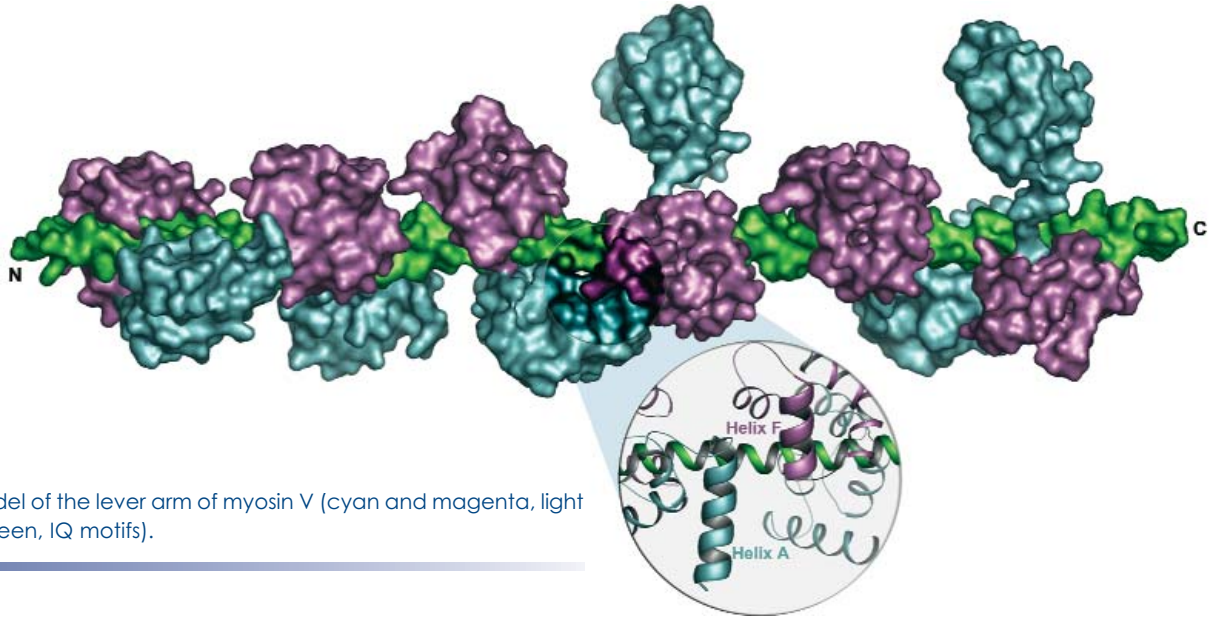

Fig. 1. Model of the lever arm of myosin V (cyan and magenta, light chains; green, IQ motifs).

The investigators concentrated on the myosin V molecule, which boasts two heads and had been shown to be involved in cellular transport in mammals and yeast cells. The myosin V motor turned out to have two really interesting aspects to its structure. First, it has what the researchers called processivity, which can be likened to a procession along a route, as in a parade. The myosin V motor can proceed along the surface of the actin molecule with its payload. And in doing so, it exhibits a second remarkable attribute by taking large steps—for a molecule, that is. The myosin can take linear steps as long as 36 nm, which is equal to one turn of the helical track of the actin molecule. Obviously, this myosin is not messing around when it decides to move forward.

What allows the myosin molecule to take such long steps? The researchers provided an elegant answer to that question by investigating the crystal structure of a myosin light chain bound to a myosin V from yeast. The myosin V light chain-binding domain, with its six tandem sequences, called "IQ motifs," is the key to the giant strides.

Using an array of techniques—including the crystallography done at the APS—and incorporating data from previous work, the team built a fascinating model for the light chain-binding domain of myosin V. If you took a look at the overall structure of the molecule, you would see two heavy chains and twelve light chains. There is a motor domain, with the actin-binding site, at the head of each heavy chain. Then comes the light chain-binding domain with its six tandem IQ motifs followed by the tail domain, which is involved in binding cargo.

The model developed by the researchers reveals why the myosin motor is such a powerhouse and capable of staying attached to actin for a large part of the movement cycle (Fig. 1). A slow rate of energy release—by forming adenosine diphosphate (ADP) from adenosine triphosphate (ATP)—is one factor

Continued on next page

responsible for allowing the myosin to hang on so long. Another factor is that the six IQ motifs of the light chain-binding domain are yoked in three separate pairs. Within each pair, the molecules cooperate, but there does not seem to be interaction between pairs, so that there is flexibility, just like there would be between links of a metal watchband.

The researchers describe the myosin V molecule as being able to essentially walk across the actin filament (the roadway) in a straight line, while carrying large cargoes in its cargo-binding domain connected to the long lever arm—and avoiding collisions with other components of the cell. That is quite a feat for a molecule that is driving itself and, along with actin, efficiently moving cellular components. With a detailed picture of the myosin V motor in hand, future research can focus on cellular functions of the molecule and mutants. — *Mona Mort*

See: M. Terrak, G. Rebowski, R.C. Lu, Z. Grabarek, and R. Dominguez, "Structure of the Light Chain-Binding Domain of Myosin V," Proc. Nat. Acad. Sci. USA **102**(36), 12718 (2005).
Author Affiliation: Boston Biomedical Research Institute
Correspondence: rdominguez@bbri.org

This work was supported by the National Institutes of Health, the U.S. Department of Energy, and the National Science Foundation. Use of the Advanced Photon Source was supported by the U.S. Department of Energy, Office of Science, Office of Basic Energy Sciences, under Contract No. W-31-109-ENG-38.

FINDING WAYS TO FIGHT ANTHRAX

The anthrax bacterium has received extensive attention as a biological weapon, because the anthrax spore is durable, and because after being ingested or inhaled, the resulting bacterial infection is highly toxic. Current treatment for anthrax exposure is limited to antibiotics that must be taken very early in the infection cycle, often when the flu-like symptoms may be too mild to identify as an infection. Even this treatment does not address the systemic toxicity that accompanies the infection and that would still be present after the bacteria had been killed by antibiotics. Any information about how to improve treatments for anthrax infection—and to make more likely the survival of those infected—constitutes great progress. A research team using the IMCA-CAT 17-ID beamline at the APS characterized a molecule that inhibits the factor responsible for making the anthrax infection lethal (Fig. 1). Their work is an important step in the discovery of treatments for controlling anthrax infection.

When the bacterium *Bacillus anthracis* infects cells, the primary disease effect comes from an enzyme toxin, a zinc-dependent metalloprotease called lethal factor. This factor, secreted into the cellular machinery of the host, wreaks havoc.

The researchers from Merck Research Laboratories, the United States Army Medical Research Institute of Infectious Diseases, and the Massachusetts Institute of Technology wanted to find a lethal factor inhibitor that could specifically block the ability of lethal factor to prevent macrophages—the cell's vacuum cleaners—from eliminating anthrax spores early in the infection (Fig. 2). Such an inhibitor could be administered when intentional release of anthrax is suspected and would help prevent the disease from developing. Or, if infection is already under way, the inhibitor could be used, together with an antibiotic, to make it less virulent and give the host a better chance of survival.

To pursue these goals, the team worked on the crystal structure of a proposed lethal factor inhibitor—a hydroxamate—bound to lethal factor at its active site. By studying this interaction in detail and by performing relevant bioassays, the group was able to show several promising inhibitory effects of the hydroxamate. Most important, when in complex with the hydroxamate, enzyme activity of the lethal factor decreased. The presence of the hydroxamate also helped keep the natural defenses intact; macrophages could carry out their eviction of the anthrax spores despite lethal factor. In mice, the presence of the hydroxamate provided complete protection against a recombinant form of lethal factor. Mice and rabbits exposed to a lethal dose of anthrax showed a significant survival advantage and a longer average time to death. And, in rabbits, using the hydroxamate treatment in combination with the antibiotic ciprofloxacin completely protected against anthrax infection. This is a significant improvement over the 50% protection demonstrated by giving the antibiotic alone.

All of these results support the research team's conclusion that they have discovered a small molecule that can significantly impair the virulence of lethal factor in anthrax infection. The group achieved their goal of finding a way to arrest the rate at which the infection takes over the organisms and leads to circulatory shock. The hydroxamate even shows promise as a prophylactic monotherapy against anthrax, in addition to being effective in a late stage of the disease when used with an antibiotic. Inhibiting anthrax lethal factor, when combined with an antibiotic administered during and immediately after anthrax

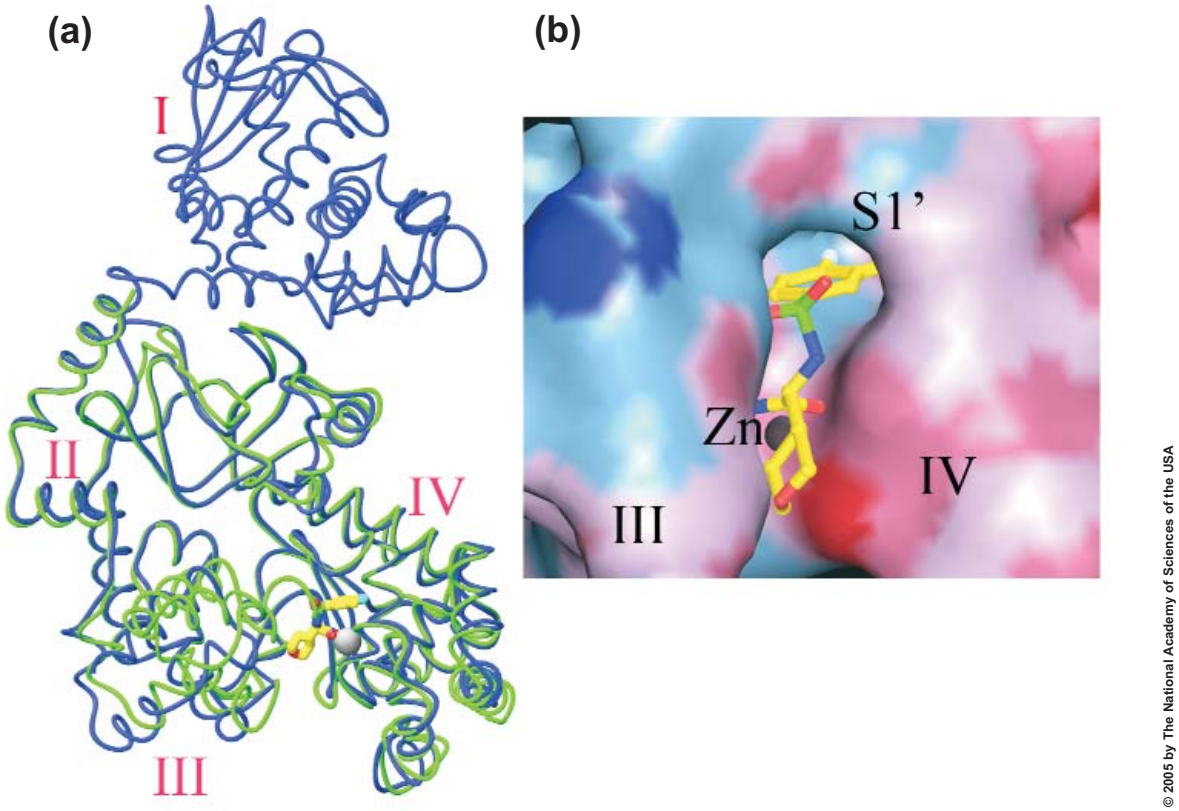

Fig. 1. Crystal structure of lethal factor inhibitor bound to lethal factor. (a): Overlay of full-length (blue) and truncated (green) lethal factor used in the study; domains numbered in red; lethal factor inhibitor and zinc ion represented as ball-and-stick models. (b): Molecular surface around the inhibitor binding site.

infection, shows great promise for saving people from the fatal effects of the disease. — *Mona Mort*

See: W.L. Shoop[1], Y. Xiong[1], J. Wiltsie[1], A. Woods[1], J. Guo[1], J.V. Pivnichny[1], T. Felcetto[1], B.F. Michael[1], A. Bansal[1], R.T. Cummings[1], B.R. Cunningham[1], A.M. Friedlander[2], C.M. Douglas[1], S.B. Patel[1], D. Wisniewski[1], G. Scapin[1], S.P. Salowe[1], D.M. Zaller[1], K.T. Chapman[1], E.M. Scolnick[3], D.M. Schmatz[1], K. Bartizal[1], M. MacCoss[1], and J.D. Hermes[1], "Anthrax Lethal Factor Inhibition," Proc. Natl. Acad. Sci. USA **102**, 7958 (2005).

Author Affiliations: [1]Merck Research Laboratories, [2]United States Army Medical Research Institute of Infectious Diseases, [3]Massachusetts Institute of Technology

Correspondence: jeffrey_hermes@merck.com

Use of the Industrial Macromolecular Crystallography Association Collaborative Access Team beamline 17-ID was supported by the Industrial Macromolecular Crystallography Association through a contract with the Illinois Institute of Technology. Use of the Advanced Photon Source was supported by the U.S. Department of Energy, Office of Science, Office of Basic Energy Sciences, under Contract No. W-31-109-ENG-38.

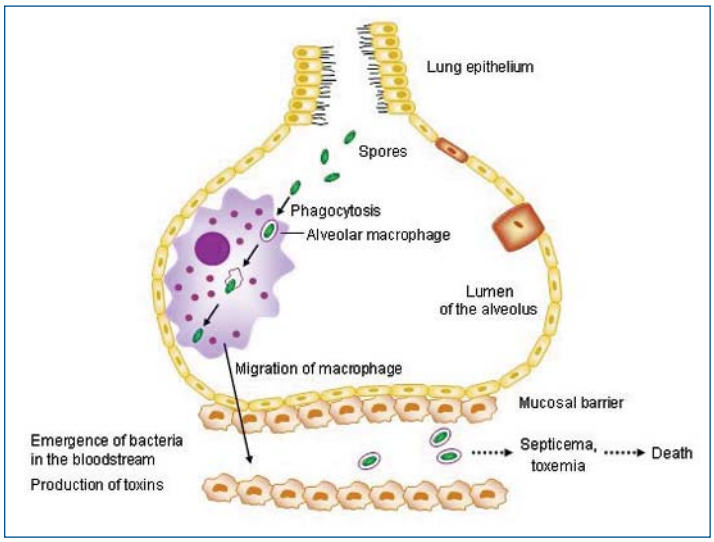

Fig. 2. Lethal factor disables the antibacterial effects of host macrophage and allows anthrax bacteria to gain access to the bloodstream.

Making Methanol: How Bacteria Do It

With oil reserves rapidly dwindling, finding a way to tap the fuel potential of extensive natural gas reserves is becoming critical. Converting methane to its liquid form, methanol, would make natural gas a desirable energy alternative to petroleum. Humans have yet to come up with an efficient method for converting methane to methanol. Certain bacteria, on the other hand, have long been capable of living on methane by turning it into methanol. Researchers from Northwestern University used the DND-CAT 5-ID beamline at the APS to characterize the first enzyme in the pathway that bacteria use to convert methane to methanol. Their work provides a clear picture of the enzyme's structure and is an important breakthrough in understanding how to improve the synthesis of methanol.

The investigators determined the elegant structure (Fig. 1) of particulate methane monooxygenase (pMMO) from the methanotrophic bacterium *Methylococcus capsulatus* (Bath) to a resolution of 2.8 Å. The architecture of the membrane-bound enzyme follows the rule of three. There are three subunits, with each subunit consisting of one copy of each of three different amino acid chains, called α (pmoA), β (pmoB), and γ (pmoC). The enzyme is partly soluble (primarily pmoB) and partly within the membrane (primarily pmoA and pmoC). Two metal centers in pmoB contain copper ions—either one or two. The pmoB subunit is also interesting because it looks a lot like an enzyme in the respiratory metabolic pathway. In the crystal, the membrane-bound section of the enzyme contains zinc ions in a third metal center. In living bacteria, this third metal center would most likely contain another metal ion, such as copper or iron.

One of the most promising aspects of this research is that the enzyme studied is one that is capable of converting methane to methanol at room temperature. That is important because a real stumbling block in synthetic production of methanol from methane has been the high temperatures needed to catalyze the reaction—temperatures at which the product methanol was not stable. Because methane is also a greenhouse gas and has been implicated in global warming, understanding how bacteria can convert dangerous methane into useful methanol is an added environmental benefit of knowing the structure of pMMO, which is one of the few enzymes capable of modifying methane.

Another important set of questions—about the number and nature of pMMO's metal centers—has also been answered by this study. Knowing how many and what type of metal ions the enzyme utilizes is integral to understanding how to manipulate its activity. Previous studies presented conflicting models of pMMO's metal binding properties, with some reports of up to 15 copper ions present in each subunit. The researchers conducting this study were able to provide data that nicely put the controversy to rest. In each of the three subunits of pMMO, there are three metal centers that, taken together, carry three copper ions and a fourth metal ion, with its exact identity in living systems yet to be determined.

With the structure of pMMO known in detail, the next question is: Which of the metal centers is the active site responsible for the oxidation activity of the enzyme? Because it is unusual and resembles other active double-copper-ion centers (such as in hemocyanin), the metal center that carries two copper ions is a plausible candidate. Or, because it resembles part of a cytochrome oxidase subunit, the two-copper-ion pmoB site could be involved in electron transfer, in which case the metal center carrying one copper ion could be the active site for oxidation of methane. Following the rule of three dictated by the enzyme's structure, there is a third possibility—the third metal center occupied by the zinc ion in the crystal could be the active site. Because of the enzyme picture revealed by this study, the answers to such questions, and others, are now within reach.

— Mona Mort

< Fig. 1. The structure of pMMO, showing the three subunits and metal centers (cyan: copper; magenta: zinc). A semi-transparent molecular surface is superimposed.

See: R.L. Lieberman and A.C. Rosenzweig, "Crystal Structure of a Membrane-bound Metalloenzyme that Catalyses the Biological Oxidation of Methane," Nature **434**, 177 (10 March 2005).

Author Affiliation: Northwestern University
Correspondence: amyr@northwestern.edu

This work was supported by the American Chemical Society Petroleum Research Fund (to A.C.R.), the David and Lucile Packard Foundation (to A.C.R.), and the NIH (to A.C.R. and R.L.L.). Use of the Advanced Photon Source was supported by the U.S. Department of Energy, Office of Science, Office of Basic Energy Sciences, under Contract No. W-31-109-ENG-38.

A GROWING UNDERSTANDING OF FETAL-MATERNAL IMMUNITY

It's a simple problem with a complex solution. A developing fetus is also a foreign body in the maternal womb. How does the fetus protect itself from the maternal immune response that is designed to eliminate foreign cells? A large number of immune system molecules are involved to varying degrees in a process not clearly understood. The APS helped shed light on the fetal immune response when researchers from Monash University and the University of Melbourne utilized the BioCars beamline 14-BM to characterize the crystal structure of the protein HLA-G. Their work points to a role for HLA-G in fetal immunological tolerance and paves the way for a deeper understanding of immune responses in general.

In terms of overall structure, HLA-G is similar to known major histocompatibility class I (MHC-I) molecules in that there is a heavy chain with three domains (α1, α2, and α3) associated with β_2M [Fig. 1(A)]. An amino acid chain—or peptide—from histone H2A protein attaches in a groove created by the helices α1 and α2, with a floor formed by an antiparallel β sheet [Fig. 1(B)]. Detailed analysis of the HLA-G binding constraints leads to an understanding of why HLA-G exhibits restricted amino acid specificity [Fig. 1(C)].

The investigators used a resolution of 1.9 Å to study an HLA-G molecule attached to the peptide from histone H2A. The intricacies of the peptide binding are not typical of related MHC-Ia (classical) structures and are more similar to those found in the nonclassical (class Ib) HLA-E. An array of contacts between the peptide and the HLA-G antigen-binding cleft result in restricted binding similar to that found in the HLA-E molecule. HLA-G shares high (78%) sequence similarity with HLA-E and equal or higher sequence similarity with related molecules (Qa-2, HLA-A2, HLA-B44, and HLA-CW3).

HLA-G exhibits its specificity by binding to a limited suite of peptides; it also interacts with LIR-1 and LIR-2, inhibitory leukocyte Ig-like receptors, and perhaps with some natural killer cell receptors. The binding constraints point to a structural basis for the limited number of peptides that are bound by HLA-G. In addition, the α3 domain of HLA-G, which may be the binding site for the LIR-1 and LIR-2 inhibitory receptors, is structurally different from α3 domains of classical MHC-I molecules. Different structures may explain why different peptides are bound by the two types of molecules.

The human choriocarcinoma cell line JEG-3 provided the gene for HLA-G*0101. Site-directed mutagenesis produced a variant of HLA-G*0101 in which Cys-42 of the heavy chain was changed to serine; this procedure improved the yield of correctly folded HLA-G. The two HLA-G forms were expressed separately in *E. coli* and purified. The 14-BM BioCars beamline allowed structural measurement, at 1.9 Å, of a flash-frozen crystal of the Cys42-Ser42 variant. Diffracting crystals, obtained by hanging drop vapor diffusion, belong to the space group $P322_1$ (unit cell dimensions a = b = 77.15 Å; c = 151.72 Å). The Cys-42 is unique to HLA-G relative to other MHC-I molecules and is the site for disulfide bond formation when HLA-G attaches to another molecule of its own kind, thus forming double molecules. Nevertheless, crystals of wild-type HLA-G,

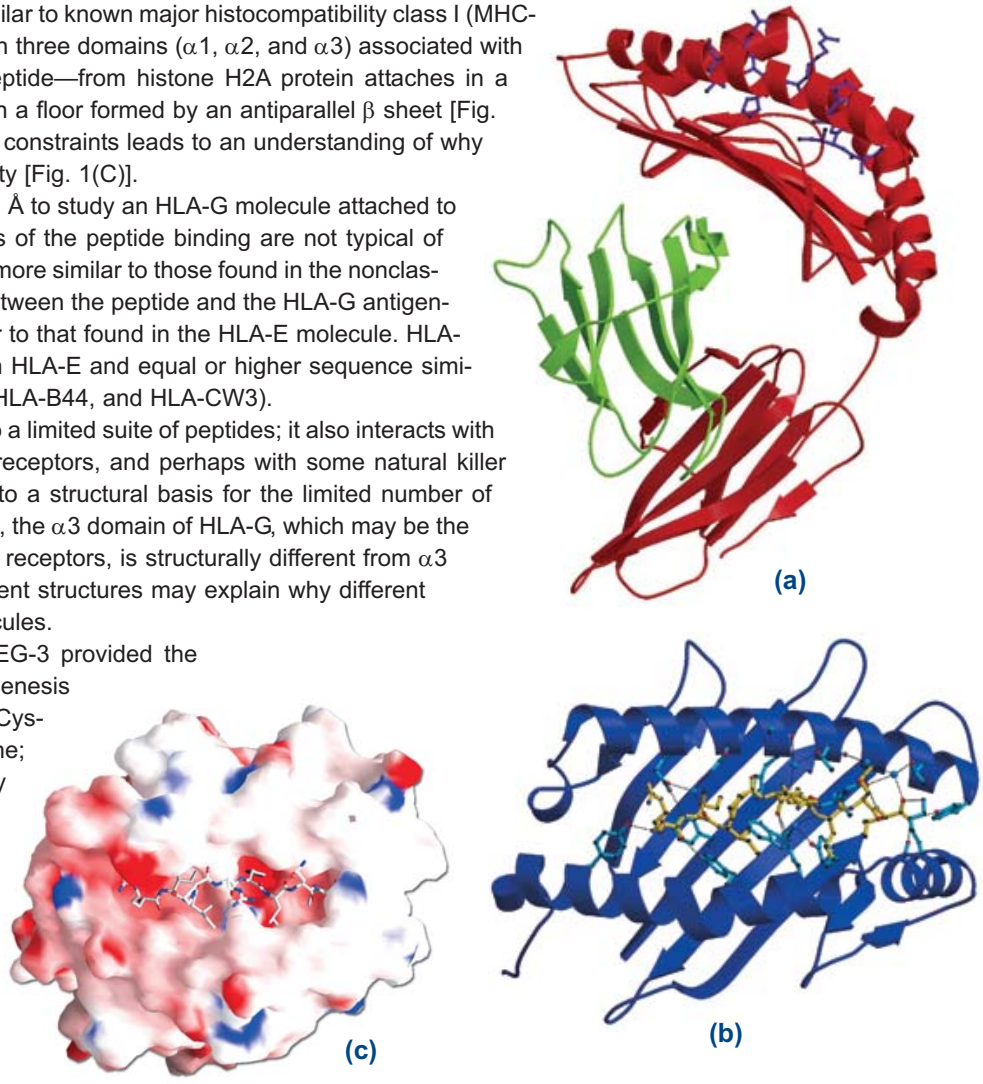

Fig. 1(a). Overall structure of HLA-G. The heavy chain is shown in red, β2M in green, and the peptide in purple. (b) Interactions between the peptide (yellow) and the HLA-G antigen binding cleft, illustrating the extensive network of contacts that impose structural constraints on the peptide. (c) Electrostatic representation of HLA-G with the peptide (ball-and-stick) bound in the antigen-binding cleft.

grown under identical conditions, exhibited the same unit cell dimensions as the variant and did not form double molecules under the experimental conditions.

The limited peptide repertoire of HLA-G, in addition to its high expression in the placenta and unusual promoter elements, point to a unique functional role in fetal-maternal immune responses. The researchers suggest that HLA-G makes a significant contribution to the immunological tolerance of the fetus. Future work will undoubtedly focus on how HLA-G interacts with inhibitory killer and LIR-1/2 receptors, following the trail of a novel mode of interaction suggested by the present data. — *Mona Mort*

See: C.S. Clements[1], L. Kjer-Nielsen[2], L. Kostenko[2], H.L. Hoare[1], M.A. Dunstone[1], E. Moses[2], K. Freed[2], A.G. Brooks[2], J. Rossjohn[1], and J. McCluskey[2], "Crystal Structure of HLA-G: A Nonclassical MHC Class I Molecule Expressed at the Fetal-maternal Interface," PNAS **102**, 3360 (2005).

Author Affiliations: [1]Monash University, [2]University of Melbourne

Correspondence: craig.clements@med.monash.edu.au

This work was supported by a Wellcome Trust Senior Research Fellowship in Biomedical Science in Australia (to J.R.), a Monash University Research Fellowship (to C.S.C.), the National Health and Medical Research Council, the Australian Research Council, the Australian Synchrotron Research Program and the Roche Organ Transplantation Research Foundation. Use of the Advanced Photon Source was supported by the U.S. Department of Energy, Office of Science, Office of Basic Energy Sciences under Contract No. W-31-109-ENG-38.

AROUND THE EXPERIMENT HALL

THE SILK ROAD LEADS TO THE APS

Lori Khatchadourian (University of Michigan) and Adam Smith (The University of Chicago) switch sample mounts at the ChemMatCARS 15-ID-D beamline. The samples are from one of Smith's excavations in Armenia and date to 1300 B.C. They were recovered from a shrine destroyed in a violent conflagration that ended occupation in the region for several hundred years. Smith's group is analyzing relics from northern China, the southern Urals, and the south Caucasus. These materials date to three distinct phases, from the early third millennium B.C. to the mid-first millennium B.C. The other team members, all from The University of Chicago, are Alan Greene, Charles Hartley, and David Peterson.

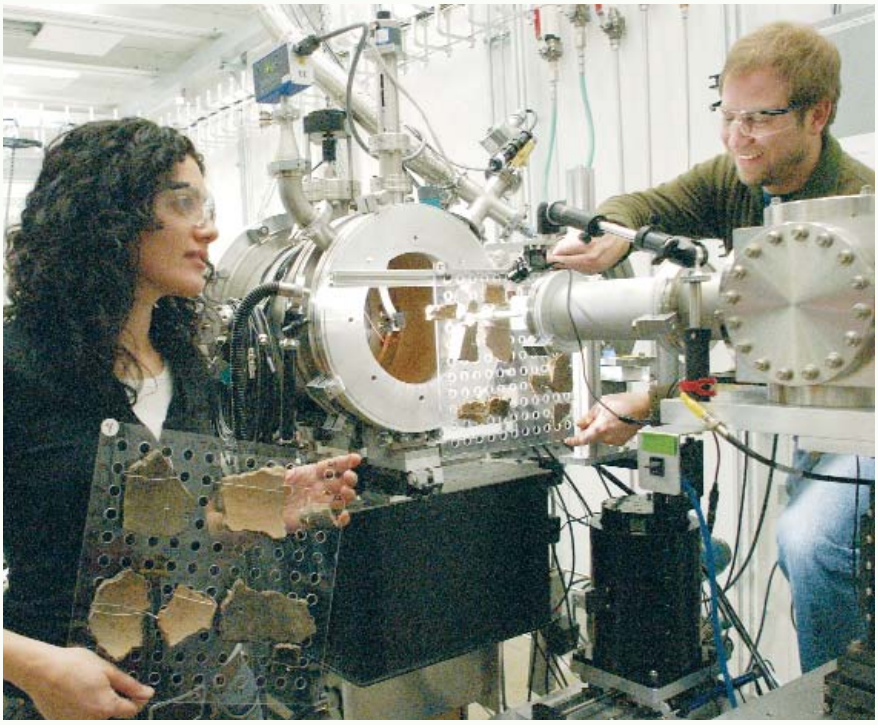

Smith: "Archaeologists, on the rare occasions when they have turned to the APS, have traditionally used it to describe a single remarkable 'treasure' in great depth. While this approach sheds much light on unique finds, it focuses attention on the extraordinary, singular find at the expense of the vast corpus of ordinary materials that make up most archaeological assemblages. Our group's goal is to determine the utility of APS analysis to examining large assemblages of mundane objects from different parts of the past. Eurasia—the vast continent that stretches from the Caucasus to China—is our geographic focus because, first, it is best known through archaeological methods; historical records from the Bronze and Iron Ages are rare. And second, the links between China, the Russian Steppe, and the Caucasus would later form the basis for the complex exchange networks known as the Silk Road. There was clearly an earlier material basis for these connections that we think is still visible in the artifacts of the three regions. But such connections will not be visible in the unique art historical treasures. They will only emerge from close analyses of everyday things." *Contact: atsmith@uchicago.edu*

How DNA-modifying Enzymes Find Their Place

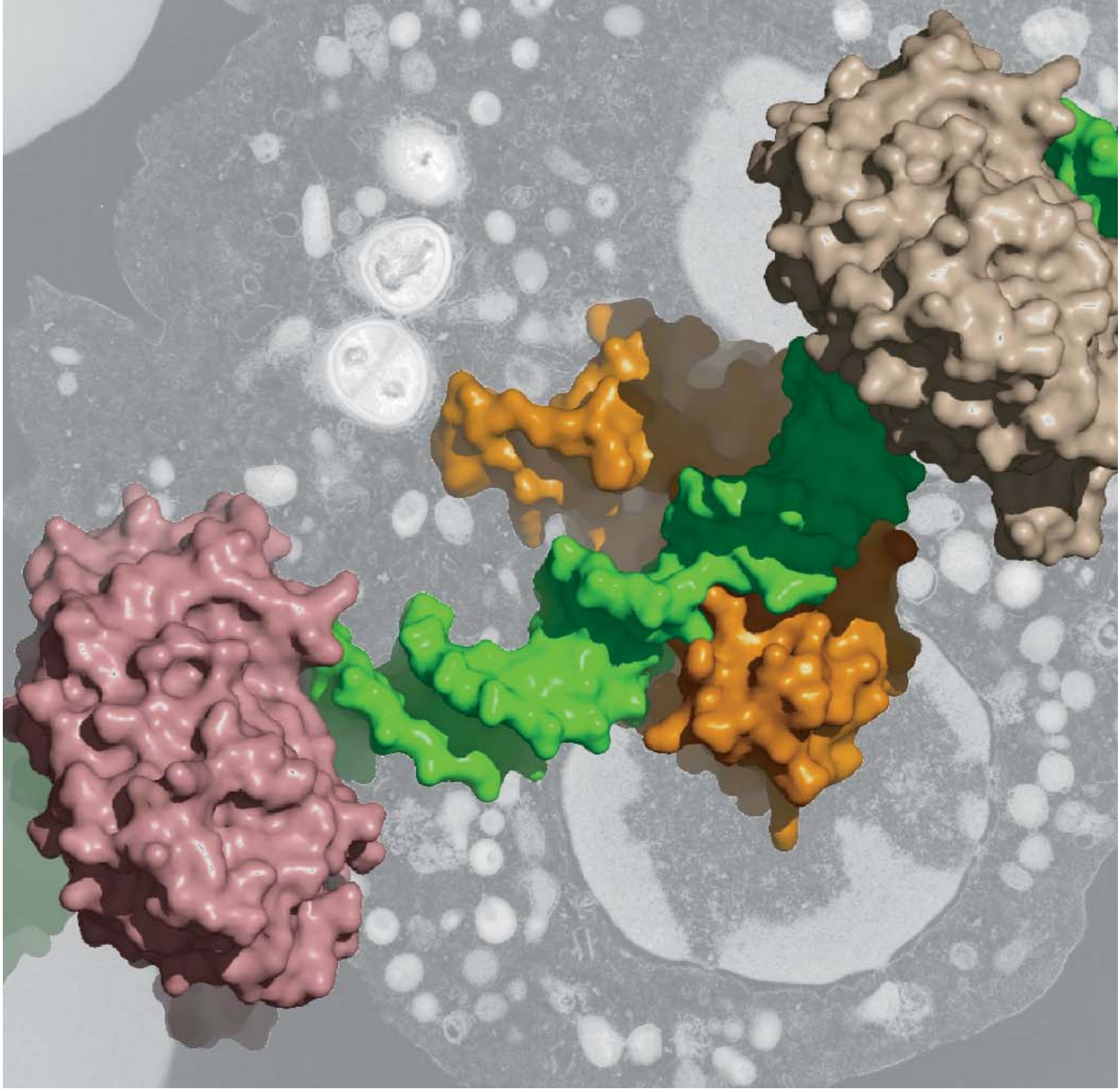

Given the large size and intricate structure of DNA molecules, it is a wonder that binding proteins ever find their target location. But they do, with the help of sophisticated chemical bonding events and rearrangements. The DNA methyltransferases, a particularly interesting group, exhibit elegant specificity in terms of where they bind DNA. Some particulars of this process were already known. Now, investigators from Emory University, International University Bremen, and University of Rochester, aided by the IMCA-CAT 17-ID and SER-CAT 22-ID beamlines at the APS in have carried out studies of bacteriophage and related bacterial DNA-adenine methyltransferase. Their results reveal telling detail about the suite of steps involved in binding. Since the resulting methylation is linked to the virulence of pathogenic bacteria, such as *Salmonella*, refined understanding of the process shows promise for inhibiting the spread of disease that is bacterial in origin.

The researchers determined structures for bacteriophage T4 DNA-adenine methyltransferase (T4Dam) and studied the effects of substitutions in the related *Escherichia coli* DNA-adenine methyltransferase (EcoDam). The researchers examined T4Dam in complex with partially and fully specific DNA and a methyl-donor analog. Altered residues in EcoDam were those that correspond to that observed in the interaction with the T4Dam GATC (Gua-Ade-Thy-Cyt) target sequence. Two types of protein-DNA interactions emerged from this work. Discriminatory contacts are responsible for stabilizing the transition state and accelerating methylation of the cognate site. Antidiscriminatory contacts work by disfavoring activity at noncognate sites while not having a large influence on methylation at the cognate site. The beauty of the structural transitions is that they show how the enzyme-DNA interaction moves from nonspecific to specific, with a strong suggestion of a temporal order for forming specific contacts.

The IMCA-CAT and SER-CAT beamlines facilitated collection of crystallographic data in three sets. Data set 1 used crystals from a 13-mer oligonucleotide (protein/DNA ratio ~2:1) and the methylation reaction product S-adenosyl-L-homocysteine (AdoHcy). Data set 2 used an orthorhombic-form crystal from the 15-mer oligonucleotide (protein/DNA ratio ~1:1) and AdoHcy; since this reaction mix could produce several forms of crystal within the same drop, the protein/DNA ratio and PEG 6000 concentration were varied to create a predominance of one form. Data set 3 used crystals from the blunt-end 16-mer DNA (protein/DNA ratio ~2:1) and sinefungin [adenosyl ornithine, an S-adenosyl-L-methionine (AdoMet) analog]. DNA methylation and binding experiments allowed tracking of how the variants performed with respect to specificity.

< Fig. 1. Three DNA adenine methyltransferases (Dam) molecules (grey, orange, salmon) move linearly along the DNA (green) and rotate up and down as rigid bodies searching for the specific DNA sequence GATC. In the background, electron micrograph (courtesy of Dr. Robert P. Apkarian, Emory University) shows polymorphonuclear leukocytes harvested from human peripheral blood containing the bacterium *Staphylococcus aureus*. *(Image courtesy of Drs. John R. Horton and Xiaodong Cheng, Emory University.)*

The 13-mer oligonucleotide, in complex with T4Dam and AdoHcy, had one GATC binding site. In a surprising result, the two DNA molecules in the crystal showed shifting, so that the helical axes were offset by ~12 Å. Each DNA molecule in the crystallographic asymmetric unit was bound to two Dam monomers. One monomer generally binds nonspecifically to eight base pairs in a single DNA duplex, while another binds in the joint between the two DNA duplexes.

The end sequence of the 15-mer duplex represents part of the GATC target. One type of Dam molecule occupied all the joints between adjacent DNA molecules; two other types of Dam molecule appear to be more restricted in terms of where they will bind. Intermediate stages in specificity are seen by conformations that mimic partial site recognition. For full site recognition, a protein side chain intercalation is involved. The 16-mer oligonucleotide-sinefungin binding revealed extensive detail about the active-site conformation.

The substrate-recognition pathway exhibited six unique T4Dam-DNA interactions that occur without much conformational change in the proteins or the DNA. The transition stages strongly suggest a time component for forming specific binding while T4Dam slides along the DNA (Fig. 1) and also suggest how proteins and enzymes could have acquired DNA specificity during evolution. Enzyme activity was strongly reduced after disrupting the discriminatory contact, suggesting a way to debilitate the metabolism of bacterial pathogens.

— *Mona Mort*

See: J.R. Horton[1], K. Liebert[2], S. Hattman[3], A. Jeltsch[2], and X. Cheng[1], "Transition from Nonspecific to Specific DNA Interactions Along the Substrate-recognition Pathway of Dam Methyltransferase," Cell **121**, 349 (6 May 2005).

Author Affiliations: [1]Emory University, [2]International University Bremen, [3]University of Rochester
Correspondence: xcheng@emory.edu

This work was supported by the U.S. Public Health Services (to S.H. and X.C.), the Georgia Research Alliance (to X.C.), and the German BMBF and DFG (to A.J.). Use of the Advanced Photon Source was supported by the U.S. Department of Energy, Office of Science, Office of Basic Energy Sciences, under Contract No. W-31-109-ENG.-38.

Peering into the Geological Past: Crystal Signatures in Magma

Photo: "Nyiragongo" by Jacques Durieux (jdurieux@chello.fr)
Observatoire Volcanologique de Goma - Goma RDCongo

Where, when, how—three questions that are often asked about volcanic eruptions in the distant past. One way to find answers to those questions lies in examining magma—the molten rock under the Earth's crust that turns to igneous rock upon cooling at the surface. In the enormous Long Valley Caldera near Mammoth Lakes, California, the Bishop Tuff is a prime example of erupted magma. Researchers from The University of Chicago employed the GSECARS bending magnet beamline 13-BM to examine the size and distribution of crystals and bubbles in the Bishop Tuff. Their results are making it possible to reconstruct the volcanic events that rearranged the landscape, leading to refined knowledge of how magma behaves before reaching the Earth's surface—information that could help predict volcanic activity.

Focusing on quartz, because it was the most abundant mineral in their sample, the researchers combined their microscope observations and x-ray images to reconstruct processes in the Bishop magma. Two types of glass-coated quartz crystals occurred: crystals showing bipyramidal shapes (euhedral) and round crystals. Commonly found were whole crystals greater than 200 μm in size, with no whole crystals under 100 μm. The higher the density of the pumice, the greater was the weight fraction composed of crystals.

Because fragmentation of crystals is thought to be important in magma formation, the size distribution of crystals lends itself to interpretations of magmatic processes. The data suggest that before or during eruption, crystals in the Bishop magma underwent pronounced fragmentation. Since small whole crystals are less likely to fragment than large crystals, it was assumed that, if they had formed in great numbers, small whole crystals would have been present in the sample. But the small crystals were not present in abundance, leading to the

conclusion that seeding, or nucleation, of crystals was not important in the later stages of crystallization of this particular magmatic body.

A high-silica pyroclastic rhyolite, the Bishop Tuff was the source of five pumice samples from three early-erupted stratigraphic units. Using facilities at the APS, the researchers studied crystal size classes via: crushing, sieving, and winnowing (for crystals >100 μm); optical microscopy of pumice fragments (for crystals <100 μm); and computerized x-ray microtomography (for crystals >100 μm, using ~1 cm^3 pumice pieces). The observed crystal size distributions can be explained by crystal fragmentation. Frequently found were embedded fragments coated with glass, showing that fragmentation happened prior to eruption.

The size distribution for whole crystals, characteristic of a group of high-density pumice with high crystal content, indicates late-stage growth with limited nucleation (Fig. 1). Another group of pumice samples exhibited low density, low crystal content, and few large crystals; nucleation appeared to be locally significant, perhaps near the walls (Fig. 2). A third group exhibited characteristics intermediate between the first two groups. The larger the number of crystals, the smaller the volume of bubbles; this result is compatible with sinking of large crystals and rise of bubbles in the magma. All of these features are consistent with a large, gas-saturated, slowly cooling, stably stratified magma.

X-ray tomography produced three-dimensional images of crystals and crystal fragments and was used to determine their spatial distributions, as well as size distributions. The GSECARS bending magnet beamline was used for collection of x-ray tomographic data. The tomography data were important because they revealed the characteristics of the pumice samples prior to any significant laboratory processing, unlike the other techniques used.

A pattern of relationships among density, crystal abundance, and size and shape of the Bishop Tuff samples allowed three different kinds of pumice to be identified in the pre-eruptive magma. Study of crystal fragmentation, nucleation, and growth can be used to retrace the temporal and spatial paths by which magma journeyed to the Earth's surface and became the history-laden treasure of hard rock now visible. — *Mona Mort*

See: G.A.R. Gualda, D.L. Cook, R. Chopra, L. Qin, A.T. Anderson, Jr., and M. Rivers, "Fragmentation, Nucleation and Migration of Crystals and Bubbles in the Bishop Tuff Rhyolitic Magma," T. Roy. Soc. Edin-Earth **95**, 375 (2004).
Author Affiliation: The University of Chicago
Correspondence: ggualda@uchicago.edu

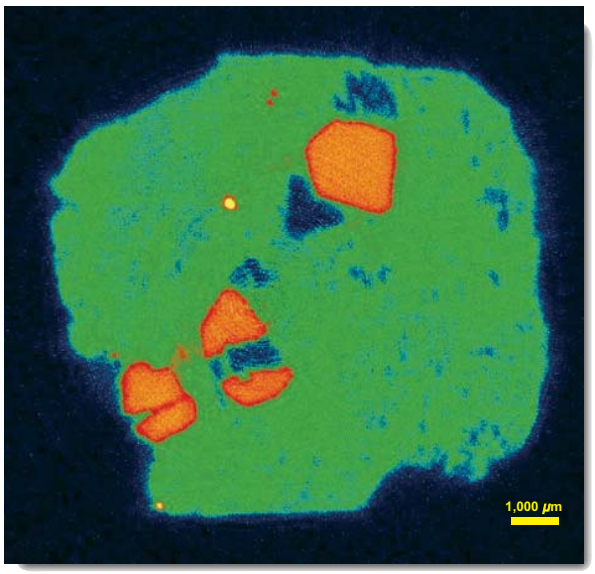

Fig. 1 (above). A small magnetite crystal (yellow) and three quartz crystals (orange)—one of which is nearly broken in two—in a glass matrix with small vesicles (green) and a few large vesicles (black) that are remnants of large bubbles in the magma.

Fig. 2 (below). A feldspar crystal (bright orange) with a tiny inclusion of magnetite.

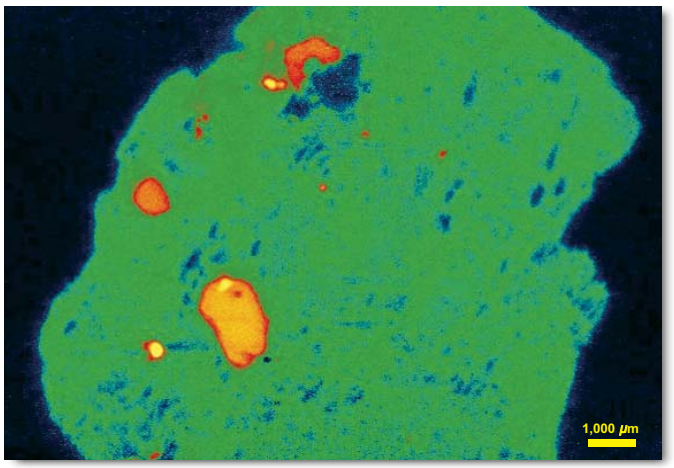

This work was supported by NSF grants to A.T.A. GSECARS-CAT is supported by the NSF (EAR-0217473) and the U.S. DOE (DE-FG02-94ER14466). Use of the Advanced Photon Source was supported by the U.S. DOE, Office of Science, Office of Basic Energy Sciences, under Contract No. W-31-109-ENG-38.

HEMATITE SURFACES

Chemical reactions occurring at the interface between minerals and water are among the most important factors controlling the fate of contaminants in the environment. Therefore, having a fundamental understanding of how water interacts with mineral surfaces is critical to the fields of environmental chemistry and geochemistry. As a common iron oxide, hematite provides an excellent model system in which to study how aqueous solutions affect the structure and reactivity of mineral surfaces. An extensive research project, based at the University of Alaska Fairbanks and aided by the GSECARS facilities at the APS, has now resulted in a detailed description of the structure and reactivity of the hydrated hematite (0001) surface. These new data advance our understanding of the factors controlling surface structure under aqueous conditions; they also provide experimental and theoretical constraints for developing models that predict contaminant fate in aquatic systems.

The hydroxylated (0001) surface of hematite (α-Fe_2O_3) served as the main focus of the study, which relied on crystal truncation rod (CTR) diffraction and density functional theory (DFT). Combining experimental and theoretical results, the researchers propose that two chemically distinct hydroxyl units—singly and doubly coordinated with Fe—dominate the surface. Distinct domains of the surface species appeared, with one domain corresponding to the hydroxylation of the surface Fe-cation predicted to be most stable under ultra-high vacuum. In a second domain, complete removal of the surface Fe leaves the hydroxylated oxygen layer. In addition, at high water partial pressures, the hydroxylated hematite surface structures prove to be more stable than the dehydroxylated versions previously observed in ultra-high vacuum studies of the same surface. Interestingly, when compared to the same type of stability transition for α-alumina, the hematite transition occurs at water pressures that are orders of magnitude lower. The latter finding helps explain why hematite and alumina (0001) surfaces react differently with water and aqueous metal cations.

A CTR is a diffuse streak of x-ray intensity that arises from the abrupt termination of a crystal lattice. CTR diffraction data, measured on a natural specular hematite specimen from Brazil, were obtained at the GeoSoilEnviroCARS 13-ID beamline (Fig.1). Density functional theory calculations allowed predictions of surface structure that could then be compared directly with the experimental CTR results, and they provide detailed information about the energetics of the surface.

The DFT results predicted that a single-layer Fe-terminated surface (Fe-O_3-Fe-R, or charge-balanced termination) should be most stable under ultra-high vacuum conditions (Fig. 2). The application of *ab initio* thermodynamic calculations to predict the surface energy in the presence of water suggested, however, that environmental conditions would strongly influence both the structure and composition of the most stable surface configuration.

A refinement of the CTR data set led to a best-fit structural model consistent with hydroxylation of the charge-balanced Fe_2O_3 (0001) surface but showed a partial occupancy of the terminating Fe-cation (Fig. 1). Detailed comparison of the experimental structural model with optimized DFT surface models suggested that the surface consisted of two distinct

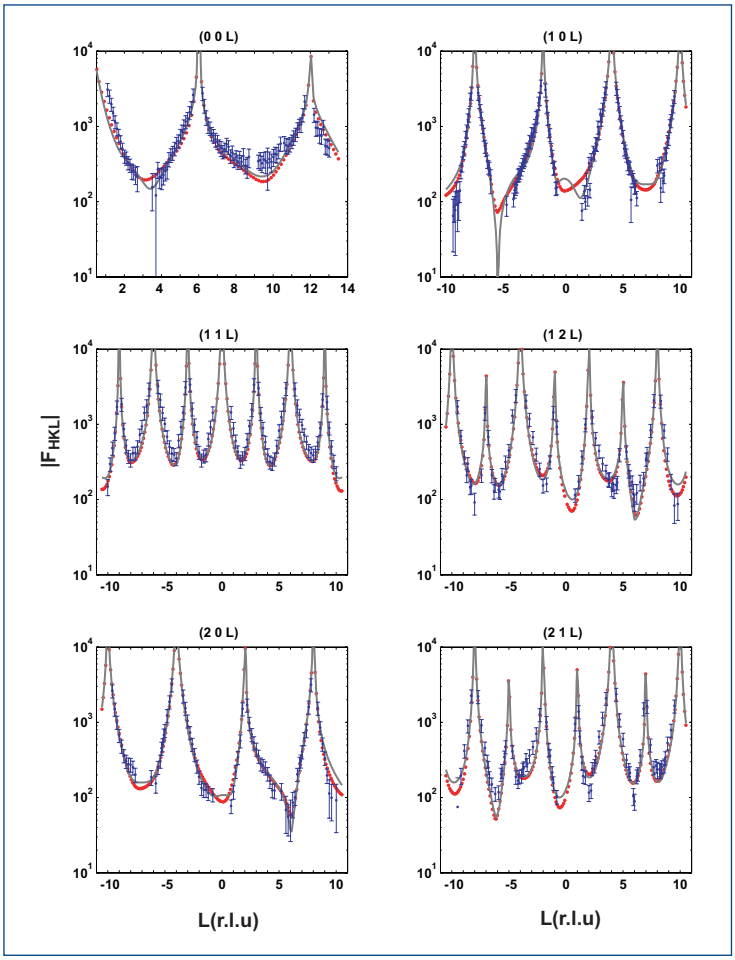

Fig. 1. Experimental structure factors (F_{HKL}) as a function of perpendicular momentum transfer (L, in reciprocal lattice units) for the α-Fe_2O_3 (0001) surface and calculated CTR profiles for best-fit model.

hydroxylated domains: one in which the surface structure is consistent with adsorption of three waters at the Fe-cation site on the charge-balanced surface and a second consistent with complete removal of this cation, leading to a single hydroxyl layer (Fig. 3). While the thermodynamic calculations predict that a single domain should be most stable, the researchers speculate that kinetic factors prevent complete conversion of the surface. Future experimental and theoretical work will refine the factors influencing the dynamics of the surface transformation.

By providing a sophisticated analysis of the surface and structure of hydrated hematite, the present study contributes immensely to our knowledge of how minerals respond to interaction with water. Using this knowledge, more accurate predictions can be made about how structural chemistry controls the fate of surface and groundwater contamination. — *Mona Mort*

See: T.P. Trainor[1], A.M. Chaka[2], P.J. Eng[3], M. Newville[3], G.A. Waychunas[4], and J.G. Catalano[5], and G.E. Brown, Jr.[5,6], "Structure and Reactivity of the Hydrated Hematite (0001) Surface," Surf. Sci. **573**, 204 (2004).

Author Affiliations: [1]University of Alaska Fairbanks, [2]National Institute of Standards and Technology, [3]The University of Chicago, [4]Lawrence Berkeley National Laboratory, [5]Stanford University, [6]Stanford Synchrotron Radiation Laboratory
Correspondence: fftpt@uaf.edu

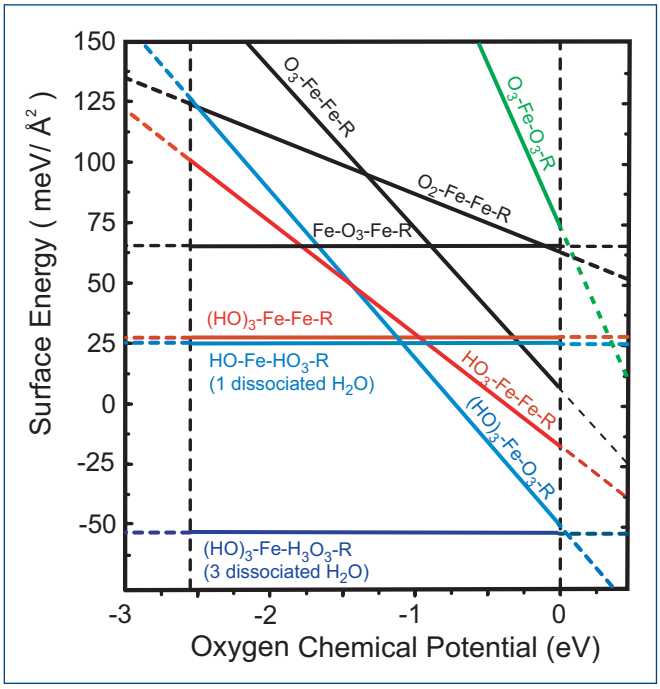

Fig. 2. Surface energy diagram based on DFT calculations at 0K; calculations using μ_H at 1 bar H_2O (ideal gas) are shown.

This work was supported by DOE-Geosciences, NSF-CHE and NSF-BES, and the University of Alaska Fairbanks. Use of the Advanced Photon Source was supported by the U.S. Department of Energy, Office of Science, Office of Basic Energy Sciences, under Contract No. W-31-109-ENG-38.

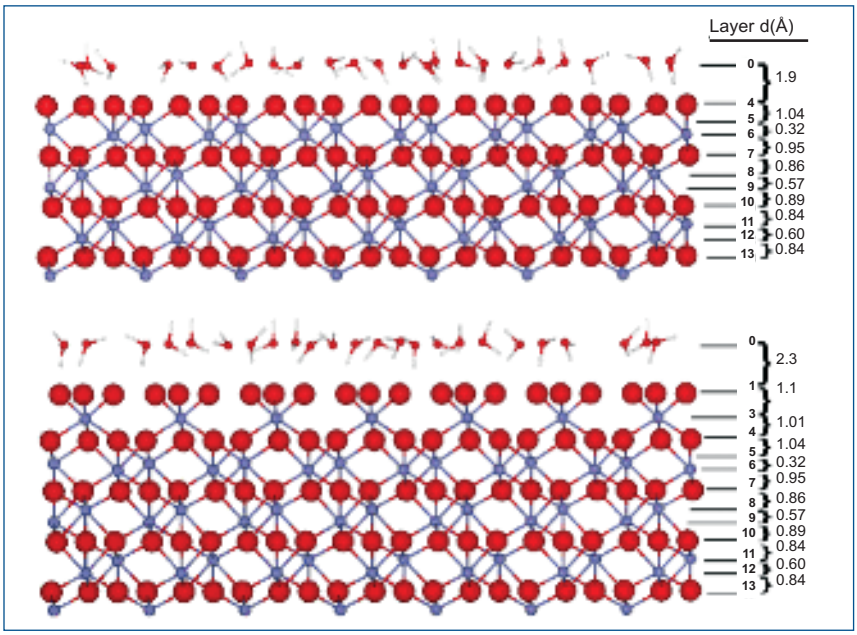

Fig. 3. Atomic layering sequence and layer spacings (d) along the [0001] direction for the best-fit relaxed surface models. Top panel, O_3-Fe-Fe-R; bottom panel, O_3-Fe-O_3-R; large spheres, O atoms; small spheres, Fe atoms. Adsorbed water layers (layer 0) drawn with arbitrary in-plane positions and water molecule orientations. The analysis gives layer 0 oxygen densities for surfaces: 1.2 ± 0.3 (O/unit cell), O_3-Fe-Fe-R, and 2.0 ± 0.3 (O/unit cell), O_3-Fe-O_3-R.

IRON AT THE D″ LAYER

At the boundary between the Earth's silicate mantle and iron-rich core lies the enigmatic D" layer. This layer is approximately 2,600 km to 2,900 km below the Earth's surface, and it has intrigued scientists because of its many complex seismic features, which include ultralow-velocity zones. Recent work has suggested that $MgSiO_3$ perovskite, the most abundant phase in the lower mantle, undergoes a transition to a post-perovskite (ppv) phase at pressures and temperatures comparable to those of the D" layer. Researchers from the The University of Chicago, the Carnegie Institution of Washington, and HP-CAT have studied the solubility of iron in this phase, which was previously unknown. They found that iron-rich (Fe_xMg_{1-x}) SiO_3 with x as high as 0.8 was stable, forming a single-phase ppv silicate (rather than decomposing into oxides). The iron-rich phase is up to 20% denser than any known silicate at the core mantle boundary, and if present in the D" layer, could explain the large reductions in seismic velocity observed in ultralow-velocity zones.

The researchers began with orthopyroxenes samples with x = 0.2, 0.4, 0.6, and 0.8 (designated as Fs20, Fs40, Fs60, and Fs80, respectively) and compressed them to 120 to 150 GPa in symmetrical diamond-anvil cells. The samples were heated by using double-sided laser systems and examined via x-ray diffraction on the 13-ID-D (GSECARS) and 16-ID-B (HP-CAT) beamlines at the APS. Laser-heating of Fs40 and Fs60 at 30 GPa to 100 GPa produced silicate perovskite, magnesiowustite, and stishovite. Heating samples compressed directly to 120 GPa to 150 GPa at 2,000K, Fs20, Fs40, Fs60, and Fs80 transformed to ppv without a trace of silicate perovskite or mixed oxides.

The research team found that the increase in volume with iron content was fairly small, so the density of the ppv was essentially dependent on the amount of iron—as iron content increased, so did the density of the ppv. For Fs80 ppv, this translates into a density increase of 20% relative to other iron-poor lower mantle phases. Such high density in the silicates would have a major impact on the seismic and geodynamic properties of the D" layer. As a first approximation, seismic velocities are reduced inversely proportional to the square root of the increasing density because of the iron enrichment. For instance, a ppv silicate with x= 0.66 would be sufficient to lower seismic velocities by the amount observed in ultralow-velocity zones found at the base of the D" layer.

Contrary to beliefs that the composition of lower mantle silicates was essentially unchanged by contact with the iron-rich core (i.e., that the D" layer would be fairly iron-poor), this study shows that this boundary layer may consist of denser silicates with a high iron content. At the core-mantle boundary, ppv silicate would be in contact with a huge iron reservoir, which may provide favorable conditions for the formation of high-iron ppv silicate (Fig. 1). This may provide an alternate explanation for the cause of ultralow velocity zones and some of the other intriguing seismic properties of the D" layer. — *Karen Fox*

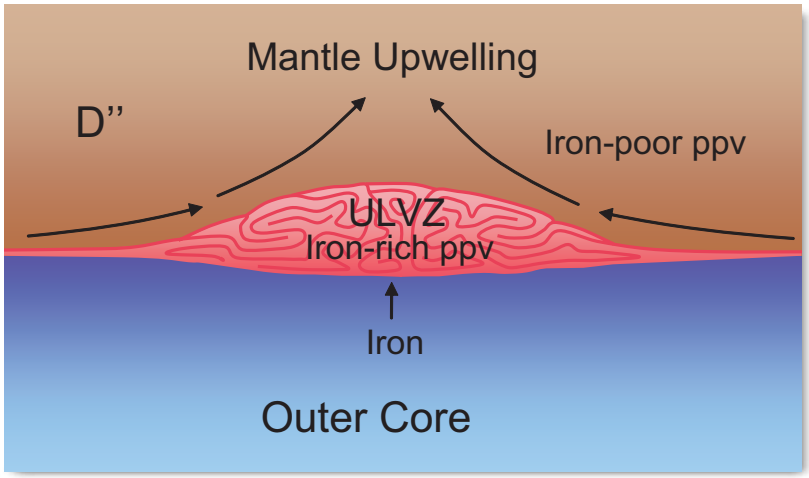

Fig. 1. Schematic diagram of the reaction boundary between an Fe-poor mantle and Fe-rich core, and the accumulation of Fe-rich ppv in ultralow-velocity zones.

See: Wendy L. Mao[1,2], Yue Meng[3], Guoyin Shen[1], Vitali B. Prakapenka[1], Andrew J. Campbell[1], Dion L. Heinz[1], Jinfu Shu[2], Razvan Caracas[2], Ronald E. Cohen[2], Yingwei Fei[2], Russell J. Hemley[2], and Ho-kwang Mao[1,2,3], "Iron-rich Silicates in the Earth's D" Layer," Proc. Natl. Acad. Sci. U.S.A. **102**, 9751 (12 July 2005).

Author Affiliations: [1]The University of Chicago, [2]Carnegie Institution of Washington, [3]High Pressure Collaborative Access Team

Correspondence: wmao@uchicago.edu

Work supported by the National Science Foundation (NSF) Earth Sciences Geochemistry, Geophysics, and Instrumentation and Facility Programs. GeoSoilEnviroCARS is supported by NSF–Earth Sciences Grant EAR-0217473, the U.S. Department of Energy (DOE) Geosciences Grant DE-FG02-94ER14466, and the State of Illinois. HP-CAT facility supported by the DOE Office of Science, Office of Basic Energy Sciences (BES), the DOE National Nuclear Security Administration (Carnegie/DOE Alliance Center), the NSF, the Department of Defense Tank-Automotive and Armaments Command, and the W.M. Keck Foundation. Use of the Advanced Photon Source was supported by the DOE-BES, under Contract No. W-31-109-ENG-38.

WHAT LIES AT THE EARTH'S CORE-MANTLE BOUNDARY?

The lowest level of the Earth's mantle, some 2,700 km below the surface, has recently been the subject of some intrigue. Known as the D" layer, this thin boundary between the Earth's mantle and its core shows unexplained seismological properties. Seismic waves change speed as they cross the layer in a variety of interesting and not well understood ways: speed varies from region to region within the layer and also varies with the polarization of the seismic wave. Understanding the composition and crystal structure of the mantle is a key first step to interpreting these seismic features. Researchers using the GSECARS 13-ID beamline at the APS have uncovered some tantalizing clues that point to transformed perovskite as a major component at the boundary between the Earth's mantle and core.

The mantle is made of rock, the core is made of metal, but the composition of the D" layer in between is not completely understood. Understanding the composition and crystal structure is a key first step to interpreting the seismic features. The dominant mineral in the lower mantle is known to be $MgSiO_3$ with a perovskite-type structure—a mineral which is also found in many superconducting materials. In the 1990s, the first synchrotron *in situ* high pressure-temperature experiment on $MgSiO_3$ perovskite (Mg-Pv) suggested that at pressures of 1,500-km depth, it separated into two minerals: MgO and SiO_2. Shim et al examined the stability of Mg-Pv at a wide range of pressures and temperatures and found no such transition. Instead, they found evidence that Mg-Pv undergoes a major phase transition at much deeper depth conditions (2,700-3,000 km). This is consistent with the post-perovskite phase proposed by Murakami et al. in 2004 [1] and it may account for the oddities of the D" layer.

The research was conducted by researchers from the Massachusetts Institute of Technology; Princeton University, the University of California, Berkeley; and The University of Chicago. $MgSiO_3$ glass was loaded into a rhenium gasket with an insulating layer of argon. This was then put into a diamond anvil and then examined with angle-dispersive diffraction on the GSECARS 13-ID beamline. The researchers studied the samples at pressures from 90 to 144 GPa. (90 GPa is comparable to a depth of 2,000 km from the Earth's surface; 144 GPa is comparable to 3,000 km.)

For the lower pressure range, they used a double-side laser heating system to heat the samples to more than 1,500K for 30 to 45 min. A new peak was consistently visible above 88 GPa during heating. (Shim et al. [2] reported this peak initially, though in that paper it only appeared in 50% of the measurements.) This new peak was not consistent with any of the known or postulated structures in the sample—including MgO and SiO_2. It could, however, be associated with Mg-Pv or a material of similar compressibility.

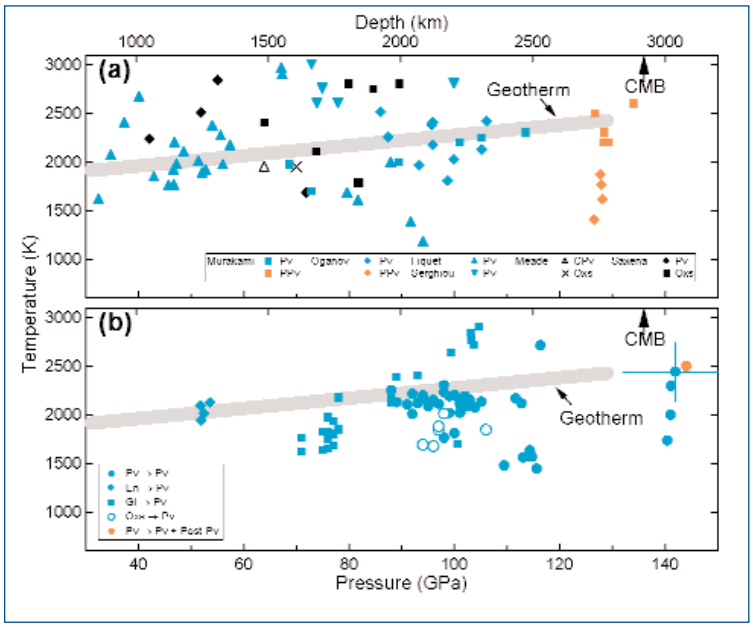

Fig. 1. Top: Reported pressure and temperature conditions for perovskite and postperovskite. Bottom: the data points obtained in this study over three-year period (1999-2001) at GSECARS. The data points are color coded based on the observed phase (blue = perovskite and orange = post-perovskite). The thick gray line is the expected pressure-temperature profile of the mantle. Most of the data points are very close to the P-T conditions of the mantle.

For the higher pressure range (130-140 GPa), the temperature was held at 2,500K. These samples showed many additional new peaks, which also did not correlate to MgO or SiO_2. Nor did they correspond to a simple tilting of the octahedrons of perovskite. Many of these peaks showed good agreement with the peak of the recently proposed post-perovskite phase structure. The observed patterns may indicate an incomplete transition from modified Mg-Pv to the post-perovskite phase. The fact that only Mg-Pv was observed below 2,500K may indicate that Mg-Pv is still stable at such temperatures, and at pressures comparable to the D" layer. In addition to the appear-

Continued on next page

ance of the new peaks, the diffraction peaks for standard perovskite decreased in intensity at the pressures, offering additional support for a post-perovskite phase transition.

These results offer the hypotheses that previous evidence of peaks suggesting that $MgSiO_3$ separated into MgO and SiO_2 was probably due to thermal gradients—not seen in this instance because the insulating argon layer protected against such gradients. Instead the peaks here support the existence of a major phase transition under conditions close to those at the base of the Earth's mantle—suggesting the D" layer may be made of this post-perovskite material. — *Karen Fox*

References

[1] M. Murakami, K. Hirose, K. Kawamura, N. Sata, and Y. Ohishi, "Post-perovskite Phase Transition in MgSiO3," Science **304**, 855 (7 May 2004).

[2] S.-H. Shim, T. S. Duffy, and G. Shen, "Stability and Structure of $MgSiO_3$ Perovskite to 2300-km Depth Conditions," Science **293**, 2437 (2001).

See: S.-H. Shim[1], T.S. Duffy[2], R. Jeanloz[3], and G. Shen[4], "Stability and Crystal Structure of $MgSiO_3$ Perovskite to the Core-Mantle," Geophys. Res. Lett. **31**, L10603 (2004).

Author Affiliations: [1]Massachusetts Institute of Technology; [2]Princeton University; [3]University of California, Berkeley; [4]The University of Chicago

Correspondence: sangshim@mit.edu

This study is supported by the National science foundation. S.S. and R.J. thank the Miller Institute for support. T.D. thanks the Packard Foundation for support. Use of the Advanced Photon Source was supported by the U.S. Department of Energy, Office of Science, Office of Basic Energy Sciences, under Contract No. W-31-109-ENG-38.

Using NRIXS to Peer into the Earth's Core

Estimating the composition of the Earth's iron-rich core is often a matter of making inferences from data that have been extrapolated to Earth-core conditions. Not surprisingly, different methodologies often produce conflicting results, creating controversies in the process. Recently, researchers from Carnegie Institution of Washington, Argonne National Laboratory, and The University of Chicago entered the fray by conducting a static nuclear-resonant inelastic x-ray scattering (NRIXS) study of sound velocities in hexagonal close-packed (hcp) Fe samples at pressures up to 73 GPa and temperatures as high as 1,700K in a laser-heated diamond anvil cell at the XOR 3-ID beamline at the APS (Fig. 1). The measurements revealed the temperature dependence of the compressional-wave velocity (V_p) and shear-wave velocity (V_s) of hcp Fe for the first time.

The properties of the Earth's core have been inferred from estimates of iron densities at high pressures and temperatures and from measurements of V_p and V_s for sound waves passing through the core. These data have indicated that the Earth's core is less dense than pure iron by about 10% for the outer core and 3% for the inner core, suggesting the existence of light elements in the core. On the other hand, Birch's law, which is a linear sound velocity-density relation that has also been used to extrapolate measured sound velocities at high pressures and room temperature to inner core conditions, suggests that the inner core is mainly made of Fe-Ni alloy; Birch's law performs the extrapolation without considering a temperature effect.

The NRIXS technique is a direct probe of the phonon density of states (DOS) of the resonant isotope, which in this case is ^{57}Fe. Energy spectra were obtained by tuning the x-ray energy (±70 meV) around the nuclear transition energy of 14.4125 keV and collecting the Fe K-fluorescence radiation that was emitted. The researchers used a quasiharmonic model to extract the phonon DOS from the NRIXS spectra (Fig. 2). Parabolic fitting of the low-energy regime of the DOS yielded the Debye sound velocity, and vibrational, elastic, and thermodynamic parameters were obtained by integrating the DOS. The rest of the parameters needed to calculate the shear modulus and V_p and V_s were then obtained by use of a thermal equation of state (EOS) from previous studies and the Birch-Murnaghan EOS.

These calculations showed that the bulk sound velocity followed Birch's law at high temperatures but that V_p, V_s, and the shear modulus did not. At a pressure of ~54 GPa and over a temperature increase of 1,000K, Vp decreased by ~7%, while Vs decreased by ~14%, and the shear modulus decreased by ~28%. X-ray diffraction spectra showed that the samples maintained a polycrystalline hcp structure at high pressures without a significant preferred orientation, suggesting that the strong effect of temperature on the sound velocities cannot be

explained simply by elastic anisotropy in highly textured hcp Fe.

The extrapolated sound velocities of hcp Fe at 3,000K and 6,000K, obtained by combining the researchers' study results with those of a previous NRIXS study at high pressures and 300K and with shock-wave data at high pressure and high temperature, showed that the effect of temperature on the sound velocities of Fe is significant at moderate pressures, but weakens under inner core pressures, because highly compressed Fe has a smaller thermal expansion. This implies that the extrapolated V_s values in the inner core should actually be corrected to even lower values, because the temperature of the inner core is believed to be close to the melting curve of Fe. The extrapolated data also suggest that the temperature effect on V_p is suppressed under inner core conditions, whereas temperature continues to have a strong effect on V_s, even under core pressures.

Previous studies have shown that the addition of a light element (such as Si or S) to Fe would increase V_p and V_s under high pressures. In light of the temperature effect on the V_p and V_s of hcp Fe at inner core pressures and 6,000K, the APS research showed that an additional few percent of light elements alloyed with Fe are needed in the inner core to increase V_p to match seismic models. This suggests the presence of more light elements in the Earth's inner core than has been suggested from the application of Birch's law.

— Vic Comello

See: J.-F. Lin[1,†], W. Sturhahn[2], J. Zhao[2], G. Shen[3], H.-k. Mao[1], and R. J. Hemley[1], "Sound Velocities of Hot Dense Iron: Birch's Law Revisited," Science **308**, 1892 (2005).

Author Affiliations: [1]Carnegie Institution of Washington, [2]Argonne National Laboratory, [3]The University of Chicago
([†]Present address: Lawrence Livermore National Laboratory)
Correspondence: lin24@llnl.gov

This work and use of the APS were supported by U.S. Department of Energy, Office of Science, Office of Basic Energy Sciences, under Contract No. W-31-109-ENG-38, and the State of Illinois, under HECA. We thank GSECARS at the APS for the use of the ruby fluorescence system. Work at the Carnegie Institution of Washington was supported by DOE/BES, DOE/NNSA (CDAC), NSF, and the W.M. Keck Foundation.

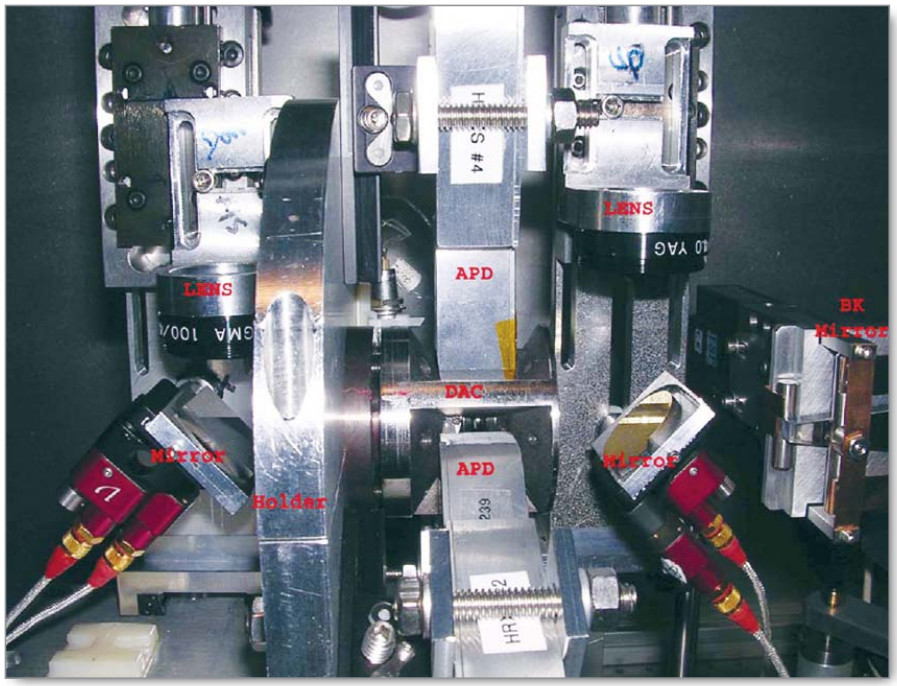

Fig. 1. NRIXS setup with a double-sided laser heating system for high-pressure experiments on hcp Fe. Two infrared laser beams were focused by the laser lenses (LENS) and reflected off mirrors onto samples in a diamond anvil cell (DAC). An x-ray beam of 14.4125 keV was used to resonate iron samples in the DAC, and Fe K-fluorescence radiation was collected by three avalanche photodiode detectors (APD) surrounding the DAC.

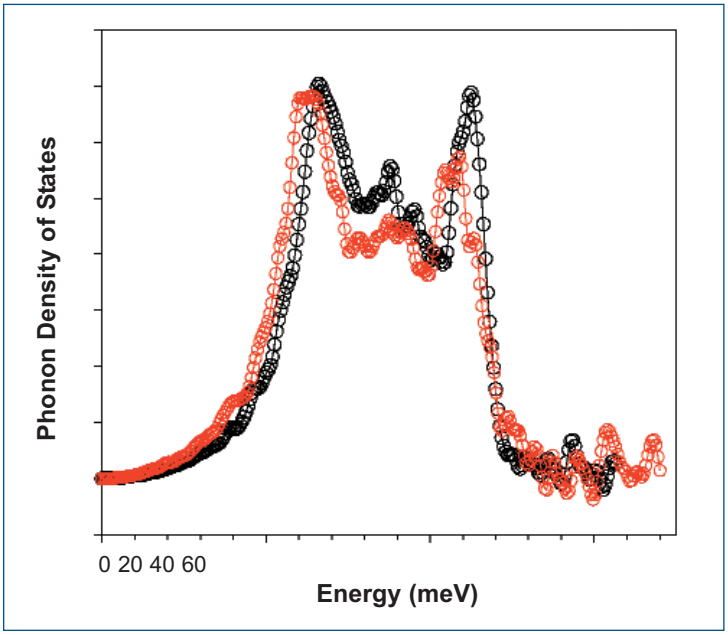

Fig. 2. Phonon density of states (DOS) of hcp Fe at high pressures and temperatures. Red curve: 46.5 GPa and 1,100K; black curve: 43.3 GPa and 300K. The initial slope of the low-energy regime increases significantly at 1,100K, indicating a softening of the lattice excitation and a decrease in the Debye sound velocity. Debye sound velocities, derived from parabolic fitting of the low-energy regime of the DOS, were then used to calculate compressional and shear wave velocities of hcp Fe under high pressures and temperatures.

SAMMS Soak Up Toxic Actinides to Benefit the Environment

SAMMS (short for self-assembled monolayers on mesoporous supports) are high-efficiency, high-capacity sorbent materials that can be used to sequester toxic materials from the environment, a key component of environmental remediation. The SAMMS technique, which is easy to use, less expensive, much faster, and much more effective than traditional sorption methods, has been developed by researchers from the Pacific Northwest National Laboratory (PNNL) for the sequestration of mercury and other heavy metals (Fig. 1). This research effort was later extended to include anions, cesium, radioiodine, and other toxic metallic species; and is now the basis for their latest work: the sequestration of actinides. The SAMMS technique is an important aspect in reducing the volume of radioactive waste (which includes actinides)that must undergo the waste vitrification process as a part of the U.S. Department of Energy's (DOE's) environmental cleanup efforts.

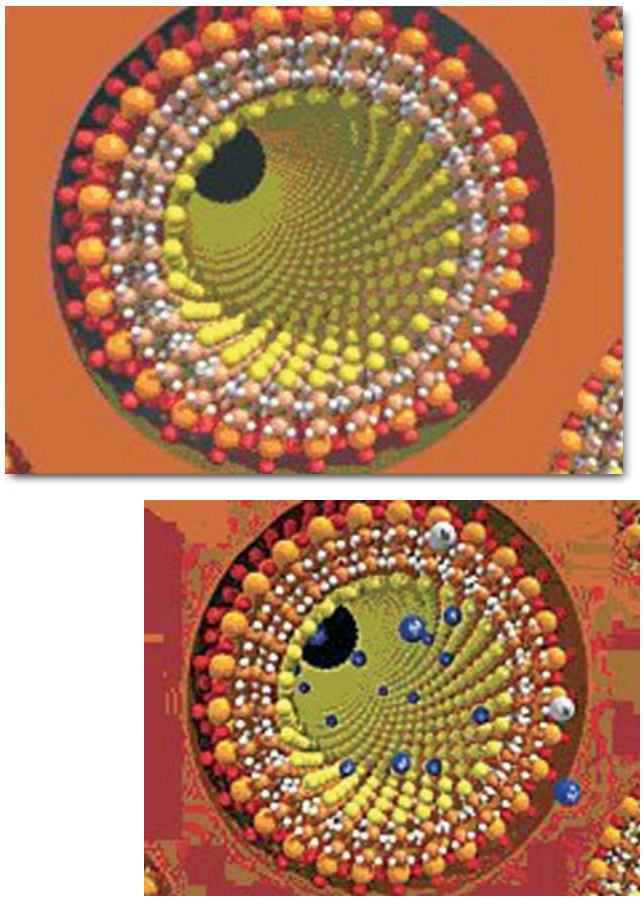

Fig. 1. SAMMS (top) without heavy metals and (bottom) with heavy metals (in this case, mercury [Hg]). Molecular self-assembly allows for the construction of highly organized arrays of binding sites available to bind heavy metals inside of a nanoporous ceramic matrix. This combination makes for a very effective, and very fast, method for removing heavy metals and radionuclides.

SAMMS materials, which were originally synthesized by PNNL scientists, bring together a nanoporous ceramic (silica-based) substrate and a technique for attaching a functional monolayer onto the pore surfaces throughout the porous substrate. Each “flavor” of SAMMS is specifically designed to sequester large amounts of a specific target contaminant (such as arsenic, cadmium, chromium, lead, mercury, or radionuclides) in a very small volume of sorbent material. In this study, the SAMMS were tailored specifically to bind actinides.

Actinide-selective SAMMS were developed by the collaborators in such a way that a variety of chemically different monolayer interfaces could be easily installed onto various substrates, allowing subtle differences in chemical selectivity to be exploited for different separation needs. In this particular study, a number of different actinide-selective ligands were employed, including glycinyl-urea (Gly-UR), salicylamide (Sal), and a couple of related phosphonate-based ligands (Phos).

Gly-UR-SAMMS were prepared by combining an isocyanate-terminated silane and a triethylamine-buffered solution of glycine, which results in the amino acid joining with the silane through a urea linkage. The resulting Gly-UR-SAMMS covered a surface area of about 4.0 silanes per square nanometer (silanes/nm^2). Sal-SAMMS were prepared by combining the carboxylic acid, carbonyl diimidazole, and 3-aminopropyltrimethoxysilane, which results in the salicylate ligand joining with aminopropylsiloxane through an amide linkage. In this case, Sal-SAMMS were attached to the surface at a population of about 1.1 silanes/nm^2. Phos-SAMMS were prepared by displacing trifluoroethanol by 3-aminopropyltrimethoxysilane from the corresponding ester, with the resulting material covering the surface at a level from 2.0 to 2.2 silanes/nm^2.

To test the effectiveness of the resulting SAMMS, the actinide (isotopic) target materials of ^{241}Am(III) (americium), ^{237}Np(V) (neptunium), ^{239}Pu(IV) (plutonium), ^{230}Th(IV) (thorium), and ^{233}U(VI) (uranium) were used. Because these actinide materials normally produce insoluble polymeric oxides or hydroxides in an alkaline environment, the collaborators performed binding studies in a pH range from 1.0 to 6.5. The actinide binding affinity of these SAMMS was found to be pH-dependent. In general, Sal-SAMMS were found to be only moderately effective. The affinity of the Gly-UR-

SAMMS was found to be highly effective at higher pH values, but rapidly decreased below a pH of 2. In addition, the Gly-UR-SAMMS were determined to bind easily with all of the actinides except Np(V) and to bind over a broader range of pH values (well below a pH of 4) than the other two SAMMS. The acetamide phosphonate (Ac-Phos) SAMMS ester was found to be effective at separating actinides that were in both aqueous and nonaqueous waste streams, while the affinity of the propionamidephosphonate (Prop-Phos) SAMMS ester was more selective over the tested actinides, especially at low pH values. Am(III) and Pu(IV) were easily and almost totally separated by a single treatment with the Prop-Phos-SAMMS ester. Overall, the phosphonic acid SAMMS were found to be excellent materials for actinide separations.

In order to better understand the structure and stability of the metal-laden SAMMS, the researchers subjected certain representative adducts to extended x-ray absorption fine structure characterization at the MR-CAT beamline 10-ID at the APS. These studies provided valuable insight into the geometry and structure of the macromolecular chelation these metal ions experience at the monolayer interface.

The SAMMS study demonstrates the superior ability of SAMMS to sequester actinides from complex toxic mixtures, even when competing ions or complexants are present. According to the collaborators, directing the SAMMS technology toward actinides could significantly reduce the volume of high-level waste that must be run through the vitrification process. As a result, these actinide SAMMS offer potentially substantial cost savings for DOE's remediation efforts.

— *William Arthur Atkins*

See: Glen E. Fryxell[1], Yuehe Lin[1], Sandy Fiskum[1], Jerome C. Birnbaum[1], Hong Wu[1], Ken Kemner[2], and Shelley Kelly[2], "Actinide Sequestration Using Self-Assembled Monolayers on Mesoporous Supports," Enviro. Sci. Tech. **39** (5), 1324 (2005). (See also Environ. Sci. Tech. **39**, 1332 [2005], which outlines the chemistry developed to effectively bind Np.)

Author Affiliations: [1]Pacific Northwest National Laboratory, [2]Argonne National Laboratory

Correspondence: glen.fryxell@pnl.gov

Research was supported by the U.S. DOE, Environmental Management Science Program. Portions of this work were performed at Pacific Northwest National Laboratory, which is operated for the DOE by Battelle Memorial Institute under Contract DE AC06-76RLO 1830. MR-CAT is supported by the DOE under Contract DE-FG02-94-ER45525 and the member institutions. Use of the Advanced Photon Source was supported by the U.S. DOE, Office of Science, Office of Basic Energy Sciences, under Contract No. W-31-109-ENG-38.

AROUND THE EXPERIMENT HALL

NANOPARTICLES IN THE ENVIRONMENT

Matt Newville (The University of Chicago) and Juyoung Ha (Stanford University) at the GSECARS 13-BM-D beamline.

Ha: "Nanoparticles are widespread in a range of different natural environmental settings despite their predicted instability based on the classical thermodynamic analysis. Nanoparticles can arise from a variety of mechanisms: chemical weathering processes, precipitation from relatively saturated solutions in hydrothermal and acid mine drainage environments, evaporation of aqueous solutions in soils, and biological formation by a variety of microorganisms.

"When compared to bulk materials, environmentally occurring nanoparticles possess distinctive properties with respect to their reactivity toward different ionic species in natural waters. However, the molecular-scale characterization of structures and compositions of reactive sites on mineral nanoparticles in contact with aqueous solutions are poorly understood, mainly due to the complexities of the interfaces and scarcity of appropriate analytical tools for probing such complex systems.

"Here, we are studying the nanoparticles of laboratory-synthesized hematite particles and their interaction with different organic acids and heavy metal ions in the solution phase at different environmental conditions. Investigating the surface structures of ligands in interface between hematite nanoparticles and water at a molecular level can give indirect information on the reactivitiy of the mineral phases. This is because the reactivity of a mineral phase is controlled, in part, by the types and concentrations of surface structure, sites exposed to the aqueous solution, and the different surface complex that forms at the interface."

Contact: juyoung@gmail.com, newville@cars.uchicago.edu

An X-ray Window on Nanoparticles in Flame

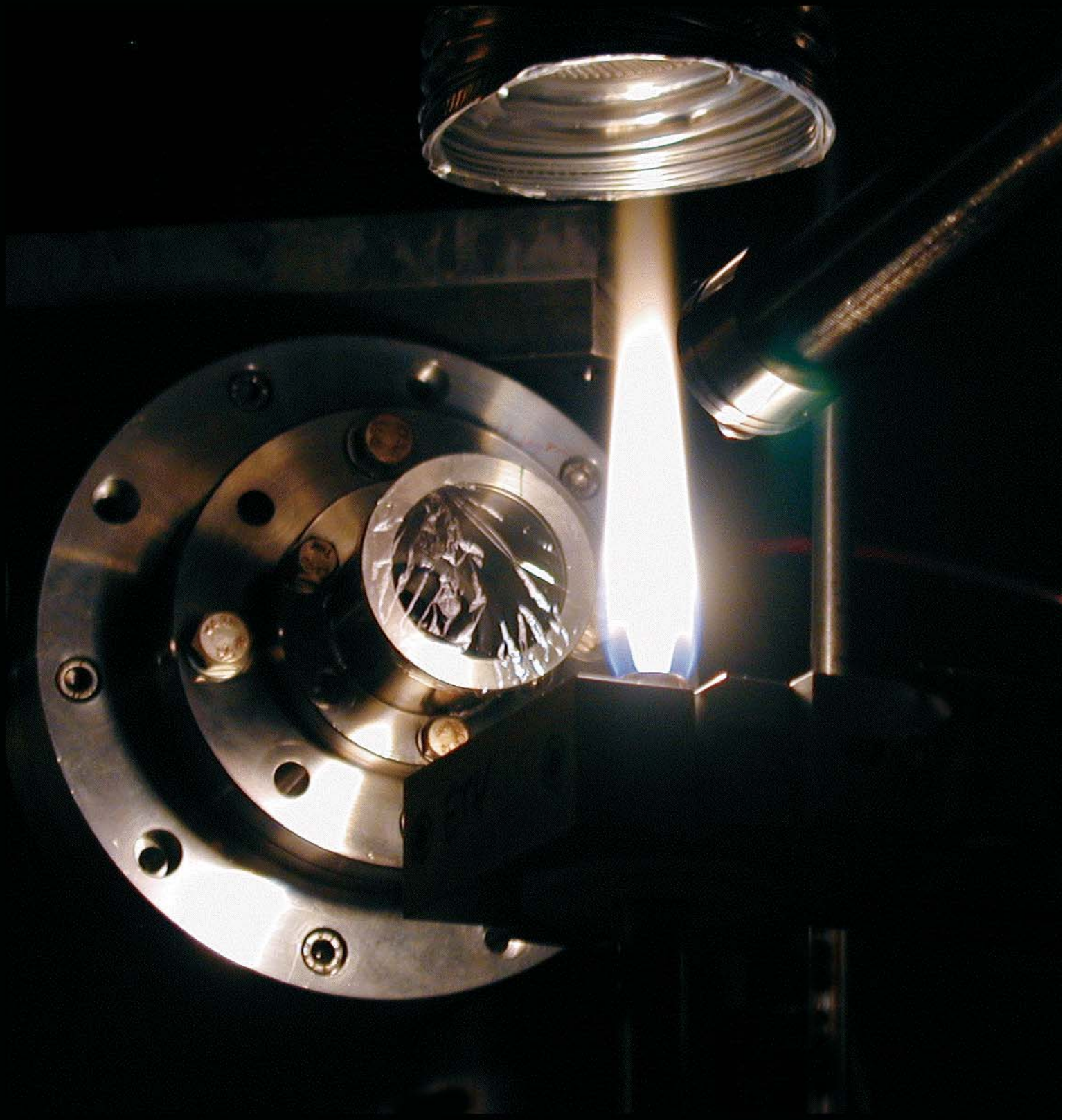

For nanotechnology to fulfill its commercial potential, efficient ways to create large numbers of very tiny things must be developed and perfected. Currently, the most viable mass production technique for nanotechnology is pyrolysis, or flame synthesis—producing nanomaterials such as nanotubes and quantum dots by doping a highly-controlled flame with the appropriate raw materials. To properly control and employ such a process, however, the process must first be fully understood. The same high-temperature, kinetically busy, and extremely bright conditions in the depths of a flame that make it an ideal environment for nanosynthesis also make direct observation of the process a considerable challenge. A team from the University of Cincinnati, Institut für Verfahrenstechnik at the ETH Zentrum in Zurich, and the European Synchrotron Radiation Facility (ESRF) has succeeded in using synchrotron x-ray scattering to probe the secrets of nanoparticle formation in a flame, even at volume fractions as small as 10^{-6}.

The researchers conducted *in situ* studies of nanoparticle growth in flames using both the XOR/UNI 33-ID beamline at the APS and the ID2 beam line at the ESRF. With the diffusion flame apparatus installed in the beamline, a 12.46-keV monochromatic x-ray beam, 300 μm in diameter with an exposure time of 0.3 s, entered the flame from the right. The beam, including the scattered x-rays, continued into a 10-m evacuated chamber, which contains a small-angle x-ray scattering (SAXS) detector consisting of an image-intensified charge-coupled device detector above the diffusion burner. The nanoparticles created in the flame were collected on a filter, on which they were later examined by means of electron microscopy, nitrogen gas adsorption, and SAXS. The burner is fed by three temperature-controlled streams using mass flow controllers (with nitrogen and methane as carrier gases) and then doped with hexamethyldisiloxane (HMDSO) to produce silica nanoparticles. Computer control of the flame and burner motion allowed various scattering patterns to be observed and recorded.

The SAXS studies show that nanoparticles initially form in the diffusion flame at about 5 mm above the burner. After the initial 300 μs of particle growth, diffusion fronts in the flame allow continued particle nucleation and coalescence in higher regions of the flame. The size of the nanoparticles depends upon both the position at which they form and the amount of time spent within the highest-temperature regions of the flame. At the 5-mm height, silica nanoparticles coalesce to very small diameters of about 20 nm, with high polydispersity. The growth of nanoparticles within the flame can be mapped by using a least-squares method to fit the data to a global scattering function based on polydisperse, smooth spheres. This mapping reveals a diffusion front where precursor converts to oxide at about 10 mm to 30 mm above the burner, with a high volume of silica and consequent high density of nanoparticles. The largest nanoparticles form in the regions of least polydisperse particles, whereas nanoparticles are relatively uniform in shape and size further downstream. The flame temperature profile was measured by means of infrared spectroscopy. From this profile, the axial velocity of the laminar gas stream can be determined by using the ideal gas law, which confirms that the size of the nanoparticles is a function of time within the flame.

The experimenters have proven that nanoparticle nucleation and growth can be directly studied *in situ* by using SAXS for particle sizes ranging from 0.5 nm to 500 nm, at a time scale as short as 100 μs. Their success paves the way both for more accurate modeling and simulation of nanoparticle formation and a method to directly confirm such models. With the greater understanding of nanoscale phenomena that such tools will afford, we will be much closer to creating nanomaterials with the precision and confidence that a Swiss watchmaker brings to bear on the finest watch movement. — *Mark Wolverton*

See: Gregory Beaucage[1], Hendrikk Kammler[2], Roger Mueller[2], Reto Strobel[2], Nikhil Agashe[1], Sotirise Pratsinis[2], and Theyencheri Narayanan[3], "Probing the Dynamics of Nanoparticle Growth in a Flame Using Synchrotron Radiation," Nat. Mater. **3**, 370 (1 June 2004).

Author Affiliations: [1]University of Cincinnati, [2]Institut für Verfahrenstechnik, [3]European Synchrotron Radiation Facility
Correspondence: beaucage@uc.edu

This work was supported by the National Science Foundation (CTS-0070214), the Swiss National Science Foundation (200021-101901/1), the Swiss Commission for Technology and Innovation (TopNano21-5487.1), and the synchrotron facilities at ESRF (beam-time allocation ME421). Use of the Advanced Photon Source was supported by the U.S. Department of Energy, Office of Science, Office of Basic Energy Sciences, under Contract No. W-31-109-ENG-38.

< A supported silica diffusion flame in a SAXS camera at the ESRF.

COPOLYMER/NANOPARTICLE MIXTURES EXHIBIT SELF-DIRECTED SELF-ASSEMBLY

Researchers using the XOR 1-BM beamline at the APS have derived a process for nanoparticle self-assembly that provides for exceptional control and flexibility over the fabrication of nanostructured materials with applications including chemical sensing, separation, catalysis, high-density data storage and photonic materials. The group used grazing incidence small-angle x-ray scattering (GISAXS) measurements at the APS to show that mixtures of diblock copolymers and either cadmium selenide- or ferritin-based nanoparticles exhibit cooperative, coupled self-assembly on the nanoscale. In thin films, the copolymers assembled into cylindrical domains that dictated the spatial distribution of the nanoparticles. Segregation of the particles to the interfaces, in turn, mediated interfacial interactions and reoriented the copolymer domains normal to the surface of the substrate, even when one of the blocks was strongly attracted to the substrate. Organization of both the polymeric and particulate entities was achieved without the use of external fields, demonstrating a simple and general route for fabricating nanostructured materials with hierarchical order.

Block copolymer/nanoparticle films were prepared by spin coating toluene solutions of a mixture of 3- or 5-wt% polystyrene-*block*-poly(2-vinylpyridine) copolymer (PS-*b*-P2VP) and 1-wt% tri-*n*-octylphosphine oxide-covered CdSe nanoparticles (4 nm in diameter) onto silicon wafers. The 150- to 600-nm-thick films were annealed thermally at 170° C under vacuum in either a supercritical fluid CO_2 environment at 70° C or in chloroform vapors at room temperature. Each treatment imparted mobility to the thin-film mixtures, allowing them to attain their equilibrium morphologies within about two days.

The researchers—from the University of Massachusetts, Universität Bayreuth, Argonne National Laboratory, the University of South Carolina, and the University of Pittsburgh—carried out GISAXS measurements at the 1-BM beamline. The measurements were made before and after thermal annealing, and included measurements at several incident angles to provide quantitative information on the depth dependence of the thin-film morphologies (Fig. 1). These measurements were supplemented with data derived from scanning force microscopy, scanning electron microscopy, and transmission electron microscopy.

To indicate that a corresponding interplay between assembly processes could apply to a wide variety of other systems, the researchers also examined a blend of poly(ethylene glycol) (PEG)-tagged ferritin bio-nanoparticles (ferritin-PEG) and a lamella-forming diblock copolymer of poly(2-vinylpyridine) and poly(ethylene oxide) (P2VP-*b*-PEO). Thin-film samples of the block copolymer with and without ferritin-PEG particles were prepared and annealed in saturated benzene vapor. Without the ferritin-PEG particles, the P2VP-*b*-PEO microphase separated into lamellae oriented parallel to the surface, with the crystalline PEO located at the surface. With the ferritin-PEG particles, PEO crystallization was suppressed, and the lamellar microdomains were oriented normal to the surface. Thus, the ferritin-PEG bio-nanoparticles were incorporated into the PEO microdomains, where they suppressed crystallization, medi-

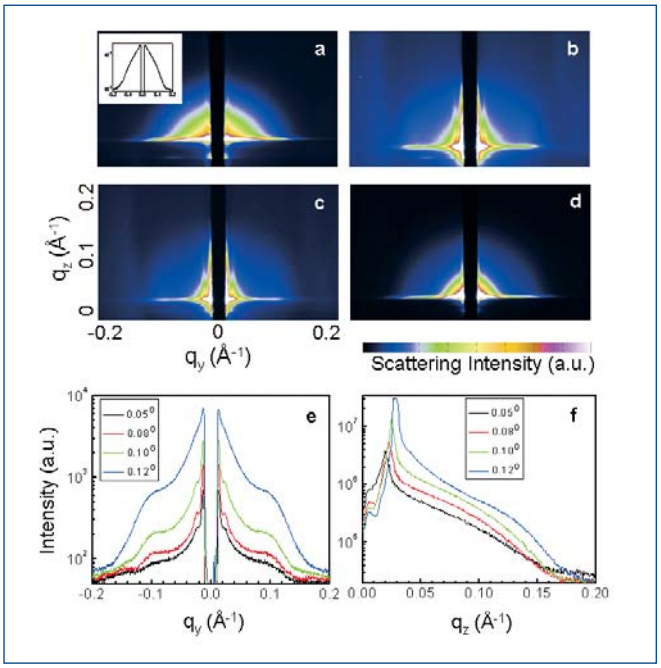

Fig. 1. GISAXS data for thin-film PS-*b*-P2VP/CdSe nanoparticle composites. (a) Data from a freshly spin-coated thin film of diblock copolymer and nanoparticles at an incidence angle of 0.06° with a penetration depth of 44 Å. Data from a thin film thermally annealed for 48 hrs at 170°C at incidence angles and penetration depths of (b) 0.08° and 54 Å, (c) 0.09° and 61 Å, and (d) 0.12° and full thickness, respectively. (e) q_y linescan at q_z = 0.0376 Å^{-1} at four different x-ray incident angles of 0.058°, 0.088°, 0.108°, and 0.12°, with penetration depths of 44 Å, 54 Å, 73 Å, and full thickness, respectively. (f) q_z linescan along the first-order peak (1 0) for the four incident angles. The critical angle of the thin film was measured to be 0.11°, and q_y and q_z are the momentum transfers normal to the diffraction plane and sample surface, respectively.

ated interfacial interactions, and reoriented the microdomains. This result was similar to the reorientation seen in the PS-*b*-P2VP/CdSe nanoparticle mixtures.

The researchers thereby provided examples of synthetic and biologically inspired systems wherein one-step hierarchical self-organizations occur via interplays between distinct self-assembling processes—producing spatially ordered, organic-inorganic and organic-bioparticle hybrid materials. The inherent synergy that was demonstrated represents a significant advance over other processes that rely on sequential fabrication steps to incorporate functionality into pre-organized templates. Furthermore, microdomain orientation, which is built into the system by the segregation of the nanoparticles to the interfaces, is independent of film thickness, the nature of the interfaces, and the geometry of the system—eliminating the need for external fields to manipulate the orientation. This is particularly important for systems like PS-*b*-P2VP, where interfacial interactions are so strong that even large external fields could not reorient the domains through the entire film.

Coupled with recent advances in the synthesis of nanocrystals and the large variety of bionanoparticles that can be surface-modified and biomineralized, the synergistic assembly process the researchers demonstrated could provide control and flexibility over the fabrication of nanostructured materials.

— Vic Comello

See: Y. Lin[1], A. Böker[1,2], J. He[1], K. Sill[1], H. Xiang[1], C. Abetz[2], X. Li[3], J. Wang[3], T. Emrick[1], S. Long[4], Q. Wang[4], A. Balazs[5], and T.P. Russell[1], "Self-directed Self-assembly of Nanoparticle/Copolymer Mixtures," Nature **434**, 55 (3 March 2005).

Author Affiliations: [1]University of Massachusetts, [2]Universität Bayreuth, [3]Argonne National Laboratory, [4]University of South Carolina, [5]University of Pittsburgh

Correspondence: russell@mail.pse.umass.edu

This research was supported by the National Science Foundation through the Materials Research Science and Engineering Center and the Cooperative Research in Chemistry program; the Army Office of Research through the Multi-University Research Initiative; and the U.S. Department of Energy. Use of the Advanced Photon Source was supported by the U.S. Department of Energy, Office of Science, Office of Basic Energy Sciences, under Contract No. W-31-109-ENG-38.

PEERING INTO POLYMER NANOCOMPOSITES

Engineered composite materials are becoming a mainstay for nanotechnology applications and may also find wide use in microelectronics and biomedical applications. To this end, a substantial effort has been devoted to developing nanocomposites based on functionalized nanoparticles embedded in a stable polymer matrix. Recently, researchers from McGill University used XOR beamline 8-ID to learn more about the properties of capped nanoparticles and nanoparticles in polymer matrices.

Many of the currently available methods for synthesizing nanocomposites based on functionalized nanoparticles embedded in a stable polymer matrix have shortcomings. These include producing unwanted contaminants, poor dispersion, or uncontrolled nanoparticle size distributions. One method gaining interest is the use of polymer-capped metal or semiconductor nanoparticles that are blended into a pre-made polymer matrix by using a solvent (Fig. 1). Nanoparticle capping is an attractive synthesis route because the interaction between the particle coating and the polymer matrix can be fine tuned, while offering full control of the composition of the nanoparticle and the matrix. The challenge then is to be able to observe and control the subsequent aggregation and miscibility of the nanoparticles in the matrix.

To study nanoparticle dispersion in a polymer matrix, the researchers used gold cores with diameters ranging from 3.6 to 6.2 nm, capped with polystyrene (PS) and polyethylene oxide (PEO) shells of different degrees of polymerization (the ratio of the molecular weight of the polymer to that of a monomer unit). The capping layer can be described as a polymer brush, where one end of the polymer chain is grafted onto the gold nanoparticles with the polymer extending outward into the solvent or matrix. These capped nanoparticles were then blended into PS and PEO matrices of the same or differing molecular weight to examine the degree of dispersion or aggregation of particles in the nanocomposite. The researchers used a suite of tools to characterize the nanocomposites: transmission electron microscopy (TEM), ultraviolet-visible spectroscopy (UV-vis), and small-angle x-ray scattering (SAXS). The TEM images yielded the distances between nanoparticles, an estimate of the number of particles per unit volume, and an estimate of the extent of aggregation. helped detecting aggregation. Aggregation of the gold particles in drop-cast and spin-coated samples was examined with UV-vis (300-nm to 800-nm) spectroscopy.

Small-angle x-ray scattering is a valuable technique for determining the details of colloidal systems because of the sensitivity of the scattering structure factor to particle aggregation. The SAXS measurements were carried out at beamline 8-ID of the APS with an incident beam energy of 7.66 keV, which was collimated to a 20-μm × 20-μm beam. The diffrac-

Continued on next page

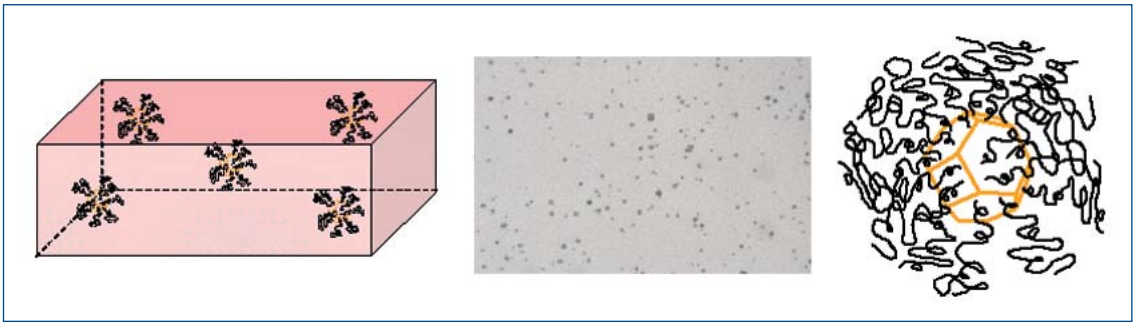

Fig. 1. Left: Schematic representing polymer-stabilized gold nanoparticles embedded in a polymer matrix. Middle: TEM image of a 60-nm-thick section of nanocomposite (dispersed gold nanoparticles stabilized with short PS_{19}-SH ligands in a short PS_{20} matrix). Right: Schematic representing a polymer-stabilized gold nanoparticle (truncated octahedral gold core with thiol-terminated polymeric chains covalently attached to the core).

tion patterns from the nanocomposite samples were detected with a charge-coupled device array. The scattering cross section as a function of Q was calculated by assuming an electron density model based on a gold metal core surrounded by a lower-density polymer shell, with the capped particle dissolved in solvent or bulk polymer (Fig. 2).

The researchers found a rich and complex set of aggregation phenomena for the different capped structures and different molecular weight polymer matrices. In particular, TEM shows that the gold nanoparticles have a faceted geometry at the diameters used in the study (Fig. 1), and this has a large influence on the wettability of the polymer cap by the matrix polymer. Theoretically, highly dense polymer brushes should not be wetted by high-molecular-weight matrices, but the gold faceting causes a large volume fraction of voids in the brush, which, in turn, improves the dispersion of the nanoparticles in the matrix, as observed in the experiments. As suggested by theory, in the case of lower-density polymer brushes, the nanoparticles were observed to disperse in both high- and low-molecular-weight matrices. These observations highlight how geometries (in this case of the faceted gold nanoparticle) at the nanoscale introduce new properties to materials.

These results show the importance of detailed analysis via complementary probes of capped nanoparticle dispersion in polymer matrices, in this case a combination of TEM, optical spectroscopy, and x-ray scattering. In addition, the SAXS data indicate the value of third-generation synchrotron facilities, such as the APS, where the high beam brightness can make small-angle scattering feasible. Such studies open an important window on the properties of nanomaterials and what factors control their composition. — *David Voss*

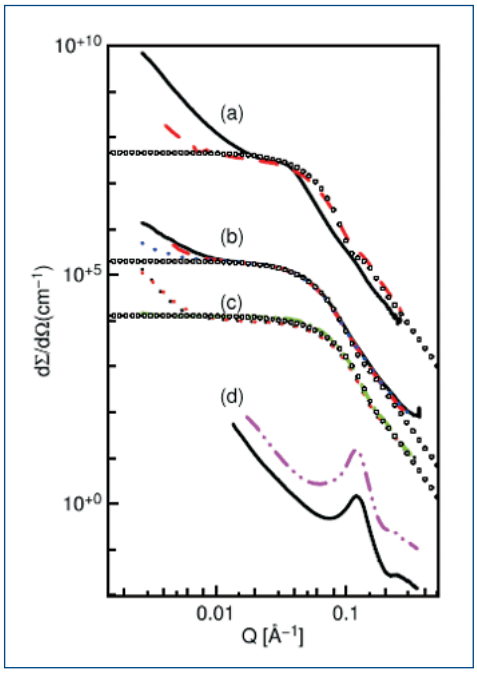

Fig. 2. SAXS data obtained from gold nanoparticles. Circles correspond to the calculated cross sections from the core-shell model used by the authors. (a) PEO_{45}-Au (offset by 10^5). The matrices are PEO_{340} (M_n = 15,000 g/mol) (black solid) and PEO_{25} (1,000 g/mol) (red dashed). (b) PS_{125}-Au (offset by 10^3), with matrices PS_{760} (Mn = 80,000 g/mol) (black solid), PS_{440} (Mn = 46,400 g/mol) (red dashed), and PS_{20} (Mn = 2,000 g/mol) (blue dotted). (c) PS_{19}-Au (offset by 10^2) with matrices PS_{20} (Mn = 2,000 g/mol) (blue dotted), PS_{19}-SH (red dotted), and toluene (green dot-dashed). (d) C_{14}-Au, with matrices PS_{440} (pink dash-dotted), and PS_{760} (black solid).

See: Muriel K. Corbierre, Neil S. Cameron, Mark Sutton, Khalid Laaziri, and R. Bruce Lennox, "Gold Nanoparticle/Polymer Nanocomposites: Dispersion of Nanoparticles as a Function of Capping Agent Molecular Weight and Grafting Density," Langmuir **21**, 6063 (2005).
Author Affiliation: McGill University
Correspondence: bruce.lennox@mcgill.ca

Funding for this research was provided by NSERC (R.B.L., M.S.), Merck Frosst Canada (R.B.L.), and FCAR (R.B.L., M.S.). Use of the Advanced Photon Source was supported by the U.S. Department of Energy, Office of Science, Office of Basic Energy Sciences, under Contract No. W-31-109-ENG-38.

WATCHING NANOPARTICLES ASSEMBLE IN REAL TIME

Self-assembly of metal particles in polymer materials is an important approach for synthesizing nanocomposites for electronic, spintronic, and photonic applications. To be effective, however, precise control has to be maintained over the aggregation of nanoparticles into larger engineered nanostructures. To achieve this level of control, especially in ultrathin film systems, monitoring of lateral diffusion and transport of the particles is essential. Such measurements are difficult because of the small number of particles in a given volume (less than one monolayer) and these particles are often randomly distributed before self-assembly. Recently, researchers from Argonne National Laboratory; Northwestern University; the University of California, San Diego; and Los Alamos National Laboratory overcame these limitations in studies of gold nanoparticles in thin film polymers using a combination of x-ray scattering techniques at two APS beamlines.

Resonance enhancement of the x-ray scattering in a waveguide structure was the key development that enabled the researchers to obtain high sensitivity in such a sparse sample. In the vicinity of the surface, x-rays incident on a metal mirror at grazing incidence (Fig. 1) form a standing wave normal to the surface by total external reflection. If a low electron density film, such as a polymer layer, is applied to the mirror surface and has a thickness that is a multiple of the x-ray wavelength, then the electromagnetic field at the surface can be enhanced by one to two orders of magnitude. The use of such a resonant waveguide to increase the x-ray scattering probability means that even very weakly scattering structures can be observed. Moreover, the higher sensitivity allows changes in the particle ordering to be observed in a time-resolved manner.

To create the nanostructures, a 35-nm layer of polytert-butylacetate (PtBA) was applied to a silver/chromium x-ray mirror. A submonolayer of gold nanoparticles was deposited by thermal evaporation onto this polymer surface and covered by another layer of PtBA of equal thickness. The gold nanoparticles had diameters of between 2 and 4 nm separated by an average distance of approximately 6 nm. Grazing incidence small-angle x-ray scattering (GISAXS) measurements were carried out at XOR beamline 1-BM (8-keV incident energy) and XOR beamline 8-ID (7.66-keV incident energy) at the APS. The scattering patterns were recorded by an image plate detector. X-ray reflectivity measurements were undertaken to confirm the presence of the resonance enhancement in the thin film structure, and these results agreed well with calculated electric field values inside the waveguide structure.

Diffusion of the gold was probed with GISAXS by first heating the polymer film to 65° C, well above the glass transition temperature (49° C), to allow the two PtBA layers to melt into a single layer. Then, with the sample at 75°C allowing nanoparticle diffusion, x-ray scattering measurements at 0 min, 10 min, and 47 min intervals revealed significant lateral

Continued on next page

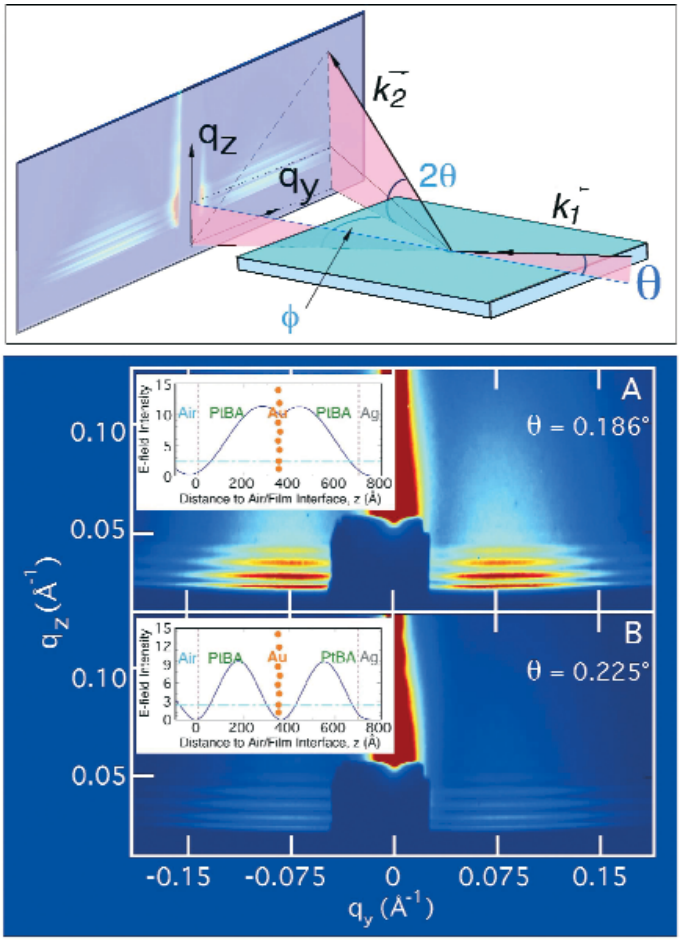

Fig. 1. Top: Schematic of GISAXS experiment setup and (lower panel) resonance-enhanced GISAXS patterns of gold nanoparticles in an ultrathin polymer x-ray waveguide (A) at the first resonance mode and (B) at an off-resonance condition. The insets depict the corresponding calculated electric-field intensity distributions in the waveguide. The enhancement of the scattering intensity at the resonance condition is readily observable.

motion of the gold particles. Plots of the scattering intensity in reciprocal space (I vs. q) indicated that the in-plane motion along the film dimensions was not Brownian, but was instead dominated by attractive van der Waals forces between the gold particles. This lateral mobility was more than an order of magnitude higher than the motion perpendicular to the plane of the film, which can be attributed to both the anisotropic nature of the gold nanoparticle distribution (being in a two-dimensional layer) and the mobility of the polymer chains perpendicular to the film, which is reduced by confinement.

The results show that resonantly enhanced scattering carried out in a thin-film waveguide structure may offer greatly improved sensitivity for observing real-time phenomena in dilute or weakly scattering samples. This is especially the case when carried out at third-generation synchrotron facilities such as the APS, where waveguide enhancement can complement the high brightness of the incident x-ray beam. In particular, these studies of particle mobility may yield important information for controlling particle aggregation in nanotechnological materials.

— David Voss

See: Suresh Narayanan[1], Dong Ryeol Lee[1], Rodney S. Guico[1,2], Sunil K. Sinha[3,4], and Jin Wang[1], "Real-Time Evolution of the Distribution of Nanoparticles in an Ultrathin-Polymer-Film-Based Waveguide," Phys. Rev. Lett. **94**, 145504 (2005).

Author Affiliations: [1]Argonne National Laboratory; [2]Northwestern University; [3]University of California, San Diego; [4]Los Alamos National Laboratory

Correspondence: wangj@aps.anl.gov

This work and use of the Advanced Photon Source was supported by the U.S. Department of Energy, Office of Science, Office of Basic Energy Sciences, under Contract No. W-31-109-ENG-38. The work was also partially funded by NSF Grant No. DMR-0209542.

Novel Nonspherical Nanoparticles

In the quest to develop new materials at the nanoscale with useful electronic, chemical, and optical properties, a major challenge has been how to prepare wire- or rod-shaped metal nanoparticles, because synthesizing nonspherical shapes has required many painstaking interventions using a hard matrix as a template. A team of researchers from Argonne National Laboratory has recently discovered that a soft, ionogel template impregnated with a gold salt and subjected to reducing ultraviolet radiation produces a large collection of nonspherical nanoparticles in a variety of shapes and sizes without requiring tedious, multi-step manipulations. Using small-angle x-ray scattering (SAXS) at the XOR/BESSRC 12-ID-C beamline, scanning electron microscopy (SEM), and optical spectroscopy, the team was able to confirm for the first time the structures of these particles.

In the quest to develop new materials with useful electronic, chemical, and optical properties, a major challenge has been to prepare wire- or rod-shaped metal nanoparticles. But synthesis of nonspherical shapes requires many painstaking interventions using a hard matrix as a template. A team of researchers from Argonne National Laboratory recently discovered that a soft, ionogel template impregnated with a gold salt and subjected to reducing ultraviolet radiation produces a large collection of nonspherical nanoparticles in a variety of shapes and sizes without requiring tedious, multi-step manipulations. By using small-angle x-ray scattering (SAXS) at the XOR/BESSRC 12-ID-C beamline, scanning electron microscopy (SEM), and optical spectroscopy, the researchers were able to confirm the intriguing morphologies of these particles in the soft template, including trigonal prismatic nanorods, which had never before been synthesized (Fig. 1).

The template was prepared by adding a small concentration of a gold salt solution to an ionic liquid, creating a viscous gel phase that adopted a two-dimensional (2-D) hexagonal structure. Irradiation of the composite with ultraviolet light caused the photochemical reduction of the gold salt to nanoparticles without destroying the liquid crystalline texture of the ionogel. An interesting feature of the template is its distinct channels that likely contribute to the formation of nanosized particles.

Incident x-ray beams directed perpendicular to the long axis of the capillary containing the nanoparticles revealed three distinct Bragg peaks, indicative of the formation of a 2-D hexagonal lattice structure at the intermediate, or mesoscopic, scale over the entire sample volume probed by the x-ray beam. It is most unusual to observe such order in a self-assembled material without further intervention.

To further explore the structure of the sample, the team used optical spectroscopy, which revealed three surface plasmon bands consistent with the formation of nonspherical nanoparticle shapes such as cylinders or rods. When the gold particles were freed from the ionogel by simply dissolving the gel in ethanol, the midwavelength and near-infrared spectral features disappeared, suggesting that the process of liberating the nanoparticles altered their shape, or that the organization or aggregation of the particles was disrupted in the process.

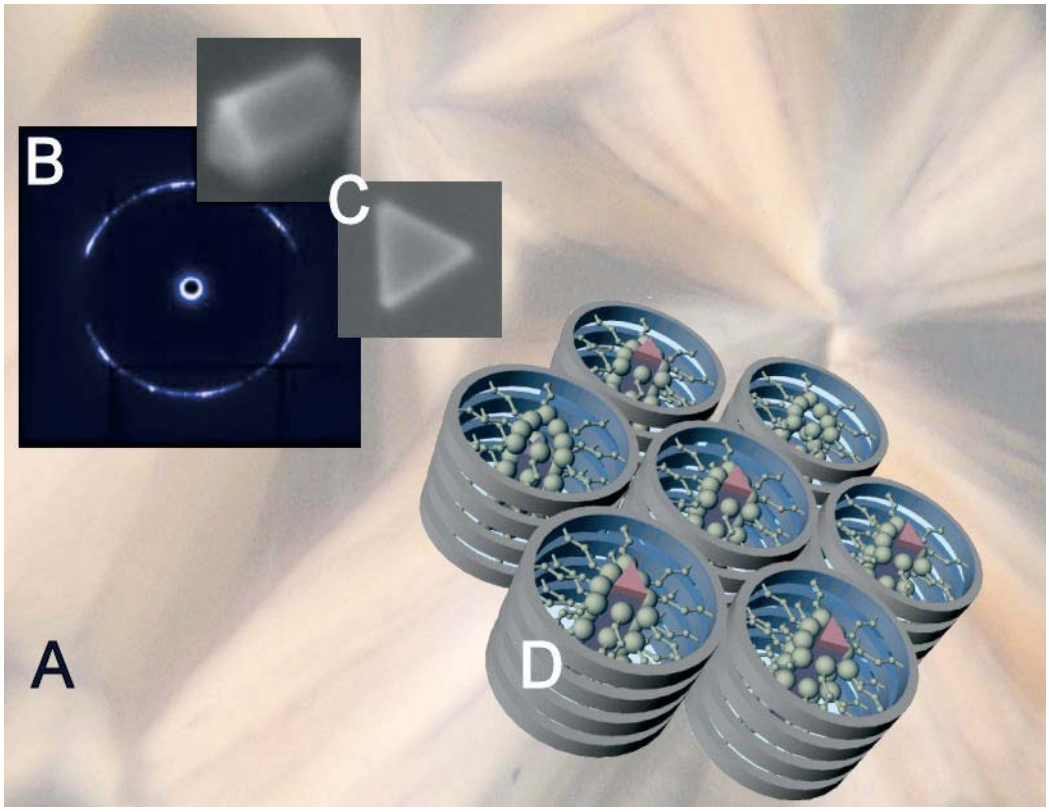

Fig. 1. (A) Polarized optical micrograph of a gold nanoparticle-ionogel composite. (B) SAXS pattern showing 2-D hexagonal symmetry of the composite. (C) Scanning electron micrographs of representative gold particles formed within ionogel. (D) Schematic diagram of self-assembled ionogel illustrating the possible arrangement of encapsulated gold particles.

Further examination of the samples used SEM to directly observe the morphology of the nanoparticles. The images revealed particles 100 to 1,000 nm in size adopting a surprising variety of shapes, including hexagonal and triangular plates, prisms, and trigonal prismatic rods. Of particular interest are trigonal prismatic nanorods, which differ from the thin, triangular nanoparticle plates observed in previous studies. These particles fit the description of true nanorods; that is, they are thicker than plates, having an aspect ratio greater than 1 but less than 20.

Although the morphologies and sizes of the nanoparticles were well documented in this suite of experimental probes, the exact mechanism that allows their formation remains to be determined, as does the nature of the interaction between the guest nanoparticles and the host ionogel template. When these questions are answered, it may be possible to control the shape and spacing of the nanoparticles and harness the materials for use in plasmonics and other applications that depend on the precise control of these characteristics for their electronic, optical, and catalytic properties.— *Elise LeQuire*

See: M.A. Firestone, M.L. Dietz, S. Seifert, S. Trasobares, D.J. Miller, and N. J. Zaluzec, "Ionogel-templated Synthesis and Organization of Anisotropic Gold Nanoparticles," Small **1**(7), 754 (2005).

Author Affiliation: Argonne National Laboratory
Correspondence: firestone@anl.gov

This work was performed under the auspices of the Office of Basic Energy Sciences, Divisions of Materials Sciences (M.A.F., S.S., S.T., D.J.M., N.J.Z.) and Chemical Sciences (M.L.D.), United States Department of Energy. Use of the Advanced Photon Source was supported by the U.S. Department of Energy, Office of Science, Office of Basic Energy Sciences, under Contract No. W-31-109-ENG-38.

BIMETALLIC NANOPARTICLES PARALLEL BULK ALLOYING CHARACTERISTICS

Metallic nanoparticles are of increasing interest due to their use in many applications, from catalysis to electronic devices. Bimetallic nanoparticles, comprising two different metallic elements, are of even greater interest. They hold promise as biosensors, which can be used for disease prevention and treatment, ensuring a safe food supply, and environmental monitoring. Researchers from the University of Notre Dame, the University of Missouri-Rolla, and the Illinois Institute of Technology studied the mixing behavior of metallic nanoparticle materials composed of two metallic elements. The impetus for this study came from theoretical comparisons of excess surface free energy versus elastic relaxation within bimetallic nanoparticles. The investigators showed that the metals alloyed in ways that paralleled how their bulk form alloyed; that is, two metals possessing the ability to thoroughly mix and form a single homogeneous phase in their large bulk form (i.e., complete miscibility) also displayed that ability as bimetallic nanoparticles. Likewise, two metals that were completely immiscible in bulk also remained as separate phases when mixed as bimetallic nanoparticles.

Specifically, the group studied bimetallic nanoparticles of platinum-silver (Pt-Ag), which is completely immiscible in bulk, and palladium-silver (Pd-Ag), which is entirely bulk-miscible. In these two systems, the atomic sizes of the components differed (i.e., were mismatched) by 15% and 16%, respectively.

The effect of morphology on the degree of alloying was examined at a core size of 2 nm for spherical shaped Pt-Ag nanoparticles (Fig. 1) and in a diameter of 20 nm for cylindrical-shaped Pd-Ag nanoparticles (or nanowires). Both systems were synthesized radiolytically (irradiated), which allowed for structural control of the particles when experimental parameters were varied.

To determine the alloying of the two disordered bimetallic nanoparticle systems, as well as analyze their local structures (such as interatomic distances, coordination numbers, bond lengths, and bond-length distributions), the collaborators used the technique of x-ray-absorption fine structure (XAFS). The XAFS measurements—taken at the Pt L_3, Ag K, and Pd K edges—were performed at the MR-CAT beamline 10-ID at the APS.

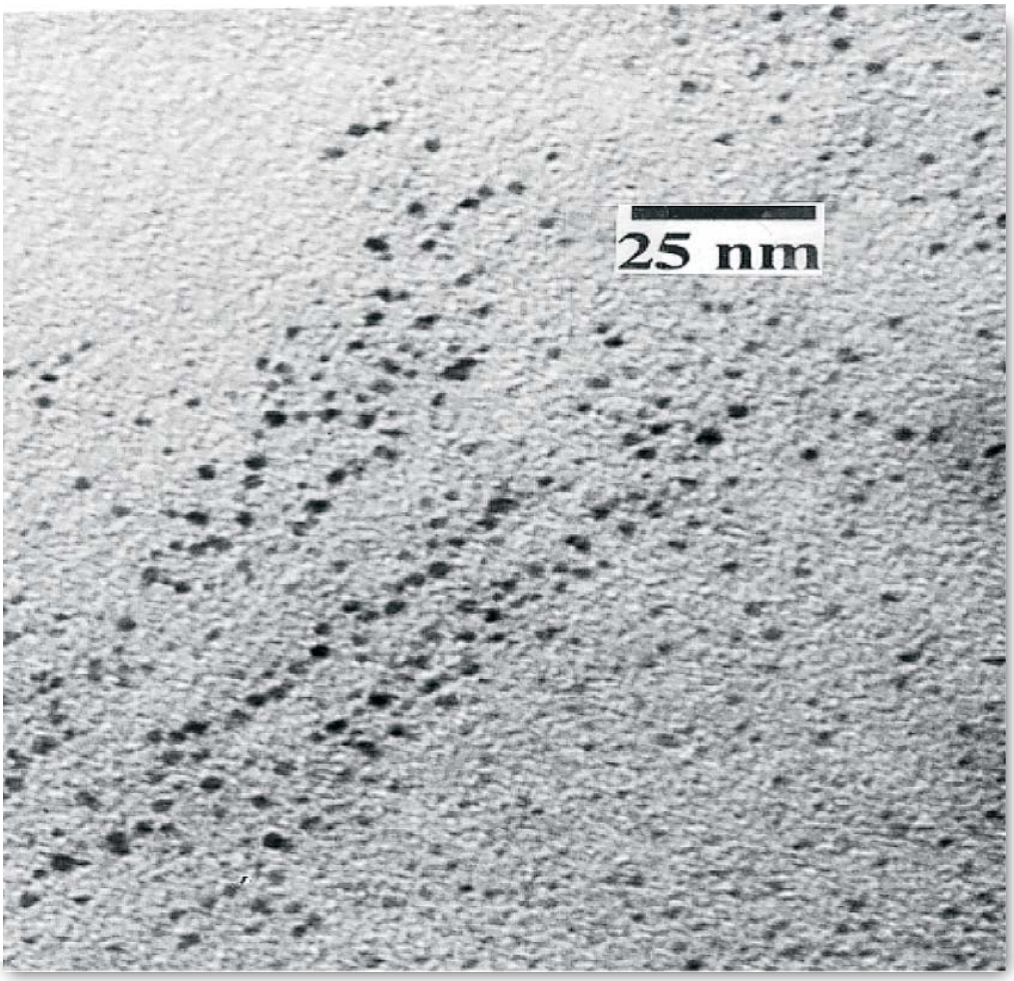

Fig. 1. TEM Image of the 2-nm Pt nanoparticles. The particles were synthesized radiolytically and were used as core for the Pt-Ag particles.

In addition, x-ray appearance near-edge structure (XANES) was used to determine that the absorbing metal atoms of the samples did not oxidize during the measurements, and transmission electron microscopy (TEM) was used to determine the composition, shape, and size of the samples (Fig. 2).

According to the collaborators, when the two bimetallic nanoparticles were mixed, the materials followed their bulk alloying characteristics in all cases. Specifically, the collaborators found—with bimetallic Pt-Ag—that at a diameter of two nanometers and larger, Pt and Ag did not alloy in the nanosized system. Instead, the two metals remained separated in both spherical and cylindrical forms because the tension produced in the Ag-Pt lattice from crystallographic mismatch was greater than the excess surface free energy found in the particle pair. In the case of bimetallic Pd-Ag, the research showed that the cylindrical rods of the nanowires alloy in the nanosized system (as was the case with their spherical equivalents from other, similar studies). With Pd-Ag, the mismatch-induced strain was less than the excess surface free energy found in the small particles. Thus, the two metals did not remain separated.

The collaborators concluded that the morphology of the nanostructures did not directly influence their ability to alloy in these systems and at these very small sizes. The information learned in this study will be important in future research, especially with regard to (1) providing a method to control energies of plasmon absorption bands of metallic mixtures, (2) improving catalytic activities of particles, which sometimes produce new catalysts unknown in bulk form, and (3) alloying component metals in order to make structural alterations that affect the electronic properties of composites, as well as possibly increasing or decreasing Fermi-level equilibration in those composites. Future applications of bimetallic nanoparticles are growing in many diverse fields such as catalysis, biosensing, and electronics. — *William Arthur Atkins*

See: Debdutta Lahiri[1], Bruce Bunker[1], Bhoopesh Mishra[1], Zhenyuan Zhang[1], Dan Meisel[1], C.M. Doudna[2], M.F. Bertino[2], Frank D. Blum[2], A.T. Tokuhiro[2] Soma Chattopadhyay[3], Tomohiro Shibata[3], and Jeff Terry[3], "Bimetallic Pt-Ag and Pd-Ag Nanoparticles," J. Appl. Phys. **97**, 094304 (2005).

Author Affiliations: [1]University of Notre Dame, [2]University of Missouri-Rolla, [3]Illinois Institute of Technology
Correspondence: bunker.1@nd.edu

Work performed at MR-CAT is supported in part by funding from the U.S. Department of Energy under Grant No. DE-FG02-04ER46106. The work done at the Notre Dame Radiation Laboratory has been funded by the U.. Department of Energy under Contract No. 4568. Use of the Advanced Photon Source was supported by the U.S. Department of Energy, Office of Science, Office of Basic Energy Sciences, under Contract No. W-31-109-ENG-38.

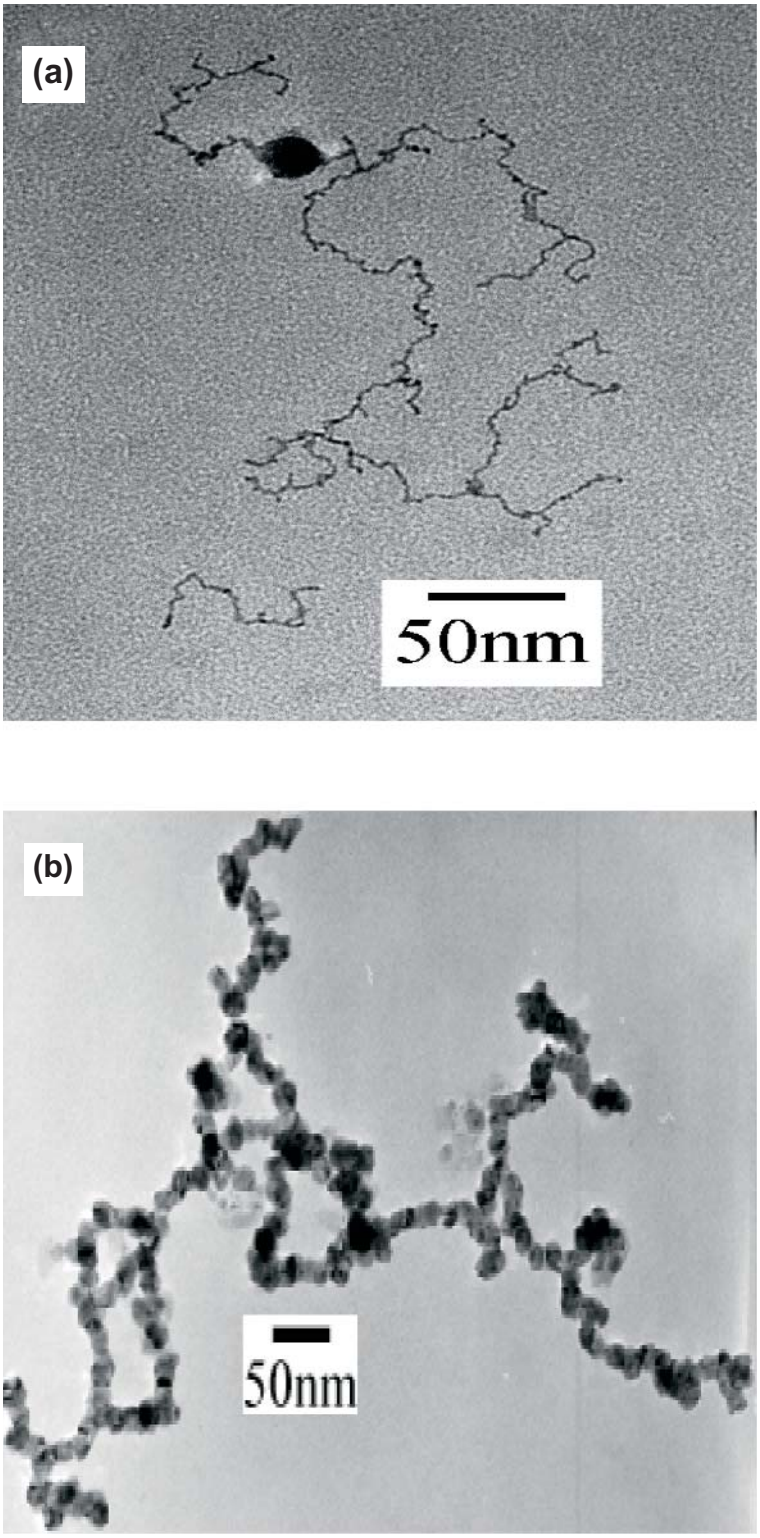

Fig. 2. (a) Bright-field TEM micrographs of Pt-Ag nanowires: A large (20 nm) particle of 85 ± 5% Ag can be seen at the top of the figure; thin filaments (3-nm diameter) of 50% Ag extend out of the particle. (b) Pd-Ag nanowires: The wire-like particles have a diameter of 20-25 nm and a length of up to 1.5 μm.

Novel X-ray Techniques & Instrumentation

Phasing Out the Problem in Interfacial Crystallography

Paul Fenter (left) and Zhan Zhang at the mineral-fluid interface spectrometer on the XOR/BESSRC 12-ID-D beamline.

X-ray diffraction and scattering have been applied to study a broad range of materials, from proteins and interfaces, and now to nanoparticles. But the "phase problem" of crystallography limits these applications. The phase problem arises because the complete description of a structure requires a complex structure factor with both a magnitude and a phase. Because the measured x-ray intensities are proportional to the structure factor magnitude, phase information is lost in the measurement. If the phase information were recovered, the data could be inverted directly to "image" the structure. Researchers from Argonne's Chemistry Division have demonstrated the applicability of error correction algorithms as an effective method for one-dimensional imaging of buried interfacial structures, less than 1-Å spatial resolution.

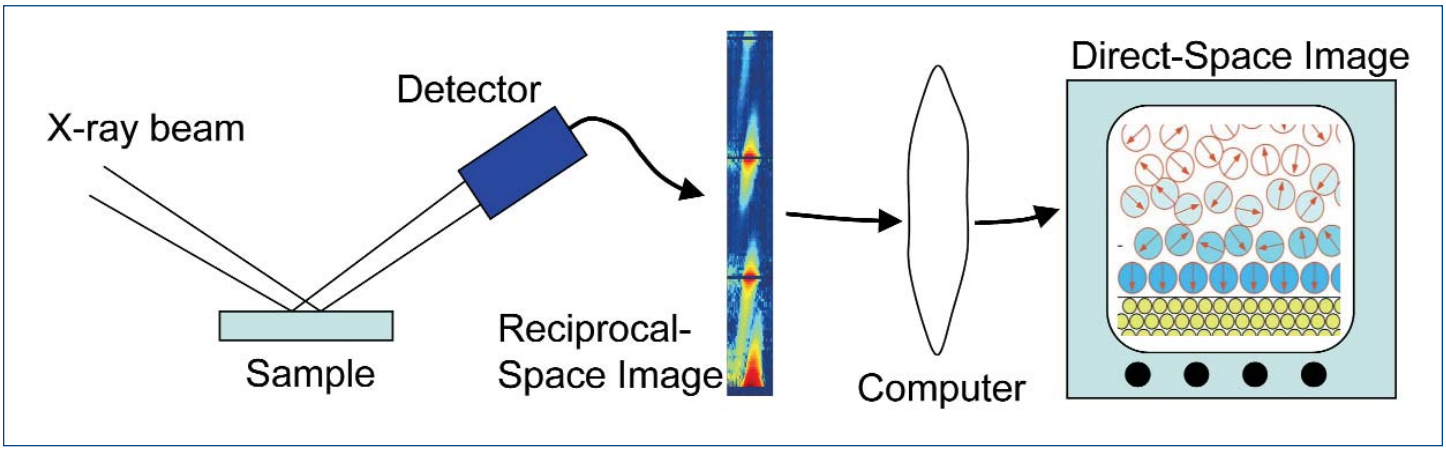

Fig. 1. A schematic of the inversion process (left to right): The reflectivity of an interface is probed by normal procedures revealing a reciprocal space image of the "crystal truncation rod." This is inverted to a direct-space density profile by use of a computer algorithm which acts as a lens that images the interfacial structure.

Since the advent of dedicated synchrotron radiation facilities, the applications of x-ray diffraction and scattering for structure determination have expanded to include a broad range of materials, from proteins and interfaces to nanoparticles. However, the well-known "phase problem" of crystallography limits these applications. The phase problem arises because the complete description of a structure requires a complex structure factor having both a magnitude and a phase. The measured x-ray intensities, however, are proportional to the structure factor magnitude, and phase information is lost in the measurement. If the phase information were retained, the data could be inverted directly to "image" the structure. Over the years, several methods have been developed that effectively bypass the phase problem in traditional crystallography (e.g., multiwavelength anomalous diffraction phasing, direct methods) and in coherent diffraction. Various approaches have been developed for inverting interfacial scattering data, including coherent Bragg rod analysis (COBRA) and holographic inversion techniques, but so far, these have been demonstrated for only a relatively narrow range of systems (e.g., thin-film structures, or inversion of data in the Fresnel regime). Consequently, the "brute-force" least-squares fitting approach is still the most widely used method of data analysis for interfacial systems, but it can require several months of effort for a successful analysis.

Researchers from Argonne's Chemistry Division have recently demonstrated the applicability of error correction (i.e., Fienup) algorithms as an effective approach for one-dimensional imaging of buried interfacial structures. They applied this approach to the determination of the hydration structures of oxide-water interfaces at high resolution. This topic was particularly challenging because no approach had yet been demonstrated to invert one-dimensional data with sub-Å resolution. The Argonne researchers' approach derives from a similar one that had been applied to the inversion of coherent diffraction data of larger meso- and nanoscale structures. Here, the computer in effect acts as a lens, converting the reciprocal space image of the crystal truncation rod into a one-dimensional direct-space image of the interface (Fig. 1). Application to high-resolution specular reflectivity data measured at the XOR/BESSRC 12-BM-B, 11-ID-D, 12-ID-D; and XOR 1-BM beamlines at the APS demonstrates the efficacy of this approach, in which individual layers of water molecules at the oxide-water interface are directly imaged. Comparisons of interfacial structures derived with model-dependent and model-independent approaches show that this approach provides a reliable first-order indication of the interfacial structure, revealing atomic locations within ~0.2 Å of those derived using model-dependent approaches. The success of this approach, coupled with previous developments in this area, suggests that the inversion of diffraction data need not be the rate-limiting step, and that real-time analysis of x-ray scattering data for complex interfaces may be possible. — *Paul Fenter and Zhan Zhang Contact: fenter@anl.gov*

See: P. Fenter and Z. Zhang, "Model-Independent One-Dimensional Imaging of Interfacial Structures at <1 Å resolution," Phys. Rev. B, Rapid Communications, **72** 081401R (2005).

Author Affiliation: Argonne National Laboratory

Use of the Advanced Photon Source was supported by the U.S. Department of Energy, Office of Science, Office of Basic Energy Sciences, under Contract No. W-31-109-ENG-38.

VIBRATIONAL MODES OF ^{57}Fe IN HEME AND HEME PROTEINS

The synchrotron-based technique of nuclear resonance vibrational spectroscopy (NRVS) has been applied to an investigation of the vibrational modes of ^{57}Fe in heme and heme proteins. Hemes are the complex molecules that contain ferrous-state iron and are important contributors to a variety of biochemical processes. The new technique, which can be thought of as Mössbauer spectroscopy with vibrational sidebands, is possible now because of high-brightness third-generation synchrotron sources like the APS. The selectivity of NRVS is reminiscent of that of resonance Raman spectroscopy, but with the significant advantage of not being subject to the optical selection rules of Raman or infrared spectroscopy. NRVS may be said to provide the ultimate limit in selectivity, because only the vibrational dynamics of the probe nucleus contribute to the observed signal. Moreover, the NRVS intensity is directly related to the magnitude and direction of the motion of the probe nucleus; so, the method provides a uniquely quantitative view of the measured vibrational spectrum.

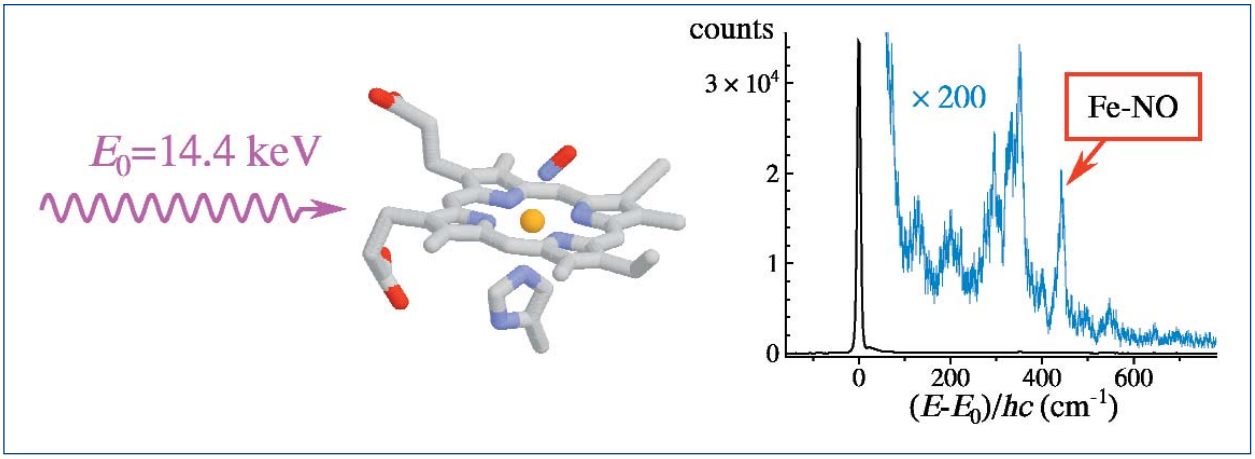

Fig. 1. Plot of the NRVS spectrum of nitrosylmyoglobin and the corrected assignment of the Fe-NO vibration.

The radiation from third-generation synchrotron sources helps circumvent previous experimental limitations by enabling measurements in a time-resolved fluorescence excitation mode. The subnanosecond duration of the synchrotron pulse, together with fast detectors, allows the nuclear resonance signal to be distinguished from the background signal, because of the ^{57}Fe signal arrives with a delay on the order of the nuclear lifetime (141 ns). The high source brilliance at the XOR 3-ID-D undulator beamline at the APS allowed researchers from the University of Notre Dame, Purdue University, and Northeastern University to use a tunable, ultra-high-resolution monochromator to produce a beam with an extremely narrow energy bandwidth (0.001 eV) and acceptable photon fluxes, which resulted in an experimental resolution of the vibrational spectrum of 7–8 cm^{-1}. The energy of the incident photons was tuned in the vicinity of the nuclear resonance at 14.413 keV, and photons that were absorbed by ^{57}Fe at any given wavelength were determined by measuring the resulting 6.4-keV atomic fluorescence emitted from the excited ^{57}Fe atoms with an avalanche photodiode detector. Thus, the observed fluorescence signal was proportional to the number of photons absorbed by nuclei within the excited sample volume.

The NRVS experiments provided the complete set of bands corresponding to the modes of motion of the iron atom (Fig. 1). All iron-ligand modes were observed, including many that had not been previously observed. For hemes, these included in-plane iron vibrations that have not yet been reported by resonance Raman studies and the iron-imidazole stretch, which was not previously identified in six-coordinate porphyrins. The data demonstrated the importance of peripheral substituents on the vibrational spectrum of heme derivatives.

Although the NRVS technique has been available for a relatively short time, the early progress achieved by these and other researchers indicates that NRVS has significant potential for elucidating the role of Fe in biology. This is important

because many physiologically essential proteins incorporate Fe, often at the center of a planar heme group. The best-known heme proteins (such as hemoglobin and cytochrome c oxidase) are involved in the transport and usage of molecular oxygen. Heme proteins also mediate the function of another diatomic molecule, nitric oxide (NO), a signaling molecule involved in diverse physiological processes, including neurotransmission, immune function, and regulation of blood pressure. Both O_2 and NO bind to Fe, and this atom is believed to play a fundamental role in protein control of active-site reactivity. Conventional Mössbauer studies, although they provide insight into Fe dynamics in proteins, only characterize the averaged fluctuations of the Fe nucleus. In contrast, NRVS resolves the contributions of individual vibrational modes to Fe fluctuations in proteins. — *Vic Comello*

See: W.R Scheidt[1], S.M. Durbin[2], and J.T. Sage[3], "Nuclear Resonance Vibrational Spectroscopy-NRVS," J. Inorg. Biochem. **99**, 60 (2005).

Author Affiliations: [1]University of Notre Dame, [2]Purdue University, [3]Northeastern University
Correspondence: scheidt.1@nd.edu

W.R.S. thanks the National Institutes of Health (NIH) for the long-term support of his porphyrin research under Grant GM-38401-32. S.M.D. acknowledges support by National Science Foundation (NSF) grant PHY-9983180. J.T.S. acknowledges grants from NIH (GM-52002) and NSF (PHY-0240955). Use of the Advanced Photon Source was supported by the U.S. Department of Energy, Office of Science, Office of Basic Energy Sciences, under Contract No. W-31-109-ENG-38.

Self-assembly of Metal Islands on Oxygen-coated Surfaces

Many technologies, especially those based on nanoscale magnetism, require the ability to fabricate patterned surfaces and structures on an industrial scale. One attractive route for accomplishing this is self-assembly, in which a material spontaneously arranges itself into structures of useful sizes or shapes. In self-assembly, large quantities of nanoscale structures can be created quickly, although the ability to control their size and placement is currently limited. A variety of structures have been created via self-assembly of metals into nanowires and dots, but the formation mechanisms remain poorly understood. Moreover, a great deal of important surface physics can be studied by examining the behavior of metal nanostructures on surfaces. Recently, a team of researchers from Argonne National Laboratory and Lawrence Berkeley National Laboratory used the XOR-4-ID-C beamline at the APS to understand the surface features necessary for achieving controlled self-assembly of cobalt nanodots on an oxidized ruthenium (0001) surface.

To study the growth of cobalt islands, the researchers used a combination of x-ray photoemission electron microscopy (XPEEM) and low-energy electron microscopy (LEEM). Precise resolution of the chemical structure and magnetism of the cobalt nanodots was obtained by means of XPEEM, in which soft x-rays strike the sample and photo-emitted electrons are collected to form a surface image. In LEEM, electrons backscattered from a surface are collected and focused to form an image of the surface. LEEM is especially sensitive to surface morphology and chemical composition.

Sample preparation and surface investigation were carried out in an ultrahigh-vacuum chamber at 5×10^{-11} mbar. Single crystals of ruthenium (0001) with the surface exposed were cleaned of oxygen by flash heating at 1600K. Partial oxidation of the surface was achieved by flashing to lower temperatures. The substrate was held at 650K to 800K for cobalt deposition. During the deposition process, LEEM was used to monitor the formation of "nanoislands." X-ray photoemission electron microscopy images were collected with x-ray excitation at a cobalt resonance energy of 778.1 eV to create chemical contrast. In addition, x-ray magnetic circular dichroism was used to obtain images of the magnetic domain structure of the islands.

For the unoxidized substrate, the team found that at temperatures above 700K, cobalt deposition results in the growth of ribbons aligned with step edges. With continued deposition, the ribbons grow laterally until they coalesce to form a perfect monolayer of cobalt. More deposition leads to nucleation and lateral growth of cobalt islands that are anchored to the step edges.

Cobalt island growth on a partially oxidized ruthenium (0001) substrate at 800K resulted in formation of a much different pattern. Based on the XPEEM images, the partial oxygen

Continued on next page

termination of the substrate before cobalt deposition appears to create rhombus-shaped ruthenium oxide regions on top of the clean Ru(0001) surface. For eight-monolayer equivalents of cobalt deposited, the XPEEM data with elemental contrast show that the cobalt islands begin nucleating on the clean Ru region but do not stick at all to the Ru oxide zones. Deposition with the substrate at a lower temperature of 730K indicated that dense island growth occurred in the clean Ru regions with small amounts of growth on the oxidized areas, but with much lower density. Magnetic imaging showed that the island domains were randomly distributed, indicating that the islands were well separated and there was very little magnetic communication among the islands.

All of these data point to clear differences in deposition and growth behavior that the researchers attribute to temperature dependence of the sticking coefficients for cobalt on the oxidized versus the clean ruthenium surfaces. The results illustrate the power of combining multiple techniques, such as *in situ* self-assembly, XPEEM, LEEM, and x-ray magnetic circular dichroic imaging, for unraveling the puzzle of directed self-assembly on complex surfaces. Moreover, the findings show the importance of high-brightness third-generation synchrotron facilities, such as the APS, which offer x-ray beams of sufficient brightness and polarization characteristics to enable such chemical and magnetic imaging experiments.

— *David Voss*

See: H.F. Ding[1], A.K. Schmid[2], D.J. Keavney[1], Dongqi Li[1], R. Cheng[1], J.E. Pearson[1], F.Y. Fradin[1], and S.D. Bader[1], "Selective Growth of Co Nanoislands on an Oxygen-patterned Ru(0001) Surface," Phys. Rev. B **72**, 035413 (2005).

Author Affiliations: [1]Argonne National Laboratory, [2]Lawrence Berkeley National Laboratory
Correspondence: keavney@aps.anl.gov

This work was supported by the U.S. DOE BES-Materials Sciences under Contract No. W-31-109-ENG-38 at ANL and No. DE-AC03-76SF00098 at LBNL. S.D.B. and H.F.D. acknowledge support from the ANL-University of Chicago Consortium for Nanoscience Research CNR. Use of the Advanced Photon Source was supported by the U.S. Department of Energy, Office of Science, Office of Basic Energy Sciences, under Contract No. W-31-109-ENG-38.

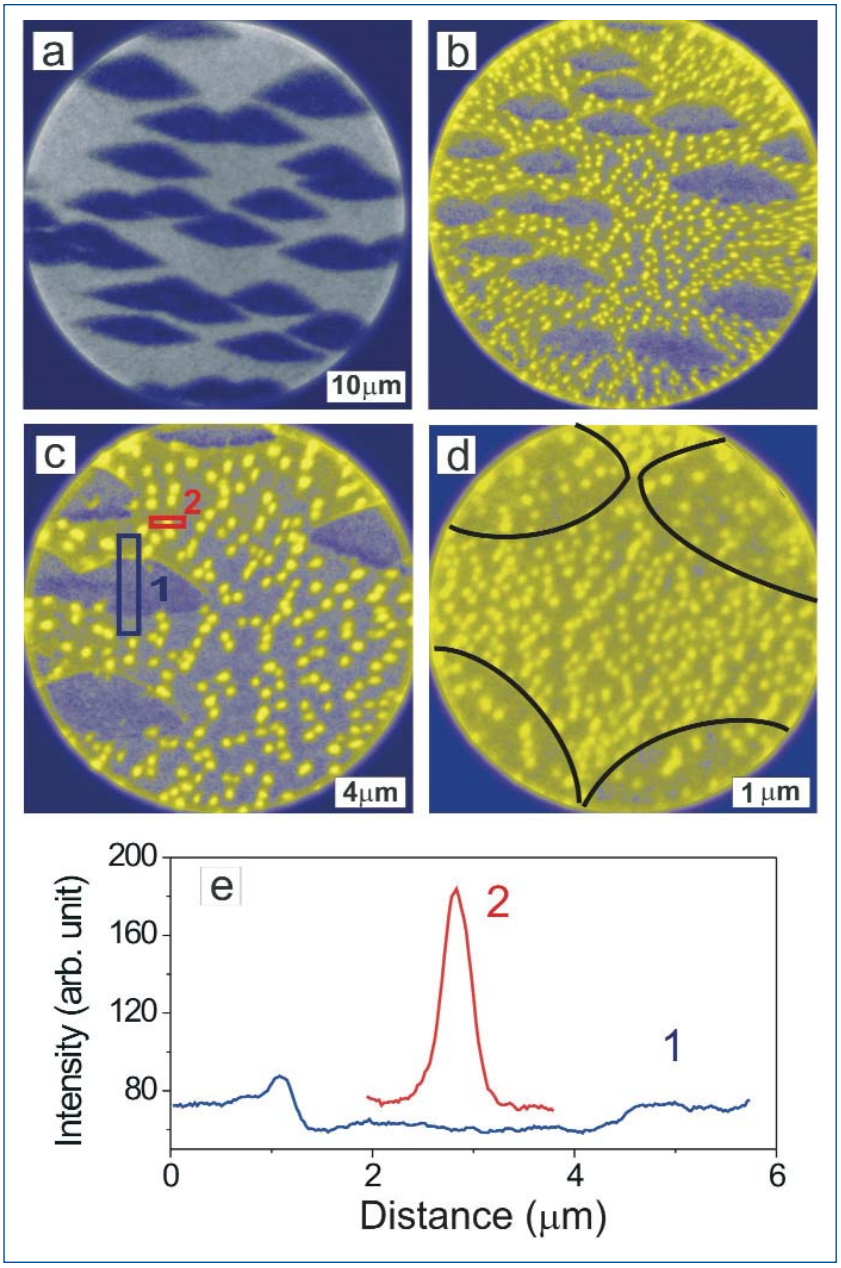

Fig. 1. X-ray photoemission electron microscopy images of partially oxidized ruthenium (0001) surfaces. (a) The dark rhombus-shaped patterns are ruthenium oxide and the lighter regions are clean ruthenium substrate. (b) Cobalt elemental map of eight-monolayer-equivalent cobalt film. (c) Magnified view of image (b). (d) Ten monolayers of cobalt with boundaries between pure ruthenium and ruthenium oxide marked by black lines. (e) Profile of cobalt elemental signal shown in (c), where 1 is across a rhombus and 2 is across a cobalt island.

Mapping X-ray Fluorescence Datasets to Elemental Distributions Using PCA and Fitting

Combining principal component analysis (PCA) with spectral fitting can significantly improve data analysis in x-ray fluorescence mapping of a biological specimen. This is achieved by reducing the processing time and providing better discrimination between background and signal. Using this technique at the XOR sector 2 beamlines 2-ID-D and 2-ID-E, members of the XSD X-ray Microscopy Group, in collaboration with colleagues from the Veterans' Affairs Medical Center in Durham, NC, carried out analysis on the elemental distribution in *Leishmania donovani* parasites that were treated with a therapeutic drug containing antimony.

X-ray fluorescence microscopy (XRF) is a powerful technique for the mapping and quantification of elemental distributions in biological specimens, such as cells and bacteria. The sample is raster-scanned through a focused x-ray beam; element-specific x-ray fluorescence excited in the sample is then detected by an energy-dispersive detector. Per-pixel dwell times are chosen to compromise between high spatial resolution (corresponding to many sampling points) and good counting statistics in order to achieve reasonable scan times. However, interpretation of elemental maps can be difficult when spectral signatures overlap. Ideally, therefore, full spectra are acquired and saved at each scan position to allow a later deconvolution of overlapping peaks and removal of the background.

Several approaches are possible to map the fluorescence counts detected by the energy-dispersive detector to quantify element concentrations. Spectral filtering based on spectral regions of interest (ROI) is the simplest and fastest method, but it lacks precision when there is interference by other peaks or by overall background. Fitting of the single spectra at every pixel can better account for these interferences, but this can be a slow process, as many spectra need to be fit. For example, in a 100 × 100 pixel scan, fits of 10,000 spectra need to be calculated and potentially inspected. Also, because the photon statistics in a single-pixel spectrum are low, the number of fit parameters has to be lim-

Continued on next page

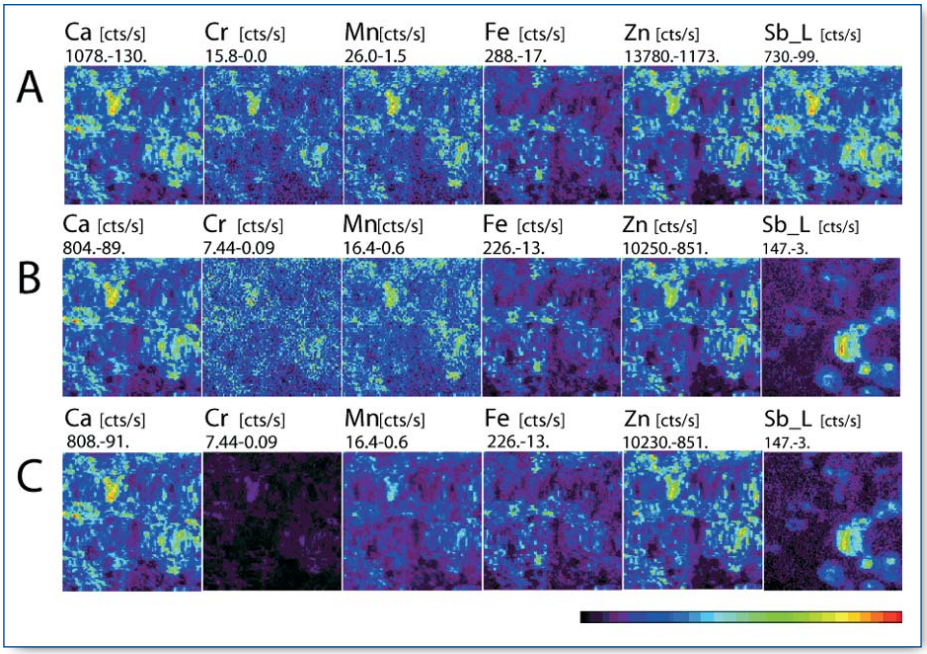

Fig. 1. Maps of selected elements of a cluster of several *Leishmania donovani* amastigote forms [4], generated from a full (x,y, energy) x-ray fluorescence dataset. Elemental maps in A were generated using only spectral filtering (ROIs). The signal in the Sb $L_{\alpha,\beta}$ map is dominated by bleed-through from the Ca $K_{\alpha,\beta}$-lines and does not show the true Sb distribution. In B, the maps were calculated using per-pixel fitting; Ca and Sb are well deconvoluted. The Sb distribution is quite distinct from the other elements and shows that the Sb content of different *L. donovani* cells varies significantly. However, the background in low count-rate regions cannot be distinguished from true signal. The Cr map, for example, is dominated by detector artifacts, such as incomplete charge collection. In C, the maps were calculated using a combination of principal component analysis and fitting. Elemental maps of high count-rate elements are reproduced, as well as those generated using only fitting, but with a shorter processing time. Additionally, uncorrelated signal (i.e., noise and background) are better recognized as such, as is apparent in the much lower apparent level of Cr in the image (Cr is not actually present in this sample).

ited, and in regions of low count rate, detector background and "true" fluorescence signal may be indistinguishable.

Principal component analysis provides a method to correlate an XRF dataset with full spectra at each scan point and to weigh each component of the spectrum, and its corresponding eigenimage, according to its respective significance in the dataset [1-3]. In particular, photon noise is not correlated among pixels and therefore does not contribute to the principal components. By fitting the eigenspectra of the principal components, one can then generate maps of fitted elemental components with high accuracy, without the need to fit the spectra of single pixels. This drastically reduces the number of spectra that need to be fit, typically to less than 20. In addition, the correlation of elemental distributions can be used to reveal information about the number and composition of the different major constituents of a cell.

Using this technique, the members of the XSD X-ray Microscopy Group carried out analysis on the elemental distribution in *Leishmania donovani* parasites that were treated with a therapeutic drug containing antimony (Pentostam, The Wellcome Foundation, London, UK). The Sb L-lines overlap significantly with the Ca K-lines, so that the naturally occurring Ca content of *L. donovani* makes an accurate analysis and mapping of the Sb difficult. Region of interest-based spectral filtering is not able to distinguish between Ca and Sb; instead, the Sb map is dominated by "bleed-through" from Ca (Fig. 1). Fitting the spectra at every pixel visualizes the differences in spatial distribution between Ca and Sb well but is comparatively slow (~15 min for the image shown). Principal component analysis-based fitting is able to deconvolute Sb and Ca as well as direct fitting and it is ~5 times faster. Moreover, it better distinguishes background from signal, as evidenced by the reduced apparent Cr signal, which can be attributed to detector artifacts.

Contact: Stefan Vogt (vogt@aps.anl.gov)

References

[1] E.R. Malinowski, *Factor Analysis in Chemistry* (J. Wiley, New York, 1991).

[2] A. Osanna and C. Jacobsen, "Principal Component Analysis for Soft X-ray Spectromicroscopy," X-ray Microscopy, AIP Conference Proceedings **507** (American Institute of Physics, Melville, 2000), 350.

[3] S. Vogt, J. Maser, and C. Jacobsen, "Data Analysis for X-ray Fluorescence Imaging," Journal de Physique IV **104**, 617, 2003.

[4] A. LeFurgey, M. Gannon, J. Blum, and P. Ingram, "*Leishmania donovani* amastigotes mobilize organic and inorganic osmolytes during regulatory volume decrease," J. Eukaryotic Microbiology, in press.

This work was was supported by the U.S. Department of Energy, Office of Science, Office of Basic Energy Sciences, under Contract No. W-31-109-ENG-38.

Around the APS

An R&D 100 Award for the Multilayer X-ray Laue Lens

Argonne researchers (l. to r.) Chian Liu, Raymond Conley, and Albert Macrander, all of the XSD Optics Fabrication and Metrology Group, received one of four prestigious R&D 100 Awards presented to Argonne scientists in 2005. The awards are given each year, by *R&D Magazine*, to the world's top 100 scientific and technological innovations. Liu, Conley, and Macrander were recognized for their development of the multilayer x-ray lens wafer technology (see article on the next page). This year's awards bring to 90 Argonne's total since the magazine began presenting them in 1964.

Contact: atm@aps.anl.gov

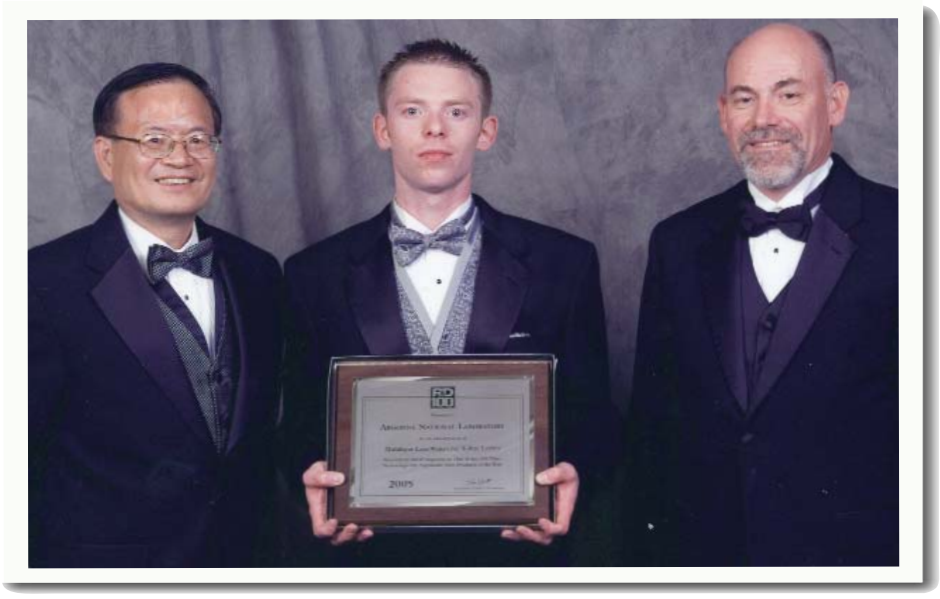

Nanometer Linear Focusing of Hard X-rays by a Multilayer Laue Lens

Focusing of light to near atomic resolution using hard x-rays has been a dream ever since the nature of x-rays was understood a century ago. A new type of x-ray optic, dubbed Multilayer Laue Lens (MLL), developed in collaboration between the Center for Nanoscale Materials and APS, promises to fulfill this dream. The optical depth of an MLL can be many times the depth that can be achieved for nanometer-scale zone plates by using lithographic techniques, resulting in many-fold higher efficiencies for hard x-rays.

To produce an MLL [1], a flat substrate is first coated with thousands of alternating layers with nanometer-scale thicknesses. The layer thicknesses gradually increase through the multilayer to form the zones of a linear Fresnel zone plate. Thin cross sections of the multilayer are then made, which focus x-rays when illuminated in transmission (Laue) diffraction geometry. As shown in Fig. 1, a pair of cross sections can be used to focus in one dimension. A second pair (not shown) can be used to focus in the perpendicular dimension. Unlike earlier sputtered-sliced zone plates, in which the thinnest layers were grown last, in fabricating an MLL, these critical thinnest layers are grown first, so that any cumulative roughening of layer interfaces is less consequential.

The properties of these new x-ray focusing structures have been investigated theoretically [2]. As a result of the large depth of the MLL, the diffraction physics differ from the thin-optic Fresnel diffraction employed for standard zone plates; volume diffraction effects occur, akin to those applicable to a crystal. For example, local diffraction efficiency is highest when the incidence angle matches the local Bragg condition. But, unlike a periodic crystal, the optimum incidence angle matching the Bragg condition varies across the optic, corresponding to the varying layer thicknesses in the structure. Each half of the MLL can be tilted with respect to the incident beam to maximize overall efficiency. A diffraction-limited 5-nm line focus with 30% efficiency at 20-keV x-ray energy is predicted for a multilayer structure having a thinnest layer thickness of 5 nm, at the optimum depth and tilt. At higher x-ray energies, the predicted efficiency increases. A near-atomic resolution of below 2 nm is predicted for an idealized structure in which each layer is tilted so that the Bragg condition can be achieved for all layers simultaneously.

Experimental studies of MLL structures at XOR beamlines 12-BM and 8-ID have yielded results that corroborate the theory [2]. A scanning-electron-microscope image of a multilayer cross section is shown in Fig. 2 [3]. This sample consists of 728 tungsten silicide (~WSi_2) and silicon layers with thicknesses graded from 10 nm to 58 nm, for a total thickness of 12.4 μm. This materials combination is found to have the correct properties to allow deposition of such thick and accurate multilayer structures and to allow its preservation during subsequent sec-

Continued on next page

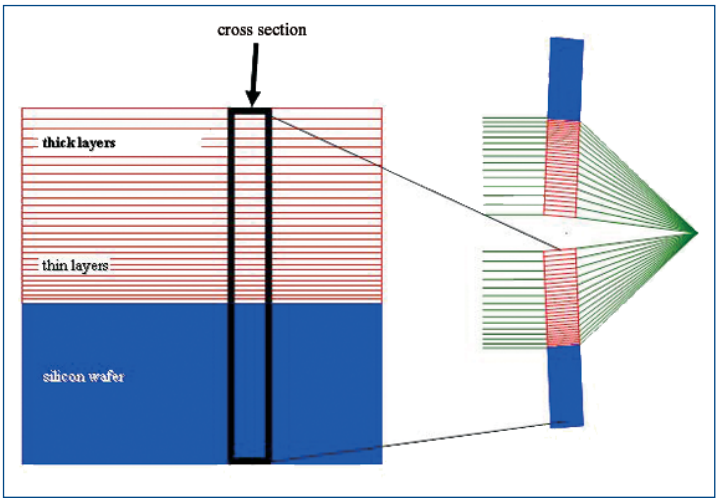

Fig. 1. Schematic view of a cross section cut from a multilayer wafer, and a pair of cross sections positioned to focus x-rays.

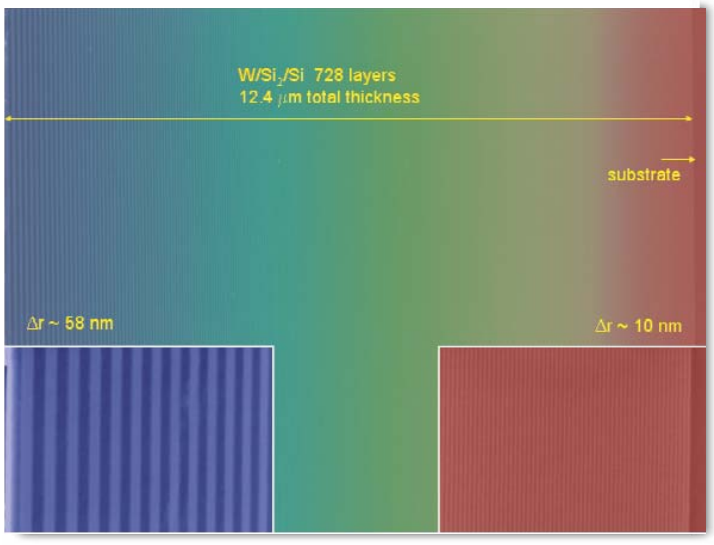

Fig. 2. An image of one side of a cross section obtained with a scanning electron microscope.

tioning. As shown in Fig. 3, a single cross-section of this multilayer produces a nearly diffraction-limited line focus of 30.6 nm (full width at half maximum) and 44% efficiency at 19.5 keV. This measurement is made by scanning a 10-nm-thick Pt film section edgewise through the focal plane and measuring the Pt fluorescence [2]. Because the predicted resolution improves as the layer thicknesses decrease and the total thickness increases, further experiments in this direction are planned. A structure having 1,588 layers with a 5-nm smallest thickness has recently been deposited, and focusing measurements are underway.

Contact: Hyon Chol Kang (kang@anl.gov), Chian Liu (cliu@aps.anl.gov), Jörg Maser (maser@aps.anl.gov), G.B. Stephenson (stephenson@anl.gov), A.T. Macrander (atm@aps. anl.gov).

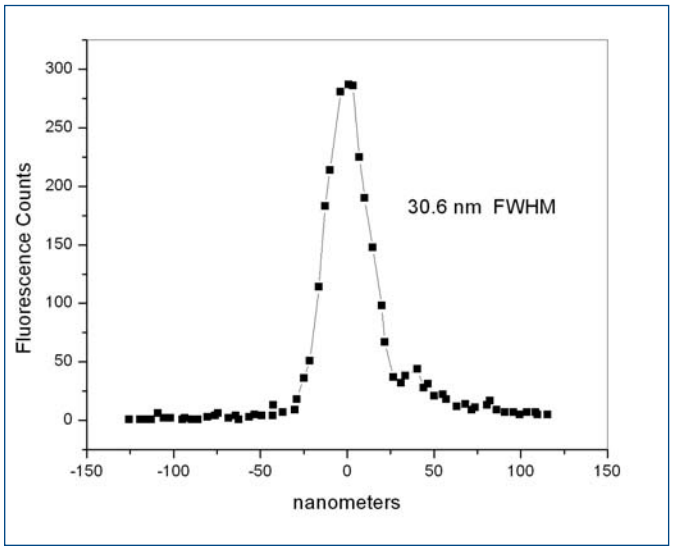

Fig. 3. Fluorescence signal obtained by scanning a 10-nm-thick Pt film turned on edge. The scan reveals a full width half maximum of 30.6 nm for the focus.

REFERENCES

[1] J. Maser, G.B. Stephenson, S. Vogt, W. Yun, A. Macrander, H.C. Kang, C. Liu, and R. Conley, "Multilayer Laue Lenses as High-Resolution X-ray Optics,' SPIE Proc. **5539**, 185 (2004).

[2] H.C. Kang, J. Maser, G.B. Stephenson, C. Liu, R. Conley, A.T. Macrander, and S. Vogt, "Nanometer Focusing of Hard X-rays by a Multilayer Laue Lens," Phys. Rev. Lett, in press.

[3] Chian Liu, R. Conley, A.T. Macrander, J. Maser, H.C. Kang, M.A. Zurbuchen, and G.B. Stephenson, "Depth-graded Multilayers for Application in Transmission Geometry as Linear Zone Plates," J. Appl. Phys. **98**(11), 113519 (2005).

AGISAXS STUDIES OF PLATINUM NANOPARTICLES FORMED BY CLUSTER DEPOSITION

Metallic nanoparticles are the subject of much interest, not least because of their extraordinary catalytic properties. However, these properties can be strongly altered, and catalytic activity can be lost. Size and shape measurements of metallic nanoparticles in certain matrices or on substrates are crucial for understanding their physical and chemical properties. The anomalous grazing incident small-angle x-ray scattering (AGISAXS) technique has proven to be a highly effective tool for overcoming barriers to a greater understanding of these particles, as demonstrated by recent studies at XOR/BESSRC beamline 12-ID-C.

The extraordinary catalytic properties of metallic nanoparticles can be strongly altered and catalytic activity can be lost because of the sintering process that takes place at elevated temperatures or upon exposure to mixtures of reactive gases. Therefore, understanding the physical and chemical properties of these nanoparticles as a function of size and shape in a certain matrixes or on substrates is crucial.

Unfortunately, only a limited number of tools are available to observe particles on the nanoscale. The small-angle x-ray scattering (SAXS) technique gives better resolution as the particle size grows smaller; with microscopy, the opposite is true. Grazing incident small-angle x-ray scattering (GISAXS), which is a branch of SAXS, is a useful *in situ* technique because it can enhance the scattering signal and deliver the size and shape of particles in multiple dimensions. However, in the case of supported nanoparticles on a substrate, often the roughness of the substrate can be of the order of the particle dimensions, and its scattering signal will be mixed with the GISAXS signal of the particles of interest.

To overcome this limitation, AGISAXS studies were carried out on platinum (Pt) clusters deposited on a silicon wafer by means of a laser ablation method. The AGISAXS results demonstrated that the signals that do not originate from a particle could be separated out from the total signal. Coverages of Pt on samples S1, S2, S3, and S4 were 1.4×10^{14}, 3.4×10^{15}, 6.8×10^{15}, and 1.4×10^{16} atoms/cm^2, respectively.

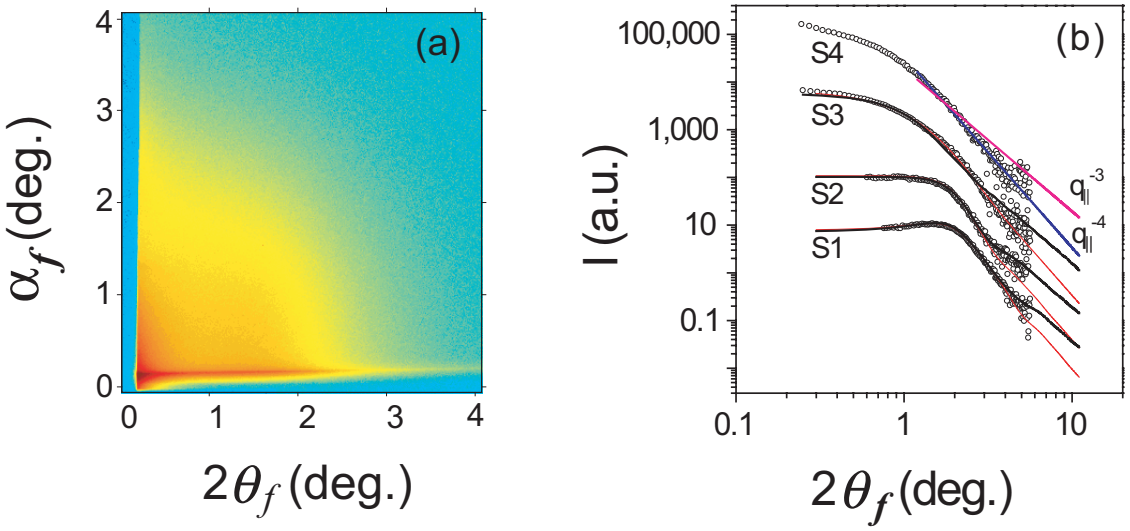

Fig. 1. Scheme of the GISAXS geometry used in the experiment. (a) the fluorescence-subtracted horizontal cuts, (b) for samples 1(S1), 2(S2), 3(S3), and 4(S4).

The AGISAXS experiments were performed at XOR/BESSRC beamline 12-ID-C by using monochromatic x-rays with energies near the L_3-absorption edge of Pt (E = 11.564 keV). Prior to the scattering measurement, energies were calibrated by using the absorption edge of a standard Pt foil. Three detectors were used: an ion chamber for the measurement of incoming beam flux, a pin diode for the transmitted or reflected primary beam, and a 2048 × 2048 pixel two-dimensional MarCCD detector for recording AGISAXS images from the sample. The detector was positioned about 0.9 m from the sample. The incident angle was kept at 0.14°, close to the critical angle of the SiO_2/Si(111) substrate for total reflection.

As shown in Fig.1(c), the anomalous effect is clear; scattering at the smallest angle region is almost energy independent, indicating that it is from the surface of the substrate and not from the particle. Figure 1(d) shows the variations of GISAXS intensities of the particle as a function of the incident x-ray energy. With this AGISAXS measurement, the particle scattering is separated from the total scattering signal and summarized in Fig. 1(e-f). In a low-coverage sample, the ISAXS signal fits to a small cylindrical shape. As the coverage goes higher, it fits well to the larger spherical shape. This AGISAXS result is understood as follows: A single Pt cluster, which is composed of a small number of Pt atoms, probably has an anisotropic shape or a facet. The clusters are agglomerated to a nanoparticle whose size gets larger as the amount of the deposited clusters is increased. When the nanoparticle is small and composed of a single or low number of clusters, the nanoparticle might still maintain the shape of a cluster that is probably far from spherical, but close to a cylinder or a hemisphere. As more clusters are agglomerated—randomly oriented on the surface of a nanoparticle—nanoparticles will be larger in size and isotropic in shape.

Byeongdu Lee, Sönke Seifert, Stephen J. Riley, George Tikhonov, Nancy A. Tomczyk, Stefan Vajda, and Randall E. Winans. Contact: blee@aps.anl.gov

See: B. Lee, S. Seifert; S.J. Riley, G. Tikhonov, N.A. Tomczyk, S. Vajda, and R.E. Winans, "Anomalous Grazing Incidence Small-angle X-ray Scattering Studies of Platinum Nanoparticles Deposition," J. Chem. Phys. **123**(7), 074701 (2005); and R.E. Winans, S. Vajda, B. Lee, S.J. Riley, S. Seifert, G.Y. Tikhonov, and N.A. Tomczyk, "Thermal Stability of Supported Platinum Clusters Studied by *in situ* GISAXS," J. Phys. Chem. B **108**(47), 18105 (2004); and S. Vajda, R.E. Winans, J.W. Elam, B. Lee, M. J. Pellin, S. Seifert, G.Y. Tikhonov, and N.A. Tomczyk, "Supported Gold Clusters and Cluster-Based Nanomaterials: Characterization, Stability and Growth Studies by *In Situ* GISAXS under Vacuum Conditions and in the Presence of Hydrogen," Top. Catal. In press. (2006).

This work was supported by the U.S. Department of Energy, Office of Science, Office of Basic Energy Sciences, under Contract No. W-31-109-ENG-38.

A Curved Image-plate Detector for High-resolution, Fast, Powder Diffraction Measurements

Knowledge of the specific atomic arrangement of materials (such as ceramics, metals and alloys, thin films, semiconductors, superconductors, bio-materials, catalysts and polymers) is essential to understanding their physical properties, chemical reactivity, or biological function. Many of these important materials are either unavailable in single-crystal form or are fabricated and used in a powder form. For these reasons, powder diffraction techniques are critical for solving crystal structures. Researchers at the University of Illinois at Urbana-Champaign (UIUC) Materials Science Department have collaborated with researchers at HASYLAB and XOR/UNI to develop a curved image-plate (CIP) detector that allows the collection and reading of the x-ray diffraction pattern to a data file in seconds [1,2].

Traditional powder diffraction methods that step-scan a fine slit or analyzing crystal over a range of angles are inefficient because they collect only a small part of the diffracted spectrum at any time and can take several hours to collect a complete spectrum.

Not only is this an inefficient method (only a small fraction of the available diffracted intensity spectrum is measured at each point), but measurements on samples that change in time are difficult and sometimes impossible. For example, it is not practical to study phase transitions by using a measurement technique that inherently takes hours to collect a single diffraction spectrum. Furthermore, samples that experience radiation damage can change during the course of the measurement.

Position-sensitive detectors have been employed to collect large parts of the diffraction pattern at once, but these are often limited in terms of either resolution, count rate, or angular range.

By contrast, the CIP detector developed by the UIUC-HASYLAB-XOR/UNI group is a linear-sensitive x-ray detector with intrinsic resolution as high as 0.006° and fast data acquisition times. The system is based on proven image-plate technology, and permits simultaneous measurement of the powder diffraction spectrum over the range of scattering angles up to nearly 40°. With a read-out time of about 6 s, the duty cycle of this detector is much

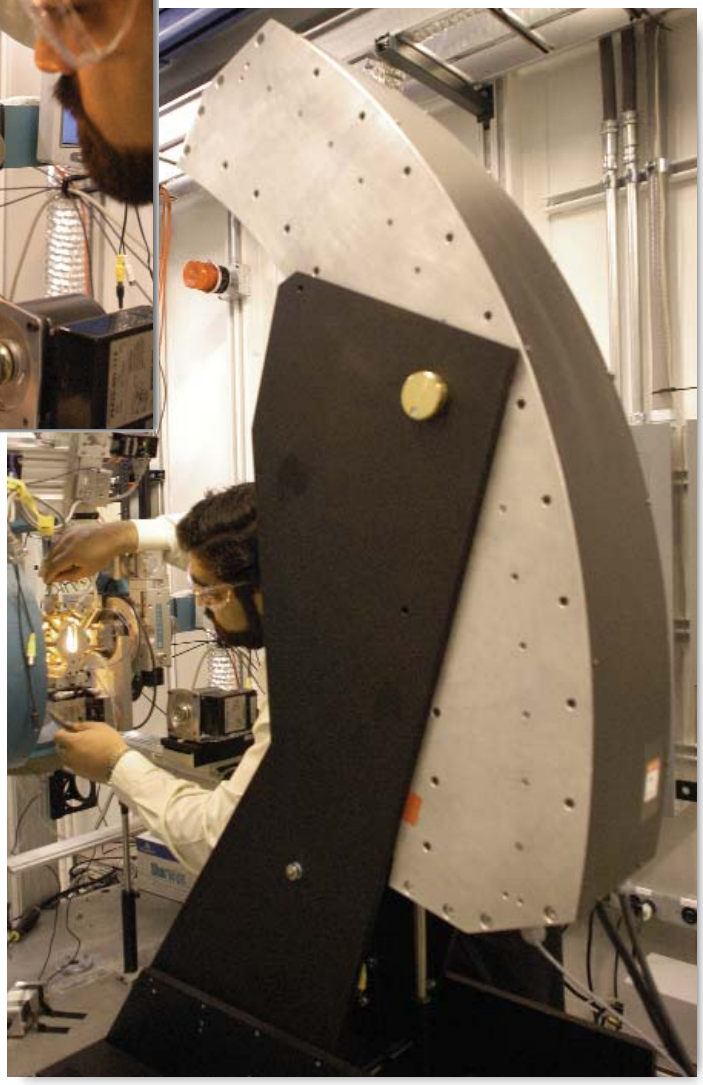

Fig. 1. The curved image plate detector system (right) at the XOR/UNI 33-BM-C beamline is used in conjunction with the quadrupole lamp furnace (inset) for rapid *in situ* XRD measurements, up to 2000° C in air.

less than 1 min., thereby increasing the measurement throughput by two to three orders of magnitude. The image plate is mounted to an arc with an ~1-m radius. The read laser and photomultiplier tube are mounted on a carriage that moves rapidly along an encoded track that provides excellent position resolution. Once positioned and calibrated, this detector enables a variety of time-resolved studies and permits more efficient use of the XOR/UNI 33-BM bending magnet beamline. Once fully commissioned, this unique detector will support studies in high-temperature ceramic material properties and phase diagrams, and will represent a paradigm shift in how high-temperature ceramic phase diagrams will be determined.

In addition, the details of phase transformations can now be studied directly *in situ*. For example, martensitic transformations, and the subsequent relaxation phenomena that immediately follow these displacive transformations, can be examined in detail as they occur. And of course, the kinetics of other phase transformations (or of chemical reactions) can also be directly investigated by using this fast detector while the sample is held in a high-temperature furnace or a reaction cell.

Contact: Waltraud M. Kriven (kriven@uiuc.edu),
Paul Zschack (zschack@anl.gov)

REFERENCES

[1] P. Sarin, R.P. Haggerty, W. Yoon, P. Zschack, M. Knapp, and W.M. Kriven, "Rapid *In situ* Ultra-high-temperature Investigations of Ceramics Using Synchrotron X-ray Diffraction," *Ceramic Engineering and Science Proceedings* **30** (in press).

[2] M. Knapp, V. Joco, C. Baehtz, H. H. Brecht, A. Berghaeuser, H. Ehrenberg, H. von Seggern, and H. Fuess, "Position-sensitive Detector System OBI for High-resolution X-ray Powder Diffraction Using On-site Readable Image Plates," Nucl. Instrum. Methods Phys. Res. Sect. A-Accel. Spectrom. Dect. Assoc. Equip. **521** 565 (2004).

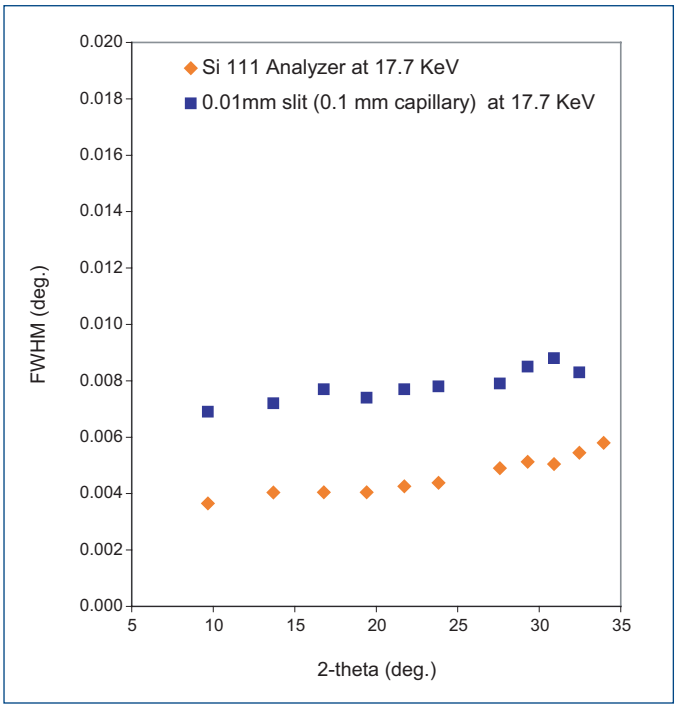

Fig. 2. Comparison of full width at half maximum of LaB6 powder sample (NIST-SRM660a) XRD patterns measured by using the CIP detector and a Si 111 analyzer. Note: The sample was mounted in a 0.1- mm glass capillary.

CIP detector development was funded by an AFOSR-DURIP Award FA9550-04-1-0345 to the University of Illinois at Urbana-Champaign. High-temperature XRD studies were supported by the National Science Foundation (DMR 02-11139). The XOR/UNI facility at the APS was supported by the U.S. DOE under Award No. DEFG02-91ER45439. Use of the Advanced Photon Source supported by the U.S. Department of Energy, Office of Science, Office of Basic Energy Sciences, under Contract No. W-31-109-ENG-38.

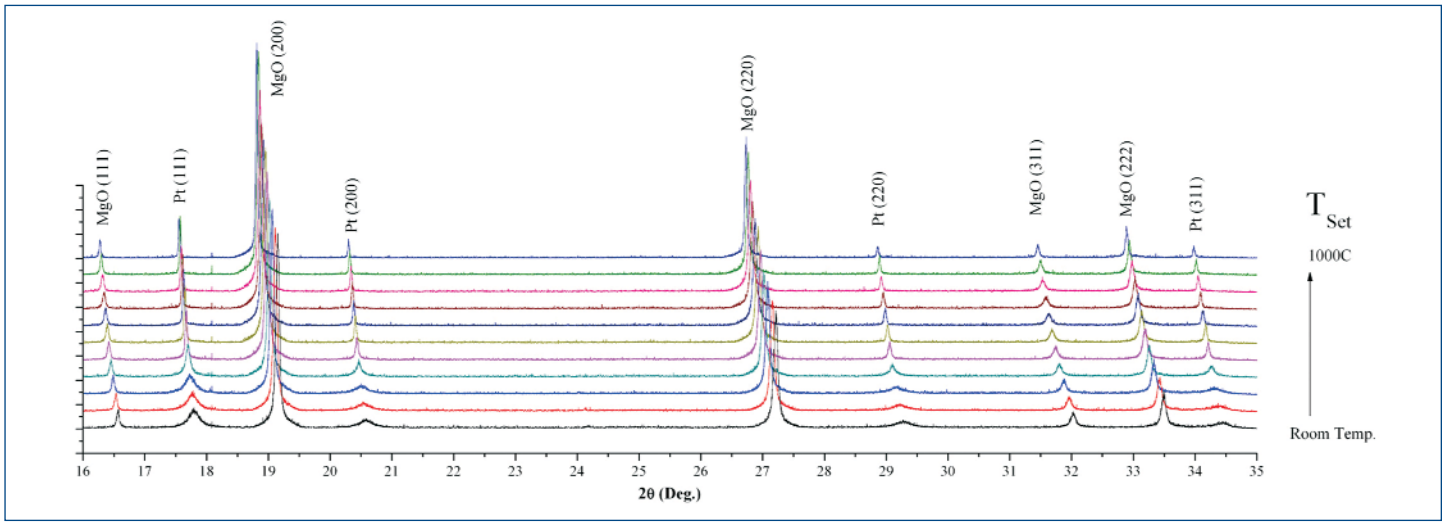

Fig. 3. High-temperature XRD studies of MgO coated with Pt using the CIP detector and quadrupole lamp furnace from T_{Set} = 25 to 1100°C in steps of 100°C. The entire experiment was completed in 72 minutes; temperature change was the slowest step, and accounted for 49 min; each scan was from a 60-s exposure [1].

Thin-film Growth by Pulsed Laser Deposition

Pulsed laser deposition (PLD) has emerged as an important approach for the growth of high-quality thin films of complex materials. In PLD, non-equilibrium growth occurs as a plume of laser-ablated material is ejected from a suitable target and impinges on the growth substrate. Researchers from the Oak Ridge National Laboratory (ORNL) Condensed Matter Sciences Division and the University of Illinois at Urbana-Champaign (UIUC) Materials Research Laboratory have developed instrumentation to allow the real-time investigation of the epitaxial surface growth process. These experiments utilize a focused excimer laser to ablate target material onto the substrate inside a growth chamber.

A central problem in nonequilibrium materials synthesis is the nature of epitaxial growth and the relationship between deposition parameters and the resulting film structure. The high-brightness x-ray beams available at the APS permit studies that can lead to an understanding of both the nature of this growth and the parameters affecting the growth of high-quality thin-films.

The ORNL-UIUC PLD chamber (Fig. 1), now installed at XOR/UNI beamline 33-ID-D, was designed around the (2+2) circle diffractometer geometry and is optimized for surface x-ray diffraction (Fig. 2). The chamber is integrated with the goniometer, and a load lock sample and target-changing mechanism permits quick sample and target turnaround. With suitable alignment procedures, the specular and off-specular truncation rods can be monitored simultaneously, providing structural information about the growing film both in-plane and perpendicular to the growing surface.

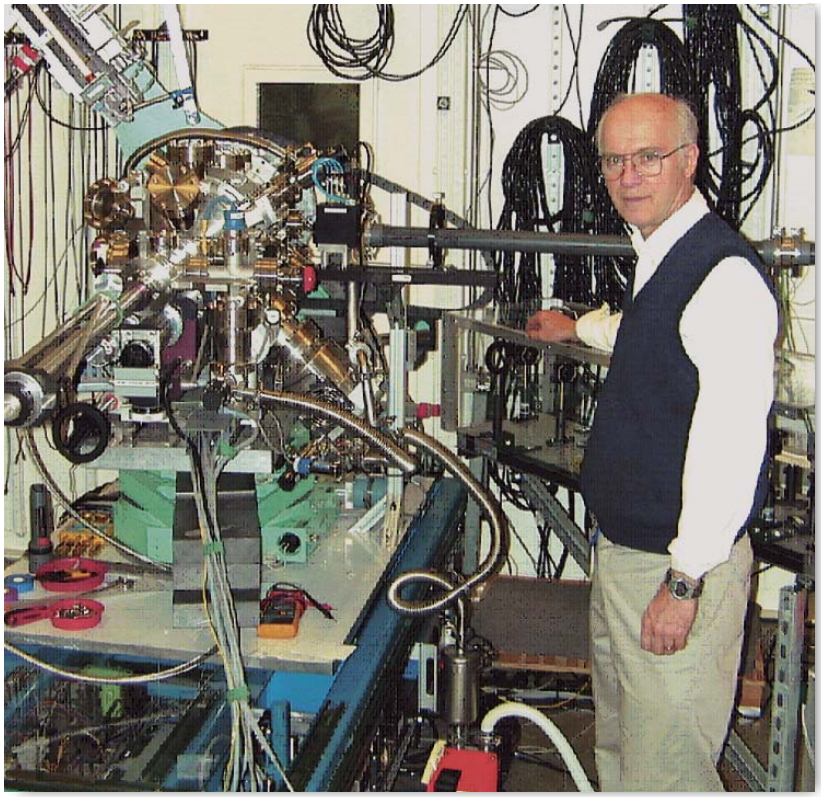

Fig. 1. (above) Ben Larson (ORNL) inspects the installation and scattering geometry of the PLD chamber at 33-ID-D.

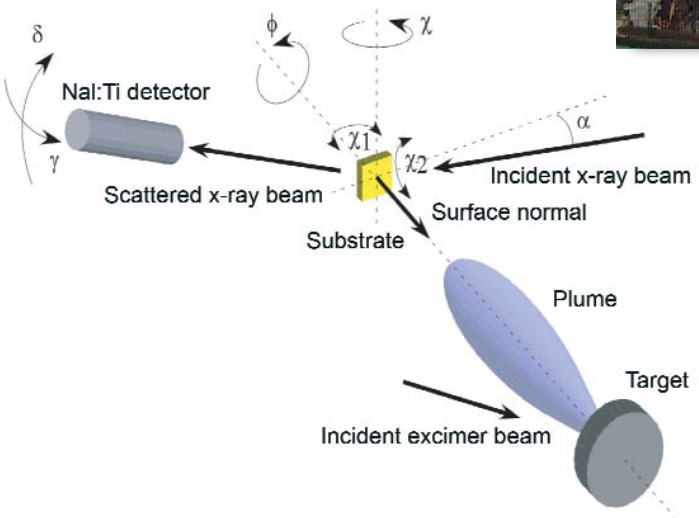

Fig. 2. (left) Pulsed laser deposition schematic.

Sub-millisecond time-resolved surface x-ray diffraction measurements are used to study the deposition, aggregation, and surface evolution phases of pulsed-deposition growth using x-rays at the undulator beamline in sector 33 of the APS. Direct analysis of pulsed-deposition epitaxial growth transients is used to construct an overall framework for the synthesis of nonequilibrium materials and structures by manipulation of epitaxial growth parameters. While the materials focus is currently on perovskites, the PLD technique is

well suited to many classes of materials encompassing wide-ranging structures and properties of both fundamental and technological interest.

Detailed measurements of the time scales of crystallization, aggregation, and surface evolution are critical to developing a fundamental understanding of the growth mechanisms and for practical applications of nonequilibrium film growth methods (Fig. 3.). The ability to measure and control interlayer transport can lead to the discovery of new approaches to synthesis of high-quality oxide films that will be required for future device functionality.

Contact: Jon Tischler (tischlerjz@ornl.gov),
Paul Zschack (zschack@anl.gov)

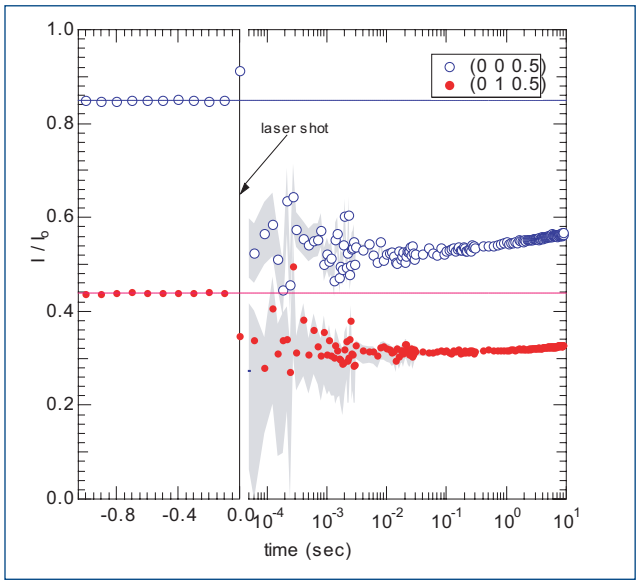

Fig. 3. Time dependence of specular (0 0 0.5) and off-specular (0 1 1.5) crystal truncation rods during homoepixatial $SrTiO_3$ PLD showing simultaneous in-plane and perpendicular registry.

The SER-CAT Remote-user Participation Program

Striving to meet the growing demands for timely access to its beamlines, the Southeast Regional Collaborative Access Team at APS sector 22 has developed an innovative program for secure remote user participation in data collection on its bending magnet beamline.

The SER-CAT remote-user participation system consists of (1) an automated crystal mounter originally developed at the Advanced Light Source and modified by SER-CAT; (2) a custom user interface, SERGUI, developed by SER-CAT; and (3) an Access Grid technology (www.accessgrid.org)-based communication link between the remote observer/user and the beamline.

The automounter (Fig. 1) allows for uninterrupted screening or data collection of up to 96 samples at a time. Mounting of the crystal takes less than five seconds, during which the crystal temperature is maintained well below 120K. The crystal (loop) can be centered either manually or automatically within SERGUI, using a remote-controlled xyz goniometer head.

The SERGUI user interface (Fig. 2) provides tab notebook-style access to all beamline control and data collection functions, as well as access to data reduction and analysis software.

The remote user workstation (Fig. 3) consists of three active screens: environment, experiment, and processing. The environment screen is used for Access Grid control functions (audio, video, and text messaging) and allows the remote user

Continued on next page

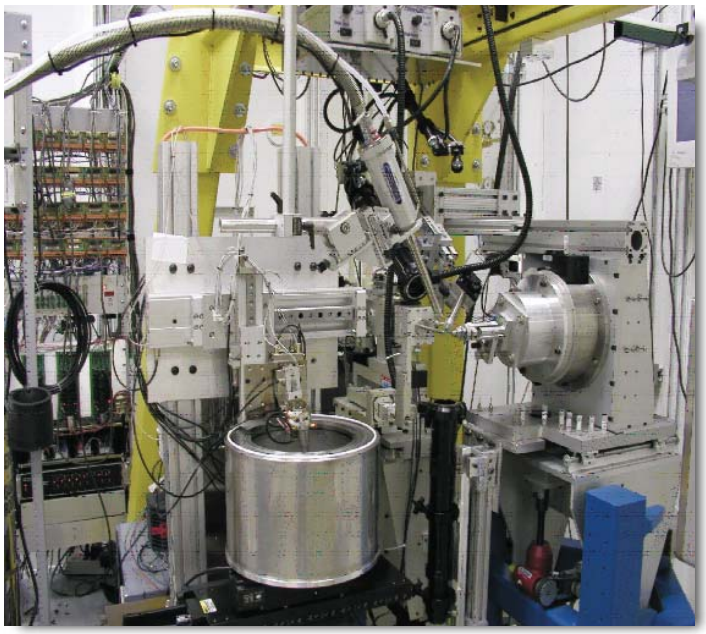

Fig. 1. The SER-CAT automounter installed on 22-BM.

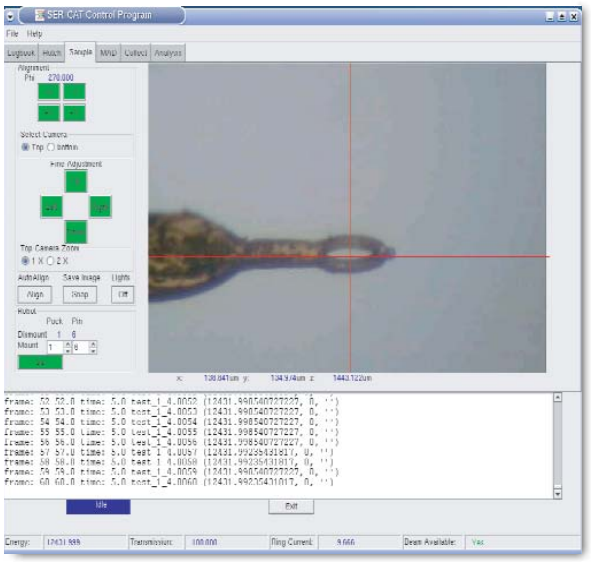

Fig. 2. The SERGUI2 user interface.

Fig. 3. The Access Grid remote user workstation.

to communicate with associates at SER-CAT or beamline staff. The experiment screen is used to set up and carry out data collection via the SERGUI interface. The processing screen is used to run HKL2000 and other data reduction and analysis software remotely at the beamline using VNC connections. Because all data remains on SER-CAT computers, the communications overhead is dramatically reduced. After processing, the resulting structure factors or experimental models can be quickly moved to the remote site for further analysis.

A key component of the system is the Access Grid communications backbone developed by the Argonne's Mathematics and Computer Science Division. This backbone allows for secure communication (audio, video, and VNC-based software applications) between the beamline and the remote user workstation. Each remote user must be registered in the Access Grid database and verified via a certificate in order to access the SER-CAT beamlines. Thus, only those users scheduled for data collection will have access to the beamline.

The remote access system was alpha tested by researchers at the University of Georgia for nine months, with a planned release to the SER-CAT membership in mid-2006. The automounter, coupled with the ability to initiate or supervise data collection remotely via SERGUI and Access Grid, will enable SER-CAT to begin exploring the possibility of restructuring its current 24-h minimum beam time allocation into smaller but more frequent 4-, 6-, or 8-h shifts. This would give SER-CAT members better access to the facility and allow them to plan their experiments and beamline use more efficiently.
Contact: John Rose (rose@BCL4.bmb.uga.edu)

Around the APS

Distinguished Performances in X-ray Imaging

Jin Wang (left in photo) and Wah-Keat Lee (both XSD) were among five Argonne scientists who received the 2005 University of Chicago Board of Governors for Argonne Distinguished Performance Award, which recognizes outstanding scientific or technical achievements or a distinguished record of achievements.

Wang and Lee were honored for their success in using x-rays in a wide range of imaging. Jin Wang is a world-renowned expert in the application of x-ray scattering to a variety of materials science problems. He is best known for his research into the dynamics of fuel sprays, where he applied an innovative research approach and achieved unique results. Wah-Keat Lee, after many years of developing successful high-heat-load x-ray optics, switched fields and became an expert in phase contrast x-ray imaging. The results of his *in vivo* imaging of breathing insects have been acclaimed worldwide. The two have recently developed an ultra-fast x-ray phase-contrast imaging technique with submicrosecond exposure times using the APS.
Contact: wangj@aps.anl.gov, wklee@aps.anl.gov

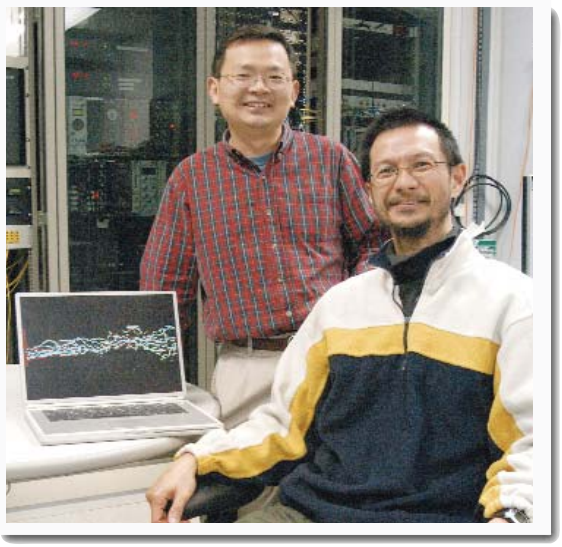

A DEDICATED GISAXS BEAMLINE AT THE APS

A dedicated grazing-incidence small-angle x-ray scattering (GISAXS) beamline has been designed and constructed as a part of the XOR 8-ID-E beamline at the APS. This dedicated beamline allows structural and dynamic characterization not only of a wide array of nanoparticles, but also of organic/organic nanocomposites that possess only weak scattering contrast. This new capability presents a unique research opportunity in the field of soft-condensed matter research at the APS.

Complex nanocomposites are believed to be associated with novel electronic, magnetic, and photonic properties of organic and inorganic components. In these nanocomposite systems, highly ordered structures can often form in a self-assembled fashion, but the formation of the structures can be extremely dynamic, far from the commonly accepted near-equilibrium conditions even at the end of the ordering processes. Therefore, a controlled self-assembling of the nanostructure has to be guided by a thorough understanding of ordering kinetics and nanoparticle dynamics in the complex matrices.

For probing the systems involving dynamical structure of surfaces and buried interfaces, many x-ray surface and interfacial characterization techniques provide a unique scientific opportunity to study the principle of formation of ordered nanostructures. As an increasingly important structural-characterization technique, GISAXS finds vast applications for *in situ* and real-time studies of nanostructures and nano-composites at surfaces and interfaces because of its probing *q*-range (10^{-3} - 1 nm^{-1}) and temporal resolution (10^{-3} - 1 s).

At synchrotron sources worldwide, dedicated in-vacuum and *in situ* GISAXS instruments have been set up, facilitating highly sensitive, time-resolved measurement of nanostructure formation. At the APS, research-ers have pioneered the use of GISAXS techniques under thin-film waveguide-based resonance conditions to study nanoparticle/polymer nanocomposites (Fig. 1) and the kinematics of ordered nanoparticle formation at air/liquid interfaces. However, with an in-air setup, only a very limited number of experiments involving intense scattering particles—such as gold nanoparticles—can be effectively performed because the signal-to-noise ratio is limited by background scattering from air, beam-defining and collimating slits, and flight-pipe windows.

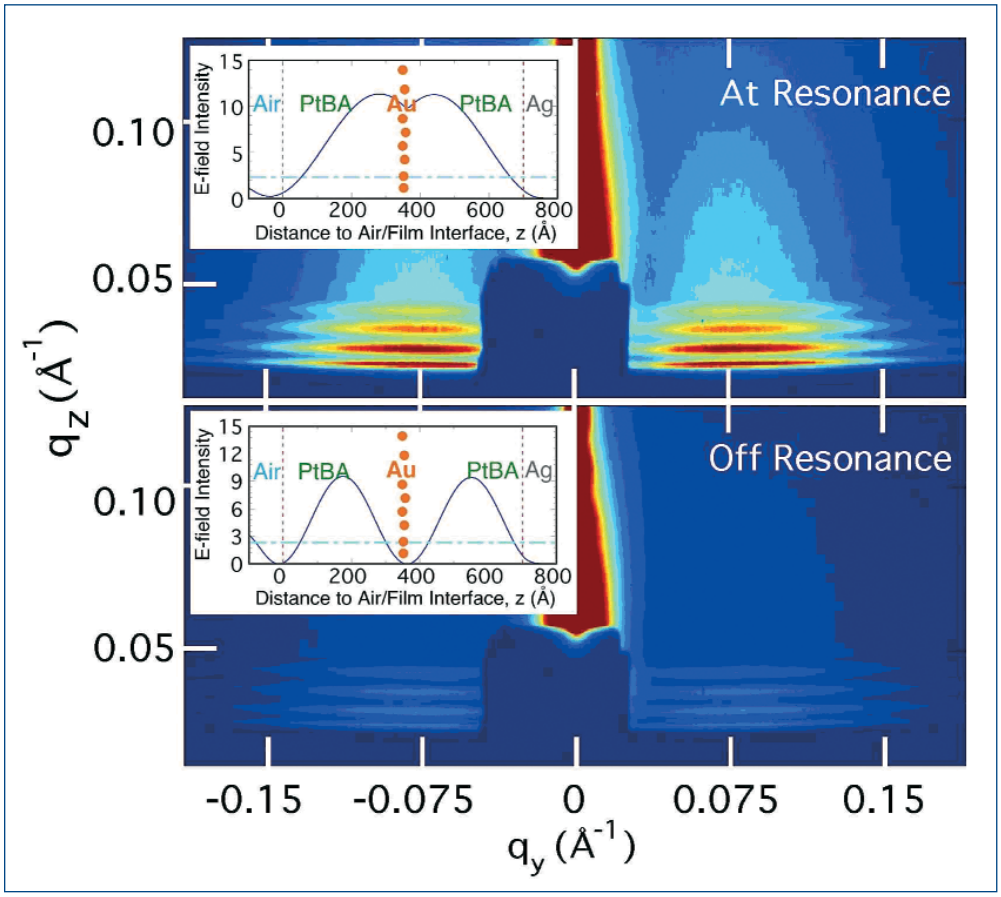

Fig. 1. Normalized 2-D GISAXS patterns of a nanoparticle monolayer embedded in a polymer ultrathin film measured at the first resonance condition (TE0 mode, top panel) and at off-resonance condition (bottom panel), respectively. The insets depict the corresponding calculated E-field intensity distribution in the film.

Continued on next page

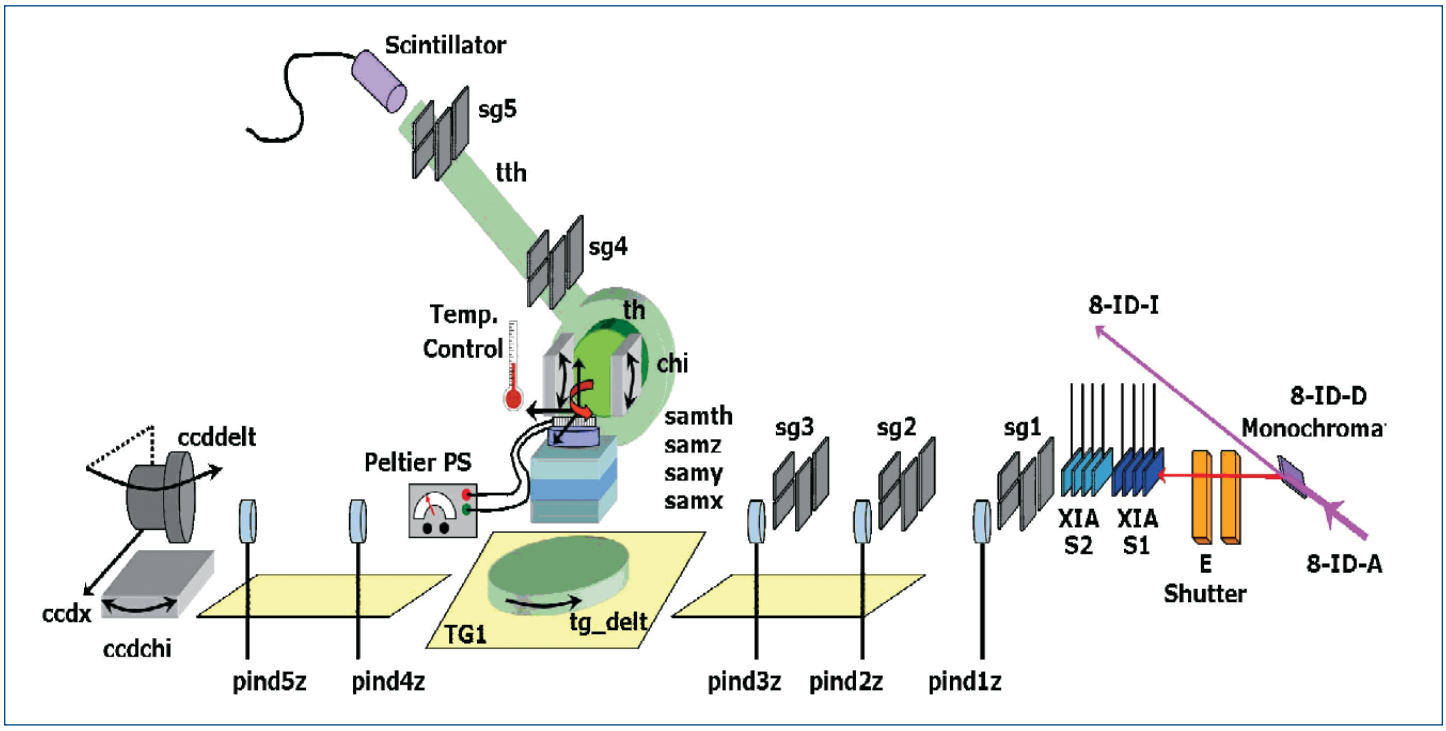

Fig. 2. Layout of the dedicated GISAXS beamline developed as a part of the APS 8-ID-E station.

To meet the strong demand from the nanoscience community, a dedicated GISAXS beamline has been designed and constructed as a part of the 8-ID-E beamline at the APS (Fig. 2). Taking advantage of the high-brilliance x-ray beam from an APS undulator, this beamline is designed with both simplicity and flexibility in mind to achieve high resolution in both reciprocal and real spaces, as well as high temporal resolution in measurement. The simplicity is associated with a fixed photon energy of 7.4 keV with three sets of stable, upstream, in-vacuum slits to ensure a high-throughput, user-friendly operation. The flexibility comes from many aspects, such as a four-circle diffractometer-based sample holder for freedom and precision of sample manipulations, together with the ability to provide various types of sample environments in which the samples can be situated in an integrated vacuum chamber on a high-precision heating and cooling stage. The sample chamber can also be isolated from the beamline to allow solvent flows and to accommodate other mechanical systems, such as *in situ* dip-coating devices.

This new dedicated GISAXS beamline has allowed structural and dynamic characterization not only of vast varieties of nanoparticles, but also of organic/organic nanocomposites that possess only weak scattering contrast. This new capability presents a unique research opportunity in the soft-condensed matter research field. A list of new and exciting research programs has been built around the x-ray measurements:

- Kinetics of block copolymer thin films under thermal and/or solvent annealing,
- Methods for obtaining mesoscaled ordered nanostructures using the phase properties of the polymer blocks,
- Sol-gel processes to form highly-ordered nanostructures, which are affected by solvent, temperatures and other sample environments,
- Formation of organic/inorganic nanocomposites; for example, using organic materials as the templates for inorganic nanocrystals to form superlattices,
- Preparation and characterization of quantum dots,
- Magnetic nanomaterials and their assembly at surfaces and interfaces,
- Dynamics of surfaces, interfaces, and nanoparticles in ultrathin films,
- Dynamics of two-dimensional (2-D) nanocrystals and their domain walls: rotational, translational motions, and
- Characteristics of true 2-D systems: phases, phase transitions.

Xuefa Li, Suresh Narayanan, Michael Sprung, Alec Sandy, Dong Ryeol Lee, Jin Wang. Contact: wangj@ aps.anl.gov

This work was supported by the U.S. Department of Energy, Office of Science, Office of Basic Energy Sciences, under Contract No. W-31-109-ENG-38.

A Remote-access, Automated X-ray Tomography System at XOR 2-BM

X-ray microtomography is an established tool for three-dimensional (3-D) imaging of thick structures at the 1-10-μm scale. The fast microtomography system developed at XOR beamline 2-BM offers near video-rate acquisition of tomographic data, pipelined processing, and 3-D visualization combined with fully automated and remotely controlled capability. At its maximum throughput, the system can image hundreds of specimens a day. Every sample is fully analyzed within 2-3 min, giving the user immediate feedback on the quality of the results. The system has use in both biological applications and materials science, such as the recent study of corrosion propagation in industrially important metals.

The entire instrument, including the tomography setup, automatic sample loader, beamline, and a dedicated 32-node computer cluster for data analysis (Fig.1), is also remotely accessible via Access Grid (AG) technology, giving a user full remote control of every aspect of the experiment.

During the last year the 2-BM microtomography system has been used extensively to resolve the density distribution of biological and material samples at 1-μm spatial resolution. The final results are usually presented as a 3-D volume or as slices. The quasi-real-time feature of the system has been instrumental in both biological applications—where a statistical approach is needed to characterize a broad population of samples—and in materials science, where time-dependent 3-D sample evolution can be studied on practical time scales.

An automatic sample changer into which a user can preload up to 70 samples has also been installed at 2-BM.

Another major improvement in remote beamline operation is the implementation of AG technology at the experimental station to allow external users the capability for full remote control of the instrument, with the goal of creating a virtual environment in which collaborators at geographically distributed sites can perform high resolution x-ray tomography measurements. The same tool is used by the beamline staff to remotely support user operation.

The ability to generate time-dependent 3-D images of sample evolution has been applied to study the corrosion of aluminum alloys (Fig. 2). In wet environments, aluminum alloys are susceptible to corrosion along grain boundaries (intergranular corrosion, or IGC). This is a problem because the narrow regions of attack along grain boundaries can be sites where cracks initiate, leading to structural failure. The use of x-ray microtomography allows real-time monitoring of the development of IGC *in situ* in an aqueous environment. This offers remarkable insight into the

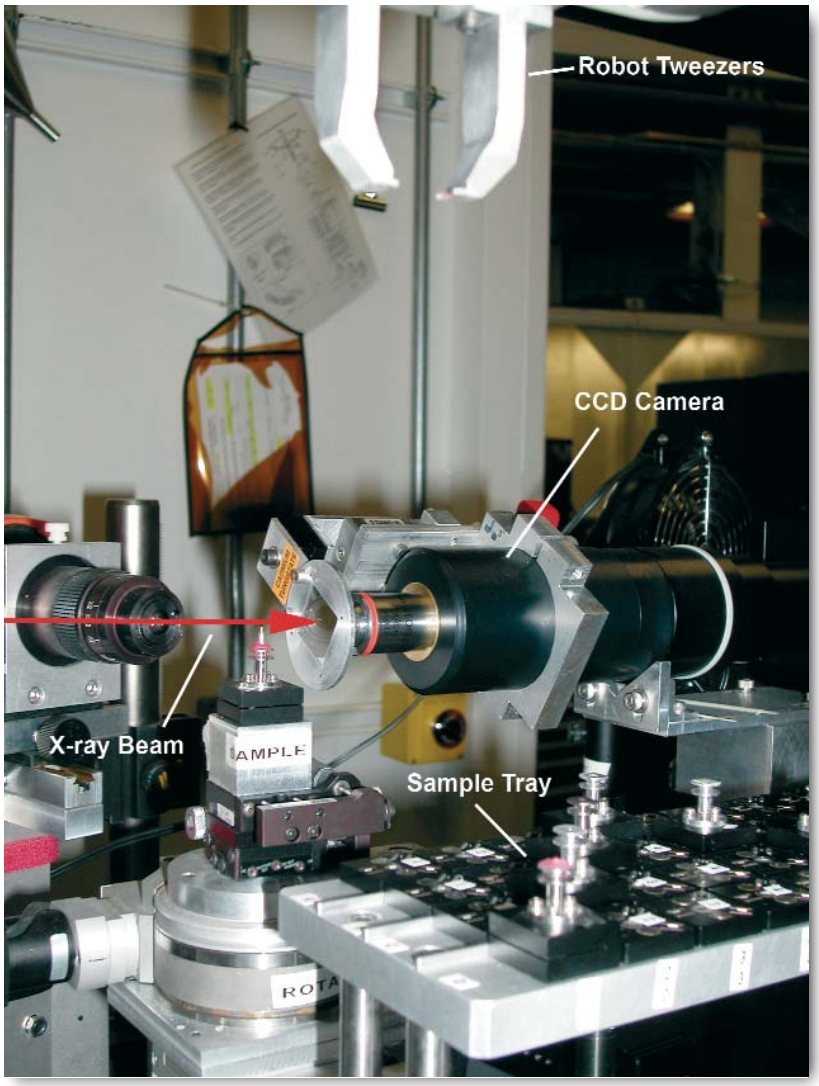

Fig. 1. A row of samples preloaded on the tomography automatic sample loader, in queue to be measured.

Continued on next page

evolution of corrosion, and enables the measurement of the rate of attack along individual grain boundaries as well as the rate of growth of the width of the cavities compared with their length. Furthermore, this sheds light on the interaction of the corrosion front with microstructural features such as intermetallic particles. Even the role of surface corrosion products and hydrogen bubbles produced during corrosion can be examined. Prior to this, information could only be obtained from mechanical cross sectioning of *ex situ* corroded samples, a labor-intensive process that does not give any time-dependent information.

Comparison of the characteristics of attack and propagation rates for the different alloys will provide data that can be correlated with electrochemical corrosion measurements and high-resolution microstructural characterization of the alloys. The rate of corrosion propagation through the metal will, in future, be used in models to predict the life of aluminum components in aircraft, ships, and land vehicles.

Contact; Francesco De Carlo (decarlo@aps.anl.gov)

See: B.J. Connolly, D.A. Horner, S.J. Fox, A.J. Davenport, M. Preuss, N.P. Stevens, T.J. Marrow, M. Stampanoni, and A. Groso, "*In Situ*, 3D Observations of Localized Corrosion in Aluminum Aerospace Alloy 2024," PSI Scientific Report 2004 **VII**, *Synchrotron Radiation / Micro- and Nanotechnology* (2005).

B.J. Connolly, S.J. Fox, D.A. Horner, C. Padovani, A.J. Davenport, M. Preuss, N.P. Stevens, J.-Y. Buffiere, T.J. Marrow, M. Stampanoni, and A. Groso, "3D Investigation of Localised Corrosion in Aluminum Aerospace Alloys via High-resolution, *in situ* Synchrotron X-ray Tomography," 16th International Corrosion Congress, (2005).

G. Svenningsen, M.H. Larsen, J.H. Nordlien, and K. Nisancioglu, "Effect of High Temperature Heat Treatment on Intergranular Corrosion of AlMgSi(Cu) Model Alloy," Corros. Sci. **48**(1), 258 (2005).

A.J. Davenport, R. Ambat, M. Jariyaboon, P.C. Morgan, D.A. Price, A. Wescott, and S.W. Williams, "Corrosion of Friction Stir Welds in High Strength Aluminum Alloys," *Corrosion in the 21st Century*, Manchester (2003).

This work was funded by the governments of the United Kingdom, Switzerland, and Norway, and by the U.S. Department of Energy, Office of Science, Office of Basic Energy Sciences, under Contract No. W-31-109-ENG-38.

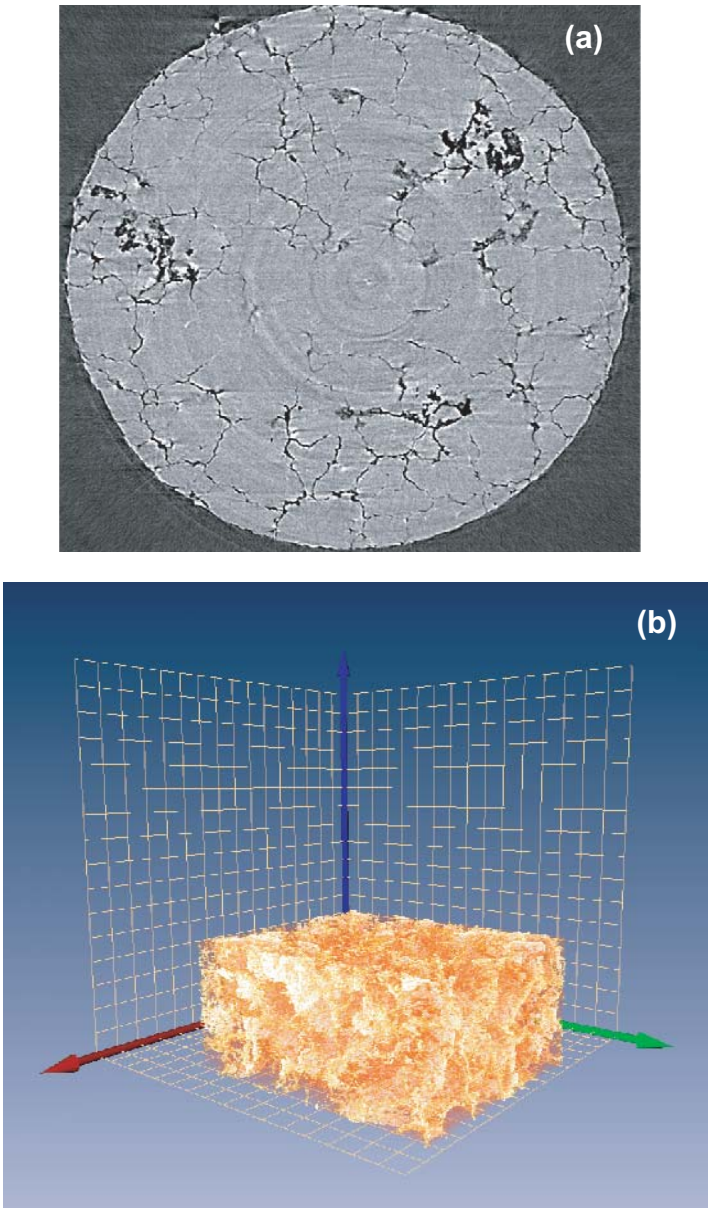

Fig. 2. An AlMgSi alloy after grain boundary corrosion in a chloride-containing environment. (a) cross-section, diameter ~2 mm; (b) 3-D rendering of 1-mm cube extracted from the center of the sample. *(Courtesy of Alison Davenport, University of Birmingham, UK; and Magnus Hurlen Larsen, NTNU, Norway)*

Time-resolved Magnetic Imaging Using PEEM

Researchers at XOR sector 4 have recently developed element-specific time-resolved magnetic imaging using a soft x-ray photoemission microscope. This technique can determine the response of magnetic domain patterns in nanoscale magnets to fast external field excitations. Dynamical information such as this contributes to our understanding of finite size effects in magnetism and is important for new magneto-electronic device applications.

Researchers at the APS have recently developed time-resolved magnetic imaging at 300-nm spatial and 90-ps time resolution using the soft x-ray photoemission electron microscope (PEEM) at XOR beamline 4-ID-C. In recent years, the ability to fabricate magnetic structures with micron and submicron dimensions has advanced substantially. These nano-scale magnets form the building blocks for a host of potential new applications in electronic de-vices, such as magnetic random access memories. However, as the size of magnetic structures is reduced, the boundaries of the objects begin to influence both their static and dynamic behavior very profoundly, and this interplay between boundary and bulk effects is not always understood, even in simple geometries. One of the principal questions is the behavior of magnetic vortices (regions of circulating magnetic polarization). Vortex phenomena offer insight into magnetization dynamics on a fundamental level, and they also govern the magnetic reversal of device structures. In magnetic devices, the shape of the structures can also have a strong effect on the fields needed and the time required for switching, with a corresponding impact on their real-world applicability. Therefore, techniques to characterize magnetic nanostructures that yield high spatial and time resolution are crucial to understanding how these structures respond to fast, time-dependent external magnetic field pulses, and to the more fundamental influence of finite-size effects on magnetism.

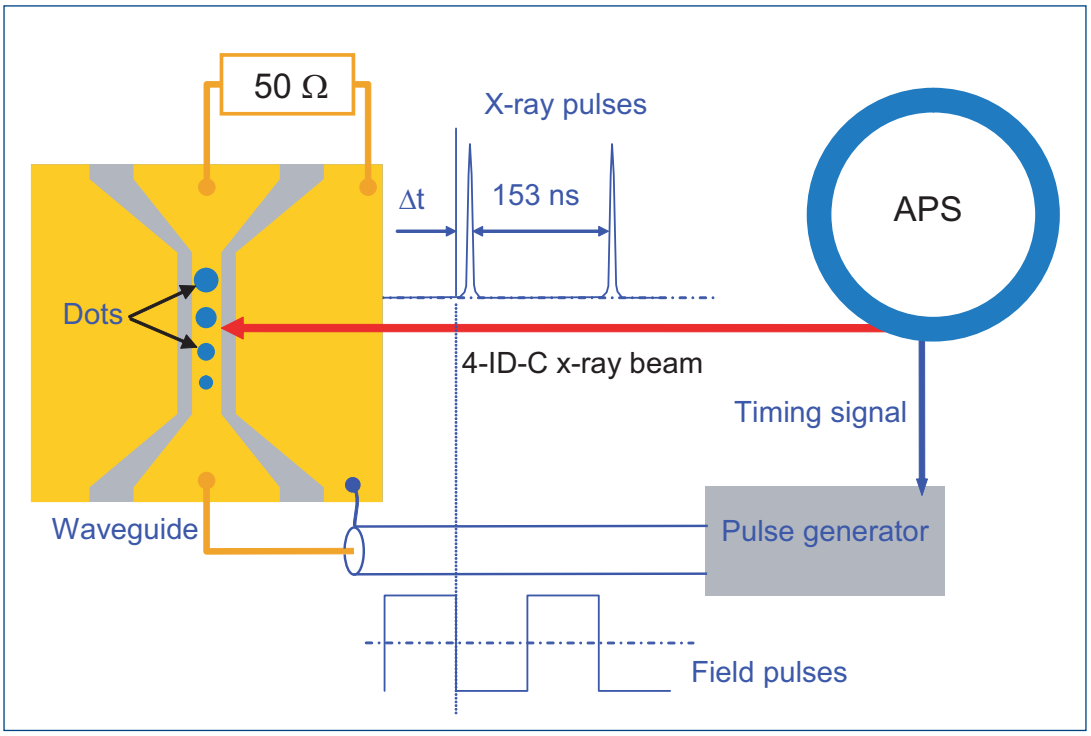

Fig. 1. Diagram of the timing arrangement for stroboscopic PEEM imaging. Magnetic field pulses are introduced at the nanostructures using a coplanar waveguide. The pulse generator is driven with a timing signal from the synchrotron such that an x-ray pulse always arrives at a time Δt after a field pulse. The resulting photoelectrons are imaged with the PEEM optics (not shown), and the delay time is scanned to map the time response of the dots.

The approach discussed here uses the pulsed nature of the radiation from the APS to map out time-dependent domain patterns in lithographic NiFe alloy structures grown on top of a waveguide. A schematic of the timing arrangement is shown in Fig. 1. Working in the 24-bunch mode of the APS storage ring, a pulse train synchronized with the x-ray pulses is sent down the waveguide, creating fast magnetic field-induced transitions in the nanostructures. In this mode, the x-ray pulse width is ~90 ps and the separation is 153 ns, which is ideal for studies

Continued on next page

of magnetization dynamics because it allows high time resolution and sufficient time between pulses to study low-frequency effects. By varying the delay between the x-ray and field pulses, the time response of the structures can be imaged stroboscopically. Magnetic contrast is achieved by taking the difference of two photoelectron images with left- and right-circularly-polarized radiation at the Ni L_3 absorption edge. These difference images have a strong contrast from the resonant x-ray magnetic circular dichroism effect, thus areas with opposite magnetization show up as light or dark.

In collaboration with Argonne's Materials Science Division and Center for Nanoscale Materials, this technique has been used to examine the fundamental dynamics of magnetic vortices in circular structures and the effect of shape on the magnetization reversal in elongated structures. In the vortex dynamics experiment, the relaxation behavior of the vortex state was imaged after abrupt removal of a bias field. In addition, since these elementary circular structures can be treated analytically, the team performed theoretical calculations that further contribute to our understanding of how the finite size influences magnetization dynamics in confined structures. The researchers were able to observe how the vortex oscillation frequencies depend on the disk geometry and to help address outstanding questions regarding the trajectory of the center of the vortex [1]. In Fig. 2, selected snapshots of the vortex motion in a 5.3-μm disk (after the removal of the bias field) are shown, along with the displacements of the vortex core.

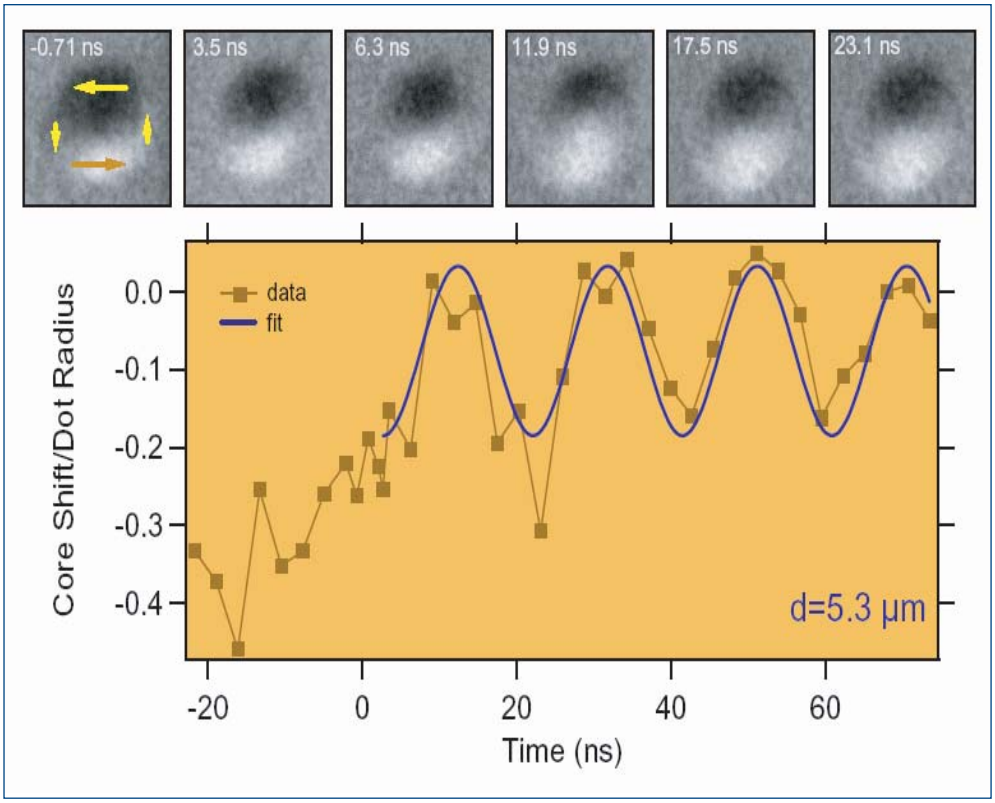

Fig. 2. Selected vortex images (upper panels) from the first oscillation of the 5.3-μm disk (0 to ~23 ns). The dark (light) region indicates magnetization to the left (right), thus the counterclockwise circulating magnetization pattern (indicated by arrows) shows up with dark/light contrast between the top and bottom and grey lobes on the left and right. The location of the vortex core, defined as the transition point between light and dark, is seen to oscillate after removal of the bias field. In the lower panel is plotted the vertical position of the core with time along with a sinusoidal fit, showing a period of 18 ns.

In another experiment, the researchers examined the role of end tapering in making elongated magnets reverse their magnetic directions. Previous work had found that tapering these structures results in a more uniform switching field, making them desirable as magnetic memory elements. Using a positive-to-negative field transition, the researchers found that in rectangles, with no end tapering, the magnetization reversal starts at multiple points along the length of the structure, including the ends, and proceeds in a disordered way. These multiple starting points allow for local variations in the field required to begin the magnetization reversal, which leads to problems with reproducibility of the switching field in large arrays of dots, as would be found in many applications. As the ends become tapered, the structures begin to reverse in the center only before moving out to the ends. This explains the more uniform switching field in tapered dots and shows how the destabilizing influence of the end domains can be remediated by adjusting their shape.

Contact: David Keavney (keavney@aps.anl.gov)

Reference

[1] K. Yu. Guslienko, X.F. Han, D.J. Keavney, R. Divan, and S. D. Bader, "Magnetic Vortex Core Dynamics in Cylindrical Ferromagnetic Dots," Phys. Rev. Lett. **96**, 067205 (2006).

The work was supported by the U.S. Department of Energy, Office of Science, Office of Basic Energy Sciences, under Contract No. W-31-109-ENG-38.

The Sector 7 Ultrafast Laser Lab for Time-resolved Research

A recently completed laser laboratory located at the end of the XOR 7-ID beamline will benefit the users of femtosecond lasers at the APS by improving existing research programs, making more efficient use of available beam time, and increasing safety.

The laser-only room, designated 7-ID-E, (Fig. 1), is complemented by a new ultrafast laser amplifier that was funded jointly by the XSD Time-Resolved X-ray Research Group and the Argonne Chemistry Division's Atomic Physics Group. The amplified femtosecond laser is unique to the APS (2.5 W, < 50 fs pulse duration, 1 or 5 KHz repetition rate). Its stability, beam quality, and high pulse energy have resulted in several successful experiments since its installation in the fall of 2004.

The new laser enclosure (Fig. 2) provides additional space that will make possible future development of a number of new instruments, such as a high-repetition-rate ultrafast laser to match the standard APS fill pattern, an adaptive optical system for generating custom laser waveforms, and dedicated doubled and tripled light laser beam paths, etc. Beamline 7-ID-E is currently delivering laser beam directly to 7-ID-D for general time-resolved x-ray experiments, but eventually the laser will be delivered via beam pipes to x-ray-technique-specific upstream hutches for microprobe, surface science, and white beam studies. Placing the laser in a separate lab has not only been good for the laser (which needs a fair amount of regular maintenance), but has also freed up valuable x-ray hutch real estate. The arrangement also permits simultaneous "tweaking up" or reconfiguration of the laser while x-ray setup is under way, thus saving a considerable amount of time.

The major justification for a new separate laser enclosure is the potential user community for such a facility: the hundreds of research groups worldwide that build or use femtosecond lasers. The transient phenomena studied by time-resolved researchers cannot be preprepared and transported as a sample to a beamline. Instead, this research requires duplication at a beamline of the same type of conditions under study at a scientist's home institution. Proper use of an ultrafast laser as a measurement instrument takes as much time to set up as an x-ray experiment. The value of an ultrafast laser as a tool to study time-resolved phenomena is essentially lost unless a laboratory is available that can be set up and used off-line (i.e., not during x-ray beam time). To illustrate this, the laser system has been on for a large fraction of the January 2006 shutdown, with users commissioning a new mass spectrometer.

Contact: Eric Landahl (elandahl@anl.gov)

This work supported by the U.S. DOE, Office of Science, Office of Basic Energy Sciences, under Contract No. W-31-109-ENG-38.

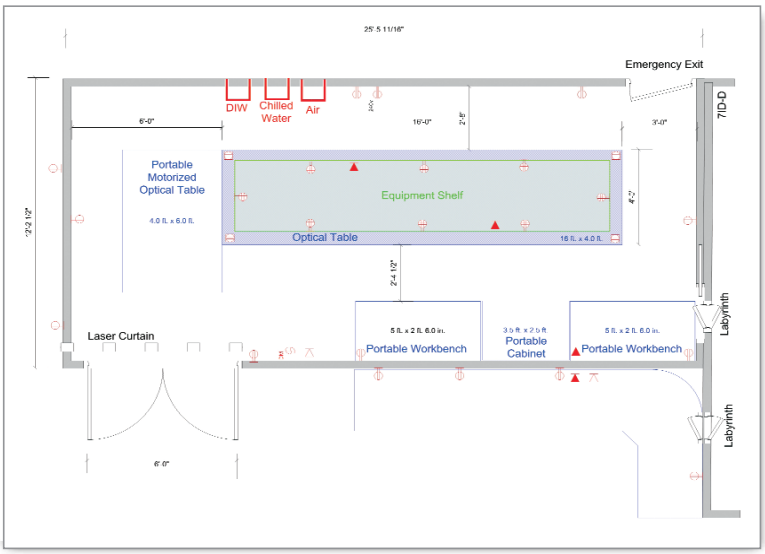

Fig. 1. Drawing of the laser enclosure.

Fig. 2. Emily Peterson (Chemistry Division) inside the new sector 7 laser lab (right). The amplified laser system is at the far end of the main photo and in the inset.

A DUAL-DIAMOND TRANSMISSION PHASE-RETARDER INSTRUMENT AT XOR 4-ID-D

A technique utilizing two transmission phase retarders to produce circularly polarized x-rays has been developed on XOR beamline 4-ID-D. The simultaneous use of two thin-diamond phase retarders reduces experimental artifacts in measured dichroic spectra by eliminating intensity changes upon helicity reversal. Furthermore, using two phase retarders in-series yields an effectively thicker optic, enabling measurements at higher-energy absorption edges.

The use of polarized x-rays offers unique capabilities in the study of magnetic materials. In particular, the element specificity of resonant x-ray scattering and absorption provides a key tool to decipher the different magnetic contributions in multiconstituent materials. Circularly polarized x-rays have proven particularly useful, because they couple directly to the ferromagnetism of a sample. On beamline 4-ID-D, transmission phase-retarding optics (PRs), consisting of thin, single-crystal diamond plates, have been used effectively to obtain circularly polarized x-rays for a wide variety of experiments. If the diamond PR is oriented near (but not exactly on) a Bragg reflection, the beam transmitted through the diamond becomes circularly polarized (Fig.1). Furthermore, the helicity of the transmitted x-ray beam can be easily reversed by rotating the PR to either side of the Bragg reflection. Most circularly polarized x-ray experiments measure the differential absorption or scattering signal upon this helicity reversal. As can be seen in Fig. 1, however, this change in helicity is accompanied by a small

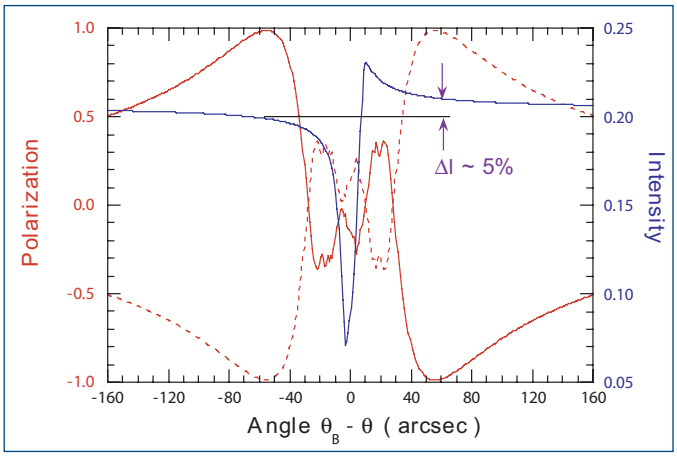

Fig. 1. Circular polarization (red) and intensity (blue) of the beam transmitted through a 400-μm-thick diamond as a function of angular offset from the Bragg condition (8 keV). Solid (dashed) line indicates the beam polarization with the scattering plane at +45°(-45°) from vertical.

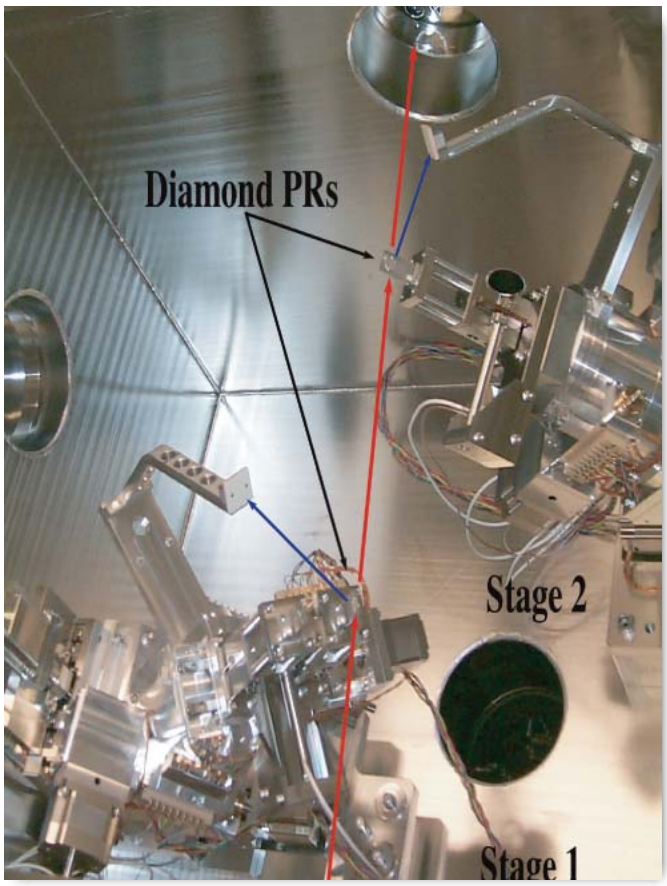

Fig. 2. Picture of the two in-series phase-retarders and orienting stages showing scattered beam (blue) and transmitted beam (red) used for experiment further downstream.

change (~5%) in the transmitted beam intensity. This asymmetric beam intensity can typically be compensated for, by normalizing the detected signal with an incident beam intensity monitor, such as an ion chamber. This normalization, however, can introduce systematic errors into the measurement, especially when detecting minute signals. A method of using two PRs in series to compensate for this intensity asymmetry has been developed on XOR beamline 4-ID-D, thereby reducing systematic errors and permitting the detection of smaller dichroic signals.

Figure 2 shows the phase-retarder setup on beamline 4-ID-D. It consists of two separate in-vacuum goniometers for aligning phase-retarding crystals in the beam path. The scattering planes of each of the rotation stages are oriented at ± 45° with respect to the vertical (i.e., one scatters up and inboard and the other out and outboard). In this geometry, the sense of the circular polarization produced by each PR as a function of the deviation from the Bragg condition is inverted (Fig. 1), while the transmitted intensity asymmetry remains constant. Thus, the intensity asymmetry can be eliminated by rotating each PR an equal amount in opposite directions and adjusting the angular offset such that each PR provides half the necessary phase lag (1/8 wave plate condition).

The phase-retarder setup on 4-ID-D is also equipped with piezoelectric transducer rotational stages to rapidly oscillate the PR crystals between opposite beam helicities. This enables the use of lock-in detection methods to measure extremely small dichroic signals. Figure 3 shows a scope trace of an ion-chamber signal, as two phase retarders are oscillated in opposing directions at 11.7 Hz. The two minima in the signal demonstrate that the rotation of the two PR crystals is synchronized to less than 2 ms. The red line indicates the total time for reversing the helicity (~8 ms) and the constant beam intensity on either side of the Bragg reflection.

A further advantage of using two phase retarders is that it enables dichroism measurements at higher-energy edges. Higher energies require thicker diamond crystals, which can be both difficult to obtain and prohibitively expensive. Using two PRs in series effectively mimics a single, thicker PR optic with the added advantage of eliminating the intensity asymmetry. This technique extends the circular polarization capabilities of 4-ID-D up to energies as high as 16 keV, enabling the study of the spin-polarization of valence electrons in 4p and 5d systems. Figure 4 shows an example of such a XMCD measurement taken at the Ge K edge (11.114 keV) in a $GdGe_2Si_2$ sample. *Contact: Jonathan Lang (lang@aps.anl.gov)*

This work was supported by the U.S. Department of Energy, Office of Science, Office of Basic Energy Sciences, under Contract No. W-31-109-ENG-38.

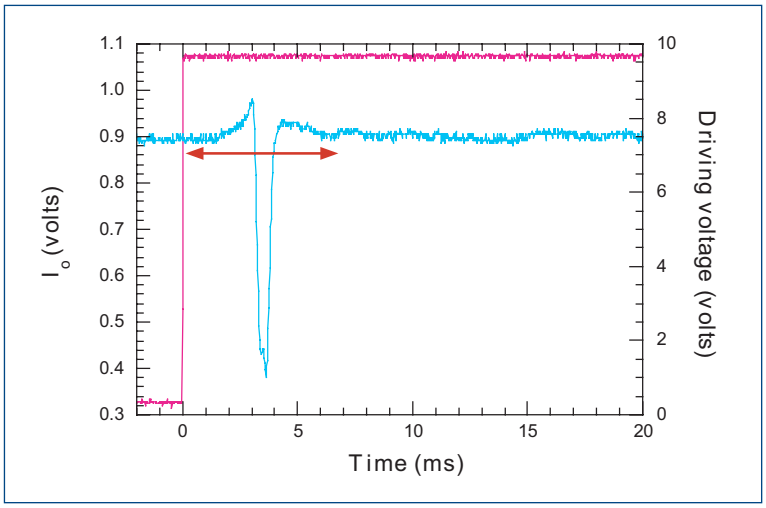

Fig. 3. Scope trace for the incident beam (aqua) as both phase retarders are oscillated in opposite directions.

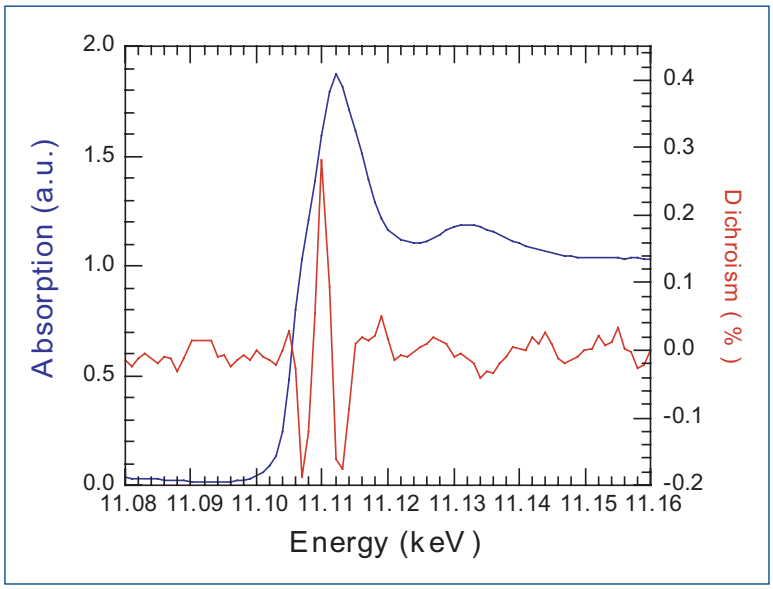

Fig. 4. Ge K edge absorption (blue) dichroism (red) taken using two PRs in lock-in mode.

A YLF LASER-HEATING SYSTEM FOR X-RAY DIFFRACTION STUDIES UNDER EXTREME CONDITIONS

A double-sided yttrium lithium fluoride (YLF) laser heating system has been developed and installed at the HP-CAT undulator beamline 16-ID-B for *in situ* x-ray diffraction measurements at simultaneous high-pressure and high-temperature conditions. Integration of the laser-heated diamond anvil cell (DAC) technique with a microfocused, third-generation synchrotron x-ray source provides a unique opportunity for users to probe the novel behavior of materials subjected to high pressures (up to several megabar) and high temperatures (up to thousands of degrees).

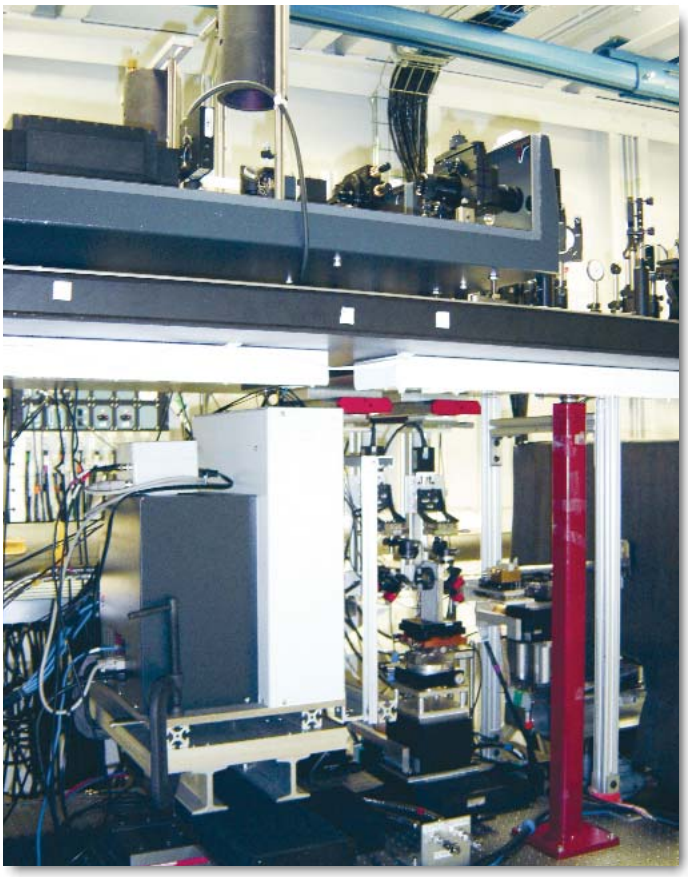

Fig. 1. The integrated laser heating and microfocused x-ray diffraction setup at the undulator beamline of HP-CAT.

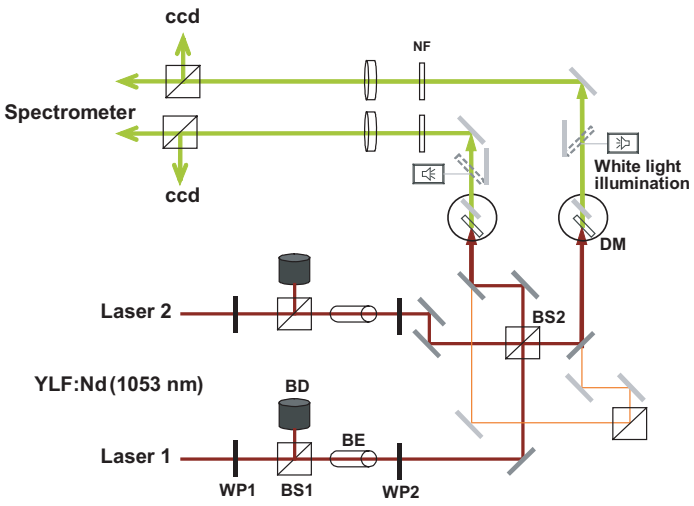

Fig. 2 (above). Schematic of the laser heating optics on the top experimental table. "WP" denotes wave plate; "BS," beam splitter; "BE," beam expander; "BD," beam dump; "DM," dichroic mirror; "ccd," CCD camera. The red lines represent the YLF-laser path; orange lines, the He-Ne alignment laser; and green lines, the thermal radiation from the heating spot. The heating optics below the top experimental table are shown in the photo at right.

Figure 1 shows the laser heating system as part of an integrated high-pressure/high-temperature x-ray diffraction setup. The major portion of the heating optical components is located on the top experimental table, shown schematically in Fig. 2. This double-sided laser heating system has two identical Nd:YLF lasers (Photonics GS40, wavelength = 1053 nm) operating in horizontally polarized donut mode (TEM_{01} mode) and

providing a total maximum output of 170 W with a power stability greater than 99%. The heating laser beam is split by a cube beam splitter into two beams that pass through the opposing diamond anvils to heat the high-pressure sample simultaneously from both sides (Fig. 3). The heating spot size is typically 30 to 50 μm in diameter.

Temperatures can be measured simultaneously from both sides with an imaging spectrograph. The power ratio of two laser beams to each side of a diamond anvil cell can be controlled by changing the polarization direction of the incident beam with a waveplate. All controls can be handled through the motif editor and display manager computer interface. Laser heating and x-ray diffraction measurement can be conducted simultaneously; at the same time, the sample and the heating alignment, as well as the coupling between the heating spot and temperature measurement, can be monitored from both sides (using charge-coupled device cameras) and adjusted as needed.

In addition to opening the way to state-of-the-art techniques, this system is also optimized for user-friendly operation and is capable of accommodating a variety of user demands, such as different heating configurations and DAC dimensions.

Contact: Yue Meng (ymeng@hpcat.aps.anl.gov)

See: Sebastien Merkel, Atsushi Kubo, Lowell Miyagi, Sergio Speziale, Thomas S. Duffy, Ho-kwang Mao, and Hans-Rudolf Wenk, "Plastic Deformation of $MgGeO_3$ Post-Perovskite at Lower Mantle Pressures," Science **311**, 644 (2006).

W.L. Mao, Y. Meng, G. Shen, V. Prakapenka, A.J. Campbell, D.L. Heinz, J. Shu, R. Caracas, R.E. Cohen, Y. Fei, R.J. Hemley, and H.-k. Mao, "Iron-rich Silicates in the Earth's D" Layer," Proc. Natl. Acad. Sci. USA **102**(28), 9751 (2005).

W.L. Mao, G. Shen, V.V. Prakapenka, Y. Meng, A.J. Campbell, D.L. Heinz, J. Shu, R.J. Hemley, and H.-k. Mao, "Ferromagnesian Postperovskite Silicates in the D" Layer of the Earth," Proc. Natl. Acad. Sci. USA **101**(45), 15867 (2004).

Crowhurst et al., "Synthesis and Characterization of the Nitrides of Platinum and Iridium," (Science, accepted).

This work is supported by the U.S. Department of Energy (DOE)-Basic Energy Sciences, DOE-National Nuclear Security Administration, NSF, Department of Defense-Tank-Automotive and Armaments Command, and the W.M. Keck Foundation.

Around the Experiment Hall

Hemley and Mao of HP-CAT Receive Balzan Prize for Mineral Physics

Russell J. Hemley (second from right) and Ho-kwang (David) Mao (far right) were awarded the 2005 International Balzan Foundation Prize for Mineral Physics. The ceremony, shown here, was held in Berne, Switzerland, on Friday, November 11, 2005, in The Federal Parliament Building Chamber of the Swiss National Council. The presenter was Mr. Pascal Couchepin, Federal Councillor (far left).

Much of the research that garnered this award was carried out at the HP-CAT beamlines, APS sector 16. Mao is HP-CAT director. Hemley and Mao (both from The Carnegie Institution of Washington and affiliated with the Carnegie/ DOE Alliance Center) were honored "For the impressive impact of their joint work leading to fundamental breakthroughs, theoretical and experimental, in the field of minerals submitted to extreme physical conditions. They have operated as a highly effective team, characterized by 20 years of research contributions at the highest level. They have developed techniques which allow them to study the behavior of a wide range of materials, such as hydrogen, the most abundant 'mineral' in the universe. Their results have deep implications for our understanding of nature." The Balzan Prize comes with a stipend of 1,000,000 Swiss francs (approximately 650,000 euros). The prizes are given annually to persons who have earned international distinction in their fields. See http://www.balzan.it/News_eng.aspx?ID=1951for more on the Balzan Prize.

A High-field Magnet Facility for Scattering Studies of Condensed Matter

A wide range of magnetic fields and x-ray techniques is required for the study of materials. A vertical-field cryogenic magnet capability with a maximum field of 13 T has been commissioned on the hard x-ray branch beamline of XOR sector 4. Several scattering techniques are available for studying magnetic-field-induced phenomena in diverse classes of materials. This facility will serve a growing need for high-field magnets at third generation synchrotron facilities.

The range of magnetic fields and types of x-ray techniques required to study materials are diverse. While magnetostriction in magnetic nanoparticles requires the use of powder diffraction in intermediate fields, studies of metamagnetic states or Bose-Einstein condensation of integer-spin particles call for magnetic scattering with polarization analysis in fields of ~10 T and beyond. On the other hand, short-range correlations associated with competing phases in correlated electron systems—such as the cuprates and manganites—require high-energy diffuse scattering studies in a wide range of fields. A 13 T magnet that has been successfully commissioned by the XOR sector 4 beamline staff in collaboration with a group from the Massachusetts Institute of Technology will serve a growing need for high-field magnets at third-generation synchrotron facilities by enabling studies of magnetic-field-induced phenomena on the hard x-ray branch beamline at XOR sector 4.

The high-field cryogenic magnet, manufactured by Oxford Instruments (Fig. 1) for studies of materials in magnetic fields, provides vertical fields with a maximum strength of 13 T. It has four asymmetrically placed kapton windows, each of which has 40° of opening angle in the horizontal plane. In the vertical direction, the opening angle is ± 5°. These windows allow for a significant range of optical access and scattering angles. The magnet can be tilted as allowed by the windows during measurements. The magnet is supported by an APS-designed mount. The mount has a rotation bearing and two translation stages. The mount is fully integrated into a two-circle diffractometer with an arc, making a true four-circle scattering geometry available for experiments. A high-throughput rotary pump is utilized to attain 13 T.

The sample is mounted at the end of a rod (~1.5 m long) by using an *in situ* goniometer and top-loaded into a sample chamber filled with He exchange gas. Several mini-goniometers, made with low-magnetic-impurity materials such as copper and phosphor-bronze, are used. The sample rod has a thermal link to a variable-temperature insert that can regulate the sample temperature in the range of ~1.6K up to room temperature. In addition, the sample rod can be rotated a complete 360° while inside the magnet. In order to adjust the sample height and

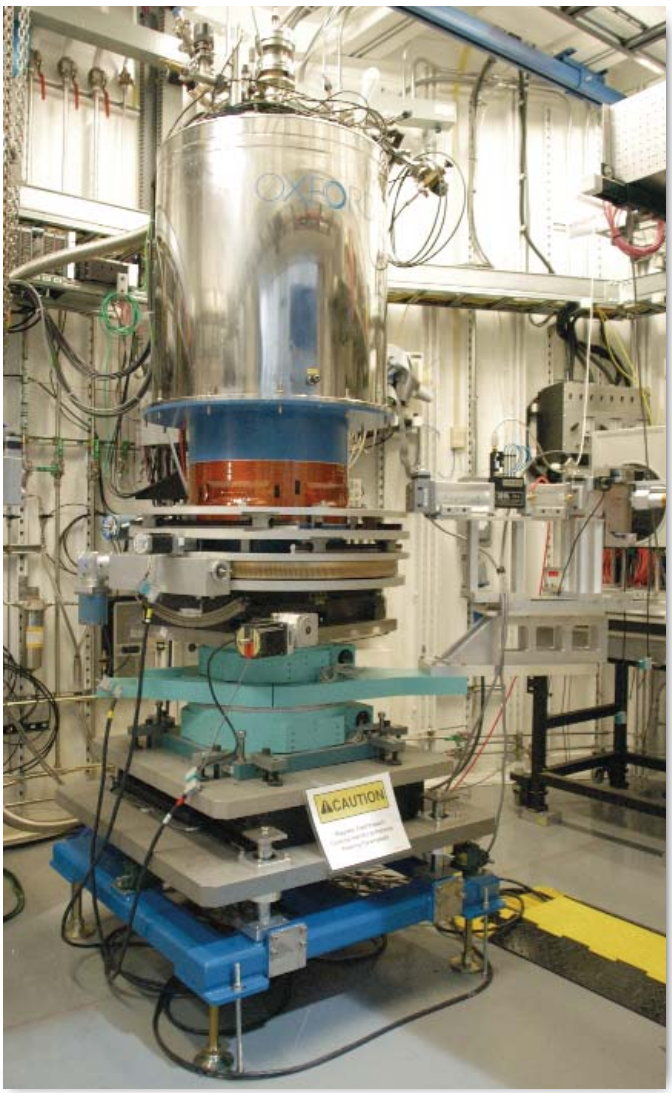

Fig. 1. The 13-T vertical-field cryogenic magnet shown mounted on a diffractometer. A polarization analyzer is mounted after two sets of slits on the 2θ arm. A two-dimensional image plate is placed downstream to quickly collect diffraction patterns.

compensate for thermal contraction/expansion, the sample rod is mounted on a translation stage. In the case of single-crystal samples, a table-top goniometer is placed upstream of the magnet to facilitate prealignment of the sample, as shown in Fig. 2.

In summary, the 13-T vertical-field *cryogenic* magnet is complementary to existing intermediate-field (4-T) *cryogen-free* magnets, which have been in operation for a few years. As a set, these magnets offer the user community a unique capability at the APS for in-field studies of a wide range of problems in condensed matter physics and materials science.

Contact: Zahir Islam (zahir@aps.anl.gov)

This work was supported by the Massachusetts Institute of Technology, and the U.S. Department of Energy, Office of Science, Office of Basic Energy Sciences, under Contract No. W-31-109-ENG-38.

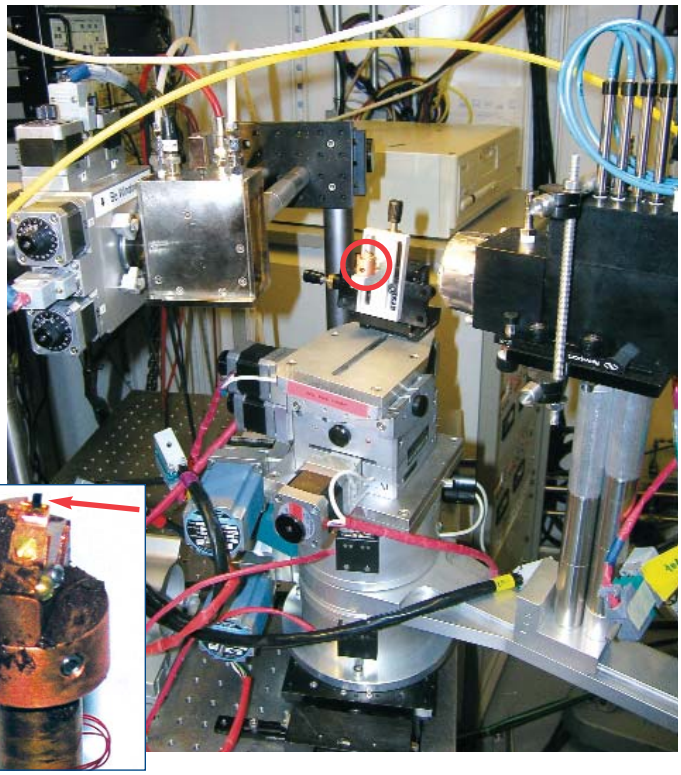

Fig. 2. A table-top diffractometer was assembled to precisely prealign single-crystal samples. Inset and circled on large photo: A minigoniometer machined from OFHC copper holding a tiny single crystal (red arrow). It consists of two tilts and a rotation in order to orient the crystal using the table-top diffractometer as required with a precision of ~0.5°.

A Sample Holder for SAXS Static and Flow Cell Measurements

A sample holder has been devised that can be used for both static and flow cell measurements with small-angle x-ray scattering (SAXS) using the same cell mount and different sample cells. This new device expedites the experimental set-up process and enables the study of extremely small samples.

Small-angle x-ray scattering is an important technique for the study of the size, shape, and interactions of biological macromolecules and other polymer or detergent systems [1,2]. Small-angle x-ray scattering and anomalous small-angle x-ray scattering (ASAXS) enable investigations of macromolecules under (near) physiological conditions in solution without the need to crystallize the sample. These techniques can also be used to study unfolded and/or denatured conformations [1] and to follow conformational changes as a function of time.

A sample holder has been developed that can be used for both static and flow cell measurements using the same cell mount and different sample cells (Fig. 1). This holder allows the user to switch between static and flow cell measurements without the need to realign the detector and camera geometry. The device makes possible high-signal-to-noise experiments with sample volumes as small as 16 μl (static cell) and can be thermocontrolled using a standard recirculating water bath. The device has recently been used by the authors' group and collaborators for SAXS studies carried out at the XOR/BESSRC beamline 12-ID.

In the flow cell set-up, fresh solution is continuously pumped, through the observation volume, allowing for long integration times without incurring radiation damage, which enables measurements on low-molecular-weight samples and samples particularly susceptible to radiation damage. It was employed in several studies on peptides, such as ≈ 0.9 kDa, 11-residue alanine peptide [3], and in a series of alanine- and lysine-rich peptides [4]. Static cell measurements have been used in a study on membrane proteins solubilized by micelle-forming detergents, where it is difficult to obtain large sample quantities because of the difficulty of over-expressing membrane proteins [5], and in several studies of nucleic acid samples. A construct of tethered DNA duplexes was studied by probing their interac-

Continued on next page

Fig. 1. Photograph of the sample cells: Flow cell with tubing (left) and static cell (right). A quarter is shown for comparison.

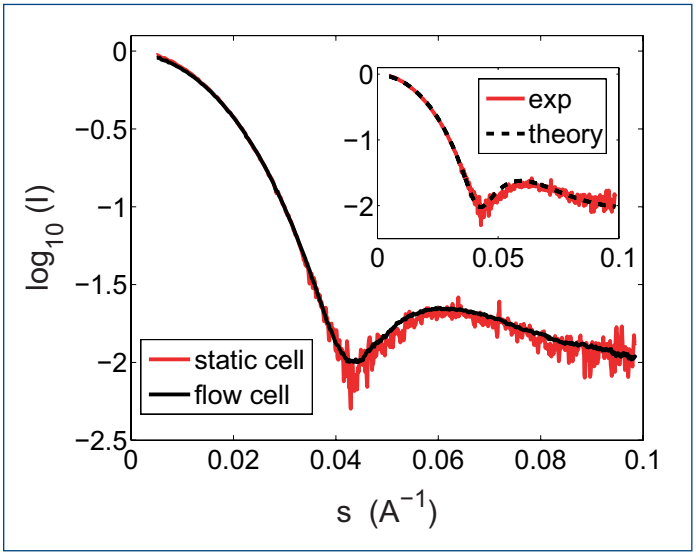

Fig. 2. Scattering profiles of horse heart cytochrome c. Average over 5 profiles with 0.1-s exposure time for static cell measurement (red, solid line) and over 40 profiles with 1-s exposure time for a flow cell measurement (black, solid line). Inset: Experimental (static cell) scattering profile (red, solid line) and theoretical profiles obtained from the crystal structure (PDB accession code 1CRC) using the software crysol[7] (black, dashed line). $s = 2 \sin\theta/\lambda$ where 2θ is the total scattering angle and λ the x-ray wavelength.

tions under different salt conditions [6], an RNA riboswitch was studied as a function of salt and ligand concentration, and gold-labeled DNA was utilized to probe molecular distances (work in preparation).

As a performance test, Fig 2 presents typical flow cell and static cell data collected at beamline 12-ID on horse heart cytochrome *c*, which is a readily available protein that the authors employ routinely as a molecular weight standard. The differences in signal to noise for the two measurement types are apparent. The design drawings for the sample holder and sample cells are available from the authors upon request and are discussed in more detail in a forthcoming publication.

Jan Lipfert[1], Ian S. Millett, Sönke Seifert, and Sebastian Doniach. Contact: lipfert@stanford.edu

REFERENCES

[1] S. Doniach, "Changes in Biomolecular Conformations Seen by Small Angle X-ray Scattering," Chem. Rev. **101**, 1763 (2001).

[2] Dmitri I. Svergun and Michel H.J. Koch, "Small-angle Scattering Studies of Biological Macromolecules in Solution," Rep. Prog. Phys. **66**, 1735 (2003).

[3] Bojan Zagrovic, Jan Lipfert, Eric J. Sorin, Ian S. Millett, Wilfred F. van Gunsteren, Sebastian Doniach, and Vijay S. Pande, "Unusual Compactness of a Polyproline Type II Structure," Proc. Natl. Acad. Sci. USA **102**, 11698 (2005).

[4] Bojan Zagrovic, Guha Jayachandran, Ian S. Millett, Sebastian Doniach, and Vijay S. Pande, "How Large is an α-Helix? Studies of the Radii of Gyration of Helical Peptides by Small-angle X-ray Scattering and Molecular Dynamics," J. Mol. Biol. **353**, 232 (2005).

[5] L. Columbus, J. Lipfert, H. Klock, I.S. Millett, S. Doniach, and S. Lesley, "Expression, Purification and Characterization of *Thermotoga maritima* α-helical Membrane Proteins for Structure Determination," Prot. Sci., in press.

[6] Yu Bai, Rhiju Das, Ian S. Millett, Daniel Herschlag, and Sebastian Doniach, "Probing Counterion Modulated Repulsion and Attraction between Nucleic Acid Duplexes in Solution," Proc. Natl. Acad. Sci. USA **102**, 1035 (2005).

[7] D. I. Svergun, C. Barberato, and M. Koch, "CRYSOL—a Program to Evaluate X-ray Solution Scattering of Biological Macromolecules from Atomic Coordinates," J. Appl. Cryst. **28**, 768 (1995).

This research was supported by the National Science Foundation Grant PHY-0140140 and the National Institutes of Health Grant PO1 GM0066275.

GROWING AND PROBING TINY CRYSTALS

The crystalline form of many molecules and nanoclusters provides researchers with invaluable information about materials. However, such traditional tools as spectroscopy and x-ray diffraction require relatively large crystals. Newer tools, such as atomic force microscopy, can image microscopic crystals, but those crystals are typically grown randomly on a substrate amid other microstructures. A new method for growing microscopic crystals has been verified using the DND-CAT 5-ID-C beamline at the APS. This method will provide researchers with a tool for investigating difficult-to-grow macromolecule crystals, as well as an efficient way to determine the best crystal-growing conditions for these molecules.

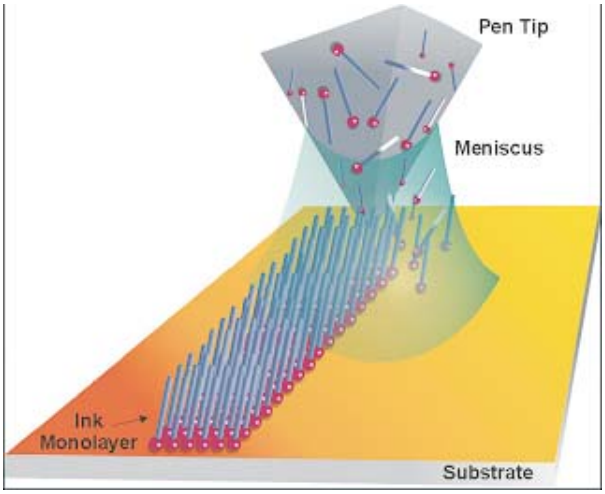

Fig. 1. Depiction of DPN nanolithography [1], in which an extremely narrow strip of molecules in solution is transferred from an AFM tip to a substrate surface.

Researchers from Northwestern University used dip-pen nanolithography (DPN, Fig.1) with an atomic force microscope (AFM) tip to grow single crystals with specific crystal orientations on a substrate, as well as both controlling and imaging their growth to micrometer sizes. Just as a pen transfers ink to paper using capillary forces, the tip of an AFM can transfer molecules with an affinity for the substrate. Coating the AFM tip with a molecular solution and then writing the desired pattern leaves behind a relatively small collection of molecules in submicrometer dimensions. Dip-pen nanolithography was developed by the Northwestern University group reporting this work. It has been used to study monolayer formation and as a massively parallel writing method; both applications provide potential benefits for crystal-growers.

In this study, the research team grew triangular prisms of the polymer poly-DL-lysine hydrobromide (PLH) on mica substrates. Polylysine attaches well to inorganic substrates, so it has been used to coat inorganic substrates employed for biological purposes. By raster-scanning the lysine-coated AFM tip across the substrate, the researchers controlled the growth rate of the crystals.

Crystals of PLH in solution or microcontact-printed on the substrate form all sorts of structures. In contrast, DPN nanolithography with the AFM operated in tapping mode (which is less likely to damage the surface than contact mode) resulted in the growth of equilateral triangular prisms. The researchers found that prisms initiated at the same time grew at very similar rates. All the prisms grew in one of two orientations, which differed by 180° (Fig.1). This suggests that the prisms' growth was oriented to the substrate's lattice.

The researchers used 5-ID-C to perform x-ray diffraction studies on the PLH prisms,to confirm that the structures were crystalline and to investigate their relationship to the substrate. Two patterns were obtained: one for mica and one for PLH-covered mica. The diffraction spots were found to be consistent with single crystals, with the lattice oriented to the oxygen on the surface of the mica substrate. Had the PLH not been in the form of many similarly-oriented single crystals, it would not have been possible to obtain diffraction spots from the material.

See "Tiny Crystals" on page 157

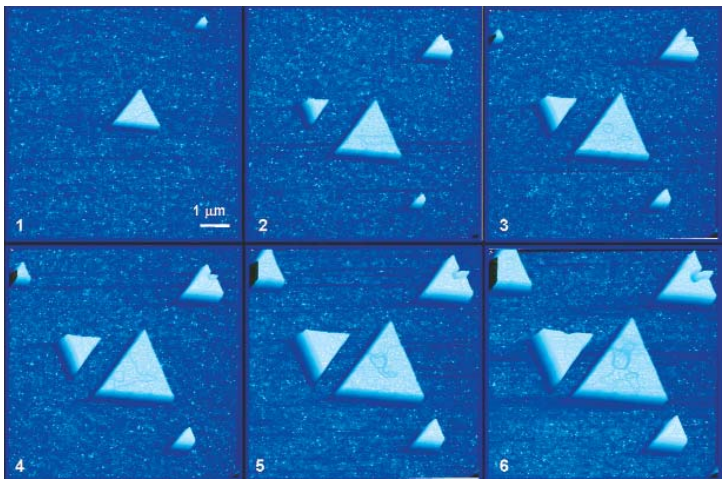

Fig. 2. Time sequence of 8 × 8 μm AFM images taken at 512-s intervals, showing growth of PLH prisms on a freshly cleaved mica surface. Subsequent x-ray diffraction analysis showed that the prisms were single crystals with the outer equilateral triangular shape and two opposing orientations dictated by the underlying pseudo-hexagonal symmetry of the mica surface.

Exploring Materials under Simultaneous High-pressure and High-temperature Conditions

Studies of vibrational and thermodynamic properties of materials at high pressure (~1 Mbar) and high temperature (~3000K) have been very limited. Now, nuclear resonant spectroscopy (NRS)—which benefited tremendously from the development of (1) x-ray monochromatization to meV bandwidth and (2) focusing techniques to micron beam size—has become a truly unique method to study the vibrations, magnetism, and elastic properties of materials containing Mössbauer isotopes under Mbar pressure in diamond anvil cells (DACs). By integrating a laser-heating system at XOR beamline 3-ID at the APS, NRS was recently found to be the only method available for the study of sound velocities and magnetic properties of materials under conditions similar to those found in the deep interior of planets. Some crucial issues in geophysics and geology could be addressed utilizing this new capability.

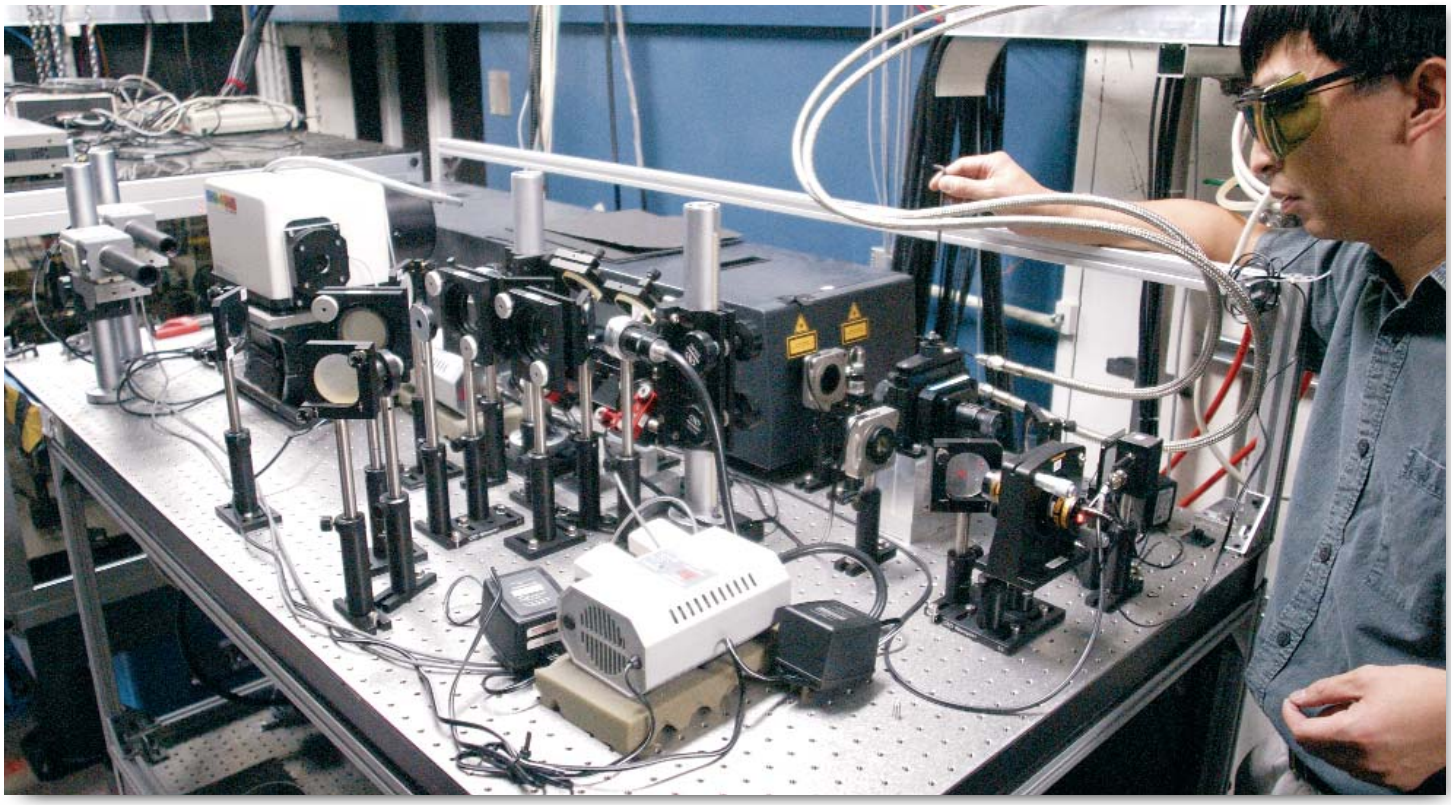

Fig. 1. X-ray Science Division staff member Jiyong Zhao at laser-heated diamond anvil cell system on XOR beamline 3-ID. The top tier (shown) is for the laser and laser optics, while the lower tier holds the diamond anvil cell and x-ray optics. The system can produce temperatures up to 3000K at the center of a diamond anvil cell.

Nuclear resonant scattering techniques, including nuclear resonant inelastic x-ray scattering (NRIXS) and synchrotron Mössbauer spectroscopy (SMS), have been successfully applied at highly-brilliant third-generation synchrotron radiation light sources such as the APS to study materials under high pressure in DACs. The NRIXS technique provides a direct probe of the phonon density-of-states of a resonant isotope; the SMS technique probes the magnetic properties of a sample. Both NRIXS and SMS have been applied at ambient temperatures and Mbar pressures. Higher temperatures can be obtained by using the laser-heated diamond-anvil cell (LHDAC) technique, which is a unique, static method for generating extreme pressures (above 1 Mbar) and temperatures (above 3000K). The LHDAC technique has been widely used in com-

bination with x-ray diffraction to conduct melting point and phase equilibrium studies based on structural analysis. The combination of NRS and LHDAC techniques now make it possible to extract thermodynamic and elastic information from materials under simultaneous high-pressure and high-temperature conditions, which are of fundamental importance to our understanding of the physical and chemical state of planetary interiors.

Combine the two techniques is not an easy task, mainly because of the low counting rates in many NRS experiments. The typical collection time for a reasonably accurate NRIXS spectrum of a sample in the DAC is at least 6 h. Previously operated LHDAC systems were only required to provide stable heating conditions for times on the order of minutes for *in situ* x-ray diffraction experiments. It was thus very challenging to design an LHDAC system for NRS applications that would be highly stable over hours of operation. The use of high-resolution monochromators and avalanche photodiode timing detectors raised the bar even higher for a design that would eventually maintain a thermally and mechanically stable environment near the DAC and in the experimental hutch.

The solution to the stability challenge of an LHDAC system for NRS studies is shown in Fig. 1 [1]. A two-tier structure was devised to make the system compact and stable. The idea has now been used in new designs at HP-CAT (sector 16) and at GSECARS (sector 13). In this system, the laser and most of the laser optics are located on the top tier, while the DAC and the x-ray optics are located on the bottom tier. An Nd:YLF laser (1.053-μm wavelength) operated in continuous donut mode (TEM_{01}) provides a maximum output power of 80 w. In order to minimize the thermal effects on the detector and high-resolution monochromator, the laser, the beam stop, and the DAC are water cooled. The temperature of the DAC stays below 310K even during extended hours of data collection, which ensures mechanical stability. Temperatures of the sample inside the DAC during laser heating are measured by means of spectral radiometry and by the detailed balance principle of the NRIXS spectra. By utilizing this system, researchers have studied sound velocities in hexagonal, close-packed Fe via NRIXS up to a pressure of 73 GPa and up to temperatures of 1700K [2]. The data revealed the separate temperature and density dependence of the sound velocities of hcp Fe for the first time.

The combination of sophisticated experimental techniques such as laser-heating, diamond anvil cells, and nuclear resonant spectroscopy has extended the research capabilities at beamline 3-ID to extreme conditions: Mbar and 3000K. Scientists in the fields of high-pressure material science, mineralogy, and geophysics can count on a new tool in the fascinating quest to understand the thermodynamic, elastic, and magnetic properties of materials under these extreme conditions.

Contact: Jiyong Zhao (jzhao@aps.anl.gov)

References:

[1] J.Y. Zhao, W. Sturhahn, J. Lin, G .Shen, E. Alp, and H.-k. Mao, "Nuclear Resonant Scattering at High Pressure and High Temperature," High Pressure Res. **24**, 447 (2004).

[2] J.F. Lin, W. Sturhahn, J.Y. Zhao, G. Shen, H. Mao, and R. Hemley, "Sound Velocities of Hot Dense Iron: Birch's Law Revisited," Science **308**, 1892 (2005).

This work was supported by the U.S. Department of Energy, Office of Science, Office of Basic Energy Sciences, under Contract No W-31-109-ENG-38.

"Tiny Crystals" from page 155

The researchers also found that prisms increased in two-dimensional area faster than they grew in thickness. This disparity may arise because more molecules are required to increase a layer of depth than to increase the length of the sides.

By changing the temperature during growth, the researchers changed the shape of the crystals in a reproducible way. Thus, the technique can be used to investigate structural effects of changes in environmental conditions. Understanding such effects is important because scientists often struggle with the process of growing crystals of macromolecules. By using DPN as a massively parallel writing tool, this method allows researchers to quickly find good conditions for growing the crystals of a molecule. — *Yvonne Carts-Powell*

Reference

[1] R.D. Piner, J. Zhu, F. Xu, S. Hong, and C.A. Mirkin, "Dip-Pen Nanolithography," Science **283**, 661 (1999).

See: Xiaogang Liu, Yi Zhang, Dipak K. Goswami, John S. Okasinski, Khalid Salaita, Peng Sun, Michael J. Bedzyk, and Chad A. Mirkin, "The Controlled Evolution of a Polymer Single Crystal," Science **307**, 1763 (18 March 2005).

Author Affiliation: Northwestern University.
Correspondence: chadnano@northwestern.edu,
bedzyk@ northwestern.edu

The research was supported by the Nanoscale Science and Engineering Initiative of the NSF under NSF Award No. EEC-0118025, the NIH through Award No. GM62109-02, a Director's Pioneer Award to C.A.M., the Institute for BioNanotechnology in Medicine, Baxter Healthcare Corp, and the Air Force Office of Scientific Research (AFOSR) through a Multidisciplinary University Research Initiative (MURI) Award. Use of the Advanced Photon Source was supported by the U.S. Department of Energy, Office of Science, Office of Basic Energy Sciences, under Contract No. W-31-109-ENG-38.

MIRRORS TO PRODUCE ACHROMATIC, nm-SIZE X-RAY BEAMS

Thanks to the successful development of highly precise elliptical mirrors for achromatic nanofocusing of hard x-ray beam, a focal spot of 95 nm has been achieved using an APS undulator beam. Analyses indicate that vibration control and precision positioning of the mirrors should lead to a spot size approaching 30 nm. For comparison, analyses show that a perfect mirror would ideally provide a focal spot of 26 nm.

Essential to the study of materials is an understanding of their atomic structure, elemental composition, and local mesoscopic structure, including grain boundaries and defects. While a variety of techniques are available for examining bulk properties, local, non-destructive three-dimensional (3-D) methods with submicron resolution are essential to addressing fundamental and long-standing issues of materials science. Ultra-small, intense, hard x-ray beams provide a unique non-destructive means of characterizing materials. These beams can be produced by focusing x-rays generated by powerful synchrotron radiation sources.

Hard x-rays can be focused by zone plates, compound refractive lenses, capillary optics, crystals, or mirrors, depending on the application. Mirrors provide a means for *achromatic* focusing: photons of all energies are focused at the same location. This attribute, on the one hand, and advances in high-precision mirror fabrication on the other, have made using mirrors to focus x-ray beams to submicron and nanometer levels an attractive option.

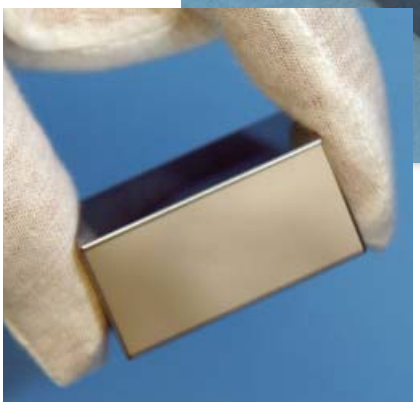

Fig. 1. Four state-of-the-art, elliptically shaped mirrors were produced from one parent substrate (top photo). The backside of the parent is shown here. After figuring the mirror front surface, the area between the channels is cut from the parent, and it is further cut perpendicular to the channel length to produce the four mirrors. Inset: The 40-mm-long palladium-coated mirror tested at the APS is shown. This is one of the four identical mirrors cut from the parent shown.

A typical set-up to produce focused x-ray beams consists of placing a pair of elliptically figured short-focal-length mirrors orthogonal to each other in the Kirkpatrick-Baez arrangement. The mirrors are located at a sufficient distance from the source to provide high-demagnification, point-to-point focusing. For example, at the APS, a 60-mm focal length elliptical mirror placed at 60 m from the source demagnifies the latter by 1,000 times. A 30-μm source size can thus be focused to 30 nm under ideal conditions.

However, producing x-ray beams on the order of 100 nm and smaller requires elliptical mirrors that are precise and

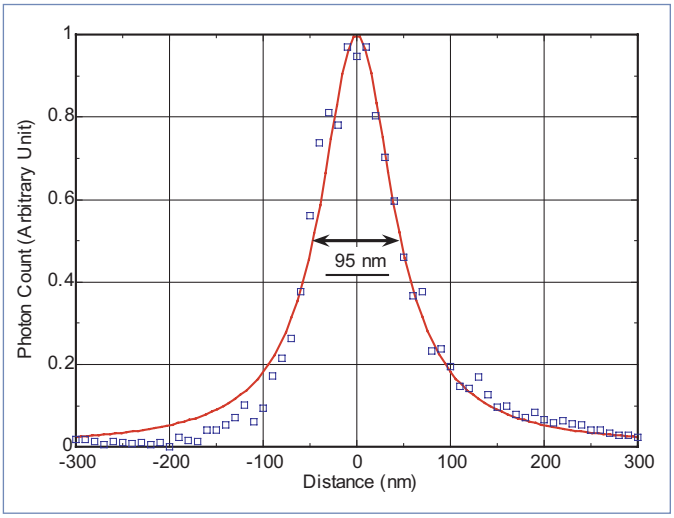

Fig. 2. A Lorentzian curve fit through the experimental data showing the vertical profile of the focused beam at 60 mm from the mirror. The FWHM is 95 nm for the white incident beam. Results were the same for monochromatic (7-20 keV) beams.

smooth. Small surface deviations from a perfect ellipse can result in a much larger focal spot size. For instance, a root-mean-square (rms) slope-error deviation from an ideal elliptical surface of only σ = 0.5 μrad in the above example can result in the expansion of the image by as much as 2 $\sigma \times$ 60 mm = 60 nm rms or 140 nm full width half maximum (FWHM)—approximately five times the geometrical demagnification of 30 nm. This is why producing high-performance mirrors that work near their theoretical limits is vital and requires both very precise fabrication tools and extremely accurate metrology.

State-of-the-art mirror surfaces can be produced in a number of ways. One approach involves polishing the precise elliptical profile into the surface by means of a chemical/plasma process, magneto-rheological finishing, ion etching, or computer-controlled optical surfacing (CCOS).

The proprietary CCOS process used to fabricate APS mirrors has recently been successfully employed in the fabrication of a series of increasingly demanding optical systems for extreme ultraviolet lithography for use in the production of future generations of microelectronics devices. Against this backdrop, and working with Tinsley Laboratory and in collaboration with Oak Ridge National Laboratory and ASML Optics, APS has successfully spearheaded the four-year program for the development of a set of precisely figured elliptical mirrors for x-ray nanofocusing. A set of four identical elliptical mirrors on a single substrate was fabricated using a well-characterized 20-mm-thick, single-crystal, float-zone silicon disk of 150-mm diameter. At the APS, the substrate was oriented, ground, lapped, etched, and topographed to ensure low residual stress. Channels were then configured along crystallographic planes on the backside of the substrate, as shown in Fig. 1. The substrate was etched and topographed again to make sure it was free of any discernible strain. The role of these channels is to reduce the potential distortion of the mirrors caused by a redistribution of any residual internal stress when they are cut from the figured parent substrate. The mirror surface was then manufactured via a series of alternating figuring and finishing steps to approach the final specifications. The parent was then cut into four mirrors, such as the one shown in the Fig. 1 inset. Prior to cutting out the mirrors from the parent, an independent set of metrology measurements was made at ASML Optics showing comparable results. After cutting from the parent, the mirrors were individually evaluated by Tinsley Laboratory, the APS, and, more recently, Osaka University. It is important to note that accurate metrology, with sub-nanometer accuracy and repeatability, is essential for the fabrication and measurements of these mirrors.

Developing multiple mirrors on the same substrate was demonstrated in the course of this program. This not only results in a substantial reduction in cost per mirror but, more importantly, it allows working with a larger circular substrate, which is advantageous for fabrication and in making the critical metrology easier and more precise.

One of these mirrors was coated with a thin layer of platinum and installed and evaluated on an XOR/UNI sector 34 beamline at the APS to vertically focus an incident undulator beam. Figure 2 shows the profile of the focal spot obtained. Its FWHM is 95 nm. Subsequent metrology measurements and simulations carried out at Osaka University indicate that these mirrors should provide near-diffraction-limited performance, reaching 30-nm FWHM focal size compared with 26 nm for an ideal elliptical mirror. The difference between prediction and measurements is thought to be largely due to vibration. A plan to mitigate this problem through a combined effort of reducing noise at its source and using vibration-damping pads has been developed for the next round of experiments at APS.

Ali Khounsary, Gene Ice, Wenjun Liu, Jay Daniel, Lahssen Assoufid, Kazuto Yamauchi, Al Macrander
Contact: amk@aps.anl.gov

Reference

[1] W. Liu, G. Ice, J.Z. Tischler, A. Khounsary, C. Liu, L. Assoufid, and A. Macrander, "Short Focal Length Kirkpatrick-Baez Mirrors for a Hard X-ray Nanoprobe," Rev. Sci. Instrum. **76**, 113701 (2005).

Support for this project was provided by the APS, which is funded by the U.S. Department of Energy, Office of Science, Office of Basic Energy Sciences (DOE-BES) under Contract No. W-31-109-ENG-38. The work was also sponsored by the U.S. DOE Division of Materials Sciences and Engineering through a contract with the Oak Ridge National Laboratory, which is operated by UT-Battelle, LLC, for the U.S. Department of Energy under contract DE-AC05-00OR22725. Experiments were performed on XOR/UNI beamline 34-ID at the APS, which is funded by the DOE-BES.

FIRST LIGHT FROM THE SECOND GM/CA-CAT CANTED UNDULATOR

The General Medicine and Cancer Institutes Collaborative Access Team (GM/CA-CAT) has completed installation of the second of two canted-undulator beamlines for macromolecular crystallography that were described in *APS Science 2003* (ANL-04/07, pg. 115). In February 2005, staff members from GM/CA; ACCEL Instruments, GmbH; and the APS celebrated first monochromatic light from the second insertion device (ID) beamline (Fig.1).

Fig. 1. GM/CA, ACCEL, and APS staff members pose with the simultaneous images of the monochromatic beams form the dual-canted undulators. Left to right are: (front row) Sergey Stepanov and Derek Yoder, (back row) Glenn Decker (ASD), Rich Benn, Leif Schroeder (ACCEL), Bob Fischetti, Ward Smith, Chitra Venkataraman (ACCEL), Shenglan Xu, Steve Corcoran, Sheila Rossi, Satish Devarapalli, and Alex Urakhchin.

Light was demonstrated by simultaneously observing x-ray beams on YAG crystals positioned in-vacuum immediately after each monochromator. During 2005, the commissioning of the first ID beamline was completed and the user program was ramped up. The beamline was declared operational and is accepting general users and users from the special projects of our sponsors, the National Institute of General Medical Sciences and the National Cancer Institute of the National Institutes of Health. The end station for the second line was installed and, after initial crystallographic commissioning, the first data set was recorded in December 2005.

Hahn Bui (left) and Adam Brill (right), both ASD, checking diagnostics near the canted undulators at sector 23.

Independent operation was a critical aspect of developing two ID beamlines based on the canted-undulator geometry. The new front-end design incorporates particle-beam position monitors and corrector magnets before, between, and after the undulators. The APS developed software to steer the two ID lines independently and incorporated the three beam position monitors into the storage ring feedback system. The gap of one ID device or the steering of one line can now be changed without affecting the other beamline. This completes the proof-of-principle that canted undulators can provide truly independent ID beamlines, thereby doubling the capacity of an APS straight section.

The standard APS undulator A (3.3-cm period with 72 poles, or 62 poles for canted-undulator beamlines) has been the workhorse for macromolecular crystallography beamlines at the APS. The small beam size and low divergence have significantly improved the quality of crystallographic data obtained. Many structures have been solved using multiwavelength anomalous diffraction (MAD) about the Se K-edge (12.658 keV), where diffraction data are recorded at energies corresponding to the edge inflection point, the peak, and a third point well above the edge. However, the 3.3-cm device is not optimal for these experiments because the intensity output of the undulator falls off rapidly above 12 keV. Thus, the experimenter must decide whether to stay on the undulator's first harmonic with its decreasing intensity or switch to the undulator's high-power third harmonic, with the potential for inducing thermal drift of the monochromator.

Fig. 2. These plots compare the measured intensity vs energy for the first and third harmonics of the 3.3- and 3.0-cm period undulators. The vertical lines indicate the energy of the K-edges of Se-Met and Br. The intensity was measured in the focused beam at the sample position. The beamline optics include a double-crystal monochromator with Si(111) crystals and a pair of mirrors oriented in a Kirkpatrick-Baez geometry. The rhodium strip of the mirrors intercepts the beam at a grazing angle of 3.0 mrad.

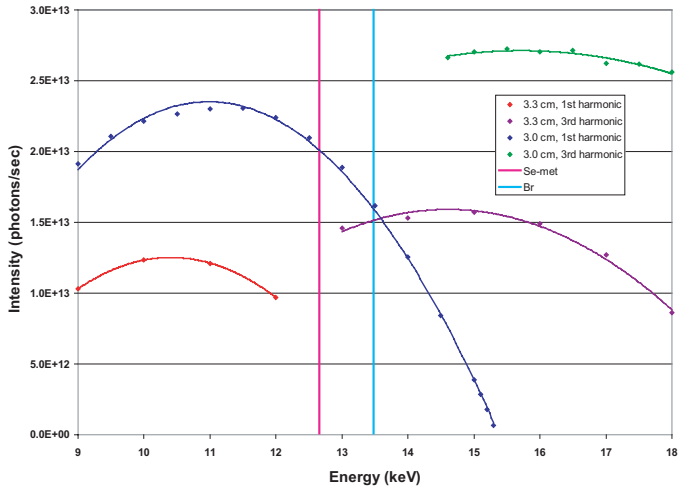

The GM/CA-CAT investigated other undulator periods and concluded that a device with a 3.0-cm period would be more appropriate for MAD experiments about the K-edges of Se and Br (13.446 keV). The XSD Magnetic Devices Group did the design work and, in August 2005, replaced the existing undulator on the first of GM/CA's ID lines with a 3.0-cm, 69-pole device (Fig 2). The device performs well and provides approximately two-fold greater measured flux at the sample when compared to the 62-pole, 3.3-cm device (Fig 2). Of particular interest is the region between 12 and 15 keV. One can clearly see that, with the 3.0-cm device, the fundamental emission curve extends to 15 keV, allowing experimenters to use the first harmonic for Se and Br MAD experiments and to collect data under lower-power conditions in which the monochromator is more stable.

Contact: Robert Fischetti (rfischetti@anl.gov), Janet Smith (janetsmith@umich.edu)

GM/CA-CAT has been funded in whole or in part with Federal funds from the National Cancer Institute (Y1-CO-1020) and the National Institute of General Medical Sciences (Y1-GM-1104).

AROUND THE EXPERIMENT HALL

GM/CA-CAT DEDICATES NEWEST APS BEAMLINES

The General Medicine and Cancer Institutes Collaborative Access Team marked the beginning of a new era in structural biology research with the dedication of the GM/CA-CAT beamline facility at the APS. "The need for structural biology beam time continues to grow," GM/CA-CAT Director Janet Smith told the crowd gathered in the APS experiment hall in August, 'and this facility will help provide researchers from the National Institutes of Health and other organizations the tools to discover how proteins and biomolecules work." The GM/CA-CAT facility is a collaboration between the U.S. Department of Energy, the National Institutes of Health's National Institute of General Medical Sciences (NIGMS), and the National Cancer Institute. Shown cutting the ribbon are (l. to r.): Janet Smith; Jeremy Berg, Director of the NIGMS; Murray Gibson, Associate Laboratory Director for Scientific User Facilities; Marvin Cassman, Past Director of the NIGMS; Bob Fischetti, GM/CA-CAT Project Manager; and Dinah Singer, Director of the National Cancer Institute's Division of Cancer Biology. *Contact: janetsmith@umich.edu, rfischetti@anl.gov*

APS Users

The APS User Program

The APS User Community: Trending Up

Continued growth characterized the APS user community during the past year: growth in the number of individuals carrying out experimentation at the APS, and growth in opportunities for research, communication, and collaboration.

During FY2005, more than 3,200 researchers came to the APS, 917 of whom were first-time users. In total, these users made 9,640 visits and conducted 2,660 experiments in disciplines ranging from materials science and biology, to geoscience, high-pressure research, environmental remediation, and archaeology. In addition, several opportunities for users to mail in samples were introduced, primarily in the areas of macromolecular crystallography and powder diffraction. Research conducted by remote users either mailing in samples or actually manipulating the beamline remotely is expected to grow significantly in the coming years.

A full spectrum of research affiliations was represented in this year's user community, with approximately 70% of the users coming from academic institutions (both U.S. and foreign), and the rest from industry, other national laboratories, private research institutions, and medical centers.

Research opportunities also continued to grow, with five new beamlines (8-BM, 9-BM, 22-ID, 31-ID, and 33-BM) becoming available for research by general users (GUs), who submit proposals for peer review to obtain beam time. During 2005, 81,464 hours were available for peer-reviewed competition, 11% more than were available in 2004.

Opportunities for communication increased as well. During the past few years, informal scientific interest groups (SIGs) have begun to spring up in the APS user community. These groups meet during lunch time in various locations at Argonne, where they listen to speakers, discuss issues of general or specific interest, and eat lunch-time fare ranging from pizza to Thai food. At present, these SIGs meet regularly: “High-Pressure,” “Interface Scattering,” “Liquid and Soft-Matter Surface Scattering,” “Macromolecular Crystallography,” “Small-Angle Scattering,” “Tomography,” and “X-ray Absorption Spectroscopy.” Information about these groups is located on the APS Web site under “Meetings and Seminars” at (http://www.aps.anl.gov/Users/Meeting/2005/Program/index.html).

An increasing number of users have registered to come to more than one of Argonne's national user facilities (APS, the Center for Nanoscale Materials [CNM], the Electron Microscopy Center, and the Intense Pulsed Neutron Source). Of the almost 9,000 users currently registered, more than a quarter expect to use at least two of these facilities for their research. The back-to-back users meetings for the the APS and the CNM sparked some of these potential collaborations. Joint workshops for all four of the facilities are being planned for the 2006 APS Users Meeting.

The 2005 APS/CNM Users Meeting

The 2005 Users Meeting for the Advanced Photon Source and the Center for Nanoscale Materials was in every way a celebration of science: past, present, and future. U.S. Senator Dick Durbin (D-IL), the Senate Minority Whip, opened the APS meeting with his views on the current state of science funding and called for a “sound, sustainable national energy policy that protects our national security, strengthens our economy, and preserves the health of the world and its people for generations to come." The Senator was followed by Pedro A. Montano (Department of Energy, Office of Basic Energy Sciences [DOE-BES]), who outlined the DOE-BES perspective on its user facilities and the ongoing BES initiatives and goals. Next came facility updates from APS Director J. Murray Gibson and CNM Director Eric D. Isaacs.

The morning session, chaired by Mark Rivers (University of Chicago/CARS) included the presentation of the APS Compton Award to Günter Schmahl (University of Göttingen) and Janos Kirz (SUNY-Stony Brook/LBNL-ALS) for pioneering work in the field of x-ray microscopy using Fresnel zone plates. They each presented scientific and historical perspectives on their work, which has had exceptionally wide impact, both in terms of optics hardware and scientific applications. Because March of 2005 also marked first light at the newly constructed hard x-ray nanoprobe beamline station on APS sector 26, the recognition of the work the Schmahl and Kirz on zone plates generated much enthusiasm in the audience. The opening session concluded with David Moncton presenting an overview of the impact of the APS on current and future synchrotron sources.

Continued on next page

This photo: A full house in the APS conference center for the opening session of the 2005 APS/CNM Users Meeting. Above right: U.S. Senator Dick Durbin. Top: Presentation of the Compton Prize; left to right: Mark Rivers Janos Kirz, Günter Schmahl, Murray Gibson.

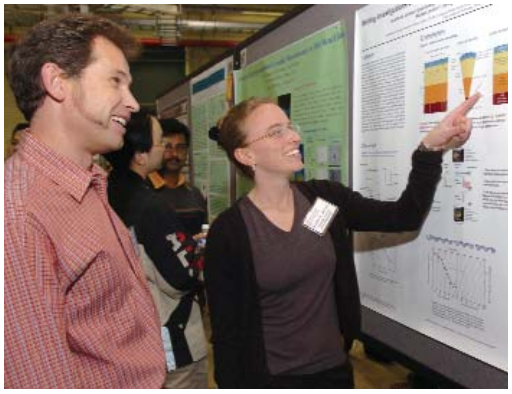

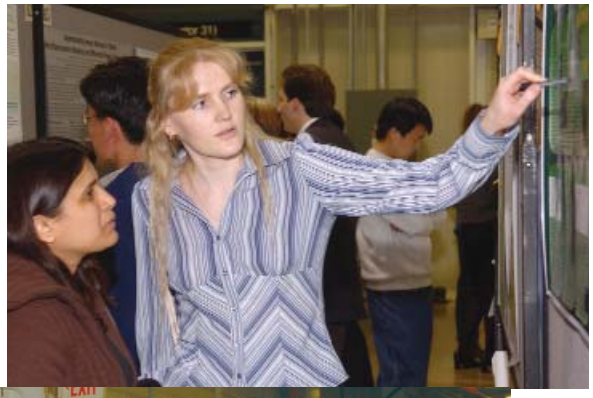

Top photo: The poster session on the APS experiment hall floor. (Middle row) Poster presenters and their attentive audiences. Bottom photo: A tour of the APS experiment hall capped off the CNM groundbreaking ceremony on the last day of the user meeting. Murray Gibson (third from right) regales (left to right) Illinois Governor Rod Blagojevich; Marvin E. Gunn, Jr., Manager, U.S. DOE Chicago Operations Office; U.S. Secretary of Energy Samuel Bodman; Don Randel, President, The University of Chicago; Jack Lavin, Director, Illinois Department of Commerce and Economic Opportunity; and Argonne Director Robert Rosner.

The week concluded on Friday with a dedication and cornerstone ceremony for the CNM. Robert Rosner, Director of Argonne National Laboratory, welcomed the 100 or so invited guests to the CNM site, then introduced Don Randel, President of The University of Chicago); Raymond Orbach (Director, Office of Science, Department of Energy); U.S. Representative Judy Biggert (R-IL-13), Rod Blagojevich (Governor, State of Illinois), and Samuel Bodman (U.S. Secretary of Energy), each of whom spoke briefly and offered congratulations to the project team.

The record-setting 600-plus attendees heard outstanding science talks, view more than 140 posters, choose among nine half- or full-day workshops, and attend a number of social functions, including the traditional mid-week banquet—a "Celebration of Light" commemorating the tenth anniversary of first light at the APS and the first nanoprobe light.

Plenary science talks were: Simon Bare on "Uniform Catalytic Site in Sn-beta Zeolite Determined Using X-ray Absorption Fine Structure," Peggy O'Day on "It's Not As Easy As It Looks: Application of Synchrotron-Based Techniques to the Analysis of Environmental Contaminants," Brian Newbury on "The APS and Archaeometallurgy: Studying the Alloys and Forming Techniques of the Medieval Brass Industry," Alfonso Mondragon on "Structural Studies of Catalytic RNA Molecules," Peter Abbamonte on "Imaging Electronic Motion in Water with Attosecond Time Resolution," Michael Borland on "A Survey of Possible Near-Term Accelerator Improvements," and Aled Edwards on "Structural Biology and Genomes." Student poster prize winners (Jeremy Robinson from the University of California, Berkeley, for "Metal-Induced Assembly of a Semiconductor-Island Lattice: Ge Islands on Au-Patterned Si," Anthony Escuadro of Northwestern University for "XSW Imaging of Submonolayer Vanadium Oxides on α-Fe_2O_3 (0001)," and Marcus Young of Northwestern University for "Internal Strain Measurements in Ultrahigh-Carbon Steels" spotlighted APS science, and scientists, of the future.

Workshop topics included nanoscale bio-hybrid materials, advanced nanopatterning, and scientific applications of the hard x-ray nanoprobe, all conducted jointly by APS and CNM. Workshops conducted solely by the APS addressed collection of good diffraction data, scattering from liquid surfaces and interfaces, metals and metalloids in cell biology, deep x-ray lithography and LIGA, applications of grazing incidence small-angle x-ray scattering, and generation and use of short x-ray pulses at the APS. *Contact: Susan Strasser (strasser@aps.anl.gov)*

Users Who Visited the APS at Least Once in FY05, by Geographic Distribution

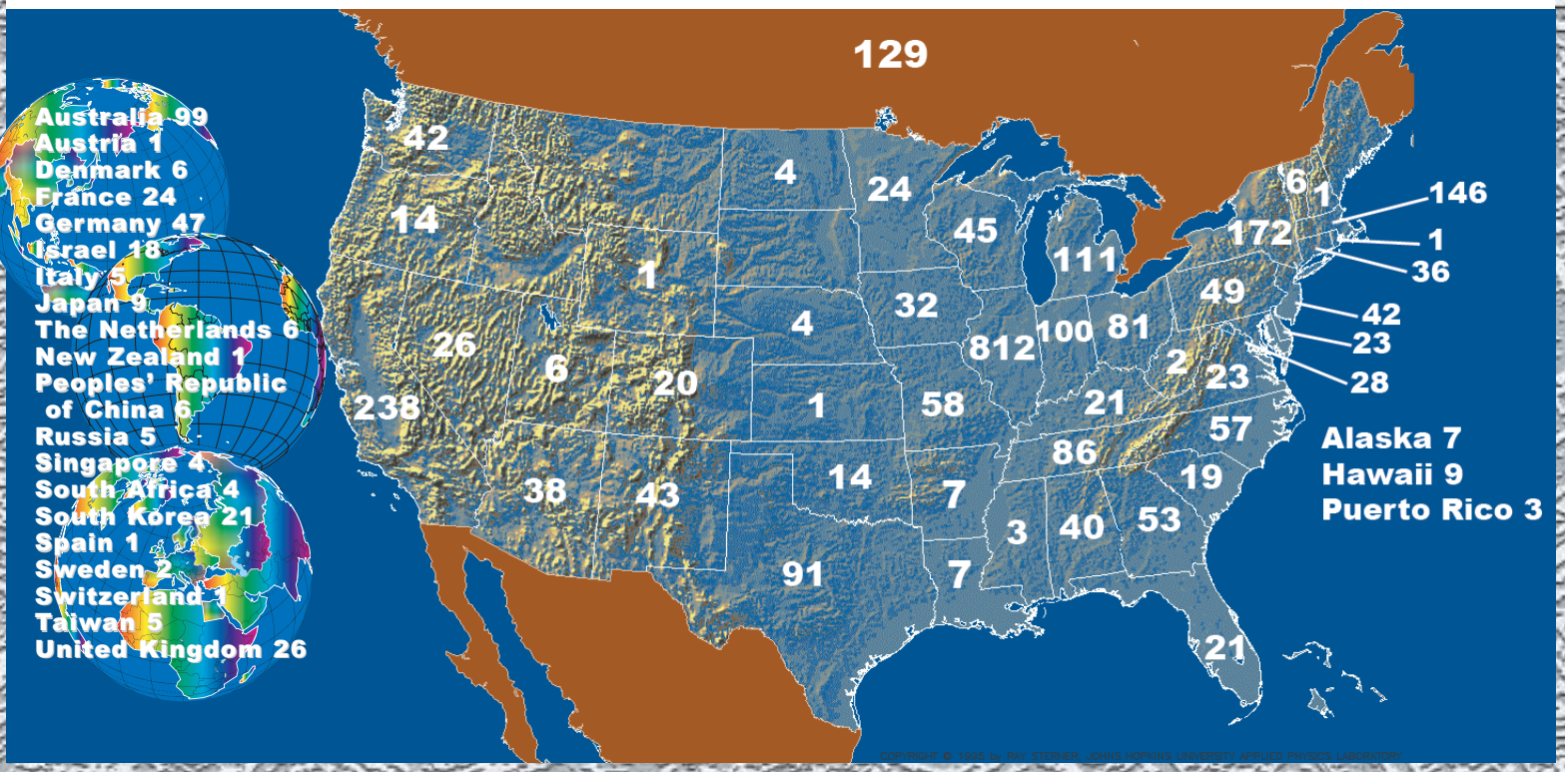

Experiments at the APS by Fiscal Year

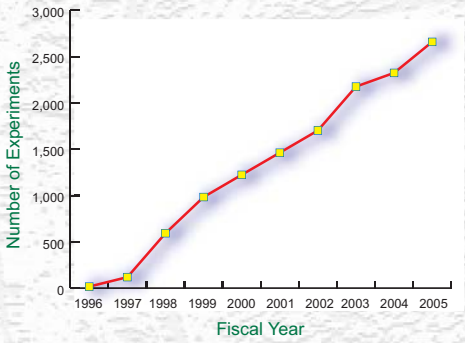

User Visits to the APS by Fiscal Year

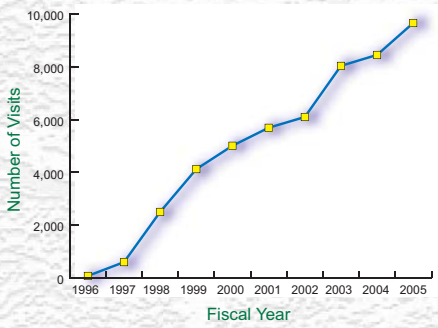

Number of Visits to the APS by User Type

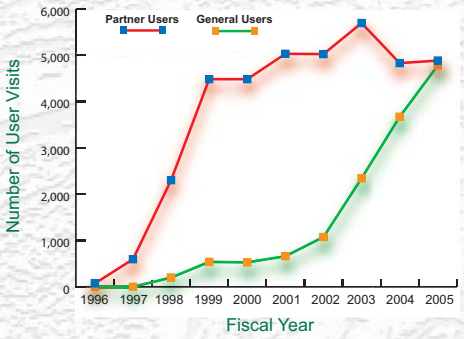

APS Publications by Calendar Year (99-05)

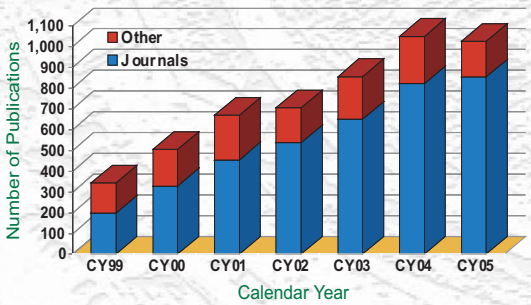

APS Users by Employment Level (FY05)

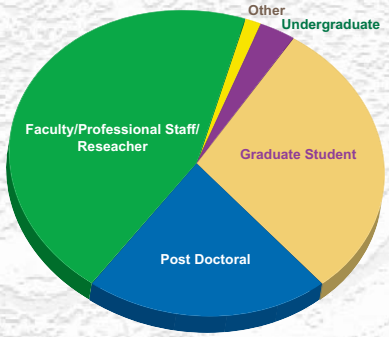

APS Users by Institution Type (FY05)

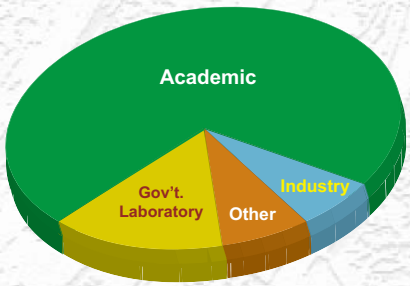

USER SUPPORT

NEW CONTROLS FOR 8-ID

When XOR beamline 8-ID became part of the APS, its antiquated, PC-based control system was replaced with standard hardware and software tools from the AES Beamline Controls and Data Acquisition (BCDA) Group, based on the Experimental Physics and Industrial Control System (EPICS) software toolkit. These changes led to improved functionality, improved ease of use, significantly faster data acquisition, and markedly greater beamline automation and reliability.

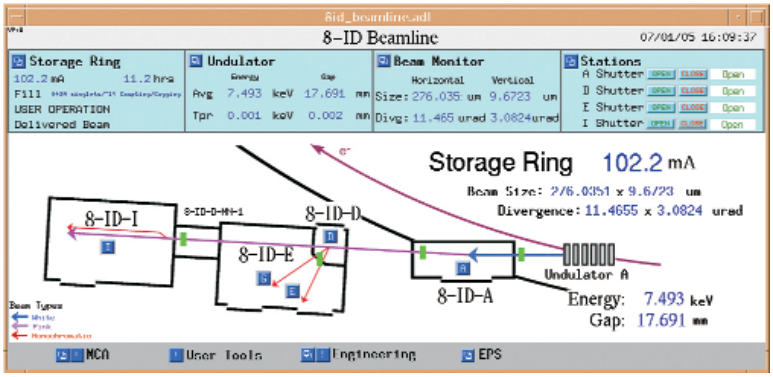

Fig. 1. Top-level 8-ID beamline schematic implemented in MEDM.

The original control and data acquisition system at XOR sector 8 was based on **spec** running on Linux PCs. Motor control and some data acquisition were done in or near the experiment enclosures, using PCs with legacy Industry Standard Architecture (ISA) cards and bus extenders. The ISA-based PC workstations and associated control hardware were obsolete, but the task of upgrading and replacing them was too difficult and time-consuming for the beamline staff to accomplish. The 8-ID beamline staff decided to convert to BCDA-standard hardware and software tools at that time. The BCDA Group recommended VME-based processor and control hardware and an EPICS-based software package (synApps) for this large-scale beamline control application. Because XOR sector 8 had become part of the APS, BCDA would be primarily responsible for implementing the control system upgrade.

A primary goal of the XOR sector 8 control system conversion was to ensure that no scheduled experiments would be disrupted. This goal was accomplished by using an incremental approach that involved converting one hutch per shutdown period. Other goals were for existing beamline motor stages and stand-alone control and data acquisition devices to be reused, and for compatibility with **spec** to be maintained. The beamline staff and the BCDA Group were successful in achieving all of the project goals. Over the span of three shutdown periods, all four 8-ID hutches were converted to an EPICS/VME-based control system running the synApps beamline control package.

The A station control conversion supported all the existing optical components (two tables, white-beam slits, and mirror stage). The beamline control system was enhanced by adding a direct interface to the beamline equipment protection system and remote shutter control (with an auto-open feature). Since the initial control conversion, improvements have continued in the A station. Position data for all the optical components are now fed back into the control system.

The D station (monochromator) conversion supported the existing motors. Support was added for an existing rotation position feedback device. In addition, APS-provided storage ring status information was made available to 8-ID by adding the bunch clock generator and machine status link interface cards to the D station. The 21-slot VME card cage used for the D station was also capable of controlling the E experimental station.

The I station was the first one converted from PC-based control to EPICS. The station contains several motor-driven optical components (one table and four slits), a digitally controlled filter stage, and a multitude of serial-interfaced devices (current preamplifiers, slits, a power supply, and a temperature controller). Support for all of the I-station devices—except the programmable power supply, which was added to synApps as part of the switchover—was already contained in synApps. General-purpose input/output was added to the VME control platform to provide flexibility in designing experiments.

The standalone E station has many of the same optical and data acquisition devices as the I station. The VME-based control hardware and software for these devices was installed in the combination D-E control VME crate. In addition, synApps support was created for a scanning electrometer and a sub-micron-accuracy, three-axis positioning system. For this latter application, synApps general motor support software maintained "closed-loop" control to encure submicron accuracy with this stage.

In summary, the BCDA Group has efficiently and effectively upgraded the beamline 8-ID control scheme to a modern VME-based control system and provided many benefits to 8-ID, such as greater automation, reliability, and data acquisition rates. Moreover, and perhaps more important, the successful conversion demonstrates that the BCDA Group can effectively support and enhance the many new beamlines that the APS is charged with operating. *Contact: Joe Sullivan (sullivan@aps.anl.gov)*

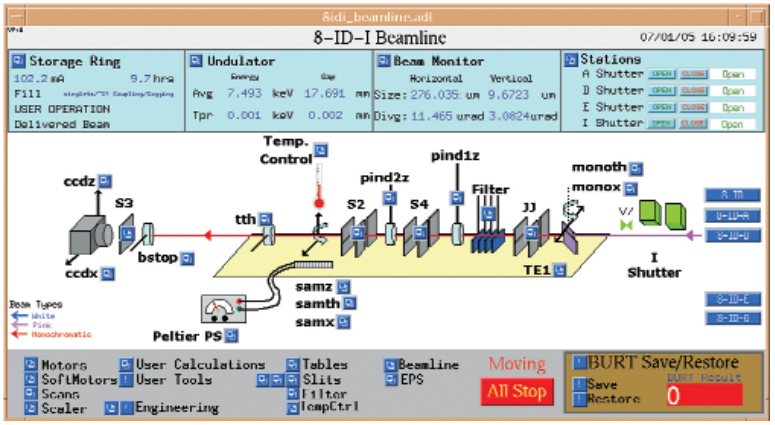

Fig. 2. Top-level control screen for the I station (implemented in MEDM).

SUPPORTING SPEC

Jonathan Lang (left) of the XSD X-ray Magnetic Materials Group confers with Xuesong Jiao, AES BCDA Group **spec** specialist, in the XOR 4-ID control room.

In response to requests from scientists at numerous APS beamlines, the AES Beamline Control and Data Acquisition (BCDA) Group has initiated a program to support **spec** (Fig. 1), software from Certified Scientific Software that is used for x-ray diffraction and data acquisition. The APS purchased a site license and has installed **spec** at a number of instrument stations around the experiment hall. While the Experimental Physics and Industrial Control System (EPICS) is the major hardware control platform at APS beamlines, **spec** remains an essential front-end data acquisition program because of its compatibility with EPICS. Many APS users prefer **spec** because of its extensive built-in functionalities for numerous experimental geometries and its versatile macro command language, through which scientists can expand and customize **spec**'s built-in capabilities. In 2005, the BCDA Group added an engineer to provide technical support to the **spec** community.

One of the major goals of the BCDA **spec** support program is the development of a central **spec** repository for macro command sequences. Site-dependent macros are tailored to meet the specific needs for each instrument, as researchers at various beamlines develop macros for their specific controls; some of these macros might be useful to others, with minor modifications, and there are many general-purpose macros that can be shared amongst the community, such as those for charge-coupled device detector control and user-defined header and data columns. The BCDA Group implements, collects, and sorts these common macros; maintains and expands the repository; and distributes these macros throughout the APS-managed file system. The BCDA repository helps to reduce duplication of effort in the creation of macros, while the APS users benefit by having the same interface at different beamlines.

In addition to assisting beamline staff on **spec** configuration based on a beamline's EPICS control system, the BCDA Group develops and evaluates **spec**-related tools and applications, installs and upgrades **spec** for APS beamline research stations, and surveys beamline needs for future development. The support staff also writes site-specific macros in a timely manner for the beamlines. For instance, in 2005, many macros were written for beamlines 4-ID and 8-ID per requests from the beamline personnel.

Some of the BCDA-developed macros in use at various beamlines include a package to control multi-channel analyzers (MCA) on top of the EPICS interface that allows users to trigger multiple MCAs and save the spectra and regions of interest into the **spec** file during scans. This package has been deployed at

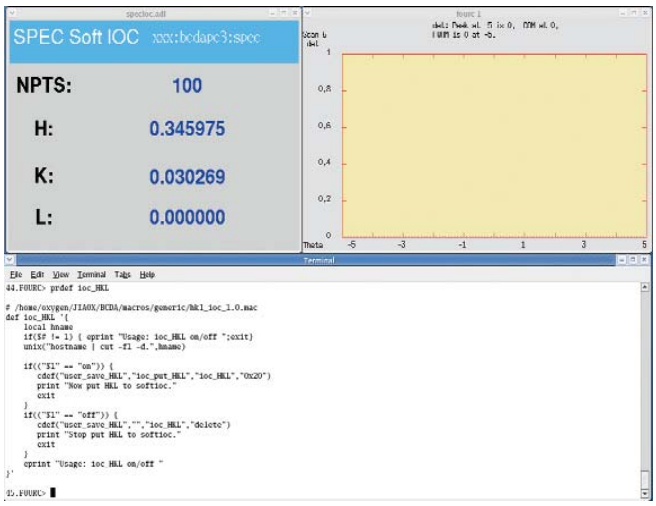

Fig. 1. A typical **spec** graphical user interface.

XOR 4-ID and XOR/UNI. It can be used at any other beamline if the EPICS-based MCA DXP server is installed for hardware control.

The BCDA Group also assists with the integration of **spec** into the EPICS control system. For example, a soft input/output controller tool (**spec**IOC) was implemented to allow **spec** to send out the Miller indices and the orientation matrix as EPICS PVs. Other applications can monitor these values in real time via the channel access.

All of these macros, complete with documentation, can be accessed from the BCDA **spec** macro repository at http://www.aps.anl.gov/aod/bcda/**spec**.

Contact: Xuesong Jiao (jiaox@aps.anl.gov)

Information Technology Support for the APS Beamlines

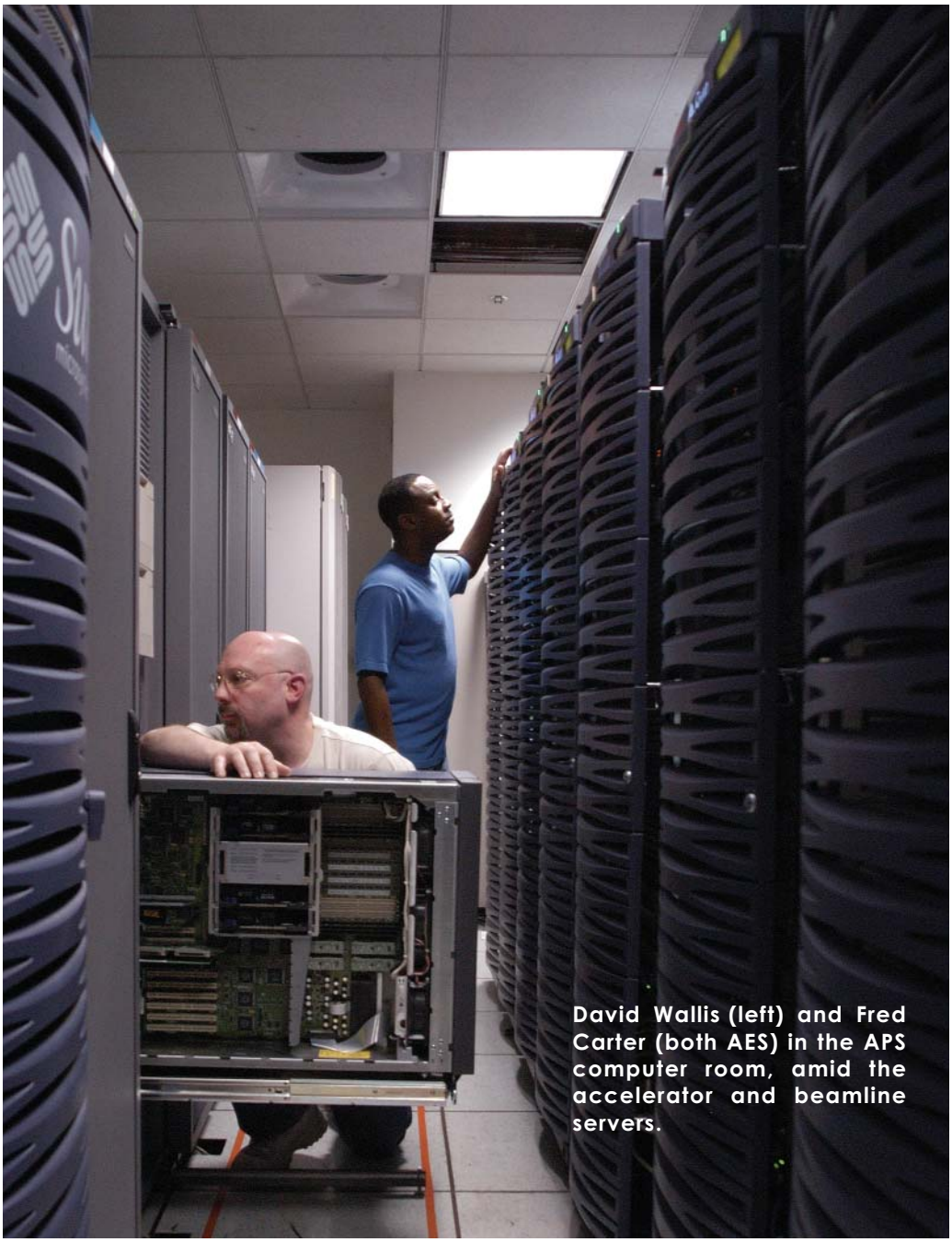

David Wallis (left) and Fred Carter (both AES) in the APS computer room, amid the accelerator and beamline servers.

Providing a computing environment suitable for a state-of-the-art user facility such as the APS is the challenge for the AES Information Technology (IT) Group. Users of the APS constantly push the limits of computing technology, with faster and higher-resolution imaging detectors and faster computers that generate data at ever-increasing speeds and quantities. Beamlines operating 24 hours per day for up to three months at a time host thousands of visiting scientists and experiments each year, resulting in a dynamic and ever-changing computing environment. The IT Group has developed a systematic approach to designing and maintaining a network and computing environment that meets the current and future needs of APS users.

When the first APS beamlines were commissioned, IT supported three sectors (five beamlines). Data storage consisted of two disk array systems with an aggregate of about 30 gigabytes (GB) of storage. The data output of most experiments was measured in megabytes (MB) per day. Today, IT services 12 beamlines (9 sectors), and that number is expected to grow to about 21 beamlines (16 sectors) within a year. During 2005, the IT Group completed a number of projects aimed at increasing the reliability of IT support systems, as well as improving the ability of APS users to store and access data from these experiments.

Beamline Networking Cyber Security Cyber security for beamline networks that meets U.S. Department of Energy and Argonne requirements is provided by APS-managed firewalls. Three levels of firewall protection mitigate risks from vendor vulnerabilities and leverage the security capabilities of different vendors. The firewalls, which are placed at different tiers of the network to provide multilayer security, include antivirus, anti-spam, and URL filtering to prevent intrusions. Network traffic is analyzed by using APS-developed programs that detect network intrusion attempts and automatically block the source address of the attacker.

Moving Data The first APS beamline network consisted of 10-megabit (Mb)/s shared bandwidth. The IT Group has upgraded those networks to a level that will meet user needs for many years. Network components have been used to construct a backbone comprising multiple redundant 1-gigabit (Gb)/s optical fiber connections. Switches located at each sector provide gigabit connectivity to the desktop, allowing the newest computers to access the network and move data files at maximum speed. The switches were engineered for easy upgrade to a 10-Gb/s backbone network. The wireless network was upgraded and expanded in the APS experiment hall and laboratory/office module buildings and now provides 802.11G 54-Mb/s connectivity to all user beamlines, offices, and labs at the facility.

Managing Data File servers are the heart of beamline data storage. During 2005, file servers for beamline support were

upgraded to a pair of Enterprise servers configured as a high-availability cluster. Each server monitors the other; if one server fails or is shut down for maintenance, the other automatically takes over. Each server also has redundant hardware configurations to ensure that it can stay on line in the event of even the most common failures.

Storing Data During 2005, an aging assortment of disk arrays was replaced with a new storage system that provides 20 terabytes (TB) (20,000 GB) of high-performance, high-availability storage. The system connects to file servers via a 2-Gb/s optical fiber technology and features redundant RAID-5 controllers in 10 disk trays, a number of warm spare disk drives, and a storage management controller that automates many of the operations required to configure and maintain the storage system. Hot-swap capability allows replacement of components without storage system shutdown. The system can be expanded to a total of 60 TB of storage. A near-term goal for the IT Group is developing a system that will allow users to archive all of their beamline data nearly indefinitely and retrieve historical data easily and automatically.

Distributed Network Services New workgroup servers provide better access to a number of network information services, including distributed domain name service, dynamic host configuration protocol, and network time protocol. These servers are configured so that in the event of a network failure, beamlines will have access to necessary services so that experiments can continue.The servers are also a platform for distributing Experimental Physics and Industrial Control System and locally developed beamline control and data analysis software.

Taking Data Home In response to requests from beamline users, the IT Group is upgrading a single file transfer protocol (FTP) server with two new servers and expanded storage. Visiting scientists often generate more data than can be conveniently written to DVDs that they transport to home institutions. Or a user might submit experiment samples to be processed by APS personnel without the user actually visiting the APS. File transfer protocol provides a simple and reliable method of transferring data files from the APS to an external user's computer. Typically, more than 1,000 files per week are transferred from the FTP server when experiments are generating data. The new FTP servers are configured as a high-availability pair. In order to support the large amount of data that users generate, each server provides 1 TB of storage. Users also have the option of accessing the FTP servers via their web browsers.
Contact: Kenneth Sidorowicz (kvs@aps.anl.gov)

AROUND THE EXPERIMENT HALL

THE DEDICATED INELASTIC X-RAY SCATTERING PROGRAM AT THE APS

The dedicated inelastic x-ray scattering beamline at the APS that could only be described in the 2004 APS annual report (*APS Science 2004*, ANL-05/04, pg. 138) can now be visited as it draws closer to completion in 2006, with a general user program starting in 2007. The gleaming silver 9-m-long movable arm of the HERIX spectrometer (photo at right) has been installed in the research station at beamline 30-ID. HERIX and the companion MERIX instrument will enable a scientific program that covers a range of exciting research areas, including correlated electron systems, high-melting-temperature liquids, biologically important DNA solutions or proteins, and nanophase materials. The microfocusing capability will enable high-pressure experiments in diamond-anvil cells. HERIX will be used predominantly to study phonon excitations in solids, while MERIX is designed to study electronic excitations. Construction of the Inelastic X-ray Scattering Collaborative Development Team sector 30 is funded by the National Science Foundation; the U.S. Department of Energy, Office of Basic Energy Sciences; and participating universities. See: http://www.ixs.aps.anl.gov/. *Contact: John Hill (hill@bnl.gov), Ercan Alp (eea@aps.anl.gov), Harald Sinn (HERIX, sinn@aps.anl.gov), or Clem Burns and and Yuri Shvydko (MERIX, burnsc@wmich.edu, shvydko@aps.anl.gov).*

Present at the installation of the HERIX spectrometer (all ANL unless otherwise indicated). First row: Ayman Said, Jacques Van Zyl (Oxford Danfysik), Harald Sinn, Ian Campton (Oxford Danfysik), Bran Brajuskovic, Tim Roberts. Second row: Mike Bosek, Scott Wesling, Kristine Mietsner, Stan Johnson. Third row: Keith Knight, Ahmet Alatas, Bill Jansma. Last row: Mike Johnson, John Wozniak, Ed Theres.

The APS Light Source

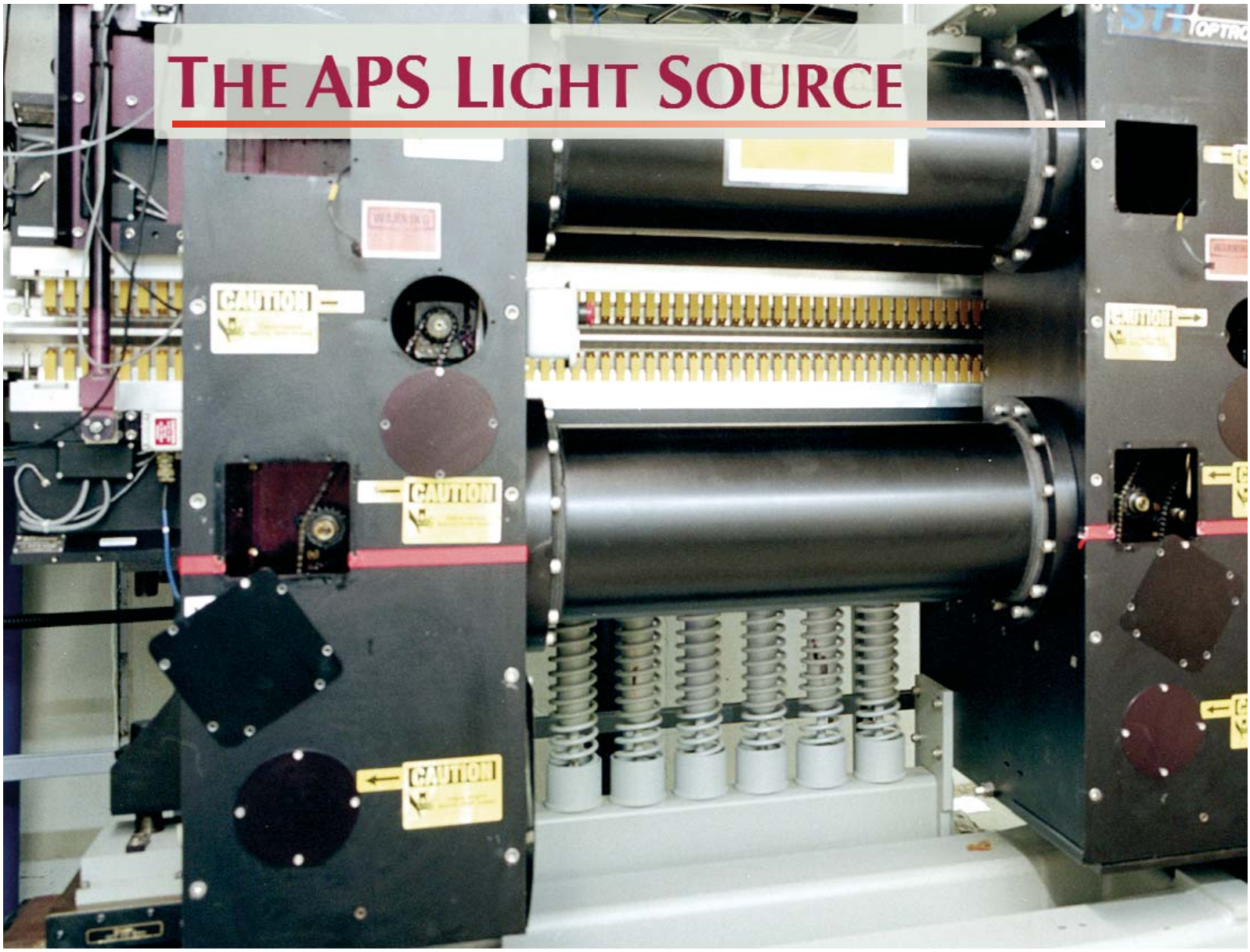

The Accelerator

Light Source Operations

In calendar year (CY) 2005, the APS scheduled 5024.4 h for user-beam operations and delivered 4925.3 h. The emphasis on meeting established availability and reliability goals has continued to yield impressive results, with the reliability—expressed as the mean time between faults (MTBF)—climbing to 86.4 h. The focus of accelerator R&D has moved in the direction of identifying and addressing accelerator issues to support the APS tactical plan.

Beam Availability and MTBF

During 2005, accelerator operation, as quantified by availability and MTBF, was exceptional (see Table 1). The APS has, since 2000, routinely exceeded the goal of 95% availability. A concerted effort has been made to maintain this level of availability while reducing the number of faults. These efforts have resulted in a reliability figure-of-merit of 88.4 h MTBF, an increase from 68.1 in CY 2004. Although the number of faults has remained low, the accelerator complex (now in operation for nearly 10 years) is experiencing end-of-life aging on many components. The facility cannot afford to preemptively replace the larger, more costly components, resulting in a longer "mean time to recovery" when these devices fail. (A storage ring radio frequency [rf] system klystron failed during Run 2005-3.)

User Operation Fill Patterns

Various storage ring operation modes have been developed to meet different user-beam requirements. The operating modes used in 2005 were:

- Top-up, 24 singlets fill pattern
- Top-up, 1 + 7 x 8 hybrid (singlet) fill pattern
- Non-top-up, 324 multibunch
- Non-top-up, 1296 multibunch

See Fig. 1 for relative utilization.

Continued on page 172

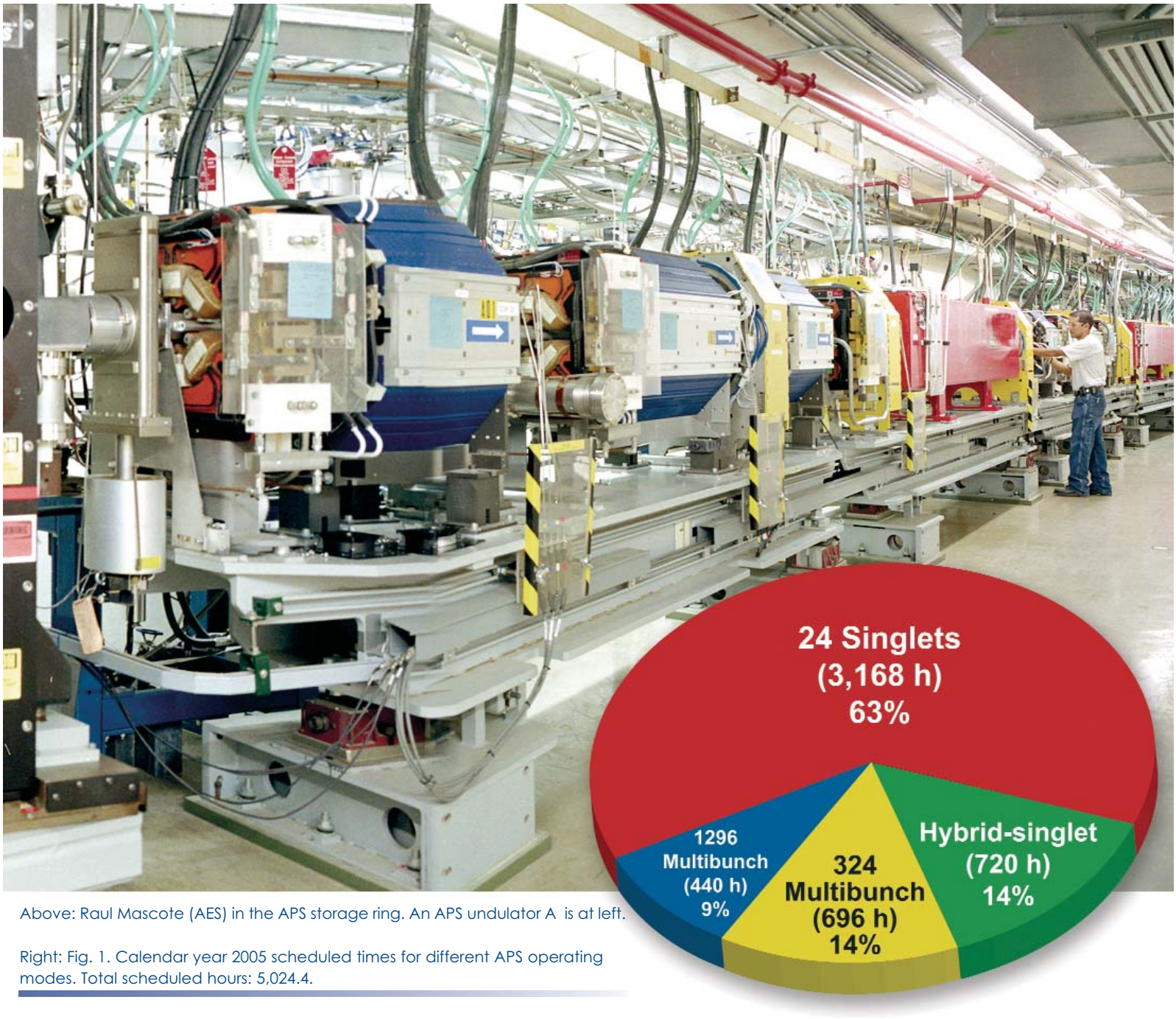

Above: Raul Mascote (AES) in the APS storage ring. An APS undulator A is at left.

Right: Fig. 1. Calendar year 2005 scheduled times for different APS operating modes. Total scheduled hours: 5,024.4.

Table 1. Operations statistics—CY 2004-CY 2005.

	CY2004				CY2005
Run number		**Run 05-1**	**Run 05-2**	**Run 05-3**	
Start		1/31/05	6/1/05	10/4/05	
End		4/21/05	8/25/05	12/22/05	
Total hours scheduled (h)	5,128.3	1,639.3	1,792.1	1,593.0	5,024.4
Beam available for users (h)	5,039.3	1,617.0	1,764.8	1,543.6	4925.3
Beam availability (%)	98.3	98.6	98.48	96.9	98.03
Total downtime (h)	88.9	22.4	27.4	49.4	99.2
Average current (mA)	99.4	99.6	100.88	100.3	100.3
Number of faults	74	15	20	22	57
Mean time between faults (h)	68.1	107.8	88.2	70.2	86.4
Mean time to recovery (h)	1.2	1.5	1.4	2.2	1.7
Injector availability (%)	98.4	98.76	97.60	95.47	97.28

Typical APS Machine Operations Parameters

Linac

Output energy	325 MeV
Output beam charge	1–3 nC
Normalized emittance	10–20 mm-mrad
Frequency	2.856 GHz
Modulator pulse rep rate	30 Hz
Gun rep rate (1–6 pulses, 33.3 ms apart every 0.5 sec)	2–12 Hz
Beam pulse length	8–30 ns
Bunch length	1–10 ps FWHM

Particle Accumulator Ring (PAR)

Nominal energy	450 MeV
Circumference	30.66 m
Cycle time	500 ms
Fundamental rf frequency (RF1)	9.77 MHz
12th harmonic rf frequency (RF12)	117.3 MHz
RMS bunch length (after compression)	0.34 ns

Injector Synchrotron (Booster)

Nominal extraction energy	7.0 GeV
Injection energy	325 MeV
Circumference	368.0 m
Lattice structure	10 FODO cells/ quadrant
Ramping rep rate	2 Hz
Natural emittance	65 nm-rad
Radio frequency	351.930 MHz

Storage Ring System

Nominal energy	7.0 GeV
Circumference	1,104 m
Number of sectors	40
Length available for insertion device	5.0 m
Nominal circulating current, multibunch	100 mA
Natural emittance	2.5 nm-rad
Momentum spread	0.096%
Effective emittance	3.1 nm-rad
Vertical emittance	0.025 nm-rad
Coupling	1%
Revolution frequency	272 kHz
Radio frequency	351.930 MHz
Number of bunches	24 to 1296
Time between bunches	153 to 2.8 ns
Bunch length	70 ps to 23 ps
Bunch length in hybrid mode @ 16 mA	70 ps to 23 ps

"The Accelerator" from page 170

Note that all operations now utilize the low-emittance lattice developed over the last several years, CY 2004 being the first year in which this was the case (see Table 2).

Table 2. APS beam parameters at radiation points, 2.5-nm horizontal emittance, 1% coupling.

		ID	BM
Horiz. beta function	(m)	19.4	2.39
Horiz. dispersion	(m)	0.172	0.059
Horiz. rms beam size	(μm)	275	95.3
Horiz. rms divergence	(mrad)	11.3	56.7
Vert. beta function	(m)	2.98	24.6
Vert. rms beam size	(μm)	8.8	25.2
Vert. rms divergence	(mrad)	2.9	1.2

The most common fill pattern was 24 singlets spaced by 154 ns. Top-up injection (injecting beam into the storage ring every two minutes.) is utilized for this fill pattern.

The hybrid singlet pattern is used by the timing community to perform dynamic biological, chemical, and condensed matter/materials science studies. This pattern is defined as a single bunch containing a maximum of 16 mA isolated from the remaining bunches by symmetrical 1.59-μsec gaps. The maximum current in the single bunch has been increased this year to the 16-mA level from 8 mA in the previous year. (See page 176.) The remaining current is distributed in 8 groups of 7 consecutive bunches and a spacing of 48 ns between groups. Top-up is also utilized in this mode, but in order to maintain the higher current in the single bunch, injection is scheduled every 60 s as opposed to the 2-min interval in the normal sing-let fill pattern.

Non-top-up operation (refilling the storage ring twice every 24 h) is mainly used to provide injector beam time for parasitic injector study, operator training, and injector maintenance and improvement. A 324-multibunch fill pattern (bunch spacing of 11.4 ns) has been utilized; in CY2005, the APS began using a fill pattern in which all rf buckets (1,296) in the storage ring are populated. This mode was developed primarily as a reliability initiative; the particle accumulator ring (PAR) is used to manipulate the time structure of the beam to contain all of the incoming charge into one 352-MHz storage ring bucket. If the requirement for clean single bunches (no charge in neighboring rf buckets) is relaxed, the PAR is not needed. Thus, the 1,296-bunch fill pattern was created primarily as a backup plan in case a major failure occurs in the PAR during operation. However, the lower per-bunch current results in a much longer lifetime (about 100 h as opposed to 60 h for the 324-bunch mode) and, therefore, more constant current across the refills. There is about 92 mA remaining after 12 h (with 324 bunches, this has been approximately 83 mA). Non-top-up operation in CY 2006 will continue to use a mix of these two modes.

Beam current is 102 mA for all modes. The APS has continued to explore a program of raising the current during short

They are "machine operators" in more ways than one. Personnel in the APS Main Control Room (photo above) are not only highly skilled at operating the APS accelerator and beamline systems—they have also been trained to provide limited after-hours machine shop support for users in dire need of drill-press services at 3:00 a.m. Shown are (l. to r.): Bryan Oakley (ASD), Shane Flood (ASD), John Forrestal (AES), and Joe Sutton (ASD).

periods of operation as part of a strategy for raising normal operational current. This has been put on hold while a thorough analysis is done on the reliability and performance of all front-end and beamline components that are exposed to insertion device x-rays. This work is ongoing.

ACCELERATOR R&D IN SUPPORT OF THE APS STRATEGIC PLAN

The APS Strategic Plan has a number of implications for accelerator innovation. The notable implications are requests for longer straight sections (see the article on page 175) that allow space for additional insertion devices, and for customized lattice functions—reducing the horizontal beam size—in the insertion device straight sections. Both of these issues have been studied in stand-alone cases. However, as the strategic plan is developed, there will be multiple requests for each of these types of accelerator modification, and the requests will come from arbitrary sectors (from an accelerator symmetry perspective). Because of the significant beamline infrastructure in place on the experimental hall floor, it is desirable to leave that infrastructure where it is and apply the accelerator modifications where needed. This will mean asymmetric accelerator modifications—perhaps in consecutive sectors, perhaps in combinations of the modifications in adjacent sectors. It is this problem that has been studied in both simulations and on the storage ring. (See the article, "A High-throughput Interface for Storage Ring Modeling," on the next page). The storage ring is proving to be a very flexible accelerator, but specific steps forward have not yet been defined.

Time domain science is another component of the strategic plan that affects the accelerator. There is considerable interest in producing x-ray pulses on the order of 1 ps. A method for producing these short pulses using rf manipulation of the circulating electron beam and x-ray optics has been proposed by Zholents of Lawrence Berkeley Laboratory. The parameters of the APS storage ring make it a very good candidate for implementation of this scheme. Accelerator physicists at the APS have demonstrated the feasibility of the scheme. Research and development on the rf systems is under way.

Contact: Rod Gerig (rod@aps.anl.gov)

Accelerator Operations and Improvements

Accelerator physicists Louis Emery (l.) and Michael Borland (both ASD) contemplate the interface.

A High-throughput Interface for Storage Ring Modeling

Researchers in the APS Accelerator Systems Division have developed a graphical user interface (GUI) to a popular APS-developed accelerator simulation code that provides physicists with high-throughput analysis of storage ring designs. The interface allows the physicist to concurrently and easily use many nodes of a Linux cluster. With this interface, physicists can perform, in less than an hour, analyses that used to take days. It also produces some eye-catching graphics.

The simulation code in question is known as "**elegant**" (***ele***ctron ***g***eneration ***an***d ***t***racking), and it is the basic tool used by accelerator physicists at the APS for accelerator design and simulation. In fact, all of the accelerator configurations presently in use at the APS—from the linac to the storage ring—were designed using this code. The code is also used at the APS and worldwide for research into next-generation light sources, including storage rings, energy recovery linacs, and free-electron lasers.

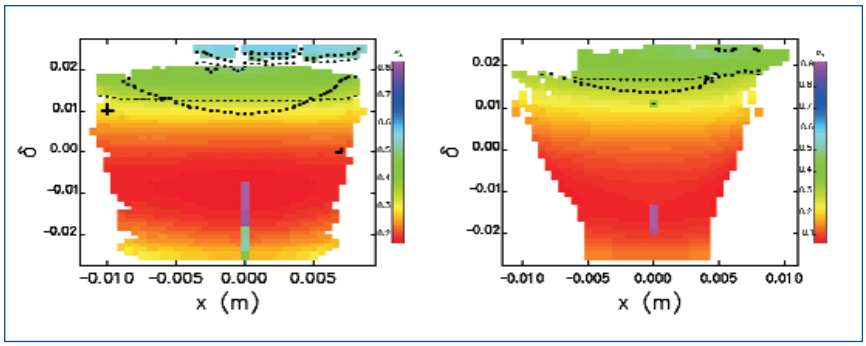

Fig. 1. Frequency map analysis for candidate combo-lattice configurations from the **elegant** Ring Analysis GUI. The left-hand plot shows a lattice with inadequate momentum aperture, indicated by a gap in the colored region near d=0.02, which is caused by a resonance. The right-hand plot shows a revised configuration that extends the energy aperture above the 2% boundary. The black symbols show various resonances that may cause performance problems in a poorly corrected lattice.

One of the salient features of **elegant** is that it uses the APS-developed SDDS (Self-Describing Data Sets) file protocol for input and output, which means that the powerful SDDS Toolkit is available for pre- and post-processing of data. As a result, any scripting language—such as Tcl/Tk—can be used to configure and run **elegant** and process the data. These are, not coincidentally, the same tools used for development of much of the software that is used to operate the APS. However, whereas in the case of the APS a wealth of GUIs are provided, the individual **elegant** user is left to develop private scripts.

Owing, again, to its use of SDDS files, **elegant** is well suited for a Linux-cluster-based batch queue, which permits running many jobs simultaneously. With SDDS files and scripts, the results of these jobs can be easily monitored, collated, and post-processed. The newly developed GUI makes it unnecessary for users to develop their own scripts for certain common time-consuming calculations, such as phase space tracking, dynamic aperture tracking, and frequency map analysis. It also permits the user to make efficient use of a large cluster because it allows simultaneous submittal and monitoring of many tasks, each consisting of a multitude of jobs.

The **elegant** software was used in many APS lattice development efforts in the last year to gain insight into which lattices can be expected to work well and how to improve those that work poorly. For example, work on mocked-up long straight section (LSS) lattices and lattices providing reduced horizontal beam size (RHB) all made use of the new interface. Figure 1 shows an example of frequency map analysis for the "combo lattice," which is a developmental lattice for determining whether one can eventually provide a mixture of LSS and RHB straight sections.

Contact: Michael Borland (borland@aps.anl.gov)

LONG STRAIGHT SECTIONS

Thanks to the foresight of those who designed it, the APS storage ring has a great deal of built-in flexibility, which opens up many avenues of improvement. In particular, unlike any previous storage ring light source, the APS has independent power supplies for every one of its 400 quadrupole magnets and 280 sextupole magnets. This allows physicists to more readily contemplate such things as beta-function customization or increased straight-section length, because the electron beam optics can be adjusted (within limits) on a sector-by-sector basis. In addition, because the APS performs top-up, it can be operated with such customizations even if they may result in decreased beam lifetime.

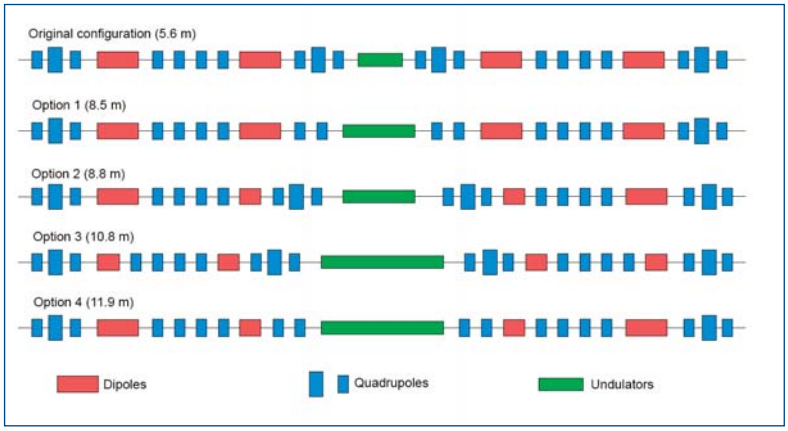

Fig. 1. Diagrams of two sectors, showing various possible configurations for lengthened straight sections. The values in parentheses indicate the maximum distance between the gate values on either side of the straight section.

History and Options

APS straight sections provide space for two 2.4-m-long insertion devices and associated hardware. Following a question raised by a beamline scientist during the APS Strategic Planning Meeting in 2001, on-the-spot electron optics calculations on a laptop showed that a configuration providing 7.7 m for undulators was possible with relatively simple modifications. About a year later, interest was expressed in having four 2.4-m-long undulators in a single straight section. This configuration was investigated, and a possibility was found for providing space for up to 10.8 m of undulators [1], albeit with extensive modifications. A detailed design study and cost estimate was undertaken by a group of APS accelerator physicists, mechanical engineers, and project managers.

Figure 1 shows, in schematic form, the various arrangements that were investigated, along with the amount of free space for each. Option 1 involves the fewest changes to the ring. Essentially, a large quadrupole magnet is removed from each side of the undulator, and the existing small quadrupole magnet is moved into its place, increasing the free space from 5.6 m to 8.5 m. Options 2, 3, and 4 involve shortening the existing dipole magnets and building new magnet girders, which makes them considerably more expensive.

Figure 2 shows the brightness one could achieve with Option 4 and four 2.4-m-long U27 undulators in a single long straight section. The improvement is slightly less than a factor of four, because the beta functions for the long straight section optics do not match the undulator radiation as well as the normal beta functions.

Experimental Tests

Given the flexibility of the APS ring, one can mock-up an Option-1-type long straight section by turning off some quadrupole magnets on either side of a straight section. (Of course, one must also make other adjustments.) The first tests were conducted just after the 2001 APS Strategic Planning Meeting and showed that the idea was workable in a single straight section. Further tests in 2003 explored the dynamic aperture and other aspects of the lattice.

In 2005, it became known that several sectors might benefit from having an Option 1 long straight section. A workable lattice was developed that mocked up long straight sections in sectors 1, 3, 9, 11, 30, and 32. Subsequently, a similar lattice—that also includes smaller beam size in three other sectors—was tested and also appears workable, although the lifetime is reduced from ~7 h to ~4 h. This limitation is readily handled with faster top-up injection. In addition, the effective beam emittance increases from 3.1 nm to 3.8 nm, an unfortunate trade-off that must be made for such extensive lattice changes.

Contact: M. Borland (borland@aps.anl.gov), Louis Emery (emery@aps.anl.gov), Efim Gluskin (gluskin@aps.anl.gov), Kathy Harkay (harkay@ aps.anl.gov), Vadim Sajaev (sajaev@ aps.anl.gov)

REFERENCE

[1] L. Emery et al., "Progress and Prospects Toward Brightness Improvements at the APS," Proc. of PAC 2001, p. 2602 (2001).

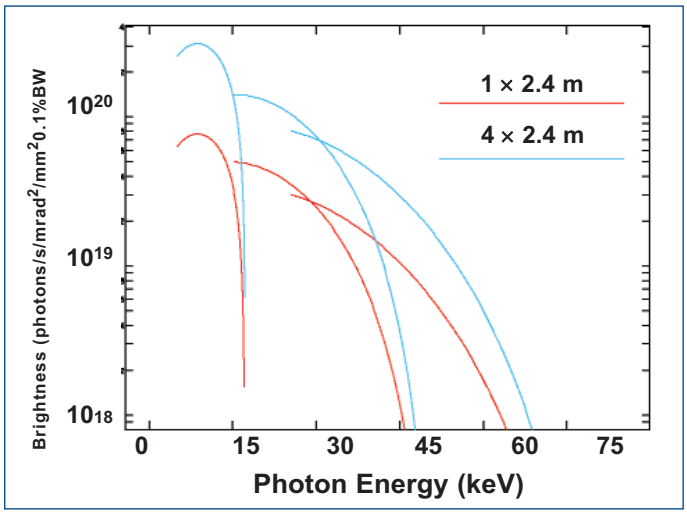

Fig. 2. Brightness curves for U27 undulators for a normal APS straight section with one undulator, and a long straight section with four undulators.

ENHANCED HYBRID MODE DELIVERED TO USERS

Stored beam at the APS consists of a set of up to 1,296 circulating electron bunches. The injection system is flexible enough to allow filling of any pattern in the 1,296 available slots, although not all of the possible patterns or modes are compatible with good operation of the ring. Among the modes used at the APS are 1,296-, 324-, and 24-bunch patterns with equispaced bunches of nominally the same intensity. The storage ring also routinely operates in the so-called "hybrid mode."

Hybrid mode refers to a bunch pattern in which there is one intense bunch on one side of the ring and a train of 56 less-intense bunches on the other side of the ring. The intensity of the single bunch and the space between it and the other bunches are important for certain types of time-resolved experiments. The intensity of the single bunch is limited by a collective instability that originates in the electromagnetic interaction of the bunch with the walls of the vacuum chamber, particularly the small-gap chambers at beamlines 3-ID (now removed) and 4-ID. Overcoming this instability requires increasing the strength of the sextupole magnets in the ring, which stabilizes the beam by introducing a spread in resonant frequencies for different electrons in the intense bunch. However, increasing the sextupole strength also reduces the beam lifetime for both types of bunches. It has long been known that decreasing the top-up interval would compensate for shorter lifetime. What was not known is how high the single bunch current could go and at what cost in increased top-up rate.

Following the removal of the 3-ID vacuum chamber (for other reasons), it was expected that the single-bunch current limit would increase. Furthermore, improvements to the storage ring optics made the sextupole magnet stabilization more effective. In other words, one could achieve a given stable bunch current for a lower sextupole strength and, hence, longer lifetime. Increasing the sextupole strengths further than before possible made it feasible to go as high as 20.7 mA, a new record for the APS and significantly higher than the normal 8-mA hybrid bunch.

However, there is a downside. The effective horizontal emittance of the hybrid bunch increases with increasing current, due to a phenomenon known as the microwave instability (which cannot be cured with sextupoles). Figure 1 shows the ratio of hybrid-bunch current to hybrid-bunch emittance, which is roughly proportional to the brightness delivered by the hybrid bunch. It continues to increase even as the 21-mA limit is approached. Backing off to 16 mA permitted the establishment of a conservative new operating point with twice the former hybrid bunch intensity. This was found to be consistent with a 60-s top-up interval, with about 3 of every 4 top-up shots going to replenish the hybrid bunch.

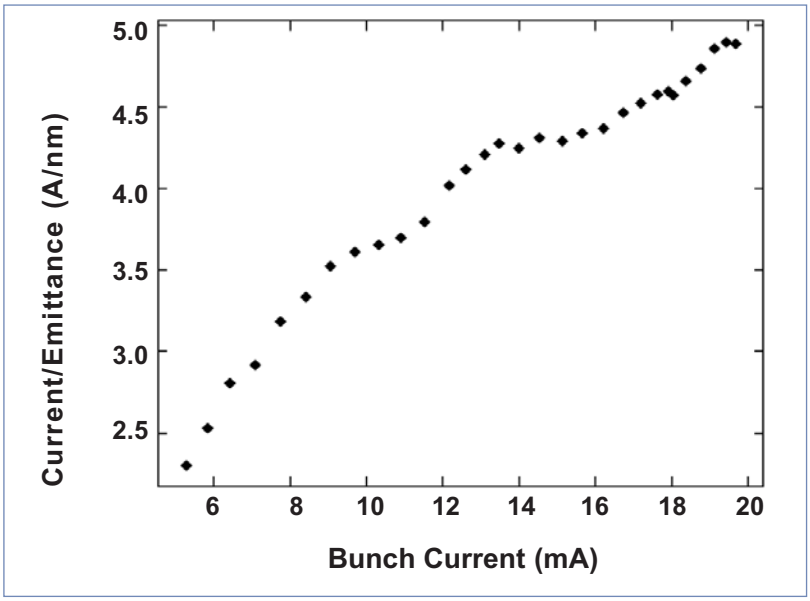

Fig. 1. Hybrid bunch current over hybrid bunch emittance as a bunch of current. This demonstrates that the brightness continues increasing even up to the instability limit at about 21 mA.

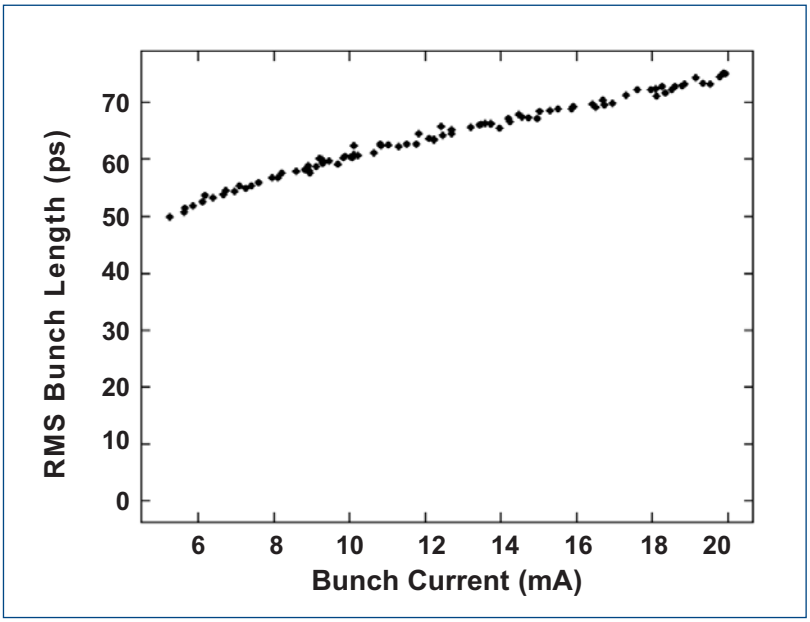

Fig. 2. Measured rms bunch duration of the hybrid bunch as a function of its current

Contact: M. Borland (borland@aps.anl.gov), L. Emery (emery@aps.anl.gov), K. Harkay (harkay@aps.anl.gov), V. Sajaev (sajaev@aps.anl.gov)

NEW PHASE DETECTORS AND SOFTWARE TO REDUCE LINAC DRIFT AND TOP-UP INTERRUPTIONS

The APS storage ring creates x-rays by sending a beam of electrons through the magnetic fields of undulators and bending magnets. Those electrons originate in the APS linear accelerator (linac) and go through a complex chain of acceleration and conditioning before injection into the storage ring. In top-up mode, the linac is required to provide beam at intervals of 60 or 120 s. This process is highly automated and has recently become more reliable owing to the addition of new diagnostics and feedback loops.

Like all high-energy electron linacs, the APS linac uses radio frequency (rf) electromagnetic fields to accelerate electrons. This process starts in one of two rf electron guns and continues through a long series of accelerating structures. Both the guns and the structures have a resonant frequency of 2856 MHz. How much energy the beam picks up from any structure depends on the phase of rf in these resonant structures when the beam arrives. If the beam is "misphased," the result is not only less energy, but a large energy spread. Such a condition will create difficulties in the transport and capture of the beam, resulting in a poor fill rate or failure to keep up with beam losses during top-up.

Traditionally, direct feedback was used on the measured rf phase relative to a reference signal to attempt to control this. However, these measurements were subject to drift. Occasionally, operators would have to interrupt top-up in order to maximize the beam energy and minimize the energy spread. In addition, operators would have to adjust phases manually whenever starting the linac.

As a result of several years of development by the ASD Diagnostics Group, the APS linac now supplies measurements of the rf phases relative to the beam itself. This eliminates problems with drift of a reference signal, since the beam now generates the reference for each structure. Using these signals, the ASD Operations and Analysis Group, working with the Diagnostics Group and the ASD Main Control Room Group, set up feedback loops that regulate the beam-to-rf phases. These obviate the need to interrupt beam and to make manual adjustments at startup. This provides more reliable beam and faster recovery from linac shutdowns.

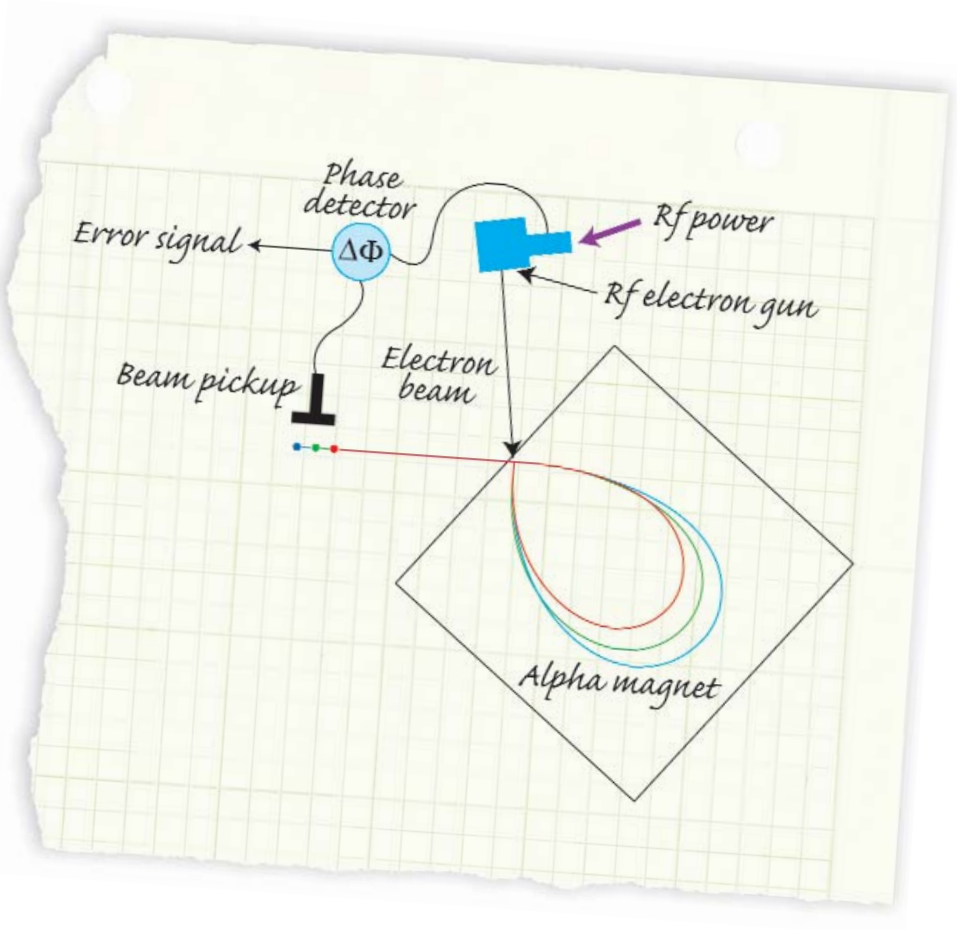

Fig. 1. Schematic of the concept behind rf gun energy regulation using an alpha magnet and phase detector, an idea originated and first applied at APS. The time-of-flight through the alpha magnet varies with changing beam energy, as illustrated by the three different colors. This is detected as a change in beam-to-rf phase between the rf power into the gun and the beam after the alpha magnet. The phase error signal is used in a feedback loop to correct the beam energy error.

In addition, an unusual feature of the APS linac was utilized, namely the existence of special bunch-compression magnets, known as alpha magnets, following the rf guns. These magnets have a unique property: if the beam energy changes, so does the time required for the beam to travel through the magnet. Hence, one can detect energy changes by looking for arrival time changes (i.e., by looking for beam-to-rf phase changes when the beam arrives at the accelerating structure). This is illustrated in Fig. 1. Using this analysis, feedback on the beam energy from the gun was also established, a method that is much more precise and reliable than the old method of feeding back directly on the detected rf power.

Contact: Nick Sereno (sereno@aps.anl.gov),
M. Borland (borland@aps.anl.gov)

THE PARTICLE ACCUMULATOR RING GETS CLEANER

For users who perform certain types of time-resolved studies, storage ring bunch purity is an important measure of performance. Bunch purity is defined as the ratio of the number of particles in the unwanted bucket to that in the main buckets. The principal responsibility for generating pure bunches rests with the particle accumulator ring (PAR), one of the accelerator systems in the APS injector. The PAR is a 325-MeV electron storage ring that has two functions: First, it accumulates charge from the injector linear accelerator in order to make a bunch with the desired intensity; second, it reduces the duration of that bunch in order to make it acceptable for further acceleration in the synchrotron.

To accomplish these tasks, the PAR employs two radio frequency (rf) systems, a low-frequency ("fundamental') system and a higher-frequency ("12th harmonic") system. The fundamental system is used to capture long beam pulses from the linac, while the harmonic system is used to compress the bunch

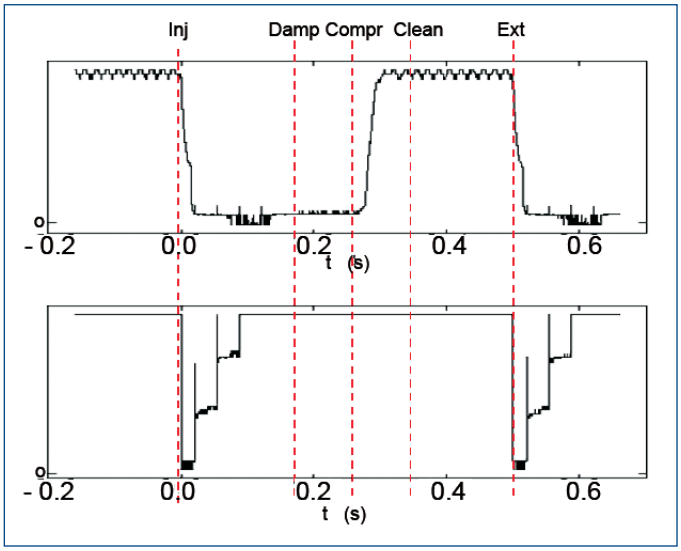

Fig.1. PAR operation cycle. The top trace is a harmonic rf waveform; the bottom trace is a beam current waveform. The marks indicate the beginning of a time segment.

length to make it acceptable to the synchrotron. During the compression process, satellite bunches with very low charge may form during the harmonic rf capture and bunch-length compression processes if the rf phase or beam charge of the rf systems vary. Once injected into the storage ring, these satellites have much longer lifetimes than the main bunches and, hence, they build up as top-up runs.

In order to maintain good storage ring bunch purity, the injector beam needs to be "clean" before it is injected into the storage ring. The new PAR bunch cleaning system is designed to ensure that this is the case.

Figure 1 shows a PAR cycle. The first 167 ms is used for fundamental rf beam capture. The next 80 ms is used for bunch-length damping under fundamental rf. Rms bunch length is reduced to about 0.9 ns by the end of this period. The harmonic rf is then turned on, and beam is again captured into the much shorter harmonic rf bucket. The bunch is further compressed to about 0.34 ns in length. At this point, the bunch cleaning system is turned on. It applies a high-frequency horizontal kick to the beam that preferentially affects the satellites and so drives out the unwanted satellites in 20 ms. After cleaning, the bunch in the PAR continues to damp its beam size and bunch length and is then extracted into the booster synchrotron.

Figure 2 shows the bunch cleaning waveform. The basic waveform is synchronized with the PAR revolution frequency and consists of two pulses with opposite polarity. The basic waveform is amplitude-modulated by a sinusoidal signal with a frequency that matches the natural horizontal frequency (or "tune") of the beam. The main bunch is timed at the zero crossing part of the basic waveform and therefore is not driven. The satellite bunches are timed at the top of the basic waveform and

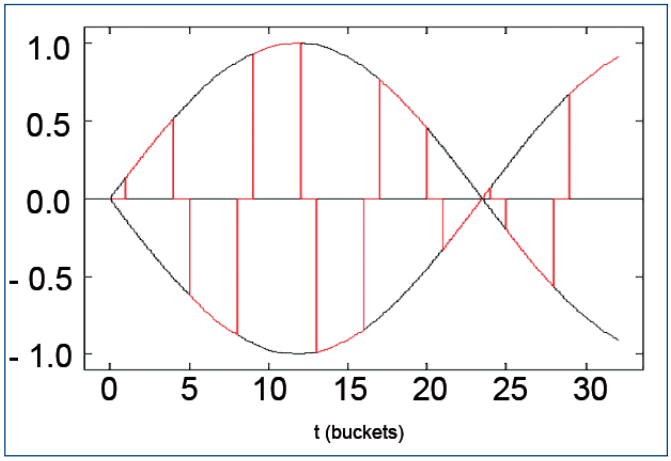

Fig.2. A bunch-cleaning drive signal The red trace is the drive signal and the black trace is the amplitude modulation signal.

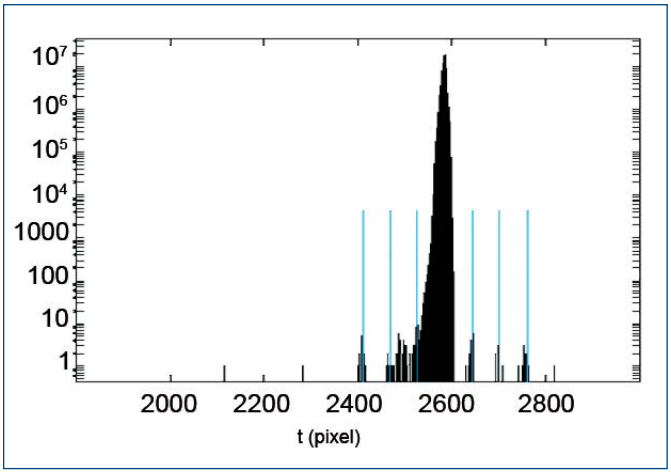

Fig. 3. A bunch purity measurement result. The main peak reflects the change in the main bucket. The blue lines mark the location of the satellites. Left is the later side in time.

are driven by the modulating tune signal. The oscillation amplitude of the satellite bunches grows with time due to resonant excitation and these bunches are eventually lost. The effectiveness of the system depends strongly on the timing accuracy and consistency between beam bunches and the drive waveform. Substantial effort was spent on improving beam stability in order to achieve better bunch cleaning performance.

Bunch purity in the storage ring is measured by an x-ray avalanche photon detector. Bunch purity of the storage ring has improved from a few $\times 10^{-6}$ to 2×10^{-7} since the installation and operation of the PAR bunch cleaning system. The consistency of the bunch purity has also improved greatly. Figure 3 shows a plot of a recent storage ring bunch purity measurement.
Contact: C.-Y. Yao (cyao@aps.anl.gov)

IMPROVING INJECTOR RELIABILITY

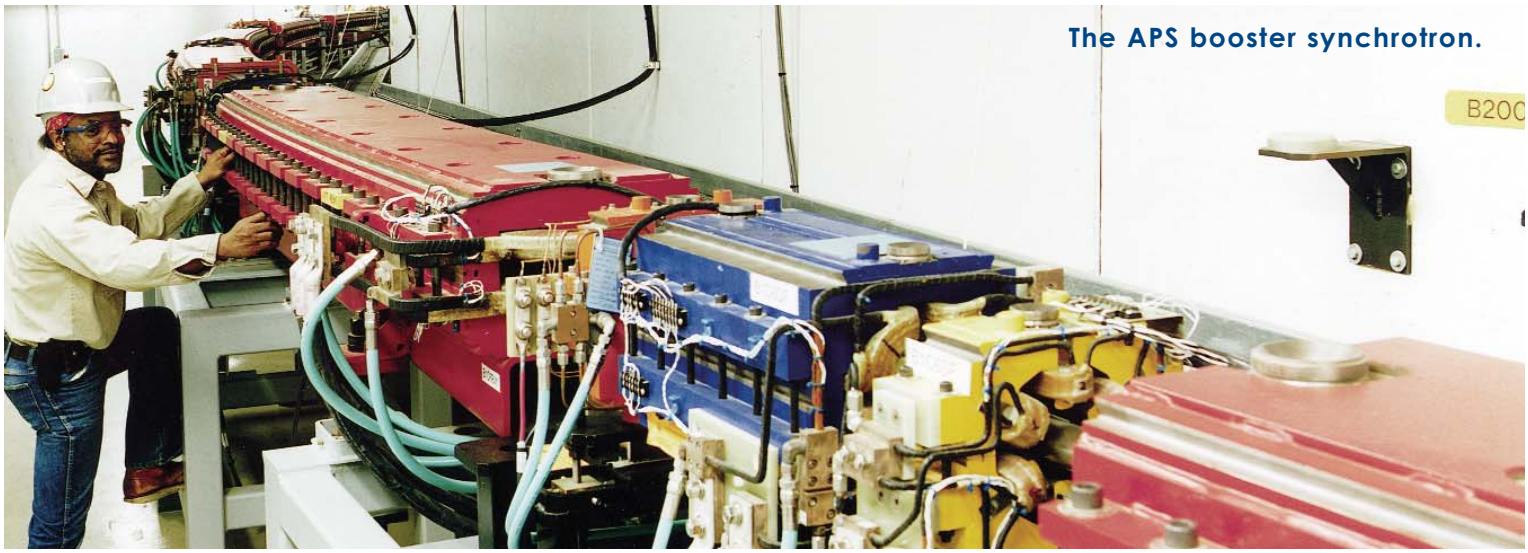

The APS booster synchrotron.

Three injector accelerators must work together to provide the stable, reliable, high-energy electron beam that the APS storage ring uses to produce x-rays for user science. The APS booster synchrotron (the third and final stage in the acceleration process) injects electron beam into the ring at 7 GeV. In top-up mode, the booster is required to provide beam at intervals of 60 s or 120 s. This represents the most demanding APS operations mode. Injector operation is now highly automated and has recently become more reliable owing to the addition of new automatic software to correct errors in the booster magnet power supply outputs.

The booster accelerates the electron beam from low energy (usually 325 MeV) to 7 GeV in 223 ms. The booster magnets, which are families of dipoles, quadrupoles, and sextupoles, must ramp from low to high current in 223 ms during the acceleration process. As these magnets ramp, the current in each must follow a linear trend within a tight tolerance so that the electron beam is not lost as it accelerates.

In the past, human operators were required to monitor each magnet power supply and manually operate software to correct the magnet power supply current. This would sometimes lead to poor efficiency until an operator could correct the supplies manually. Now, new software operates in a watchdog mode, detects when the booster power supplies require feedback correction, and corrects the supplies immediately as required, thereby relieving operations personnel of the need to constantly monitor the power supplies. Routine booster operation is now fully automated, thanks to the addition of this software. Other tasks previously requiring manual intervention, such as optimization of the injection trajectory, injection energy, and injection phase, were automated in 2004.
Contact: N. Sereno (sereno@aps.anl.gov)

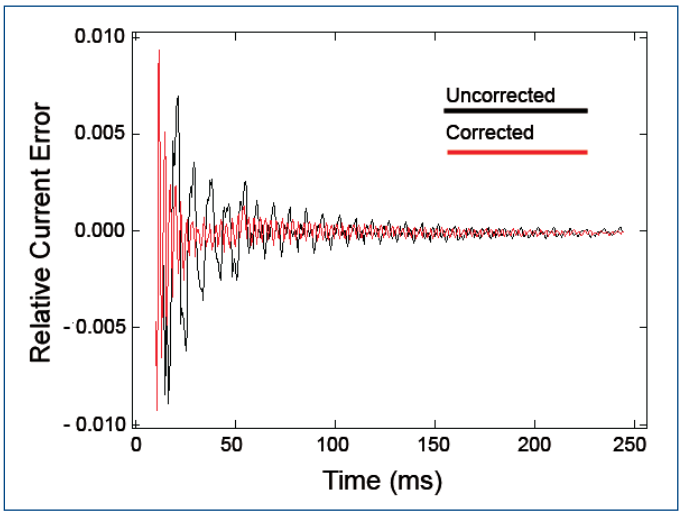

Fig. 1. Relative current error of the booster dipole before and after correction. The large ripples in the uncorrected trace would result in a loss of beam in the booster, making top-up injection difficult. The new software automatically detects and corrects problems such as these.

A MULTILAB COLLABORATION TOWARD A SUPERCONDUCTING UNDULATOR

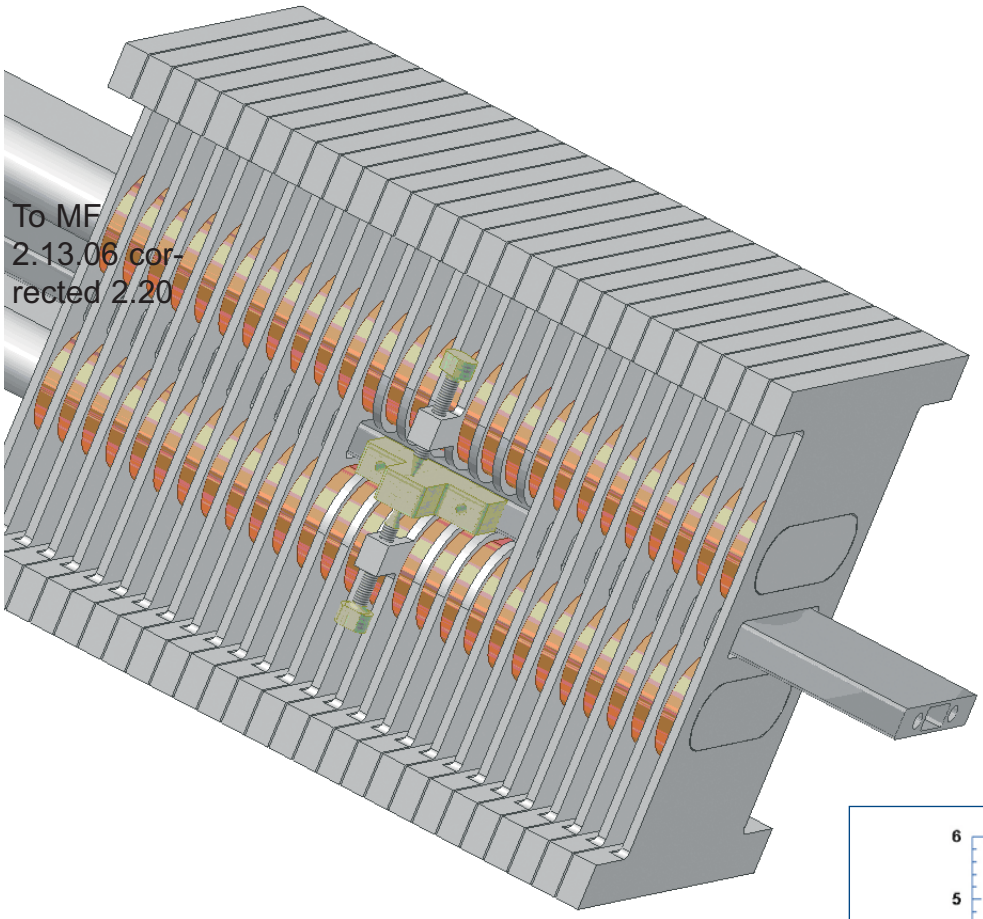

< Fig. 2. A conceptual design for the superconducting undulator. The superconducting coils are above and below the beam tube. Thermal standoffs maintain the vacuum gap between the 77K beam tube and the 4K superconductor.

The APS is working with the National High Magnetic Field Lab (NHMFL, in Tallahassee, FL), and with Lawrence Berkeley National Laboratory (LBNL) on the challenges involved in building a superconducting undulator for the APS.

APS Science 2004 (ANL-05/04) carried a report ("Superconducting Undulator R&D," page 153) on successful tests at the APS of an undulator segment using NbTi superconductor. The possibility of using the alternative Nb_3Sn superconducting material is now being investigated. Nb_3Sn superconductor offers a higher superconducting quench temperature, a higher critical field, and higher critical current density. An undulator built with Nb_3Sn wire would be expected to reach higher field strength. The drawback is that Nb_3Sn conductor requires heat treatment, after which the superconductor strands become brittle. (The advantage of a Nb_3Sn undulator can be seen in Fig. 1.)

A conceptual design for a Nb_3Sn 15-cm-period superconducting undulator and cryosystem for the APS was completed at the NHMFL [1], and a follow-on project is now under way to demonstrate the feasibility of the design and to test two differ-

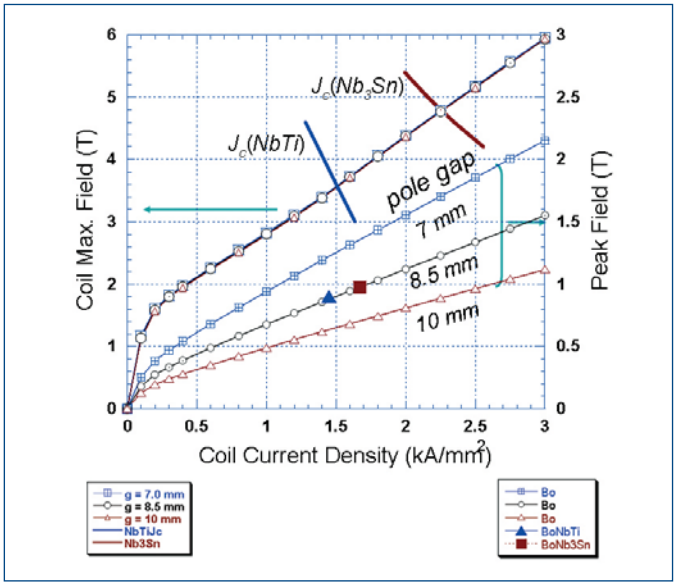

Fig. 1. Calculated peak field on the beam axis (right) and the maximum field in the coil (left) for a 14.5-mm-period undulator are shown as a function of the average current density in the coil for three pole gaps: 7, 8.5, and 10 mm. The critical current densities Jc and maximum coil fields of the two superconductor coils at 4.2K are also shown. The filled triangle on the peak field curve for the 8.5-mm gap was achieved for the NbTi test. The filled rectangle was achieved in the Nb_3Sn test.

ent assembly schemes. A schematic is shown in Fig. 2. Superconducting coils above and below the beam axis are thermally isolated from the beam tube by a small vacuum gap. The beam tube will be held at liquid nitrogen temperature so that much of the beam heat load will be removed without affecting the ~4K environment of the superconductor. The smaller heat load at 4K—and absence of beam tube heating and pressure bursts in the storage ring vacuum in the event of a superconductor quench—make this design attractive for a storage ring that demands high reliability. The slightly larger pole gap required for thermal isolation is compensated for by using Nb_3Sn superconductor, which has a higher critical current as compared to NbTi.

Two different assembly schemes are being tested. One starts with a single-piece iron yoke (Fig. 3). The superconducting wire is wound around the yoke, with all periods being wound continuously. This avoids joints in the superconducting wire that would add slightly to the heat load at 4K.

The other scheme, shown in Fig. 4, is to make the undulator modular. Individual coils are manufactured, each wrapped around its own stainless steel core. The coils would be stacked on a pair of assembly rods, alternating with iron pole pieces. Joints would have to be made between the coils after assembly. This scheme may allow more adjustment possibilities than the monolithic core, and a coil with problems could simply be discarded.

One of the potential challenges with Nb_3Sn conductor is flux jumping, which results in the coil quenching at currents well below what was expected from quench measurements of short sections of wire. Some tests were run at the APS with Nb_3Sn conductor wound on the same design of low-carbon steel cores that was used in the earlier NbTi tests. In these initial tests, the expected critical current was not reached, as shown in Fig. 1, because flux jumping intervened.

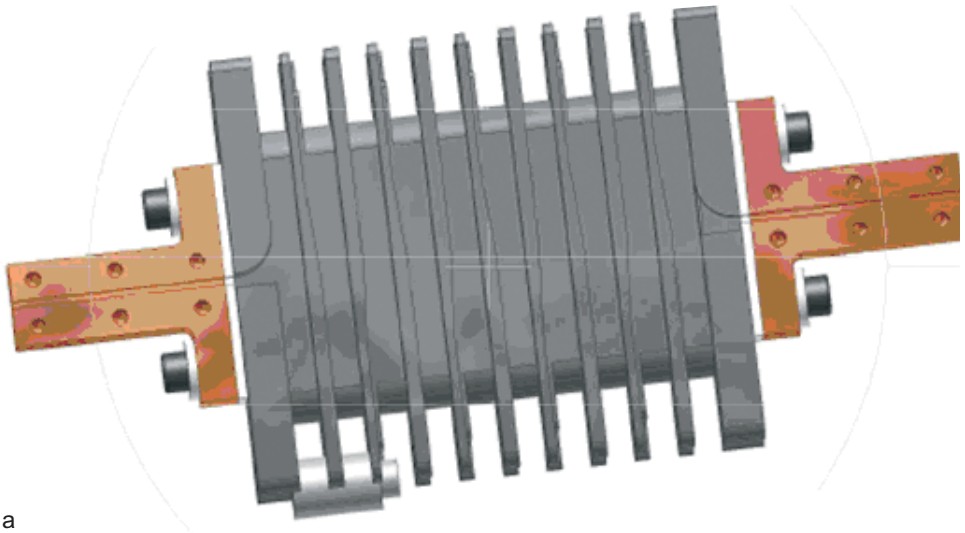

Fig. 3. Five-period-long test yoke. After the winding is complete in one groove, the wire is wrapped around a "button,", seen on the lower edge, to reverse the winding direction for the next groove. This use of buttons was developed at LBNL [3].

A common cure for flux jumping is to make the conductors smaller in diameter. The usual fiberglass insulation is thick, so when the strands get smaller the fraction of superconductor in the coil pack drops. Less superconductor means less current and a smaller field on the undulator axis. In Fig. 1., the critical current J_c for Nb_3Sn would be higher than what is shown if the wire could be packed more compactly than the ~56% packing assumed. With NbTi, the packing factor exceeded 90% because of the thin Formvar insulation. However, the insulation

Continued on next page

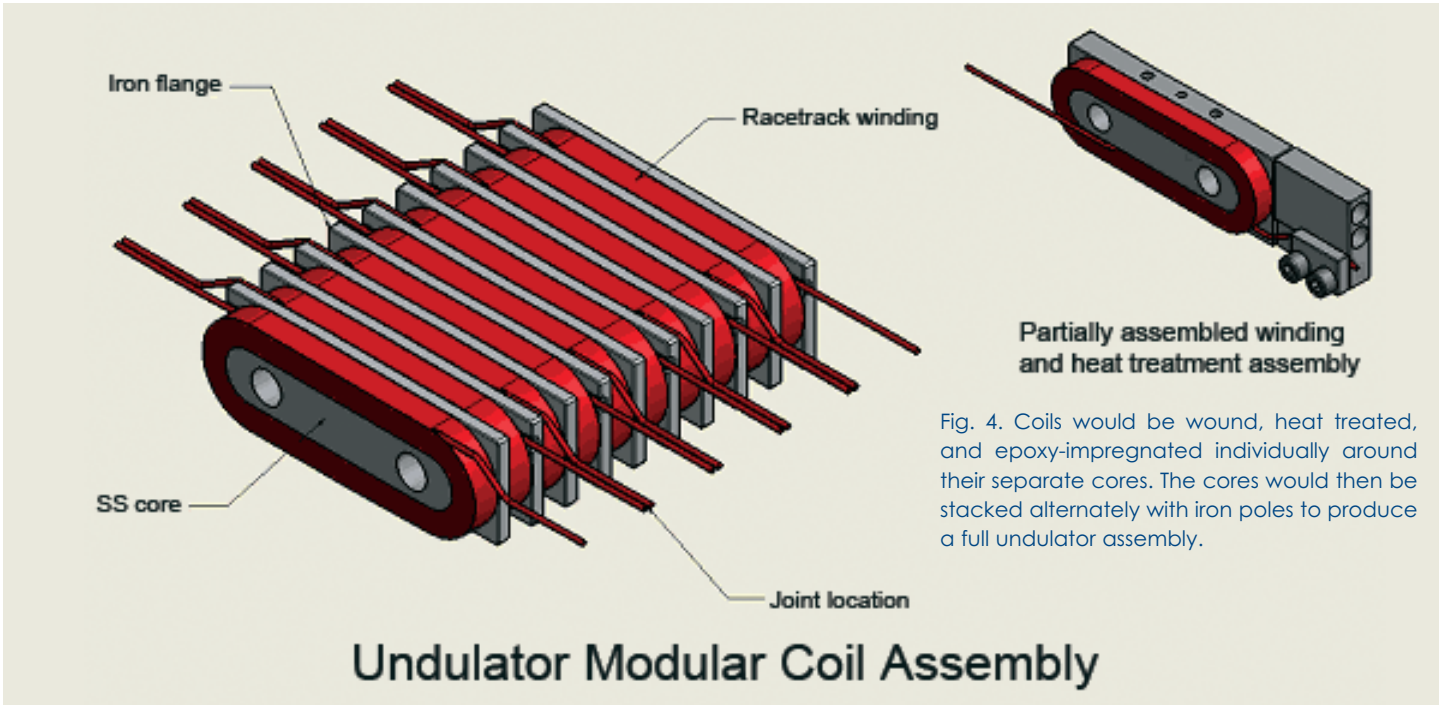

Fig. 4. Coils would be wound, heat treated, and epoxy-impregnated individually around their separate cores. The cores would then be stacked alternately with iron poles to produce a full undulator assembly.

APS Source Parameters

Undulator A

Period: 3.30 cm
Length: 2.4 m
K_{max}: 2.74 (effective; at minimum gap)
Minimum gap: 10.5 mm
Tuning range: 3.0–13.0 keV (1st harmonic)
3.0–45.0 keV (1st-5th harmonic)
On-axis peak brilliance:
5.0×10^{19} ph/s/mrad²/mm²/0.1%bw at 7 keV
Source size and divergence at 8.0 keV:
Σ_x: 275 μm Σ_y: 9 μm
$\Sigma_{x'}$: 12.6 μrad $\Sigma_{y'}$: 6.4 μrad

2.70-cm Undulator (sector 3)

Period: 2.70 cm
Length: 2.4 m
K_{max}: 1.78 (effective; at minimum gap)
Minimum gap: 10.5 mm
Tuning range: 6.7–16.0 keV (1st harmonic)
6.7–60.0 keV (1st-5th harmonic, non-contiguous)
On-axis peak brilliance:
7.0×10^{19} ph/s/mrad²/mm²/0.1%bw at 8.5 keV
Source size and divergence at 8.0 keV:
Σ_x: 275 μm Σ_y: 9 μm
$\Sigma_{x'}$: 12.6 μrad $\Sigma_{y'}$: 6.4 μrad

3.00-cm Undulator (sector 30)

Period: 3.00 cm
Length: 2.4 m
K_{max}: 2.20 (effective; at minimum gap)
Minimum gap: 10.5 mm
Tuning range: 4.6–14.5 keV (1st harmonic)
4.6–50.0 keV (1st-5th harmonic)
On-axis peak brilliance:
5.9×10^{19} ph/s/mrad²/mm²/0.1%bw at 8 keV
Source size and divergence at 8.0 keV:
Σ_x: 275 μm Σ_y: 9 μm
$\Sigma_{x'}$: 12.6 μrad $\Sigma_{y'}$: 6.4 μrad

3.50-cm SmCo Undulator (sector 4)

Period: 3.50 cm
Length: 2.4 m
K_{max}: 3.08 (effective; at minimum gap)
Minimum gap: 9.5mm
Tuning range: 2.3–12.5 keV (1st harmonic)
2.3–42.0 keV (1st-5th harmonic)
On-axis peak brilliance:
4.5×10^{19} ph/s/mrad²/mm²/0.1%bw at 7 keV
Source size and divergence at 8.0 keV:
Σ_x: 275 μm Σ_y: 9 μm
$\Sigma_{x'}$: 12.6 μrad $\Sigma_{y'}$: 6.4 μrad

5.50-cm Undulator (sector 2)

Period: 5.50 cm
Length: 2.4 m
K_{max}: 4.97 (effective; at minimum gap)
Minimum gap: 14.0 mm
Tuning range: 0.6–7.0 keV (1st harmonic)
0.6–25.0 keV (1st-5th harmonic)
On-axis peak brilliance:
2.0×10^{19} ph/s/mrad²/mm²/0.1%bw at 4 keV
Source size and divergence at 4.0 keV:
Σ_x: 275 μm Σ_y: 9 μm
$\Sigma_{x'}$: 13.9 μrad $\Sigma_{y'}$: 8.6 μrad

Fig. 5. A test section of undulator, designed, wound, and heat treated at LBNL. Another section is being prepared using ceramic-insulated wire. The LBNL design includes endshoes, at the top and bottom in the photo above, that provide additional support to the coil and help fill in voids.

for Nb_3Sn must be able to survive the ~700° C heat treatment.

A group of researchers at LBNL has been working on the development of a Nb_3Sn-based superconducting undulator for ALS [2,3]. The group is funded by the APS to investigate an alternative type of ceramic insulation that is much thinner. They are winding test sections of undulator using the same conductor, but with the two types of insulation in order to compare the properties. The fiberglass ("S-glass") thickness is ~70 μm, whereas the thickness of the ceramic is ~15 μm. If the ceramic-insulated wire works well, it would be a good choice for a full-size undulator. Figure 5 shows the fiberglass test section after winding and heat treating.

Another aspect of the work at LBNL is examination of the Nb_3Sn reaction process. The raw material must be heated for the Nb and Sn to react and make the brittle superconducting material. If the temperature stays hot for too long, the Sn begins to contaminate the Cu matrix. (The superconducting wire consists of small strands of superconductor embedded in a Cu matrix.) Sn contamination raises the resistivity of the Cu at cryogenic temperature. A low resistivity in the Cu matrix at cryogenic temperature contributes to a more stable superconducting coil and can help reduce instability from flux jumping. It may be advantageous to incompletely react the Nb and Sn, even though that reduces the superconducting critical current, if the current where flux jumping begins is increased.

Ultimately, results of these studies will be used to construct a superconducting undulator to be installed in the APS storage ring. The first goal is an undulator that produces first-harmonic radiation ranging from 19 to 28 keV.

Contact: Liz Moog (moog@aps.anl.gov)
Suk Hong Kim (shkim@aps.anl.gov)

References

[1] H.W. Weijers, K.R. Cantrell, A.V Gavrilin, and J.R. Miller, "A short-period high-field Nb3Sn undulator study," 19th Magnet Technology Conference (MT-19), Genova, Italy, Sept 19-23 (2005); and H.W. Weijers, A.V. Gavrilin, K.R. Cantrell, and J.R. Miller, "A Short Period High Field Nb_3Sn Undulator Demonstration," Int. Workshop on Undulator Systems for Free Electron Lasers (WUS), DESY, Hamburg, Germany, June 6-8 (2005).

[2] S.O. Prestemon, D.R. Dietderich, S.E. Bartlett, M. Coleman, S.A. Gourlay, A.F. Lietzke, S. Marks, S. Mattafirri, R.M. Scanlan, R.D. Schlueter, B. Wahrer, and B. Wang, "Design, Fabrication, and Test Results of Undulators Using Nb_3Sn Superconductor," *IEEE Transactions on Applied Superconductivity* **15**, (2005), 1236, and refs. therein.

[3] S. Prestemon, D.R. Dietderich, S.A. Gourlay, P. Heimann, S. Marks, G. Sabbi, R.M. Scanlan, R. Schlueter, B. Wahrer, and B. Wang, "Design and Evaluation of a Short Period Nb_3Sn Superconducting Undulator Prototype," *Proceedings of the 2003 Particle Accelerator Conference* **2**, Joe Chew, Peter Lucas, and Sara Webber, eds. (Portland, OR, 2003), 1032.

APS Source Parameters

Circularly Polarized Undulator (sector 4)

Period: 12.8 cm
Length: 2.1 m
Circular mode:
K_{max}: 2.65 (effective; for both horizontal and vertical fields at maximum currents of 1.2 kA horizontal and 0.34 kA vertical)
B_{max}: 0.26 T (peak fields)
Tuning range: 0.5–3.0 keV (1st harmonic)
On-axis peak circular brilliance:
3.6×10^{18} ph/s/mrad^2/mm^2/0.1%bw at 1.8 keV
Linear mode:
K_{max}: 2.80 (effective; for both horizontal and vertical fields at maximum currents 1.4 kA horizontal and 0.40 kA vertical)
B_{max}: 0.29 T (peak fields)
Tuning range: 0.8–3.0 keV (1st harmonic)
0.8–10.0 keV (1st–5th harmonic)
On-axis peak linear brilliance:
2.7×10^{18} ph/s/mrad^2/mm^2/0.1%bw at 2.1 keV
Switching frequency: 0-5 Hz
Switching rise time: 20 ms
Source size and divergence at 1.5 keV:
Σ_x: 275 μm Σ_y: 9 μm
$\Sigma_{x'}$: 18.0 μrad $\Sigma_{y'}$: 14.3 μrad

Elliptical Multipole Wiggler (sector 11)

Period length: 16.0 cm
Number of poles: 34 permanent magnets, 36 electromagnets
Length: 2.8 m
$K_{x\text{-}max}$: 1.3 (effective; at maximum current 1.15 kA)
$K_{y\text{-}max}$: 14.4 (peak; at minimum gap 24.0 mm)
Switching frequency: 0–10 Hz
Critical energy: 31.4 keV (at minimum gap)
Energy range: 5–200 keV
Elliptical mode (K_x = 1.3, K_y = 14.4)
Degree of circular polarization (P_c) ~90%
On-axis peak brilliance:
1.0×10^{17} ph/s/mrad^2/mm^2/0.1%bw at 7 keV
On-axis peak angular flux density:
1.6×10^{15} ph/s/mrad^2/mm^2/0.1%bw at 7 keV
Linear mode (K_x = 0, K_y = 14.4)
On-axis peak brilliance:
2.0×10^{17} ph/s/mrad^2/mm^2/0.1%bw at 26 keV
On-axis peak angular flux density:
3.1×10^{15} ph/s/mrad^2/mm^2/0.1%bw at 26 keV
Source size and divergence at the critical energy:
Σ_x: 275 μm Σ_y: 9 μm
$\Sigma_{x'}$: 820 μrad (FWHM 1.9 mrad; non-Gaussian; linear mode)
$\Sigma_{y'}$: 47 μrad (linear mode)

APS Bending Magnet

Critical energy: 19.51 keV
Energy range: 1–100 keV
On-axis peak brilliance:
6.5×10^{15} ph/s/mrad^2/mm^2/0.1%bw at 16 keV
On-axis peak angular flux density:
9.6×10^{13} ph/s/mrad^2/0.1%bw at 16 keV
On-axis peak horizontal angular flux density:
1.6×10^{13} ph/s/mradh/0.1%bw at 6 keV
Source size and divergence at the critical energy:
Σ_x: 92 μm Σ_y: 26 μm
$\Sigma_{x'}$: 6 mrad $\Sigma_{y'}$: 47 μrad

A NEW, BLUE SmCo INSERTION DEVICE

The first undulator at the APS to be made using SmCo permanent magnets was installed in XOR sector 4 in December 2005. It is a planar hybrid device with a 3.5-cm-period length. It was designed and fabricated at the APS (Fig. 1). Sector 4 is one of two APS sectors where radiation damage to undulators has been a significant issue in recent years, as reported in *APS Science 2003* (May 2004, ANL-04/07). Those two sectors were the only ones with small-gap (5-mm beam clearance) insertion device (ID) vacuum chambers installed. The radiation damage in one of the two sectors was addressed successfully by replacing the small-gap vacuum chamber with a standard 7.5-mm-aperture ID vacuum chamber during the May 2005 shutdown. No further radiation damage to the undulators in that sector has been observed.

Replacing the vacuum chamber was not an option for sector 4, however, because the circularly polarizing undulator also installed in sector 4 requires the smaller gap. It is hoped that the greater radiation resistance of the SmCo magnets, as compared to the NdFeB used in other APS undulators, will significantly reduce the radiation damage rate. The magnets used in the undulator are of grade R32HS from Shin-Etsu Magnetics, Inc., a grade that offers a remanent field of 1.12 to 1.2 T and a coercivity H_{cJ} of 20 to 30 kOe. A high H_{cJ} is correlated with higher radiation resistance.

The period length chosen for the undulator is longer than for the standard undulator A so that photon energies at the *L* edges of ruthenium and molybdenum can be reached. Figure 2 shows the on-axis brilliance tuning curves for the first, third, and fifth harmonics of the 3.5-cm-period ID compared to undulator A (3.3-cm-period length). Although the on-axis brilliance is lower by ~5% at low harmonic energies, the 3.5-cm device offers the advantage of being able to tune to lower photon energies.

The ruthenium oxides exhibit a wide variety of fascinating properties, ranging from superconductivity to itinerant ferromagnetism to negative magnetoresistance. As such, they represent an important complement to the more familiar transition metal oxides, though they are much less well studied or understood. In many of the ruthenates, the spin, charge, and orbital degrees of freedom are believed to contribute to their complex behaviors. The best and most direct way to study this complex behavior is to perform resonant x-ray scattering at the Ru L_2-edge (2.967 keV).

Another important class of problems is one-dimensional inorganic materials that show a charge density wave, such as the molybdenum-containing blue bronze ($K_{0.3}MoO_3$). Recent measurements on the blue bronze provided evidence for a complicated many-electron quantum state. In order to provide further insight, resonant x-ray diffraction at the Mo L_2-edge (2.625 keV) can provide detailed information on the electronic structure of the Mo.

Fig. 1. The new SmCo undulator (3.5-cm-period length) in the magnet measurement laboratory prior to installation. The blue color is from anodizing of the clamps and not from the SmCo magnets. (Photo: Kurt Boerste [ASD])

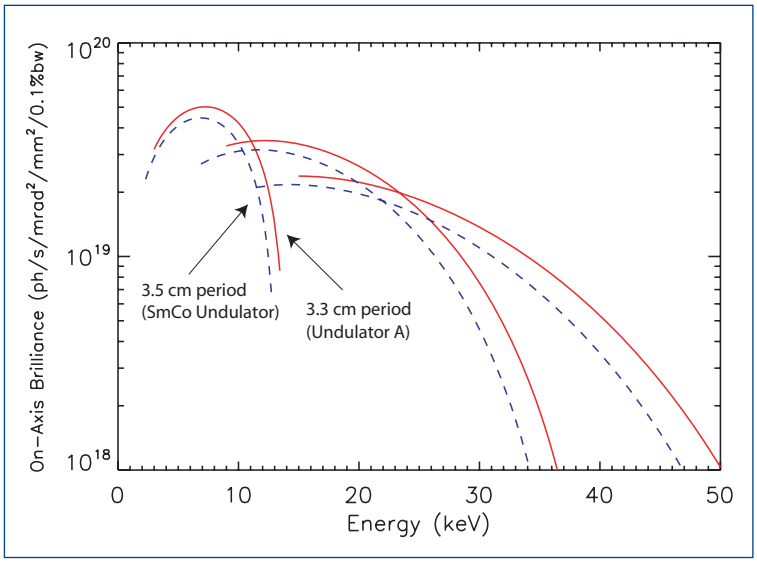

Fig. 2. On-axis brilliance tuning curves for the first, third, and fifth harmonics of the 3.5-cm-period SmCo undulator and for undulator A (3.3-cm-period) at 7.0-GeV beam energy and 100-mA beam current. The minimum gap is 9.5 mm for the SmCo undulator and 10.5 mm for undulator A. Both devices are 2.4-m long. The lowest reachable energy in the first harmonic is 2.3 keV for the SmCo device and 3.0 keV for undulator A.

Contact: L. Moog (moog@aps.anl.gov)
George Srajer (srajerg @aps.anl.gov)

This work was was supported by the U.S. Department of Energy, Office of Science, Office of Basic Energy Sciences, under Contract No. W-31-109-ENG-38.

A TUNABLE RF WAVEGUIDE WINDOW

The APS linac uses long runs of radio frequency (rf) transmission waveguide for the accelerating structures. The original structures were fabricated with WR-284-size copper waveguide. However, the power loss inherent in the waveguide was always a limiting factor in making power available to the accelerating structures. A new, lower-loss, WR340-size copper waveguide was developed that uses ceramic in-line windows. Because the windows were not stock items, the industry price was extremely high. The APS RF and Vacuum Technology groups decided to design and fabricate a window that could be produced at a lower cost and would solve a number of operational limitations, such as insertion loss, high-power performance, and the need to discard a complete window in the event of a failure.

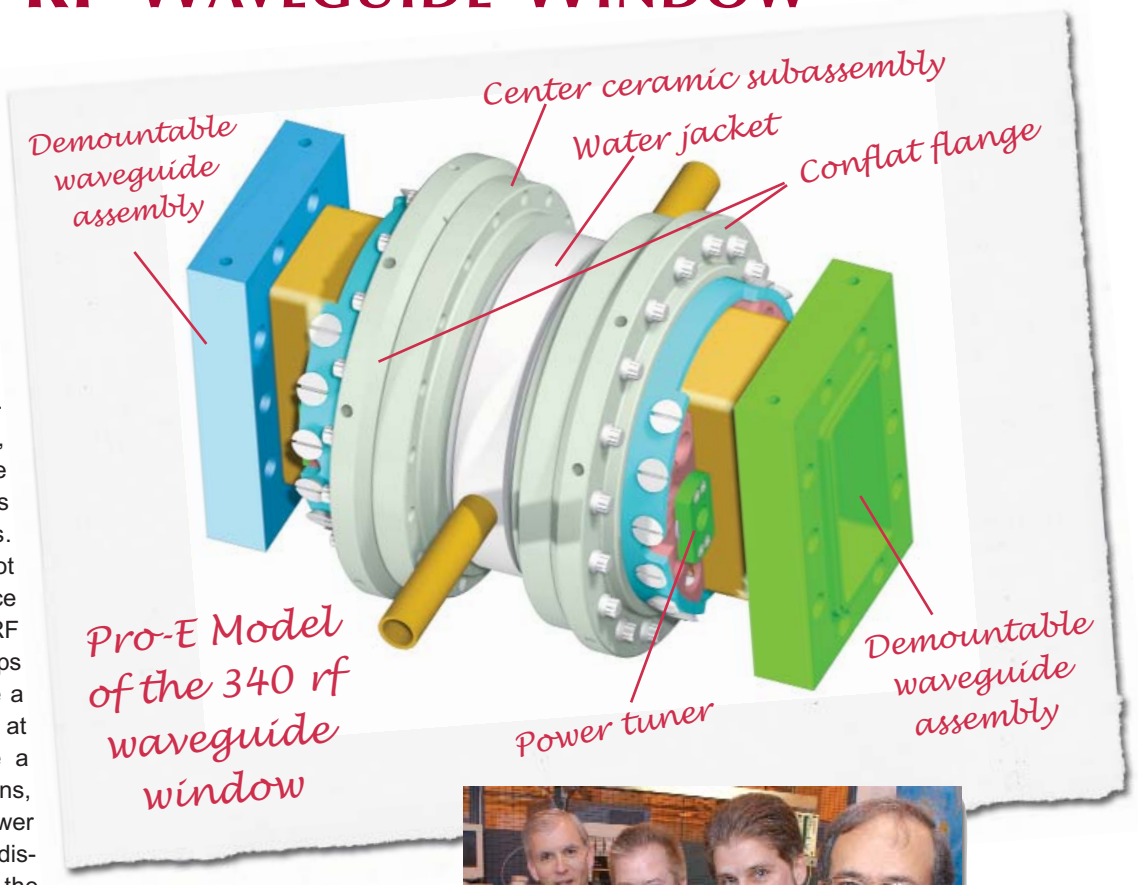

The APS has now successfully produced WR340 ceramic windows that exhibit a measured loss between 40 and 54 dB when tested at 2856 MHz, which is the linac operating frequency. A simple linear actuator is used to adjust the power transmission through the window. In high-power testing, 42 MW of peak power was safely transmitted through the window. This is well above the 35-MW peak power available for windows produced by commercial vendors.

In addition, the APS-designed window is made with replaceable subassemblies. A ceramic window is brazed to ConFlat flanges. Separate assemblies are fabricated to mate with the waveguide flanges. If any one of the subassemblies is damaged, only that component must be replaced.

The window is now in routine operation in the APS linac transmission system, both in the vacuum section and as isolation between 10^{-9}-torr vacuum sections and 30-psig sulfur hexafluoride (SF_6) pressurized sections.

Recently, Mega Industries, a manufacturer of rf components and equipment, has purchased the licensing rights to sell the APS 340 window commercially. They were impressed with the low return loss, elimination of fixed brazing posts, the single-braze-cycle fabrication of the window, and the fact that the window design is adaptable to other waveguide sizes besides WR340.

The production 340 waveguide window and the APS personnel who collaborated on the project. Front to back: Art Grelick, Terry Smith, Steve Berg (all ASD), and George Goeppner (AES).

Contact: T. Smith (tls@aps.anl.gov), G. Goeppner (gag@aps.anl.gov), A. Grelick (grelick@aps.anl.gov)

APS DATA

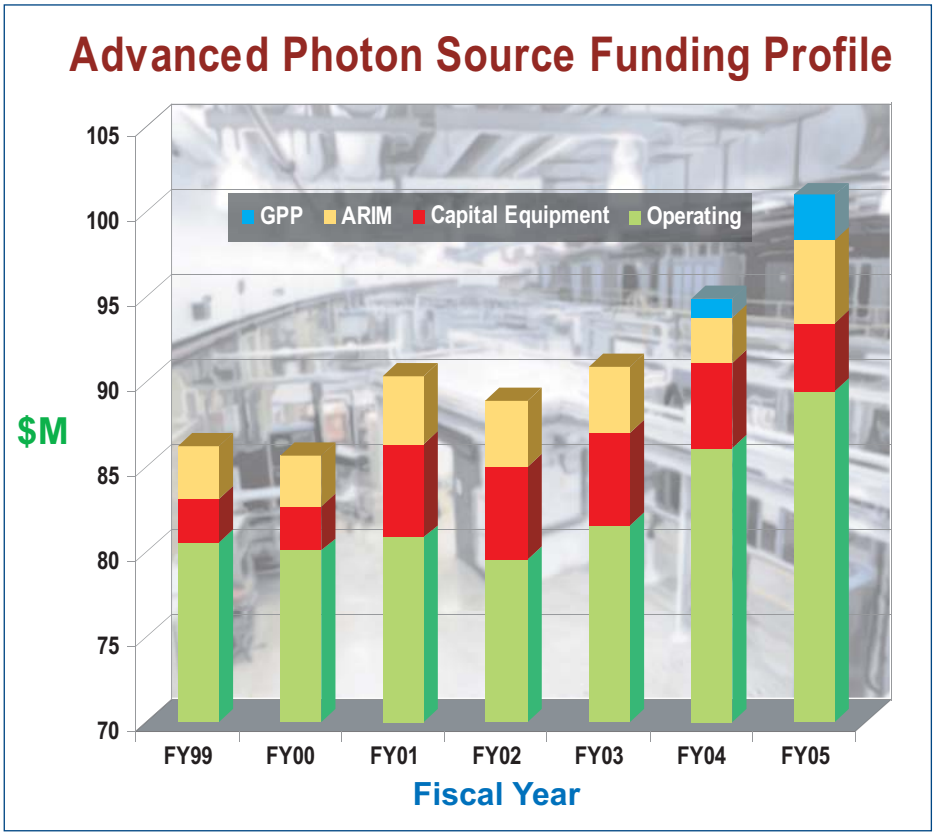
Advanced Photon Source Funding Profile
105
100
95
90
85
80
75
70
$M
GPP
ARIM
Capital Equipment
Operating
FY99
FY00
FY01
FY02
FY03
FY04
FY05
Fiscal Year

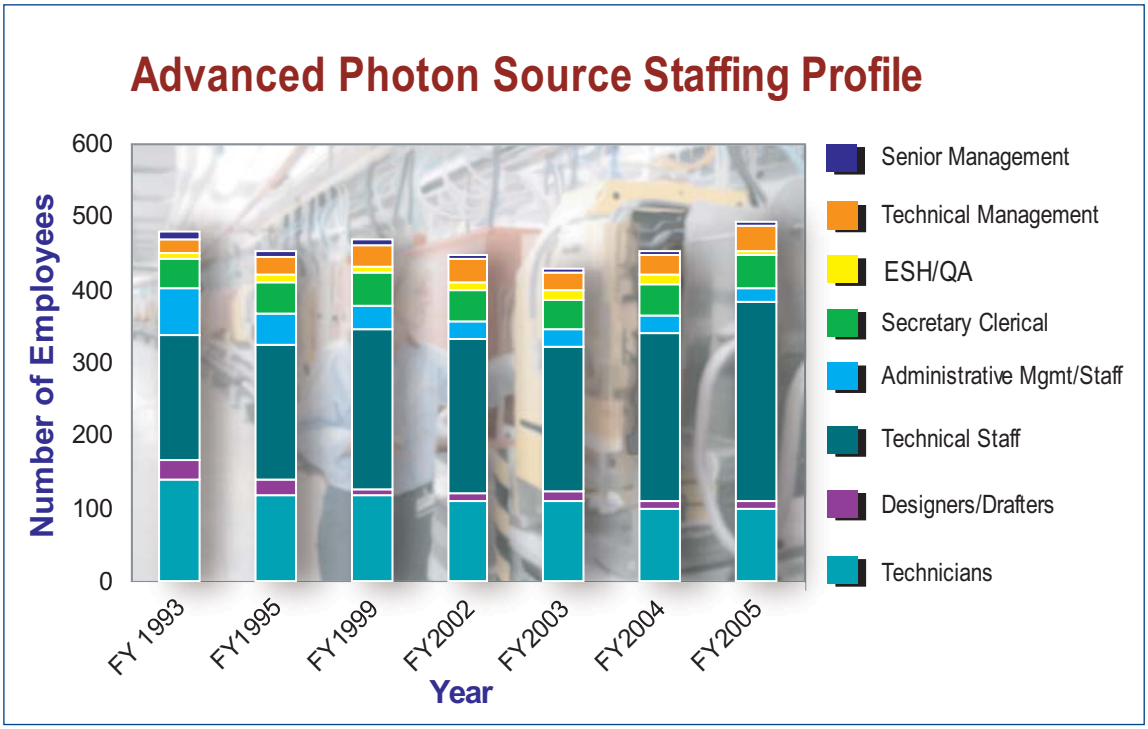
Advanced Photon Source Staffing Profile
600
500
400
300
200
100
0
Number of Employees
FY 1993
FY1995
FY1999
FY2002
FY2003
FY2004
FY2005
Year
Senior Management
Technical Management
ESH/QA
Secretary Clerical
Administrative Mgmt/Staff
Technical Staff
Designers/Drafters
Technicians

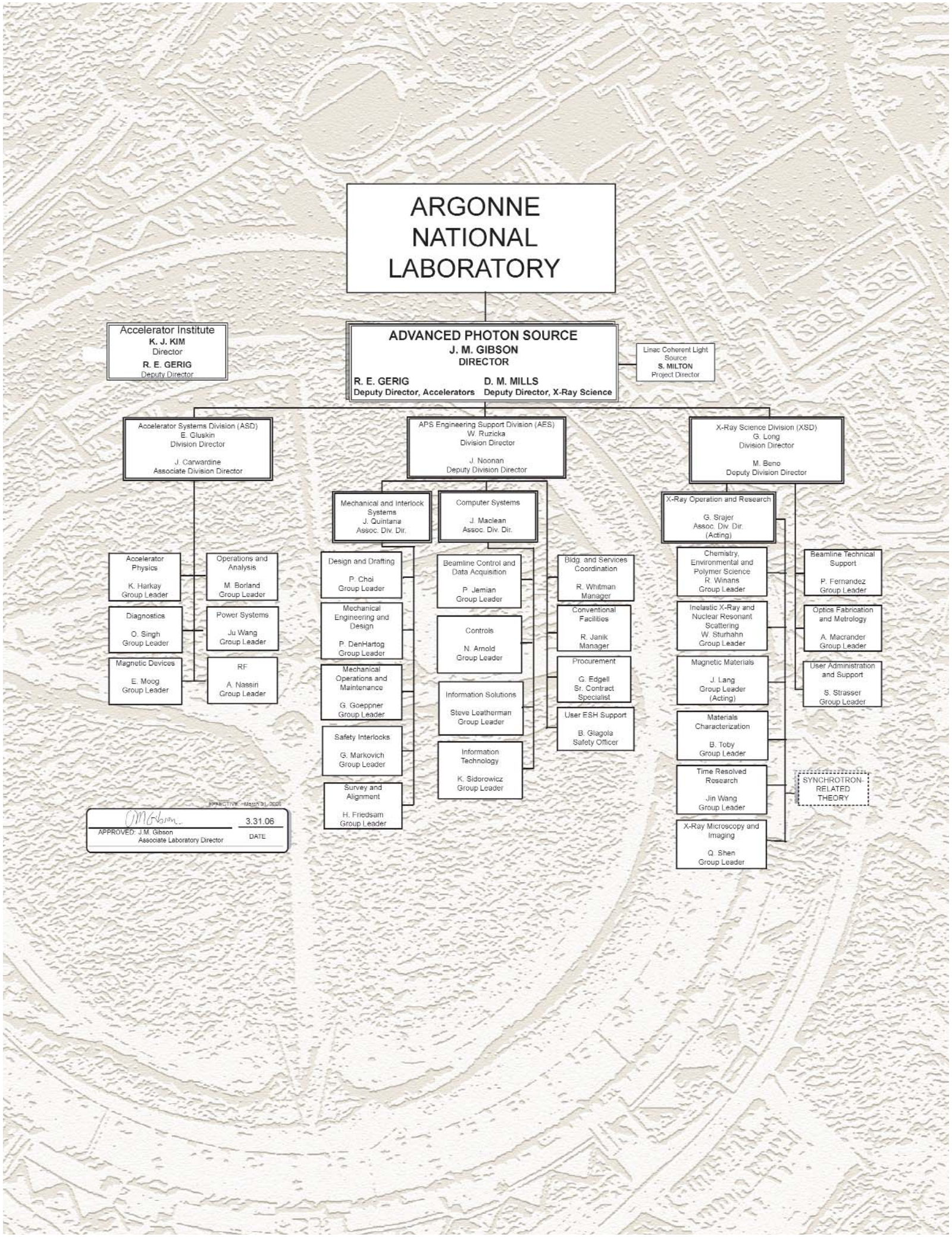
ARGONNE NATIONAL LABORATORY
Accelerator Institute
K. J. KIM
Director
R. E. GERIG
Deputy Director
ADVANCED PHOTON SOURCE
J. M. GIBSON
DIRECTOR
R. E. GERIG
Deputy Director, Accelerators
D. M. MILLS
Deputy Director, X-Ray Science
Linac Coherent Light Source
S. MILTON
Project Director
Accelerator Systems Division (ASD)
E. Gluskin
Division Director
J. Carwardine
Associate Division Director
APS Engineering Support Division (AES)
W. Ruzicka
Division Director
J. Noonan
Deputy Division Director
X-Ray Science Division (XSD)
G. Long
Division Director
M. Beno
Deputy Division Director
Accelerator Physics
K. Harkay
Group Leader
Operations and Analysis
M. Borland
Group Leader
Diagnostics
O. Singh
Group Leader
Power Systems
Ju Wang
Group Leader
Magnetic Devices
E. Moog
Group Leader
RF
A. Nassiri
Group Leader
Mechanical and Interlock Systems
J. Quintana
Assoc. Div. Dir.
Computer Systems
J. Maclean
Assoc. Div. Dir.
Design and Drafting
P. Choi
Group Leader
Mechanical Engineering and Design
P. DenHartog
Group Leader
Mechanical Operations and Maintenance
G. Goeppner
Group Leader
Safety Interlocks
G. Markovich
Group Leader
Survey and Alignment
H. Friedsam
Group Leader
Beamline Control and Data Acquisition
P. Jemian
Group Leader
Controls
N. Arnold
Group Leader
Information Solutions
Steve Leatherman
Group Leader
Information Technology
K. Sidorowicz
Group Leader
Bldg. and Services Coordination
R. Whitman
Manager
Conventional Facilities
R. Janik
Manager
Procurement
G. Edgell
Sr. Contract Specialist
User ESH Support
B. Glagola
Safety Officer
X-Ray Operation and Research
G. Srajer
Assoc. Div. Dir. (Acting)
Chemistry, Environmental and Polymer Science
R. Winans
Group Leader
Inelastic X-Ray and Nuclear Resonant Scattering
W. Sturhahn
Group Leader
Magnetic Materials
J. Lang
Group Leader (Acting)
Materials Characterization
B. Toby
Group Leader
Time Resolved Research
Jin Wang
Group Leader
X-Ray Microscopy and Imaging
Q. Shen
Group Leader
Beamline Technical Support
P. Fernandez
Group Leader
Optics Fabrication and Metrology
A. Macrander
Group Leader
User Administration and Support
S. Strasser
Group Leader
SYNCHROTRON-RELATED THEORY
EFFECTIVE March 31, 2006
APPROVED: J.M. Gibson
Associate Laboratory Director
3.31.06
DATE

Partner User Proposals Approved for Beam Time

Investigators	Partner User Proposal Title (PUP number)	Beamline	Beam Time Award
T.A. Calcott, D.L. Ederer J. Freeland, G. Srajer	Soft X-ray Spectroscopy for the Study of Complex Magnetic Materials (PUP-1)	4-ID-C	10%/run for three years beginning with run 2003-3 through 2006-2
J. Wang, S. E. Parrish R. Poola, P.V. Farrell M.-C. Lai, S. Gruner	Fuel Spray Research at the 1-BM Beamline at the APS (PUP-3)	1-BM	30%/run for three years beginning with run 2003-3 through 2006-2
J. Lang, D. Haskel Z. Islam, G. Srajer	Enhanced Sensitivity of X-ray Magnetic Circular Dichroism Measurements Using Phase Lock-in Detection (PUP-7)	4-ID-D	15%/run for two years beginning with run 2003-3 through 2005-2
D. Keavney, J. Freeland R. Rosenberg	Incorporation of a High-Field Magnet on Beamline 4-ID-C (PUP-8)	4-ID-C	15%/run for one year beginning with run 2003-3 through 2004-2 (completed)
S. Shastri, D. Haeffner W.-K. Lee, U. Lienert	High-Energy X-ray Optics Development (50-100 keV) at the XOR 1-ID Beamline at the APS (PUP-9)	1-ID	10%/run for three years beginning with run 2003-3 through 2005-2
W. Sturhan, J. Zhao J.-F. Lin, J. Jackson G. Shen	Nuclear Resonant Scattering under High Pressure and High Temperature (PUP-10)	3-ID	15%/run for one year beginning with run 2003-3 through 2004-2 (completed)
S. Mochrie, L. Lurio A. Sandy, S. Narayanan	Development of X-ray Photon Correlation Techniques to Probe Soft Matter and Complex Fluids (PUP-17)	8-ID-I	15%/run for one year beginning with run 2003-3 through 2004-2 (completed)
U. Lienert H. Poulson R. Suter	*In Situ* Structural Characterization of Bulk Polycrystalline Materials on the Single-Grain Length Scale by High-Energy Synchronization (PUP-19)	1-ID	10%/run for two years beginning with run 2004-1 through 2005-3
D. Reis, P. Bucksbaum R. Clarke, E. Dufresne	Ultrafast X-ray Science: A Partner User Proposals for Establishing a User Base for Time-Resolved Science at MHATT-CAT, Sector 7 (PUP-20)	7-ID	20%/run for one year beginning with run 2004-1 through 2004-3
E.D. Crozier	Pacific Northwest Consortium Synchrotron Radiation Facility-XOR Partnership Proposal (PUP-21)	20-ID	15%/run for three years beginning with run 2004-1 through 2006-3
E. Stern, E.D. Crozier S. Heald, G. Seidler Y. Yacoby, D. Brewe J. Cross	Novel X-ray Spectroscopies and Microscopies for the Determination of Structure with Atomic Resolution (PUP-24)	20-ID 20-BM	30% for two years on both lines beginning with run 2004-3 through 2006-2
S. Mochrie, A. Sandy L. Lurio, S. Narayanan	Development of Small-Angle X-ray Photon Correlation Spectroscopy for Studies of the Dynamics of Soft Matter (PUP-35)	8-ID-I	20% for three years beginning with run 2004-3 through 2007-2
L. Young, S. Southworth D. Ederer, E. Landahl E. Kanter, B. Kraessig R. Dunford	Ultrafast and Ultrasmall Laser X-ray Techniques (PUP-37)	7-ID	15% for three years beginning with run 2004-3 through 2007-2
L. Soderholm S. Skanthakumar J. Neuefeind P. Burns, M. Beno	Short-range Order in Solution: Development of a Dedicated Beam Line for Pair-Distribution Functions Studies at the APS (PUP-42)	11-ID-B	10% per run for two years beginning with run 2005-1
Y. Lee, B. Khaykovich Z. Islam, G. Srajer J. Hill, J. Lang	Establishing a High-Magnetic-Field Capability at the APS (PUP-43)	4-ID-D	10% per run for two years beginning with run 2005-1
D. Keavney	Implementation of Low-Temperature Magnetic Imaging Using Photoemission Electron Microscopy at 4-ID-C (PUP-44)	4-ID-C	10%/run for one year beginning with run 2005-1
D. Reis, R. Clarke P. Bucksbaum, D. Arms E. Landahl, D. Walko	Ultrafast X-ray Science: a Partner User Proposal for Establishing a User Base for Time-Resolved Science at MHATT-CAT, Sector 7 (PUP-47 [update of PUP-20])	7-ID	15% of each run for one year
L. Soderholm, P. Burns J. Neuefeind, M. Beno S. Skanthakumar	Short-range order in solution: development of a Dedicated Beamline for Pair-distribution Functions (PDF) studies at the APS (PUP-52)	11-ID-B	20% beginning 2005-3 through 2008-2
J. Miao, M. Glimcher	Three-dimensional Imaging of Nanoscale Systems Using Coherent X-rays (PUP-53)	2-ID-B	15% beginning 2005-3 through 2008-2
S. Risbud, J Amonette I. McNulty, D. Paterson E. Stern, E. D. Crozier S. Heald, G. Seidler D. Brewe, J. Cross	Novel X-ray Spectroscopies and Microscopies for the Determination of Structure with Atomic Resolution (extension of PUP-24) (PUP-55)	20-ID	Various allocations for different programs
L. Chen, K. Attenkofer G. Jennings, D. Tiede	Developing Laser Initiated Time-resolved X-ray Facility at 11-ID-D for Photochemical Research using XAS and WAXS (PUP-56)	11-ID-D	20% beginning 2006-2 through 2007-3
E. D. Crozier, T.-K. Sham R. Gordon	Pacific Northwest Consortium Synchrotron Radiation Facility-XOR Partnership Proposal (PUP-57)	20-BM	10% beginning 2006-1 through 2006-3

Abstracts for these proposals are at http://www.aps.anl.gov/Users/Scientific_Access/Partner_User_Information/Results/index.html

APS BEAMLINE GUIDE

As of 3.1.06. Source: *DOE-BES Program Review of the Advanced Photon Source at Argonne National Laboratory*, Volume 2 - Beamlines & Publications, 2005; and addt'l.

(KEY: UA: 3.3 Undulator A; BM: Bending Magnet; CPU: Circularly Polarized Undulator; CU: Canted undulator; EMW: Elliptical Multipole Wiggler; GU: General Users)

Beamline	Sector	Discipline	Supported Techniques	Source	Status
1-BM	XOR	Materials Sci., Physics, Chemistry, Geo. Sci.	Powder diffraction, Radiography (not GU) • Reflectivity/grazing incidence small-angle x-ray scattering	BM	Operational/GU
1-ID	XOR	Materials Sci., Chemistry, Physics, Geo. Sci., Instrumentation	High-energy x-ray scattering • Phase contrast imaging • High-pressure pair distribution function analysis	UA	Operational/GU
2-BM	XOR	Materials Sci., Life Sci.	Microtomography • Diffraction microscopy	BM	Operational/GU
2-ID-B	XOR	Materials Sci., Life Sci.	Scanning transmission/fluorescence x-ray microscopy • Coherent x-ray scattering	5.5-cm und.	Operational/GU
2-ID-D	XOR	Materials Sci., Life Sci.	Scanning fluorescence x-ray microscopy • Micro/nanodiffraction	UA	Operational/GU
2-ID-E	XOR	Materials Sci., Life Sci.	Scanning fluorescence x-ray microscopy	3.3-, 5.5-cm unds.	Operational/GU
3-ID	XOR	Physics, Geosci., Materials Sci, Optics Biochemistry	Nuclear resonant inelastic x-ray scattering • Momentum-resolved inelastic x-ray scattering • Synchrotron Mössbauer spectroscopy	2.7-cm unds. (x 2)	Operational/GU
4-ID-C	XOR	Physics, Materials Sci.	Photoemission electron microscopy • X-ray excited optical luminescence • X-ray magnetic circular dichroism • X-ray resonant magnetic scattering	CPU (canted)	Operational/GU
4-ID-D	XOR	Physics, Materials Sci.	X-ray magnetic circular dichroism • Anomalous & resonant scattering • Magnetic x-ray scattering	3.5-cm CU	Operational/GU
5-BM-C	DND-CAT	Materials Sci., Polymer Sci.	Tomography • Powder diffraction • White-beam experiments	BM	Operational/GU
5-BM-D	DND-CAT	Materials Sci., Polymer Sci.	X-ray absorption fine structure (XAFS) • High-energy x-ray scattering • Polymer scattering • White/pink beam	BM	Operational/GU
5-ID	DND-CAT	Materials Sci., Polymer Sci.	Macromolecular crystallography • Powder diffraction • Polymer scattering • Small-angle x-ray scattering • X-ray optics development • Inorganic crystallography • Simultaneous SAXS/WAXS	UA	Operational/GU
6-ID	MU-CAT	Materials Sci.	Liquid surface diffraction • Resonant & nonresonant magnetic x-ray scattering • Solid surface diffraction	UA	Operational/GU
6-ID-D	MU-CAT	Materials Sci.	High-energy/high-Q scattering • Powder diffraction	UA	Operational/GU
7-ID	XOR	Materials Sci.	Time-resolved x-ray scattering & spectroscopy following a 50-fs-laser-pulse excitation • Microprobe • Ultrafast x-ray imaging • General interface & surface diffraction w/a 6-circle diffractometer	UA	Operational/GU

Continued on next page

APS Beamline Guide cont'd.

(KEY: UA: 3.3 Undulator A; BM: Bending Magnet; CPU: Circularly Polarized Undulator; CU: Canted undulator; EMW: Elliptical Multipole Wiggler; GU: General Users)

Beamline	Sector	Discipline	Supported Techniques	Source	Status
8-BM	NE-CAT	Life Sci.	Macromolecular crystallography • Multiwavelength anomalous dispersion (MAD)	BM	Operational/GU
8-ID	XOR	Materials Sci.	X-ray photon correlation spectroscopy (transmission & reflection geometries) • Time-resolved small-angle x-ray scattering • Small-angle x-ray scattering • Grazing-incidence small-angle x-ray scattering	UA	Operational/GU
9-BM	XOR/CMC	Materials Sci., Chemistry	X-ray absorption spectroscopy • X-ray absorption near-edge spectroscopy	BM	Operational/GU
9-ID	XOR/CMC	Materials Sci., Physics	Momentum resolved inelastic x-ray scattering • Liquid surface/interface scattering	UA	Operational/GU
10-ID	MR-CAT	Materials Sci., Enviro. Sci.	X-ray absorption fine structure microscopy • X-ray absorption fine structure • Powder diffraction • Reflectivity • X-ray optics development • Grazing incidence x-ray diffraction & XAFS	UA	Operational/GU
11-BM	XOR	Materials Sci., Geo. Sci., Chemistry, Physics	High-resolution, high-throughput powder diffraction	BM	Construction
11-ID-B	XOR/BESSRC	Materials Sci., Geo. Sci. Chemistry, Physics	High-energy x-ray scattering	EMW	Operational/GU
11-ID-C	XOR/BESSRC	Materials Sci., Geo. Sci. Chemistry, Physics	High-energy x-ray scattering	EMW	Operational/GU
11-ID-D	XOR/BESSRC	Materials Sci., Geo. Sci. Chemistry, Physics	X-ray absorption spectroscopy (XAFS) • X-ray absorption near-edge spectroscopy (XANES) • General diffraction • Time-dependent XAFS & XANES	EMW	Operational/GU
12-BM	XOR/BESSRC	Materials Sci., Geo. Sci. Chemistry, Physics	X-ray absorption spectroscopy • Surface scattering • General diffraction	BM	Operational/GU
12-ID	XOR/BESSRC	Materials Sci., Geo. sci. Chemistry, Physics	Small-angle x-ray scattering • Surface & interface scattering	UA	Operational/GU
13-BM	GSECARS	Geo. Sci., Enviro. Sci.	Microtomography • Brillouin spectroscopy • X-ray absorption fine structure • Diamond anvil cell diffraction • Multi-anvil press diffraction & imaging	BM	Operational/GU
13-ID	GSECARS	Geo. Sci., Enviro. Sci.	Surface diffraction • Microdiffraction • Microprobe & micro-XAFS • Inelastic scattering • Diamond anvil cell diffraction & spectroscopy • Multi-anvil press diffraction & imaging	UA	Operational/GU
14-BM-C	BioCARS	Life Sci.	Macromolecular crystallography	BM	Operational/GU
14-BM-D	BioCARS	Life Sci.	Macromolecular crystallography (MAD)	BM	Operational/GU
14-ID	BioCARS	Life Sci.	Macromolecular crystallography (MAD & Laue) • Time-resolved crystallography	UA	Operational/GU
15-ID	ChemMatCARS	Materials Sci., Chemistry	Anomalous scattering • Chemical crystallography • Small-angle & wide-angle x-ray scattering • Liquid & solid surface & interface scattering	UA	Operational/GU

APS BEAMLINE GUIDE CONT'D.

(KEY: UA: 3.3 Undulator A; BM: Bending Magnet; CPU: Circularly Polarized Undulator; CU: Canted undulator; EMW: Elliptical Multipole Wiggler; GU: General Users)

Beamline	Sector	Discipline	Supported Techniques	Source	Status
16-BM	HP-CAT	Materials Sci., Geo. Sci.	Powder diffraction • Single-crystal diffraction	BM	Construction
16-ID-B	HP-CAT	Physics, Chemistry, Materials Sci., Geo. Sci. Biology	Angular dispersive x-ray diffraction • Nuclear resonant forward x-ray scattering • Nuclear resonant inelastic x-ray scattering • High-resolution x-ray emission spectroscopy • Light-element K-edge inelastic scattering • Non-resonant inelastic x-ray scattering • Resonant inelastic x-ray scattering	UA	Operational/GU
16-ID-D	HP-CAT	Physics, Chemistry Materials Sci., Geo. Sci. Biology	Angular dispersive x-ray diffraction • Nuclear resonant forward x-ray scattering • Nuclear resonant inelastic x-ray scattering • High-resolution x-ray emission spectroscopy • Light-element K-edge inelastic scattering • Non-resonant inelastic x-ray scattering • Resonant inelastic x-ray scattering	UA	Operational/GU
17-BM	IMCA-CAT	Life Sci.	Macromolecular crystallography • Multiwavelength anomalous dispersion	BM	Recommissioning
17-ID	IMCA-CAT	Life Sci.	Macromolecular crystallography • Multiwavelength anomalous dispersion	UA	Operational/GU
18-ID	Bio-CAT	Life Sci.	X-ray absorption fine structure • Fluorescence spectroscopy • Small-angle x-ray scattering • Time-resolved x-ray scattering • Fiber & powder diffraction • High-resolution inelastic x-ray • scattering spectroscopy • μ diffraction • μ XAS imaging	UA	Operational/GU
19-BM	SBC-CAT	Life Sci.	Macromolecular crystallography • Multiwavelength anomalous dispersion (MAD/SAD)	BM	Operational/GU
19-ID	SBC-CAT	Life Sci.	Macromolecular crystallography • Multiwavelength anomalous dispersion (MAD/SAD)	UA	Operational/GU
20-BM	XOR/PNC	Materials Sci., Enviro. Sci. Chemistry, Physics	X-ray absorption fine structure • Diffraction anomalous fine structure • General diffraction • X-ray microprobe	BM	Operational/GU
20-ID	XOR/PNC	Materials Sci., Enviro. Sci. Chemistry	X-ray absorption fine structure • Microfluorescence • Time-resolved XAFS • EXAFS microscopy • Diffraction anomalous fine structure • Microprobe • General diffraction • X-ray Raman spectroscopy	UA	Operational/GU
21-ID-D	LS-CAT	Life Sci.	Macromolecular crystallography • Multiwavelength anomalous dispersion (MAD/SAD)	CU	Construction
21-ID-E	LS-CAT	Life Sci.	Macromolecular crystallography • Multiwavelength anomalous dispersion (MAD/SAD)	CU	Construction
22-BM	SER-CAT	Life Sci.	Macromolecular crystallography • Multiwavelength anomalous dispersion	BM	Operational

Continued on next page

APS Beamline Guide cont'd.

(KEY: UA: 3.3 Undulator A; BM: Bending Magnet; CPU: Circularly Polarized Undulator; CU: Canted undulator; EMW: Elliptical Multipole Wiggler; GU: General Users)

Beamline	Sector	Discipline	Supported Techniques	Source	Status
22-BM	SER-CAT (cont'd.)		Macromolecular structure determinations • Single-wavelength anomalous scattering (SAD) macromolecular structure determinations		
22-ID	SER-CAT	Life Sci.	Macromolecular crystallography • Multiwavelength anomalous dispersion macromolecular structure determinations • Single-wavelength anomalous scattering • macromolecular structure determinations	UA	Operational
23-BM	GM/CA-CAT	Life Sci.	Macromolecular crystallography • Multiwavelength anomalous dispersion (MAD/SAD)	BM	Commissioning
23-ID-B	GM/CA-CAT	Life Sci	Macromolecular crystallography • Multiwavelength anomalous dispersion (MAD/SAD)	CU	Commissioning
23-ID-D	GM/CA-CAT	Life Sci	Macromolecular crystallography • Multiwavelength anomalous dispersion (MAD/SAD)	CU	Operatiional/GU
24-ID-C	NE-CAT	Life Sci.	Macromolecular crystallography • Multiwavelength anomalous dispersion	CU	Commissioning
24-ID-E	NE-CAT	Life Sci.	Macromolecular crystallography • Multiwavelength anomalous dispersion	CU	Construction
24-BM	NE-CAT	Life Sci.	Macromolecular crystallography • Multiwavelength anomalous dispersion	BM	Construction
26-ID	CNM-CDT	Nanoscience, Energy Science, Materials Science, Optics Development	Fluorescence, diffraction, & transmission imaging • Tomography • Small-angle scattering • Polarization dependent scattering	UA (x 2)	Commissioning
30-ID	IXS-CDT	Physics, Geo. Sci., Materials Sci.	Medium-energy resolution inelastic x-ray scattering • High-energy resolution inelastic x-ray scattering • Nuclear inelastic x-ray scattering	U 3.0 (x2)	Construction
31-ID	SGX-CAT	Life Sci.	Macromolecular crystallography • Multiwavelength anomalous dispersion	UA	Operational/GU
32-ID	XOR	Materials Sci. Life Sci.	Full-field microscopy & diffraction imaging • Phse contrast imaging	UA	Construction/GU
33-BM	XOR/UNI	Materials Sci., Condensed Matter Physics	X-ray topography • Diffraction & scattering • Powder diffraction • XAFS • Single-crystal diffraction • General diffraction	BM	Operational/GU
33-ID	XOR/UNI	Materials Sci. Condensed Matter Physics	Anomalous & resonant scattering • Inelastic scattering • Ultra-small-angle x-ray scattering • Surface diffraction • General diffraction • Pulsed laser deposition film growth	UA	Operational/GU
34-ID	XOR/UNI	Materials Sci. Condensed Matter Physics	Coherent x-ray scattering & diffraction • Microbeam diffraction • Microprobe	UA	Operational/GU

APS User Committees

2005 APS Scientific Advisory Committee

Pierre E. Wiltzius *(Chair)*
Director, Beckman Institute for Advanced Science and Technology,
Professor, Departments of Materials Science & Engineering and Physics
University of Illinois at Urbana-Champaign

William A. Bassett
Director, Mineral Physics Laboratory
Cornell University

Paul M. Bertsch
Director, Savannah River Ecological Laboratory;
Technical Director, Advanced Analytical Center for Environmental Sciences
University of Georgia

Jennifer A. Doudna
Department of Molecular Biochemistry and Molecular Biology
University of California, Berkeley

Katherine T. Faber
Department of Materials Science and Engineering
Northwestern University

John R. Helliwell
Department of Chemistry
University of Manchester

Peter Ingram
Department of Pathology
Duke University Medical Center

Miles V. Klein
Department of Physics
University of Illinois at Urbana-Champaign

Gerhard T. Materlik
Director, Diamond Light Source
Rutherford Appleton Laboratory

Denis B. McWhan
Associate Laboratory Director (Retired)
Brookhaven National Laboratory

James R. Norris
Department of Chemistry
The University of Chicago

Michael J. Rowe
Director [Retired], Center for Neutron Research,
National Institute of Standards and Technology

Joachim Stöhr
Professor and Deputy Director, Stanford Accelerator Center,
Stanford Synchrotron Radiation Laboratory
Stanford University

Source:
http://www.aps.anl.gov/About/Committees/Scientific_Advisory_Committee/Members/index.html

2005 APS Users Organization Steering Committee

Carol Thompson *Northern Illinois University (Chair)*
Gene Ice *Oak Ridge National Laboratory (Vice Chair)*
Simon Billinge, *Michigan State University*
Keith Brister, *Northwestern University*
Malcolm Capel, *Cornell University*
Julie Cross, *University of Washington*
Millicent Firestone, *Argonne National Laboratory*
Stephan Ginell, *Argonne National Laboratory*
Thomas Gog, *Argonne National Laboratory*
Barbara Golden, *Purdue University*
Tim Graber, *The University of Chicago*
David Reis, *University of Michigan*
Ward Smith, *Argonne National Laboratory*
Ex-Officio
Mark Rivers, *The University of Chicago*

Source:http://www.aps.anl.gov/About/Committees/APS_Users_Organization/Members/index.html

2005 Partner User Council

Bruce A. Bunker *(sector 10, University of Notre Dame, Chair)*
Dean R. Haeffner *(sector 1, Argonne National Laboratory)*
Qun Shen *(sector 2, Argonne National Laboratory)*
Wolfgang Sturhahn *(sector 3, Argonne National Laboratory)*
George Srajer *(sector 4, Argonne National Laboratory)*
Denis T. Keane *(sector 5, Northwestern University)*
Douglas S. Robinson *(sector 6, Iowa State University)*
Roy Clarke *(sector 7, University of Michigan)*
Simon G.J. Mochrie *(sector 8, Yale University)*
J. Kent Blasie *(sector 9, University of Pennsylvania)*
Mark A. Beno *(sector 11, Argonne National Laboratory)*
Randall E. Winans *(sector 12, Argonne National Laboratory)*
Mark L. Rivers *(sector 13, The University of Chicago)*
Keith Moffat *(sector 14, The University of Chicago)*
P. James Viccaro *(sector 15, The University of Chicago)*
David Mao *(sector 16, Carnegie Institution of Washington)*
Lisa J. Keefe *(sector 17, The University of Chicago)*
Thomas C. Irving *(sector 18, Illinois Institute of Technology)*
Andrzej Joachimiak *(sector 19, Argonne National Laboratory)*
Edward A. Stern *(sector 20, University of Washington)*
Wayne F. Anderson *(sector 21, Northwestern University)*
John J. Chrzas *(sector 22, University of Georgia)*
Robert F. Fischetti *(sector 23, Argonne National Laboratory)*
Malcolm Capel *(sector 24, Cornell University)*
G. Brian Stephenson *(sector 26, Argonne National Laboratory)*
John P. Hill *(sector 30, Brookhaven National Laboratory)*
Kevin L. D'Amico *(sector 31, SGX Pharmaceuticals, Inc.)*
Paul Zschack *(sector 33-34, University of Illinois at Urbana-Champaign)*

Source: http://www.aps.anl.gov/About/Committees/Partner_Users_Council/Members/puc_list.htm

Continued on next page

APS User Committees (cont'd.)

2005 Proposal Review Panels

High Pressure
Guoyin Shen *Carnegie Institution of Washington (Chair)*
Thomas Duffy *Princeton University*
Dion Heinz *The University of Chicago*
Kurt Leinenweber *Arizona State University*
Viktor Struzhkin *Carnegie Institution of Washington*

Instrumentation
Eric Dufresne *Argonne National Laboratory (Chair)*
Peter Eng *The University of Chicago*
Sarvjit Shastri *Argonne National Laboratory*

Imaging/Microbeam
George Cody *Carnegie Institution of Washington (Chair)*
Henry Chapman *Lawrence Livermore National Laboratory*
Tatjana Paunesku *Northwestern University*
Steve Sutton *The University of Chicago*

Macromolecular Crystallography
Karl Volz *University of Illinois at Chicago (Chair)*
Anne Mulichak *The University of Chicago*
John Rose *University of Georgia*

Scattering/Applied Materials
Robert Winholtz *University of Missouri (Chair)*
Sean Brennan *Stanford Linear Accelerator Center*
Slade Cargill *Lehigh University*
George Fenske *Argonne National Laboratory*

Scattering/Condensed Matter
Haskell Taub *University of Missouri-Columbia (Chair)*
Peter Abbamonte *Brookhaven National Laboratory*
Valery Kiryukhin *Rutgers University*
Karl Ludwig *Boston University*
Christie Nelson *Brookhaven National Laboratory*

Scattering/Chemistry/Biology/ Environmental Science
David Tiede *Argonne National Laboratory (Chair)*
Peter Burns *University of Notre Dame*
Jean-Francois Gaillard *Northwestern University*
Lois Pollack *Cornell University*
Mark Schlossman *University of Illinois at Chicago*

Small-Angle Scattering
Pappannan Thiyagarajan *Argonne National Laboratory (Chair)*
Peter Jemian *University of Illinois*
Joanna Krueger *University of North Carolina at Charlotte*
Byeongdu Lee *Argonne National Laboratory*

Surya K. Mallapragada *Ames Laboratory*
Hiro Tsuruta *Stanford Linear Accelerator Center*

Spectroscopy (EXAFS)
Matt Newville *The University of Chicago (Chair)*
Raul Barrea *Illinois Institute of Technology*
Lin X. Chen *Argonne National Laboratory*
Daniel Haskel *Argonne National Laboratory*
Jeff Kortright *Lawrence Berkeley National Laboratory*

Source: http://www.aps.anl.gov/About/Committees/Proposal_Review_Panel/index.html

2005 Beam Time Allocation Committees

Macromolecular Crystallography
Robert Fischetti *Argonne National Laboratory (Chair)*
Keith Brister *Northwestern University*
Vukica Srajer *The University of Chicago*

All Other Science
Jonathan Tischler *Oak Ridge National Laboratory (Chair)*
Julie Cross *Argonne National Laboratory*
Denis Keane *Northwestern University*
G. Brian Stephenson *Argonne National Laboratory*

Source: http://www.aps.anl.gov/About/Committees/Beam_Time_Allocation_ Committees/index.html

2005 APS InterCAT Technical Workgroup

Subgroups:
Top-off Subgroup: John Quintana, *Argonne National Laboratory*

Beam Stability Subgroup: Paul Zschack, *Argonne National Laboratory*

Detector Subgroup: Thomas Irving, *Illinois Institute of Technology*

Diagnostics Subgroup: Jonathan Lang, *Argonne National Laboratory*

Source: http://www.aps.anl.gov/About/Committees/InterCAT_Technical_ Workgroup/index.html

APS Safety Committees

Safety Overview Committee

Safety Committee for Design Reviews

Radiation Safety Policy & Procedures Committee

Radiation Safety Shielding Committee for Design Reviews

Chemical Safety Committee

Electrical Safety Committee

Laser Safety Committee

APS PUBLICATIONS 2005*

***As of 3.21.06. For an up-to-date listing, see the searchable, publicly available database of all APS-related scientific and technical publications from APS users and personnel at: http://beam.aps.anl.gov/pls/apsweb/pub_v2_0006.review_start_page**

EXPERIMENTAL RESULTS: JOURNAL ARTICLES

C.C. Abnet, B. Lai, Y.-L. Qiao, S. Vogt, X.-M. Luo, P.R. Taylor, Z.-W. Dong, S.D. Mark, S.M. Dawsey, "Zinc concentration in esophageal biopsy specimens measured by x-ray fluorescence and esophageal cancer risk," J. Natl. Cancer I. 97 (4), February, 301-306 (2005).

F.M. Abuzaina, A.J. Patel, S.G.J. Mochrie, S. Narayanan, A.R. Sandy, B.A. Garetz, N.P. Balsara, "Structure and Phase Behavior of Block Copolymer Melts near the Sphere-Cylinder Boundary," Macromolecules 38 (16), August, 7090-7097 (2005).

Melanie Adams, Zongchao Jia, "Structural and Biochemical Analysis Reveal Pirins to Possess Quercetinase Activity," J. Biol. Chem. 280 (31), August, 28675-28682 (2005).

Rakhi Agarwal, Thomas Binz, Subramanyam Swaminathan, "Structural Analysis of Botulinum Neurotoxin Serotype F Light Chain: Implications on Substrate Binding and Inhibitor Design," Biochemistry-US 44 (35), August, 11758-11765 (2005).

Ilana Agmon, Anat Bashan, Raz Zarivach, Ada Yonath, "Symmetry at the active site of the ribosome: structure and functional implications," Biol. Chem. 386 (9), September, 833-844 (2005).

Muhtar Ahart, Ronald E. Cohen, Viktor Struzhkin, Eugene Gregoryanz, Daniel Rytz, Sergey A. Prosandeev, Ho-kwang Mao, Russell J. Hemley, "High-pressure Raman scattering and x-ray diffraction of the relaxor ferroelectric 0.96Pb(Zn[subscript 1/3]Nb[subscript 2/3])O[subscript 3]-0.04PbTiO[subscript 3]," Phys. Rev. B 71, 144102-1-144102-7 (2005).

I. Ahmad, J.C. Banar, J.A. Becker, T.A. Bredeweg, J.R. Cooper, D.S. Gemmell, A. Kraemer, A. Mashayekhi, D.P. McNabb, G.G. Miller, E.F. Moore, P. Palmer, L.N. Pangault, R.S. Rundberg, J.P. Schiffer, S.D. Shastri, T.-F. Wang, J.B. Wilhelmy, "Search for x-ray induced decay of the 31-yr isomer of [superscript 178]Hf using synchrotron radiation," Phys. Rev. C 71 (2), February, 024311-1-024311-16 (2005).

R.I. Al-Raoush, C.S. Willson, "A Pore-scale Investigation of a Multiphase Porous Media System," J. Contam. Hydrol. 77 ((1-2)), 67-89 (2005).

R.I. Al-Raoush, C.S. Willson, "Extraction of Physically-Representative Pore Networks from Unconsolidated Porous Media Systems Using Synchrotron Microtomography," J. Hydrol. 300/1-4, 44-64 (2005).

Shabnam Alam, Valerie Grum-Tokars, Jolanta Krucinska, Melisa L. Kundracik, Joseph E. Wedekind, "Conformational Heterogeneity at Position U37 of an All-RNA Hairpin Ribozyme with Implications for Metal Binding and the Catalytic Structure of the S-Turn," Biochemistry-US 44, October, 14396-14408 (2005).

A. Alatas, A. H. Said, H. Sinn, E.E. Alp, C. N. Kodituwakku, B. Reinhart, M.-L. Saboungi, D. L. Price, "Elastic modulus of supercooled liquid and hot solid silicon measured by inelastic X-ray scattering," J. Phys. Chem. Solids 66 (12), December, 2230-2234 (2005).

M.M.C. Allain, B.J. Heuser, "Lattice strain measurements of deuteride (hydride) formation in epitaxial Nb: Additional results and further insights into past measurements," Phys. Rev. B 72, August, 54102-1-54102-11 (2005).

Simon T.M. Allard, Craig A. Bingman, Kenneth A. Johnson, Gary E. Wesenberg, Eduard Bitto, WonBae Jeon, George N. Phillips JR., "Structure at 1.6 Å resolution of the protein from gene locus At3g22680 from Arabidopsis thaliana," Acta Crystallogr. F 61 (7), July, 647-650 (2005).

Andrew J. Allen, "Characterization of Ceramics by X-Ray and Neutron Small-Angle Scattering," J. Am. Ceram. Soc. 88 (6), June, 1367-1381 (2005).

John S. Allingham, Robert Smith, Ivan Rayment, "The structural basis of blebbistatin inhibition and specificity for myosin II," Nature Struct. Biol. 12, March, 378-379 (2005).

John S. Allingham, Angela Zampella, Maria Valeria D'Auria, Ivan Rayment, "Structures of microfilament destabilizing toxins bound to actin provide insight into toxin design and activity," Biochemistry-US 102 (41), October, 14527-14532 (2005).

N. Allison, A.A. Finch, M. Newville, S.R. Sutton, "Strontium in coral aragonite: 3. Sr coordination and geochemistry in relation to skeletal architecture," Geochim. Cosmochim. Acta 69 (15), 3801-3811 (2005).

N. Allison, A.A. Finch, A.W. Tudhope, M. Newville, S.R. Sutton, R.M. Ellam, "Reconstruction of deglacial sea surface temperature in the tropical Pacific from selective analysis of a fossil coral," Geophys. Res. Lett. 32, L17609-L17612 (2005).

J.D. Almer, S.R. Stock, "Internal strains and stresses measured in cortical bone via high-energy x-ray diffraction," J. Struct. Biol. 152 (1), October, 14-27 (2005).

J.D. Almer, E. Üstündag, G.A. Swift, J.A. Nychka, C.C. Aydiner, D.R. Clarke, "In situ synchrotron measurements of oxide growth strains," Mater. Sci. Forum 490-491, 287-293 (2005).

E. Ercan Alp, Arun Bansil, "5th International Conference on Inelastic X-ray Scattering (IXS2004)," J. Phys. Chem. Solids 66 (12), December, vii (2005).

S.J. Altman, W.J. Peplinski, M.L. Rivers, "Evaluation of synchrotron X-ray computerized microtomography for the visualization of transport processes in low-porosity materials," J. Contam. Hydrol. 78, 167-183 (2005).

Susan J. Altman, Mark L. Rivers, Marissa D. Reno, Randall T. Cygan, Angela A. McLain, "Characterization of Adsorption Sites on Aggregate Soil Samples Using Synchrotron X-ray Computerized Microtomography," Environ. Sci. Technol. 39 (8), March, 2679-2685 (2005).

Maya Amita, Rita Berisiob, David Barama, Joerg Harms, Anat Bashana, Ada Yonath, "A crevice adjoining the ribosome tunnel: Hints for cotranslational folding," FEBS Lett. 579 (15), June, 3207-3213 (2005).

George M. Amulele, Murli H. Manghnani, "Compression studies of TiB[subscript 2] using synchrotron x-ray diffraction," J. Appl. Phys. 97, 023506-1-023506-6 (2005).

Spencer Anderson, Vladimira Dragnea, Shinji Masuda, Joel Ybe, Keith Moffat, Carl Bauer, "Structure of a Novel Photoreceptor, the BLUF Domain of AppA from Rhodobacter sphaeroides," Biochemistry-US 44 (22), May, 7998-8005 (2005).

M. Angst, A. Kreyssig, Y. Janssen, J.-W. Kim, L. Tan, D. Wermeille, Y. Mozharivskyij, A. Kracher, A.I. Goldman, P.C. Canfield, "Distinct order of Gd 4f and Fe 3d moments coexisting in GdFe[subscript 4]Al[subscript 8]," Phys. Rev. B 72 (17), November, 174407-1-174407-13 (2005).

Todd C. Appleby, Cynthia Kinsland, Tadhg P. Begley, Steven E. Ealick, "The crystal structure and mechanism of orotidine 5'-monophosphate decarboxylase," Proc. Natl. Acad. Sci. USA 97 (5), February, 2005-2010 (2005).

Paul I. Archer, Pavle V. Radovanovic, Steve M. Heald, Daniel R. Gamelin, "Low-Temperature Activation and Deactivation of High-Curie-Temperature Ferromagnetism in a New Diluted Magnetic Semiconductor: Ni[superscript 2+]-Doped SnO[subscript 2]," J. Am. Chem. Soc. 127 (41), October, 14479-14487 (2005).

L. Arleth, B. Bashok, H. Onyuksel, P. Thiyagarajan, J. Jacob, R.P. Hjelm, "Detailed Structure of Hairy Mixed Micelles Formed by Phosphatidylcholine and PEGylated Phospholipids in Aqueous Media," Langmuir 21 (8), April, 3279-3290 (2005).

D.A. Arms, T.J. Graber, A.T. Macrander, R.O. Simmons, M. Schwoerer-Böhning, Y. Zhong, "Excitons in bulk liquid [superscript 4]He," Phys. Rev. B 71, 233107-1-233107-4 (2005).

J.W. Arndt, R. Schwarzenbacher, R. Page, P. Abdubek, E. Ambing, T. Biorac, J.M. Canaves, H.J. Chiu, X. Dai, A.M. Deacon, M. Didonato, M.A. Elsliger, A. Godzik, C. Grittini, S.K. Grzechnik, J. Hale, E. Hampton, G.W. Han, J. Haugen, M. Hornsby, H.E. Klock, E. Koesema, A. Kreusch, P. Kuhn, L. Jaroszewski, S.A. Lesley, I. Levin, D. McMullan, T.M. McPhillips, M.D. Miller, A. Morse, K. Moy, E. Nigoghossian, J. Ouyang, W.S. Peti, K. Quijano, R. Reyes, E. Sims, G. Spraggon, R.C. Stevens, H. vanden Bedem, J. Velasquez, J. Vincent, F. von Delft, X. Wang, B. West, A. White, G. Wolf, Q. Xu, O. Zagnitko, K.O. Hodgson, J. Wooley, I.A. Wilson, "Crystal structure of an [alpha]/[beta] serine hydrolase (YDR428C) from Saccharomyces cerevisiae at 1.85 Å resolution.," Proteins 58 (3), 755-758 (2005).

J.W. Arndt, W. Yu, F. Bi, R.C. Stevens, "Crystal structure of botulinum neurotoxin type G light chain: serotype divergence in substrate recognition," Biochemistry-US 44 (28), July, 9574-9580 (2005).

M.L. Auad, M.D. Kempe, J.A. Kornfield, S. Rendon, W.R. Burghardt, K. Yoon, "Effect of Mesophase Order on the Dynamics of Side Group Liquid Crystalline Polymers," Macromolecules 38, 6946-6953 (2005).

Tamar Auerbach-Nevo, Raz Zarivach, Moshe Peretz, Ada Yonath, "Reproducible growth of well diffracting ribosomal crystals," Acta Crystallogr. D 61 (6), May, 713-719 (2005).

Thierry C. Auperin, Gilles R. Bolduc, Miriam J. Baron, Annie Heroux, David J. Filman, Lawrence C. Madoff, James M. Hogle, "Crystal Structure of the N-terminal Domain of the Group B Streptococcus Alpha C Protein," J. Biol. Chem. 280 (18), May, 18245-18252 (2005).

S.S. Babu, E.D. Specht, S.A. David, E. Karapetrova, P. Zschack, M. Peet, H.K.D.H. Bhadeshia, "In-Situ Observations of Lattice Parameter Fluctuations in Austenite and Transformation to Bainite," Metall. Mater. Trans. A 36A, December, 3281-3289 (2005).

J. Badger, J.M. Sauder, J.M. Adams, S. Antonysamy, K. Bain, M.G. Bergseid, S.G. Buchanan, M.D. Buchanan, Y. Batiyenko, J.A. Christopher, S. Emtage, A. Eroshkina, I. Feil, E.B. Furlong, K.S. Gajiwala, X. Gao, D. He, J. Hendle, A. Huber, K. Hoda, P. Kearins, C. Kissinger, B. Laubert, H.A. Lewis, J. Lin, K. Loomis, D. Lorimer, G. Louie, M. Maletic, C.D. Marsh, I. Miller, J. Molinari, H.J. Muller-Dieckmann, J.M. Newman, B.W. Noland, B. Pagarigan, F. Park, T.S. Peat, K.W. Post, S. Radojicic, A. Ramos, R. Romero, M.E. Rutter, W.E. Sanderson, K.D. Schwinn, J. Tresser, J. Winhoven, T.A. Wright, L. Wu, J. Xu, T.J.R. Harris, "Structural analysis of a set of proteins resulting from a bacterial genomics project," Proteins 60 (4), September, 787-796 (2005).

Nathan J. Baird, Eric Westhof, Hong Qin, Tao Pan, Tobin R. Sosnick, "Structure of a Folding Intermediate Reveals the Interplay Between Core and Peripheral Elements in RNA Folding," J. Mol. Biol. 352, 712-722 (2005).

Y. Bai, R. Das, I.S. Millett, D. Herschlag, S. Doniach, "Probing counterion modulated repulsion and attraction between nucleic acid duplexes in solution," Proc. Natl. Acad. Sci. USA 102 (4), January, 1035-1040 (2005).

Duhee Bang, Georgel. Makhatadze, Valentina Tereshko, Anthony A. Kossiakoff, Stephen B. Kent, "Total Chemical Synthesis and X-ray Crystal Structure of a Protein Diastereomer: [D-Gln 35]Ubiquitin," Angew. Chem. Int. Ed. 44 (25), April, 3852-3856 (2005).

R.I. Barabash, G.E. Ice, W. Liu, S. Einfeldt, D. Hommel, A.M. Roskovski, R.F. Davis, "White X-ray Microbeam Analysis of Strain and Crystallographic Tilt in GaN Layers Grown by Maskless Pendeoepitaxy," Phys. Status Solidi. a. 202 (5), April, 732-783 (2005).

R.I. Barabash, G.E. Ice, W. Liu, S. Einfeldt, A.M. Roskovski, R.F. Davis, "Local Strain, Defects and Crystallographic Tilt in GaN(0001) Layers Grown by Maskless Pendeoepitaxy from X-ray Microdiffraction," J. Appl. Phys. 97, 013504-1-013504-5 (2005).

David Baram, Erez Pyetan, Assa Sittner, Tamar Auerbach-Nevo, Anat Bashan, Ada Yonath, "Structure of trigger factor binding domain in biologically homologous complex with eubacterial ribosome reveals its chaperone action," Proc. Natl. Acad. Sci. USA 102 (34), August, 12022-12017 (2005).

David Baram, Ada Yonath, "From peptide-bond formation to cotranslational folding: dynamic, regulatory and evolutionary aspects," FEBS Lett. 579, 948-954 (2005).

J.R. Bargar, U. Bergmann, B.M. Tebo, S.M. Webb, M. Villalobos, V. Chiu, "Biotic and Abioic Products of Mn(II) Oxidation by Spores of the Marine Bacillus sp., strain SG-1," Am. Mineral. 90, 143-154 (2005).

R.A. Barrea, R. Fischetti, S. Stepanov, G. Rosenbaum, E. Kondrashkina, G.B. Bunker, E. Black, K. Zhang, D. Gore, R. Heurich, M. Vukonich, C. Karanfil, A.J. Kropf, S. Wang, T.C. Irving, "Biological XAFS at the BioCAT Undulator Beamline 18ID at the APS," Phys. Scripta. T115, 867-869 (2005).

David G. Barrett, David N. Deaton, Anne M. Hassell, Robert B. McFadyen, Aaron B. Miller, Larry R. Miller, J.Alan Payne, Lisa M. Shewchuk, Derril H. Willard, Jr., Lois L. Wright, "Acyclic cyanamide-based inhibitors of cathepsin K," Bioorg. Med. Chem. Lett. 15 (12), June, 3039-3043 (2005).

Anat Bashan, Ada Yonath, "Ribosome crystallography: catalysis and evolution of peptide-bond formation, nascent chain elongation and its co-translational folding," Biochem. Soc. T. 33 (3), June, 488-492 (2005).

Dolly Batra, Stefan Vogt, Phillip D. Laible, Millicent A. Firestone, "Self-Assembled, Mesoporous Polymeric Networks for Patterned Protein Arrays," Langmuir 21 (23), 10301-10306 (2005).

Richard H.G. Baxter, Brandon-Luke Seagle, Nina Ponomarenko, James R. Norris, "Cryogenic structure of the photosynthetic reaction center of Blastochloris viridis in the light and dark," Acta Crystallogr. D 61 (5), May, 605-612 (2005).

James R. Bayrer, Wei Zhang, Michael A. Weiss, "Dimerization of Doublesex Is Mediated by a Cryptic Ubiquitin-associated Domain Fold: Implications for Sex-Specific Gene Regulation," J. Biol. Chem. 280 (38), September, 32989-32996 (2005).

Lesa J. Beamer, Xuchu Li, Christopher A. Bottoms, Mark Hannink, "Conserved solvent and side-chain interactions in the 1.35 Å structure of the Kelch domain of Keap1," Acta Crystallogr. D 61, 1335-1342 (2005).

Jessica K. Bell, Istvan Botos, Pamela R. Hall, Janine Askins, Joseph Shiloach, David M. Segal, David R. Davies, "The molecular structure of the Toll-like receptor 3 ligand-binding domain," Proc. Natl. Acad. Sci. USA 102 (31), August, 10976-10980 (2005).

C.J. Benmore, R.T. Hart, Q. Mei, D.L. Price, J. Yarger, C.A. Tulk, D.D. Klug, "Intermediate range chemical ordering in amorphous and liquid water, Si and Ge," Phys. Rev. B 72 (13), October, 132201-1-132201-4 (2005).

Douglas A. Bernstein, James L. Keck, "Conferring Substrate Specificity to DNA Helicases: Role of the RecQ HRDC Domain," Structure 13 (8), August, 1173-1182 (2005).

N.S.P. Bhuvanesh, J.H. Reibenspies, M.L. Golden, M.Y. Darensbourg, Y. Zhang, P.L. Lee, "The vapochromic behavior, desulfoxidation and structural characterization of the SO[subscript 2] adducts of Ni(BME-DACH) from powder data," Synth. React. Inorg. Me. 35 (1), 11-17 (2005).

N.S.P. Bhuvanesh, J.H. Reibenspies, Y. Zhang, P.L. Lee, "A novel strategy for ab initio structure determination using micro-powder X-ray diffraction: structure solution and refinement of 3-bromophenylboronic acid and tris(4-bromo-phenyl) boroxine," J. Appl. Crystallogr. 38, 632-638 (2005).

Simon J.L. Billinge, Emily J. McKimmey, Mouath Shatnawi, HyunJeong Kim, Valeri Petkov, Didier Wermeille, Thomas J. Pinnavaia, "Mercury Binding Sites in Thiol-Functionalized Mesostructured Silica," J. Am. Chem. Soc. 127, 8492-8498 (2005).

Tapan Biswas, Hideki Aihara, Marta Radman-Livaja, David Filman, Arthur Landy, Tom Ellenberger, "A structural basis for allosteric control of DNA recombination by [lambda] integrase," Nature 435, June, 1059-1066 (2005).

Eduard Bitto, Craig A. Bingman, Simon T.M. Allard, Gary E. Wesenberg, David J. Aceti, Russell L. Wrobel, Ronnie O. Frederick, Hassan Sreenath, Frank C. Vojtik, Won Bae Jeon, Craig S. Newman, John Primm, Michael R. Sussman, Brian G. Fox, John L. Markley, George N. Phillips, Jr., "The structure at 2.4 Å resolution of the protein from gene locus At3g21360, a putative Fe[superscript II]/2-oxoglutarate-dependent enzyme from Arabidopsis thalinia," Acta Crystallogr. F 61 (5), April, 469-472 (2005).

Eduard Bitto, Craig A. Bingman, Jason G. McCoy, Simon T.M. Allard, Gary E. Wesenberg, George N. Phillips, Jr., "The structure at 1.6 Å resolution of the protein product of the At4g34215 gene from Arabidopsis thaliana," Acta Crystallogr. D 61, 1655-1661 (2005).

Eduard Bitto, Eduard A. Bingman, Simon T.M. Allard, Gary E. Wesenberg, George N. Phillips, Jr., "The structure at 1.7 Å resolution of the protein product of the At2g17340 gene from Arabidopsis thaliana," Acta Crystallogr. F 61 (7), June, 630-635 (2005).

C.J. Blamey, C. Ceccarelli, U.P. Naik, B.J. Bahnson, "The crystal structure of calcium- and integrin-binding protein 1: Insights into redox regulated functions," Protein Sci. 14 (5), May, 1214-1221 (2005).

Randy K. Bledsoe, Kevin P. Madauss, Jason A. Holt, Christopher J. Apolito, Millard H. Lambert, Kenneth H. Pearce, Thomas B. Stanley, Eugene L. Stewart, Ryan P. Trump, Timothy M. Willson, Shawn P. Williams, "A Ligand-mediated Hydrogen Bond Network Required for the Activation of the Mineralocorticoid Receptor," J. Biol. Chem. 28035, September, 31283-31293 (2005).

T.A. Blizzard, F. DiNinno, J.D. Morgan II, H.Y. Chen, J.Y. Wu, S. Kim, W. Chan, E.T. Birzin, Y.T. Yang, L.-Y. Pai, P.M.D. Fitzgerald, N. Sharma, Y. Li, Z. Zhang, E.C. Hayes, C.A. DaSilva, W. Tang, S.P. Rohrer, J.M. Schaeffer, M.L. Hammond, "Estrogen receptor ligands. Part 9: Dihydrobenzoxathiin SERAMs with alkyl substituted pyrrolidine side chains and linkers," Bioorg. Med. Chem. Lett. 15, 107-113 (2005).

S. Bluskov, J.M. Arocena, O.O. Omotoso, J.P. Young, "Uptake, Distribution, and Speciation of Chromium in Brassica Juncea," Int. J. Phytoremediat. 7 (2), 153-165 (2005).

Kevin M. Bobofchak, Agustin O. Pineda, F.Scott Mathews, Enrico Di Cera, "Energetic and Structural Consequences of Perturbing Gly-193 in the Oxyanion Hole of Serine Proteases," J. Biol. Chem. 280 (27), July, 25644-25650 (2005).

Philippe R.J. Bois, Robert A. Borgon, Clemens Vonrhein, Tina Izard, "Structural Dynamics of [alpha]-Actinin-Vinculin Interactions," Mol. Cell Biol. 25 (14), July, 6112-6122 (2005).

Daniel N. Bolon, Robert A. Grant, Tania A. Baker, Robert T. Sauer, "Specificity versus stability in computational protein design," Proc. Natl. Acad. Sci. USA 102 (36), June, 12724-12729 (2005).

C.J. Bond, C. Wiesmann, J.C. Marsters, Jr., S.S. Sidhu, "A structure-based database of antibody variable domain diversity," J. Mol. Biol. 348, 699-709 (2005).

Istvan Botos, Edward E. Melnikov, Scott Cherry, Serguei Kozlov, Oksana V. Makhovaskaya, Joseph E. Tropea, Alla Gustchina, Tatyana V. Rotanova, Alexander Wlodawer, "Atomic-resolution Crystal Structure of the Proteolytic Domain of Archaeoglobus fulgidus Lon Reveals the Conformational Variability in the Active Sites of Lon Proteases," J. Mol. Biol. 351, 144-157 (2005).

Julie Bouckaert, Jenny Berglund, Mark Schembri, Erwin De Genst, Lieve Cools, Manfred Wuhrer, Chia-Suei Hung, Jerome Pinkner, Rikard Slättegard, Anton Zavialov, Devapriya Choudhury, Solomon Langermann, Scott J. Hultgren, Lode Wyns, Per Klemm, Stefan Oscarson, Stefan D. Knight, Henri De Greve, "Receptor binding studies disclose a novel class of high-affinity inhibitors of the Escherichia coli FimH adhesin," Mol. Microbiol. 55 (2), January, 441-455 (2005).

Richard Bourgault, Aaron J. Oakley, J.Derek Bewley, Matthew C.J. Wilce, "Three-dimensional structure of (1,4)-[superscript beta]-D-mannan mannanohydrolase from tomato fruit," Protein Sci. 14 (5), May, 1233-1241 (2005).

Dominique Bourgeois, Antoine Royant, "Advances in kinetic protein crystallography," Curr. Opin. Struct. Biol. 15 (5), October, 538-547 (2005).

N. Boyard, M. Vayer, C. Sinturel, S. Seifert, R. Erre, "Investigation of Phase Separation Mechanisms of Thermoset Polymer Blends by Time-Resolved SAXS," Eur. Polym. J. 416 (6), June, 1333-1341 (2005).

Artur Braun, Jan Ilavsky, Brian C. Dunn, Pete R. Jemian, Frank E. Huggins, Edward M. Eyring, Gerald P. Huffman, "Ostwald ripening of cobalt precipitates in silica aerogels? An ultra-small-angle X-ray scattering study," J. Appl. Crystallogr. 38, 132-138 (2005).

Artur Braun, Jan Ilavsky, Sönke Seifert, Pete R. Jemian, "Deformation of diesel soot aggregates as a function of pellet pressure: A study with ultra-small-angle x-ray scattering," J. Appl. Phys. 98, October, 073513-1-073513-5 (2005).

A. Braun, N. Shah, F.E. Huggins, K.E. Kelly, A. Sarofim, C. Jacobsen, S. Wirick, H. Francis, J. Ilavsky, G.E. Thomas, G.P. Huffman, "X-ray scattering and spectroscopy studies on diesel soot from oxygenated fuel under various engine load conditions," Carbon 43 (12), October, 2588-2599 (2005).

Chad A. Brautigam, Jacinta L. Chuang, Diana R. Tomchick, Mischa Machius, David T. Chuang, "Crystal Structure of Human Dihydrolipoamide Dehydrogenase: NAD[superscript +]/NADH Binding and the Structural Basis of Disease-causing Mutations," J. Mol. Biol. 350, 543-552 (2005).

J. Breger, N. Dupre, P.J. Chupas, P.L. Lee, T. Proffen, J.B. Parise, C.P. Grey, "Short- and long-range order in the positive electrode material Li(NiMn)[subscript 0.5]O[subscript 2]: A joint x-ray and neutron diffraction, pair distribution function analysis and NMR study," J. Am. Chem. Soc. 127, 7529-7537 (2005).

Julien Breger, Meng Jiang, Nicolas Dupre, Ying S. Meng, Yang Shao-Horn, Gerbrand Ceder, Clare P. Grey, "High-resolution X-ray diffraction, DIFFaX, NMR and first principles study of disorder in the Li[subscript 2]MnO[subscript 3]-Li[Ni[subscript 1/2]Mn[subscript 1/2]O[subscript 2] solid solution," J. Solid State Chem. 178 (9), September, 2575-2585 (2005).

Ashraf Brik, Jerry Alexandratos, Ying-Chuan Lin, John H. Elder, Arthur J. Olson, Alexander Wlodawer, David S. Goodsell, Chi-Huey Wong, "1,2,3-Triazole as a Peptide Surrogate in the Rapid Synthesis of HIV-1 Protease Inhibitors," ChemBioChem 6, June, 1167-1169 (2005).

K.L. Brinker, A.H. Lebovitz, J.M. Torkelson, W.R. Burghardt, "Porod Scattering Study of Coarsening in Immiscible Polymer Blends," J. Polym. Sci. Pol. Phys. 43 (23), October, 3413-3420 (2005).

Alistair K. Brown, Sudharsan Sridharan, Laurent Kremer, Sandra Lindenberg, Lynn G. Dover, James C. Sacchettini, Gurdyal S. Bes, "Probing the Mechanism of the Mycobacterium tuberculosis [beta]-Ketoacyl-Acyl Carrier Protein Synthase III mtFabH: Factors Influencing Catalysis and Substrate Specificity," J. Biol. Chem. 280 (37), September, 32539-32547 (2005).

G.E. Brown, J.G. Catalano, A.S. Templeton, T.P. Trainor, F. Farges, B.C. Bostick, T. Kendelewicz, C.S. Doyle, A.M. Spormann, K. Revill, G. Morin, F. Juillot, G. Calas, "Environmental interfaces, heavy metals, microbes, and plants: Applications of XAFS spectroscopy and related synchrotron radiation methods to environmental sciences," Phys. Scripta. T115, 80-87 (2005).

Richard J. Brown, Julian J. Adams, Rebecca A. Pelekanos, Yu Wan, William J. McKinstry, Kathryn Palethorpe, Ruth M. Seeber, Thea A. Monks, Karin A. Eidne, Michael W. Parker, Michael J. Waters, "Model for growth hormone receptor activation based on subunit rotation within a receptor dimer," Nat. Struct. Mol. Biol. 12, August, 814-821 (2005).

S. Bruhne, E. Uhrig, C. Gross, W. Assmus, A.S. Masadeh, S.J.L. Billinge, "The local atomic quasicrystal structure of the icosahedral Mg[subscript 25]Y[subscript 11]Zn[subscript 64] alloy," J. Phys. Condens. Matter 17 (10), February, 1561-1572 (2005).

Stefan Bruhne, Eckhard Uhrig, Klaus-Dieter Luther, Wolf Assmus, Michela Brunelli, Ahmad S. Masadeh, Simon Billinge, "PDF from X-ray powder diffraction for nanometer-scale atomic structure analysis of quasicrystalline alloys," Z. Kristallogr. 220, 962-967 (2005).

Robert A. Bubeck, Petar R. Dvornic, Jin Hu, Alexander Hexemer, Xuefa Li, Steven E. Keinath, Daniel A. Fischer, "Near Edge X-Ray Absorption Fine Structure (NEXAFS) Studies of Copper Ion-Containing PAMAMOS Dendrimer Networks," Macromol. Chem. Phys. 206 (11), May, 1146-1153 (2005).

P.S. Budnik, R.A. Gordon, E.D. Crozier, "Structure of the Magnetic Trilayer System FePdFe Epitaxially Grown on GaAs(001)-4x6," Phys. Scripta. T115, 495-497 (2005).

Greg Buhrman, Benjamin Parker, Jungsan Sohn, Johannes Rudolph, Carla Mattos, "Structural Mechanism of Oxidative Regulation of the Phosphatase Cdc25B via an Intramolecular Disulfide Bond," Biochemistry-US 44, 5307-5316 (2005).

Grant Bunker, Ncholas Dimakis, Gocha Khelashvili, "New methods for EXAFS analysis in structural genomics," J. Synchrotron Rad. 12 (1), January, 53-56 (2005).

T. Buonassisia, A. Istratov, S. Peters, C. Ballif, J. Isenberg, S. Riepe, W. Warta, R. Schindler, G. Willeke, Z. Cai, B. Lai, E.R. Weber, "Impact of metal silicide precipitate dissolution during rapid thermal processing of multicrystalline silicon solar cells," Appl. Phys. Lett. 87, 121918-1-121918-3 (2005).

T. Buonassisi, A.A. Istratov, M. Heuer, M.A. Marcus, R. Jonczyk, J. Isenberg, B. Lai, Z. Cai, S. Heald, W. Warta, R. Schindler, G. Willeke, E.R. Weber, "Synchrotron-based investigations of the nature and impact of iron contamination in multicrystalline silicon solar cells," J. Appl. Phys. 97, April, 074901-1-074901-11 (2005).

T. Buonassisi, A. Istratov, M.A. Marcus, B. Lai, Z. Cai, S.M. Heald, E.R. Weber, "Engineering metal-impurity nanodefects for low-cost solar cells," Nat. Mater. 4, September, 676-679 (2005).

T. Buonassisi, M.A. Marcus, A.A. Istratov, M. Heuer, T.F. Ciszek, B. Lai, Z. Cai, E.R. Weber, "Analysis of copper-rich precipitates in silicon: Chemical state, gettering, and impact on multicrystalline silicon solar cell material," J. Appl. Phys. 97, 063503: 1-9 (2005).

W.R. Burghardt, E.F. Brown, M.L. Auad, J.A. Kornfield, "Molecular Orientation of a Commercial Thermotropic Liquid Crystalline Polymer in Simple Shear and Complex Flow," Rheol. Acta 44, 445-456 (2005).

Peter C. Burns, Karrie-Ann Kubatko, Ginger Sigmon, Brian J. Fryer, Joel E. Gagnon, Mark R. Antonio, L. Soderholm, "Actinyl Peroxide Nanospheres," Angew. Chem. Int. Ed. 44 (14), March, 2135-2139 (2005).

W. Bu, E.C. Settembre, M.H el Kouni, S.E. Ealick, "Structural Basis for Inhibition of Escherichia coli Uridine Phosphorylase by 5-substituted Acyclouridines," Acta Crystallogr. D 61 (7), July, 863-872 (2005).

W. Bu, D. Vaknin, A. Travesset, "Monovalent counterion distributions at highly charged water interfaces: Proton-transfer and Poisson-Boltzmann theory," Phys. Rev. E 72, December, 060501-1-060501-4 (2005).

A. Cady, D. Haskel, J.C. Lang, G. Srajer, P. Chupas, R. Osborn, J.F. Mitchell, J.S. Ahn, N. Hur, S. Park, S.-W. Cheong, "Scanning low-temperature element-specific magnetic microscopy," Rev. Sci. Instrum. 76 (6), June, 063702-1-063702-6 (2005).

Y.Q. Cai, H.-k. Mao, P.C. Chow, J.S. Tse, Y. Ma, S. Patchovskii, J.F. Shu, V. Struzhkin, R.J. Hemley, H. Ishii, C.C. Chen, I. Jarrige, C.T. Chen, S.R. Shieh, E.P. Huang, C.C. Kao, "Ordering of Hydrogen Bonds in High-Pressure Low-Temperature H[subscript 2]O," Phys. Rev. Lett. 94, January, 025502-1-025502-4 (2005).

G. Caliskan, C. Hyeon, U. Perez-Salas, R. M. Briber, S. A. Woodson, D. Thirumalai, "Persistence Length Changes Dramatically as RNA Folds," Phys. Rev. Lett. 95 (26), December, 268303-1-268303-4 (2005).

R. Callens, C. L'abbe, J. Meersschaut, I. Serdons, W. Sturhahn, T.S. Toellner, "Phase determination in nuclear resonant scattering using a velocity drive as an interferometer and phase shifter," Phys. Rev. B 72 (8), 081402-1-081402-4 (2005).

E.A. Campbell, O. Pavlova, N. Zenkin, F. Leon, K. Severinov, S.A. Darst, "Structural, functional, and genetic analysis of sorangicin inhibition of bacterial RNA polymerase," EMBO J. 24, 674-682 (2005).

D. Cao, R.H. Heffner, F. Bridges, I.-K. Jeong, E.D. Bauer, W.M. Yuhasz, M.B. Maple, "Local Distortion Induced Metal-to-Insulator Phase Transition in PrRu[subscript 4]P[subscript 12]," Phys. Rev. Lett. 94, January, 036403-1-036403-4 (2005).

C.Britt Carlson, Douglas A. Bernstein, Douglas S. Annis, Tina M. Misenheimer, "Structure of the calcium-rich signature domain of human thrombospondin-2," Nat. Struct. Mol. Biol. 12, September, 910-914 (2005).

E.N. Caspi, B. Pokroy, P.L. Lee, J.P. Quintana, E. Zolotoyabko, "On the structure of aragonite," Acta Crystallogr. B 61, 129-132 (2005).

N. Castagnola, A.J. Kropf, C.L. Marshall, "Studies of Cu-ZSM-5 by X-ray absorption spectroscopy and its application for the oxidation of benzene to phenol by air," Appl. Catal. A-Gen. 290 (1-2), August, 110-122 (2005).

M. Castro-Colin, W. Donner, S.C. Moss, Z. Islam, S.K. Sinha, R. Nemanich, H.T. Metzger, P. Boesecke, T. Shuelli, "Synchrotron x-ray studies of vitreous SiO[subscript 2] over Si(001). I. Anisotropic glass contribution," Phys. Rev. B 71, 045310-1-045310-7 (2005).

M. Castro-Colin, W. Donner, S.C. Moss, Z. Islam, S.K. Sinha, R. Nemanich, "Synchrotron x-ray studies of vitreous SiO[subscript 2] over Si(001). II. Crystalline contribution," Phys. Rev. B 71, 045311-1-045311-7 (2005).

J.G. Catalano, T.P. Trainor, P.J. Eng, G.A. Waychunas, G.E. Brown, Jr., "CTR diffraction and grazing-incidence EXAFS study of U(VI) adsorption onto alpha-Al2O3 and alpha-Fe[subscript 2]O[subscript 3] (1-102) surfaces," Geochim. Cosmochim. Acta 69 (14), July, 3555-3572 (2005).

K.A. Cavicchi, K.J. Berthiaume, B. Ocko, L. Yang, T.P. Russell, "Solvent Annealing Thin Films of Poly(Isoprene-B-Laftide)," Polymer 46 (25), November, 11635-11639 (2005).

Eleonora Cesareo, Lorien J. Parker, Jens Z. Pedersen, Marzia Nuccetelli, Anna P. Mazzetti, Anna Pastore, Giorgio Federici, Anna M. Caccuri, Giorgio Ricci, Julian J. Adams, Michael W. Parker, Mario Lo Bello, "Nitrosylation of Human Glutathione Transferase P1-1 with Dinitrosyl Diglutathionyl Iron Complex in Vitro and in Vivo," J. Biol. Chem. 280 (51), December, 42172-42180 (2005).

Preethi Chander, Kari M. Halbig, Jamie K. Miller, Christopher J. Fields, Heather K.S. Bonner, Gail K. Grabner, Robert L. Switzer, Janet L. Smith, "Structure of the Nucleotide Complex of PyrR, the pyr Attenuation Protein from Bacillus caldolyticus, Suggests Dual Regulation by Pyrimidine and Purine Nucleotides," J. Bacteriol. 187 (5), March, 1773-1782 (2005).

Anita Changela, Alexandra Martin, Stewart Shuman, Alfonso Mondragon, "Crystal Structure of Baculovirus RNA Triphosphatase Complexed with Phosphate," J. Biol. Chem. 280 (18), May, 17848-17856 (2005).

B.D. Chapman, E.A. Stern, S.-W. Han, J.O. Cross, G.T. Seidler, V. Gavrilyatchenko, R.V. Vedrinskii, V.L. Kraizman, "Diffuse x-ray scattering in perovskite ferroelectrics," Phys. Rev. B 71 (2), January, 20102-1-20102-4 (2005).

K.W. Chapman, P.J. Chupas, C.J. Kepert, "Selective Recovery of Dynamic Guest Structure in a Nanoporous Prussian Blue Through in situ X-ray Diffraction: a Differential Pair Distribution Function Analysis," J. Am. Chem. Soc. 127 (32), August, 11232-11233 (2005).

K.W. Chapman, P.J. Chupas, C.J. Kepert, "Direct Observation of a Transverse Vibrational Mechanism for Negative Thermal Expansion in Zn(CN)[subscript]2: an Atomic Pair Distribution Function Analysis.," J. Am. Chem. Soc. 127 (44), November, 15630-15636 (2005).

E. Chase, B.L. Golden, "Crystallization and preliminary diffraction analysis of a group I ribozyme from bacteriophage Twort," Acta Crystallogr. F 61 (1), January, 71-74 (2005).

Soma Chattopadhyay, Deniz Erdemir, James M.B. Evans, Jan Ilavsky, Heinz Amenitsch, Carlo U. Segre, Allan S. Myerson, "SAXS Study of the Nucleation of Glycine Crystals from a Supersaturated Solution," Cryst. Growth Des. 5 (2), 532-527 (2005).

S. Chattopadhyay, S.D. Kelly, V.R. Palkar, L. Fan, C.U. Segre, "Investigation of Size Effects in Magnetoelectric BiFeO[subscript 3]," Phys. Scripta. T115, 709-713 (2005).

Seema Chauhan, Gokhan Caliskan, Robert M. Briber, Ursula Perez-Salas, Prashanth Rangan, D. Thirumalai, Sarah A. Woodson, "RNA Tertiary Interactions Mediate Native Collapse of a Bacterial Group I Ribozyme," J. Mol. Biol. 353, 1199-1209 (2005).

Bing Chen, Erik M. Vogan, Haiyun Gong, John J. Skehel, Don C. Wiley, Stephen C. Harrison, "Structure of an unliganded simian immunodeficiency virus gp120 core," Nature 433, February, 834-841 (2005).

Bing Chen, Erik M. Vogan, Haiyun Gong, John J. Skehel, Don C. Wiley, Stephen C. Harrison, "Determining the Structure of an Unliganded and Fully Glycosylated SIV gp120 Envelope Glycoprotein," Structure 13, 197-211 (2005).

L.X. Chen, "Probing Transient Molecular Structures in Photochemical Processes Using Laser-Initiated Time-Resolved X-ray Absorption Spectroscopy," Annu. Rev. Phys. Chem. 56, February, 221-254 (2005).

L.X. Chen, G.B. Shaw, T. Liu, G. Jennings, K. Attenkofer, "Capturing Excited State Molecular Structures in Disordered Media with 100 ps Time Resolution by Laser Pump X-ray Probe XAFS," Phys. Scripta. T115, May, 93-96 (2005).

L.X. Chen, G.B. Shaw, D.M. Tiede, X. Zuo, P. Zapol, P.C. Redfern, L.A. Curtiss, T. Sooksimuang, B.K. Mandal, "Excited State Dynamics and Structures of Functionalized Phthalocyanines. 1. Self-Regulated Assembly of Zinc Helicenocyanine," J. Phys. Chem. B 109 (35), September, 16598-16609 (2005).

X-J. Chen, M.V. Struzhkin, Z. Wu, M. Somayazulu, J. Qian, S. Kung, A. Christensen, Y. Zhao, R.E. Cohen, H.-k. Mao, R.J. Hemley, "Hard superconducting nitrides," Proc. Natl. Acad. Sci. USA 102 (9), March, 3198-3201 (2005).

Y. Chen, J.L. Fulton, J.C. Linehan, T. Autrey, "In-situ XAFS and NMR Study of Rhodium Catalyst Structure during Dehydrocoupling of Dimethylamine Borane," J. Am. Chem. Soc. 127 (10), February, 3254-3255 (2005).

Yongsheng Chen, John L. Fulton, Walter Partenheimer, "The Structure of the Homogeneous Oxidation Catalyst, Mn(II)(Br[superscript -1])[subscript x], in Supercritical Water: An X-ray Absorption Fine-Structure Study," J. Am. Chem. Soc. 127 (40), September, 14085-14093 (2005).

Yongsheng Chen, John L. Fulton, Walter Partenheimer, "A XANES and EXAFS Study of Hydration and Ion Pairing in Ambient Aqueous MnBr[subscript 2] Solutions," J. Solution Chem. 34 (9), September, 993-1007 (2005).

David Chereau, Frederic Kerff, Philip Graceffa, Zenon Grabarek, Knut Langsetmo, Roberto Dominguez, "Actin-bound structures of Wiskott-Aldrich syndrome protein (WASP)-homology domain 2 and the implications for filament assembly.," Proc. Natl. Acad. Sci. USA 102 (46), November, 16644-16649 (2005).

P.T. Chiu, B.W. Wessels, D.J. Keavney, J.W. Freeland, "Local environment of ferromagnetically ordered Mn in epitaxial InMnAs," Appl. Phys. Lett. 86, 072505- 1-072505- 3 (2005).

Thang K. Chiu, Jan Kubelka, Regine Herbst-Irmer, William A. Eaton, James Hofrichter, David R. Davies, "High-resolution x-ray crystal structures of the villin headpiece subdomain, an ultrafast folding protein," Proc. Natl. Acad. Sci. USA 102 (21), May, 7517-7522 (2005).

Jill E. Chrencik, Jillian Orans, Linda B. Moore, Yu Xue, Li Peng, Jon L. Collins, G. Bruce Wisely, Millard H. Lambert, Steven A. Kliewer, Matthew R. Redinbo, "Structural Disorder in the Complex of Human Pregnane X Receptor and the Macrolide Antibiotic Rifampicin," Mol. Endocrinol. 19 (7), May, 1125-1134 (2005).

Craig S. Clements, Lars Kjer-Nielsen, Lyudmila Kostenko, Hilary L. Hoare, Michelle A. Dunstone, Eric Moses, Katy Freed, Andrew G. Brooks, Jamie Rossjohn, James McCluskey, "Crystal structure of HLA-G: A nonclassical MHC class I molecule expressed at the fetal-maternal interface," Proc. Natl. Acad. Sci. USA 102 (9), February, 3360-3365 (2005).

Violina A. Cocalia, Mark P. Jensen, John D. Holbrey, Scott K. Spear, Dominique C. Stepinski, Robin D. Rogers, "Identical Extraction Behavior and Coordination of Trivalent or Hexavalent f-Element Cations using Ionic Liquid and Molecular Solvents," Dalton T. - (11), June, 1966-1971 (2005).

Diana M. Colleluori, Robert S. Reczkowski, Frances A. Emig, Evis Cama, J. David Cox, Laura R. Scolnick, Kevin Compher, Kevin Jude, Shoufa Han, Ronald E. Viola, David W. Christianson, David E. Ash, "Probing the role of the hyper-reactive histidine residue of arginase," Arch. Biochem. Biophys. 444, 15-26 (2005).

Jean-Francois Collet, Daniel Peisach, James C.A. Bardwell, Zhaohui Xu, "The crystal structure of TrxA(CACA): Insights into the formation of a [2Fe-2S] iron-sulfur cluster in an Escherichia coli thioredoxin mutant," Protein Sci. 14, 1863-1869 (2005).

J.F. Collingwood, A. Mikhaylova, M. Davidson, C. Batich, W.J. Streit, J. Terry, J. Dobson, "In-situ Characterization and Mapping of Iron Compounds in Alzheimer's Tissue," J. Alzheimers Dis. 7, 267-272 (2005).

P. Coppens, B. Iversen, F.K. Larsen, "The use of synchrotron radiation in X-ray charge density analysis of coordination complexes," Coordin. Chem. Rev. 249, 179-195 (2005).

P. Coppens, I.V. Novozhilova, "DFT calculations of light-induced excited states and comparison with time-resolved crystallographic results," Int. J. Quant. Chem. 101, 611-632 (2005).

Philip Coppens, Ivan L. Vorontsov, Tim Graber, Milan Gembicky, Andrey Yu. Kovalevsky, "The structure of short-lived excited states of molecular complexes by time-resolved X-ray diffraction," Acta Crystallogr. A 61 (2), 162-172 (2005).

M.K. Corbierre, N.S. Cameron, M. Sutton, K. Laaziri, R.B. Lennox, "Gold Nanoparticle/Polymer Nanocomposites: Dispersion of Nanoparticles as a Function of Capping Agent Molecular Weight and Grafting Density," Langmuir 21 (13), June, 6063-6072 (2005).

Daniel P. Core, Stephen E. Kesler, Eric J. Essene, Eric B. Dufresne, Roy Clarke, Dohn A. Arms, Don Walko, Mark L. Rivers, "Copper and zinc in silicate and oxide minerals in igneous rocks from the Bingham-Park City belt, Utah: synchrotron x-ray fluorescence data," Can. Mineral. 43, 1781-1796 (2005).

James V. Corino, T. Robertson, N. Dutton, D. Halas, A. Boyd, J. Bentel, J. Papadimitriou, "Early diagnosis of breast cancer by hair diffraction," Int. J. Cancer 114 (6), May, 969-972 (2005).

Julien J.H. Cotelesage, Lata Prasad, J.Gregory Zeikus, Maris Laivenieks, Louis T.J. Delbaere, "Crystal structure of Anaerobiospirillum succiniciproducens PEP carboxykinase reveals an important active site loop," Int. J. Biochem. Cell B. 37 (9), November, 1829-1837 (2005).

Jean-François Couture, Evys Collazo, Joseph S. Brunzelle, Raymond C. Trieve, "Structural and functional analysis of SET8, a histone H4 Lys-20 methyltransferase," Gene Dev. 19, June, 1455-1465 (2005).

Bryan Cox, MaMay Chit, Todd Weaver, Christine Gietl, Jaclyn Bailey, Ellis Bell, Leonard Banaszak, "Organelle and translocatable forms of glyoxysomal malate dehydrogenase: The effect of the N-terminal presequence," FEBS Lett. 272, 643-654 (2005).

Christopher D. Cox, Michael J. Breslina, Brenda J. Mariano, Paul J. Coleman, Carolyn A. Buser, Eilee S. Walsh, Kelly Hamilton, Hans E. Huber, Nanc E. Kohl, Maricel Torrent, Youwei Yan, Laurence C. Kuo, George D. Hartman, "Kinesin spindle protein (KSP) inhibitors. Part 1: The discovery of 3,5-diaryl-4,5-dihydropyrazoles as potent and selective inhibitors of the mitotic kinesin KSP," Bioorg. Med. Chem. Lett. 15 (8), April, 2041-2045 (2005).

J.W. Crawford, J.A. Harris, K. Ritz, I.M. Young, "Towards an evolutionary ecology of life in soil," Trends Ecol. Evol. 20 (2), 81-87 (2005).

Carrie A. Crot, Chunping Wu, Mark L. Schlossman, Thomas P. Trainor, Peter. Eng, Luke Hanley, "Determining the Conformation of an Adsorbed Br-PEG-Peptide by Long Period X-Ray Standing Wave Fluorescence," Langmuir 21 (17), July, 7899-7906 (2005).

J.W. Crotty, C. Etzkorn, C.F. Barbas III, D.J. Segal, N.C. Horton, "Crystallization and preliminary X-ray crystallographic analysis of Aart, a designed six-finger zinc-finger peptide, bound to DNA," Acta Crystallogr. F 61 (6), June, 573-576 (2005).

James D. Crowley, Brice Bosnich, "Molecular Recognition: Use of Metal-Containing Molecular Clefts for Supramolecular Self-Assembly and Host-Guest Formation," Eur. J. Inorg. Chem. 2005 (11), 2015-2025 (2005).

J.D. Crowley, I.M. Steele, B. Bosnich, "An examination of Weak Metal-Metal Interactions in Host-Guest Formation," Inorg. Chem. 44, 2989-2991 (2005).

Louise M. Cunane, John D. Barton, Zhi-wei Chen, K.H.Diep Le, David Amar, Florence Lederer, F.Scott Mathews, "Crystal Structure Analysis of Recombinant Rat Kidney Long Chain Hydroxy Acid Oxidase," Biochemistry-US 44 (5), January, 1521-1531 (2005).

Louise M. Cunane, Zhi-wei Chen, William S. McIntire, F.Scott Mathews, "p-Cresol Methylhydroxylase: Alteration of the Structure of the Flavoprotein Subunit upon Its Binding to the Cytochrome Subunit," Biochemistry-US 44, 2963-2973 (2005).

Nicholas C. Cunningham, Nenad Velisavljevic, Yogesh K. Vohra, "Crystal grain growth at the [alpha]-uranium phase transformation in praseodymium," Phys. Rev. B 71, January, 012108-1-012108-4 (2005).

Edmund W. Czerwinski, Terumi Midoro-Horiuti, Mark A. White, Edward G. Brooks, Randall M. Goldblum, "Crystal Structure of Jun a 1, the Major Cedar Pollen Allergen from Juniperus ashei, Reveals a Parallel [beta]-Helical Core," J. Biol. Chem. 280 (5), February, 3740-3746 (2005).

P. Czoschke, Hawoong Hong, L. Basile, T.-C. Chiang, "Quantum size effects in the surface energy of Pb/Si(111) film nanostructures studied by surface x-ray diffraction and model calculations," Phys. Rev. B 72, 075402-1-075402-13 (2005).

P. Czoschke, Hawoong Hong, L. Basile, T.-C. Chiang, "Surface x-ray-diffraction study and quantum well analysis of the growth and atomic-layer structure of ultrathin Pb/Si(111) films," Phys. Rev. B 72, 035305-1-035305-11 (2005).

Han Dai, Diana R. Tomchick, Jesus Garcia, Thomas C. Sudhof, Mischa Machius, Josep Rizo, "Crystal Structure of the RIM2 C[subscript 2]A-Domain at 1.4 Å Resolution," Biochemistry-US 44 (41), October, 13533-13542 (2005).

M. Daniel, S.-W. Han, C.H. Booth, A.L. Cornelius, P.G. Pagliuso, J.L. Sarrao, J.D. Thompson, "X-ray absorption studies of the local structure and f-level occupancy in CeIr[subscript 1-x]Rh[subscript x]In[subscript 5]," Phys. Rev. B 71, 054417-1-054417-8 (2005).

Arvin C. Dar, Thomas E. Dever, Frank Sicheri, "Higher-Order Substrate Recognition of eIF2[alpha] by the RNA-Dependent Protein Kinase PKR," Cell 122 (6), September, 887-900 (2005).

Zbigniew Dauter, Istvan Botos, Nicole LaRonde-LeBlanc, Alexander Wlodawer, "Pathological crystallography: case studies of several unusual macromolecular crystals," Acta Crystallogr. D 61, April, 967-975 (2005).

J.M. Davies, H. Tsuruta, A.P. May, W.I. Weis, "Conformational Changes of p97 during Nucleotide Hydrolysis Determined by Small-Angle X-ray Scattering," Structure 13, February, 183-195 (2005).

Tara L. Davis, Tabetha M. Bonacci, Stephen R. Sprang, Alan V. Smrcka, "Structural and Molecular Characterization of a Preferred Protein[beta[subscript gamma]] Interaction Surface on G Protein Subunits," Biochemistry-US 44 (31), July, 10593-10604 (2005).

Luigi De Colibus, Min Li, Claudia Binda, Ariel Lustig, Dale E. Edmondson, Andrea Mattevi, "Three-dimensional structure of human monoamine oxidase A (MAO A): Relation to the structures of rat MAO A and human MAO B," Proc. Natl. Acad. Sci. USA 102 (36), August, 12684-12689 (2005).

D. de Fontaine, V. Ozolins, Z. Islam, S.C. Moss, "On the origin of modulated structures in YBa[subscript 2]Cu[subscript 3]O[subscript 6.63]: A first-principles approach," Phys. Rev. B 71 (21), June, 212504-1-212504-4 (2005).

Frank de Groot, "Multiplet effects in X-ray spectroscopy," Coordin. Chem. Rev. 249 (1-2), January, 31-63 (2005).

Frank M.F. de Groot, Pieter Glatzel, Uwe Bergmann, Peter A. van Aken, Raul A. Barrea, Stephan Klemme, Michael Havecker, Axel Knop-Gericke, Willem M. Heijboer, Bert M. Weckhuysen, "1s2p Resonant Inelastic X-ray Scattering of Iron Oxides," J. Phys. Chem. B 109 (44), 20751-20762 (2005).

M.D. de Jonge, C.Q. Tran, C.T. Chantler, Z. Barnea, B.B. Dhal, D.J. Cookson, W.-K. Lee, A. Mashayekhi, "Measurement of the x-ray mass attenuation coefficient and determination of the imaginary component of the atomic form factor of molybdenum over the 13.5-41.4-keV energy range," Phys. Rev. A 71, March, 032702-1-032702-16 (2005).

Alexandra M. Deaconescu, Seth A. Darst, "Crystallization and preliminary structure determination of Escherichia coli Mfd, the transcription-repair coupling factor," Acta Crystallogr. F 61, November, 1062-1064 (2005).

A. Deb, U. Bergmann, S.P. Cramer, E.J. Cairns, "In situ x-ray absorption spectroscopic study of the Li[Ni[subscript 1/3]Co[subscript 1/3]Mn[subscript 1/3]]O[subscript 2]," J. Appl. Phys. 97, 113523-1-113523-11 (2005).

Matthew F. DeCamp, David A. Reis, David M. Fritz, Philip H. Bucksbaum, Eric M. Dufresne, Roy Clarke, "X-ray synchrotron studies of ultrafast crystalline dynamics," J. Synchrotron Rad. 12 (2), 177-192 (2005).

O. Degtyareva, E. Gregoryanz, H.-k. Mao, R.J. Hemley, "Crystal structure of sulfur and selenium at pressures up to 160 GPa," High Pressure Res. 25 (1), March, 17-33 (2005).

O. Degtyareva, E. Gregoryanz, M. Somayazulu, P. Dera, H.-k. Mao, R.J. Hemley, "Novel chain structures in group VI elements," Nat. Mater. 4, January, 152-155 (2005).

Olga Degtyareva, Eugene Gregoryanz, Maddury Somayazulu, Ho-kwang Mao, Russell J. Hemley, "Crystal structure of the superconducting phases of S and Se," Phys. Rev. B 71 (21), 214104-1-214104-6 (2005).

V.F. Degtyareva, O. Degtyareva, M.K. Sakharov, N.I. Novokhatskaya, P. Dera, H.-k. Mao, R.J. Hemley, "Stability of Hume-Rothery phases in Cu-Zn alloys at pressures up to 50 GPa," J. Phys. Condens. Matter 17, December, 7955-7962 (2005).

Byron DeLaBarre, Axel T. Brunge, "Nucleotide Dependent Motion and Mechanism of Action of p97/VCP," J. Mol. Biol. 347 (2), March, 437-452 (2005).

M.A. Denecke, K. Dardenne, C.M. Marquardt, "Np(IV)/Np(V) valence determinations from Np L3 edge XANES/EXAFS," Talanta 65 (4), February, 1008-1014 (2005).

Melissa A. Denecke, Andre Rossberg, Petra J. Panak, Michael Weigl, Bernd Schimmelpfennig, Andreas Geist, "Characterization and Comparison of Cm(III) and Eu(III) Complexed with 2,6-Di(5,6-dipropyl-1,2,4-triazin-3-yl)pyridine Using EXAFS, TRFLS, and Quantum-Chemical Methods," Inorg. Chem. 44 (23), October, 8418-8425 (2005).

Junpeng Deng, Nancy Lewis Ernst, Stewart Turley, Kenneth D. Stuart, Wim G.J. Hol, "Structural basis for UTP specificity of RNA editing TUTases from Trypanosoma brucei," EMBO J. 24 (23), 4007-4017 (2005).

Lu Deng, Eugene S. Vysotski, Svetlana V. Markova, Zhi-Jie Liu, John Lee, John Rose, Bi-Cheng Wang, "All three Ca[superscript 2+]-binding loops of photoproteins bind calcium ions: The crystal structures of calcium-loaded apo-aequorin and apo-obelin," Protein Sci. 14, 663-675 (2005).

Ilia G. Denisov, Mark A. McLean, Andrew W. Shaw, Yelena V. Grinkova, Stephen G. Sligar, "Thermotropic Phase Transition in Soluble Nanoscale Lipid Bilayers," J. Phys. Chem. B 109 (32), July, 15580-15588 (2005).

Sanghamitra Dey, Gregory A. Grant, James C. Sacchettini, "Crystal Structure of Mycobacterium tuberculosis D-3-Phosphoglycerate Dehydrogenase: Extreme Asymretry in a Tertamer of Identical Subunits," J. Biol. Chem. 280 (15), April, 14892-14899 (2005).

M. Dickinson, G. Farman, M. Frye, T. Bekyarova, D. Gore, D. Maughan, T. Irving, "Molecular dynamics of cyclically contracting insect flight muscle in vivo," Nature 433 (7023), January, 330-333 (2005).

J. Diefenbacher, M. McKelvy, A.V. Chizemeshya, G.H. Wolf, "Externally controlled pressure and temperature microreactor for in situ x-ray diffraction, visual and spectroscopic reaction investigations under supercritical and subcritial conditions," Rev. Sci. Instrum. 76, 015103-1-015103-7 (2005).

N. Dimakis, G. Bunker, "Initial Results of the OneDimensional XAFS DebyeWaller Models for Active Sites of Cu Histidine and Cystein Metalloproteins," Phys. Scripta. T115, 175-178 (2005).

N. Dimakis, G. Bunker, "3D Molecular Graphical user Interface AddOn for Analysis Program for EXAFS A New Prospect," Phys. Scripta. T115, 226-228 (2005).

H.F. Ding, A.K. Schmid, D.J. Keavney, D. Li, R. Cheng, J.E. Pearson, F.Y. Fradin, S.D. Bader, "Selective growth of Co nanoislands on an oxygen-patterned Ru(0001) surface," Phys. Rev. B 72, 035413-1-035413-5 (2005).

Yang Ding, Haozhe Liu, Maddury Somayazulu, Yue Meng, Jian Xu, Charles T. Prewitt, "Zone-axis x-ray diffraction of single-crystal Fe[subscript 1-x]O under pressure," Phys. Rev. B 72, 174109-1-174109-6 (2005).

Yang Ding, Haozhe Liu, Jian Xu, Charles T. Prewitt, Russell J. Hemley, Ho-kwang Mao, "Zone-axis diffraction study of pressure-induced inhomogeneity in single-crystal Fe[subscript 1-x]O," Appl. Phys. Lett. 87 (4), July, 041912-1-041912-3 (2005).

Yang Ding, Jian Xu, Charles T. Prewitt, Russell J. Hemley, Ho-kwang Mao, John A. Cowan, Jianzhong Zhang, Jiang Qian, Sven C. Vogel, Konstantin Lokshin, Yusheng Zhao, "Variable pressure-temperature neutron diffraction of wüstite (FeO): Absence of long-range magnetic order to 20 GPa," Appl. Phys. Lett. 86, January, 052505-1-052505-3 (2005).

D.Eric Dollins, Robert M. Immormino, Daniel T. Gewirth, "Structure of Unliganded GRP94, the Endoplasmic Reticulum Hsp90: Basis for Nucleotide-Induced Conformatinal Change," J. Biol. Chem. 280 (34), August, 30438-30447 (2005).

Jill D. Dombrauckas, Bernard D. Santarsiero, Andrew D. Mesecar, "Structural Basis for Tumor Pyruvate Kinase M2 Allosteric Regulation and Catalysis," Biochemistry-US 44 (27), June, 9417-9429 (2005).

G. Dong, A.H. Hutagalung, C. Fu, P. Novick, K.M. Reinisch, "The structures of exocyst subunit Exo70p and the Exo84p C-terminal domains reveal a common motif," Nat. Struct. Mol. Biol. 12 (12), December, 1094-1100 (2005).

Jianbo Dong, Ning Shi, Ian Berke, Liping Chen, Youxing Jiang, "Structures of the MthK RCK Domain and the Effect of Ca[superscript 2+]on Gating Ring Stability," J. Biol. Chem. 280 (50), December, 41716-41724 (2005).

Christian J. Doonan, Limei Zhang, Charles G. Young, Simon J. George, Aniruddha Deb, Uwe Bergmann, Graham N. George, Stephen P. Cramer, "High-Resolution X-ray Emission Spectroscopy of Molybdenum Compounds," Inorg. Chem. 44 (8), March, 2579-2581 (2005).

Michaeleen Doucleff, Baoyu Chen, Ann E. Maris, David E. Wemmer, Elena Kondrashkina, B.Tracy Nixon, "Negative Regulation of AAA+ ATPase Assembly by Two Component Receiver Domains: A Transcription Activation Mechanism that is Conserved in Mesophilic and Extremely Hyperthermophilic Bacteria," J. Mol. Biol. 353 (2), September, 242-255 (2005).

T. Droubay, S.M. Heald, V. Shutthanandan, S. Thevuthasan, S.A. Chambers, "Cr-doped TiO[subscript 2] anatase: A ferromagnetic insulator," J. Appl. Phys. 97, February, 046103-1-046103-3 (2005).

James L. Drummond, DeCarlo Francesco, Boaz J. Super, "Three-dimensional tomography of composite fracture surfaces," J. Biomed. Mater. Res.-B 74B (2), June, 665-668 (2005).

N. Dubrovinskaia, L. Dubrovinsky, I. Kantor, W.A. Crichton, V. Dmitriev, V. Prakapenka, G. Shen, L. Vitos, R. Ahuja, B. Johansson, I.A. Abrikosov, "Beating the Miscibility Barrier between Iron Group Elements and Magnesium by High-Pressure Alloying," Phys. Rev. Lett. 95, December, 245502-1-245502-4 (2005).

N. Dubrovinska, L. Dubrovinsky, F. Langehorst, S. Jacobsen, C. Liebske, "Nanocrystalline diamond synthesized from C60," Diam. Relat. Mater. 14 (1), January, 16-22 (2005).

David N. Duda, Helen Walden, John Sfondouris, Brenda A. Schulman, "Structural Analysis of Escherichia Coli ThiF," J. Mol. Biol. 349, June, 774-786 (2005).

T. Duffy, "Synchrotron facilities and the study of the Earth's deep interior," Rep. Prog. Phys. 68, 1811-1859 (2005).

Erica M. Duguid, Phoebe A. Rice, Chuan He, "The Structure of the Human AGT Protein Bound to DNA and its Implications for Damage Detection," J. Mol. Biol. 350 (4), June, 657-666 (2005).

K.V. Dunlop, R.T. Irvin, B. Hazes, "Pros and cons of cryocrystallography: should we also collect a room-temperature data set?," Acta Crystallogr. D 61 (1), January, 80-87 (2005).

Martin B. Duriska, Stuart R. Batten, Jinzhen Lu, Paul Jensen, Harry Adams, Graham M. Davies, John C. Jeffery, Graham R. Motson, Michael D. Ward, "Crystal engineering with scorpionate ligands," Acta Crystallogr. A A61, C356 (2005).

David H. Dyer, Karen S. Lyle, Ivan Rayment, Brian G. Fox, "X-ray structure of putative acyl-ACP desaturase DesA2 from Mycobacterium tuberculosis H37Rv," Protein Sci. 14, 1508-1517 (2005).

J.A. Eastman, P.H. Fuoss, L.E. Rehn, P.M. Baldo, G.-W. Zhou, D.D. Fong, L.J. Thompson, "Early-stage suppression of Cu (001) oxidation," Appl. Phys. Lett. 87 (5), August, 051914-1-051914-3 (2005).

Martin Egli, George Minasov, Valentina Tereshko, Pradeep S. Pallan, Marianna Teplova, Gopal B. Inamati, Elena A. Lesnik, Steve R. Owens, Bruce S. Ross, Thazha P. Prakash, Muthiah Manoharan, "Probing the Influence of Stereoelectronic Effects on the Biophysical Properties of Oligonucleotides: Comprehensive Analysis of the RNA Affinity, Nuclease Resistance, and Crystal Structure of Ten 2'-O-Ribonucleic Acid Modifications," Biochemistry-US 44 (25), June, 9045-9057 (2005).

A.G. Eguiluz, O.D. Restrepo, B.C. Larson, J.Z. Tischler, P. Zschack, G.E. Jellison, "Electron-hole excitations in NiO: LSDA+U-based calculations vs. inelastic X-ray scattering and ellipsometry measurements," J. Phys. Chem. Solids 66 (12), December, 2281-2289 (2005).

Youssef Elias, Raven H. Huang, "Biochemical and Structural Studies of A-to-I Editing by tRNA:A34 Deaminases at the Wobble Position of Transfer RNA," Biochemistry-US 44 (36), August, 12057-12065 (2005).

J.W. Elmer, T.A. Palmer, S.S. Babu, E.D. Specht, "In situ observations of lattice expansion and transformation rates of [alpha] and [beta] phases in Ti-6Al-4V," Mat. Sci. Eng. A 391 (1-2), January, 104-113 (2005).

J.W. Elmer, T.A. Palmer, S.S. Babu, E.D. Specht, "Low temperature relaxation of residual stress in Ti-6Al-4V," Scripta Mater. 52 (10), May, 1051-1056 (2005).

Lauren K. Ely, Katherine J. Green, Travis Beddoe, Craig S. Clements, John J. Miles, Stephen P. Bottomley, Danielle Zernich, Lars Kjer-Nielsen, Anthony W. Purcell, James McCluskey, Jamie Rossjohn, Scott R. Burrows, "Antagonism of antiviral and allogeneic activity of a human public CTL clonotype by a single altered peptide ligand: implications for allograft rejection," J. Immunol. 175 (9), May, 5593-5601 (2005).

D. Errandonea, Y. Meng, M. Somayazulu, D. Hausermann, "Pressure-induced alpha to omega transition in titanium metal: a systematic study of the effects of uniaxial stress," Physica B 355, January, 116-125 (2005).

D. Errandonea, J. Pellicer-Porres, F.J. Manjón, A. Segura, Ch. Ferrer-Roca, R.S. Kumar, O. Tschauner, P. Rodríguez-Hernández, J. López-Solano, S. Radescu, A. Mujica, A. Munoz, G. Aquilanti, "High-pressure structural study of the scheelite tungstates CaWO[subscript 4] and SrWO[subscript 4]," Phys. Rev. B 72, 174106-1-174106-14 (2005).

P.G. Evans, P.P. Rugheimer, M.G. Lagally, C.H. Lee, A. Lal, Y. Xiao, B. Lai, Z. Cai, "Microfabricated strained substrates for Ge epitaxial growth," J. Appl. Phys. 97, April, 103501-1-103501-5 (2005).

P.G. Evans, D.S. Tinberg, M.M. Roberts, M.G. Lagally, Y. Xiao, B. Lai, Z. Cai, "Germanium hut nanostressors on freestanding thin silicon membranes," Appl. Phys. Lett. 87 (7), August, 073112-1-073112-3 (2005).

W.J. Evans, M.J. Lipp, H. Cynn, C.S. Yoo, M. Somayazulu, D. Hausermann, G. Shen, V. Prakapenka, "X-ray diffraction and Raman studies of beryllium: Static and elastic properties at high pressure," Phys. Rev. B 72 (9), September, 094113-1-094113-6 (2005).

P. Falus, M.A. Borthwick, S.G.J. Mochrie, "Fluctuation Dynamics of Block Copolymer Vesicles," Phys. Rev. Lett. 94 (2), January, 016105-1-016105-4 (2005).

L. Fan, I. McNulty, D. Paterson, M.M.J. Treacy, J.M. Gibson, "Fluctuation microscopy - a tool for examining medium-range order in non-crystalline systems," Nucl. Instrum. Methods B 238 (1-4), 196-199 (2005).

Qing R. Fan, Wayne A. Hendrickson, "Structure of human follicle-stimulating hormone in complex with its receptor," Nature 433, January, 269-277 (2005).

Frederic A. Fellouse, Bing Li, Deanne M. Compaan, Andrew A. Peden, Sarah G. Hymowitz, Sachdev S. Sidhu, "Molecular Recognition by a Binary Code," J. Mol. Biol. 348 (5), May, 1153-1162 (2005).

R. Feng, E.H. Conrad, C. Kim, P.F. Miceli, M.C. Tringides, "The evolution of the structure of quantum size effect Pb nanocrystals on Si(111) 7x7," Physica B 357, 175-179 (2005).

Y. Feng, M.S. Somayazulu, R. Jaramillo, T.F. Rosenbaum, E.D. Isaacs, J. Hu, H.-k. Mao, "Energy dispersive x-ray diffraction of charge density waves via chemical filtering," Rev. Sci. Instrum. 76, 063913-1-063913-4 (2005).

P. Fenter, Z. Zhang, "Model-Independent One-Dimensional Imaging of Interfacial Structures at <1 Å resolution," Phys. Rev. B 72, August, 081401-1-081401-4 (2005).

Bradley Finnigan, Kevin Jack, Kayleen Campbell, Peter Halley, Rowan Truss, Phil Casey, David Cookson, Stephen King, Darren Martin, "Segmented Polyurethane Nanocomposites: Impact of Controlled Particle Size Nanofillers on the Morphological Response to Uniaxial Deformation," Macromolecules 38 (17), June, 7386-7396 (2005).

Millicent A. Firestone, Mark L. Dietz, Sonke Seifert, Susana Trasobares, Dean J. Miller, Nestor J. Zaluzec, "Ionogel-Templated Synthesis and Organization of Anisotropic Gold Nanoparticles," Small 1 (7), 754-760 (2005).

John F. Flanagan, Li-Zhi Mi, Maksymilian Chruszcz, Marcin Cymborowski, Katrina L. Clines, Youngchang Kim, Wladek Minor, Fraydoon Rastinejad, Sepideh Khorasanizadeh, "Double chromodomains cooperate to recognize the methylated histone H3 tail," Nature 438 (22), December, 1181-1185 (2005).

Christopher D. Fleming, Sompop Bencharit, Carol C. Edwards, Janice L. Hyatt, Lyudmila Tsurkan, Feng Bai, Charles Fraga, Christopher L. Morton, Escher L. Howard-Williams, Philip M. Potter, Matthew R. Redinbo, "Structural Insights into Drug Processing by Human Carboxylesterase 1: Tamoxifen, Mevastatin, and Inhibition by Benzil," J. Mol. Biol. 352, 165-177 (2005).

J.F. Flores, S.L. Carney, B.N. Green, J.K. Freytag, S.W. Schaeffer, C.R. Fisher, W.E. Royer, "Sulfide binding is mediated by zinc ions discovered in the crystal structure of a hydrothermal vent tubeworm hemoglobin," Proc. Natl. Acad. Sci. USA 102 (8), February, 2713-2718 (2005).

A. Fluerasu, M. Sutton, E.M. Dufresne, "X-Ray Intensity Fluctuation Spectroscopy Studies on Phase-Ordering Systems," Phys. Rev. Lett. 94 (5), February, 055501-1-055501-4 (2005).

Andrei Fokine, Petr G. Leiman, Mikhail M. Shneider, Bijan Ahvazi, Karen M. Boeshans, Alasdair C. Steven, Lindsay W. Black, Vadim V. Mesyanzhinov, Michael G. Rossmann, "Structural and functional similarities between the capsid proteins of bacteriophages T4 and HK97 point to a common ancestry," Proc. Natl. Acad. Sci. USA 102 (20), May, 7163-7168 (2005).

D.D. Fong, C. Cionca, Y. Yacoby, G.B. Stephenson, J.A. Eastman, P.H. Fuoss, S.K. Streiffer, Carol Thompson, R. Clarke, R. Pindak, E.A. Stern, "Direct structural determination in ultrathin ferroelectric films by analysis of synchrotron x-ray scattering measurements," Phys. Rev. B 71, April, 144112-1-144112-11 (2005).

D.D. Fong, J.A. Eastman, G.B. Stephenson, P.H. Fuoss, S.K. Streiffer, C. Thompson, O. Auciello, "In situ synchrotron X-ray studies of ferroelectric thin films," J. Synchrotron Rad. 12 (2), March, 163-167 (2005).

S. Forster, A. Timmann, M. Konrad, C. Schellbach, A. Meyer, S.S. Funari, H. Nakamura, P. Mulvaney, R. Knott, "Scattering-curves of ordered mesoscopic materials," J. Phys. Chem. B 109 (4), January, 1347-1360 (2005).

A.E. Forsyth, C.G. Weisener, P.C. Burns, D.A. Fowle, "Reductive dissolution of zippeite group minerals by Desulfovibrio desulfuricans," Geochim. Cosmochim. Acta 69 (10), A419-A419 (2005).

J.O. Fossum, E. Gudding, D.M. Fonseca, Y. Meheust, E. DiMasi, T. Gog, C. Venkataraman, "Observation of orientational ordering in aqueous suspensions of a nano-layered silicate," Energy 30, 873-883 (2005).

Brian G. Fox, Thomas E. Malone, Kenneth A. Johnson, Stacey E. Madson, David Aceti, Craig A. Bingman, Paul G. Blommel, Blake Buchan, Brendan Burns, John Cao, Claudia Cornilescu, Jurgen Doreleijers, Jason Ellefson, Ronnie Frederick, Holokere Geetha, David Hruby, Won Bae Jeon, Todd Kimball, John Kunert, John L. Markley, Craig Newman, Andew Olson, Francis C. Peterson, George N. Phillips, Jr., John Primm, Bryan Ramirez, Nathan S. Rosenberg, Mike Runnels, Kory Seder, Jeff Shaw, David W. Smith, Hassan Sreenath, Jikui Song, Michael R. Sussman, Sandy Thao, Donna Troestler, Ejan Tyler, Robert Tyler, Eldon Ulrich, Dimitriy Vinarov, Frank Vojtik, Brian F. Volkman, Gary Wesenberg, Russell L. Wrobel, Jie Zhang, Qin Zhao, Zolt Zolnai, "X-ray structure of Arabidopsis At1g7768, 12-oxophytodienoate reductase isoform 1," Proteins 61 (1), 206-208 (2005).

G.E. Fryxell, Y. Lin, S. Fiskum, J.C. Birnbaum, H. Wu, K.M. Kemner, S.D. Kelly, "Actinide Sequestration Using Self-Assembled Monolayers on Mesoporous Supports," Environ. Sci. Technol. 39 (5), January, 1324-1331 (2005).

Masahiro Fujihashi, Angelica M. Bello, Ewa Poduch, Lianhu Wei, Subhash C. Annedi, Emil F. Pai, Lakshmi P. Kotra, "An Unprecedented Twist to ODCase Catalytic Activity," J. Am. Chem. Soc. 127 (43), October, 15048-15050 (2005).

Norio Fukuda, Yiming Wu, Gerrie Farman, Thomas C. Irving, Henk Granzier, "Titin-based modulation of active tension and interfilament lattice spacing in skinned rat cardiac muscle," Pflug. Arch. Eur. J. Phy. 449 (5), February, 449-457 (2005).

M.J. Fuller, L.E. Sinks, B. Rybtchinski, J.M. Giaimo, X. Li, M.R. Wasielewski, "Ultrafast Photoinduced Charge Separation Resulting from Self-assembly of a Green Perylene-based Dye into [pi]-Stacked Arrays," J. Phys. Chem. A 109 (6), January, 970-975 (2005).

Kate F. Fulton, Ashley M. Buckle, Lisa D. Cabrita, James A. Irving, Rebecca E. Butcher, Ian Smith, Shane Reeve, Arthur M. Lesk, Stephen P. Bottomley, Jamie Rossjohn, James C. Whisstock, "The high resolution crystal structure of a native thermostable serpin reveals the complex mechanism underpinning the stressed to relaxed transition," J. Biol. Chem. 280 (9), 8435-8432 (2005).

Zheng-Qing Fu, John Rose, Bi-Cheng Wang, "SGXPro: a parallel workflow engine enabling optimization of program performance and automation of structure determination," Acta Crystallogr. D D (61), July, 951-959 (2005).

K.J. Gaffney, A.M. Lindenberg, J. Larsson, K. Sokolowski-Tinten, C. Blome, O. Synnergren, J. Sheppard, C. Caleman, A.G. MacPhee, D. Weinstein, D.P. Lowney, T. Allison, T. Matthews, R.W. Falcone, A.L. Cavalieri, D.M. Fritz, S.H. Lee, P.H. Bucksbaum, D.A. Reis, J. Rudati, A.T. Macrander, P.H. Fuoss, C.C. Kao, D.P. Siddons, R. Pahl, K. Moffat, J. Als-Nielsen, S. Duesterer, R. Ischebeck, H. Schlarb, H. Schulte-Schrepping, J. Schneider, D. von der Linde, O. Hignette, F. Sette, H.N. Chapman, R.W. Lee, T.N. Hansen, J.S. Wark, M. Bergh, G. Huldt, D. van der Spoel, N. Timmeanu, J. Hajdu, R.A. Akre, E. Bong, P. Krejcik, J. Arthur, S. Brennan, K. Luening, J.B. Hastings, "Observation of structural anisotropy and the onset of liquidlike motion during the nonthermal melting of InSb," Phys. Rev. Lett. 95 (12), September, 125701-1-125701-5 (2005).

Susan J. Gagnon, Oleg Y. Borbulevych, Rebecca L. Davis-Harrison, Tiffany K. Baxter, John R. Clemens, Kathryn M. Armstrong, Richard V. Turner, Marale Damirjian, William E. Biddison, Brian M. Baker, "Unraveling a Hotspot for TCR Recognition on HLA-A2: Evidence Against the Existence of Peptide-independent TCR Binding Determinants," J. Mol. Biol. 353, 556-573 (2005).

Lokesh Gakhar, Zulfiqar A. Malik, Christopher C.R. Allen, David A. Lipscomb, Michael J. Larkin, S. Ramaswamy, "Structure and Increased Thermostability of Rhodococcus sp. Naphthalene 1,2-Dioxygenase," J. Bacteriol. 187 (21), November, 7222-7231 (2005).

Vannakambadi K. Ganesh, Suresh Kumar Muthuvel, Scott A. Smith, Girish J. Kotwal, Krishna H.M. Murthy, "Structural Basis for Antagonism by Suramin of Heparin Binding to Vaccinia Complement Protein," Biochemistry-US 44, July, 10757-10765 (2005).

Jianhua Gan, Joseph E. Tropea, Brian P. Austin, Donald L. Court, David S. Waugh, Xinhua Ji, "Intermediate States of Ribonuclease III in Complex with Double-Stranded RNA," Structure 13, October, 1435-1442 (2005).

Lawrencede Garavilla, Michael N. Greco, Narayanasami Sukumar, Zhi-Wei Chen, Agustin O. Pineda, F.Scott Mathews, Enrico Di Cera, Edward C. Giardino, Gracel. Wells, Barbara J. Haertlein, Jack A. Kauffman, Thomas W. Corcoran, Claudia K. Derian, Annette J. Eckardt, Bruce P. Damiano, Patricia Andrade-Gordon, Bruce E. Maryanoff, "A novel, potent dual inhibitor of the leukocyte proteases cathepsin G and chymase: Molecular mechanisms and anti-inflammatory activity in vivo," J. Biol. Chem. 280 (18), May, 18001-18007 (2005).

Miguel Garcia-Diaz, Katarzyna Bebenek, Joseph M. Krahn, Thomas A. Kunkel, Lars C. Pedersen, "A closed conformation for the Pol (lamda) catalytic cycle," Nat. Struct. Mol. Biol. 12 (1), January, 97-98 (2005).

Bruce C. Garrett, David A. Dixon, Donald M. Camaioni, Daniel M. Chipman, Mark A. Johnson, Charles D. Jonah, Gregory A. Kimmel, John H. Miller, Thomas N. Rescigno, Peter J. Rossky, Sotiris S. Xantheas, Steven D. Colson, Allan H. Laufer, Douglas Ray, Paul F. Barbara, David M. Bartels, Kurt H. Becker, Kit H. Bowen, Stephen E. Bradforth, Ian Carmichael, James V. Coe, L.Rene Corrales, James P. Cowin, Michel Dupuis, Kenneth B. Eisenthal, James A. Franz, Maciej S. Gutowski, Kenneth D. Jordan, Bruce D. Kay, Jay A. LaVerne, Sergei V. Lymar, Theodore E. Madey, C.William McCurdy, Dan Meisel, Shaul Mukamel, Anders R. Nilsson, Thomas M. Orlando, Nikolay G. Petrik, Simon M. Pimblott, James R. Rustad, Gregory K. Schenter, Sherwin J. Singer, Andrei Tokmakoff, Lai-Sheng Wang, Curt Wittig, Timothy S. Zwier, "Role of Water in Electron-Initiated Processes and Radical Chemistry: Issues and Scientific Advances," Chem. Rev. 105 (1), January, 355-390 (2005).

M. Gateshki, V. Petkov, G. Williams, S.K. Pradhan, Y. Ren, "Atomic-scale structure of nanocrystalline ZrO[subscript2] prepared by high-energy ball milling," Phys. Rev. B 71, 224107-1-224107-9 (2005).

A.G. Gavriliuk, V.V. Struzhkin, I.S. Lyubutin, M.Y. Hu, H.-k. Mao, "Phase Transition with Suppression of Magnetism in BiFeO[subscript 3] at High Pressure," J. Exp. Theor. Phys. 84 (2), July, 224-227 (2005).

Brian V. Geisbrecht, Brent Y. Hamaoka, Benjamin Perman, Adam Zemla, Daniel J. Leahy, "The Crystal Structures of EAP Domains from Staphylococcus aureus Reveal an Unexpected Homology to Bacterial Superantigens," J. Biol. Chem. 280 (17), April, 17243-17250 (2005).

K.L. Genson, J. Holzmueller, D. Vaknin, O.F. Villavicencio, D.V. McGrath, V.V. Tsukruk, "Langmuir monolayers from functionalized amphiphiles with epoxy terminal groups," Thin Solid Films 493 (1-2), December, 237-248 (2005).

K.L. Genson, J. Holzmuller, O.F. Villacencio, D.V. McGrath, D. Vaknin, V.V. Tsukruk, "Langmuir and Grafted Monolayers of Photochromic Amphiphilic Monodendrons of Low Generations," J. Phys. Chem. B 109 (43), October, 20393-20402 (2005).

Holly R. Gentry, Alex U. Singer, Laurie Betts, Cheng Yang, Joseph D. Ferrara, John Sondek, Leslie V. Parise, "Structural and Biochemical Characterization of CIB1 Delineates a New Family of EF-hand-containing Proteins," J. Biol. Chem. 280 (9), March, 8407-8415 (2005).

M. Ginder-Vogel, T. Borch, M.A. Mayes, P.M. Jardine, S. Fendorf, "Chromate Reduction and Retention Processes within Arid Subsurface Environments," Environ. Sci. Technol. 39, 7833-7839 (2005).

P. Glatzel, U. Bergmann, "High resolution 1s core hole x-ray spectroscopy in 3d transition metal complexes - Electronic and Structural Information," Coordin. Chem. Rev. 249, 65-95 (2005).

P. Glatzel, U. Bergmann, F.M.F. de Groot, B.M. Weckhuysen, S.P. Cramer, "A Study of Transition Metal K Absorption PreEdges by Resonant Inelastic XRay Scattering RIXS," Phys. Scripta. T115, 1032-1034 (2005).

P. Glatzel, F.M.F. de Groot, O. Manoilova, D. Grandjean, B.M. Weckhuysen, U. Bergmann, R. Barrea, "Range-extended EXAFS at the L edge of rare earths using high-energy-resolution fluorescence detection: A study of La in LaOCl," Phys. Rev. B 72 (1), 014117-1-014117-7 (2005).

M.L. Glówka, A. Olczak, J. Bojarska, M. Szczesio, W.L. Duax, B.M. Burkhart, W.A. Pangborn, D.A. Langs, Z. Wawrzak, "Structure of gramicidin D-RbCl complex at atomic resolution from low-temperature synchrotron data: interactions of double-stranded gramicidin channel contents and cations with channel wall," Acta Crystallogr. D 61, April, 433-441 (2005).

Gali Golan, Dmitry O. Zharkov, Hadar Feinberg, Andrea S. Fernandes, Elenal. Zaika, Jadwiga H. Kycia, Arthur P. Grollman, Gil Shoham, "Structure of the uncomplexed DNA repair enzyme endonuclease VIII indicates significant interdomain flexibility," Nucleic Acids Res. 33 (15), September, 5006-5016 (2005).

Barbara L. Golden, Elaine Chase, Hajeong Kim, "Crystal structure of a phage Twort group I ribozyme-product complex," Nat. Struct. Mol. Biol. 12 (1), January, 82-89 (2005).

Adam Golebiowski, Jennifer A. Townes, Matthew J. Laufersweiler, Todd A. Brugel, Michael P. Clark, Cynthia M. Clark, Jane F Djung, Steven K. Laughlin, Mark P. Sabat, Roger G. Bookland, John C. VanRens, Biswanath De, Lily C. Hsieh, Michael J. Janusz, Richard L. Walter, Mark E. Webster, Marlene J. Mekel, "The development of monocyclic pyrazolone based cytokine synthesis inhibitors," Bioorg. Med. Chem. Lett. 15 (9), May, 2285-2289 (2005).

A.F. Goncharov, M.R. Manaa, J.M. Zaug, R.H. Gee, L.E. Fried, W.B. Montgomery, "Polymerization of formic acid under high pressure," Phys. Rev. Lett. 94, February, 065505-1-065505-4 (2005).

Alexander F. Goncharov, Joseph M. Zaug, Jonathan C. Crowhurst, "Optical calibration of pressure sensors for high pressures and temperatures," J. Appl. Phys. 97, April, 094917-1-094917-5 (2005).

G. Gonzalez-Gil, J. Amonette, M. Romine, Y. Gorby, G. Geesey, "Bioreduction of natural specular hematite under flow conditions," Geochim. Cosmochim. Acta 69 (5), 1145-1155 (2005).

D.M. Goodner, D.L. Marasco, A.A. Escuadro, L. Cao, M.J. Bedzyk, "X-ray standing wave investigation of submonolayer barium and strontium surface phases on Si(001)," Phys. Rev. B 71, 165426-1-165426-5 (2005).

Kristie D. Goodwin, Eric C. Long, Millie M. Georgiadi, "A host-guest approach for determining drug-DNA interactions: an example using netropsin," Nucleic Acids Res. 33 (13), July, 4106-4116 (2005).

W. Good, J. Kim, A.I. Goldman, D. Wermeille, P.C. Canfield, C. Cunningham, Z. Islam, J.C. Lang, G. Srajer, I.R. Fisher, "Magnetic structure of GdCo[subscript 2]Ge[subscript 2]," Phys. Rev. B 71, 224427-1-224427-6 (2005).

Darren J. Goossens, T.Richard Welberry, Aidan P. Heerdegen, Alison J. Edwards, "Modelling disorder in 3,3' -dimethoxybensil, C[subscript 16]H[subscript 14]O[subscript 4]," Z. Kristallogr. 220 (12), 1035-1042 (2005).

V. Gopalakrishnan, S.A. Shah, C.F. Zukoski, "Cage melting and viscosity reduction in dense equilibrium suspensions," J. Rheol. 49 (2), March, 383-400 (2005).

R.A. Gordon, P.S. Budnik, D.T. Jiang, E.D. Crozier, "Evolution of an Iron Film on GaAs(001)-4x6," Phys. Scripta. T115, 492-494 (2005).

R.A. Gordon, E.D. Crozier, D.-T. Jiang, P.S. Budnik, T.L. Monchesky, B. Heinrich, "In-situ XAFS study of Fe epitaxially grown by MBE on GaAs(001)-4x6," Surf. Sci. 581 (1), April, 47-57 (2005).

Jason Gorman, Lawrence Shapiro, "Crystal structures of the tryptophan repressor binding protein WrbA and complexes with flavin mononucleotide," Protein Sci. 14, 3004-3012 (2005).

Andrea Gorrell, Sarah H. Lawrence, James G. Ferry, "Structural and Kinetic Analyses of Arginine Residues in the Active Site of the Acetate Kinase from Methanosarcina thermophila," J. Biol. Chem. 280 (11), March, 10731-10742 (2005).

Eugene Gregoryanz, Olga Degtyareva, Maddury Somayazulu, Russell J. Hemley, Ho-kwang Mao, "Melting of Dense Sodium," Phys. Rev. Lett. 94, May, 185502-1-185502-4 (2005).

S. Grenier, J.P. Hill, V. Kiryukhin, W. Ku, Y.-J. Kim, K.J. Thomas, S.-W. Cheong, Y. Tokura, Y. Tomioka, D. Casa, T. Gog, "d-d Excitations in Manganites Probed by Resonant Inelastic X-ray Scattering," Phys. Rev. Lett. 94, February, 047203-1-047203-4 (2005).

Anna Gribun, Matthew S. Kimber, Reagan Ching, Remco Sprangers, Klaus M. Fiebig, Walid A. Houry, "The ClpP Double Ring Tetradecameric Protease Exhibits Plastic Ring-Ring Interactions, and the N Termini of Its Subunits Form Flexible Loops That Are Essential for ClpXP and ClpAP Complex Formation," J. Biol. Chem. 280 (16), April, 16185-16196 (2005).

K.A. Griffin, A.B. Pakhomov, C.M. Wang, S.M. Heald, Kannan M. Krishnan, "Intrinsic Ferromagnetism in Insulating Cobalt Doped Anatase TiO[subscript 2]," Phys. Rev. Lett. 94 (15), April, 157204-1-157204-4 (2005).

K.A. Griffin, A. Pakhomov, C.M. Wang, S.M. Heald, K.M. Krishnan, "Cobalt-Doped Anatase - a Room Temperature Dilute Magnetic Dielectric," J. Appl. Phys. 97 (10), May, 10D320-1-10D320-3 (2005).

Alexei Grigoriev, Oleg Shpyrko, Christoph Steimer, Peter S. Pershan, Benjamin M. Ocko, Moshe Deutsch, Binhua Lin, Mati Meron, Timothy Graber, Jeffrey Gebhardt, "Surface oxidation of liquid Sn," Surf. Sci. 575 (3), February, 223-232 (2005).

G. Gualda, D.L. Cook, R. Chopra, L. Qin, A.T. Anderson, M. Rivers, "Fragmentation, nucleation and migration of crystals and bubbles in the Bishop Tuff rhyolitic magma," T. Roy. Soc. Edin.-Earth 95, February, 375-390 (2005).

Baohua Gu, Wei-Min Wu, Matthew A. Ginder-Vogel, Hui Yan, Matthew W. Fields, Jizhong Zhou, Scott Fendorf, Craig S. Criddle, Philip M. Jardine, "Bioreduction of Uranium in a Contaminated Soil Column," Environ. Sci. Technol. 39 (13), June, 4841-4847 (2005).

Qing Guo, Yuequan Shen, Young-Sam Lee, Craig S. Gibbs, Milan Mrksich, Wei-Jen Tang, "Structural basis for the interaction of Bordetella pertussis adenylyl cyclase toxin with calmodulin," EMBO J. 224 (18), September, 3190-3201 (2005).

I.G. Gurtubay, J.M. Pitarke, Wei Ku, A.G. Eguiluz, B.C. Larson, J. Tischler, P. Zschack, K.D. Finkelstein, "Electron-hole and plasmon excitations in 3d transition metals: Ab initio calculations and inelastic x-ray scattering measurements," Phys. Rev. B 72 (`), 125117-1-125117-11 (2005).

Wen-Zhen Gu, Ingrid Joseph, Yi-Chun Wang, David Frost, Gerard M. Sullivan, Le Wang, Nan-Horng Lin, Jerry Cohen, Vincent S. Stoll, Clarissa G. Jakob, Steven W. Muchmore, John E. Harlan, Tom Holzman, Karl A. Walten, Uri S. Ladror, Mark G. Anderson, Paul Kroeger, Luis E. Rodriguez, Kenneth P. Jarvis, Debra Ferguson, Kennan Marsh, Shichung Ng, Saul H. Rosenberg, Hing L. Sham, Haiying Zhang, "A highly potent and selective farnesyltransferase inhibitor ABT-100 in preclinical studies," Anti-Cancer Drug 16 (10), November, 1059-1069 (2005).

D.R. Haeffner, J.D. Almer, U. Lienert, "The use of high energy X-rays from the Advanced Photon Source to study stresses in materials," Mat. Sci. Eng. A 399 (1-2), June, 120-127 (2005).

Byung Woo Han, Craig A. Bingman, Donna K. Mahnke, Richard L. Sabina, George N. Phillips, Jr., "Crystallization and preliminary X-ray crystallographic analysis of adenosine 5'-monophosphate deaminase (AMPD) from Arabidopsis thaliana in complex with coformycin 5'-phosphate," Acta Crystallogr. F F61, 740-742 (2005).

Gye Won Han, Robert Schwarzenbacher, Rebecca Page, Lukasz Jaroszewski, Polat Abdubek, Eileen Ambing, Tanya Biorac, Jaume M. Canaves, Hsiu-Ju Chiu, Xiaoping Dai, Ashley M. Deacon, Michael DiDonato, Marc-André Elsliger, Adam Godzik, Carina Grittini, Slawomir K. Grzechnik, Joanna Hale, Eric Hampton, Justin Haugen, Michael Hornsby, Heath E. Klock, Eric Koesema, Andreas Kreusch, Peter Kuhn, Scott A. Lesley, Inna Levin, Daniel McMullan, Timothy M. McPhillips, Mitchell D. Miller, Andrew Morse, Kin Moy, Edward Nigoghossian, Jie Ouyang, Jessica Paulsen, Kevin Quijano, Ron Reyes, Eric Sims, Glen Spraggon, Raymond C. Stevens, Henry vanden Bedem, Jeff Velasquez, Juli Vincent, Frank von Delft, Xianhong Wang, Bill West, Aprilfawn White, Guenter Wolf, Qingping Xu, Olga Zagnitko, Keith O. Hodgson, John Wooley, Ian A. Wilson, "Crystal structure of an alanine-glyoxylate aminotransferase from Anabaena sp. at 1.70 Å resolution reveals a noncovalently linked PLP cofactor," Proteins 58 (4), 971-975 (2005).

Qing Han, Qiang Zhao, Sarah Fish, Klaus B. Simonsen, Dionisios Vourloumis, Jamie M. Froelich, Daniel Wall, Thomas Hermann, "Molecular Recognition by Glycoside Pseudo Base Pairs and Triples in an Apramycin-RNA Complex," Angew. Chem. Int. Ed. 44 (18), April, 2694-2700 (2005).

B. Hao, N. Zheng, B.A. Schulman, G. Wu, J.J. Miller, M. Pagano, N.P. Pavletich, "Structural basis of the Cks1-dependent recognition of p27(Kip1) by the SCF(Skp2) ubiquitin ligase," Mol. Cell 20, 9-19 (2005).

J.K. Harper, D.H. Barich, E.M. Heider, D.M. Grant, R.R. Franke, J.H. Johnson, Y. Zhang, P.L. Lee, R.B. Von Dreele, B. Scott, D. Williams, G.B. Ansell, "A combined solid-state NMR and x-ray powder diffraction study of a stable polymorph of paclitaxel," Cryst. Growth Des. 5 (5), 1737-1742 (2005).

H.H. Harris, A. Levina, C.T. Dillon, I. Mulyani, B. Lai, Z. Cai, P.A. Lay, "Time-dependent uptake, distribution and biotransformation of chromium(VI) in individual and bulk human lung cells: application of synchrotron radiation techniques," J. Biol. Inorg. Chem. 10, March, 105-118 (2005).

Philip A. Harris, Mui Cheung, Robert N. Hunter III, Matthew L. Brown, James M. Veal, Robert T. Nolte, Liping Wang, Wendy Liu, Renae M. Crosby, Jennifer H. Johnson, Andrea H. Epperly, Rakesh Kumar, Deirdre K. Luttrell, Jeffrey A. Stafford, "Discovery and Evaluation of 2-Anilino-5-aryloxazoles as a Novel Class of VEGFR2 Kinase Inhibitors," J. Med. Chem. 48 (5), February, 1610-1610 (2005).

D. Haskel, J.C. Lang, Z. Islam, A. Cady, G. Srajer, M. van Veenendaal, P.C. Canfield, "Atomic Origin of Magnetocrystalline Anisotropy in Nd[subscript 2]Fe[subscript 14]B," Phys. Rev. Lett. 95 (21), November, 217207-1-217207-4 (2005).

Alshaimaa Hassan-Abdallah, Guohua Zhao, Michael Eschenbrenner, Zhi-wei Chen, F.Scott Mathews, Marilyn Schuman Jorns, "Cloning, expression and crystallization of heterotetrameric sarcosine oxidase from Pseudomonas maltophilia," Protein Expres. Purif. 43 (1), September, 33-43 (2005).

S. Hayashi, S.I. Ford, D.J. Young, D.J. Sordelet, M.F. Besser, B. Gleeson, "[alpha]-NiPt(Al) and phase equilibria in the Ni-Al-Pt system at 115[degrees]C," Acta Mater. 53, 3319-3328 (2005).

Franklin A. Hays, Amy Teegarden, Zebulon J.R. Jones, Michael Harms, Dustin Raup, Jeffrey Watson, Emily Cavaliere, P. Shing Ho, "How sequence defines structure: A crystallographic map of DNA structure and conformation," Proc. Natl. Acad. Sci. USA 102 (20), May, 7157-7162 (2005).

S.M. Heald, S.A. Chambers, T. Droubay, "XAFS Study of Epitaxial CoxTi1-xO[subscript 2]-x Anatase," Phys. Scripta. T115, June, 597-599 (2005).

Gen He, Sivakumar Gajjeraman, David Schultz, David Cookson, Chunlin Qin, William T. Butler, Jianjun Hao, Anne George, "Spatially and Temporally Controlled Biomineralization Is Facilitated by Interaction between Self-Assembled Dentin Matrix Protein 1 and Calcium Phosphate Nuclei in Solution," Biochemistry-US 44 (49), November, 16140-16148 (2005).

Gen He, Amsaveni Ramachandra, Tom Dahl, Sarah George, David Schultz, David Cookson, Arthur Veis, Anne George, "Phosphorylation of Phosphophoryn Is Crucial for Its Function as a Mediator of Biomineralization," J. Biol. Chem. 280 (39), September, 33109-33114 (2005).

W.M. Heijboer, D.C. Koningsberger, B.M. Weckhuysen, F.M.F. de Groot, "New frontiers in X-ray spectroscopy in heterogeneous catalysis: Using Fe/ZSM-5 as test-system," Catal. Today 110 (3-4), December, 228-238 (2005).

Russell J. Hemley, Ho-kwang Mao, Viktor V. Struzhkin, "Synchrotron radiation and high pressure: new light on materials under extreme conditions," J. Synchrotron Rad. 12, 135-154 (2005).

J. Nathan Henderson, S. James Remington, "Crystal structures and mutational analysis of amFP486, a cyan fluorescent protein from Anemonia majano," Proc. Natl. Acad. Sci. USA 102 (36), August, 12712-12717 (2005).

L. Hennet, S. Krishnan, A. Bytchkov, T. Key, D. Thiaudière, P. Melin, I. Pozdnyakova, M.-L. Saboungi, D.L. Price, "X-ray Diffraction on High-Temperature Liquids. Towards Time-Resolved Studies," Int. J. Thermophys. 26 (4), July, 1127-1136 (2005).

J. Hershberger, O.O. Ajayi, G.R. Fenske, "Zinc Content of ZDDP Films Formed Thermally and Mechanically," Tribol. Int. 38 (3), March, 299-303 (2005).

J. Hershberger, O.O. Ajayi, G.R. Fenske, "Phase Transformation in Nickel during Tribotesting," Scripta Mater. 53 (12), December, 1449-1453 (2005).

J. Hershberger, O.O. Ajayi, J. Zhang, H. Yoon, G.R. Fenske, "Evidence of scuffing initiation by adiabatic shear instability," Wear 258 (10), May, 1471-1478 (2005).

Alison B. Hickman, Zhanita N. Perez, Liqin Zhou, Primrose Musingarimi, Rodolfo Ghirlando, Jenny E. Hinshaw, Nancy L. Craig, Fred Dyda, "Molecular architecture of a eukaryotic DNA transposase," Nat. Struct. Mol. Biol. 12 (8), August, 715-721 (2005).

L.J. Higgins, F. Yan, P. Liu, H.W. Liu, C.L. Drennan, "Structural insight into antibiotic fosfomycin biosynthesis by a mononuclear iron enzyme," Nature 437, October, 838-844 (2005).

Daniel M. Himmel, Kalyan Das, Arthur D. Clark, Jr., Stephen H. Hughes, Abdellah Benjahad, Said Oumouch, Jerome Guillemont, Sophie Coupa, Alain Poncelet, Imre Csoka, Christophe Meyer, Koen Andries, Chi Hung Nguyen, David S. Grierson, Eddy Arnold, "Crystal Structures for HIV-1 Reverse Transcriptase in Complexes with Three Pyridinone Derivatives: A New Class of Non-Nucleoside Inhibitors Effective against a Broad Range of Drug-Resistant Strains," J. Med. Chem. 48 (24), November, 7582-7591 (2005).

Francis Hindle, Eric Fertein, Soenke Seifert, Christophe Przygodski, Robin Bocquet, Marc Douay, Eugene Bychkov, "Anomalous small-angle X-ray scattering of a femtosecond irradiated germano silicate fibre preform," J. Non-Cryst. Solids 351 (27-29), August, 2200-2204 (2005).

William L. Holstein, H.David Rosenfeld, "In-Situ X-ray Absorption Spectroscopy Study of Pt and Ru Chemistry during Methanol Electrooxidation," J. Phys. Chem. B 109 (6), February, 2176-2186 (2005).

M. Holt, Kh. Hassani, M. Sutton, "Microstructure of Ferroelectric Domains in BaTiO[subscript 3] Observed via X-Ray Microdiffraction," Phys. Rev. Lett. 95 (8), August, 085504-1-085504-4 (2005).

John R. Horton, Kirsten Liebert, Stanley Hattman, Albert Jeltsch, Xiaodong Cheng, "Transition from Nonspecific to Specific DNA Interactions along the Substrate-Recognition Pathway of Dam Methyltransferase," Cell 121 (3), May, 349-361 (2005).

Nobuyoshi Hosoito, Takuo Ohkochi, "Depth-Resolved Induced Magnetic Polarization in the Cu layer of the Gd/Cu Multilayer Investigated by Resonant X-ray Magnetic Diffraction at the Cu K Absorption Edge," J. Phys. Soc. Jpn. 74 (11), November, 3060-3065 (2005).

Zhonggang Hou, Douglas A. Bernstein, Catherine A. Fox, James L. Keck, "Structural basis of the Sir1-origin recognition complex interaction in transcriptional silencing," Proc. Natl. Acad. Sci. USA 102 (24), June, 8489-8494 (2005).

Maria Hrmova, Victor A. Streltsov, Brian J. Smith, Andrea Vasella, Joseph N. Varghese, Geoffrey B. Fincher, "Structural Rationale for Low-Nanomolar Binding of Transition State Mimics to a Family GH3 [beta]-D-Glucan Glucohydrolase from Barley," Biochemistry-US 44 (50), November, 16529-16539 (2005).

Chih-chin Huang, Francois Stricher, Loic Martin, Julie M. Decker, Shahzad Majeed, Phillippe Barthe, Wayne A. Hendrickson, James Robinson, Christian Roumestand, Joseph Sodroski, Richard Wyatt, George M. Shaw, Claudio Vita, Peter D. Kwong, "Scorpion-Toxic Mimics of CD4 in Complex with Human Immunodeficiency Virus gp120: Crystal Structures, Molecular Mimicry, and Neutralization Breadth," Structure 13, May, 755-768 (2005).

Chih-chin Huang, Min Tang, Mei-Yun Zhang, Shahzad Majeed, Elizabeth Montabana, Robyn L. Stanfield, Dimiter S. Dimitrov, Bette Korber, Joseph Sodroski, Ian A. Wilson, Richard Wyatt, Peter D. Kwong, "Structure of a V3-containing HIV-1 gp120 core," Science 310, November, 1025-1028 (2005).

Thomas D. Hurley, Stephanie Stout, Emily Miner, Jing Zhou, Peter J. Roach, "Requirements for Catalysis in Mammalian Glycogenin," J. Biol. Chem. 280 (25), June, 23892-23899 (2005).

X. Hu, X. Jiao, S. Narayanan, Z. Jiang, S.K. Sinha, L.B. Lurio, J. Lal, "Resonantly enhanced off-specular X-ray scattering from polymer/polymer interfaces," Eur. Phys. J. E 17 (3), July, 353-359 (2005).

Sarah G. Hymowitz, Darshana R. Patel, Heidi J.A. Wallweber, Steven Runyon, Minhong Yan, Jian Ping Yin, Stephanie K. Shriver, Nathaniel C. Gordon, Borlan Pan, Nicholas J. Skelton, Robert F. Kelley, Melissa A. Starovasnik, "Structures of APRIL-Receptor Complexes: Like BCMA, TACI Employs Only a Single Cysteine-Rich Domain for High Affinity Ligand Binding," J. Biol. Chem. 288 (8), February, 7218-7227 (2005).

Gene Ice, "Amorphous materials: Characterizing amorphous strain," Nat. Mater. 4, January, 17-18 (2005).

Gene E. Ice, Rozaliya I. Barabash, Wenjun Liu, "Diffuse X-ray scattering from tiny sample volumes," Z. Kristallogr. 220, 1076-1081 (2005).

G.E. Ice, R.I. Barabash, F.J. Walker, "Characterization of Nano and Mesoscale Deformation Structures with Intense X-ray Synchrotron Sources," Compos. Sci. Tech. 36, 271-277 (2005).

Gene E. Ice, Przemyslaw Dera, Wenjun Liu, Ho-kwang Mao, "Adapting polychromatic X-ray microdiffraction techniques to high-pressure research: energy scan approach," J. Synchrotron Rad. 12, 608-617 (2005).

G.E. Ice, B.C. Larson, J.Z. Tischler, W. Liu, W. Yang, "X-ray microbeam measurements of subgrain stress distributions in polycrystalline materials," Mat. Sci. Eng. A 399 (1-2), June, 43-48 (2005).

G.E. Ice, B.C. Larson, W. Yang, J.D. Budai, J.Z. Tischler, J.W.L. Pang, R.I. Barabash, W. Liu, "Polychromatic X-ray Microdiffraction Studies of Mesoscale Structure and Dynamics," J. Synchrotron Rad. 12, December, 155-162 (2005).

K.I. Ignatiev, W.-K. Lee, K. Fezzaa, S.R. Stock, "Phase contrast stereometry: fatigue crack mapping in three dimensions," Philos. Mag. 85 (28), October, 3273-3300 (2005).

Hyotcherl Ihee, Sudarshan Rajagopal, Vukica Srajer, Reinhard Pahl, Spencer Anderson, Marius Schmidt, Friedrich Schotte, Philip A. Anfinrud, Michael Wulff, Keith Moffat, "Visualizing reaction pathways in photoactive yellow protein from nanoseconds to seconds," Proc. Natl. Acad. Sci. USA 102 (20), May, 7145-7150 (2005).

Young Jun Im, Sumana Raychaudhuri, William A. Prinz, James H. Hurley, "Structural mechanism for sterol sensing and transport by OSBP-related proteins," Nature 437, September, 154-158 (2005).

A.F. Isakovic, P.G. Evans, Z. Cai, B. Lai, J. Kmetko, K. Cicak, R.E. Thorne, "Transverse correlations and plasticity in the CDW conductor NbSe[subscript 3] studied by X-ray microbeam diffraction," J. Phys. IV France 131, 139-142 (2005).

Z. Islam, D. Haskel, J.C. Lang, G. Srajer, X. Liu, S.K. Sinha, B.W. Veal, "High-resolution polarization analysis study of long-range magnetic order in cuprates," Phys. Rev. B 71 (21), June, 212506-1-212506-4 (2005).

S.A. Ismail, H.W. Park, "Structural analysis of human liver glyceraldehyde-3-phosphate dehydrogenase," Acta Crystallogr. D 61, 1508-1513 (2005).

J.M. Jackson, W. Sturhahn, G. Shen, J. Zhao, M.Y. Hu, D. Errandonea, J.D. Bass, Y. Fei, "A synchrotron Mössbauer spectroscopy study of (Mg, Fe)SiO[subscript 3] perovskite up to 120 GPa," Am. Mineral. 90, 199-205 (2005).

Jennifer M. Jackson, Jianzhong Zhang, Jinfu Shu, Stanislav V. Sinogeikin, Jay D. Bass, "High-pressure sound velocities and elasticity of aluminous MgSiO[subscript 3] perovskite to 45 GPa: Implications for lateral heterogeneity in Earth's lower mantle," Geophys. Res. Lett. 32 (21), November, L21305-1-L21305-4 (2005).

S.D. Jacobsen, J.-F. Lin, R.J. Angel, G. Shen, V.B. Prakapenka, P. Dera, H.-K. Mao, R.J. Hemley, "Single-crystal synchrotron X-ray diffraction study of wustite and magnesiowustite at lower-mantle pressures," J. Synchrotron Rad. 12, 577-583 (2005).

Deepti Jain, Youngchang Kim, Karen L. Maxwell, Steven Beasley, Rongguang Zhang, Gary N. Gussin, Aled M. Edwards, Seth A. Darst, "Crystal Structure of Bacteriophage [lambda]cII and Its DNA Complex," Mol. Cell 19, July, 259-269 (2005).

G. Jain, J. Yang, M. Balasubramanian, J.J. Xu, "Synthesis, Electrochemistry, and Structural Studies of Lithium Intercalation of a Nanocrystalline Li[subscript 2]MnO[subscript 3]-like Compound," Chem. Mater. 17 (15), 3850-3860 (2005).

Rinku Jain, Bing Hao, Ren-peng Liu, Michael K. Chan, "Structures of E. coli Peptide Deformylase Bound to Formate: Insight into the Preference for Fe[superscript 2+] over Zn[superscript 2+] as the Active Site Metal," J. Am. Chem. Soc. 127 (13), 4558-4559 (2005).

Veronica J. James, Jill C. Richardson, Terry A. Robertson, John M. Papadimitriou, Nichole S. Dutton, Moira A.L. Maley, Lev M. Berstein, Olga E. Lantseva, Ralph N. Martins, "Fibre diffraction of hair can provide a screening test for Alzheimer's Disease: a human and animal model study," Med. Sci. Mon. 11 (2), February, CR53-CR57 (2005).

Srinivas Janaswamy, Rengaswami Chandrasekaran, "Cation-induced polymorphism in iota-carrageenan," Carbohyd. Polym. 60, May, 499-505 (2005).

Michael C. Jaye, John A. Krawiec, Nino Campobasso, Angela Smallwood, Chunyan Qiu, Quinn Lu, John J. Kerrigan, Maite De Los Frailes Alvaro, Bryan Laffitte, Wu-Schyong Liu, Joseph P. Marino, Jr., Craig R. Meyer, Jason A. Nichols, Derek J. Parks, Paloma Perez, Lea Sarov-Blat, Sheila D. Seepersaud, Klaudia M. Steplewski, Scott K. Thompson, Ping Wang, Mike A. Watson, Christine L. Webb, David Haigh, Justin A. Caravella, Colin H. Macphee, Timothy M. Willson, Jon L. Collins, "Discovery of Substituted Maleimides as Liver X Receptor Agonists and Determination of a Ligand-Bound Crystal Structure," J. Med. Chem. 48 (17), August, 5419-5422 (2005).

C. Jiang, M.F. Besser, D.J. Sordelet, B. Gleeson, "A combined first-principles and experimental study of the lattice site preference of Pt in B[subscript 2] NiAl," Acta Mater. 53 (7), April, 2101-2109 (2005).

J.S. Jiang, J.E. Pearson, Z.Y. Liu, B. Kabius, S. Trasobares, D.J. Miller, S.D. Bader, D.R. Lee, D. Haskel, G. Srajer, J.P. Liu, "A new approach for improving exchange-spring magnets," J. Appl. Phys. 97 (10), 10K311-1-10K311-3 (2005).

Tengchuan Jin, Andrew Howard, Erica A. Golemis, Yingtong Wanga, Yu-Zhu Zhang, "Overproduction, purification, crystallization and preliminary X-ray diffraction studies of the human transcription repressor ERH," Acta Crystallogr. F 61, April, 531-533 (2005).

T. Jin, A.J. Howard, E.A. Golemis, Y. Wang, Y.-Z. Zhang, "Overproduction, purification, crystallization and preliminary X-ray diffraction studies of the human spliceosomal protein TXNL4B," Acta Crystallogr. F 61 (3), March, 282-284 (2005).

Xiangshu Jin, Miguel A Ballicora, Jack Preiss, James H. Geiger, "Crystal structure of potato tuber ADP-glucose pyrophosphorylase," EMBO J. 24 (4), 694-704 (2005).

Amy Wagoner Johnson, Nilda Juan Serrano, Abby Whittington Morang, Russell Jamison, Young Bin Choy, Hyungsoo Choi, Kyekyoon Kim, Francesco DeCarlo, "Imaging Therapeutic Proteins in Gelatin for Controlled Drug Release," Macromol. Symp. 227, 295-305 (2005).

Steven M. Johnson, H.Michael Petrassi, Satheesh K. Palaninathan, Nilofar N. Mohamedmohaideen, Hans E. Purkey, Christopher Nichols, Kyle P. Chiang, Traci Walkup, James C. Sacchettini, K.Barry Sharpless, Jeffery W. Kelly, "Bisaryloxime Ethers as Potent Inhibitors of Transthyretin Amyloid Fibril Formation," J. Med. Chem. 48 (5), 1576-1578 (2005).

Christopher A. Johnston, Francis S. Willard, Mark R. Jezyk, Zoey Fredericks, Erik T. Bodor, Miller B. Jones, Rainer Blaesius, Val J. Watts, T.Kendall Harden, John Sondek, J.Kevin Ramer, David P. Siderovski, "Structures of G alpha i 1 Bound to a GDP-Selective Peptide Provides Insight into Guanine Nucleotide Exchange," Structure 13, July, 1069-1080 (2005).

Ryan S. Justice, Dale W. Schaefer, Richard A. Vaia, David W. Tomlin, Timothy J. Bunning, "Interface morphology and phase separation in polymer-dispersed liquid crystal composites," Polymer 46 (12), 4465-4473 (2005).

Mebrahtu A. Kahsai, Bernhard Vogler, Andrew T. Clark, Stephen P. Edmondson, John W. Shriver, "Solution Structure, Stability, and Flexibility of Sso10a: A Hyperthermophile Coiled-Coil DNA-Binding Protein," Biochemistry-US 44 (8), January, 2822-2832 (2005).

Lara S. Kallander, Qing Lu, Wenfang Chen, Thaddeus Tomaszek, Guang Yang, David Tew, Thomas D. Meek, Glenn A. Hofmann, Christina K. Schulz-Pritchard, Ward W. Smith, Cheryl A. Janson, M.Dominic Ryan, Gui-Feng Zhang, Kyung O. Johanson, Robert B. Kirkpatrick, Thau F. Ho, Paul W. Fisher, Michael R. Mattern, Randall K. Johnson, Michael J. Hansbury, James D. Winkler, Keith W. Ward, Daniel F. Veber, Scott K. Thompson, "4-Aryl-1,2,3-triazole: A Novel Template for a Reversible Methionine Aminopeptidase 2 Inhibitor, Optimized To Inhibit Angiogenesis in Vivo," J. Med. Chem. 48 (18), August, 5644-5647 (2005).

Hendrik K. Kammler, Gregory Beaucage, Douglas J. Kohls, Nikhil Agashe, Jan Ilavsky, "Monitoring simultaneously the growth of nanoparticles and aggregates by in situ ultra-small-angle x-ray scattering," J. Appl. Phys. 97, March, 054309-1-054309-11 (2005).

Khanita Karaveg, Aloysius Siriwardena, Wolfram Tempel, Zhi-Jie Liu, John Glushka, Bi-Cheng Wang, Kelley W. Moremen, "Mechanism of Class 1 (Glycosylhydrolase Family 47) a-Mannosidases Involved in N-Glycan Processing and Endoplasmic Reticulum Quality Control," J. Biol. Chem. 280 (16), April, 16197-16207 (2005).

T.C. Kaspar, T. Droubay, C.M. Wang, S.M. Heald, A.S. Lea, S.A. Chambers, "Co-doped anatase TiO[subscript 2] heteroepitaxy on Si"(001)," J. Appl. Phys. 97, April, 073511-1-073511-10 (2005).

Masato Kato, Jacinta L. Chuang, Shih-Chia Tso, R.Max Wynn, David T. Chuang, "Crystal structure of pyruvate dehydrogenase kinase 3 bound to lipoyl domain 2 of human pyruvate dehydrogenase complex," EMBO J. 24 (10), April, 1763-1774 (2005).

D.J. Keavney, S.T. King, S.H. Cheung, M. Weinert, L. Li, "The role of defect sites and Ga polarization in the magnetism of Mn-doped GaN," Phys. Rev. Lett. 95 (25), December, 257201-1-257201-5 (2005).

S.D. Kelly, K.M. Kemner, S.C. Brooks, J.K. Fredrickson, S.L. Carroll, D.W. Kennedy, J.M. Zachara, A.E. Plymale, S. Fendorf, "Ca-UO[subscript 2]-CO[subscript 3] complexation- Implications for bioremediation of U(VI)," Phys. Scripta. T115, 915-917 (2005).

K.F. Kelton, A.K. Gangopadhyay, "Getting the hot structures," Powder Diffr. 20 (2), June, 87-93 (2005).

K.M. Kemner, S.D. Kelly, E.J. O'Loughlin, T. Khare, Y. Londer, M. Schiffer, L.A. Moe, B.G. Fox, M.I. Donnelly, Y. Londer, M. Schiffer, C.S. Gionetti, "XRF and XAFS Analysis of Electrophoretically Isolated Nondenatured Proteins," Phys. Scripta. T115, 940-942 (2005).

Ivan M. Kempson, K.Paul Kirkbride, William M. Skinner, John Coumbaros, "Applications of synchrotron radiation in forensic trace evidence analysis," Talanta 67 (2), August, 286-303 (2005).

S.B. Kennedy, K. Littrell, P. Thiyagarajan, D.A. Tirrell, T.P. Russell, "Controlled Structure in Artificial Protein Hydrogels," Macromolecules 38 (17), August, 7470-7475 (2005).

S. Kewalramani, G. Evmenenko, C.-J. Yu, K. Kim, J. Kmetko, P. Dutta, "Evidence of surface reconstruction during 'bioinspired' inorganic nucleation at an organic template," Surf. Sci. 591, L286-L291 (2005).

Jason Key, Keith Moffat, "Crystal Structures of Deoxy and CO-Bound bjFixLH Reveal Details of Ligand Recognition and Signaling," Biochemistry-US 44 (12), March, 4627-4635 (2005).

P.-S.G. Kima, Y.-F. Hub, Y.M. Yiua, T.K. Sham, "X-ray absorption and X-ray excited optical luminescence (XEOL) studies of KAu(CN)[subscript 2] at the C, N and K K-edge and the Au L[subscript 3]-edge-comparison with density functional theory (DFT) calculation," J. Electron. Spectrosc. 144-147, June, 811-815 (2005).

Chang Soo Kim, Stephen J. Lombardo, Robert A. Winholtz, "Strain-Induced Deformation in Magnesia-Alumina Layered Composites," J. Am. Ceram. Soc. 88 (8), August, 2064-2070 (2005).

Hye-Kyung Kim, Jian-Wei Liu, Paul D. Carra, David L. Ollis, "Following directed evolution with crystallography: structural changes observed in changing the substrate specificity of dienelactone hydrolase," Acta Crystallogr. D 61 (7), July, 920-931 (2005).

Hyeonjae Kim, Haining Zhang, Suresh Narayanan, Jin Wang, Oswald Prucker, Jürgen Rühe, Mark D. Foster, "Surface fluctuations of polymer brushes probed by diffuse X-ray scattering," Polymer 46 (7), March, 2331-2337 (2005).

J.W. Kim, A. Kreyssig, L. Tan, D. Wermeille, S.L. Bud'ko, P.C. Canfield, A.I. Goldman, "Imaging antiferromagnetic domains in GdNi[subscript 2]Ge[subscript 2] with x-ray resonant magnetic scattering," Appl. Phys. Lett. 87 (20), September, 202505-1-202505-3 (2005).

J.W. Kim, Y. Lee, D. Wermeille, B. Sieve, L. Tan, S.L. Bud'ko, S. Law, P.C. Canfield, B.N. Harmon, A.I. Goldman, "Systematics of x-ray resonant scattering amplitudes in RNi[subscript 2]Ge[subscript 2] (R=Gd,Tb,Dy,Ho,Er,Tm): The origin of the branching ratio at the L edges of the heavy rare earths," Phys. Rev. B 72, 064403-1-064403-6 (2005).

Jaewon Kim, Sujatha Sitaraman, Aitor Hierro, Bridgette M. Beach, Greg Odorizzi, James H. Hurley, "Structural basis for endosomal targeting by the bro1 domain," Dev. Cell 8 (6), June, 937-947 (2005).

J.W. Kim, L. Tan, D. Wermeille, S.L. Bud'ko, P.C. Canfield, A.I. Goldman, "Magnetic powder diffraction from GdNi[subscript 2]Ge[subscript 2] using x-ray resonant magnetic scattering," J. Phys. Condens. Matter 17 (46), November, L493-L497 (2005).

Man-Ho Kim, Charles J. Glinka, "Application of in situ vapor sorption small-angle neutron scattering (SANS) to semicrystalline polymers: vapor pathway and structure evolution in semicrystalline linear polyethylene," J. Appl. Crystallogr. 38, 734-739 (2005).

P.-S.G. Kim, S. Naftel, T.K. Sham, I. Coulthard, Y.-F. Hu, A. Moewes, J.W. Freeland, "Photon-in photon-out studies of Alq[subscript]3 (tris-aluminum-8-hydroxyquinolinate): Synchrotron light excited optical luminescence and X-ray emission," J. Electron. Spectrosc. 144, June, 901-904 (2005).

T.H. Kim, A.K. Gangopadhyay, L.Q. Xing, G.W. Lee, Y.T. Shen, K.F. Kelton, A.I. Goldman, R.W. Hyers, J.R. Rogers, "Role of Ti in the formation of Zr-Ti-Cu-Ni-Al glasses," Appl. Phys. Lett. 87, December, 251924-1-251924-3 (2005).

T.H. Kim, G.W. Lee, B. Sieve, A.K. Gangopadhyay, R.W. Hyers, T.J. Rathz, J.R. Rogers, D.S. Robinson, K.F. Kelton, A.I. Goldman, "In situ High-Energy X-Ray Diffraction Study of the Local Structure of Supercooled Liquid Si," Phys. Rev. Lett. 95, August, 085501-1-085501-4 (2005).

Matt J. Kipper, Sheng-Shu Hou, Soenke Seifert, P. Thiyagarajan, Klaus Schmidt-Rohr, Balaji Narasimhan, "Nanoscale Morphology of Polyanhydride Copolymers," Macromolecules 38 (20), 8468-8472 (2005).

M.J. Kipper, S. Seifert, P. Thiyagarajan, B. Narasimhan, "Morphology of Polyanhydride Copolymers: Time Resolved SAXS Studies of Polyanhydride Crystallization," J. Polym. Sci. Pol. Phys. 43 (4), January, 463-477 (2005).

Iris Koch, Angela Duso, Corinne Haug, Christy Miskelly, Melanie Sommerville, Paula Smith, Kenneth J. Reimer, "Distinguishing Between Naturally and Anthropogenically Elevated Arsenic at an Abandoned Arctic Military Site," Environ. Forensics 6 (4), December, 335-344 (2005).

Vladimir Komanicky, Andreas Menzel, Kee-Chul Chang, Hoydoo You, "Nanofaceted Platinum Surfaces: A New Model System for Nanoparticle Catalysts," J. Phys. Chem. B 109 (49), November, 23543-23549 (2005).

Vladimir Komanicky, Andreas Menzel, Hoydoo You, "Investigation of Oxygen Reduction Reaction Kinetics at (111)-(100) Nanofaceted Platinum Surfaces in Acidic Media," J. Phys. Chem. B 109, November, 23550-23557 (2005).

Geoffrey K.-W Kong, Denise Galatis, Kevin J. Barnham, Galina Polekhina, Julian J. Adams, Colin L. Masters, Roberto Cappai, Michael W. Parker, William J. McKinstry, "Crystallization and preliminary crystallographic studies of the copper-binding domain of the amyloid precursor protein of Alzheimer's disease," Acta Crystallogr. F F61 (1), 93-95 (2005).

Chong Min Koo, Lifeng Wu, Lisa S. Lim, Mahesh K. Mahanthappa, Marc A. Hillmyer, Frank S. Bates, "Microstructure and Mechanical Properties of Semicrystalline-Rubbery-Semicrystalline Triblock Copolymers," Macromolecules 38 (14), May, 6090-6098 (2005).

Nicole M. Koropatkin, W. Wallace Cleland, Hazel M. Holden, "Kinetic and Structural Analysis of [alpha]-D-Glucose-1-phosphate Cytidylyltransferase from Salmonella typhi," J. Biol. Chem. 280 (11), March, 10774-10780 (2005).

Nicole M. Koropatkin, Hazel M. Holden, "Structure of CDP-D-glucose 4,6-dehydratase from Salmonella typhi complexed with CDP-D-xylose," Acta Crystallogr. D 61 (4), 365-373 (2005).

Rumiana Koynova, Li Wang, Yury Tarahovsky, Robert C. MacDonald, "Lipid phase control of DNA delivery," Bioconjugate Chem. 16 (6), October, 1335-1339 (2005).

B.J. Kozioziemski, J.A. Koch, A. Barty, H.E. Martz, Jr., Wah-Keat Lee, Kamel Fezzaa, "Quantitative characterization of inertial confinement fusion capsules using phase contrast enhanced x-ray imaging," J. Appl. Phys. 97 (6), March, 063103- 1-063103-9 (2005).

Julia Kraineva, R.Aravinda Narayanan, Elena Kondrashkina, Pappannan Thiyagarajan, Roland Winter, "Kinetics of Lamellar-to-Cubic and Intercubic Phase Transitions of Pure and Cytochrome c Containing Monoolein Dispersions Monitored by Time-Resolved Small-Angle X-ray Diffraction," Langmuir 21 (8), March, 3559-3571 (2005).

M.J. Kramer, D.J. Sordelet, "Polymorphism in the short-range order of Zr[subscript 70]Pd[subscript 30] metallic glasses," J. Non-Cryst. Solids 351 (19-20), July, 1586-1593 (2005).

S. Krishnan, L. Hennet, S. Jahn, T.A. Key, P.A. Madden, M.-L. Saboungi, D.L. Price, "Structure of Normal and Supercooled Liquid Aluminum Oxide," Chem. Mater. 17 (10), May, 2662-2666 (2005).

A.J. Kropf, J.A. Fortner, R.J. Finch, J.C. Cunnane, C. Karanfil, "A Bent Silicon Crystal in the Laue Geometry to Resolve Actinide X-ray Fluorescence for X-ray Absorption Spectroscopy," Phys. Scripta. T115, 998-1000 (2005).

A.J. Kropf, C.S. Johnson, J.T. Vaughey, M.M. Thackeray, "XAFS Analysis of Layered Li[subscript x]Ni[subscript 0.5]Mn[subscript 0.5]O[subscript 2] (0<x <= 2) Electrodes for Lithium Batteries," Phys. Scripta. T115, 274-277 (2005).

Irina N. Krylova, Elena P. Sablin, Jamie Moore, Robert X. Xu, Gregory M. Waitt, J.Andrew MacKay, Dalia Juzumiene, Jane M. Bynum, Kevin Madauss, Valerie Montana, Lioudmila Lebedeva, Miyuki Suzawa, Jon D. Williams, Shawn P. Williams, Rodney K. Guy, Joseph W. Thornton, Robert J. Fletterick, Timothy M. Willson, Holly A. Ingraham, "Structural Analyses Reveal Phosphatidyl Inositols as Ligands for the NR5 Orphan Receptors SF-1 and LRH-1," Cell 123 (3), February, 343-355 (2005).

A.A. Kulkarni, A. Goland, H. Herman, A.J. Allen, J. Ilavsky, G.G. Long, F. De Carlo, "Advanced microstructural characterization of plasma-sprayed zirconia coatings over extended length scales," J. Therm. Spray Techn. 14 (2), June, 239-250 (2005).

Anand A. Kulkarni, Sanjay Sampath, Allen Goland, Herbert Herman, Andrew J. Allen, Jan Ilavsky, Wenquan Gong, Shrikant Gopalan, "Plasma spray coatings for producing next-generation supported membranes," Top. Catal. 32 (3-4), March, 241-249 (2005).

Ravhi S. Kumar, Andrew L. Cornelius, "Structural transitions in NaBH[subscript 4] under pressure," Appl. Phys. Lett. 87 (26), December, 261916-1-261916-3 (2005).

Ravhi S. Kumar, Andrew L. Cornelius, Eunja Kim, Yongrong Shen, S. Yoneda, Changfeng Chen, Malcolm F. Nicol, "Pressure induced structural phase transition in AgSbTe[subscript 2]," Phys. Rev. B 72 (6), 060101-1-060101-4 (2005).

R.S. Kumar, A.L. Cornelius, Y. Shen, T.G. Kumary, J. Janaki, M.C. Valsakumar, M.F. Nicol, "Structural behavior of non-oxide perovskite superconductor MgCNi[subscript 3] at pressures up to 32 GPa," Physica B 363, 190-195 (2005).

R.S. Kumar, H. Kohlmann, B.E. Light, A.L. Cornelius, V. Raghavan, T.W. Darling, J.L. Sarrao, "The crystal structure of CeRhIn[subscript 5] under pressure," Physica B 359-361, 407-409 (2005).

R.S. Kumar, S. Rekhi, A.L. Cornelius, M.W. Barsoum, "Compressibility of Nb[supscript 2]AsC to 41 GPa," Appl. Phys. Lett. 86, March, 111904-1-111904-5 (2005).

Jennifer Kung, Baosheng Li, Takeyuki Uchida, Yanbin Wang, "In-situ elasticity measurement for the unquenchable high-pressure clinopyroxene phase: Implication for the upper mantle," Geophys. Res. Lett. 32, L01307-1-L01307-4 (2005).

Seo-Young Kwak, Elaine DiMasi, Yong-Jin Han, Joanna Aizenberg, Ivan Kuzmenko, "Orientation and Mg Incorporation of Calcite Grown on Functionalized Self-Assembled Monolayers: A Synchrotron X-ray Study," Cryst. Growth Des. 5 (6), 2139-2145 (2005).

Debdutta Lahiri, Bruce Bunker, Bhoopesh Mishra, Zhenyuan Zhang, Dan Meisel, C.M. Doudna, M.F. Bertino, Frank D. Blum, A.T. Tokuhiro, Soma Chattopadhyay, Tomohiro Shibata, Jeff Terry, "Bimetallic Pt-Ag and Pd-Ag nanoparticles," J. Appl. Phys. 97, May, 094304-1-094304-8 (2005).

D. Lahiri, S. Chattopadhyay, B.A. Bunker, C.M. Doudna, M.F. Bertino, F. Blum, A. Tokuhiro, J. Terry, "EXAFS Studies of Bimetallic Ag-Pt and Ag-Pd Nanorods," Phys. Scripta. T115, 776-780 (2005).

Dmitry L. Lakshtanov, Carine B. Vanpeteghem, Jennifer M. Jackson, Jay D. Bass, Guoyin Shen, Vitali B. Prakapenka, Konstantin Litasov, Eiji Ohtani, "The equation of state of Al,H-bearing SiO[subscript 2] stishovite to 58 GPa," Phys. Chem. Miner. 32 (7), November, 466-470 (2005).

F.J. Lamelas, Z.A. Dreger, Y.M. Gupta, "Raman and X-Ray Scattering Studies of High-Pressure Phases of Urea," J. Phys. Chem. B 109 (16), April, 8206-8215 (2005).

Michael Douglas Lane, Hyun-Joo Nam, Eric Padron, Brittney Gurda-Whitaker, Eric Kohlbrenner, George Aslanidi, Barry Byrne, Robert McKenna, Nicholas Muzyczka, Sergei Zolotukhin, Mavis Agbandje-McKenna, "Production, purification, crystallization and preliminary X-ray analysis of adeno-associated virus serotype 8," Acta Crystallogr. F 61, 558-561 (2005).

Paul Langan, Narayanasami Sukumar, Yoshiharu Nishiyama, Henri Chanzy, "Synchrotron X-ray structures of cellulose I[subscript beta] and regenerated cellulose II at ambient temperature and 100 K," Cellulose 12 (6), December, 551-562 (2005).

Nicole LaRonde-LeBlanc, Tad Guszczynski, Terry Copeland, Alexander Wlodawer, "Autophosphorylation of Archaeoglobus Fulgidus Rio2 and Crystal Structures of its Nucleotide-Metal Ion Complexes," FEBS Lett. 272, June, 2800-2810 (2005).

Nicole LaRonde-LeBlanc, Tad Guszczynski, Terry Copeland, Alexander Wlodawer, "Structure and activity of the atypical serine kinase Rio1," FEBS J. 272, June, 3698-3713 (2005).

Heather N. Larson, Henry Weiner, Thomas D. Hurley, "Disruption of the Coenzyme Binding Site and Dimer Interface Revealed in the Crystal Structure of Mitochondrial Aldehyde Dehydrogenase," J. Biol. Chem. 280 (34), August, 30550-30556 (2005).

Michael V. Lasker, Mark M. Gajjar, Satish K. Nair, "Cutting Edge: Molecular Structure of the IL-1R-Associated Kinase-4 Death Domain and Its Implications for TLR Signaling," J. Immunol. 175, 4175-4179 (2005).

Steven K. Laughlin, Michael P. Clark, Jane F. Djung, Adam Golebiowski, Todd A. Brugel, Mark Sabat, Roger G. Bookland, Matthew J. Laufersweiler, John C. VanRens, Jennifer A. Townes, Biswanath De, Lily C. Hsieh, Susan C. Xu, Richard L. Walter, Marlene J. Mekel, Michael J. Janusz, "The development of new isoxazolone based inhibitors of tumor necrosis factor-alpha (TNF-alpha) production," Bioorg. Med. Chem. Lett. 15 (9), May, 2399-2403 (2005).

Ruby H.P. Law, James A. Irving, Ashley M. Buckle, Katya Ruzyla, Marguerite Buzza, Tanya A. Bashtannyk-Puhalovich, Travis C. Beddoe, Kim Nguyen, D.Margaret Worrall, Stephen P. Bottomley, Phillip I. Bird, Jamie Rossjohn, James C. Whisstock, "The High Resolution Crystal Structure of the Human Tumor Suppressor Maspin Reveals a Novel Conformational Switch in the G-helix," J. Biol. Chem. 208 (23), June, 22356-22364 (2005).

A.C. Lawson, J.A. Roberts, B. Martinez, R.B. Von Dreele, B. Storey, H.T. Hawkins, M. Ramos, F.G. Hampel, C.C. Davis, R.A. Pereyra, J.N. Mitchell, F. Freibert, S.M. Valone, T.N. Claytor, D.A. Viskoe, F.W. Schonfeld, "Lattice constants and anisotropic microstrain at low temperature in [superscript 242]Pu-Ga alloys," Philos. Mag. 85 (18), June, 2007-2022 (2005).

Kristi L. Lazar, Helene Miller-Auer, Godfrey S. Getz, Joseph P.R.O. Orgel, Stephen C. Meredith, "Helix-Turn-Helix Peptides That Form [alpha] -Helical Fibrils: Turn Sequences Drive Fibril Structure," Biochemistry-US 44 (38), August, 12681-12689 (2005).

A. Lazicki, B. Maddox, W.J. Evans, C.-S. Yoo, A.K. McMahan, W.E. Pickett, R.T. Scalettar, M.Y. Hu, P. Chow, "New Cubic Phase of Li[subscript 3]N: Stability of the N[superscript 3-] Ion to 200 GPa," Phys. Rev. Lett. 95, October, 165503-1-165503-4 (2005).

Pierre Le Magueres, Hookang Im, Jerry Ebalunode, Ulrich Strych, Michael J. Benedik, James M. Briggs, Harold Kohn, Kurt L. Krause, "The 1.9 Å Crystal Structure of Alanine Racemase from Mycobacterium tuberculosis Contains a Conserved Entryway into the Active Site," Biochemistry-US 44 (5), 1471-1481 (2005).

Yvonne A. Leduc, Lata Prasad, Marvis Laivenieks, J. Gregory Zeikus, LouisT.J. Delbaere, "Structure of PEP carboxykinase from the succinate-producing Actinobacillus succinogenes: a new conserved active-site motif," Acta Crystallogr. D 61, 903-912 (2005).

Richard Ledwidge, Bijal Patel, Aiping Dong, David Fiedler, Mat Falkowski, Jane Zelikova, Anne O. Summers, Emil F. Pai, Susan M. Miller, "NmerA, the Metal Binding Domain of Mercuric Ion Reductase, Removes Hg[superscript 2+] from Proteins, Delivers It to the Catalytic Core, and Protects Cells under Glutathione-Depleted Conditions," Biochemistry-US 44 (34), August, 11402-11416 (2005).

Andre Lee, Jun Xiao, Frank J. Feher, "New Approach in the Synthesis of Hybrid Polymers Grafted with Polyhedral Oligomeric Silsesquioxane and Their Physical and Viscoelastic Properties," Macromolecules 38 (2), 438-444 (2005).

B. Lee, W. Oh, J. Yoon, Y. Hwang, J. Kim, B.G. Landes, J.P. Quintana, M. Ree, "Scattering Studies of Nanoporous Organosilicate Thin Films Imprinted with Reactive Star Porogens," Macromolecules 38 (22), September, 8991-8995 (2005).

B. Lee, S.J. Riley, S. Seifert, G.P. Tikhonov, S. Vajda, A.N. Tomczyk, R.E. Winans, "Anomalous grazing incidence small-angle scattering studies of platinum nanoparticles formed by cluster deposition," J. Chem. Phys. 123, August, 074701-1-074701-7 (2005).

B. Lee, S. Seifert, S.J. Riley, G.Y. Tikhonov, N.A. Tomczyk, S. Vajda, R.E. Winans, "Anomalous Grazaing Incidence Small Angle X-ray Scattering Studies of Platinum Nanopraticles Formed by Cluster Deposition," American Chemical Society, Division of Fuel Chemistry 50 (1), March, 188-189 (2005).

Jae Young Lee, Judy Chang, Nimesh Joseph, Rodolfo Ghirlando, Desirazu N. Rao, Wei Yang, "MutH Complexed with Hemi- and Unmethylated DNAs: Coupling Base Recognition and DNA Cleavage," Mol. Cell 20 (1), October, 155-166 (2005).

Jihun Lee, Vikash Kumar Dubey, Thayumanasamy Somasundaram, Michael Blaber, "Conversion of type I 4:6 to 3:5 [beta]-turn types in human acidic fibroblast growth factor: Effects upon structure, stability, folding, and mitogenic function," Proteins 62 (3), December, 686-697 (2005).

Ji Hyun Lee, Constance J. Jeffery, "The crystal structure of rabbit phosphoglucose isomerase complexed with D-sorbitol-6-phosphate, an analog of the open chain form of D-glucose-6-phosphate," Protein Sci. 14, 727-734 (2005).

Julia C. Lee, B. Ravel, "Determining the Grain Composition of the Interstellar Medium with High-Resolution X-Ray Spectroscopy," Astrophysical Journ. 622 (Part 1), April, 970-976 (2005).

Kyoung Lee, Rosmarie Friemann, Juan V. Parales, David T. Gibsona, S. Ramaswamy, "Purification, crystallization and preliminary X-ray diffraction studies of the three components of the toluene 2,3-dioxygenase enzyme system," Acta Crystallogr. F 61, 669-672 (2005).

Shinwoo Lee, Paul R. Anderson, "EXAFS study of Zn sorption mechanisms on hydrous ferric oxide over extended reaction time," J. Colloid Interf. Sci. 286 (1), June, 82-89 (2005).

S.H. Lee, A.L. Cavalieri, D.M. Fritz, M.C. Swan, R.S. Hegde, M. Reason, R.S. Goldman, D.A. Reis, "Generation and Propagation of a Picosecond Acoustic Pulse at a Buried Interface: Time-Resolved X-Ray Diffraction Measurements," Phys. Rev. Lett. 95 (24), December, 246104-1-246104-4 (2005).

Sung Kuen Lee, Peter J. Eng, Ho-Kwang Mao, Yue Meng, Matthew Newville, Michael Y. Hu, Jinfu Shu, "Probing of bonding changes in B[subscript 2]O[subscript 3] glasses at high pressure with inelastic X-ray scattering," Nat. Mater. 4, October, 851-854 (2005).

Y.J. Lee, E.J. Elzinga, R.J. Reeder, "Cu(II) adsorption at the calcite-water interface in the presence of natural organic matter: kinetic studies and molecular-scale characterization," Geochim. Cosmochim. Acta 69 (1), January, 49-61 (2005).

Yongbin Lee, Jong-Woo Kim, Alan I. Goldman, Bruce N. Harmon, "X-ray resonant magnetic scattering and x-ray magnetic circular dichroism branching ratios, L[subscript 3] / L[subscript 2], for heavy rare earths," J. Appl. Phys. 97, 10A311-1-10A311-3 (2005).

Christopher Lehmann, Sadhana Pullalarevu, Wojciech Krajewski, Mark A. Willis, Andrey Galkin, Andrew Howard, Osnat Herzberg, "Structure of HI0073 from Haemophilus influenzae, the nucleotide-binding domain of a two-protein nucleotidyl transferase," Proteins 60 (4), July, 807-811 (2005).

Ming Lei, Michael A. Robinson, Stephen C. Harrison, "The Active Conformation of the PAK1 Kinase Domain," Structure 13 (5), May, 769-778 (2005).

Michael J. Lenaeus, Magdalini Vamvouka, Pamela J. Focia, Adrian Gross, "Structural basis of TEA blockade in a model potassium channel," Nat. Struct. Mol. Biol. 12, April, 454-459 (2005).

Bryan W. Lepore, Frank J. Ruzicka, Perry A. Frey, Dagmar Ringe, "The x-ray crystal structure of lysine-2,3-aminomutase from Clostridium subterminale," Proc. Natl. Acad. Sci. USA 102 (39), September, 13819-13824 (2005).

M. Lerotic, C. Jacobsen, J.B. Gillow, A.J. Francis, S. Wirick, S. Vogt, J. Maser, "Cluster analysis in soft X-ray spectromicroscopy: Finding the patterns in complex specimens," J. Electron. Spectrosc. 144-147, June, 1137-1143 (2005).

Bogdan M. Leu, Marek Z. Zgierski, Graeme R. A. Wyllie, Mary K. Ellison, W. Robert Scheidt, Wolfgang Sturhahn, E. Ercan Alp, Stephen M. Durbin, J. Timothy Sage, "Vibrational dynamics of biological molecules: Multi-quantum contributions," J. Phys. Chem. Solids 66 (12), November, 2250-2256 (2005).

Igor Levchenko, Robert A. Grant, Julia M. Flynn, Robert T. Sauer, Tania A. Baker, "Versatile modes of peptide recognition by the AAA+ adaptor protein SspB," Nat. Struct. Mol. Biol. 12, May, 520-525 (2005).

A. Levina, R.S. Armstrong, P.A. Lay, "Three-Dimensional Structure Determination using Multiple-Scattering Analysis of XAFS: Applications to Metalloproteins and Coordination Chemistry," Coordin. Chem. Rev. 249, 141-160 (2005).

A. Levina, P.A. Lay, "Mechanistic Studies of Relevance to the Biological Activities of Chromium," Coordin. Chem. Rev. 249, 281-298 (2005).

Hal A. Lewis, Xun Zhao, Chi Wang, J.Michael Sauder, Isabelle Rooney, Brian W. Noland, Don Lorimer, Margaret C. Kearins, Kris Conners, Brad Condon, Peter C. Maloney, William B. Guggino, John F. Hunt, Spencer Emtage, "Impact of the [delta]F508 Mutation in First Nucleotide-binding Domain of Human Cystic Fibrosis Transmembrane Conductance Regulator on Domain Folding and Structure," J. Biol. Chem. 280, January, 1346-1353 (2005).

H. Liang, D. Harries, G.C.L. Wong, "Polymorphism of DNA-anionic liposome complexes reveals hierarchy of ion-mediated interactions," Proc. Natl. Acad. Sci. USA 102 (32), August, 11173-11178 (2005).

B. Li, J. Kung, T. Uchida, Y. Wang, "Pressure calibration to 20 GPa by simultaneous use of ultrasonic and x ray techniques," J. Appl. Phys. 98, 13521-1-13521-5 (2005).

Helga C. Lichtenegger, Henrik Birkedal, Diego M. Casa, Julie O. Cross, Steve M. Heald, J.Herbert Waite, Galen D. Stucky, "Distribution and Role of Trace Transition Metals in Glycera Worm Jaws Studied with Synchrotron Microbeam Techniques," Chem. Mater. 17 (11), April, 2927-2931 (2005).

C. Li, T. Koga, C. Li, J. Jiang, S. Sharma, S. Narayanan, L.B. Lurio, X. Hu, X. Jiao, S.K. Sinha, S. Billet, D. Sosnowik, Hyunjung Kim, J.C. Sokolov, M.H. Rafailovich, "Viscosity Measurements of Very Thin Polymer Films," Macromolecules 38 (12), May, 5144-5151 (2005).

R.L. Lieberman, A.C. Rosenzweig, "Crystal structure of a membrane-bound metalloenzyme that catalyses the biological oxidation of methane," Nature 434, March, 177-182 (2005).

H.-P. Liermann, A.K. Singh, B. Manoun, S.K. Saxena, C.S. Zha, "Compression behavior of TaC[subscript 0.98] under nonhydrostatic and quasi-hydrostatic pressures up to 76 GPa," Int. J. Refract. Met. H. 23, 109-114 (2005).

Jing Li, Z.L. Wang, J.P. Liu, S.E. Lofland, Somdev Tyagi, J.W. Freeland, D. Giubertoni, M. Bersani, M. Anderle, "Interphase exchange coupling in Fe/Sm-Co bilayers with gradient Fe thickness," J. Appl. Phys. 98 (6), 063908-1-063908-4 (2005).

Mi Li, Gary S. Laco, Mariusz Jaskolski, Jan Rozycki, Jerry Alexandratos, Alexander Wlodawer, Alla Gustchina, "Crystal structure of human T cell leukemia virus protease, a novel target for anticancer drug design," Proc. Natl. Acad. Sci. USA 102 (51), December, 18332-18337 (2005).

Binhua Lin, Mati Meron, Jeff Gebhardt, Tim Graber, Dongxu Li, Bin Yang, Stuart A. Rice, "X-ray diffuse scattering study of height fluctuations at the liquid-vapor interface of gallium," Physica B 357, 106-109 (2005).

H. Lin, E.S. Bo□in, S.J.L. Billinge, E. Quarez, M.G. Kanatzidis, "Nanoscale clusters in the high performance thermoelectric AgPb[subscript m]SbTe[subscript m+2]," Phys. Rev. B 72, November, 174113-1-174113-7 (2005).

Jung-Fu Lin, Eugene Gregoryanz, Viktor V. Struzhkin, Maddury Somayazulu, H.-K. Mao, R.J. Hemley, "Melting behavior of H[subscript 2]O at high pressures and temperatures," Geophys. Res. Lett. 32, L11306-L11309 (2005).

J-F. Lin, V.V. Struzhkin, S.D. Jacobsen, M.H. Hu, P. Chow, J. Kung, "Spin transition of iron in magnesiowüstite in the Earth's lower mantle," Nature 436, July, 377-380 (2005).

J.-F. Lin, V.V. Struzhkin, S.D. Jacobsen, G. Shen, V.B. Prakapenka, H.-K. Mao, R.J. Hemley, "X-ray emission spectroscopy with a laser-heated diamond anvil cell: a new experimental probe of the spin state of iron in the Earth's interior," J. Synchrotron Rad. 12, 637-641 (2005).

Jung-Fu Lin, Wolfgang Sturhahn, Jiyong Zhao, Guoyin Shen, Ho-kwang Mao, Russell J. Hemley, "Sound velocities of hot dense iron: Birch's Law revisited," Science 308, June, 1892-1894 (2005).

T. Lin, W. Schildkamp, K. Brister, P.C. Doerschuk, M. Somayazulu, H. Mao, J.E. Johnson, "The mechanism of high-pressure-induced ordering in a macromolecular crystal," Acta Crystallogr. D 61 (6), June, 737-743 (2005).

Yao Lin, Alexander Boker, Habib Skaff, David Cookson, A.D. Dinsmore, Todd Emrick, Thomas P. Russell, "Nanoparticle Assembly at Fluid Interfaces: Structure and Dynamics," Langmuir 21 (1), January, 191-194 (2005).

Y. Lin, A. Böker, J. He, K. Sill, H. Xiang, C. Abetz, X. Li, J. Wang, T. Emrick, S. Long, Q. Wang, A. Balazs, T.P. Russell, "Self-directed self-assembly of nanoparticle/copolymer particles," Nature 434, March, 55-59 (2005).

Yi-Lun Lin, Youssef Elias, Raven H. Huang, "Structural and Mutational Studies of the Catalytic Domain of Colicin E5: A tRNA-Specific Ribonuclease," Biochemistry-US 44 (31), July, 10494-10500 (2005).

Kristina E. Lipinska-Kalita, Gino Mariotto, Patricia E. Kalita, Yoshimichi Ohki, "Effects of high pressure on stability of the nanocrystalline LiAlSi[subscript 2]O[subscript 6] phase of a glass-ceramic composite: A synchrotron X-ray diffraction study," Physica B 365, 155-162 (2005).

Elizabeth J. Little, Nancy C. Horton, "DNA-induced Conformational Changes in Type II Restriction Endonucleases: The Structure of Unliganded HincII," J. Mol. Biol. 351 (1), August, 76-78 (2005).

Chian Liu, Ray Conley, Albert T. Macrander, J. Maser, H.C. Kang, M.A. Zurbuchen, G.B. Stephenson, "Depth-graded multilayers for application in transmission geometry as linear zone plates," J. Appl. Phys. 98 (11), 113519-1-113519-6 (2005).

Dali Liu, Bryan W. Lepore, GregoryA. Petsko, Pei W. Thomas, Everett M. Stone, Walter Fast, Dagmar Ringe, "Three-dimensional structure of the quorum-quenching N-acyl homoserine lactone hydrolase from Bacillus thuringiensis," Proc. Natl. Acad. Sci. USA 102 (33), August, 11882-11887 (2005).

Fengling Liu, Peter I. Boross, Yuan-Fang Wang, Jozsef Tozser, John M. Louis, Robert W. Harrison, Irene T. Weber, "Kinetic, Stability, and Structural Changes in High-resolution Crystal Structures of HIV-1 Protease with Drug-resistant Mutations L24I, I50V, and G73S," J. Mol. Biol. 354 (4), October, 789-800 (2005).

H.-Z. Liu, J. Chen, J. Hu, C.D. Martin, D.J. Weidner, D. Hausermann, H.-k. Mao, "Octahedral tilting evolution and phase transition in orthorhombic NaMgF[subscript 3] perovskite under pressure," Geophys. Res. Lett. 32 (4), February, L04304-1-L04304-5 (2005).

H. Liu, Y. Ding, M. Somayazulu, J. Qian, J. Shu, D. Hausermann, H.-k. Mao, "Rietveld refinement study of the pressure dependence of the internal structural parameter u in the wurtzite phase of ZnO," Phys. Rev. B 71, June, 212103-1-212103-4 (2005).

Haozhe Liu, John S. Tse, Jingzhu Hu, Zhenxian Liu, Luhong Wang, Jiuhua Chen, Don J. Weidner, Yue Meng, Daniel Hausermann, Ho-kwang Mao, "Structural Refinement of the High-Pressure Phase of Aluminum Trihydroxide: In-Situ High-Pressure Angle Dispersive Synchrotron X-ray Diffraction and Theoretical Studies," J. Phys. Chem. B 109 (18), May, 8857-8860 (2005).

Sijiu Liu, Zhibing Lu, Yin Han, Eugene Melamud, Debra Dunaway-Mariano, Osnat Herzberg, "Crystal Structures of 2-Methylisocitrate Lyase in Complex with Product and with Isocitrate Inhibitor Provide Insight into Lyase Substrate Specificity, Catalysis and Evolution," Biochemistry-US 44, 2949-2962 (2005).

T. Liu, L.X. Chen, "An Enhanced Electronic State in ZnTPP Induced by Interaction with Solvation: A Multiple-Scattering Calculation of X-ray Absorption Near-Edge Spectra," Phys. Scripta. T115, May, 864-866 (2005).

Wenjun Liu, Gene E. Ice, Bennett C. Larson, Wenge Yang, Jonathan Z. Tischler, "Nondestructive three-dimensional characterization of grain boundaries by X-ray crystal microscopy," Ultramicroscopy 103 (3), June, 199-204 (2005).

Xiangxin Liu, A.D. Compaan, Jeff Terry, "Cu K-edge X-ray fine structure changes in CdTe with CdCl[subscript 2] processing," Thin Solid Films 480-481 (1), June, 95-98 (2005).

Xiaogang Liu, Yi Zhang, Dipak K. Goswami, John S. Okasinski, Khalid Salaita, Peng Sun, Michael J. Bedzyk, Chad A. Mirkin, "The Controlled Evolution of a Polymer Single Crystal," Science 307, March, 1763-1766 (2005).

Yun Liu, Debora Berti, Piero Baglioni, Sow-Hsin Chen, Ahmet Alatas, Harald Sinn, Ayman Said, Ercan Alp, "Inelastic X-ray scattering studies of phonons propagating along the axial direction of a DNA molecule having different counter-ion atmosphere," J. Phys. Chem. Solids 66 (12), November, 2235-2245 (2005).

Yun Liu, Sow-Hsin Chen, Debora Berti, Piero Baglioni, Ahmet Alatas, Harald Sinn, Ercan Alp, Ayman Said, "Effects of counterion valency on the damping of phonons propagating along the axial direction of liquid-crystalline DNA," J. Chem. Phys. 123 (21), December, 214909-1-214909-11 (2005).

Zhi-Jie Liu, Dawei Lin, Wolfram Tempel, Jeremy L. Praissman, John P. Rose, Bi-Cheng Wang, "Parameter-space screening: a powerful tool for high-throughput crystal structure determination," Acta Crystallogr. D 61 (5), May, 520-527 (2005).

Zhi-Jie Liu, Wolfram Tempel, Joseph D. Ng, Dawei Lina, Ashit K. Shah, Lirong Chen, Peter S. Horanyi, Jeff E. Habel, Irina A. Kataeva, Hao Xu, Hua Yang, Jessie C. Chang, Lei Huang, Shu-Huey Chang, Weihong Zhou, Doowon Lee, Jeremy L. Praissman, Hua Zhang, M.Gary Newton, John P. Rose, Jane S. Richardson, David C. Richardson, Bi-Cheng Wang, "The high-throughput protein-to-structure pipeline at SECSG," Acta Crystallogr. D 61 (6), April, 679-684 (2005).

Yong Li, Mihwa Choi, Kelly Suino, Amanda Kovach, Jennifer Daugherty, Steven A. Kliewer, H.Eric Xu, "Structural and biochemical basis for selective repression of the orphan nuclear receptor liver receptor homolog 1 by small heterodimer partner," Proc. Natl. Acad. Sci. USA 102 (27), 9505-9510 (2005).

Yuanhe Li, Alan S. Fanning, James M. Anderson, Arnon Lavie, "Structure of the Conserved Cytoplasmic C-terminal Domain of Occludin: Identification of the ZO-1 Binding Surface," J. Mol. Biol. 352 (1), August, 151-164 (2005).

Yongdong Li, Xiaoli Shi, Graham Parry, Liqing Chen, Jennifer A. Callahan, Andrew P. Mazar, Mingdong Huang, "Optimization of Crystals of an Inhibitory Antibody of Urokinase Plasminogen Activator Receptor (uPAR) with Hydrogen Peroxide and Low Protein Concentration," Protein Peptide Lett. 12, December, 655-658 (2005).

C.-T. Lo, S. Seifert, P. Thiyagarajan, B. Narasimhan, "Effect of Polydispersity on the Phase Behavior of Polymer Blends," Macromol. Rapid Commun 26 (7), April, 533-536 (2005).

T.P. Lodge, J. Bang, Z. Li, M.A. Hillmyer, Y. Talmon, "Strategies for Controlling Intra- and Intermicellar Packing in Block Copolymer Solutions: Illustrating the Flexibility of the Self-Assembly Toolbox," Faraday Discuss. 128, 1-12 (2005).

Luisa Maria Lois, Christopher D. Lima, "Structures of the SUMO E1 provide mechanistic insights into SUMO activation and E2 recruitment to E1," Eur. Mol. Biol. 24 (3), January, 439-451 (2005).

I. Lonardelli, H.-R. Wenk, L. Lutterotti, M. Goodwin, "Texture analysis from synchrotron diffraction images with the Rietveld method: dinosaur tendon and salmon scale," J. Synchrotron Rad. 12 (3), May, 354-360 (2005).

Gary J. Long, Raphael P. Hermann, Fernande Grandjean, Ercan E. Alp, Wolfgang Sturhahn, Charles E. Johnson, Dennis E. Brown, Olaf Leupold, Rudolf Rüffer, "Strongly decoupled europium and iron vibrational modes in filled skutterudites," Phys. Rev. B 71, April, 140302-1-140302-4 (2005).

George T. Lountos, Kevin H. Mitchell, Joey M. Studts, Brian G. Fox, Allen M. Orville, "Crystal Structures and Functional Studies of T4moD, the Toluene 4-Monooxygenase Catalytic Effector Protein," Biochemistry-US 44, 7131-7142 (2005).

J.J. Lovelace, C.R. Murphy, H.D. Bellamy, K. Brister, R. Pahl, G.E.O. Borgstahl, "Advances in digital topography for characterizing imperfections in protein crystals," J. Appl. Crystallogr. 38 (3), June, 512-519 (2005).

Olga Y. Lubman, Raphael Kopan, Gabriel Waksman, Sergey Korolev, "The crystal structure of a partial mouse Notch-1 ankyrin domain: Repeats 4 through 7 preserve an ankyrin fold," Protein Sci. 14, March, 1274-1281 (2005).

Gang Lu, James M. Westbrooks, Amy L. Davidson, Jue Chen, "ATP hydrolysis is required to reset the ATP-binding cassette dimer into the resting-state conformation," Proc. Natl. Acad. Sci. USA 102 (50), December, 17969-17974 (2005).

L. Lu, G. Chabot-Couture, X. Zhao, J.N. Hancock, N. Kaneko, O.P. Vajk, G. Yu, S. Grenier, Y.J. Kim, D. Casa, T. Gog, M. Greven, "Charge-Transfer Excitations in the Model Superconductor HgBa[subscript 2] CuO[subscript 4 + delta]," Phys. Rev. Lett. 95, November, 217003-1-217003-5 (2005).

Guangming Luo, Sarka Malkova, Sai Venkatesh Pingali, David G. Schultz, Binhua Lin, Mati Meron, Timothy J. Graber, Jeffrey Gebhardt, Petr Vanysek, Mark L. Schlossman, "The width of the water/2-heptanone liquid-liquid interface," Electrochem. Commun. 7 (6), June, 627-630 (2005).

G. Luo, S. Malkova, S.V. Pingali, D. Schultz, M.L. Schlossman, P. Vanysek, B. Lin, M. Meron, T. Graber, J. Gebhardt, "X-ray Studies of the Interface Between Two Polar Liquids: Neat and with Electrolytes," Faraday Discuss. 129, 23-34 (2005).

Sheng-Nian Luo, Oliver Tschauner, Thomas E. Tierney, Damian C. Swift, Steve J. Chipera, Paul D. Asimow, "Novel crystalline carbon-cage structure synthesized from laser-driven shock wave loading of graphite," J. Chem. Phys. 123 (2), July, 024703-1-024703-5 (2005).

Darren A. Lytle, Michael R. Schock, "The Formation of Pb(IV) Oxides in Chlorinated Water," J. Am. Water Works Ass. 97 (11), November, 102-114 (2005).

Albert T. Macrander, Szczesny Krasnicki, Yuncheng Zhong, Jozef Maj, Yong S. Chu, "Strain mapping with parts-per-million resolution in synthetic type-Ib diamond plates," Appl. Phys. Lett. 87 (19), November, 194113-1-194113-3 (2005).

Estelle M. Maes, Sue A. Roberts, Andrzej Weichsel, William R. Montfort, "Ultrahigh Resolution Structures of Nitrophorin 4: Heme Distortion in Ferrous CO and NO Complexes," Biochemistry-US 44 (38), August, 12690-12699 (2005).

Y. Maham, M.G. Chodakowski, X. Zhang, J.M. Shaw, "Asphaltene phase behavior: prediction at a crossroads," Fluid Phase Equilibr. 227, January, 177-182 (2005).

C. Malliakas, S.J.L. Billinge, H.-J. Kim, M.G. Kanatzidis, "Square nets of tellurium: Rare-earth dependent variation in the charge-density wave of RETe[subscript 3] (RE= rare earth element)," J. Am. Chem. Soc. 127 (18), April, 6510-6511 (2005).

Thomas E. Malone, Stacey E. Madson, Russell L. Wrobel, Won Bae Jeon, Nathan S. Rosenberg, Kenneth A. Johnson, Craig A. Bingman, David W. Smith, George N. Phillips, Jr., John L. Markley, Brian G. Fox, "X-ray structure of Arabidopsis At2g06050, 12-oxophytodienoate reductase isoform 3," Proteins 58 (1), 243-245 (2005).

M.H. Manghnani, G. Amulele, J.R. Smyth, C.M. Holl, G. Shen, V. Prakapenka, D.J. Frost, "Equation of state of hydrous Fo[subscript 90] ringwoodite to 45 GPa by synchrotron powder difraction," Mineral Mag. 69 (3), 317-323 (2005).

Bouchaib Manoun, S.K. Saxena, "High pressure study of Ti[subscript 4]AlN[subscript 3] to 55 GPa," Appl. Phys. Lett. 86, 101906-1-101906-3 (2005).

W.L. Mao, Y. Meng, G. Shen, V. Prakapenka, A.J. Campbell, D.L. Heinz, J. Shu, R. Caracas, R.E. Cohen, Y. Fei, R.J. Hemley, H.-k. Mao, "Iron-rich silicates in the Earth's D" layer," Proc. Natl. Acad. Sci. USA 102 (28), July, 9751-9753 (2005).

Marina Mapelli, Santosh Panjikar, Paul A. Tucker, "The Crystal Structure of the Herpes Simplex Virus 1 ssDNA-binding Protein Suggests the Structural Basis for Flexible, Cooperative Single-stranded DNA Binding," J. Biol. Chem. 280 (4), January, 2990-2997 (2005).

I. Margiolaki, J.P. Wright, A.N. Fithch, G.C. Fox, R.B. von Dreele, "Synchrotron X-Ray Powder Diffraction Study of Hexagonal Turkey Egg-White lysozyme," Acta Crystallogr. D 61 (4), April, 423-432 (2005).

Zara Marland, Travis Beddoe, Leyla Zaker-Tabrizi, Ross L. Coppel, Paul K. Crellin, Jamie Rossjohn, "Expression, purification, crystallization and preliminary X-ray diffraction analysis of an essential lipoprotein implicated in cell-wall biosynthesis in Mycobacteria," Acta Crystallogr. F 61 (12), December, 1081-1083 (2005).

L.W. Marschand, M. Brown, L.B. Lurio, B.M. Law, S. Uran, I. Kuzmenko, T. Gog, "X-ray specular reflectivity study of a critical binary fluid mixture," Phys. Rev. E 72 (1), 011509-1-011509-5 (2005).

C.D. Martin, S.M. Antao, P.J. Chupas, P.L. Lee, S.D. Shastri, J.B. Parise, "Quantitative high-pressure pair distribution function analysis of nanocrystalline gold," Appl. Phys. Lett. 86, 061910-1-061910-3 (2005).

Maria M. Martinez-Inesta, Raul F. Lobo, "Investigation of the Negative Thermal Expansion Mechanism of Zeolite Chabazite Using the Pair Distribution Function Method," J. Phys. Chem. B 109 (19), April, 9389-9396 (2005).

M.M. Martinez-Inesta, I. Peral, T. Proffen, R.F. Lobo, "A pair distribution function analysis of zeolite beta," Micropor. Mesopor. Mat. 77, 55-66 (2005).

Philip D. Martin, Cristina Purcarea, Pengfei Zhang, Asmita Vaishnav, Sharon Sadecki, Hedeel I. Guy-Evans, David R. Evans, Brian F.P. Edwards, "The Crystal Structure of a Novel, Latent Dihydroorotase from Aquifex aeolicus at 1.7Å Resolution," J. Mol. Biol. 348 (3), May, 535-547 (2005).

R.R. Martin, I.M. Kempson, S.J. Naftel, W.M. Skinner, "Preliminary synchrotron analysis of lead in hair from a lead smelter worker," Chemosphere 58 (10), March, 1385-1390 (2005).

R.V. Martins, U. Lienert, L. Margulies, A. Pyzalla, "Determination of the radial crystallite microstrain distribution within an AlMg3 torsion sample using monochromatic synchrotron radiation," Mat. Sci. Eng. A 402 (1-2), August, 278-287 (2005).

Irimpan Mathews, Robert Schwarzenbacher, Daniel McMullan, Polat Abdubek, Eileen Ambing, Herbert Axelrod, Tanya Biorac, Jaume M. Canaves, Hsiu-Ju Chiu, Ashley M. Deacon, Michael DiDonato, Marc-André Elsliger, Adam Godzik, Carina Grittini, Slawomir K. Grzechnik, Joanna Hale, Eric Hampton, Gye Won Han, Justin Haugen, Michael Hornsby, Lukasz Jaroszewski, Heath E. Klock, Eric Koesema, Andreas Kreusch, Peter Kuhn, Scott A. Lesley, Inna Levin, Mitchell D. Miller, Kin Moy, Edward Nigoghossian, Jie Ouyang, Jessica Paulsen, Kevin Quijano, Ron Reyes, Glen Spraggon, Raymond C. Stevens, Henry vanden Bedem, Jeff Velasquez, Juli Vincent, Aprilfawn White, Guenter Wolf, Qingping Xu, Keith O. Hodgson, John Wooley, Ian A. Wilson, "Crystal structure of S-adenosylmethionine:tRNA ribosyltransferase-isomerase (QueA) from Thermotoga maritima at 2.0 Å resolution reveals a new fold," Proteins 59 (4), April, 869-874 (2005).

Allan Matte, Gordon V. Louie, J. Sivaraman, Miroslaw Cygler, Stephen K. Burley, "Structure of the pseudouridine synthase RsuA from Haemophilus influenzae," Acta Crystallogr. F 61 (4), April, 350-354 (2005).

Karen L. Maxwell, Patricia Reed, Rongguang Zhang, Steven Beasley, Adrian R. Walmsley, Fiona A. Curtis, Andrzej Joachimiak, Aled M. Edwards, Gary J. Sharples, "Functional similarities between phage [lambda] Orf and Escherichia coli RecFOR in initiation of genetic exchange," Proc. Natl. Acad. Sci. USA 102 (32), 11260-11265 (2005).

Mark L. Mayer, "Crystal Structures of the GluR5 and GluR6 Ligand Binding Cores: Molecular Mechanisms Underlying Kainate Receptor Selectivity," Neuron 45 (4), February, 539-552 (2005).

Jennifer A. McCourt, Siew Siew Pang, Luke W. Guddat, Ronald G. Duggleby, "Elucidating the Specificity of Binding of Sulfonylurea Herbicides to Acetohydroxyacid Synthase," Biochemistry-US 44 (7), January, 2330-2338 (2005).

S.A. McMahon, J.L. Miller, J.A. Lawton, D.E. Kerkow, A. Hodes, M.A. Marti-Renom, S. Doulatov, E. Narayanan, A. Sali, J.F. Miller, P. Ghosh, "The C-type lectin fold as an evolutionary solution for massive sequence variation," Nature Struct. Biol. 12 (10), October, 886-892 (2005).

D.H. McNear, Jr., E. Peltier, J. Everhart, R.L. Chaney, S. Sutton, M. Newville, M. Rivers, D.L. Sparks, "Application of Quantitative Fluorescence and Absorption-Edge Computed Microtomography to Image Metal Compartmentalization in Alyssum murale," Environ. Sci. Technol. 39 (7), 2210-2218 (2005).

D.H. McNear, Jr., R. Tappero, D.L. Sparks, "Shining light on metals in the environment," Elements 1, 211-216 (2005).

Jennifer L. Meagher, Harry C. Winter, Porscha Ezell, Irwin J. Goldstein, Jeanne A. Stuckey, "Crystal structure of banana lectin reveals a novel second sugar binding site," Glycobiology 15 (10), July, 1033-1042 (2005).

Y.S. Meng, G. Ceder, C.P. Grey, W.-S. Yoon, M. Jiang, J. Breger, Y. Shao-Horn, "Cation ordering in layered O[subscript 3]Li[Ni[subscript x]Li[subscript 1/3-2x/3]Mn[subscript 2/3-x/3]O[subscript 2] (0 less than or equal to x less than or equal to 1/2) compounds," Chem. Mater. 17, March, 2386-2394 (2005).

F.M. Michel, S.M. Antao, P.J. Chupas, P.L. Lee, J.B. Parise, M.A.A. Schoonen, "Short- To medium-range atomic order and crystallite size of the initial FeS precipitate from pair distribution function analysis," Chem. Mater. 17 (25), December, 6246-6255 (2005).

A. Mikhaylova, M. Davidson, H. Toastmann, J.E.T. Channell, Y. Guyodo, C. Batich, J. Dobson, "Detection, identification and mapping of iron anomalies in brain tissue using X-ray absorption spectroscopy," J. Roy. Soc. Inter. 2 (2), March, 33-37 (2005).

John J. Miles, Diah Elhassen, Natalie A. Borg, Sharon L. Silins, Fleur E. Tynan, Jacqueline M. Burrows, Anthony W. Purcell, Lars Kjer-Nielsen, Jamie Rossjohn, Scott R. Burrows, James McCluskey, "CTL Recognition of a Bulged Viral Peptide Involves Biased TCR Selection," J. Immunol. 175, 3826-3834 (2005).

C.E. Miller, J. Majewski, T. Gog, T.L. Kuhl, "Characterization of Biological Thin Films at the Solid-Liquid Interface by X-Ray Reflectivity," Phys. Rev. Lett. 94, June, 238104-1-238104-4 (2005).

Chad E. Miller, Jaroslaw Majewski, Thomas Gog, Tonya L. Kuhl, "Grazing incidence diffraction of cadmium arachidate multilayers," Z. Kristallogr. 220, 987-992 (2005).

Gregory J. Miller, Monita P. Wilson, Philip W. Majerus, James H. Hurley, "Specificity Determinants in Inositol Polyphosphate Synthesis: Crystal Structure of Inositol 1,3,4-Trisphosphate 5/6-Kinase," Mol. Cell 18 (2), April, 201-212 (2005).

L.M. Miller, Q. Wang, T.P. Telivala, R.J. Smith, A. Lanzirotti, J. Miklossy, "Synchrotron-based infrared and X-ray imaging shows focalized accumulation of Cu and Zn co-localized with beta-amyloid deposits in Alzheimer's disease," J. Struct. Biol. 152 (3), December, 204-211 (2005).

Mark S. Miller, Bradley M. Palmer, Stuart Ruch, Lisa A. Martin, Gerrie P. Farman, Yuan Wang, Jeffrey Robbins, Thomas C. Irving, David W. Maughan, "The Essential Light Chain N-terminal Extension Alters Force and Fiber Kinetics in Mouse Cardiac Muscle," J. Biol. Chem. 280 (41), October, 34427-34434 (2005).

L.-C. Ming, S.K. Sharma, A.J. Jayaraman, Y. Kobayashi, E. Suzuki, S. Endo, V. Prakapenka, D. Yang, "X-ray diffraction and Raman studies of the CuGeO[subscript 3](III)-(IV) transformation under high pressures," Spectrochim. Acta A 61 (10), 2418-2422 (2005).

S. Misaghi, P.J. Galardy, W.J. Meester, H. Ovaa, H.L. Ploegh, R. Gaudet, "Structure of the Ubiquitin Hydrolase UCH-L3 Complexed with a Suicide Substrate," J. Biol. Chem. 280 (2), January, 1512-1520 (2005).

Yasushi Miyazaki, Shinichiro Matsunaga, Jun Tang, Yutaka Maeda, Masato Nakano, RocherJ. Philippe, Megumi Shibahara, Wei Liu, Hideyuki Sato, Liping Wang, Robert T. Nolte, "Novel 4-amino-furo[2,3-d]pyrimidines as Tie-2 and VEGFR2 dual inhibitors," Bioorg. Med. Chem. Lett. 15 (9), May, 2203-2207 (2005).

A.T. Motta, A. Yilmazbayhan, R.J. Comstock, J. Partezana, G.P. Sabol, B. Lai, Z. Cai, "Microstructure and growth mechanism of oxide layers formed on Zr alloys studied with micro-beam synchrotron radiation," J. ASTM Intl. 2 (5), May, JAI12375-1-JAI12375-26 (2005).

Tinoush Moulaei, Tatsuya Maehigashi, George T. Lountos, Seiji Komeda, Derrick Watkins, Michael P. Stone, Luis A. Marky, Jian-sen Li, Barry Gold, Loren Dean Williams, "Structure of B-DNA with Cations Tethered in the Major Groove," Biochemistry-US 44, 7458-7468 (2005).

C.E. Murray, H.-F. Yan, I.C. Noyan, Z. Cai, B. Lai, "High-resolution strain mapping in heteroepitaxial thin-film features," J. Appl. Phys. 98 (1), July, 013504-1-013504-9 (2005).

Deepak T. Nair, Robert E. Johnson, Louise Prakash, Satya Prakash, Aneel K. Aggarwal, "Rev1 Employs a Novel Mechanism of DNA Synthesis Using a Protein Template," Science 309, September, 2219-2222 (2005).

Hyun-Joo Nam, Florence Poy, Haruo Saito, Christin A. Frederick, "Structural basis for the function and regulation of the receptor protein tyrosine phosphatase CD45," J. Exp. Med. 201 (3), 441-452 (2005).

Suresh Narayanan, Dong Ryeol Lee, Rodney S. Guico, Sunil K. Sinha, Jin Wang, "Real-Time Evolution of the Distribution of Nanoparticles in an Ultrathin-Polymer-Film-Based Waveguide," Phys. Rev. Lett. 94 (14), April, 145504-1-145504-4 (2005).

Lars-Ake Naslund, David C. Edwards, Philippe Wernet, Uwe Bergmann, Hirohito Ogasawara, Lars G.M. Pettersson, Satish Myneni, Anders Nilsso, "X-ray Absorption Spectroscopy Study of the Hydrogen Bond Network in the Bulk Water of Aqueous Solutions," J. Phys. Chem. A 109 (27), June, 5995-6002 (2005).

L.-A. Naslund, J. Luning, Y. Ufuktepe, H. Ogasawara, Ph. Wernet, U. Bergmann, L.G.M. Pettersson, A. Nilsson, "X-ray Absorption Spectroscopy Measurements of Liquid Water," J. Phys. Chem. B 109 (28), May, 13835-13839 (2005).

Christopher A. Nelson, Andrew Pekosz, Chung A. Lee, Michael S. Diamond, Daved H. Fremont, "Structure and Intracellular Targeting of the SARS-Coronavirus Orf7a Accessory Protein," Structure 13 (1), 75-85 (2005).

R.L. Newton, J.L. Davidson, G.E. Ice, W. Liu, "Synchrotron X-ray microdiffraction analysis of proton irradiated polycrystalline diamond films," Diam. Relat. Mater. 14, 1588-1591 (2005).

George Nicola, Alena Fedarovich, RobertA. Nicholas, Christopher Davies, "A large displacement of the SxN motif of Cys115-modified penicillin-binding protein 5 from E. coli," Biochem. J. 392 (1), November, 55-63 (2005).

George Nicola, Sridhar Peddi, Miglena Stefanova, Robert A. Nicholas, William G. Gutheil, Christopher Davies, "Crystal Structure of Escherichia coli Penicillin-Binding Protein 5 Bound to a Tripeptide Boronic Acid Inhibitor: A Role for Ser-110 in Deacylation," Biochemistry-US 44 (223), June, 8207-8217 (2005).

A. Nilsson, Ph. Wernet, D. Nordlund, U. Bergmann, M. Cavalleri, M. Odelius, H. Ogasawara, L.-A. Naslund, T.K. Hirsch, L. Ojamäe, P. Glatzel, L.G.M. Pettersson, "Comment on "Energetics of Hydrogen Bond Network Rearrangements in Liquid Water"," Science 308 (5723), May, 793a (2005).

N. Nishiyama, Y. Wang, T. Uchida, T. Irifune, M.L. Rivers, S.R. Sutton, "Pressure and strain dependence on the strength of sintered polycrystalline Mg[subscript 2]SiO[subscript 4] ringwoodite," Geophys. Res. Lett. 32, L04307-1-L04307-4 (2005).

B.Tracy Nixon, Hemant P. Yennawar, Michaeleen Doucleff, Jeffrey G. Pelton, David E. Wemmer, Susan Krueger, Elena Kondrashkina, "SAS Solution Structures of the Apo and Mg[superscript 2+]/BeF[subscript 3][superscript-]-Bound Receiver Domain of DctD from Sinorhizobium meliloti," Biochem. J. 44 (42), October, 13962-13969 (2005).

B. Nocek, C. Chang, H. Li, L. Lezondra, D. Holzle, F. Collart, A. Joachimiak, "Crystal Structures of [Delta superscript 1]-Pyrroline-5-carboxylate Reductase from Human Pathogens Neisseria meningitides and Streptococcus pyogenes," J. Mol. Biol. 354 (1), November, 91-106 (2005).

Thaddeus J. Norman, Jr., Christian D. Grant, Adam M. Schwartzberg, Jin Z. Zhan, "Structural correlations with shifts in the extended plasma resonance of gold nanoparticle aggregates," Opt. Mat. 27 (7), April, 1197-1203 (2005).

Marcin Nowotny, Sergei A. Gaidamakov, Robert J. Crouch, Wei Yang, "Crystal Structures of RNase H Bound to an RNA/DNA Hybrid: Substrate Specificity and Metal-Dependent Catalysis," Cell 121 (7), July, 1005-1016 (2005).

C.J. O'Neal, M.G. Jobling, R.K. Holmes, W.G.J. Hol, "Structural Basis for the Activation of Cholera Toxin by Human ARF6-GTP," Science 309 (5737), August, 1093-1096 (2005).

Aaron J. Oakley, Karin V. Loscha, Patrick M. Schaeffer, Edvards Liepinsh, Guido Pintacuda, Matthew C.J. Wilce, Gottfried Otting, Nicholas E. Dixon, "Crystal and Solution Structures of the Helicase-binding Domain of Escherichia coli Primase," J. Biol. Chem. 280 (12), March, 11495-11504 (2005).

H. Ogawa, Y. Qiu, C.M. Ogata, "Structural studies of the natriuretic peptide receptor: A novel hormone-induced rotation mechanism for transmembrane signal transduction," Peptides 26 (6), June, 957-968 (2005).

Abiodun A. Ogunjimi, Douglas J. Briant, Nadia Pece-Barbara, Christine Le Roy, Gianni M. Di Guglielmo, Peter Kavsak, Richele K. Rasmussen, Bruce T. Seet, Frank Sicheri, Jeffrey L. Wrana, "Regulation of Smurf2 Ubiquitin Ligase Activity by Anchoring the E2 to the HECT Domain," Mol. Cell 19 (3), August, 297-308 (2005).

T. Ohkochi, N. Hosoito, K. Mibu, "Depth-selective measurements of induced magnetic polarization in the Cu layer of Gd/Cu multilayers by [superscript 119] Sn Mössbauer Spectroscopy," J. Phys. Condens. Matter 17, 4023-4033 (2005).

D. Orosel, P. Balog, H. Liu, J. Qian, M. Jansen, "Sb[subscript 2]O[subscript 4] at high pressures and high temperatures," J. Solid State Chem. 178 (9), September, 2602-2607 (2005).

Kanji Oshima, Yasunori Takezawa, Yasunobu Sugimoto, Thomas Irving, Katsuzo Wakabayashi, "Intensity analysis of myosin-based x-ray meridional reflections from live skeletal muscles in relaxed and contracting states," Fibre Diffract. Rev. 13, 23-30 (2005).

Takanori Otomo, Diana R. Tomchick, Chinatsu Otomo, Sanjay C. Panchal, Mischa Machius, Michael K. Rosen, "Structural basis of actin filament nucleation and processive capping by a formin homology 2 domain," Nature 433, February, 488-494 (2005).

R.T. Ott, F. Sansoz, J.F. Molinari, J. Almer, K.T. Ramesh, T.C. Hufnagel, "Micromechanics of deformation of metallic-glass-matrix composites from in situ synchrotron strain measurements and finite element modeling," Acta Mater. 53 (7), April, 1883-1893 (2005).

Anil K. Padyana, Hongfang Qiu, Antonina Roll-Mecak, Alan G. Hinnebusch, Stephen K. Burley, "Structural Basis for Autoinhibition and Mutational Activation of Eukaryotic Initiation Factor 2[alpha] Protein Kinase GCN2," J. Biol. Chem. 280 (32), August, 29289-29299 (2005).

Pradeep S. Pallan, William S. Marshall, Joel Harp, Frederic C. Jewett III, Zdzislaw Wawrzak, Bernard A. Brown II, Alexander Rich, Martin Egli, "Crystal Structure of a Luteoviral RNA Pseudoknot and Model for a Minimal Ribosomal Frameshifting Motif," Biochemistry-US 44 (34), August, 11315-11322 (2005).

C. Pantea, G.A. Voronon, T.W. Zerda, J. Zhang, L. Wang, Y. Wang, T. Uchida, Y. Zhao, "Kinetics of SiC formation during the high P-T reaction between diamond and silicon," Diam. Relat. Mater. 14 (10), October, 1611-1615 (2005).

Matthew E. Papaconstantinou, Christopher J. Carrell, Agustin O. Pineda, Kevin M. Bobofchak, F.Scott Mathews, Christodoulos S. Flordellis, Michael E. Maragoudakis, Nikos E. Tsopanoglou, Enrico Di Cera, "Thrombin Functions through Its RGD Sequence in a Non-canonical Conformation," J. Biol. Chem. 280 (33), August, 29393-29396 (2005).

J.J. Papike, J.M. Karner, C.K. Shearer, "Comparative planetary mineralogy: Valence state partitioning of Cr, Fe, Ti, and V among crystallographic sites in olivine, pyroxene, and spinel from planetary basalts," Am. Mineral. 90 (2-3), February, 277-290 (2005).

John B. Parise, Sytle M. Antao, F.Marc Michel, C. David Martin, Peter J. Chupas, Sarvjit D. Shastri, Peter L. Lee, "Quantitative high-pressure pair distribution function analysis," J. Synchrotron Rad. 12, April, 554-559 (2005).

C. Park, P.A. Fenter, N.C. Sturchio, J.R. Regalbuto, "Probing Outer-Sphere Adsorption of Aqueous Metal Complexes at the Oxide-Water Interface with Resonant Anomalous X-Ray Reflectivity," Phys. Rev. Lett. 94 (7), February, 076104-1-076104-4 (2005).

Lauren Parker, Amy Kendall, P.H. Berger, P.J. Shiel, Gerald Stubbs, "Wheat streak mosaic virus-Structural parameters for a Potyvirus," Virology 340 (1), September, 64-69 (2005).

E.J. Park, A.J.M. Smucker, "Saturated hydraulic conductivity and porosity within macroaggregates modified by tillage," Soil Sci. Soc. Am. J. 69, 38-45 (2005).

Ha-Jeng Park, Floyd G. Adsit, Jeffrey C. Boyington, "The 1.4 Å Crystal Structure of the Human Oxidized Low Density Lipoprotein Receptor Lox-1," J. Biol. Chem. 280 (14), April, 13593-13599 (2005).

Moon Jeong Park, Kookheon Char, "Interplay between Cubic and Hexagonal Phases in Block Copolymer Solutions," Langmuir 21 (4), January, 1403-1411 (2005).

A.G. Peele, F. De Carlo, P.J. McMahon, B.B. Dahl, K.A. Nugent, "X-ray phase contrast tomography with a bending magnet source," Rev. Sci. Instrum. 76, August, 083707-1-083707-5 (2005).

A.G. Peele, A.P. Mancuso, C.Q. Tran, D. Paterson, I. McNulty, J.P. Haye, K.A. Nugent, "Phase retrieval from coherent soft X-ray optics," J. Electron. Spectrosc. 144, June, 1171-1173 (2005).

Robert Pejchal, Ryan Sargeant, Martha L. Ludwig, "Structures of NADH and CH[subscript 3]-H[subscript 4] Folate Complexes of Escherichia coli Methylenetetrahydrofolate Reductase Reveal a Spartan Strategy for a Ping-Pong Reaction," Biochemistry-US 44 (34), March, 11447-11457 (2005).

Robert Pejcha, Martha L. Ludwig, "Cobalamin-Independent Methionine Synthase (MetE): A Face-to-Face Double Barrel that Evolved by Gene Duplication," PLoS Biol. 3 (2 e31), February, 0254-0265 (2005).

E. Peltier, A.L. Dahl, J.-F. Gaillard, "Metal Speciation in Anoxic Sediments: When Sulfides Can be Construed as Oxides," Environ. Sci. Technol. 39 (1), January, 311-316 (2005).

B.-H. Peng, M.A. White, G.A. Campbell, J.J. Robert, J.C. Lee, R.B. Sutton, "Crystallization and preliminary X-ray diffraction of the ZO-binding domain of human occludin," Acta Crystallogr. F F61 ((4)), online (2005).

R.L. Peng, J. Almer, M. Oden, "Residual stress in both as-deposited and annealed CrN coatings," Mater. Sci. Forum 490-491, 643-648 (2005).

Valeri Petkov, "Atomic-Scale Structure of Glasses Using High-Energy X-Ray Diffraction," J. Am. Chem. Soc. 88 (9), September, 2528-2531 (2005).

V. Petkov, M. Gateshki, J. Choi, E.G. Gillan, Y. Ren, "Structure of nanocrystalline GaN from X-ray diffraction, Rietveld and atomic pair distribution function analyses," J. Mater. Chem. 15 (43), September, 4654-4659 (2005).

Valeri Petkov, Yong Peng, Geoff Williams, Baohua Huang, Donald Tomalia, Yang Ren, "Structure of gold nanoparticles suspended in water studied by x-ray diffraction and computer simulations," Phys. Rev. B 72, November, 195402-1-195402-8 (2005).

Tatiana Petrova, Holger Steuber, Isabelle Hazemann, Alexandra Cousido-Siah, Andre Mitschler, Roland Chung, Mitsuru Oka, Gerhard Klebe, Ossama El-Kabbani, Andrzej Joachimiak, Alberto Podjarny, "Factorizing Selectivity Determinants of Inhibitor Binding toward Aldose and Aldehyde Reductases: Structural and Thermodynamic Properties of the Aldose Reductase Mutant Leu300Pro-Fidarestat Complex," J. Med. Chem. 48 (18), 5659-5665 (2005).

Jeffrey A. Pfefferkorn, Meredith L. Greene, Richard A. Nugent, Rebecca J. Gross, Mark A. Mitchell, Barry C. Finzel, Melissa S. Harris, Peter A. Wells, John A. Shelly, Robert A. Anstadt, Robert E. Kilkuskie, Laurice A. Kopta, Francis J. Schwend, "Inhibitors of Hcv Ns5B Polymerase: Part 1: Evaluation of the Southern Region of (2Z)-2-(Benzoylamino)-3-(5-Phenyl-2-Furyl)Acrylic Acid," Bioorg. Med. Chem. Lett. 15 (10), May, 2481-2486 (2005).

Jeffrey A. Pfefferkorn, Richard Nugent, Rebecca J. Gross, Meredith Greene, Mark A. Mitchell, Matthew T. Reding, Lee A. Funk, Rebecca Anderson, Peter A. Wells, John A. Shelly, Robert Anstadt, Barry C. Finzel, Melissa S. Harris, Robert E. Kilkuskie, Laurice A. Kopta, Francis J. Schwend, "Inhibitors of HCV NS5B polymerase. Part 2: Evaluation of the northern region of (2Z)-2-benzoylamino-3-(4-phenoxy-phenyl)-acrylic acid," Bioorg. Med. Chem. Lett. 15 (11), June, 2812-2818 (2005).

Peter Pfister, Natascia Corti, Sven Hobbie, Christian Bruell, Raz Zarivach, Ada Yonath, Erik C. Bottger, "23S rRNA base pair 2057-2611 determines ketolide susceptibility and fitness cost of the macrolide resistance mutation 2058A3[converts to]G," Proc. Natl. Acad. Sci. USA 102 (14), April, 5180-5185 (2005).

Jason Phan, Zhen-Dan Shi, Terrence R. Burke, Jr., David S. Waugh, "Crystal Structures of a High-affinity Macrocyclic Peptide Mimetic in Complex with the Grb2 SH2 Domain," J. Mol. Biol. 353 (1), October, 104-115 (2005).

Kulwadee Phannachet, Youssef Elias, Raven H. Huang, "Dissecting the Roles of a Strictly Conserved Tyrosine in Substrate Recognition and Catalysis by Pseudouridine 55 Synthase," Biochemistry-US 44 (47), November, 15488-15494 (2005).

J.J. Pluth, I.M. Steele, A.R. Kampf, D.I. Green, "Redgillite, Cu[subscript 6](OH)1 0(SO[subscript 4]).2H[subscript 2]O, a new mineral from Caldbeck Fells, Cumbria, England, UK: Description and crystal structure," Mineral Mag. 69 (6), December, 973-981 (2005).

Galina Polekhina, Kara Sue Giddings, Rodney K. Tweten, Michael W. Parker, "Insights into the action of the superfamily of cholesterol-dependent cytolysins from studies of intermedilysin," Proc. Natl. Acad. Sci. USA 102 (3), January, 600-605 (2005).

Galina Polekhina, Abhilasha Gupta, Bryce J.W. van Denderen, Susanne C. Feil, Bruce E. Kemp, David Stapleton, "Structural Basis for Glycogen Recognition by AMP-Activated Protein Kinase," Structure 13 (10), October, 1453-1462 (2005).

M.L. Polizzotto, C.F. Harvey, S.R. Sutton, S. Fendorf, "Process conducive to the release and transport of arsenic into aquifers of Bangladesh," Proc. Natl. Acad. Sci. USA 102 (52), December, 18819-18823 (2005).

Owen Pornillos, Yen-Ju Chen, Andy P. Chen, Geoffrey Chang, "X-ray Structure of the EmrE Multidrug Transporter in Complex with a Substrate," Science 310, December, 1950-1953 (2005).

H.F. Poulsen, U. Lienert, W. Pantleon, "Characterisation of the Orientation Distribution of Individual Grains within Deformed Metals," Mater. Sci. Tech. Ser. 21 (12), December, 1397-1400 (2005).

V.B. Prakapenka, G. Shen, M.L. Rivers, S.R. Sutton, L. Dubrovinsky, "Grain-size control in situ at high pressures and high temperatures in a diamond-anvil cell," J. Synchrotron Rad. 12, 560-565 (2005).

Venna Prasad, Shin-Woong Kang, K.A. Suresh, Leela Joshi, Qingbing Wang, Satyendra Kumar, "Thermotropic Uniaxial and Biaxial Nematic and Smectic Phases in Bent-Core Mesogens," J. Am. Chem. Soc. 127, November, 17224-17227 (2005).

Michael G. Pravica, Edward Romano, Zachary Quine, "X-ray diffraction study of elemental erbium to 70 GPa," Phys. Rev. B 72 (21), December, 214122-1-214122-4 (2005).

Marc L. Pusey, Zhi-Jie Liu, Wolfram Tempel, Jeremy Praissman, Dawei Lin, Bi-Cheng Wang, Jose A. Gavira, Joseph D. Ng, "Life in the fast lane for protein crystallization and X-ray crystallography," Prog. Biophys. Mol. Bio. 88, 359-386 (2005).

J. Qian, C. Pantea, J. Zhang, L.L. Daemen, Y. Zhao, M. Tang, T. Uchida, Y. Wang, "Yield Strength of [alpha]-Silicon Nitride at High Pressure and High Temperature," J. Am. Ceram. Soc. 88 (4), 903-906 (2005).

Xiayang Qiu, Anthony E. Choudhry, Cheryl A. Janson, Michael Grooms, Robert A. Daines, John T. Lonsdale, Sanjay S. Khandekar, "Crystal structure and substrate specificity of the[beta]-ketoacyl-acyl carrier protein synthase III (FabH) from Staphylococcus aureus," Protein Sci. 14, June, 2087-2094 (2005).

Shen Que, "Phase problem and reference-beam diffraction," Adv. Imag. Elect. Phys. 134, 69-112 (2005).

Michael L. Quillin, David M. Anstrom, Xiaokun Shu, Shannon O'Leary, Karen Kallio, Dmitry M. Chudakov, S.James Remington, "Kindling Fluorescent Protein from Anemonia sulcata: Dark-State Structure at 1.38 Å Resolution," Biochemistry-US 44 (15), March, 5774-5787 (2005).

Sudarshan Rajagopal, Spencer Anderson, Vukica Srajer, Marius Schmidt, Reinhard Pahl, Keith Moffat, "A Structural Pathway for Signaling in the E46Q Mutant of Photoactive Yellow Protein," Structure 13 (1), 55-63 (2005).

M.N. Rao, S.R. Sutton, D.S. McKay, G. Dreibus, "Clues to Martian brines based on halogens in salts from nakhlites and MER samples," J. Geophys. Res. 110, E12S06-E120S18 (2005).

B. Ravel, M. Newville, "ATHENA, ARTEMIS, HEPHAESTUS: data analysis for X-ray absorption spectropscopy using IFEFFIT," J. Synchrotron Rad. 12, July, 537-541 (2005).

M. Reconditi, M. Linari, L. Lucii, A. Stewart, Y.-B. Sun, T. Narayanan, T. Irving, G. Piazzesi, T. Irving, V. Lombardi, "Structure-Function Relation of the Myosin Motor in Striated Muscle," Ann. NY Acad. Sci. 1047, 232-247 (2005).

S. Rendon, W.R. Burghardt, R.A. Bubeck, L.S. Thomas, B. Hart, "Mechanical and Morpological Anisotropy in Injection Molding of Thermotropic Liquid Crystalline Copolyesters," Polymer 46 (23), November, 10202-10213 (2005).

David Reverter, Christopher D. Lima, "Insights into E3 ligase activity revealed by a SUMO-RanGAP1-Ubc9-Nup358 complex," Nature 435, June, 687-692 (2005).

David Reverter, Kenneth Wu, Tudeviin Gan Erdene, Zhen-Qiang Pan, Keith D. Wilkinson, Christopher D. Lima, "Structure of a Complex between Nedd8 and the Ulp/Senp Protease Family Member Den1," J. Mol. Biol. 345, 141-151 (2005).

Christopher L. Reyes, Geoffrey Chang, "Structure of the ABC Transporter MsbA in Complex with ADP·Vanadate and Lipopolysaccharide," Science 308 (5724), May, 1028-1031 (2005).

Donald R. Ronning, Catherine Guynet, Bao Ton-Hoang, Zhanita N. Perez, Rodolfo Ghirlando, Michael Chandler, Fred Dyda, "Active Site Sharing and Subterminal Hairpin Recognition in a New Class of DNA Transposases," Mol. Cell 26, October, 143-154 (2005).

R.A. Rosenberg, G.K. Shenoy, F. Heigl, S.-T. Lee, P.-S.G. Kim, X.-T. Zhou, T.K. Sham, "Effects of in situ vacuum annealing on the surface and luminescent properties of ZnS nanowires," Appl. Phys. Lett. 86, June, 263115-1-263115-3 (2005).

R.A. Rosenberg, G.K. Shenoy, F. Heigl, S.-T. Lee, P.-S.G. Kim, X.-T. Zhou, T.K. Sham, "Determination of the local structure of luminescent sites in ZnS nanowires using x-ray excited optical luminescence," Appl. Phys. Lett. 87, December, 253105-1-253105-3 (2005).

J.R. Royer, E.I. Corwin, A. Flior, M.L. Cordero, M. Rivers, P. Eng, H.M. Jaeger, "Formation of granular jets observed by high-speed x-ray radiography," Nature Phys. 1 (2), November, 164-167 (2005).

Seth M. Rubin, Anne-Laure Gall, Ning Zheng, Nikola P. Pavletich, "Structure of the Rb C-Terminal Domain Bound to E2F1-DP1: A Mechanism for Phosphorylation-Induced E2F Release," Cell 123 (6), December, 1093-1106 (2005).

Wilhelm Rulanda, Bernd Smarsly, "SAXS of self-assembled nanocomposite films with oriented two-dimensional cylinder arrays: an advanced method of evaluation," J. Appl. Crystallogr. 38 (1), February, 78-86 (2005).

J.T. Russell, Y. Lin, A. Boker, L. Su, P. Carl, H. Zettl, J. He, K. Sill, R. Tangirala, T. Emrick, K. Littrell, P. Thiyagarajan, D. Cookson, A. Fery, Q. Wang, T.P. Russell, "Self-assembly and cross-linking of bionanoparticles at liquid-liquid interfaces," Angew. Chem. Int. Ed. 44 (16), 2420-2426 (2005).

A.V. Ryazhkin, Yu.A. Babanov, T. Miyanaga, E.D. Crozier, R.A. Gordon, T. Reich, H. Funke, "Thickness Inhomogeneity Effect in EXAFS Spectroscopy," Phys. Scripta. T115, 197-199 (2005).

B. Sahoo, W. Keune, W. Sturhahn, T.S. Toellner, E.E. Alp, "Atomic vibrational dynamics of amorphous Fe-Mg alloy thin films," J. Phys. Chem. Solids 66 (12), December, 2263-2270 (2005).

Mark E. Salvati, Aaron Balog, Weifang Shan, Donna D. Wei, Dacia Pickering, Ricardo M. Attar, Jieping Geng, Cheryl A. Rizzo, Marco M. Gottardis, Roberto Weinmann, Stanley R. Krystek, John Sack, Yongmi An, Kevin Kish, "Structure based approach to the design of bicyclic-1H-isoindole-1,3(2H)-dione based androgen receptor antagonists," Bioorg. Med. Chem. Lett. 15 (2), January, 271-276 (2005).

Parthasarathy Sampathkumar, Stewart Turley, Jonathan E. Ulmer, Ho Gun Rhie, Carol Hopkins Sibley, Wim G.J. Hol, "Structure of the Mycobacterium tuberculosis Flavin Dependent Thymidylate Synthase (MtbThyX) at 2.0 Å Resolution," J. Mol. Biol. 352, 1091-1104 (2005).

Rajesh K. Sani, Brent M. Peyton, Alice Dohnalkova, James E. Amonette, "Reoxidation of Reduced Uranium with Iron(III) (Hydr)Oxides under Sulfate-Reducing Conditions," Environ. Sci. Technol. 39 (7), March, 2059-2066 (2005).

R. Sanishvili, M. Pennycooke, J. Gu, X. Xu, A. Joachimiak, A.M. Edwards, "Crystal structure of the hypothetical protein TA1238 from Thermoplasma acidophilum: a new type of helical super-bundle," J. Struct. Funct. Geno. 5 (4), April, 231-240 (2005).

Z.V. Saponjic, N.M. Dimitrijevic, D.M. Tiede, A.J. Goshe, X. Zuo, L.X. Chen, A.S. Barnard, P. Zapol, L. Curtiss, T. Rajh, "Shaping Nanometer-Scale Architecture Through Surface Chemistry," Adv. Mater. 17 (8), April, 965-971 (2005).

Vivian Saridakis, Yi Sheng, Feroz Sarkari, Melissa N. Holowaty, Kathy Shire, Tin Nguyen, Rongguang G. Zhang, Jack Liao, Weontae Lee, Aled M. Edwards, Cheryl H. Arrowsmith, Lori Frappier, "Structure of the p53 Binding Domain of HAUSP/USP7 Bound to Epstein-Barr Nuclear Antigen 1: Implications for EBV-Mediated Immortalization," Mol. Cell 18, April, 25-36 (2005).

P.V. Satyam, S. Roy, B. Satpati, J. Ghatak, K. Bhattacharjee, J. Kamila, B.N. Dev, J. Wang, R. Guico, S. Narayanan, C. Liu, R.E. Cook, L. Assoufid, "Pattern growth of Ge films on PtBA polymer substrates," Physica E 27, January, 235-239 (2005).

Kenneth Sauer, Junko Yano, Vittal K. Yachandra, "X-ray spectroscopy of the Mn[subscript 4]Ca cluster in the water-oxidation complex of Photosystem II," Photosyn. Res. 85 (1), 73-86 (2005).

W. Robert Scheidt, Stephen M. Durbin, J.Timothy Sage, "Nuclear resonance vibrational spectroscopy - NRVS," J. Inorg. Biochem. 99, 60-71 (2005).

Gerhard Schenk, Lawrence R. Gahan, Lyle E. Carrington, Natasa Miti, Mohsen Valizadeh, Susan E. Hamilton, John de Jersey, Luke W. Guddat, "Phosphate forms an unusual tripodal complex with the Fe-Mn center of sweet potato purple acid phosphatase," Proc. Natl. Acad. Sci. USA 102 (2), 273-278 (2005).

Mark L. Schlossman, "X-ray scattering from liquid-liquid interfaces," Physica B 357 (1-2), February, 98-105 (2005).

Jason W. Schmidberger, Aaron J. Oakley, Jimmy S.H. Tsang, Matthew C.J. Wilce, "Purification, crystallization and preliminary crystallographic analysis of DehIVa, a dehalogenase from Burkholderia cepacia MBA4," Acta Crystallogr. F 61, January, 271-273 (2005).

Marius Schmidt, Karin Nienhaus, Reinhard Pahl, Angela Krasselt, Spencer Anderson, Fritz Parak, G.Ulrich Nienhaus, Vukica Srajer, "Ligand migration pathway and protein dynamics in myoglobin: A time-resolved crystallographic study on L29W MbCO," Proc. Natl. Acad. Sci. USA 102 (33), August, 11704-11709 (2005).

G. Schnaar, M.L. Brusseau, "Pore-scale characterization of organic immiscible-liquid morphology in natural porous media using synchrotron x-ray microtomography," Environ. Sci. Technol. 39 (21), September, 8403-8410 (2005).

Florian D. Schubot, Michael W. Jackson, Kerri J. Penrose, Scott Cherry, Joseph E. Tropea, Gregory V. Plano, David S. Waugh, "Three-dimensional Structure of a Macromolecular Assembly that Regulates Type III Secretion in Yersinia pestis," J. Mol. Biol. 346 (4), March, 1147-1161 (2005).

Barbara A. Schweitzer, William L. Neumanna, Hayat K. Rahman, Carrie L. Kusturin, Kirby R. Sample, Gennadiy I. Poda, Ravi G. Kurumbail, Anna M. Stevens, Roderick A. Stegeman, William C. Stallings, Michael S. South, "Structure-based design and synthesis of pyrazinones containing novel P1 'side pocket' moieties as inhibitors of TF/VIIa," Bioorg. Med. Chem. Lett. 15 (12), June, 3006-3011 (2005).

Olga Senkovich, Haley Speed, Alexei Grigorian, Kelley Bradley, ChodavarapuS. Ramarao, Bessie Lane, Guan Zhu, Debasish Chattopadhyay, "Crystallization of three key glycolytic enzymes of the opportunistic pathogen Cryptosporidium parvum," Biochim. Biophys. Acta 1750 (2), May, 166-172 (2005).

Alexander Serganov, Sonja Keiper, Lucy Malinina, Valentina Tereshko, Eugene Skripkin, Claudia Hobartner, Anna Polonskaia, AnhTuan Phan, Richard Wombacher, Ronald Micura, Zbigniew Dauter, Andres Jaschke, Dinshaw J. Patel, "Structural basis for Diels-Alder ribozyme-catalyzed carbon-carbon bond formation," Nat. Struct. Mol. Biol. 12, February, 218-224 (2005).

T.K. Sham, R.A. Gordon, S.M. Heald, "Resonant inelastic x-ray scattering at the Ce L[subscript 3] edge of CePO[subscript 4] and CeO[subscript 2]:Implications for the valence of CeO[subscript 2] and related phenomena," Phys. Rev. B 72 (3), July, 035113-1-035113-6 (2005).

T.K. Sham, P.-S.G. Kim, H. Ngo, S. Chakrabati, P.C. Adams, "An X-ray Microspectroscopy Study of Hemochromatosis Liver and Diabetic Mice Kidney Tissues: Preliminary Observations," Phys. Scripta. T115, 1047-1049 (2005).

Hui Shao, Xianzhi He, Lahoucine Achnine, Jack W. Blount, Richard A. Dixon, Xiaoqiang Wang, "Crystal Structures of a Multifunctional Triterpene/Flavonoid Glycosyltransferase from Medicago truncatula," Plant Cell 17 (11), November, 3141-3154 (2005).

N. Sharma, J.H. Toney, P.M.D. Fitzgerald, "Expression, purification, crystallization and preliminary X-ray analysis of Aeromonas hydrophilia metallo-[beta]-lactamase," Acta Crystallogr. F F61, 180-182 (2005).

Wendy J. Shaw, John C. Linehan, Anna Gutowska, David Newell, Tom Bitterwolf, John L. Fulton, Yongsheng Chen, Charles F. Windisch, "Synthesis and characterization of a recoverable rhodium catalyst with a stimulus sensitive polymer ligand," Inorg. Chem. Commun. 8, July, 894-896 (2005).

G. Shen, V.B. Prakapenka, P.J. Eng, M.L. Rivers, S.R. Sutton, "Facilities for high-pressure research with the diamond anvil cell at GSECARS," J. Synchrotron Rad. 12, 642-649 (2005).

Yuequan Shen, Natalia L. Zhukovskaya, Qing Guo, Jan Florián, Wei-Jen Tang, "Calcium-independent calmodulin binding and two-metal-ion catalytic mechanism of anthrax edema factor," EMBO J. 24, 929-942 (2005).

Steven Shia, Jennifer Stamos, Daniel Kirchhofer, Bin Fan, Judy Wu, Raquel T. Corpuz, Lydia Santell, Robert A. Lazarus, Charles Eigenbrot, "Conformational Lability in Serine Protease Active Sites: Structures of Hepatocyte Growth Factor Activator (HGFA) Alone and with the Inhibitory Domain from HGFA Inhibitor-1B," J. Mol. Biol. 346, 1335-1349 (2005).

S.R. Shieh, T.S. Duffy, G. Shen, "X-ray diffraction study of phase stability in SiO[subscript 2] at deep mantle conditions," Earth Planet Sci. Lett. 235, 273-282 (2005).

Amy Y. Shih, Ilia G. Denisov, James C. Phillips, Stephen G. Sligar, Klaus Schulten, "Molecular Dynamics Simulations of Discoidal Bilayers Assembled from Truncated Human Lipoproteins," Biophys. J. 88 (1), January, 548-556 (2005).

Ke Shi, C.Kent Brown, Zu-Yi Gu, Briana K. Kozlowicz, Gary M. Dunny, Douglas H. Ohlendorf, Cathleen A. Earhart, "Structure of peptide sex pheromone receptor PrgX and PrgX/pheromone complexes and regulation of conjugation in Enterococcus faecalis," Proc. Natl. Acad. Sci. USA 102 (51), December, 18596-18601 (2005).

W.L. Shoop, Y. Xiong, J. Wiltsie, A. Woods, J. Guo, J.V. Pivnichny, T. Felcetto, B.F. Michael, A. Bansal, R.T. Cummings, B.R. Cunningham, A.M. Friedlander, C.M. Douglas, S.B. Patel, D. Wisniewski, G. Scapin, S.P. Salowe, D.M. Zaller, K.T. Chapman, E.M. Scolnick, D.M. Schmatz, K. Bartizal, M. MacCoss, D. Hermes, "Anthrax lethal factor inhibition," Proc. Natl. Acad. Sci. USA 102 (22), April, 7958-7963 (2005).

Oleg G. Shpyrko, Alexei Yu. Grigoriev, Reinhard Streitel, Diego Pontoni, Peter S. Pershan, Moshe Deutsch, Ben Ocko, Mati Meron, Binhua Lin, "Atomic-Scale Surface Demixing in a Eutectic Liquid BiSn Alloy," Phys. Rev. Lett. 95, September, 106103-1-106103-4 (2005).

L.F. Siah, W.M. Kriven, J. Schneider, "In situ, high-temperature, synchrotron, powder diffraction studies of oxide systems in air, using a thermal-image furnace," Meas. Sci. Technol. 16 (6), June, 1291-1298 (2005).

Edyta A.L. Sieminska, Andrea Macova, David R.J. Palmera, David A.R. Sanders, "Crystallization and preliminary X-ray analysis of (1R,6R)-2-succinyl-6-hydroxy-2,4-cyclohexadiene-1-carboxylate (SHCHC) synthase (MenD) from Escherichia coli," Acta Crystallogr. F 61 (5), May, 489-492 (2005).

Miljan Simonovic, Jean-Bernard Denault, Guy S. Salvesen, Karl Volz, Peter G.W. Getti, "Lack of involvement of strand s1'A of the viral serpin CrmA in anti-apoptotic or caspase-inhibitory functions," Arch. Biochem. Biophys. 441 (1), August, 1-9 (2005).

Sasha Singh, Sergey Korolev, Olga Koroleva, Thomas Zarembinski, Frank Collart, Andrzej Joachimiak, Dinesh Christendat, "Crystal Structure of a Novel Shikimate Dehydrogenase from Haemophilus influenzae," J. Biol. Chem. 290 (17), April, 17101-17108 (2005).

Sangita C. Sinha, Martina Wetterer, Stephen R. Sprang, Joachim E. Schultz, Jurgen U. Linder, "Origin of asymmetry in adenylyl cyclases: structures of Mycobacterium tuberculosis Rv1900c," EMBO J. 24 (4), January, 663-673 (2005).

L.E. Sinks, B. Rybtchinski, M. Limura, B.A. Jones, A.J. Goshe, X. Zuo, D.M. Tiede, X. Li, M.R. Wasielewski, "Self-Assembly of Photofunctional Cylindrical Nanostructures Based on Perylene-3,4:9,10-bis(dicarboximide)," Chem. Mater. 17 (25), 6295-6303 (2005).

Husin Sitepu, Maya G. Kopylova, David H. Quirt, Jeffrey N. Cutler, Thomas G. Kotzer, "Synchrotron micro-X-ray fluorescence analysis of natural diamonds: First steps in identification of mineral inclusions in situ," Am. Mineral. 90 (11-12), December, 1740-1747 (2005).

H. Skaff, Y. Lin, R. Tangirala, K. Breitenkamp, A. Boeker, T.P. Russell, T. Emrick, "Crosslinked Capsules of Quantum Dots by Interfacial Assembly and Ligand Crosslinking,," Adv. Mater. 17 (17), August, 2082-2086 (2005).

E. Skrzypczak-Jankun, O.Y. Borbulevych, A. Melillo, R. Keck, M. Soriano-Garcia, K. Aniola, M. Niedre, L. Lilge, S.H. Sherman, J. Jankun, "Aspirin blocks binding of photosensitizer SnET2 into human serum," Int. J. Mol. Med. 15 (5), May, 777-783 (2005).

Laura R. Skubal, Sandra G. Biedron, Matthew Newville, John F. Schneider, Stephen V. Milton, Piero Pianetta, H.Jack O'Neill, "Mercury transformations in chemical agent simulant as characterized by X-ray absorption fine spectroscopy," Talanta 67, 730-735 (2005).

Eli Sloutskin, Benjamin M. Ocko, Lilach Tamam, Ivan Kuzmenko, Thomas Gog, Moshe Deutsch, "Surface Layering in Ionic Liquids: An X-ray Reflectivity Study," J. Am. Chem. Soc. 127, 7796-7804 (2005).

A.J. Slowey, S.B. Johnson, J.J. Rytuba, G.E. Brown, "Role of Organic Acids in Promoting Colloidal Transport of Mercury from Mine Tailings," Environ. Sci. Technol. 39 (20), September, 7869-7874 (2005).

R. Smither, K. Abu Saleem, M. Beno, C. Kurtz, A. Khounsary, N. Abrosimov, "Diffraction efficiency and diffraction bandwidth of thermal-gradient and composition-gradient crystals," Rev. Sci. Instrum. 76 (12), 123107-1-123107-19 (2005).

Matt C. Smith, Yuming Xiao, Hongxin Wang, Simon J. George, Dimitri Coucouvanis, Markos Koutmos, Wolfgang Sturhahn, Ercan E. Alp, Jiyong Zhao, Stephen P. Cramer, "Normal-Mode Analysis of FeCl4[superscript -] and Fe[subscript 2]S[subscript 2]Cl[subscript 4][superscript 2-] via Vibrational Mossbauer, Resonance Raman, and FT-IR Spectroscopies," Inorg. Chem. 44 (16), June, 5562-5570 (2005).

P.G. Smith, I. Koch, R.A. Gordon, D.F. Mandoli, B.D. Chapman, K.J. Reimer, "X-ray Absorption Near-Edge Structure Analysis of Arsenic Species for Application to Biological Environmental Samples," Environ. Sci. Technol. 39 (1), January, 248-254 (2005).

Jungsan Sohn, Jerry M. Parks, Gregory Burhman, Paul Brown, Kolbrun Kristjansdottir, Alexias Safi, Herbert Edelsbrunner, Weitao Yang, Johannes Rudolph, "Experimental Validation of the Docking Orientation of Cdc25 with Its Cdk2-CycA Protein Substrate," Biochemistry-US 44, December, 16563-16573 (2005).

I.H. Solomon, J.M. Hager, R. Safi, D.P. McDonnell, M.R. Redinbo, E.A. Ortlund, "Crystal structure of the human LRH-1 DBD-DNA complex reveals Ftz-F1 domain positioning is required for receptor activity," J. Mol. Biol. 354 (5), December, 1091-1102 (2005).

M. Sommerhalter, R.L. Lieberman, A.C. Rosenzweig, "X-ray crystallography and biological metal centers: is seeing believing?," Inorg. Chem. 44, February, 770-778 (2005).

Monika Sommerhalter, Lana Saleh, J. Martin Bollinger Jr., Amy C. Rosenzweig, "Structure of Escherichia coli ribonucleotide reductase R2 in space group P6[subscript 1]22," Acta Crystallogr. D 61, 1649-1654 (2005).

Gang Song, Yuting Yang, Jin-huan Liu, Jose M. Casasnovas, Motomu Shimaoka, Timothy A. Springer, Jia-huai Wang, "An atomic resolution view of ICAM recognition in a complex between the binding domains of ICAM-3 and integrin [alpha]L[superscript beta]2," Proc. Natl. Acad. Sci. USA 102 (9), March, 3366-3371 (2005).

Yang Song, Zhenxian Liu, Ho-kwang Mao, Russell J. Hemley, Dudley R. Herschbach, "High-pressure vibrational spectroscopy of sulfur dioxide," J. Chem. Phys. 122 (17), May, 174511-1-174511-9 (2005).

E.D. Specht, P.D. Rack, A. Rar, G.M. Pharr, E.P. George, J.D. Fowlkes, H. Hong, E. Karapetrova, "Metastable phase evolution and grain growth in annealed nanocrystalline Cr-Fe-Ni films," Thin Solid Films 493, 307-312 (2005).

Christopher J. Squire, James M. Dickson, Ivan Ivanovic, Edward N. Baker, "Structure and Inhibition of the Human Cell Cycle Checkpoint Kinase, Wee1A Kinase: An AtypicalTyrosine Kinase with a Key Role in CDK1 Regulation," Structure 13 (4), April, 541-550 (2005).

Bart L. Staker, Michael D. Feese, Mark Cushman, Yves Pommier, David Zembower, Lance Stewart, Alex B. Burgin, "Structures of Three Classes of Anticancer Agents Bound to the Human Topoisomerase I-DNA Covalent Complex," J. Med. Chem. 48 (7), February, 2336-2345 (2005).

Petra Stefankova, Jana Maderova, Imrich Barak, Marta Kollarova, Zbyszek Otwinowsk, "Expression, purification and X-ray crystallographic analysis of thioredoxin from Streptomyces coelicolor," Acta Crystallogr. F F61, online (2005).

H. Steinfink, R.I. Dass, V. Lynch, R.L. Harlow, P.L. Lee, "On the existence of PbBi[subscript 3]PO[subscript 8] Its synthesis and crystal structure," MRS Bull. 40, 1361-1370 (2005).

Dominique C. Stepinski, Mark P. Jensen, Julie A. Dzielawa, Mark L. Dietz, "Synergistic Effects in the Facilitated Transfer of Metal Ions into Room-Temperature Ionic Liquids," Green Chem. 7 (3), March, 151-158 (2005).

E.A. Stern, D.L. Brewe, K.M. Beck, S.M. Heald, Y. Feng, "SubNanosecond Time Resolved XAFS of Laser Excited Thin Ge Films," Phys. Scripta. T115, 1044-1046 (2005).

C. Nicklaus Steussy, Anthony A. Vartia, John W. Burgner II, Autumn Sutherlin, Victor W. Rodwell, Cynthia V. Stauffacher, "X-ray Crystal Structures of HMG-CoA Synthase from Enterococcus faecalis and a Complex with Its Second Substrate/Inhibitor Acetoacetyl-CoA," Biochemistry-US 44 (43), October, 14256-14267 (2005).

G. Stubbs, L. Parker, J. Junn, A. Kendall, "Flexible filamentous virus structures from fiber diffraction," Fibre Diffract. Rev. 13, 38-42 (2005).

W. Sturhahn, J.M. Jackson, J.-F. Lin, "The spin state of iron in minerals of Earth's lower mantle," Geophys. Res. Lett. 32 (12), June, L12307 (2005).

Hua-Poo Su, Scott C. Garman, Timothy J. Allison, Christiana Fogg, Bernard Moss, David N. Garboczi, "The 1.51-Å structure of the poxvirus L1 protein, a target of potent neutralizing antibodies," Proc. Natl. Acad. Sci. USA 102 (12), March, 4240-4245 (2005).

Michael D.L. Suits, Gour P. Pal, Kanji Nakatsu, Allan Matte, Miroslaw Cygler, Zongchao Jia, "Identification of an Escherichia coli O157:H7 heme oxygenase with tandem functional repeats," Proc. Natl. Acad. Sci. USA 102 (47), November, 16955-16960 (2005).

N. Sukumar, P. Langan, F.S. Mathews, L.H. Jones, P. Thiyagarajan, B.P. Schoenbornb, V.L. Davidson, "A preliminary time-of-flight neutron diffraction study on amicyanin from Paracoccus denitrificans," Acta Crystallogr. D 61 (5), May, 640-642 (2005).

Warren Sun, Xiaohui Xu, Marina Pavlova, Aled M. Edwards, Andrzej Joachimiak, Alexei Savchenko, Dinesh Christendat, "The crystal structure of a novel SAM-dependent methyltransferase PH1915 from Pyrococcus horikoshii," Protein Sci. 14 (12), October, 3121-3128 (2005).

S.R. Sutton, J. Karner, J. Papike, J.S. Delaney, C. Shearer, M. Newville, P. Eng, M. Rivers, M.D. Dyar, "Vanadium K edge XANES of synthetic and natural basaltic glasses and application to microscale oxygen barometry," Geochim. Cosmochim. Acta 69 (9), 2333-2348 (2005).

Yohey Suzuki, Shelly D. Kelly, Kenneth M. Kemner, Jillian F. Banfield, "Direct microbial reduction and subsequent preservation of uranium in natural near-surface sediment," Appl. Environ. Microb. 71 (4), April, 1790-1797 (2005).

R.K. Tabtiang, B.O. Cezairliyan, R.A. Grant, J.C. Cochrane, R.T. Sauer, "Consolidating critical binding determinants by noncyclic rearrangement of protein secondary structure," Proc. Natl. Acad. Sci. USA 102 (7), February, 2305-2309 (2005).

J. Tang, H. Naitow, N.A. Gardner, A. Kolesar, L. Tang, R.B. Wickner, J.E. Johnson, "The structural basis of recognition and removal of cellular mRNA 7-methyl G 'caps' by a viral capsid protein: a unique viral response to host defense," J. Mol. Recognit. 18 (2), April, 158-168 (2005).

L. Tan, A. Kreyssig, J.W. Kim, A.I. Goldman, R.J. McQueeney, D. Wermeille, B. Sieve, T.A. Lograsso, D.L. Schlagel, S.L. Budko, V.K. Pecharsky, K.A. Gschneidner, Jr., "Magnetic structure of Gd[subscript 5]Ge[subscript 4]," Phys. Rev. B 71, 214408-1-214408-6 (2005).

F. Tannazi, G. Bunker, "Determination of Chemical Speciation by XAFS," Phys. Scripta. T115, 953-956 (2005).

Qiang Tan, Timothy A. Blizzard, Jerry D. Morgan II, Elizabeth T. Birzin, Wanda Chan, Yi Tien Yang, Lee-Yuh Pai, Edward C. Hayes, Carolyn A. DaSilva, Sudha Warrier, Joel Yudkovitz, Hilary A. Wilkinson, Nandini Sharma, Paula M.D. Fitzgerald, Susan Lia, Lawrence Colwell, John E. Fisher, Sharon Adamski, Alfred A. Reszka, Donald Kimmel, Frank DiNinno, Susan P. Rohrer, Leonard P. Freedman, James M. Schaeffer, Milton L. Hammond, "Estrogen receptor ligands. Part 10: Chromanes: old scaffolds for new SERAMs," Bioorgan. Med. Chem. 15 (6), March, 1675-1681 (2005).

Alexander B. Taylor, Christopher S. Stoj, Lynn Ziegler, Daniel J. Kosman, P.John Hart, "The copper-iron connection in biology: Structure of the metallo-oxidase Fet3p," Proc. Natl. Acad. Sci. USA 102 (43), October, 15459-15464 (2005).

Patrick G. Telmer, Brian H. Shilton, "Structural Studies of an Engineered Zinc Biosensor Reveal an Unanticipated Mode of Zinc Binding," J. Mol. Biol. 354 (4), December, 829-840 (2005).

Wolfram Tempel, Zhi-Jie Liu, Peter S. Horanyi, Lu Deng, Doowon Lee, M.Gary Newton, John P. Rose, Hisashi Ashida, Su-Chen Li, Yu-Teh Li, Bi-Cheng Wang, "Three-dimesional structure of GlcNAc[alpha]1-4Gal releasing Endo-Galactosidase from Clostridium perfringens," Proteins 59 (1), 141-144 (2005).

Alexey Teplyakov, Galina Obmolova, John Toedt, Michael Y. Galperin, Gary L. Gilliland, "Crystal Structure of the Bacterial YhcH Protein Indicates a Role in Sialic Acid Catabolism," J. Bacteriol. 187 (16), August, 5520-5527 (2005).

Mohammed Terrak, Grzegorz Rebowski, Renne C. Lu, Zenon Grabarek, Roberto Dominguez, "Structure of the light chain-binding domain of myosin V," Proc. Natl. Acad. Sci. USA 102 (36), August, 12718-12723 (2005).

Michael J. Theisen, Terra B. Potocky, D.Tyler McQuade, Samue H. Gellman, Mark L. Chiu, "Crystallization of bacteriorhodopsin solubilized by a tripod amphiphile," Biochim. Biophys. Acta 1751 (2), August, 213-216 (2005).

James B. Thoden, Hazel M. Holden, "The Molecular Architecture of Human N-Acetylgalactosamine Kinase," J. Bacteriol. 280 (38), September, 32784-32791 (2005).

James B. Thoden, David J. Timson, Richard J. Reece, Hazel M. Holden, "Molecular Structure of Human Galactokinase: Implications for Type II Galactosemia," J. Biol. Chem. 280 (10), March, 9662-9670 (2005).

Nicolas H. Thoma, Bryan K. Czyzewski, Andrei A. Alexeev, Alexander A. Mazin, Stephen C. Kowalczkowski, Nikola P. Pavletich, "Structure of the SWI2/SNF2 chromatin-remodeling domain of eukaryotic Rad54," Nature Struct. Biol. 12 (4), April, 350-356 (2005).

T.B. Thompson, T.F. Lerch, R.W. Cook, T.K. Woodruff, T.S. Jardetzky, "The structure of the follistatin:activin complex reveals antagonism of both type I and type II receptor binding," Dev. Cell 9 (4), October, 535-543 (2005).

J. Thornton, S. Slater, J. Almer, "The Measurement of Residual Strains Within Thermal Barrier Coatings Using High-Energy X-Ray Diffraction," J. Am. Ceram. Soc. 88 (10), October, 2817-2825 (2005).

Yunfeng Tie, Peter I. Boross, Yuan-Fang Wang, Laquasha Gaddis, Fengling Liu, Xianfeng Chen, Jozsef Tozser, Robert W. Harrison, Irene T. Weber, "Molecular basis for substrate recognition and drug resistance from 1.1 to 1.6 Å resolution crystal structures of HIV-1 protease mutants with substrate analogs," FEBS J. 272 (20), October, 5265-5277 (2005).

T.K. Tokunaga, J. Wan, J. Pena, E.L. Brodie, M.K. Firestone, T.C. Hazen, S.R. Sutton, A. Lanzirotti, M. Newville, "Uranium reduction in sediments under diffusion-limited transport of organic carbon," Environ. Sci. Technol. 39, 7077-7083 (2005).

A.V. Toms, A.L. Haas, J.-H. Park, T.P. Begley, S.E. Ealick, "Structural Characterization of the Regulatory Proteins TenA and TenI from Bacillus subtillis and the identification of TenA as a Thiaminase II," Biochemistry-US 44, 2319-2329 (2005).

Alfredo Torres-Larios, Kerren K. Swinger, Andrey S. Krasilnikov, Tao Pan, Alfonso Mondragon, "Crystal structure of the RNA component of bacterial ribonuclease P," Nature 437, September, 584-587 (2005).

Hirohide Toyama, Zhi-Wei Chen, Megumi Fukumoto, Osao Adachi, Kazunobu Matsushita, F.Scott Mathews, "Molecular Cloning and Structural Analysis of Quinohemoprotein Alcohol Dehydrogenase ADH-IIG from Pseudomonas putida HK5," J. Mol. Biol. 352 (1), September, 91-104 (2005).

C.Q. Tran, C.T. Chantler, Z. Barnea, M.D. de Jonge, B.B. Dhal, C.T.Y. Chung, D. Paterson, J. Wang, "Measurement of the x-ray mass attenuation coefficient of silver using the x-ray-extended range technique," J. Phys. B 38, January, 89-107 (2005).

C.Q. Tran, A.G. Peele, D. Paterson, A. Roberts, I. McNulty, K.A. Nugent, "Phase space density measurement of interfering X-rays," J. Electron. Spectrosc. 144, June, 947-951 (2005).

C.Q. Tran, A.G. Peele, A. Roberts, K.A. Nugent, D. Paterson, I. McNulty, "Synchrotron beam coherence: a spatially resolved measurement," Opt. Lett. 30 (2), January, 204-206 (2005).

Chanh Q. Tran, Andrew G. Peele, Ann Roberts, Keith A. Nugent, David Paterson, Ian McNulty, "X-ray imaging: a generalized approach using phase-space tomography," J. Opt. Soc. Am. A 22 (8), August, 1691-1700 (2005).

M.M.J. Treacy, J.M. Gibson, L. Fan, D.J. Paterson, I. McNulty, "Fluctuation microscopy: a probe of medium range order," Rep. Prog. Phys. 68, 2899-2944 (2005).

Oliver Tschauner, Jason McClure, Malcolm Nicol, "Strategies for reducing preferred orientation and strain in powder samples for high-pressure synchrotron X-ray diffraction in diamond-anvil cells," J. Synchrotron Rad. 12, 626-631 (2005).

J.S. Tse, D.D. Klug, M. Guthrie, C.A. Tulk, C.J. Benmore, J. Urquidi, "Investigation of the intermediate- and high-density forms of amorphous ice by molecular dynamics calculations and diffraction experiments," Phys. Rev. B 71 (21), June, 214107-1-214107-7 (2005).

S. Tse, D.D. Klug, J.Y. Zhao, W. Sturhahn, E.E. Alp, J. Baumert, C. Gutt, M.R. Johnson, W. Press, "Anharmonic motions of Kr in the clathrate hydrate," Nat. Mater. 4, December, 917-921 (2005).

Oleg V. Tsodikov, Jacquelin H. Enzlin, Orlando D. Scharer, Tom Ellenberger, "Crystal structure and DNA binding functions of ERCC1, a subunit of the DNA structure-specific endonuclease XPF-ERCC1," Proc. Natl. Acad. Sci. USA 102 (32), August, 11236-11241 (2005).

Stephen J. Turner, Katherine Kedzierska, Helen Komodromou, Nicole L. La Gruta, Michelle A. Dunstone, Andrew I. Webb, Richard Webby, Helen Walden, Wiedong Xie, James McCluskey, Anthony W. Purcell, Jamie Rossjohn, Peter C. Doherty, "Lack of prominent peptide-major histocompatibility complex features limits repertoire diversity in virus-specific CD8+ T cell populations," Nat. Immunol. 6 (4), April, 382-389 (2005).

Fleur E. Tynan, Natalie A. Borg, John J. Miles, Travis Beddoe, Diah El-Hassen, Sharon L. Silins, Wendy J.M. van Zuylen, Anthony W. Purcell, Lars Kjer-Nielsen, James McCluskey, Scott R. Burrows, Jamie Rossjohn, "The high resolution structures of highly bulged viral epitopes bound to the major histocompatability class I: Implications for T-cell receptor engagement and T-cell immunodominance," J. Biol. Chem. 280 (25), June, 23900-23909 (2005).

Fleur E. Tynan, Scott R. Burrows, Ashley M. Buckle, Craig S. Clements, Natalie A. Borg, John J. Miles, Travis Beddoe, James C. Whisstock, Matthew C. Wilce, Sharon L. Silins, Jacqueline M. Burrows, Lars Kjer-Nielsen, Lyudmila Kostenko, Anthony W. Purcell, James McCluskey, Jamie Rossjohn, "T cell receptor recognition of a 'super-bulged' major histocompatibility complex class I-bound peptide," Nat. Immunol. 6, September, 1114 -1122 (2005).

Fleur E. Tynan, Diah Elhassen, Anthony W. Purcell, Jacqueline M. Burrows, Natalie A. Borg, John J. Miles, Nicholas A. Williamson, Kate J. Green, Judy Tellam, Lars Kjer-Nielsen, James McCluskey, Jamie Rossjohn, Scott R. Burrows, "The immunogenicity of a viral cytotoxic T cell epitope is controlled by its MHC-bound conformation," J. Exp. Med. 202 (9), November, 1249-1260 (2005).

T. Uchida, Y. Wang, M.L. Rivers, S.R. Sutton, "Yield strength and strain hardening of MgO up to 8 GPa measured in the deformation-DIA with monochromatic X-ray diffraction," Earth Planet Sci. Lett. 226, 117-126 (2005).

I.A. Vartanyants, I.K. Robinson, J.D. Onken, M.A. Pfeifer, G.J. Williams, F. Pfeiffer, H. Metzger, G. Bauer, Z. Zhong, "Coherent x-ray diffraction from quantum dots," Phys. Rev. B 71, June, 245302-1-245302-9 (2005).

Nenad Velisavljevic, Yogesh K. Vohra, Samuel T. Weir, "Simultaneous electrical and X-ray diffraction studies on neodymium metal to 152 GPa," Int. J. High-Pres. Res. 25 (2), June, 137-144 (2005).

Sascha Vensky, Lorenz Kienle, Robert E. Dinnebier, Ahmad S. Masadeh, Simon J.L. Billinge, Martin Jansen, "The real structure of Na[subscript 3]BiO[subscript 4] by electron microscopy, HR-XRD and PDF," Z. Kristallogr. 220 , February, 231-244 (2005).

J. Vincent, L. Shan, M. Fan, J.S. Brunzelle, B.M. Forman, E.J. Fernandez, "Crystallographic Analysis of Murine Constitutive Androstane Receptor Ligand-Binding Domain Complexed with 5[alpha]-androst-16-en-3[alpha]-ol," Acta Crystallogr. F F61 (1), January, 156-159 (2005).

R.B. Von Dreele, "Binding of N-acetylglucosamine oligosaccharides to hen egg-white lysozyme: a powder diffraction study," Acta Crystallogr. D 61 (1), January, 22-32 (2005).

Paul B. Vordtriede, Chuong N. Doan, Jacqueline M. Tremblay, George M. Helmkamp, Jr., Marilyn D. Yoder, "Structure of PITP Beta in Complex with Phosphatidylcholine: Comparison of Structure and Lipid Transfer to Other PITP Isoforms," Biochemistry-US 44 (45), November, 14760-14771 (2005).

Ivan I. Vorontsov, Philip Coppens, "On the refinement of time-resolved diffraction data: comparison of the random-distribution and cluster-formation models and analysis of the light-induced increase in the atomic displacement parameters," J. Synchrotron Rad. 12, 488-493 (2005).

Ivan I. Vorontsov, Andrey Yu. Kovalevsky, Yu-Sheng Chen, Tim Graber, Milan Gembicky, Irina V. Novozhilova, Mohammad A. Omary, Philip Coppens, "Shedding Light on the Structure of a Photoinduced Transient Excimer by Time-Resolved Diffraction," Phys. Rev. Lett. 94, May, 193003-1-193003-4 (2005).

Dirk Wagner, Jörg Maser, Barry Lai, Zhonghou Cai, Clifton E. Barry III, Kerstin Höner zu Bentrup, David G. Russell, Luiz E. Bermudez, "Elemental Analysis of Mycobacterium avium-, Mycobacterium tuberculosis-, and Mycobacterium smegmatis-Containing Phagosomes Indicates Pathogen-Induced Microenvironments within the Host Cell's Endosomal System," J. Immunol. 174 (3), 1491-1500 (2005).

D. Wagner, J. Maser, I. Moric, N. Boechat, S. Vogt, B. Gicquel, B. Lai, J.-M. Reyrat, L. Bermudez, "Changes of the phagosomal elemental concentrations by Mycobacterium tuberculosis Mramp," Microbiology 151, January, 323-332 (2005).

Jeremiah R. Wagner, Joseph S. Brunzelle, Katrina T. Forest, Richard D. Vierstra, "A light-sensing knot revealed by the structure of the chromophore-binding domain of phytochrome," Nature 438 (17), November, 325-331 (2005).

S. Wakimoto, Young-June Kim, Hyunkyung Kim, H. Zhang, T. Gog, R.J. Birgeneau, "Resonant inelastic x-ray scattering study of overdoped La[subscript 2-x]Sr[subscript x]CuO[subscript 4]," Phys. Rev. B 72 (22), 224508-1-224508-7 (2005).

M. Walterfang, W. Keune, E. Schuster, A. T. Zayak, P. Entel, W. Sturhahn, T. S. Sturhahn, E.E. Alp, P. T. Jochym, K. Parlinski, "Atomic vibrational density of states of crystalline [beta]-FeSi[subscript 2] and amorphous FeSi[subscript 2] thin films," Phys. Rev. B 71, January, 035309-1-035309-9 (2005).

Cheng Wan, Wolfram Tempel, Zhi-Jie Liu, Bi-Cheng Wang, Robert B. Rose, "Structure of the Conserved Transcriptional Repressor Enhancer of Rudimentary Homolog," Biochemistry-US 44, 5017-5023 (2005).

Chenchen Wang, Miranda Gibson, Jurgen Rohr, Marcos A. Oliveira, "Crystallization and X-ray diffraction properties of Baeyer-Villiger monooxygenase MtmOIV from the mithramycin biosynthetic pathway in Streptomyces argillaceus," Acta Crystallogr. F 61, October, 1023-1026 (2005).

Jin Wang, "X-ray vision of fuel sprays," J. Synchrotron Rad. 12 (2), March, 197-207 (2005).

Yimin Wang, Mary C. Long, Senthil Ranganathan, Vincent Escuyer, William B. Parker, Rongbao Li, "Overexpression, purification and crystallographic analysis of a unique adenosine kinase from Mycobacterium tuberculosis," Acta Crystallogr. F 61, June, 553-557 (2005).

Y.-D. Wang, R.L. Peng, J. Almer, M. Oden, Y.-D. Liu, J.-N. Deng, C.-S. He, L. Chen, Q.-L. Li, L. Zuo, "Grain-to-grain stress interactions in an electrodeposited iron coating," Adv. Mater. 17, 1221-1226 (2005).

G.S. Was, M. Hash, R.G. Odette, "Hardening and microstructure evolution in proton-irradiated model and commercial pressure-vessel steels," Philos. Mag. 85 (4-7), February, 703-722 (2005).

Shirley J. Wasson, William P. Linak, Brian K. Gullett, Charles J. King, Abderrahmane Touati, Frank E. Huggins, Yuanzhi Chen, Naresh Shah, Gerald P. Huffman, "Emissions of Chromium, Copper, Arsenic, and PCDDs/Fs from Open Burning of CCA-Treated Wood," Environ. Sci. Technol. 39 (22), September, 8865-8876 (2005).

G.A. Waychunas, C.S. Kim, J.F. Banfield, "Nanoparticulate oxide minerals in soils and sediments: unique properties and contaminant scavenging mechanisms," J. Nanopart. Res. 7, 409-433 (2005).

G. Waychunas, T. Trainor, P. Eng, J. Catalano, G. Brown, J. Davis, J. Rogers, J. Bargar, "Surface complexion studied via combined grazing-incidence EXAFS and surface diffraction: arsenate on hematite (0001) and (10-12)," Anal. Bioanal. Chem. 383 (1), September, 12-27 (2005).

Andrew I. Webb, Michelle A. Dunstone, Nicholas A. Williamson, Jason D. Price, Andreade Kauwe, Weisan Chen, Aaron Oakley, Patrick Perlmutter, James McCluskey, Marie-Isabel Aguilar, Jamie Rossjohn, Anthony W. Purcell, "T Cell Determinants Incorporating [beta]-Amino Acid Residues Are Protease Resistant and Remain Immunogenic In Vivo," J. Immunol. 175, 3810-3818 (2005).

Andrzej Weichsel, Estelle M. Maes, John F. Andersen, Jesus G. Valenzuela, Tatjana Kh. Shokhireva, F.Ann Walker, William R. Montfort, "Heme-assisted S-nitrosation of a proximal thiolate in a nitric oxide transport protein," Proc. Natl. Acad. Sci. USA 102 (3), January, 594-599 (2005).

M. Weigl, M.A. Denecke, P.J. Panak, A. Geist, K. Gompper, "EXAFS and time-resolved laser fluorescence spectroscopy (TRLFS) investigations of the structure of Cm(III)/Eu(III) complexed with di(chlorophenyl)dithiophosphinic acid and different synergistic agents," Dalton T. 7, May, 1281-1286 (2005).

Hua Wei, Alexander J. Ruthenburg, Seth K. Bechis, Gregory L. Verdine, "Nucleotide-dependent Domain Movement in the ATPase Domain of a Human Type IIA DNA Topoisomerase," J. Biol. Chem. 280 (44), November, 37041-37047 (2005).

C. Weisener, A. Forsyth, P. Burns, D. Fowle, "Investigation of the geochemical relationships governing dissimilatory bacterial reduction of U(VI) from solid uranyl mineral phases," Geochim. Cosmochim. Acta 69 (10), A467-A467 (2005).

Christopher G. Weisener, K.Scott Sale, David J.A. Smyth, David W. Blowes, "Field Column Study Using Zerovalent Iron for Mercury Removal from Contaminated Groundwater," Environ. Sci. Technol. 39 (16), July, 6306-6312 (2005).

T. Richard Welberry, Darren J. Goossens, Aidan P. Heerdegen, Peter L. Lee, "Problems in measuring diffuse X-ray scattering," Z. Kristallogr. 220 (12), 1052-1058 (2005).

T.-C. Weng, G.S. Waldo, J.E. Penner-Hahn, "A method for normalization of X-ray absorption spectra," J. Synchrotron Rad. 12, 506-510 (2005).

H.-R. Wenk, G. Ischia, N. Nishiyama, Y. Wang, T. Uchida, "Texture development and deformation mechanisms in ringwoodite," Phys. Earth Planet. In. 152 (3), September, 191-199 (2005).

Ph. Wernet, D. Testemale, J.-L. Hazemann, R. Argoud, P. Glatzel, L.G.M. Pettersson, A. Nilsson, U. Bergmann, "Spectroscopic characterization of microscopic hydrogen-bonding disparities in supercritical water," J. Chem. Phys. 123 (15), October, 154503-1-154503-7 (2005).

C.M. Weyant, K.T. Faber, J.D. Almer, J.V. Guiheen, "Residual Stress and Microstructural Evolution in Tantalum Oxide Coatings on Silicon Nitride," J. Am. Ceram. Soc. 88 (8), August, 2169-2176 (2005).

D. Wildenschild, J.W. Hopmans, M.L. Rivers, A.J.R. Kent, "Quantitative Analysis of Flow Processes in a Sand Using Synchrotron-Based X-ray Microtomography," Vadose Zone J. 4, 112-126 (2005).

M.C. Wilding, M. Wilson, P.F. McMillan, "X-ray and neutron diffraction studies and MD simulation of atomic configurations in polyamorphic Y[subscript 2]O[subscript 3]-Al[subscript 2]O[subscript 3] systems," Phil. Trans. R. Soc. Lond. A 363 (1827), February, 589-607 (2005).

E.W. Wilker, R.A. Grant, S.C. Artim, M.B. Yaffe, "A Structural Basis for 14-3-3[sigma] Functional Specificity," J. Biol. Chem. 280 (19), May, 18891-18898 (2005).

Richard T. Wilkin, Chunming Su, Robert G. Ford, Cynthia J. Paul, "Chromium-Removal Processes during Groundwater Remediation by a Zerovalent Iron Permeable Reactive Barrier," Environ. Sci. Technol. 39 (12), 4599-4605 (2005).

Eduardo E Wolf, Francisco Gracia, Sichem Guerrero, A. Jeremy Kropf, Jeffrey Miller, "Kinetics, Operando FTIR,and Controlled Atmosphere EXAFS Study of the Effect of Sulfur on Pt Supported Catalysts during CO Oxidation," J. Catal. 233 (2), July, 372-387 (2005).

Christine S. Wright, Li-Zhi Mi, Sangderk Lee, Fraydoon Rastinejad, "Crystal Structure Analysis of Phosphatidylcholine-GM2-Activator Product Complexes: Evidence for Hydrolase Activity," Biochem. J. 44 (41), September, 13510-13521 (2005).

D. Wu, D.J. Keavney, R. Wu, E. Johnston-Halperin, D.D. Awschalom, J. Shi, "Concentration-independent local ferromagnetic Mn configuration in Ga(1-x)Mn(x)As," Phys. Rev. B 71, 153310-1-153310-4 (2005).

Jinhua Wu, Aloke K. Bera, Richard J. Kuhn, Janet L. Smith, "Structure of the Flavivirus Helicase: Implications for Catalytic Activity, Protein Interactions, and Proteolytic Processing," J. Virol. 79 (16), August, 10268-10277 (2005).

Ruiying Wu, Eric Patrick Skaar, Rongguang Zhang, Grazyna Joachimiak, Piotr Gornicki, Olaf Schneewind, Andrzej Joachimiak, "Staphylococcus aureus IsdG and IsdI, Heme-degrading Enzymes with Structural Similarity to Monooxygenases," J. Biol. Chem. 280 (4), January, 2840-2846 (2005).

Yunkun Wu, Jingzhi Li, Zhongmin Jin, Zhengqing Fu, Bingdong Sha, "The Crystal Structure of the C-terminal Fragment of Yeast Hsp40 Ydh1 Reveals Novel Dimerization Motif for Hsp40," J. Mol. Biol. 346, 1005-1011 (2005).

Ya-Ling Wu, Xiaojing Yang, Zhong Ren, Donald P. McDonnell, John D. Norris, Timothy M. Willson, Geoffrey L. Green, "Structural Basis for an Unexpected Mode of SERM-Mediated ER Antagonism," Mol. Cell 18 (4), May, 413-424 (2005).

Chuan Xiao, Carol M. Bator-Kelly, Elizabeth Rieder, Paul R. Chipman, Alister Craig, Richard J. Kuhn, Eckard Wimmer, Michael G. Rossmann, "The Crystal Structure of Coxsackievirus A21 and Its Interaction with ICAM-1," Structure 17 (7), July, 1019-1033 (2005).

Y. Xiao, Z. Cai, B. Lai, "Development of x-ray nanodiffraction instrumentation for studies of individual nano-objects," Nanotechnology 16 (9), September, 1754-1760 (2005).

Y. Xiao, Z. Cai, Z.L. Wang, B. Lai, Y.S. Chu, "An X-ray nanodiffraction technique for structural characterization of individual nanomaterials," J. Synchrotron Rad. 12 (2), February, 124-128 (2005).

Yuming Xiao, Hongxin Wang, Simon J. George, Matt C. Smith, Michael W.W. Adams, Francis E. Jenney, Jr., Wolfgang Sturhahn, Ercan E. Alp, Jiyong Zhao, Y. Yoda, Abishek Dey, Edward I. Solomon, Stephen P. Cramer, "Normal Mode Analysis of Pyrococcus furiosus Rubredoxin via Nuclear Resonance Vibrational Spectroscopy (NRVS) and Resonance Raman Spectroscopy," J. Am. Chem. Soc. 127 (42), October, 14596-14606 (2005).

Cao Xie, Adam Prahl, Bryan Ericksen, Zhibin Wu, Pengyun Zeng, Xiangqun Li, Wei-Yue Lu, Jacek Lubkowski, Wuyuan Lu, "Reconstruction of the Conserved [beta]-Bulge in Mammalian Defensins Using D-Amino Acids," J. Biol. Chem. 280 (38), August, 32921-32929 (2005).

Min Xu, Arockiasamy Arulandu, Douglas K. Struck, Stephanie Swanson, James C. Sacchettini, Ry Young, "Disulfide Isomerization After Membrane Release of Its SAR Domain Activates P1 Lysozyme," Science 307 (5706), January, 113-117 (2005).

Ting Xu, Naomi J. Logsdon, Mark R. Walter, "Structure of insect-cell-derived IL-22," Acta Crystallogr. D 61, June, 942-950 (2005).

Maneesh K. Yadav, Cory J. Gerdts, Ruslan Sanishvili, Ward W. Smith, L. Spencer Roach, Rustem F. Ismagilov, Peter Kuhn, Raymond C. Stevens, "In situ data collection and structure refinement from microcapillary protein crystallization," J. Appl. Crystallogr. 38 (6), December, 900-905 (2005).

Maneesh K. Yadav, James E. Redman, Luke J. Leman, Julietta M. Alvarez-Gutierrez, Yanming Zhang, C.David Stout, M.Reza Ghadiri, "Structure-Based Engineering of Internal Cavities in Coiled-Coil Peptides," Biochemistry-US 44 (28), June, 9723-9732 (2005).

Taro Yamada, Junichi Komoto, Kikuko Watanabe, Yoshihiro Ohmiya, Fusao Takusagawa, "Crystal Structure and Possible Catalytic Mechanism of Microsomal Prostaglandin E Synthase Type 2 (mPGES-2)," J. Mol. Biol. 348 (5), May, 1163-1176 (2005).

J.H. Yang, J.D. Henao, C. Costello, M.C. Kung, H.H. Kung, J.T. Miller, A.J. Kropf, J.R. Regalbuto, J.-G. Kim, M. Bore, H.N. Pham, A.K. Datye, J.D. Laeger, K. Kharas, "Understanding Preparation Variables in the Synthesis of Au/Al[subscript 2]O[subscript 3] using EXAFS and Electron Microscopy," Appl. Catal. A-Gen. 291 (1-2), September, 73-84 (2005).

J.H. Yang, J.D. Henao, M.C. Raphlulu, Y. Wang, T. Caputo, A.J. Groszek, M.C. Kung, M.S. Scurrell, J.T. Miller, H.H. Kung, "Activation of Au/TiO[subscript 2] for CO Oxidation," J. Phys. Chem. B 109 (20), 10319-10326 (2005).

Liuchun Yang, Reagan McRae, Maged M. Henary, Raxit Patel, Barry Lai, Stefan Vogt, Christoph J. Fahrni, "Imaging of the intracellular topography of copper with a fluorescent sensor and by synchrotron x-ray fluorescence microscopy," Proc. Natl. Acad. Sci. USA 102 (32), August, 11179-11184 (2005).

N. Yang, K.W. Dennis, R.W. McCallum, M.J. Kramer, Y. Zhang, P.L. Lee, "Spontaneous magnetostriction in R[subscript 2]Fe[subscript 14]B (R = Y, Nd, Gd, Tb, Er)," J. Magn. Magn. Mater. 295 (1), January, 65-76 (2005).

Junko Yano, Jan Kern, Klaus-Dieter Irrgang, Matthew J. Latimer, Uwe Bergmann, Pieter Glatzel, Yulia Pushkar, Jacek Biesiadka, Bernhard Loll, Kenneth Sauer, Johannes Messinger, Athina Zouni, Vittal K. Yachandra, "X-ray damage to the Mn[subscript 4]Ca complex in single crystals of photosystem II: A case study for metalloprotein crystallography," Proc. Natl. Acad. Sci. USA 102 (34), August, 12047-12052 (2005).

Junko Yano, Yulia Pushkar, Pieter Glatzel, Azul Lewis, Kenneth Sauer, Johannes Messinger, Uwe Bergmann, Vittal Yachandra, "High-Resolution Mn EXAFS of the Oxygen-Evolving Complex in Photosystem II: Structural Implications for the Mn[subscript 4]Ca Cluster," J. Am. Chem. Soc. 127 (43), 14974-14975 (2005).

W. Yao, S.W. Martin, V. Petkov, "Structure determination of low-alkali-content Na2S + B2S3 glasses using neutron and synchrotron x-ray diffraction," J. Non-Cryst. Solids 351 (24-26), August, 1995-2002 (2005).

Jun Ye, Ashoka Kandegedara, Philip Martin, Barry P. Rosen, "Crystal Structure of the Staphylococcus aureus pI258 CadC Cd(II)/Pb(II)/Zn(II)-Responsive Repressor," J. Bacteriol. 187 (12), June, 4214-4221 (2005).

Shixin Ye, Bohdana M. Discher, Joseph Strzalka, Ting Xu, Sophia P. Wu, Dror Noy, Ivan Kuzmenko, Thomas Gog, Michael J. Therien, P.Leslie Dutton, J. Kent, "Amphiphilic Four-Helix Bundle Peptides Designed for Light-Induced Electron Transfer Across a Soft Interface," Nano Lett. 5 (9), 1658-1667 (2005).

J.M. Yi, J.H. Je, Y.S. Chu, W.G. Cullen, H. You, "Novel X-ray diffraction microscopy technique for measuring textured grains of thin-films," Nucl. Instrum. Methods A 551 (1), October, 157-161 (2005).

Hsien-Sheng Yin, Reay G. Paterson, Xiaolin Wen, Robert A. Lamb, Theodore S. Jardetzky, "Structure of the uncleaved ectodomain of the paramyxovirus (hPIV3) fusion protein," Proc. Natl. Acad. Sci. USA 102 (26), June, 9288-9293 (2005).

Ada Yonath, "Antibiotics targeting ribosomes: resistance, selectivity, synergism, and cellular regulation," Annu. Rev. Biochem. 74, 649-679 (2005).

Ada Yonath, "Ribosomal Crystallography: Peptide Bond Formation, Chaperone Assistance and Antibiotics Activity," Mol. Cells 20 (1), 1-16 (2005).

C.S. Yoo, B. Maddox, J.-H.P. Klepeis, V. Iota, W. Evans, A. McMahan, M. Hu, P. Chow, M. Somayazulu, D. Häusermann, R.T. Scalettar, W.E. Pickett, "First-Order Isostructural Mott Transition in Highly Compressed MnO," Phys. Rev. Lett. 94 (8), March, 115502-1-115502-4 (2005).

Y.K. Yoo, Q. Xue, H.-C. Lee, S. Cheng, X.-D. Xiang, G.F. Dionne, S. Xu, J. He, Y.S. Chu, S.D. Preite, S.E. Lofland, I. Takeuchi, "Bulk synthesis and high-temperatue ferromagnetism of (In[subscript 1-x]Fe[subscript x])[subscript 2]O[subscript 3-sigma] with Cu do-doping," Appl. Phys. Lett. 86 (4), January, 042506-1-042506-3 (2005).

Ping Yuan, Thomas B. Thompson, Beth A. Wurzburg, Reay G. Paterson, Robert A. Lamb, Theodore S. Jardetzky, "Structural Studies of the Parainfluenza Virus 5 Hemagglutinin-Neuraminidase Tetramer in Complex with Its Receptor, Sialyllactose," Structure 13 (5), May, 803-815 (2005).

Yu-Ren Yuan, Yi Pei, Jin-Biao Ma, Vitaly Kuryavyi, Maria Zhadina, Gunter Meister, Hong-Ying Chen, Zbigniew Dauter, Thomas Tuschl, Dinshaw J. Patel, "Crystal Structure of A. aeolicus Argonaute, a Site-Specific DNA-Guided Endoribonuclease, Provides Insights into RISC-Mediated mRNA Cleavage," Mol. Cell 19, August, 405-419 (2005).

Bojan Zagrovic, Guha Jayachandran, Ian S. Millett, Sebastian Doniach, Vijay S. Pande, "How large is an [alpha]-helix? Studies of the radii of gyration of helical peptides by SAXS and MD," J. Mol. Biol. 353 (2), October, 232-241 (2005).

Bojan Zagrovic, Jan Lipfert, Eric J. Sorin, Ian S. Millett, Wilfred F. van Gunsteren, Sebastian Doniach, Vijay S. Pande, "Unusual compactness of a polyproline type II structure," Proc. Natl. Acad. Sci. USA 102 (33), August, 11698-11703 (2005).

Hong Zang, Angela K. Goodenough, Jeong-Yun Choi, Adriana Irimia, Lioudmila J. Loukachevitch, Ivan D. Kozekov, Karen C. Angel, Carmelo J. Rizzo, Martin Egli, F. Peter Guengerich, "DNA Adduct Bypass Polymerization by Sulfolobus solfataricus DNA Polymerase Dpo4," J. Biol. Chem. 280 (33), October, 29750-29764 (2005).

I. Zegkinoglou, J. Strempfer, C.S. Nelson, J.P. Hill, J. Chakhalian, C. Bernhard, J.C. Lang, G. Srajer, H. Fukazawa, S. Nakatsuji, Y. Maeno, B. Keimer, "Orbital Ordering Transition in Ca[subscript 2]RuO[subscript 4] Observed with Resonant X-Ray Diffraction," Phys. Rev. Lett. 95 (13), September, 136401-1-136401-4 (2005).

Weiqiao Zeng, Nathan J. Silvernail, David C. Wharton, Georgi Y. Georgiev, Bogdan M. Leu, W.Robert Scheidt, Jiyong Zhao, Wolfgang Sturhahn, E.Ercan Alp, J.Timothy Sage, "Direct Probe of Iron Vibrations Elucidates NO Activation of Heme Proteins," J. Am. Chem. Soc. 127 (32), 11200-11201 (2005).

Yujia Zhai, Fei Sun, Xuemei Li, Hai Pang, Xiaoling Xu, Mark Bartlam, Zihe Rao, "Insights into SARS-CoV transcription and replication from the structure of the nsp7-nsp8 hexadecamer," Nat. Struct. Mol. Biol. 12 (11), November, 980-986 (2005).

J. Zhang, Y. Zhao, C. Pantea, J. Qiana, L.L. Daemen, P.A. Rigg, R.S. Hixson, C.W. Greeff, G.T. Gray III, Y. Yang, L. Wang, Y. Wang, T. Uchida, "Experimental constraints on the phase diagram of elemental zirconium," J. Phys. Chem. Solids 66 (7), 1213-1219 (2005).

Jianzhong Zhang, Yusheng Zhao, Hongwu Xu, Matthew V. Zelinskas, Liping Wang, Yanbin Wang, Takeyuki Uchida, "Pressure-Induced Amorphization and Phase Transformations in [beta]-LiAlSiO[subscript 4]," Chem. Mater. 17 (11), April, 2817-2824 (2005).

Peng Zhang, Xingtai Zhou, Yuanhong Tang, TsunKong Sham, "Organosulfur-Functionalized Au, Pd, and Au-Pd Nanoparticles on 1D Silicon Nanowire Substrates: Preparation and XAFS Studies," Langmuir 21 (18), August, 8502-8508 (2005).

R. Zhang, T. Minh, L. Lezondra, S. Korolev, S.F. Moy, F. Collart, A. Joachimiak, "1.6 Å crystal structure of YteR protein from Bacillus subtilis, a predicted lyase," Proteins 60 (3), August, 561-565 (2005).

Xiaohui Zhang, Martin Chodakowski, John M. Shaw, "Impact of Multiphase Behavior on Coke Deposition in a Commercial Hydrotreating Catalyst under Sedimentation Conditions," Energ. Fuel 19 (4), March, 1405-1411 (2005).

Y. Zhang, K.L. Colabroy, T.P. Begley, S.E. Ealick, "Structural studies on 3-hydroxyanthranilate-3,4-dioxygenase: the catalytic mechanism of complex oxidation involved in NAD biosynthesis," Biochemistry-US 44 (21), May, 7632-7643 (2005).

Yang Zhang, Wen-Hu Wang, Shaw-Wen Wu, Steven E. Ealick, Ching C. Wang, "Identification of a Subversive Substrate of Trichomonas vaginalis Purine Nucleoside Phosphorylase and the Crystal Structure of the Enzyme-Substrate Complex," J. Biol. Chem. 280 (23), June, 22318-22325 (2005).

Y. Zhang, A.P. Wilkinson, P.L. Lee, S.D. Shastri, D. Shu, D.-Y. Chung, M.G Kanatzidis, "Determining metal ion distributions using resonant scattering at very high-energy K-edges: Bi/Pb in Pb[subscript 5]Bi[subscript 6]Se[subscript 14]," J. Appl. Crystallogr. 38, 433-441 (2005).

Bin Zhao, F. Peter Guengerich, Aouatef Bellamine, David C. Lamb, Miho Izumikawa, Li Lei, Larissa M. Podust, Munirathinam Sundaramoorthy, John A. Kalaitzis, L.Manmohan Reddy, Steven L. Kelly, Bradley S. Moore, Donald Stec, Markus Voehler, John R. Falck, Tsutomu Shimada, Michael R. Waterman, "Binding of Two Flaviolin Substrate Molecules, Oxidative Coupling, and Crystal Structure of Streptomyces coelicolor A3(2) Cytochrome P450 158A2," J. Biol. Chem. 280 (12), February, 11599-11607 (2005).

Bin Zhao, F. Peter Guengerich, Markus Voehler, Michael R. Waterman, "Role of Active Site Water Molecules and Substrate Hydroxyl Groups in Oxygen Activation by Cytochrome P450 158A2," J. Biol. Chem. 280 (51), December, 42188-42197 (2005).

Fang Zhao, Qiang Zhao, Kenneth F. Blount, Qing Han, Yitzhak Tor, Thomas Hermann, "Molecular Recognition of RNA by Neomycin and a Restricted Neomycin Derivative," Angew. Chem. Int. Ed. 44 (33), June, 5329-5334 (2005).

Yusheng Zhao, Jianzhong Zhang, Cristian Pantea, Jiang Qian, Luke L. Daemen, Paulo A. Rigg, Robert S. Hixson, George T. Gray III, Yunpeng Yang, Liping Wang, Yanbin Wang, Takeyuki Uchida, "Thermal equations of state of the [alpha], [beta], and [omega] phases of zirconium," Phys. Rev. B 71 (18), May, 184119-1-184119-6 (2005).

Bo Zheng, Cory J. Gerdts, Rustem F. Ismagilov, "Using nanoliter plugs in microfluidics to facilitate and understand protein crystallization," Curr. Opin. Struct. Biol. 15 (5), October, 548-555 (2005).

X.G. Zheng, T. Kawae, Y. Kashitani, C.S. Li, N. Tateiwa, K. Takeda, H. Yamada, C.N. Xu, Y. Ren, "Unconventional magnetic transitions in the mineral clinoatacamite Cu[subscript 2]Cl(OH)[subscript 3]," Phys. Rev. B 71, February, 052409-1-052409-4 (2005).

Y. Zhong, S. Krasnicki, A.T. Macrander, Y.S. Chu, J. Maj, "Bragg-case limited projection topography study of surface damage in diamond-crystal plates," J. Phys. D 38, May, A39-A43 (2005).

Wei Zhou, Paul A. Heiney, Hua Fan, Richard E. Smalley, John E. Fischer, "Single-Walled Carbon Nanotube-Templated Crystallization of H[subscript 2]SO[subscript 4]: Direct Evidence for Protonation," J. Am. Chem. Soc. 127 (6), January, 1640-1641 (2005).

X.T. Zhou, T.K. Sham, Y.Y. Shan, X.F. Duan, S.T. Lee, R.A. Rosenberg, "One-dimensional zigzag gallium nitride nanostructures," J. Appl. Phys. 97, May, 104315-1-104315-6 (2005).

Jianghai Zhu, John W. Burgner, Etti Harms, Boris R. Belitsky, Janet L. Smith, "A New Arrangement of ([beta}/[alpha])[subscript 8] Barrels in the Synthase Subunit of PLP Synthase," J. Biol. Chem. 280 (30), June, 27914-27923 (2005).

Xiaobing Zuo, David M. Tiede, "Resolving Conflicting Crystallographic and NMR Models for Solution-State DNA with Solution X-ray Diffraction," J. Am. Chem. Soc. 127 (1), January, 16-17 (2005).

E. Zussman, X. Chen, W. Ding, L. Calabri, D.A. Dikin, J.P. Quintana, R.S. Ruoff, "Mechanical and structural characterization of electrospun PAN-derived carbon nanofiber," Carbon 43 (10), August, 2175-2185 (2005).

Petr Šimůnek, Markéta Pešková, Valerio Bertolasi, Vladimír Machácek, Antonín Lycka, "Synthesis, NMR and X-ray characterisation of 6-substituted 4-amino-5-aryl-diazenyl-1-arylpyridazinium salts," Tetrahedron 61 (34), August, 8130-8137 (2005).

Experimental Results: Conference Papers

L. Assoufid, G.A. Mansoori, T.F. George, G. Zhang, "Diamondoids as molecular building blocks for nanotechnology," 2005 Ianano, Lloyd L. Tran, ed., CD Rom, IAnano, October (2005), CDROM.

D. Beak, N.T. Basta, K. Scheckel, S. Traina, "Bioaccessibility of As bound to Ferrihydrite," 230th ACS National Meeting, 230, American Chemical Society, June (2005), GEOC21.

T. Buonassisi, A.A. Istratov, M.A. Marcus, M. Heuer, M.D. Pickett, B. Lai, Z. Cai, S.M. Heald, E.R. Weber, "Local Measurements of Diffusion Length and Chemical Character of Metal Clusters in Multicrystalline Silicon," Solid State Phenomena, 108-109, Trans Tech Publications (2005), 577 - 584.

T. Buonassisi, A.A. Istratov, M.A. Marcus, S. Peters, C. Ballif, M. Heuer, T.F. Ciszek, A. Cai, B. Lai, R. Schindler, E.R. Weber, "Synchrotron-Based Investigations into Metallic Impurity Distribution and Defect Engineering in Multicrystalline Silicon Via Thermal Treatments," Proceedings of the 31st IEEE Photovoltaic Specialists Conference, IEEE, January (2005), 1027 - 1030.

Roy Clarke, Codrin Cionca, Catalina Dorin, Benny Perez Rodriguez, Joanna Mirecki Millunchick, Don A. Walko, Yizhak Yacoby, "Imaging and manipulating heterostructure interfaces," Nanotechnology II, Paolo Lugli, Laszlo B. Kish, and Javier Mateos, eds., 5838, SPIE, June (2005), 10 - 20.

J.F. Collingwood, A. Mikhaylova, M.R. Davidson, C. Batich, W.J. Streit, T. Eskin, J. Terry, R. Barrea, R.S. Underhill, J. Dobson, "High-resolution x-ray absorption spectroscopy studies of metal compounds in neurodegenerative brain tissue," Journal of Physics: Conference Series, 17, Institute of Physics Publishing (2005), 54 - 60.

J.S. Delaney, M.D. Dyar, M.E. Gunter, S.R. Sutton, "Broad spectrum characterization of returned samples: Orientation constraints of small samples on x-ray and other spectroscopies," Lunar and Planetary Science XXXVI, LPI, Lunar and Planetary Institute (2005), 1130.

D.S. Ebel, R.A. Fogel, M.L. Rivers, "Tomographic location of potential melt-bearing phenocrysts in lunar glass spherules," Lunar and Planetary Science XXXVI, LPI, Lunar and Plaetary Institute (2005), 1505.

Lixin Fan, Ian McNulty, David Paterson, Michael M.J. Treacy, J. Murray Gibson, "Fluctuation x-ray microscopy for measuring medium-range order," Mater. Res. Soc. Symp. Proc., S. R. Bhatia, P. G. Khalifah, D. Pochan, P. Radaelli, eds., 840, Q6.7, Marerials Research Society (2005), Q6.7.1 - Q6.7.6.

J.M. Friedrich, K.P. Jochum, D.S. Ebel, "First results of a physicochemical survey of CV3 calcium-aluminum-rich inclusions: The refractory trace elements," Lunar and Planetary Science XXXVI, LPI., Lunar and Planetary Institute (2005), 1985.

P. Glatzel, J. Yano, H. Visser, J.H. Robblee, K. Sauer, S.P. Cramer, U. Bergmann, V.K. Yachandra, "The Electronic Structure of the Mn4Ca Cluster," hotosynthesis: Fundamental Aspects to Global Perspectives, D. Bruce, A Van der Est, eds., 1, ACG Publishing (2005), 282 - 283.

Kyungmin Ham, Clinton S. Willson, "The Application of Monochromatic Energies to Investigate Multiphase Porous Media Systems using Synchrotron X-ray Tomography," Proceedings of the Geo-Frontiers 2005 Congress, Ellen M. Rathje, ed., 130-142, ASCE Press (2005), CD-ROM.

Kyoung-Su Im, K.-C. Lin, Ming-Chia Lai, "Spray atomization of liquid jet in supersonic cross flows," 43rd AIAA Aerospace Sciences Meeting and Exhibit - Meeting Papers, 732, American Institute of Aeronautics and Astronautics Inc. (2005), 13751 - 13759.

Y.H. Joeng, J.Y. Park, H.G. Kim, J.T. Busby, E. Gartner, M. Atzmon, G.S. Was, R.J. Comstock, Y.S. Chu, M. Gomes da Silva, A. Yilmazbayhan, A.T. Motta, "Corrosion of Zirconium-based Fuel Cladding Alloys in Supercritical Water," Environmental Degradation of Materials in Nuclear Systems XII, L. Nelson, P.J. King, T.R. Allen, CD-only, TMS (2005), 1369 - 1377.

R.L. Jones, C.L. Soles, E.K. Lin, W-L. Wu, W. Hu, R.M. Reano, S.W. Pang, S.J. Weigand, D.T. Keane, J.P. Quintana, "Pattern Fidelity in Nanoimprinted Films using CD-SAXS," Proceedings of the SPIE Mimcrolithography 2005, 5751, SPIE (2005), 415 - 422.

I.M. Kempson, J.A. Denman, W.M. Skinner, K.P. Kirkbride, "Applications of Synchrotron X-Ray Sources for Forensic Characterization of Glass," Australian Institute of Physics Congress Proceedings, Max Colla, eds., Australian Institute of Physics (2005), 147.

K.E. Lipinska-Kalita, M. Pravica, M. Nicol, "High-Pressure Synchtron Radiation X-Ray Diffraction Studies of Pentaerythritol Tetranitrate C(CH[subscript 2]ONO[subscript 2])[subscript 4]," Proceedings Joint 20th AIRAPT and 43rd EHPRG International Conference on High Pressure Science and Technology, E. Dingus, ed., Forschungszentrum Karlsruhe GmbH (2005), Paper O63.

Jinyuan Liu, Eric Landahl, Jin Wang, Zenghu Chang, "Single-pulse measurement of synchrotron radiation using an ultrafast x-ray streak camera," Proceedings of the SPIE-Ultrafast X-Ray Detectors, High-Speed Imaging, and Applications, Stuart Kleinfelder, Dennis L. Paisley, Zenghu Chang, Jean-Claude Kieffer, Jerome B. Hastings, eds., 5920, SPIE, September (2005), 1 - 5.

Xiangxin Liu, A.D. Compaan, J. Terry, "X-ray absorption fine structure study of aging behavior of oxidized copper in CdTe films," Conference Record of the Thirty-First IEEE Photovoltaic Specialist Conference, IEEE (2005), 267 - 270.

Darren A. Lytle, Michael R. Schock, "The Formation of Pb(IV) Oxides in Chlorinated Water," Proceedings of the American Water Works Association Water Quality Technology Conference, CD-Rom, American Water Works Association, November (2005), CD-Rom.

M.J. McKelvy, A.V. Chizmeshya, J. Diefenbacher, H. Bearat, R.W. Carpenter, G. Wolf, D. Gormley, "Developing Atomic-Level Understanding of the Mechanisms that Govern CO[subscript 2] Sequestration Mineral Carbonation Reaction Processes," EPD Congress 2005, TMS Extraction & Processing Division (EPD) (2005), 1133 - 1147.

M.J. McKelvy, J. Diefenbacher, A.V.G. Chizmeshya, G. Wolf, R. Marzke, H. Bearat, "Enhancing the observation of above and below ground carbon sequestration processes under in situ pressure and temperature conditions," Proceedings of the International Technical Conference on Coal Utilization & Fuel Systems 2005, Barbara Sakkestad, 1, Coal Technology Association (2005), 255 - 269.

N.N. Naik, A.C. Jupe, S.R. Stock, A.P. Wilkinson, P.L. Lee, K.E. Kurtis, "Sulfate resistance of cement-based materials: Influence of composition and exposure conditions," Proc. of the International Conf. on Advances in Concrete Composites and Structures, SERC, January (2005), 189 - 196.

Yuriy Platonov, Vladimir Martynov, Alexander Kazimirov, Barry Lai, "High spectral resolution Al[subscript 2]O[subscript 3]/B[subscript 4]C, SiC/Si, SiC/B[subscript 4]C and SiC/C multilayer structures for the photon energies of 6 keV to 19 keV," X-Ray Sources and Optics, Carolyn A. MacDonald, Albert T. Macrander, Tetsuya Ishikawa, Christian Morawe, James L. Wood, 5537, SPIE, January (2005), 161 - 170.

P.R. Pokkuluri, D.K. Hanson, P.D. Laible, S.L. Ginell, G. Johnson, M. Schiffer, "Structural descriptions of compensatory mutations that restore proton transfer pathways to the 212Ala-L213Ala mutant bacterial reaction center," Photosynthesis: Fundamental Aspects to Global Perspectives, A. van der Est, D. Bruce, Allen Press, Inc. (2005), 272 - 274.

M.G. Pravica, K. Lipinska-Kalita, Z. Quine, E. Romano, M.F. Nicol, "X-Ray Diffraction Study of Elemental Erbium to 65 GPa," Proceedings Joint 20th AIRAPT and 43rd EHPRG International Conference on High Pressure Science and Technology, E. Dingus, ed., Forschungszentrum Karlsruhe GmbH (2005), Paper 358.

M.N. Rao, S.R. Sutton, D.S. McKay, "Evaporative evolution of Martian brines based on halogens in nakhlites and MER samples," Lunar and Planetary Science XXXVI, LPI, Lunar and Planetary Institute (2005), 1148.

K. Righter, S.R. Sutton, M. Newville, L. Le, C.S. Schwandt, "Micro-XANES measurements on experimental spinels and the oxidation state of vanadium in coexisting spinel and silicate melt.," Lunar and Planetary Science XXXVI, LPI, Lunar and Planetary Institute (2005), 1140.

Michael R. Schock, Kirk G. Scheckel, Michael DeSantis, Tammie L. Gerke, "Mode of Occurrence, Treatment and Monitoring Significance of Tetravalent Lead," Proceedings of the American Water Works Association Water Quality Technology Conference, CD-Rom, American Water Works Association, November (2005), CD-Rom.

S.R. Sutton, M. Newville, "Vanadium K XANES of synthetic olivine: Valence determinations and crystal orientation effects," Lunar and Planetary Science XXXVI, LPI, Lunar and Planetary Institute (2005), 2133.

K.E. Thompson, C.S. Willson, C.D. White, S. Nyman, J. Bhattacharya, A.H. Reed, "Application of a New Grain-Based Reconstruction Algorithm to Microtomography Images for Quantitative Characterization and Flow Modeling," 2005 SPE Annual Technical Conference, Editorial Committee of SPE, SPE (2005), 95887-ms.

C.Q. Tran, C.T. Chantler, M.D.de Jonge, Z. Barnea, N. Rae, "The X-ray Extended Range Technique for High Accuracy Atomic Structure in Simple Systems-," AIP 16th Biennial Congress 2005. Proc., (CD Rom), 91, Australian Institute of Physics, February (2005), 1 - 3.

S. Vajda, R.E. Winans, J.W. Elam, B. Lee, M.J. Pellin, S.J. Riley, S. Seifert, G.Y. Tikhonov, "Studies of the Thermal Stability and Temperature Induced Growth of Supported Cluster-based Platinum and Gold Nanoparticles," ACS Division Fuel Chemistry, Joe Smith, eds., 50 (1), American Chemical Society (2005), 190 - 191.

E. Zolotoyabko, J.P. Quintana, D.J. Towner, B.W. Wessels, "Stroboscopic x-ray diffraction measurements of sub-ns domain dynamics in ferroelectric films," Intergration and Packaging Issues for High-Frequency Devices II, Yong S. Cho, Don Shiffler, Clive A. Randall, Harrie A.C. Tilmans, Takaaki Tsurumi, 833, Materials Research Society (2005), G5.2.

Experimental Results: Dissertations

J. Aitken, "The Application of Synchrotron Radiation to Bioinorganic Compounds," Ph.D., University of Sydney, 2005.

M. Arora, "The Spatial Distribution of Lead in Teeth as a Biomarker of Prenatal and Neonatal Lead Exposure," Ph.D., University of Sydney, 2005.

K. Branson, "Development and application of computer aided drug design methods," Ph.D., Melbourne University, 2005.

J.G. Catalano, "Molecular Scale Studies of Uranium Speciation in Contaminated Hanford, Washington Sediments and Related Model Systems," Ph.D., Stanford University, 2005.

Karena W. Chapman, "Cyanide-bridged molecular framework materials: negative thermal expansion and host-guest properties," Ph.D., University of Sydney, 2005.

Tom Chastek, "Kinetics of Ordering in Block Copolymer Solutions," Masters, University of Minnesota, 2005.

Codrin N. Cionca, "Imaging Interfaces in Epitaxial Heterostructures," Ph.D., Michigan University, 2005.

J.D. Crowley, "Supramolecular Chemistry: Molecular Recognition and Self Assembly Using Palladium and Platinum Molecular Clefts," Ph.D., The University of Chicago, 2005.

A.L. Dahl, "Comparison of direct and operational methods for probing metal bioavailability and speciation in aquatic systems," Ph.D., Northwestern University , 2005.

M.D. de Jonge, "High-Accuracy Measurements of the X-ray Mass Attenuation Coefficients of Molybdenumm and Tin: Testing Theories of Photoabsorption," Ph.D., University of Melbourne, 2005.

Elizabeth G. Duncan, "Arsenic speciation and bioavailability in Ironite®," Masters, University of Aberdeen, 2005.

M. Dunstone, "A Structural Investigation of Human Serum Proteins," Ph.D., University of Melbourne, 2005.

B. Finnigan, "The structure and properties of thermoplastic polyurethane nanocomposites," Ph.D., University of Queensland; Australia, 2005.

D.M. Goodner, "Atomic-Scale Surface Studies of Alkaline-Earth Metals on Si(001)," Ph.D., Northwestern University, 2005.

Jeffery E. Habel, "Simulation Expansion and Structural Realization of the 1985 Sulfur-SAS Phasing Insight," Ph.D., University of Georgia, 2005.

Franklin A. Hays, P. Shing Ho, "Sequence Dependent Conformational Variations in DNA Holliday Junctions," Ph.D., Oregon State University, 2005.

K. Hope, "Crystallographic phases and anisotropic compressibility in light actinide metals at high pressures," Ph.D., University of Alabama, Birmingham, 2005.

Peter S. Horanyi, "Not a toxin but a regulator: Structure guided conclusions," Ph.D., University of Georgia, 2005.

Lei Huang, "Cloning, Expression, Purification and Crystallization of Pf-1806301," Ph.D., University of Georgia, 2005.

Gaurav Jain, "Investigation of Nanostructured Iron and Manganese Oxides as Novel Intercalation Hosts for Lithium," Ph.D., Rutgers, The State University of New Jersey, 2005.

Sumeet Jain, "Aqeous Mixtures of Block Copolymer Surfactants," Ph.D., University of Minnesota, 2005.

Y.-S. Jun, "Microscopic mechanisms of dissolution and precipitation of manganese mineralse?," Ph.D., Harvard University , 2005.

Jong Woo Kim, "Investigations of the RNi[subscript 2]Ge[subscript 2] intermetallic compounds by X-ray resonant magnetic," Ph.D., Iowa State University, 2005.

Pil-Sook Grace Kim, "X- Ray Absorption Spectroscopy and X-ray Excited Optical Luminescence Studies of Various Light Emitting Materials," Ph.D., University of Western Ontario, 2005.

Dmitry A. Kondrashov, "Protein control of a ligand: modeling," Ph.D., University of Arizona, 2005.

Bryan William Lepore, "Structural studies of several pyridoxal-5'-phosphate dependent enzymes via crystallography," Ph.D., Brandeis University, 2005.

Joseph A. Libera, "X-ray structural analysis of in situ polynucleotide surface adsorption and metal-phosphonate multilayer film self-assembly," Ph.D., Northwestern University, 2005.

R.L. Lieberman, "Biophysical and structural characterization of particulate methane monooxygenase from Methylococcus capsulatus (Bath)," Ph.D., Northwestern University, 2005.

Chieh-Tsung Lo, "Nanoscale Interfacial Crystallization Effects on Semicrystalline Polymer Adhesion," Ph.D., Iowa State University, 2005.

W. Mao, "Geophysics and geochemistry of iron in the earth's core," Ph.D., The University of Chicago, 2005.

J. McCourt, "Nanoporous Molecular Framework Materials: Host-Guest Properties, Spin Crossover and Magnetism," Ph.D., University of Sydney, 2005.

George Nicola, "X-ray crystal structure of pencillin-binding protein 5 of E.coli: implications for catalytic mechanism and rational drug design," Masters, Medical University of South Carolina, 2005.

Guirong Pan, "Morphology and Properties of Anti-Corrosion Organosilane Films," Ph.D., University of Cincinnati, 2005.

J. Pehl, "Texture analysis with TOF neutron diffraction and synchrotron X-rays and data analysis with the Rietveld method," Ph.D., University of California, Berkeley, 2005.

W. Qiu, "High-pressure high-temperature studies on Fe-Pt-Ag nanoparticles using carbon-13 pressure sensor," Ph.D., University of Alabama, 2005.

M. Schramm, "Scaffold Diversity in Small-Molecule Libraries and the Chemistry of Siloxy Alkynes," Ph.D., The University of Chicago, 2005.

Nilda M. Juan Serrano, "Imaging Therapeutic Proteins in Gelatin for Controlled Drug Release Using Microcomuted Tomography," Ph.D., University of Illinois at Urbana-Champaign, 2005.

J. Stark, "The Glass Transition in Thin Supported Polystyrene Films," Masters, Northern Illinois University, 2005.

N. Velisavljevic, "Development of the designer diamond anvils and study of structural and electrical properties of f-electron metals at ultra-high pressures," Ph.D., University of Alabama, Brimingham, 2005.

Joline R. Widmeyer, "The Effects of Food Quality and Abiotic Habitat Parameters on Metal Uptake in the Blue Mussel, Mytilus Trossulus," Ph.D., Simon Fraser University, 2005.

Kristine R. Witkowski, "Determination of Local Atomic Arrangements in a Bulk-Immiscible Surface Alloy," Ph.D., Northwestern University, 2005.

Yan Zhang, "X-Ray Crystallographic Structural Studies of Four Enzymes in the Purine and Pyrimidine Salvage Pathways," Ph.D., Cornell University, 2005.

Yang Zhang, "X-ray Crystallographic and Mechanistic Studies of Three Enzymes," Ph.D., Cornell University, 2005.

Dazhi Zheng, "Study of pore morphology and anisotropic evolution with thermal excursion of UHMWPE film," Masters, University of Cincinnati, 2005.

Experimental Results: Books

J.F. Lin, W. Sturhahn, J. Zhao, G. Shen, H.-k. Mao, R.J. Hemley, *Nuclear resonant x-ray scattering and synchrotron Mössbauer spectroscopy with laser-heated diamond anvil cells*, J. Chen, Larissa F. Dobrzhinetskaya, Thomas S. Duffy,Guoyin Shen,Yanbin Wang, eds.,Elsevier Science Ltd., 2005, 0444519793.

Experimental Results: Book Chapters

B. Li, J. Kung, T. Uchida, Y. Wang, "Simultaneous equation of state, pressure calibration, and sound velocity measurements to lower mantle pressures using multi-anvil apparatus," *Advances in High-Pressure Technology for Geophysical Applications*, J. Chen, Y. Wang, T. Duffy, G. Shen, L. Dobrzhinetskaya, eds., Elsevier Academic Press, 2005, 49 - 66.

M.J. McKelvy, A.V.G. Chizmeshya, J. Diefenbacher, H. Nearat, R.W. Carpenter, G. Wolf, D. Gormley, "Developing an Atomic-Level Understanding of the Mechanisms that Govern CO[subscript 2] Sequestration Mineral Carbonation Reaction Processes," *EPD Congress 2005*, Mark Schlesinger, ed., TMS Extraction & Processing Division of EPD, The Minerals, Metals & Materials Society., 2005, 1133 - 1147.

M. Schmidt, H. Ihee, R. Pahl, V. Srajer, "Protein-ligand interactions probed by time-resolved crystallography," *Protein-Ligand Interactions: Methods and Protocols*, U. Nienhaus, eds., Humana Press, 2005, 115 - 154.

D. Shim, "Stability of MgSio[subscript 3] Perovskite in the Lower Mantle," *Geophysical Monograph Series - Earth's Deep Mantle: Structure, Composition, and Evolution*, Rob D. van der Hilst, Jay Bass, Jan Matas, Jeannot Trampert, eds., AGU, 2005, 263 - 284.

Harold C. Smith, Joseph E. Wedekind, Kefang Xie, Mark P. Sowden, "Mammalian C to U Editing," *Topics in Current Genetics: Fine-Tuning of RNA Functions by Modification and Editing*, H. Grosjean, eds., Springer-Verlag GmbH, 2005, 1610 - 2096.

Yang Song, Russell J. Hemley, Ho-kwang Mao, Dudley R. Herschbach, "Nitrogen-containing molecular systems at high pressures and temperature," *Chemistry at Extreme Conditions*, M.R. Manaa, ed., Elsevier, 2005, 189 - 222.

G.B. Stephenson, S.K. Streiffer, D.D. Fong, M.V. Ramana Murty, O. Auciello, P. Fuoss, J.A. Eastman, A. Munkholm, C. Thompson, "In-situ synchrotron x-ray studies of processing and physics of ferroelectric thin films," *Polar Oxides : Properties, Characterization and Imaging*, R. Waiser, et al., eds., John Wiley and Sons, 2005, 121 - 131.

W. Sturhahn, "Nuclear resonant scattering," *Encyclopedia of Condensed Matter Physics*, F. Bassani, G. L. Liedl, P. Wyder, eds., Elsevier, Academic Press, 2005, 227 - 234.

T. Uchida, Y. Wang, M. Rivers, S. Sutton, "Stress and strain measurements of polycrystalline materials under controlled deformation using monochromatic synchrotron radiation," *Advances in High-Pressure Technology for Geophysical Applications*, J. Chen, Y. Wang, T. Duffy, G. Shen, L. Dobrzhinetskaya, eds., Elsevier Academic Press, 2005, 137 - 165.

D. A. Walko, "Multicircle Diffractometry Methods," *Encyclopedia of Condensed-Matter Physics*, G. Bassani, Gerald Liedl, and Peter Wyder, eds., Academic Press, 2005, 32 - 41.

Y. Wang, T. Uchida, N. Nishiyama, R. Von Dreele, A. Nozawa, K. Funakoshi, H. Kaneko, "High-Pressure Angle-Dispersive Powder Diffraction Using an Energy-Dispersive Setup and White Synchrotron Radiation," *Advances in High-Pressure Technology for Geophysical Applications*, J. Chen, Y. Wang, T. Duffy, G. Shen, L. Dobrzhinetskaya, eds., Elsevier Academic Press, 2005, 339 - 352.

D.J. Weidner, L. Ji, W. Durham, J. Chen, "High-temperature plasticity measurements using synchrotron X-rays," *Advances in High-Pressure Technology for Geophysical Applications*, J. Chen, Y. WAng, T. Duffy, G. Shen, L. Dobrzhinetskaya, eds., Elsevier Academic Press, 2005, 123 - 135.

T. Xu, M.J. Misner, S. Kim, J.D. Sievert, O. Gang, B. Ocko, T.P. Russell, "Selective Solvent Induced Reversible Surface Reconstruction of Diblock Copolymer Thin Films," *New Polymeric Materials*, L. S. Korugic-Karasz, W. J. MacKnight and E. Martuscelli, eds., American Chemical Society, ACS Symposium Series, No. 916, 2005, 158 - 170.

Choong-Shik Yoo, "High Pressure Materials Research: Novel Extended Phases of Molecular Triatomics," *Chemistry at Extreme Conditions*, M.R. Manaa, ed., Elsevier, 2005, 165 - 188.

Experimental Results: Technical Reports

Kyoung-Su Im, K.-C. Lin, Ming-Chia Lai, "Spray atomization of liquid jet in supersonic cross flows," 43rd AIAA Aerospace Sciences Meeting and Exhibit - Meeting Papers, 732, American Institute of Aeronautics and Astronautics Inc. (2005), 13751 - 13759.

E.R. Weber, "Efficiency Improvement of Crystalline Solar Cells: Final Subcontract," NREL/SR-520-37578, (February -2005).

Beamline & Accelerator: Journal Articles

M. Borland, "Simulation and Analysis of using Deflecting Cavities to Produce Short X-ray Pulses with the Advanced Photon Source," Phys. Rev. Spec. Top., Accel. Beams 8 (7), July, 074001 (2005).

Daniel P. Core, Stephen E. Kesler, Eric J. Essene, Eric B. Dufresne, Roy Clarke, Dohn A. Arms, Don Walko, Mark L. Rivers, "Copper and zinc in silicate and oxide minerals in igneous rocks from the Bingham-Park City belt, Utah: synchrotron x-ray fluorescence data," Can. Mineral. 43, 1781-1796 (2005).

A.K. Gangopadhyay, G.W. Lee, K.F. Kelto, J.R. Rogers, A.I. Goldman, D.S. Robinson, T.J. Rathz, R.W. Hyers, "Beamline electrostatic levitator for in situ high energy x-ray diffraction studies of levitated solids and liquids," Rev. Sci. Instrum. 76, 073901-1-073901-6 (2005).

Milan Gembicky, Dan Oss, Ryan Fuchs, Philip Coppens, "A fast mechanical shutter for submicrosecond time-resolved synchrotron experiments," J. Synchrotron Rad. 12, June, 665-669 (2005).

W. Guo, K. Harkay, M. Borland, "Closed Orbit Change Induced by Nonzero Dispersion RF Cavities," Phys. Rev. E 72, November, 056501 (2005).H.C. Kang, G.B. Stephenson, C. Liu, R. Conley, A.T. Macrander, J. Maser, S. Bajt, H.N. Chapman, "High-efficiency diffractive x-ray optics from sectioned multilayers," Appl. Phys. Lett. 86, 151109-1-151109-3 (2005).

Man-Ho Kim, Charles J. Glinka, Robert N. Carter, "In situ vapor sorption apparatus for small-angle neutron scattering and its application," Rev. Sci. Instrum. 76 (11), November, 113904-1-113904-10 (2005).

Suk Hong Kim, "A scaling law for the magnetic fields of superconducting undulators," Nucl. Instrum. Methods A 546 (3), July, 604-619 (2005).

Wenjun Liu, Gene E. Ice, Jonathan Z. Tischler, Ali Khounsary, Chian Liu, Lahsen Assoufid, Albert T. Macrander, "Short focal length Kirkpatrick-Baez mirrors for a hard x-ray nanoprobe," Rev. Sci. Instrum. 76 (11), November, 113701-1-13701-6 (2005).

J.A. Maj, A.T. Macrander, G.J. Waldschmidt, S.F. Krasnicki, Y. Zhong, R. Khachatryan, Y.S. Chu, E. Erck, J. Woodward, "Etching methods for improving surface imperfections of diamonds used for x-ray monochromators," Adv. X Ray Anal. 48 (176), 176-182 (2005).

T. Mizuno, T. Kamae, J.S.T. Nga, H. Tajima, J.W. Mitchell, R. Streitmatter, R.C. Fernholz, E. Groth, Y. Fukazawa, "Beam test of a prototype detector array for the PoGO astronomical hard X-ray/soft gamma-ray polarimeter," Nucl. Instrum. Methods A 540 (1), March, 158-168 (2005).

C.G. Ryana, B.E. Etschmann, S. Vogt, J. Maser, C.L. Harland, E. van Achterbergh, D. Legnini, "Nuclear microprobe - synchrotron synergy: Towards integrated quantitative real-time elemental imaging using PIXE and SXRF," Nucl. Instrum. Methods B 231, April, 183-188 (2005).

G.K. Shenoy, J.W. Lewellen, Deming Shu, N.A. Vinokurov, "Variable-period undulators as synchrotron radiation sources. Erratum," J. Synchrotron Rad. 12 (4), June, 542 (2005).

Gopal Shenoy, P. James Viccaro, "Applications of synchrotron radiation to materials research," J. Synchrotron Rad. 12 (2), March, 123 (2005).

E. Trakhtenberg, V. Tcheskidov, I. Vasserman, N. Vinokurov, M. Erdmann, J. Pfluger, "Undulator for the LCLS Project - from the prototype to the full-scale manufacturing," Nucl. Instrum. Methods A 543, 42-46 (2005).

Y. Wang, T. Uchida, F. Westferro, M.L. Rivers, J. Gebhardt, C.E. Lesher, S.R. Sutton, "High-Pressure X-ray Tomography Microscope: Synchrotron Computed Microtomography at High Pressure and Temperature," Rev. Sci. Instrum. 76, 073709-1-073709-7 (2005).

Beamline & Accelerator: Conference Papers

L. Assoufid, A. Rommeveaux, H. Ohashi, K. Yamauchi, H. Mimura, J. Qian, O. Hignette, T. Ishikawa, C. Morawe, A.T. Macrander, A. Khounsary, S. Goto, "Results of x-ray round-robin metrology measurements at the APS, ESRF, and SP-ring-8 optical metrology laboratories," Advances in Metrology for x-ray and EUV optics, L. Assoufid, P. Takacs, J. Taylor, 5921, SPIE, August (2005), 129 - 140.

J.L. Bailey, B.X. Yang, T.W. Buffington, "A Wire Scanner Design for Electron Beam Profile Measurement in the Linac Coherent Light Source Undulator," Proceedings of the 2005 Particle Accelerator Conference, IEEE (2005), 3667.

M. Borland, "elegantRingAnalysis: An Interface for High-Throughput Analysis of Storage Ring Lattices Using elegant," Proceedings of the 2005 Particle Accelerator Conference, IEEE (2005), 4200.

M. Borland, L. Emery, "Touschek Lifetime and Undulator Damage in the Advanced Photon Source," Proceedings of the 2005 Particle Accelerator Conference, IEEE (2005), 3835.

M. Borland, V. Sajaev, "Simulations of X-ray Slicing and Compression Using Crab Cavities in the Advanced Photon Source," Proceedings of the 2005 Particle Accelerator Conference, IEEE (2005), 3886.

G. Chen, J.A. Johnson, R. Webber, S. Schweizer, D. MacFarlane, J. Woodford, F. De Carlo, "ZBLAN-based X-ray storage phosphors and scintillators for digital X-ray imaging," Progress in Biomedical Optics and Imaging - Proceedings of SPIE, M. J. Flynn, eds., 5745, n II, SPIE (2005), 1351 - 1358.

Roger Dejus, "On the issue of phasing of undulators at the Advanced Photon Source," Proceedings of the 2005 Particle Accelerator Conference, C. Horak, eds., IEEE (2005), 764 - 766.

G. Decker, N. Sereno, "Transient Generation of Short Pulses in the APS Storage Ring," Proceedings of the 2005 Particle Accelerator Conference, IEEE (2005), 3247.

C. Doose, S.H. Kim, R.L. Kustom, E.R. Moog, I.B. Vasserman, "R&D of short-period superconducting undulators for the APS," Proceedings of the 2005 Particle Accelerator Conference, IEEE (2005), 2419 - 2421.

L. Emery, "Coupling Correction of a Circularly Polarizing Undulator at the Advanced Photon Source," Proceedings of the 2005 Particle Accelerator Conference, IEEE (2005), 805.

L. Emery, "Optimization and Modeling Studies for Obtaining High Injection Efficiency at the Advanced Photon Source," Proceedings of the 2005 Particle Accelerator Conference, IEEE (2005), 871.

L. Emery, "Global Optimization of Damping Ring Designs Using a Multi-Objective Evolutionary Algorithm," Proceedings of the 2005 Particle Accelerator Conference, IEEE (2005), 2962.

W. Guo, K. Harkay, B. Yang, M. Borland, V. Sajaev, "Generating Picosecond X-ray Pulses with Beam Manipulation in Synchrotron Light Sources," Proceedings of the 2005 Particle Accelerator Conference, IEEE (2005), 3898.

Ulf Griesmann, Nadia Machkour-Deshayes, Johannes Soons, Byoung Chang Kim, Quandou Wang, John R. Stoup, Lahsen Assoufid, "Uncertainties in Aspheric Profile Measurements with the Geometry Measuring Machine at NIST," Advanced Characterization Techniques for Optics, Semiconductors, and Nanotechnologies II, A. Duparree, B. Singh, Z. Gu, eds., 5878, SPIE, August (2005), 112 - 124.

J.H. Grimmer, R.T. Kmak, "Parametric Mechanical Design of New Insertion Devices at the APS," Proceedings of the 2005 Particle Accelerator Conference, IEEE (2005), 889 - 891.

K. Harkay, M. Borland, Y.-C. Chae, G. Decker, R. Dejus, L. Emery, W. Guo, D. Horan, K.-J. Kim, R. Kustom, Y. Li, D. Mills, S. Milton, G. Pile, V. Sajaev, S. Shastri, G. Waldschmidt, M. White, B. Yang, A. Zholents, "Generation of Short X-ray Pulses Using Crab Cavities at the Advanced Photon Source," Proceedings of the 2005 Particle Accelerator Conference, IEEE (2005), 668.

A. Hillman, S. Pasky, N. Sereno, R. Soliday, J. Wang, "Injector Power Supplies Reliability Improvements at the Advanced Photon Source," Proceedings of the 2005 Particle Accelerator Conference, IEEE (2005), 3804.

M. Jaski, P. Job, J. Humbert, "Radiation Damage to Magnet Water Hoses at the APS," Proceedings of MEDSI2004, ESRF (2005).

Suk Hong Kim, Chuck Doose, "Magnetic field analysis of a planar superconducting undulators with variable-field polarization," Proceedings of the 2005 Particle Accelerator Conference, C. Horak, eds., IEEE, May (2005), 2410 - 2412.

S.H. Kim, C. Doose, R.L. Kustom, E.R. Moog, K.M. Thompson, "Design and development of a short-period superconducting undulator at the APS," IEEE Transactions on Applied Superconductivity, 15, 2, Part 2, IEEE, June (2005), 1240 - 1243.

Suk Hong Kim, Chuck Doose, Robert L. Kustom, Elizabeth R. Moog, Isaac Vasserman, "R&D of short-period NbTi and Nb[subscript 3]Sn superconducting undulators for the APS," Proceedings of the 2005 Particle Accelerator Conference, C. Horak, ed., IEEE Cat # 05CH37623, IEEE Operations Center, May (2005), 2419 - 2421.

R. Lill, A. Pietryla, E. Norum, F. Lenkszus, "Design of the APS RF BPM Data Acquisition Upgrade," Proceedings of the 2005 Particle Accelerator Conference, IEEE (2005), 4156. S. Sasaki, "The possibility for a short-period hybrid staggered undulator," Proceedings of the 2005 Particle Accelerator Conference, IEEE (2005), 982 - 984.

A.H. Lumpkin, W.J. Berg, M. Borland, N.S. Sereno, "Initial Measurements of CSR from a Bunch-Compressed Beam at APS," Proceedings of the 27th International Free Electron Laser Conference, SLAC (2005), 608 - 611.

A.H. Lumpkin, W.J. Berg, N.S. Sereno, D.W. Rule, B.X. Yang, C.Y. Yao, "Nonintercepting Electron Beam Diagnostics Based on Optical Diffraction Radiation for X-Ray FELs," Proceedings of the 27th International Free Electron Laser Conference, SLAC (2005), 604 - 607.

A.H. Lumpkin, W.J. Berg, N.S. Sereno, C.Y. Yao, "Initial Imaging of 7-GeV Electron Beams with OTR/ODR Techniques at APS," Proceedings of the 2005 Particle Accelerator Conference, IEEE (2005), 4162.

A.H. Lumpkin, F. Sakamoto, B.X. Yang, "Dual-Sweep Streak Camera Measurements of the APS User Beams," Proceedings of the 2005 Particle Accelerator Conference, IEEE (2005), 4185.

L.H. Morrison, W. Berg, S. Sharma, K. Harkay, C. Putnam, M. Givens, "Performance of the Upgraded Storage Ring Injection Area at the Advanced Photon Source (APS)," Proceedings of MEDSI2004, ESRF (2005), *.

V. Sajaev, L. Emery, "Dynamic Aperture Study and Lifetime Improvement at the Advanced Photon Source," Proceedings of the 2005 Particle Accelerator Conference, IEEE (2005), 3632.

S. Sasaki, M. Petra, I. Vasserman, C. Doose, E. Moog, N.V. Mokhov, "Radiation damage to Advanced Photon Source undulators," Proceedings of the 2005 Particle Accelerator Conference, IEEE (2005), 4126 - 4128.

G.K. Shenoy, "Emerging areas of scientific research using ultra-short pulse x-ray sources," Fourth Generation X-Ray Sources and Optics III, Roman O. Tatchyn, Sandra G. Biedron, Wolfgang Eberhardt, eds., 5917, SPIE, August (2005), 55 - 68.

S. Sasaki, M. Petra, I. Vasserman, C. Doose, E. Moog, N.V. Mokhov, "Radiation damage to Advanced Photon Source undulators," Proceedings of the 2005 Particle Accelerator Conference, IEEE (2005), 4126 - 4128.

D. Shu, J. Maser, M. Holt, B. Lai, S. Vogt, Y. Wang, C. Preissner, Y. Han, B. Tieman, R. Winarski, A. Smolyanitskiy, G.B. Stephenson, "Design and Test of a Differential Scanning Stage System for an X-ray Nanoprobe Instrument," Photo-Optical Instrumentation Engineers, 5877, SPIE Optomechanics 2005 (2005), E1 - E13.

V.E. Scarpine, C.W. Lindenmeyer, G.R. Tassotto, A.H. Lumpkin, "Development of an optical transition radiation detector for profile monitoring of antiproton and proton beams at FNAL," Proceedings of the 2005 Particle Accelerator Conference, IEEE (2005), 2381.

D. Shu, J. Maser, B. Lai, S. Vogt, Y. Han, B. Tieman, R. Winarski, C. Roehrig, A. Smolyanitskiy, G.B. Stephenson, "Design of a scanning stage system with nanometer resolution for a x-ray nanoprobe instrument," ASPE 2004 Annual Meeting, 34, American Society for Precision Engineering (2005), 68 - 71.

H. Shang, M. Borland, "A Parallel Simplex Optimizer and its Application to High-Brightness Storage Ring Design," Proceedings of the 2005 Particle Accelerator Conference, IEEE (2005), 4230.

H. Shang, M. Borland, C.Y. Yao, W. Guo, "ExperimentDesigner: A Tcl/Tk Interface for Creating Experiments in EPICS," Proceedings of the 2005 Particle Accelerator Conference, IEEE (2005), 4245.

S. Sharma, B.X. Yang, A. Barcikowski, B. Rusthoven, E. Rotela, "Mechanical Design of the Pinhole Imaging System in the APS Storage Ring," Proceedings of MEDSI2004, ESRF (2005), *.

O. Singh, G. Decker, "Beam Stability at the Advanced Photon Source," Proceedings of the 2005 Particle Accelerator Conference, IEEE (2005), 3268.

Alex Smolyanitskiy, Deming Shu, Thomas Wong, "A DSP-based controller for a linear actuator system with sub-angstrom resolution and 15-millimeter travel range," Proceedings of SPIE - Optomechanics 2005, Alson E. Hatheway, eds., 5877, SPIE, August (2005), 1 - 11.

R. Soliday, "A Tcl/Tk Widget for Display of MEDM Screens," Proceedings of the 2005 Particle Accelerator Conference, IEEE (2005), 3393.

Lee Soon-Hong, Isaac Vasserman, Shigemi Sasaki, Dean Walters, "Magnetic properties of undulator vacuum chamber materials for the linac coherent light source," Proceedings of the 27th International Free Electron Laser Conference, Stanford, August (2005), 383 - 386.

E. Trakhtenberg, J. Collins, P. Den Hartog, M. White, "Design of a Precision Positioning System for the Undulators of the Linac Coherent Light Source," Proceedings of the 2005 Particle Accelerator Conference, IEEE (2005), 4099 - 4101.

E. Trakhtenberg, M. Erdmann, "Undulator for the LCLS Project -Changes in the Magnet Structure Design," Proceedings of the 2005 Particle Accelerator Conference, IEEE (2005), 4075 - 4077.

A. Xiao, L. Emery, "Characterization of a 6-km Damping Ring for the International Linear Collider," Proceedings of the 2005 Particle Accelerator Conference, IEEE (2005), 3147.

J.Z. Xu, I. Vasserman, "A New Magnetic Field Integral Measurement System," Proceedings of the 2005 Particle Accelerator Conference, IEEE (2005), 1808.

B.X. Yang, "High-resolution Undulator Measurements Using Angle-Integrated Spontaneous Radiation," Proceedings of the 2005 Particle Accelerator Conference, IEEE (2005), 2342.

B.X. Yang, M. Borland, W.M. Guo, K. Harkay, V. Sajaev, "Streak Camera Studies of Vertical Synchro-Betatron-Coupled Beam Motion in the APS Storage Ring," Proceedings of the 2005 Particle Accelerator Conference, IEEE (2005), 3694.

B.X. Yang, A.H. Lumpkin, "Visualizing Electron Beam Dynamics and Instabilities with Synchrotron Radiation at the APS," Proceedings of the 2005 Particle Accelerator Conference, IEEE (2005), 74.

B.X. Yang, J.L. Bailey, D.R. Walters, S.J. Stein, "Design of a High-Resolution Optical Transistion Radiation Imager for the Linac Coherent Light Source Undulator," Proceedings of the 2005 Particle Accelerator Conference, IEEE (2005), 4209.

C.Y. Yao, Y. Chae, N.S. Sereno, B. Yang, "Investigation of APS PAR Vertical Beam Instability," Proceedings of the 2005 Particle Accelerator Conference, IEEE (2005), 2393.

C.Y. Yao, N.S. Sereno, M. Borland, A.E. Grelick, A.H. Lumpkin, "Results of Preliminary Tests of PAR Bunch Cleaning," Proceedings of the 2005 Particle Accelerator Conference, IEEE (2005), 3307.

H. Yavas, E.E. Alp, H. Sinn, R. Khachatryan, A. Alatas, A.H. Said, J. Zhao, "A High-Resolution RIXS Spectrometer for Correlated Electron Materials," Lectures on the Physics of Highly Correlated Electron Systems IX, A. Avella, F. Mancini, eds., 789, AIP (2005), 299 - 305.

Beamline & Accelerator: Technical Reports

P.K. Job, B.J. Micklich, "Design Calculations for the Advanced Photon Source Safety Shutters," ANL/APS/LS-309, (March -2005).

B. Yang, H. Friedsam, "A Novel High-Resolution Alignment Technique for XFEL Using Undulator X-ray Beams," ANL/APS/LS-310, (November -2005).

The research highlights were written by:
William Arthur Atkins (waarc@grics.net)
Mary Beckman (mbeckman@nasw.org)
David Bradley (david@sciencebase.com)
Yvonne Carts-Powell (yvonnecp@verizon.net)
Vic Comello (TSD-MED)
Karen Fox (kfox@nasw.org)
Elise LeQuire (cygnete@mindspring.com)
JR Minkel (jrminkel@gmail.com)
Mona A. Mort (mamort@nasw.org)
David Voss (dvoss@nasw.org)
Mark Wolverton (exetermw@earthlink.net)

Mechanical editing:
Mary Fitzpatrick (TSD-MED), Catherine Eyberger (AES-ADM), Floyd Bennett (TSD-MED)
Cover design: Daniel Sarro (TSD-MED)
Photography: Wes Agresta and George Joch (TSD-MED)
Project coordination: Richard Fenner (SUF-PA), Susan Picologlou (XRS-ADM)
Publication design, photography: Richard Fenner

Our thanks to the corresponding authors who assisted in the preparation of the research highlights, to the users and APS personnel who wrote articles for the report, and our apologies to anyone inadvertantly left off this list. Your contributions are definitely appreciated.

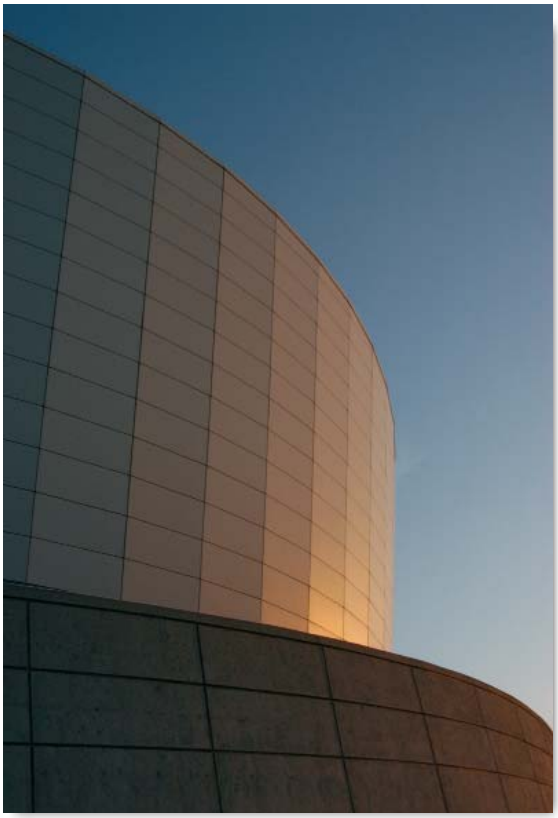

The exterior of the APS Auditorium at dusk.

Advanced Photon Source
Argonne National Laboratory
9700 S. Cass Ave.
Argonne, IL 60439 USA

www.anl.gov


A U.S. Department of Energy laboratory managed by The University of Chicago